4.55 Use the expressions given in Problem 4.54 to determine the capacitance for the configurations in Fig. 4-35(a) when the conducting plates are placed on the right and left faces of the structure.

Section 4-12: Image Method

4.56 With reference to Fig. 4-37, charge Q is located at a distance d above a grounded half-plane located in the x–y plane and at a distance d from another grounded half-plane in the x–z plane. Use the image method to

(a) Establish the magnitudes, polarities, and locations of the images of charge Q with respect to each of the two ground planes (as if each is infinite in extent).

(b) Find the electric potential and electric field at an arbitrary point $P(0, y, z)$.

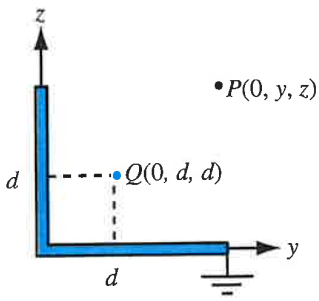


Figure 4-37: Charge Q next to two perpendicular, grounded, conducting half-planes.

4.57 Conducting wires above a conducting plane carry currents I_1 and I_2 in the directions shown in Fig. 4-38. Keeping in mind that the direction of a current is defined in terms of the movement of positive charges, what are the directions of the image currents corresponding to I_1 and I_2?



Figure 4-38: Currents above a conducting plane (Problem 4.57).

4.58 Use the image method to find the capacitance per unit length of an infinitely long conducting cylinder of radius a situated at a distance d from a parallel conducting plane, as shown in Fig. 4-39.

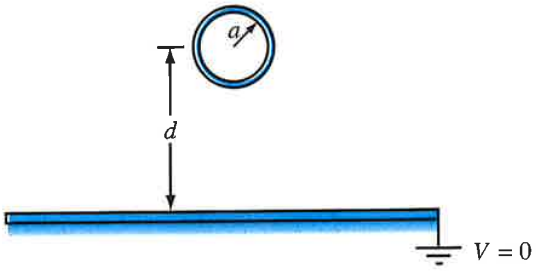
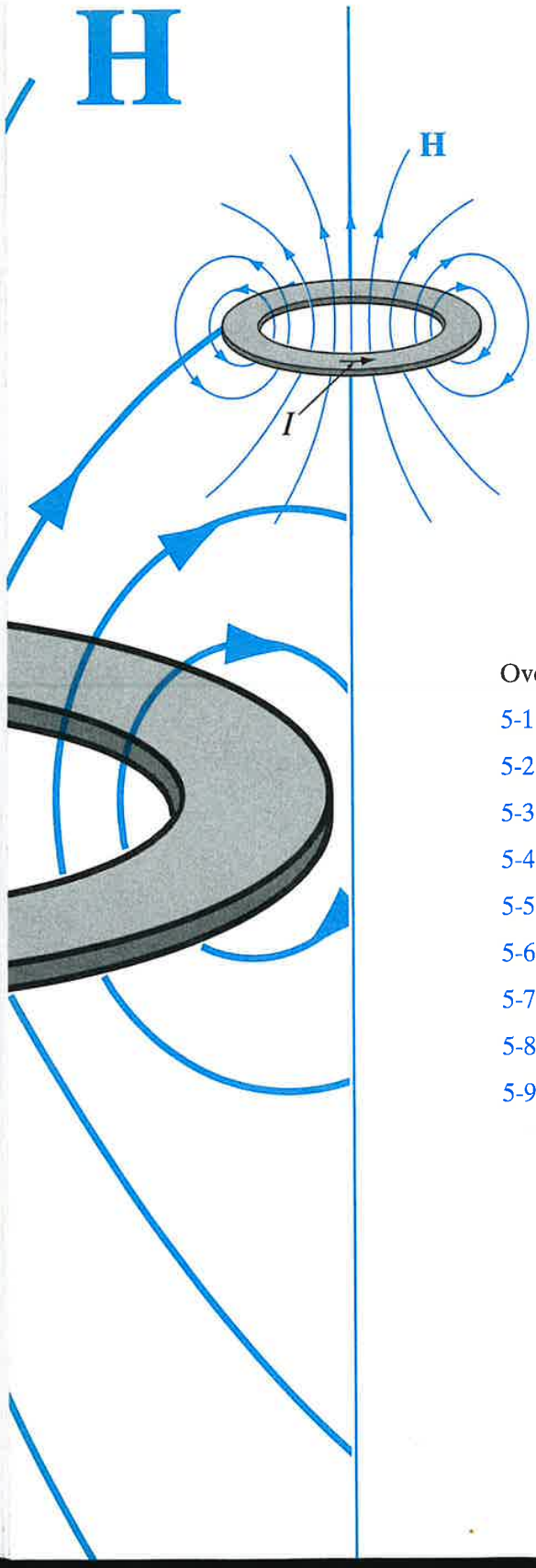


Figure 4-39: Conducting cylinder above a conducting plane (Problem 4.58).

INTEL-1014
U.S. Patent 7,151,430



CHAPTER 5

Magnetostatics

Overview

5-1 Magnetic Forces and Torques
5-2 The Biot—Savart Law
5-3 Magnetic Force between Two Parallel Conductors
5-4 Maxwell's Magnetostatic Equations
5-5 Vector Magnetic Potential
5-6 Magnetic Properties of Materials
5-7 Magnetic Boundary Conditions
5-8 Inductance
5-9 Magnetic Energy

INTEL-1014
U.S. Patent 7,151,430

OVERVIEW

This chapter on magnetostatics parallels the preceding chapter on electrostatics. Stationary charges produce static electric fields, and steady (nontime varying) currents produce magnetic fields. For $\partial/\partial t = 0$, the magnetic fields in a medium with magnetic permeability μ are governed by the second pair of Maxwell's equations, those given by Eqs. (4.3a and b):

$$\nabla \cdot \mathbf{B} = 0, \qquad (5.1a)$$

$$\nabla \times \mathbf{H} = \mathbf{J}, \qquad (5.1b)$$

where $\mathbf{J}$ is the current density. The magnetic flux density $\mathbf{B}$ and the magnetic field intensity $\mathbf{H}$ are related by

$$\mathbf{B} = \mu \mathbf{H}. \qquad (5.2)$$

When we examined electric fields in a dielectric medium in Chapter 4, we noted that the relation $\mathbf{D} = \varepsilon \mathbf{E}$ is valid only when the medium is linear and isotropic. These properties, which are true for most materials, allow us to treat the permittivity ε as a constant scalar quantity, independent of both the magnitude and direction of $\mathbf{E}$. A similar statement applies to the relation given by Eq. (5.2). With the exception of ferromagnetic materials, for which the relationship between $\mathbf{B}$ and $\mathbf{H}$ is nonlinear, most materials are characterized by constant magnetic permeabilities. *Furthermore, $\mu = \mu_0$ for most dielectrics and metals (excluding ferromagnetic materials).* Our objective in this chapter is to develop an understanding of the relationships between steady currents and the magnetic fields $\mathbf{B}$ and $\mathbf{H}$ for various types of current distributions and in various types of media and to introduce a number of related quantities, such as the magnetic vector potential $\mathbf{A}$, the magnetic energy density w_m, and the inductance of a conducting structure, L. The parallelism between these magnetostatic quantities and their electrostatic counterparts is encapsulated in Table 5-1.

5-1 Magnetic Forces and Torques

The electric field $\mathbf{E}$ at a point in space has been defined as the electric force $\mathbf{F}_e$ per unit charge acting on a test charge when placed at that point. We now define the ***magnetic flux density*** $\mathbf{B}$ at a point in space in terms of the ***magnetic force*** $\mathbf{F}_m$ that would be exerted on a charged particle moving with a velocity $\mathbf{u}$ were it to be passing through that point. Based on experiments conducted to determine the motion of charged particles moving in magnetic fields, it was established that the magnetic force $\mathbf{F}_m$ acting on a particle of charge q can be cast in the form

$$\mathbf{F}_m = q\mathbf{u} \times \mathbf{B} \quad \text{(N)}. \qquad (5.3)$$

Accordingly, the strength of $\mathbf{B}$ is measured in newtons/(C·m/s), which also is called the tesla (T) in SI units. For a positively charged particle, the direction of $\mathbf{F}_m$ is in the direction of the cross product $\mathbf{u} \times \mathbf{B}$, which is perpendicular to the plane containing $\mathbf{u}$ and $\mathbf{B}$ and governed by the right-hand rule. If q is negative, the direction of $\mathbf{F}_m$ is reversed, as illustrated in Fig. 5-1. The magnitude of $\mathbf{F}_m$ is given by

$$F_m = quB \sin\theta, \qquad (5.4)$$

where θ is the angle between $\mathbf{u}$ and $\mathbf{B}$. We note that F_m is maximum when $\mathbf{u}$ is perpendicular to $\mathbf{B}$ ($\theta = 90°$), and it is zero when $\mathbf{u}$ is parallel to $\mathbf{B}$ ($\theta = 0$ or $180°$).

INTEL-1014
U.S. Patent 7,151,430

Table 5-1: Attributes of electrostatics and magnetostatics.

Attribute	Electrostatics	Magnetostatics
Sources	Stationary charges	Steady currents
Fields	**E** and **D**	**H** and **B**
Constitutive parameter(s)	ε and σ	μ
Governing equations		
• **Differential form**	$\nabla \cdot \mathbf{D} = \rho_v$ $\nabla \times \mathbf{E} = 0$	$\nabla \cdot \mathbf{B} = 0$ $\nabla \times \mathbf{H} = \mathbf{J}$
• **Integral form**	$\oint_S \mathbf{D} \cdot d\mathbf{s} = Q$ $\oint_C \mathbf{E} \cdot d\mathbf{l} = 0$	$\oint_S \mathbf{B} \cdot d\mathbf{s} = 0$ $\oint_C \mathbf{H} \cdot d\mathbf{l} = I$
Potential	Scalar V, with $\mathbf{E} = -\nabla V$	Vector **A**, with $\mathbf{B} = \nabla \times \mathbf{A}$
Energy density	$w_e = \frac{1}{2}\varepsilon E^2$	$w_m = \frac{1}{2}\mu H^2$
Force on charge q	$\mathbf{F}_e = q\mathbf{E}$	$\mathbf{F}_m = q\mathbf{u} \times \mathbf{B}$
Circuit element(s)	C and R	L

If a charged particle is in the presence of both an electric field **E** and a magnetic field **B**, then the total *electromagnetic force* acting on it is

$$\mathbf{F} = \mathbf{F}_e + \mathbf{F}_m = q\mathbf{E} + q\mathbf{u} \times \mathbf{B} = q(\mathbf{E} + \mathbf{u} \times \mathbf{B}). \quad (5.5)$$

The force expressed by Eq. (5.5) is known as the *Lorentz force*. Electric and magnetic forces exhibit a number of important differences:

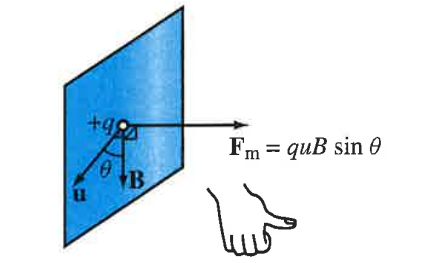
1. Whereas the electric force is always in the direction of the electric field, the magnetic force is always perpendicular to the magnetic field.
2. Whereas the electric force acts on a charged particle whether or not it is moving, the magnetic force acts on it only when it is in motion.
3. Whereas the electric force expends energy in displacing a charged particle, the magnetic force does no work when a particle is displaced.

Our last statement requires further elaboration. Because the magnetic force $\mathbf{F}_m$ is always perpendicular to **u**, $\mathbf{F}_m \cdot \mathbf{u} = 0$. Hence, the work performed when a particle is displaced by a differential distance $d\mathbf{l} = \mathbf{u}\,dt$ is

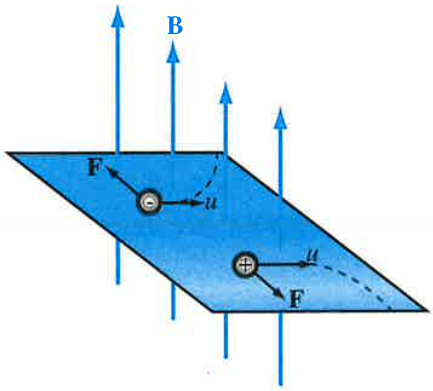
$$dW = \mathbf{F}_m \cdot d\mathbf{l} = (\mathbf{F}_m \cdot \mathbf{u})\,dt = 0. \quad (5.6)$$

Since no work is done, a magnetic field cannot change the kinetic energy of a charged particle; *the magnetic field can change the direction of motion of a charged particle, but it cannot change its speed.*

INTEL-1014
U.S. Patent 7,151,430



(a)



(b)

Figure 5-1: The direction of the magnetic force exerted on a charged particle moving in a magnetic field is (a) perpendicular to both **B** and **u** and (b) depends on the charge polarity (positive or negative).

EXERCISE 5.1 An electron moving in the positive x-direction perpendicular to a magnetic field experiences a deflection in the negative z-direction. What is the direction of the magnetic field?

Ans. Positive y-direction.

EXERCISE 5.2 A proton moving with a speed of 2×10^6 m/s through a magnetic field with magnetic flux density of 2.5 T experiences a magnetic force of magnitude 4×10^{-13} N. What is the angle between the magnetic field and the proton's velocity?

Ans. $\theta = 30°$ or $150°$.

EXERCISE 5.3 A charged particle with velocity **u** is moving in a medium containing uniform fields $\mathbf{E} = \hat{\mathbf{x}}E$ and $\mathbf{B} = \hat{\mathbf{y}}B$. What should **u** be so that the particle experiences no net force on it?

Ans. $\mathbf{u} = \hat{\mathbf{z}}E/B$.

5-1.1 Magnetic Force on a Current-Carrying Conductor

A current flowing through a conducting wire consists of charged particles *drifting* through the material of the wire. Consequently, when a current-carrying wire is placed in a magnetic field, it will experience a force equal to the sum of the magnetic forces acting on the charged particles moving within it. Consider, for example, the arrangement shown in Fig. 5-2 in which a vertical wire oriented along the z-direction is placed in a magnetic field **B** (produced by a magnet) oriented along the $-\hat{\mathbf{x}}$-direction (into the page). With no current flowing in the wire, $\mathbf{F}_m = 0$ and the wire maintains its vertical orientation, as shown in Fig. 5-2(a), but when a current is introduced in the wire, the wire deflects to the left ($-\hat{\mathbf{y}}$-direction) if the current's direction is upward ($+\hat{\mathbf{z}}$-direction), and it deflects to the right ($+\hat{\mathbf{y}}$-direction) if the current's direction is downward ($-\hat{\mathbf{z}}$-direction). The directions of these deflections are in accordance with the cross product given by Eq. (5.3).

To quantify the relationship between $\mathbf{F}_m$ and the current I flowing in the wire, let us consider a small segment of the wire of cross-sectional area A and differential length $d\mathbf{l}$, with the direction of $d\mathbf{l}$ denoting the direction of the current. Without loss of generality, we assume that the charge carriers constituting the current I are exclusively electrons, which is always a valid assumption for a good conductor. If the wire contains a free-electron

INTEL-1014
U.S. Patent 7,151,430

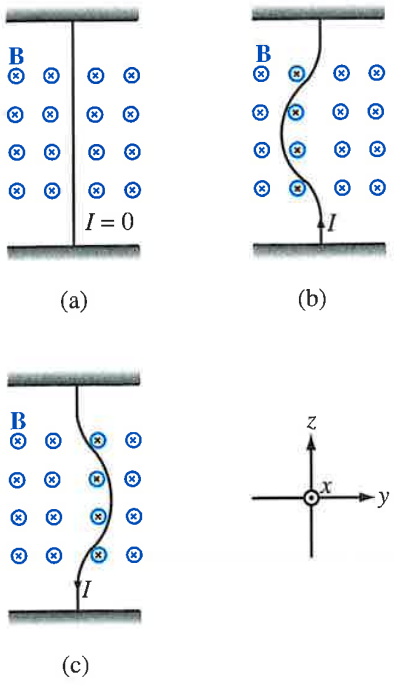


Figure 5-2: When a slightly flexible vertical wire is placed in a magnetic field directed into the page (as denoted by the crosses), it is (a) not deflected when the current through it is zero, (b) deflected to the left when I is upward, and (c) deflected to the right when I is downward.

charge density $\rho_{ve} = -N_e e$, where N_e is the number of moving electrons per unit volume, then the total amount of moving charge contained in an elemental volume of the wire is

$$dQ = \rho_{ve} A\, dl = -N_e e A\, dl, \tag{5.7}$$

and the corresponding magnetic force acting on dQ in the presence of a magnetic field $\mathbf{B}$ is

$$d\mathbf{F}_m = dQ\, \mathbf{u}_e \times \mathbf{B} = -N_e e A\, dl\, \mathbf{u}_e \times \mathbf{B}, \tag{5.8a}$$

where $\mathbf{u}_e$ is the drift velocity of the electrons. Since the direction of a current is defined as the direction of flow of positive charges, the electron drift velocity $\mathbf{u}_e$ is parallel to $d\mathbf{l}$, but opposite in direction. Thus, $dl\, \mathbf{u}_e = -d\mathbf{l}\, u_e$ and Eq. (5.8a) becomes

$$d\mathbf{F}_m = N_e e A u_e\, d\mathbf{l} \times \mathbf{B}. \tag{5.8b}$$

From Eqs. (4.11) and (4.12), the current I flowing through a cross-sectional area A due to electrons with density $\rho_{ve} = -N_e e$, moving with velocity $-u_e$, is $I = \rho_{ve}(-u_e)A = (-N_e e)(-u_e)A = N_e e A u_e$. Hence, Eq. (5.8b) may be written in the compact form

$$d\mathbf{F}_m = I\, d\mathbf{l} \times \mathbf{B} \quad \text{(N)}. \tag{5.9}$$

For a closed circuit of contour C carrying a current I, the total magnetic force is

$$\mathbf{F}_m = I \oint_C d\mathbf{l} \times \mathbf{B} \quad \text{(N)}. \tag{5.10}$$

We will now examine the application of Eq. (5.10) in each of two special situations.

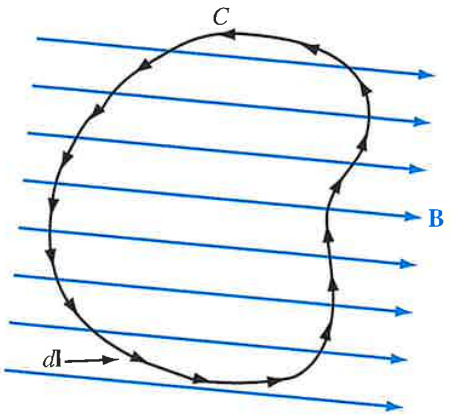
Closed Circuit in a Uniform **B** *Field*

Consider a closed wire carrying a current I and placed in a uniform external magnetic field $\mathbf{B}$, as shown in Fig. 5-3(a). Since $\mathbf{B}$ is constant, it can be taken outside the integral in Eq. (5.10), in which case we have

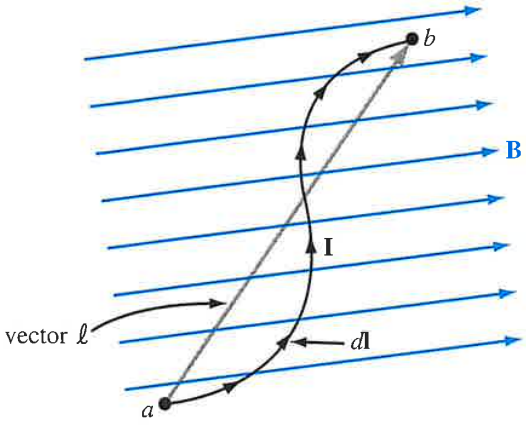
$$\mathbf{F}_m = I \left(\oint_C d\mathbf{l} \right) \times \mathbf{B} = 0. \tag{5.11}$$

This result, which is a consequence of the fact that the vector sum of the displacement vectors $d\mathbf{l}$ over a closed path is equal to zero, states that *the total magnetic force on any closed current loop in a uniform magnetic field is zero.*

INTEL-1014
U.S. Patent 7,151,430



(a)



(b)

Figure 5-3: In a uniform magnetic field, (a) the net force on a closed current loop is zero because the integral of the displacement vector $d\mathbf{l}$ over a closed contour is zero, and (b) the force on a line segment is proportional to the vector between the end point ($\mathbf{F}_m = I\boldsymbol{\ell} \times \mathbf{B}$).

Curved Wire in a Uniform **B** *Field*

If we are interested in the magnetic force exerted on a wire segment, such as that shown in Fig. 5-3(b), when placed in a uniform field **B**, then Eq. (5.10) becomes

$$\mathbf{F}_m = I\left(\int_a^b d\mathbf{l}\right) \times \mathbf{B} = I\boldsymbol{\ell} \times \mathbf{B}, \qquad (5.12)$$

where $\boldsymbol{\ell}$ is the vector directed from a to b, as shown in Fig. 5-3(b). The integral of $d\mathbf{l}$ from a to b has the same value irrespective of the path taken between a and b. For a closed loop, points a and b become the same point, in which case $\boldsymbol{\ell} = 0$ and $\mathbf{F}_m = 0$.

Example 5-1 **Force on a Semicircular Conductor**

The semicircular conductor shown in Fig. 5-4 lies in the x–y plane and carries a current I. The closed circuit is exposed to a uniform magnetic field $\mathbf{B} = \hat{\mathbf{y}}B_0$. Determine (a) the magnetic force $\mathbf{F}_1$ on the straight section of the wire and (b) the force $\mathbf{F}_2$ on the curved section.

Solution: **(a)** The straight section of the circuit is of length $2r$, and the current flowing through it is along the

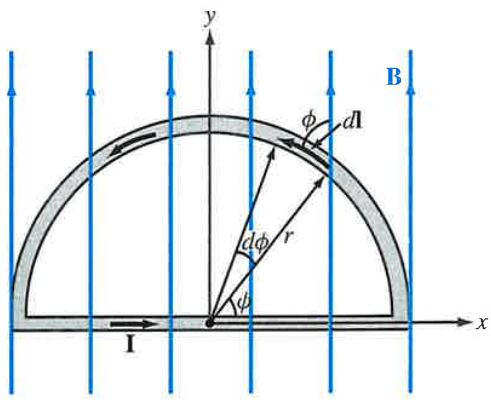


Figure 5-4: Semicircular conductor in a uniform field (Example 5-1).

INTEL-1014
U.S. Patent 7,151,430

$+x$-direction. Application of Eq. (5.12) with $\boldsymbol{\ell} = \hat{\mathbf{x}}2r$ gives

$$\mathbf{F}_1 = \hat{\mathbf{x}}(2Ir) \times \hat{\mathbf{y}}B_0 = \hat{\mathbf{z}}\,2IrB_0 \quad \text{(N)}.$$

(b) Let us consider a segment of differential length $d\mathbf{l}$ on the curved part of the circle. The direction of $d\mathbf{l}$ is chosen to coincide with the direction of the current. Since $d\mathbf{l}$ and $\mathbf{B}$ are both in the x–y plane, their cross product $d\mathbf{l} \times \mathbf{B}$ points in the negative z-direction, and the magnitude of $d\mathbf{l} \times \mathbf{B}$ is proportional to $\sin\phi$, where ϕ is the angle between $d\mathbf{l}$ and $\mathbf{B}$. Moreover, the magnitude of $d\mathbf{l}$ is $dl = r\,d\phi$. Hence,

$$\mathbf{F}_2 = I\int_{\phi=0}^{\pi} d\mathbf{l} \times \mathbf{B}$$

$$= -\hat{\mathbf{z}}I\int_{\phi=0}^{\pi} rB_0 \sin\phi\, d\phi = -\hat{\mathbf{z}}\,2IrB_0 \quad \text{(N)}.$$

We note that $\mathbf{F}_2 = -\mathbf{F}_1$, and consequently the net force on the closed loop is zero. ■

EXERCISE 5.4 A horizontal wire with a mass per unit length of 0.2 kg/m carries a current of 4 A in the $+x$-direction. If the wire is placed in a uniform magnetic flux density $\mathbf{B}$, what should the direction and minimum magnitude of $\mathbf{B}$ be in order to magnetically lift the wire vertically upward? (Hint: The acceleration due to gravity is $\mathbf{g} = -\hat{\mathbf{z}}9.8\ \text{m/s}^2$.)

Ans. $\mathbf{B} = \hat{\mathbf{y}}0.49$ T.

REVIEW QUESTIONS

Q5.1 What are the major differences between the behavior of the electric force $\mathbf{F}_e$ and the behavior of the magnetic force $\mathbf{F}_m$?

Q5.2 The ends of a 10-cm-long wire carrying a constant current I are anchored at two points on the x-axis, $x = 0$ and $x = 6$ cm. If the wire lies in the x–y plane and is present in a magnetic field $\mathbf{B} = \hat{\mathbf{y}}B_0$, which of the following arrangements produces a greater magnetic force on the wire: (a) wire is V-shaped with corners at (0, 0), (3, 4), and (6, 0), (b) wire looks like an open rectangle with corners at (0, 0), (0, 2), (6, 2), and (6, 0).

5-1.2 Magnetic Torque on a Current-Carrying Loop

When a force is applied on a rigid body pivoted about a fixed axis, the body will react by rotating about that axis. The strength of the reaction depends on the cross product of the applied force vector $\mathbf{F}$ and the distance vector $\mathbf{d}$, measured *from* a point on the rotation axis (such that $\mathbf{d}$ is perpendicular to the axis) *to* the point of application of $\mathbf{F}$ (Fig. 5-5). The length of $\mathbf{d}$ is called the ***moment arm***, and the cross product is called the ***torque***:

$$\mathbf{T} = \mathbf{d} \times \mathbf{F} \quad \text{(N·m)}. \tag{5.13}$$

The unit for $\mathbf{T}$ is the same as that for work or energy, but torque does not represent work or energy. The force $\mathbf{F}$

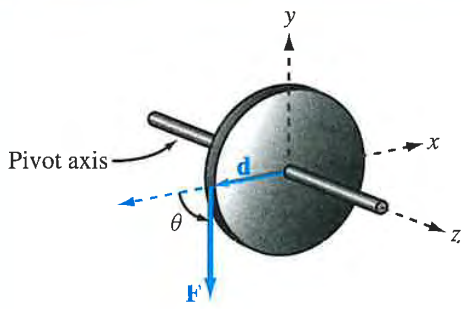


Figure 5-5: The force $\mathbf{F}$ acting on a circular disk pivoted along the z-axis generates a torque $\mathbf{T} = \mathbf{d} \times \mathbf{F}$ that causes the disk to rotate.

INTEL-1014
U.S. Patent 7,151,430

applied on the disk shown in Fig. 5-5 lies in the x–y plane and makes an angle θ with $\mathbf{d}$. Hence,

$$\mathbf{T} = \hat{\mathbf{z}} r F \sin\theta, \tag{5.14}$$

where $|\mathbf{d}| = r$, the radius of the disk, and $F = |\mathbf{F}|$. From Eq. (5.14) we see that a torque along the positive z-direction corresponds to a tendency for the cylinder to rotate in a counterclockwise direction and, conversely, a negative torque corresponds to clockwise rotation. These directions are governed by the following ***right-hand rule:*** *when the thumb of the right hand is pointed along the direction of the torque, the four fingers indicate the direction that the torque is trying to rotate the body.*

We will now consider the ***magnetic torque*** exerted on a conducting loop under the influence of magnetic forces. We begin with the simple case where the magnetic field $\mathbf{B}$ is in the plane of the loop, and then we will extend the analysis to the more general case where $\mathbf{B}$ makes an angle θ with the surface normal of the loop.

Magnetic Field in the Plane of the Loop

The rectangular conducting loop shown in Fig. 5-6(a) is made of rigid wire carrying a current I. The loop lies in the x–y plane and is pivoted about the axis shown. Under the influence of an externally generated uniform magnetic field $\mathbf{B} = \hat{\mathbf{x}} B_0$, arms 1 and 3 of the loop are subjected to forces $\mathbf{F}_1$ and $\mathbf{F}_3$, respectively, with

$$\mathbf{F}_1 = I(-\hat{\mathbf{y}} b) \times (\hat{\mathbf{x}} B_0) = \hat{\mathbf{z}} I b B_0, \tag{5.15a}$$

and

$$\mathbf{F}_3 = I(\hat{\mathbf{y}} b) \times (\hat{\mathbf{x}} B_0) = -\hat{\mathbf{z}} I b B_0. \tag{5.15b}$$

These results are based on the application of Eq. (5.12). No magnetic force is exerted on either arm 2 or 4 because $\mathbf{B}$ is parallel to the direction of the current flowing in those arms.

The end view of the loop, depicted in Fig. 5-6(b), shows that forces $\mathbf{F}_1$ and $\mathbf{F}_3$ produce a torque about the origin O, causing the loop to rotate in a clockwise direction. The moment arm is $a/2$ for both forces, but $\mathbf{d}_1$ and $\mathbf{d}_3$ are in opposite directions, resulting in a total magnetic torque of

$$\begin{aligned}\mathbf{T} &= \mathbf{d}_1 \times \mathbf{F}_1 + \mathbf{d}_3 \times \mathbf{F}_3 \\ &= \left(-\hat{\mathbf{x}}\frac{a}{2}\right) \times (\hat{\mathbf{z}} I b B_0) + \left(\hat{\mathbf{x}}\frac{a}{2}\right) \times (-\hat{\mathbf{z}} I b B_0) \\ &= \hat{\mathbf{y}} I a b B_0 = \hat{\mathbf{y}} I A B_0,\end{aligned} \tag{5.16}$$

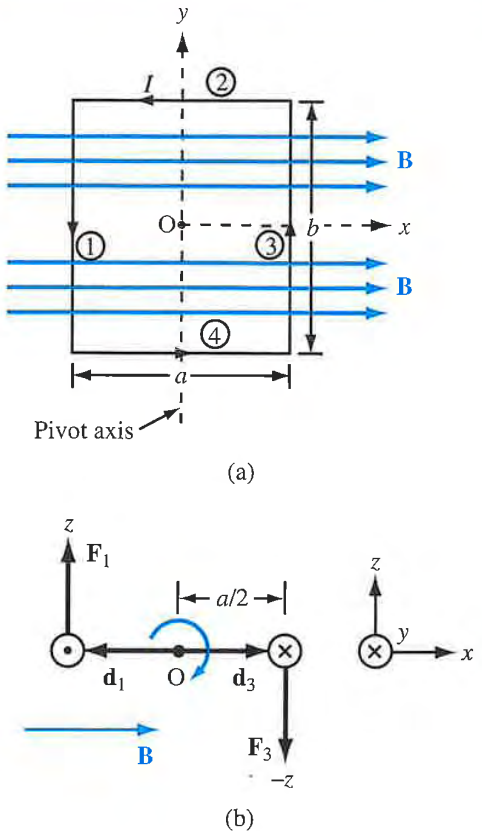


Figure 5-6: Rectangular loop pivoted along the y-axis: (a) front view and (b) bottom view. The combination of forces $\mathbf{F}_1$ and $\mathbf{F}_3$ on the loop generates a torque that tends to rotate the loop in a clockwise direction as shown in (b).

INTEL-1014
U.S. Patent 7,151,430

where $A = ab$ is the area of the loop. The right-hand rule tells us that the sense of rotation is clockwise. The result given by Eq. (5.16) is valid only when the magnetic field **B** is parallel to the plane of the loop. As soon as the loop starts to rotate, the torque **T** starts to decrease, and at the end of one quarter of a complete rotation, the torque becomes zero, as discussed next.

Magnetic Field Perpendicular to the Axis of a Rectangular Loop

For the situation represented by Fig. 5-7, where $\mathbf{B} = \hat{\mathbf{x}}B_0$, the field is still perpendicular to the loop's axis of rotation, but its direction may be at any angle θ with respect to the loop's surface normal $\hat{\mathbf{n}}$, we may now have nonzero forces on all four arms of the rectangular loop. However, forces $\mathbf{F}_2$ and $\mathbf{F}_4$ are equal in magnitude and opposite in direction and are along the rotation axis; hence, the net torque contributed by their combination is zero. The directions of the currents in arms 1 and 3 are always perpendicular to **B** regardless of the magnitude of θ. Hence, $\mathbf{F}_1$ and $\mathbf{F}_3$ have the same expressions given previously by Eqs. (5.15a and b), and their moment arm is $(a/2)\sin\theta$, as illustrated in Fig. 5-7(b). Consequently, the magnitude of the net torque exerted by the magnetic field about the axis of rotation is the same as that given by Eq. (5.16), but modified by $\sin\theta$:

$$T = IAB_0 \sin\theta. \tag{5.17}$$

According to Eq. (5.17), the torque is maximum when the magnetic field is parallel to the plane of the loop ($\theta = 90°$) and is zero when the field is perpendicular to the plane of the loop ($\theta = 0$). If the loop consists of N turns, each contributing a torque given by Eq. (5.17), then the total torque is

$$T = NIAB_0 \sin\theta. \tag{5.18}$$

The quantity NIA is called the ***magnetic moment*** m of the loop, and it may be regarded as a vector **m** with direction $\hat{\mathbf{n}}$, where $\hat{\mathbf{n}}$ is the surface normal of the loop and governed by the following ***right-hand rule:*** *when the four fingers of the right hand advance in the direction of the current I, the direction of the thumb specifies the*

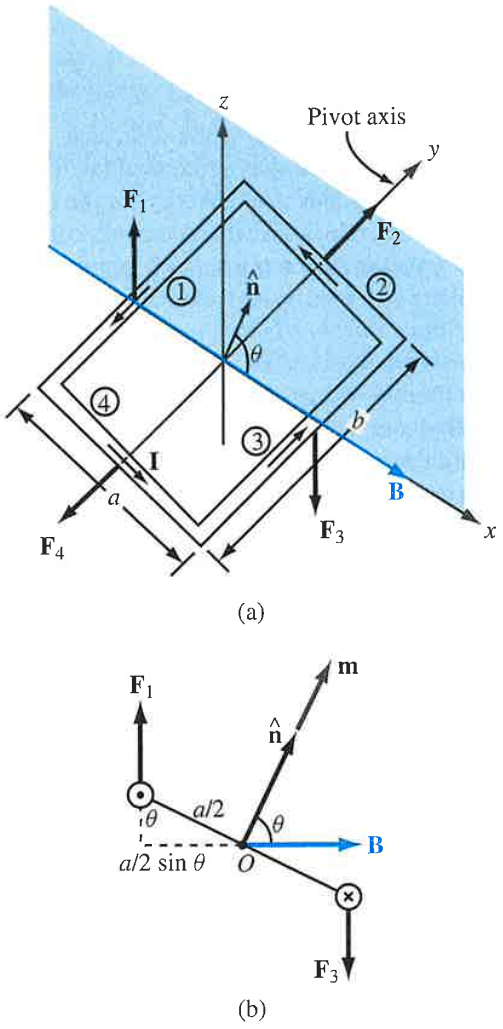


Figure 5-7: Rectangular loop in a uniform magnetic field with flux density **B** whose direction is perpendicular to the rotation axis of the loop, but makes an angle θ with the loop's surface normal $\hat{\mathbf{n}}$.

INTEL-1014
U.S. Patent 7,151,430

direction of $\hat{\mathbf{n}}$. That is,

$$\mathbf{m} \triangleq \hat{\mathbf{n}} N I A \quad (\text{A}\cdot\text{m}^2), \qquad (5.19)$$

and in terms of $\mathbf{m}$, the torque vector $\mathbf{T}$ can be written as

$$\mathbf{T} = \mathbf{m} \times \mathbf{B} \quad (\text{N}\cdot\text{m}). \qquad (5.20)$$

Even though the derivation leading to Eq. (5.20) was obtained for $\mathbf{B}$ being perpendicular to the axis of rotation of a rectangular loop, the expression is valid for any orientation of $\mathbf{B}$ and for a loop of any shape.

REVIEW QUESTIONS

Q5.3 How is the direction of the magnetic moment of a loop defined?

Q5.4 If one of two wires of equal lengths is formed into a closed square loop and the other is formed into a closed circular loop, and if both wires are carrying equal currents and both loops have their planes parallel to a uniform magnetic field, which loop would experience a greater torque?

EXERCISE 5.5 A square coil of 100 turns and 0.5-m-long sides is in a region with a uniform magnetic flux density of 0.2 T. If the maximum magnetic torque exerted on the coil is 4×10^{-2} (N·m), what is the current flowing in the coil?

Ans. $I = 8$ mA.

5-2 The Biot–Savart Law

In the preceding section, we elected to use the magnetic flux density $\mathbf{B}$ to denote the presence of a magnetic field in a given region of space. We will now work with the magnetic field intensity $\mathbf{H}$ instead. We do this in part to remind the reader that $\mathbf{B}$ and $\mathbf{H}$ are linearly related for most materials through $\mathbf{B} = \mu\mathbf{H}$, and therefore knowledge of one is synonymous with knowledge of the other (assuming that μ is known).

Through his experiments on the deflection of compass needles by current-carrying wires, Hans Oersted established that currents induce magnetic fields that form closed loops around the wires [see Section 1-2.3]. Building upon Oersted's results, Jean Biot and Felix Savart arrived at an expression that relates the magnetic field $\mathbf{H}$ at any point in space to the current I that generates $\mathbf{H}$. The *Biot–Savart law* states that the differential magnetic field $d\mathbf{H}$ generated by a steady current I flowing through a differential length $d\mathbf{l}$ is given by

$$d\mathbf{H} = \frac{I}{4\pi} \frac{d\mathbf{l} \times \hat{\mathbf{R}}}{R^2} \quad (\text{A/m}), \qquad (5.21)$$

where $\mathbf{R} = \hat{\mathbf{R}}R$ is the distance vector between $d\mathbf{l}$ and the observation point P shown in Fig. 5-8. The SI unit for $\mathbf{H}$ is ampere·m/m^2 = (A/m). It is important to remember that the direction of the magnetic field is defined such that $d\mathbf{l}$ is along the direction of the current I and the unit vector $\hat{\mathbf{R}}$ points *from* the current element *to* the observation point. According to Eq. (5.21), $d\mathbf{H}$ varies as R^{-2}, which is similar to the distance dependence of the electric field induced by an electric charge. However, unlike the electric field vector $\mathbf{E}$, whose direction is *along* the distance vector $\mathbf{R}$ joining the charge to the observation point, the magnetic field $\mathbf{H}$ is *orthogonal* to the plane containing the direction of the current element $d\mathbf{l}$ and the distance vector $\mathbf{R}$. At point P in Fig. 5-8, the direction of $d\mathbf{H}$ is out of the page, whereas at point P' the direction of $d\mathbf{H}$ is into the page.

To determine the total magnetic field $\mathbf{H}$ due to a conductor of finite size, we need to sum up the contributions

INTEL-1014
U.S. Patent 7,151,430

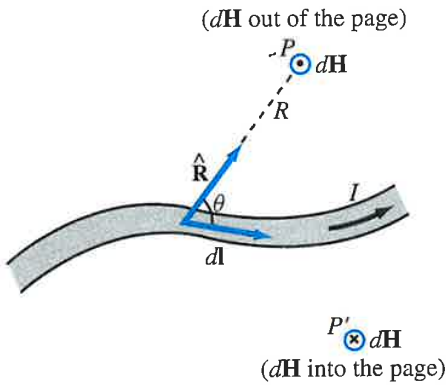


Figure 5-8: Magnetic field $d\mathbf{H}$ generated by a current element $I\,d\mathbf{l}$. The direction of the field induced at point P is opposite that induced at point P'.

due to all the current elements making up the conductor. Hence, the Biot–Savart law becomes

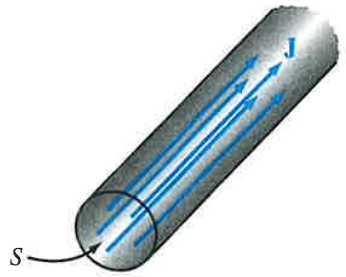
$$\mathbf{H} = \frac{I}{4\pi}\int_l \frac{d\mathbf{l}\times\hat{\mathbf{R}}}{R^2} \quad \text{(A/m)}, \qquad (5.22)$$

where l is the line path along which I exists.

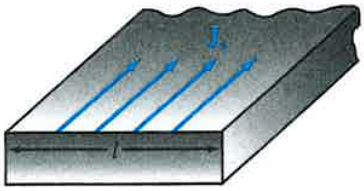
5-2.1 Magnetic Field due to Surface and Volume Current Distributions

The Biot–Savart law may also be expressed in terms of distributed current sources (Fig. 5-9) such as the ***volume current density*** $\mathbf{J}$, measured in (A/m^2), or the ***surface current density*** $\mathbf{J}_s$, measured in (A/m). The surface current density $\mathbf{J}_s$ applies to currents that flow on the surfaces of conductors in the form of sheets of effectively zero thickness. When the current sources are specified in terms of $\mathbf{J}_s$ over a surface S or in terms of $\mathbf{J}$ over a volume v, we can use the equivalence given by

$$I\,d\mathbf{l} = \mathbf{J}_s\,ds = \mathbf{J}\,dv \qquad (5.23)$$



(a) Volume current density $\mathbf{J}$ in (A/m^2)



(b) Surface current density $\mathbf{J}_s$ in (A/m)

Figure 5-9: (a) The total current crossing the cross section S of the cylinder is $I = \int_S \mathbf{J}\cdot d\mathbf{s}$. (b) The total current flowing across the surface of the conductor is $I = \int_l J_s\,dl$.

to express the Biot–Savart law as follows:

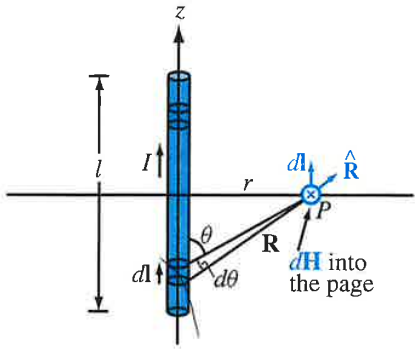
$$\mathbf{H} = \frac{1}{4\pi}\int_S \frac{\mathbf{J}_s\times\hat{\mathbf{R}}}{R^2}\,ds \quad \text{(for a surface current)}, \qquad (5.24a)$$

$$\mathbf{H} = \frac{1}{4\pi}\int_v \frac{\mathbf{J}\times\hat{\mathbf{R}}}{R^2}\,dv \quad \text{(for a volume current)}. \qquad (5.24b)$$

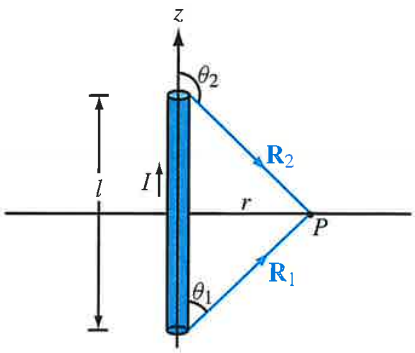
Example 5-2 Magnetic Field of a Linear Conductor

A linear conductor of length l and carrying a current I is placed along the z-axis as shown in Fig. 5-10.

INTEL-1014
U.S. Patent 7,151,430



(a)



(b)

Figure 5-10: Linear conductor of length l carrying a current I. (a) The field $d\mathbf{H}$ at point P due to incremental current element $d\mathbf{l}$. (b) Limiting angles θ_1 and θ_2, each measured between vector $I\,d\mathbf{l}$ and the vector connecting the end of the conductor associated with that angle to point P (Example 5-2).

Determine the magnetic flux density $\mathbf{B}$ at a point P located at a distance r in the x–y plane in free space.

Solution: From Fig. 5-10, current element $d\mathbf{l} = \hat{\mathbf{z}}\,dz$ and $d\mathbf{l} \times \hat{\mathbf{R}} = dz\,(\hat{\mathbf{z}} \times \hat{\mathbf{R}}) = \hat{\boldsymbol{\phi}} \sin\theta\,dz$, where $\hat{\boldsymbol{\phi}}$ is the azimuth direction and θ is the angle between $d\mathbf{l}$ and $\hat{\mathbf{R}}$. Hence, application of Eq. (5.22) gives

$$\mathbf{H} = \frac{I}{4\pi}\int_{z=-l/2}^{z=l/2}\frac{d\mathbf{l}\times\hat{\mathbf{R}}}{R^2} = \hat{\boldsymbol{\phi}}\frac{I}{4\pi}\int_{-l/2}^{l/2}\frac{\sin\theta}{R^2}\,dz. \quad (5.25)$$

For convenience, we will convert the integration variable from z to θ by using the transformations

$$R = r\csc\theta, \quad (5.26a)$$

$$z = -r\cot\theta, \quad (5.26b)$$

$$dz = r\csc^2\theta\,d\theta. \quad (5.26c)$$

Upon inserting Eqs. (5.26a) and (5.26c) into Eq. (5.25), we have

$$\begin{aligned}\mathbf{H} &= \hat{\boldsymbol{\phi}}\frac{I}{4\pi}\int_{\theta_1}^{\theta_2}\frac{\sin\theta\; r\csc^2\theta\,d\theta}{r^2\csc^2\theta}\\ &= \hat{\boldsymbol{\phi}}\frac{I}{4\pi r}\int_{\theta_1}^{\theta_2}\sin\theta\,d\theta\\ &= \hat{\boldsymbol{\phi}}\frac{I}{4\pi r}(\cos\theta_1 - \cos\theta_2), \quad (5.27)\end{aligned}$$

where θ_1 and θ_2 are the limiting angles at $z = -l/2$ and $z = l/2$, respectively. From the right triangle in Fig. 5-10(b),

$$\cos\theta_1 = \frac{l/2}{\sqrt{r^2 + (l/2)^2}}, \quad (5.28a)$$

$$\cos\theta_2 = -\cos\theta_1 = \frac{-l/2}{\sqrt{r^2 + (l/2)^2}}. \quad (5.28b)$$

Hence,

$$\mathbf{B} = \mu_0\mathbf{H} = \hat{\boldsymbol{\phi}}\frac{\mu_0 I l}{2\pi r\sqrt{4r^2 + l^2}}\ \text{(T)}. \quad (5.29)$$

For an infinitely long wire such that $l \gg r$, Eq. (5.29) reduces to

$$\mathbf{B} = \hat{\boldsymbol{\phi}}\frac{\mu_0 I}{2\pi r}\quad \text{(infinitely long wire)}. \quad (5.30)$$

INTEL-1014
U.S. Patent 7,151,430

Example 5-3 Magnetic Field of a Pie-Shaped Loop

Determine the magnetic field at the apex O of the pie-shaped loop shown in Fig. 5-11. Ignore the contributions to the field due to the current in the small arcs near O.

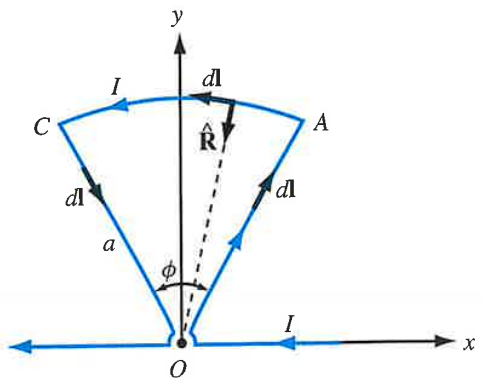


Figure 5-11: Pie-shaped loop of radius a carrying a current I (Example 5-3).

Solution: For the straight segments OA and OC, the magnetic field at O is identically zero. This is because, for all points along these segments, $d\mathbf{l}$ is parallel or antiparallel to $\hat{\mathbf{R}}$ and hence $d\mathbf{l} \times \hat{\mathbf{R}} = 0$. For segment AC, $d\mathbf{l}$ is perpendicular to $\hat{\mathbf{R}}$ and $d\mathbf{l} \times \hat{\mathbf{R}} = \hat{\mathbf{z}}\, dl = \hat{\mathbf{z}} a\, d\phi$. Consequently, Eq. (5.22) gives

$$\mathbf{H} = \frac{I}{4\pi} \int \frac{\hat{\mathbf{z}} a\, d\phi}{a^2} = \hat{\mathbf{z}} \frac{I}{4\pi a} \phi,$$

where ϕ is in radians. ■

Example 5-4 Magnetic Field of a Circular Loop

A circular loop of radius a carries a steady current I. Determine the magnetic field $\mathbf{H}$ at a point on the axis of the loop.

Solution: Let us place the loop in the x–y plane, as shown in Fig. 5-12. Our task is to obtain an expression for $\mathbf{H}$ at point $P(0, 0, z)$.

We start by noting that any element $d\mathbf{l}$ on the circular loop is perpendicular to the distance vector $\mathbf{R}$, and that all elements around the loop are at the same distance R from P, with $R = \sqrt{a^2 + z^2}$. From Eq. (5.21), the magnitude of $d\mathbf{H}$ due to element $d\mathbf{l}$ is given by

$$dH = \frac{I}{4\pi R^2} |d\mathbf{l} \times \hat{\mathbf{R}}| = \frac{I\, dl}{4\pi (a^2 + z^2)}, \qquad (5.31)$$

and the direction of $d\mathbf{H}$ is perpendicular to the plane containing $\mathbf{R}$ and $d\mathbf{l}$. As shown in Fig. 5-12, $d\mathbf{H}$ is in the r–z plane, and therefore it has components dH_r and dH_z. If we consider element $d\mathbf{l}'$, located diametrically opposite to $d\mathbf{l}$, we observe that the z-components of the magnetic

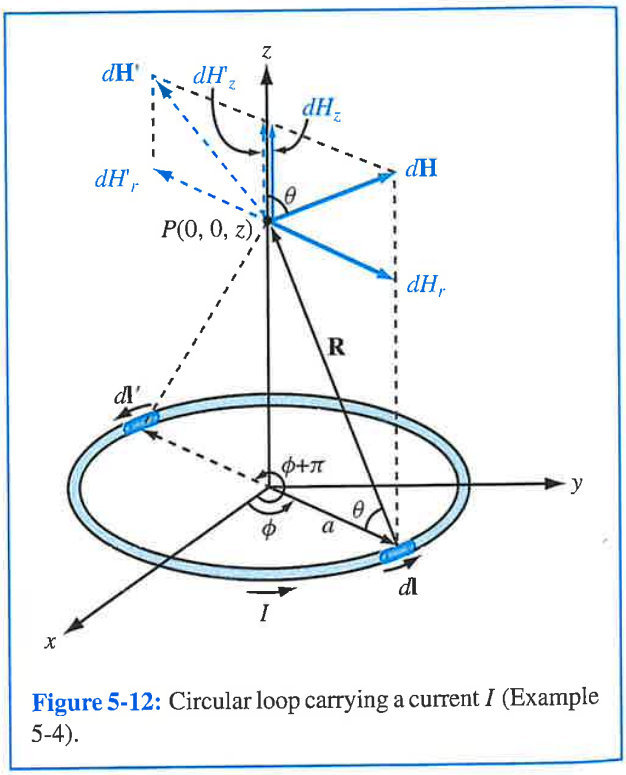


Figure 5-12: Circular loop carrying a current I (Example 5-4).

INTEL-1014
U.S. Patent 7,151,430

fields due to $d\mathbf{l}$ and $d\mathbf{l}'$ add because they are in the same direction, but their r-components cancel because they are in opposite directions. Hence, the net magnetic field is along z only. That is,

$$d\mathbf{H} = \hat{\mathbf{z}}\, dH_z = \hat{\mathbf{z}}\, dH \cos\theta = \hat{\mathbf{z}} \frac{I \cos\theta}{4\pi(a^2 + z^2)}\, dl. \quad (5.32)$$

For a fixed point $P(0, 0, z)$ on the axis of the loop, all quantities in Eq. (5.32) are constant, except for dl. Hence, integrating Eq. (5.32) over a circle of radius a gives

$$\mathbf{H} = \hat{\mathbf{z}} \frac{I \cos\theta}{4\pi(a^2 + z^2)} \oint dl = \hat{\mathbf{z}} \frac{I \cos\theta}{4\pi(a^2 + z^2)} (2\pi a). \quad (5.33)$$

Upon using the relation $\cos\theta = a/(a^2+z^2)^{1/2}$, we obtain the final expression:

$$\mathbf{H} = \hat{\mathbf{z}} \frac{Ia^2}{2(a^2 + z^2)^{3/2}} \quad \text{(A/m)}. \quad (5.34)$$

At the center of the loop ($z = 0$), Eq. (5.34) reduces to

$$\mathbf{H} = \hat{\mathbf{z}} \frac{I}{2a} \quad (\text{at } z = 0), \quad (5.35)$$

and at points very far away from the loop such that $z^2 \gg a^2$, Eq. (5.34) can be approximated as

$$\mathbf{H} = \hat{\mathbf{z}} \frac{Ia^2}{2|z|^3} \quad (\text{at } |z| \gg a). \quad (5.36)$$

5-2.2 Magnetic Field of a Magnetic Dipole

In view of the definition given by Eq. (5.19) for the magnetic moment $\mathbf{m}$ of a current loop, a loop with a single turn situated in the x–y plane, such as the one shown in Fig. 5-12, has a magnetic moment $\mathbf{m} = \hat{\mathbf{z}}m$ with $m = I\pi a^2$. Consequently, Eq. (5.36) may be expressed in the form

$$\mathbf{H} = \hat{\mathbf{z}} \frac{m}{2\pi|z|^3} \quad (\text{at } |z| \gg a). \quad (5.37)$$

This expression applies for a point P very far away from the loop, but on the axis of the loop. Had the problem been solved to find $\mathbf{H}$ at any distant point $P'(R', \theta', \phi')$ in a spherical coordinate system, where R' is the distance between the center of the loop and point P', we would have obtained the expression

$$\mathbf{H} = \frac{m}{4\pi R'^3} (\hat{\mathbf{R}}\, 2\cos\theta' + \hat{\boldsymbol{\theta}} \sin\theta') \quad (5.38)$$

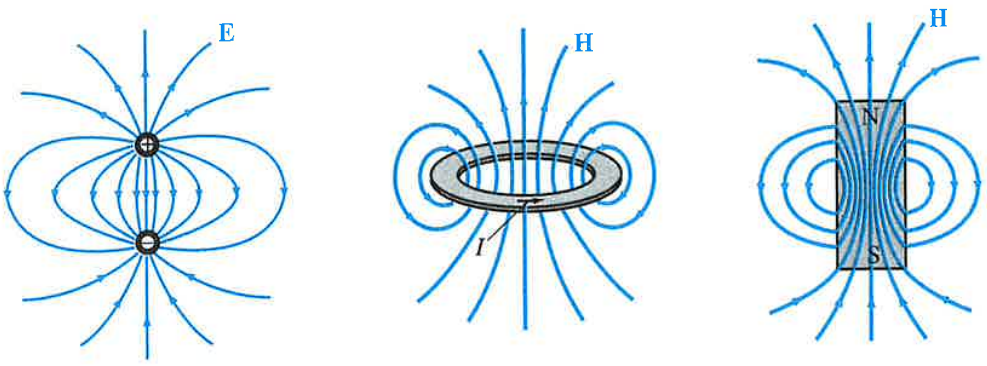
for $R' \gg a$. A current loop with dimensions much smaller than the distance between the loop and the observation point is called a *magnetic dipole*. This is because the pattern of its magnetic field is similar to that of a permanent magnet, as well as to the pattern of the electric field of the electric dipole [see Example 4-7]. The similarity is evident from the patterns shown in Fig. 5-13.

REVIEW QUESTIONS

Q5.5 Two infinitely long parallel wires carry currents of equal magnitude. What is the resultant magnetic field due to the two wires at a point midway between the wires, compared with the magnetic field due to one of them alone, if the currents are (a) in the same direction and (b) in opposite directions?

Q5.6 Devise a right-hand rule for the direction of the magnetic field due to a linear current-carrying conductor.

INTEL-1014
U.S. Patent 7,151,430



(a) Electric dipole (b) Magnetic dipole (c) Bar magnet

Figure 5-13: Patterns of (a) the electric field of an electric dipole, (b) the magnetic field of a magnetic dipole, and (c) the magnetic field of a bar magnet. Far away from the sources, the field patterns are similar in all three cases.

Q5.7 What is a magnetic dipole? Describe its magnetic field distribution.

EXERCISE 5.6 A semiinfinite linear conductor extends between $z = 0$ and $z = \infty$ along the z-axis. If the current I in the conductor flows along the positive z-direction, find $\mathbf{H}$ at a point in the x–y plane at a radial distance r from the conductor.

Ans. $\mathbf{H} = \hat{\boldsymbol{\phi}} \dfrac{I}{4\pi r}$ (A/m).

EXERCISE 5.7 A wire carrying a current of 4 A is formed into a circular loop. If the magnetic field at the center of the loop is 20 A/m, what is the radius of the loop if the loop has (a) only one turn and (b) 10 turns?

Ans. (a) $a = 10$ cm, (b) $a = 1$ m.

EXERCISE 5.8 A wire is formed into a square loop and placed in the x–y plane with its center at the origin and each of its sides parallel to either the x- or y-axes. Each side is 40 cm in length, and the wire carries a current of 5 A whose direction is clockwise when the loop is viewed from above. Calculate the magnetic field at the center of the loop.

Ans. $\mathbf{H} = -\hat{\mathbf{z}} \dfrac{4I}{\sqrt{2}\pi l} = -\hat{\mathbf{z}}11.25$ A/m.

5-3 Magnetic Force between Two Parallel Conductors

In Section 5-1.1 we examined the magnetic force $\mathbf{F}_m$ that acts on a current-carrying conductor when the conductor is placed in an external magnetic field. The current in the conductor, however, also generates its own magnetic field. Hence, if two current-carrying conductors are placed in each other's vicinity, each will exert a magnetic force on the other. Let us consider two very long (or effectively infinitely long), straight, parallel wires in free space, separated by a distance d and carrying currents I_1 and I_2 in the same direction, as shown in Fig. 5-14. Current I_1 is located at $y = -d/2$ and I_2 is located at $y = d/2$, and both point in the z-direction. We denote $\mathbf{B}_1$ as the magnetic field due to current I_1, defined

INTEL-1014
U.S. Patent 7,151,430

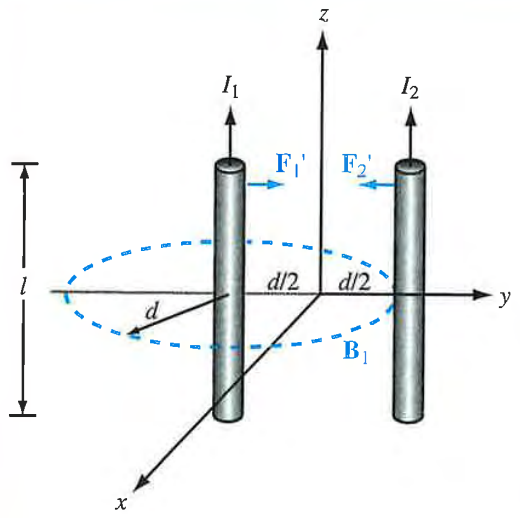


Figure 5-14: Magnetic forces on parallel current-carrying conductors.

at the location of the wire carrying the current I_2 and, conversely, $\mathbf{B}_2$ is the field due to I_2 at the location of the wire carrying current I_1. From Eq. (5.30), with $I = I_1$, $r = d$, and $\hat{\boldsymbol{\phi}} = -\hat{\mathbf{x}}$ at the location of I_2, the field $\mathbf{B}_1$ is

$$\mathbf{B}_1 = -\hat{\mathbf{x}}\frac{\mu_0 I_1}{2\pi d}. \tag{5.39}$$

The force $\mathbf{F}_2$ exerted on a length l of wire I_2 due to its presence in field $\mathbf{B}_1$ may be obtained by applying Eq. (5.12):

$$\mathbf{F}_2 = I_2 l\hat{\mathbf{z}} \times \mathbf{B}_1 = I_2 l\hat{\mathbf{z}} \times (-\hat{\mathbf{x}})\frac{\mu_0 I_1}{2\pi d}$$
$$= -\hat{\mathbf{y}}\frac{\mu_0 I_1 I_2 l}{2\pi d}, \tag{5.40}$$

and the corresponding force per unit length is

$$\mathbf{F}_2' = \frac{\mathbf{F}_2}{l} = -\hat{\mathbf{y}}\frac{\mu_0 I_1 I_2}{2\pi d}. \tag{5.41}$$

A similar analysis performed for the force per unit length exerted on the wire carrying I_1 leads to

$$\mathbf{F}_1' = \hat{\mathbf{y}}\frac{\mu_0 I_1 I_2}{2\pi d}. \tag{5.42}$$

Thus, $\mathbf{F}_1' = -\mathbf{F}_2'$, which means that the two wires attract each other with equal forces. If the currents are in opposite directions, the wires would repel each other with equal forces.

5-4 Maxwell's Magnetostatic Equations

Thus far, we have defined what we mean by a magnetic flux density **B** and the associated magnetic field **H**, we introduced the formulation provided by the Biot–Savart law for finding the fields **B** and **H** due to any specified distribution of electric currents, and we examined how magnetic fields can exert magnetic forces on moving charged particles and on current-carrying conductors. We will now examine two additional important properties of magnetostatic fields, those described mathematically by Eqs. (5.1a and b).

5-4.1 Gauss's Law for Magnetism

In Chapter 4 we learned that the net outward flux of the electric flux density **D** through a closed surface enclosing a net charge Q is equal to Q. We referred to this property as Gauss's law (for electricity), and we expressed it mathematically in differential and integral forms as

$$\nabla \cdot \mathbf{D} = \rho_v \iff \oint_S \mathbf{D} \cdot d\mathbf{s} = Q. \tag{5.43}$$

Conversion from differential to integral form was accomplished by applying the divergence theorem to a volume v enclosed by a surface S and containing charge $Q = \int_v \rho_v \, dv$ [Section 4-4]. The magnetic analogue to a point charge is a magnetic pole, but whereas electric charges can exist in isolation, magnetic poles do not. Magnetic poles always occur in pairs; no matter how

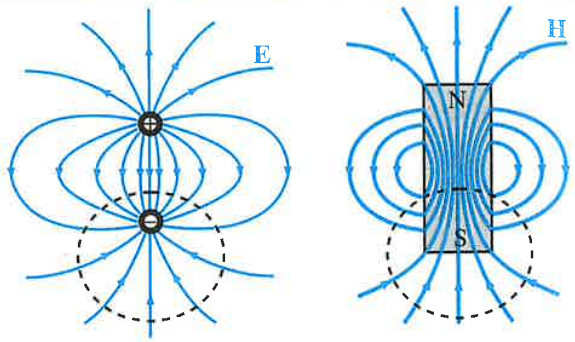
INTEL-1014
U.S. Patent 7,151,430

many times a permanent magnet is subdivided, each new piece will always have a north and a south pole, even if the process were to be continued down to the atomic level. Thus, there is no magnetic equivalence to a charge Q or a charge density ρ_v, and it is therefore not surprising that ***Gauss's law for magnetism*** is given by

$$\nabla \cdot \mathbf{B} = 0 \iff \oint_S \mathbf{B} \cdot d\mathbf{s} = 0. \quad (5.44)$$

The differential form is one of Maxwell's four equations, and the integral form is obtained with the help of the divergence theorem. Formally, the name "Gauss's law" refers to the electric case, even when no specific reference to electricity is indicated. *The property described by Eq. (5.44) has been called "the law of nonexistence of isolated monopoles," "the law of conservation of magnetic flux," and "Gauss's law for magnetism," among others.* We prefer the last of the three cited names because it reminds us of the parallelism, as well as the differences, between the electric and magnetic properties of nature.

The difference between Gauss's law for electricity and its counterpart for magnetism may be viewed in terms of field lines. Electric field lines originate from positive electric charges and terminate on negative electric charges. Hence, for the electric field lines of the electric dipole shown in Fig. 5-15(a), the electric flux through a closed surface surrounding one of the charges is not zero. In contrast, *magnetic field lines always form continuous closed loops.* As we saw in Section 5-2, the magnetic field lines due to currents do not begin or end at any point; this is true for the linear conductor of Fig. 5-10 and the circular loop of Fig. 5-12, as well as for any distribution of currents. It is also true for a magnet, as illustrated in Fig. 5-15(b) for a bar magnet. Because the magnetic field lines form closed loops, the net magnetic flux through the closed surface surrounding the south pole of the magnet (or through any other closed surface) is always zero, regardless of the shape of that surface.



(a) Electric dipole (b) Bar magnet

Figure 5-15: Whereas (a) the net electric flux through a closed surface surrounding a charge is not zero, (b) the net magnetic flux through a closed surface surrounding one of the poles of a magnet is zero.

5-4.2 Ampère's Law

We will now examine the property represented by Eq. (5.1b):

$$\nabla \times \mathbf{H} = \mathbf{J}, \quad (5.45)$$

which is the second of Maxwell's pair of equations characterizing the magnetostatic fields, **B** and **H**. The integral form of Eq. (5.45) is called ***Ampère's circuital law*** (or simply Ampère's law) under magnetostatic conditions (steady currents). It is obtained by integrating both sides of Eq. (5.45) over an open surface S,

$$\int_S (\nabla \times \mathbf{H}) \cdot d\mathbf{s} = \int_S \mathbf{J} \cdot d\mathbf{s}, \quad (5.46)$$

and then invoking Stokes's theorem given by Eq. (3.107) to obtain the result

$$\oint_C \mathbf{H} \cdot d\mathbf{l} = I \quad \text{(Ampère's law)}, \quad (5.47)$$

INTEL-1014
U.S. Patent 7,151,430

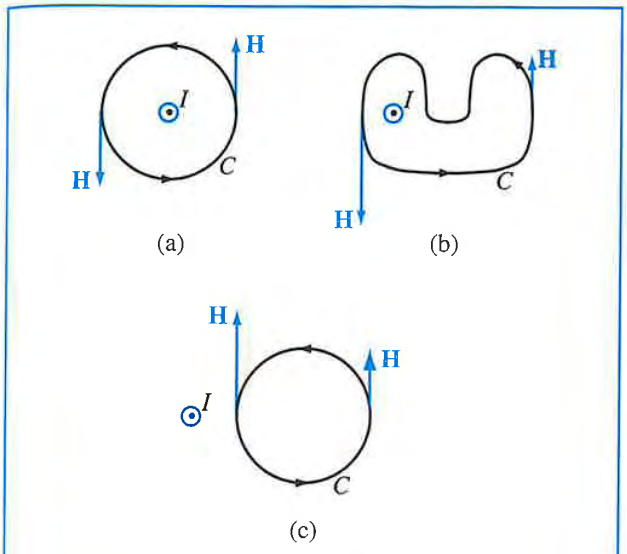


Figure 5-16: Ampère's law states that the line integral of **H** around a closed contour C is equal to the current traversing the surface bounded by the contour. This is true for contours (a) and (b), but the line integral of **H** is zero for the contour in (c) because the current I (denoted by the symbol $\odot$) is not enclosed by the contour C.

where C is the closed contour bounding the surface S and $I = \int \mathbf{J} \cdot d\mathbf{s}$ is the total current flowing through S. *The sign convention for the direction of C is taken so that I and* **H** *satisfy the right-hand rule* defined earlier in connection with the Biot–Savart law. That is, if the direction of I is aligned with the direction of the thumb of the right hand, then the direction of the contour C should be chosen to be along the direction of the other four fingers. In words, *Ampère's circuital law states that the line integral of* **H** *around a closed path is equal to the current traversing the surface bounded by that path.* By way of illustration, for both configurations shown in Figs. 5-16(a) and (b), the line integral of **H** is equal to the current I, even though the paths have very different shapes and the magnitude of **H** is not uniform along the path of configuration (b). By the same token, because path (c) in Fig. 5-16 does not enclose the current I, its line integral of **H** is identically zero, even though **H** is not zero along the path.

When we examined Gauss's law in Section 4-4, we discovered that in practice its usefulness for calculating the electric flux density **D** is limited to charge distributions that possess a certain degree of symmetry and that the calculation procedure is subject to proper choice of the Gaussian surface enclosing the charges. A similar statement applies to Ampère's law: its usefulness is limited to symmetric current distributions that allow the choice of convenient ***Ampèrian contours*** around them, as illustrated by Examples 5-5 to 5-7.

Example 5-5 Magnetic Field of a Long Wire

A long (practically infinite) straight wire of radius a carries a steady current I that is uniformly distributed over the cross section of the wire. Determine the magnetic field **H** at a distance r from the axis of the wire both (a) inside the wire ($r \leq a$) and (b) outside the wire ($r \geq a$).

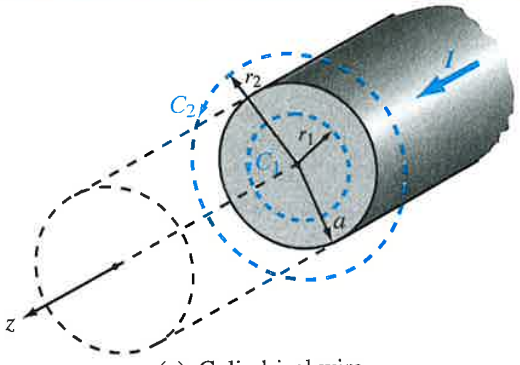
Solution: (a) We choose I to be along the $+z$-direction, as shown in Fig. 5-17(a). To determine $\mathbf{H}_1$ at a distance $r_1 \leq a$, we choose the Ampèrian contour C_1 to be a circular path of radius r_1 as shown in Fig. 5-17(b). In this case, Ampère's law takes the form

$$\oint_{C_1} \mathbf{H}_1 \cdot d\mathbf{l}_1 = I_1,$$

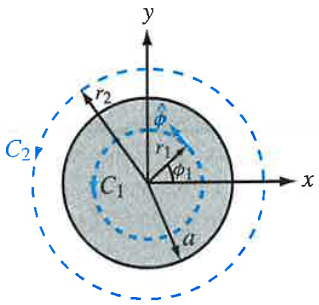
where I_1 is the fraction of the total current I flowing through C_1. From symmetry, $\mathbf{H}_1$ must be constant in magnitude and parallel to the contour at any point along the path. Furthermore, to satisfy the right-hand rule and given that I is along the z-direction, $\mathbf{H}_1$ must be along the $+\phi$-direction in a cylindrical coordinate system. Hence, $\mathbf{H}_1 = \hat{\boldsymbol{\phi}} H_1$. With $d\mathbf{l}_1 = \hat{\boldsymbol{\phi}} r_1 \, d\phi$, the left-hand side of Ampère's law gives

$$\oint_{C_1} \mathbf{H}_1 \cdot d\mathbf{l}_1 = \int_0^{2\pi} H_1 (\hat{\boldsymbol{\phi}} \cdot \hat{\boldsymbol{\phi}}) r_1 \, d\phi = 2\pi r_1 H_1.$$

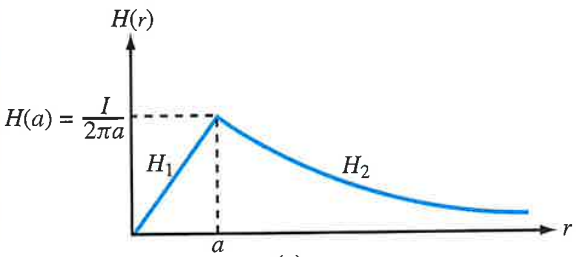
INTEL-1014
U.S. Patent 7,151,430



(a) Cylindrical wire



(b) Wire cross section



(c)

Figure 5-17: Infinitely long wire of radius a carrying a uniform current I along the $+z$-direction: (a) general configuration showing contours C_1 and C_2; (b) cross-sectional view; and (c) a plot of H versus r (Example 5-5).

The current I_1 flowing through the area enclosed by C_1 is equal to the total current I multiplied by the ratio of the area enclosed by C_1 to the total cross-sectional area of the wire:

$$I_1 = \left(\frac{\pi r_1^2}{\pi a^2}\right) I = \left(\frac{r_1}{a}\right)^2 I.$$

Equating both sides of Ampère's law and then solving for $\mathbf{H}_1$ leads to

$$\mathbf{H}_1 = \hat{\boldsymbol{\phi}} H_1 = \hat{\boldsymbol{\phi}} \frac{r_1}{2\pi a^2} I \qquad (\text{for } r_1 \le a). \tag{5.48}$$

(b) For $r_2 \ge a$, we choose path C_2, which encloses all the current I. Hence,

$$\oint_{C_2} \mathbf{H}_2 \cdot d\mathbf{l}_2 = 2\pi r_2 H_2 = I,$$

and

$$\mathbf{H}_2 = \hat{\boldsymbol{\phi}} H_2 = \hat{\boldsymbol{\phi}} \frac{I}{2\pi r_2} \qquad (\text{for } r_2 \ge a). \tag{5.49}$$

If we ignore the subscript 2, we observe that Eq. (5.49) provides the same expression for $\mathbf{B} = \mu_0 \mathbf{H}$ as Eq. (5.30), which we had derived previously on the basis of the Biot–Savart law.

The variation of the magnitude of H as a function of r is plotted in Fig. 5-17(c); H increases linearly between $r = 0$ and $r = a$ (inside the conductor), and then it decreases as $1/r$ outside the conductor. ■

EXERCISE 5.9 Current I flows in the inner conductor of a long coaxial cable and returns through the outer conductor. What is the magnetic field in the region outside the coaxial cable and why?

Ans. $\mathbf{H} = 0$ outside the coaxial cable because the net current enclosed by the Ampèrian contour is zero.

EXERCISE 5.10 The metal niobium becomes a superconductor with zero electrical resistance when it is cooled to below 9 K, but its superconductive behavior ceases when

INTEL-1014
U.S. Patent 7,151,430

the magnetic flux density at its surface exceeds 0.12 T. Determine the maximum current that a 0.1-mm-diameter niobium wire can carry and remain superconductive.

Ans. $I = 30$ A.

Example 5-6 Magnetic Field inside a Toroidal Coil

A toroidal coil (also called a torus or toroid) is a doughnut-shaped structure (called its core) with closely spaced turns of wire wrapped around it, as shown in Fig. 5-18. For clarity, we show the turns in the figure as spaced apart, but in practice they are wound in a closely spaced arrangement to form approximately circular loops. The toroid is used to magnetically couple multiple circuits and to measure the magnetic properties of materials, as illustrated later in Fig. 5-30. For a toroid with N turns carrying a current I, determine the magnetic field $\mathbf{H}$ in each of the following three regions: $r < a$, $a < r < b$, and $r > b$, all in the azimuthal plane of the toroid.

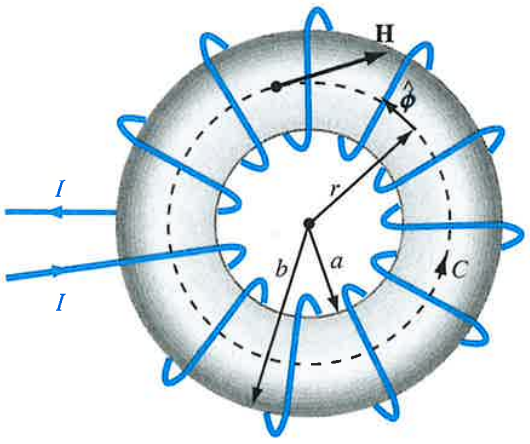


Figure 5-18: Toroidal coil with inner radius a and outer radius b. The wire loops usually are much more closely spaced than shown in the figure (Example 5-6).

Solution: From symmetry, it is clear that $\mathbf{H}$ has uniform properties in azimuth. If we construct a circular Ampèrian contour with center at the origin and of radius $r < a$, there will be no current flowing through the surface of the contour, and therefore $\mathbf{H} = 0$ for $r < a$. Similarly, for an Ampèrian contour with radius $r > b$, the *net* current flowing through its surface is zero because an equal number of current coils cross the surface in both directions. Hence, $\mathbf{H} = 0$ in the region exterior to the toroidal coil.

For the region inside the core, we construct a path of radius r, as shown in Fig. 5-18. For each loop, we know from Example 5-4 that the field $\mathbf{H}$ at the center of the loop points along the axis of the loop, which in this case is the ϕ-direction, and in view of the direction of the current I shown in Fig. 5-18, the right-hand rule tells us that $\mathbf{H}$ must be in the $-\phi$-direction. Hence, $\mathbf{H} = -\hat{\boldsymbol{\phi}}H$. The total current crossing the surface of the contour with radius r is NI and its direction is into the page. According to the right-hand rule associated with Ampère's law, the current is positive if it crosses the surface of the contour in the direction of the four fingers of the right hand when the thumb is pointing along the direction of the contour C. Hence, in the present situation the current is $-NI$. Application of Ampère's law then gives

$$\oint_C \mathbf{H} \cdot d\mathbf{l} = \int_0^{2\pi} (-\hat{\boldsymbol{\phi}}H) \cdot \hat{\boldsymbol{\phi}} r \, d\phi = -2\pi r H = -NI.$$

Hence, $H = NI/(2\pi r)$ and

$$\mathbf{H} = -\hat{\boldsymbol{\phi}}H = -\hat{\boldsymbol{\phi}}\frac{NI}{2\pi r} \quad (\text{for } a < r < b). \blacksquare \quad (5.50)$$

Example 5-7 Magnetic Field of an Infinite Current Sheet

The x–y plane of Fig. 5-19 contains an infinite current sheet with surface current density $\mathbf{J}_s = \hat{\mathbf{x}}J_s$. Find the magnetic field $\mathbf{H}$.

INTEL-1014
U.S. Patent 7,151,430

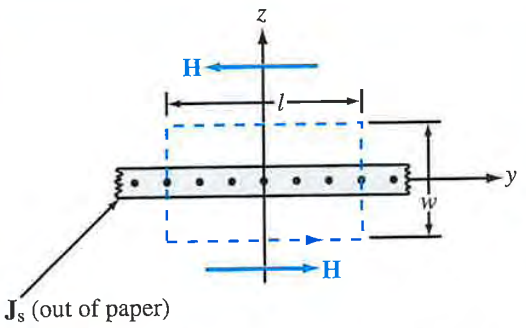


Figure 5-19: A thin current sheet in the x–y plane carrying a surface current density $\mathbf{J}_s = \hat{\mathbf{x}} J_s$ (out of the page) (Example 5-7).

Solution: From symmetry considerations and the right-hand rule, $\mathbf{H}$ must be in the direction shown in the figure. That is,

$$\mathbf{H} = \begin{cases} -\hat{\mathbf{y}} H, & \text{for } z > 0, \\ \hat{\mathbf{y}} H, & \text{for } z < 0. \end{cases}$$

To evaluate the line integral in Ampère's law, we choose a rectangular Ampèrian path around the sheet, with dimensions l and w, as shown in Fig. 5-19. Recalling that J_s represents current per unit length along the y-direction, the total current crossing the surface of the rectangular loop is $I = J_s l$. Hence, applying Ampère's law over the loop, while noting that $\mathbf{H}$ is zero along the paths of length w, we have

$$\oint_C \mathbf{H} \cdot d\mathbf{l} = 2Hl = J_s l,$$

from which we obtain the result

$$\mathbf{H} = \begin{cases} -\hat{\mathbf{y}} \dfrac{J_s}{2}, & \text{for } z > 0, \\ \hat{\mathbf{y}} \dfrac{J_s}{2}, & \text{for } z < 0. \end{cases} \tag{5.51}$$

We note that the magnetic field is uniform and everywhere parallel to the current sheet. ■

REVIEW QUESTIONS

Q5.8 What is a fundamental difference between electric field lines and magnetic field lines?

Q5.9 If the line integral of $\mathbf{H}$ over a closed contour is zero, does it follow that $\mathbf{H} = 0$ at every point on the contour? If not, what then does it imply?

Q5.10 Compare the utility of applying the Biot–Savart law versus applying Ampère's law for computing the magnetic field due to current-carrying conductors.

Q5.11 What is a toroid? What is the magnetic field at points outside the toroid?

5-5 Vector Magnetic Potential

In our treatment of electrostatic fields in Chapter 4, we introduced the electrostatic potential V and defined it in terms of the line integral of the electric field $\mathbf{E}$. In differential form, we found that V and $\mathbf{E}$ are related by $\mathbf{E} = -\nabla V$. This relationship proved useful not only in relating the electric field distribution in circuit elements (such as resistors and capacitors) to the voltage differences across them, but it also proved more convenient in certain cases to first determine the potential V due to a given charge distribution and then apply the relationship $\mathbf{E} = -\nabla V$ to find $\mathbf{E}$ than to use Coulomb's law directly to find $\mathbf{E}$. We will now explore a similar approach in connection with the magnetic flux density $\mathbf{B}$.

According to Eq. (5.44), $\nabla \cdot \mathbf{B} = 0$. We wish to define $\mathbf{B}$ in terms of a magnetic potential with the constraint that such a definition guarantees that the divergence of $\mathbf{B}$ is always equal to zero. This can be realized by taking

INTEL-1014
U.S. Patent 7,151,430

advantage of the vector identity given by Eq. (3.106b), which states that, for any vector **A**,

$$\nabla \cdot (\nabla \times \mathbf{A}) = 0. \tag{5.52}$$

Hence, by defining the ***vector magnetic potential*** **A** such that

$$\mathbf{B} = \nabla \times \mathbf{A} \quad (\text{Wb/m}^2), \tag{5.53}$$

we are guaranteed that $\nabla \cdot \mathbf{B} = 0$. The SI unit for **B** is the tesla (T). An equivalent unit used in the literature is webers per square meter (Wb/m^2). Consequently, the SI unit for **A** is (Wb/m).

With $\mathbf{B} = \mu\mathbf{H}$, the differential form of Ampère's law given by Eq. (5.45) can be written as

$$\nabla \times \mathbf{B} = \mu\mathbf{J}, \tag{5.54}$$

where **J** is the current density due to free charges in motion. If we substitute Eq. (5.53) into Eq. (5.54), we have

$$\nabla \times (\nabla \times \mathbf{A}) = \mu\mathbf{J}. \tag{5.55}$$

For any vector **A**, the Laplacian of **A** obeys the vector identity given by Eq. (3.113), that is,

$$\nabla^2\mathbf{A} = \nabla(\nabla \cdot \mathbf{A}) - \nabla \times (\nabla \times \mathbf{A}), \tag{5.56}$$

where, by definition, $\nabla^2\mathbf{A}$ in Cartesian coordinates is given by

$$\begin{aligned}\nabla^2\mathbf{A} &= \left(\frac{\partial^2}{\partial x^2} + \frac{\partial^2}{\partial y^2} + \frac{\partial^2}{\partial z^2}\right)\mathbf{A} \\ &= \hat{\mathbf{x}}\nabla^2 A_x + \hat{\mathbf{y}}\nabla^2 A_y + \hat{\mathbf{z}}\nabla^2 A_z.\end{aligned} \tag{5.57}$$

Combining Eq. (5.55) with Eq. (5.56) gives

$$\nabla(\nabla \cdot \mathbf{A}) - \nabla^2\mathbf{A} = \mu\mathbf{J}. \tag{5.58}$$

When we introduced the defining equation for the vector magnetic potential **A**, given by Eq. (5.53), the only constraint we placed on **A** is that its definition satisfy the condition $\nabla \cdot \mathbf{B} = 0$. Equation (5.58) contains a term involving $\nabla \cdot \mathbf{A}$. It turns out from vector calculus that we have a fair amount of latitude in specifying a value or a functional form for $\nabla \cdot \mathbf{A}$, without conflicting with the requirement represented by Eq. (5.52). The simplest among these allowed specifications is

$$\nabla \cdot \mathbf{A} = 0. \tag{5.59}$$

Using this choice in Eq. (5.58) leads to the ***vector Poisson's equation*** given by

$$\nabla^2\mathbf{A} = -\mu\mathbf{J}. \tag{5.60}$$

Using the definition for $\nabla^2\mathbf{A}$ given by Eq. (5.57), the vector Poisson's equation can be broken up into three scalar Poisson's equations:

$$\nabla^2 A_x = -\mu J_x, \tag{5.61a}$$

$$\nabla^2 A_y = -\mu J_y, \tag{5.61b}$$

$$\nabla^2 A_z = -\mu J_z. \tag{5.61c}$$

In electrostatics, Poisson's equation for the scalar potential V is given by Eq. (4.60) as

$$\nabla^2 V = -\frac{\rho_v}{\varepsilon}, \tag{5.62}$$

and its solution for a volume charge distribution ρ_v occupying a volume v' was given by Eq. (4.61) as

$$V = \frac{1}{4\pi\varepsilon}\int_{v'} \frac{\rho_v}{R'}\, dv'. \tag{5.63}$$

Poisson's equations for A_x, A_y, and A_z are mathematically identical in form to Eq. (5.62). Hence, for a current density **J** with x-component J_x distributed over a volume v', the solution for Eq. (5.61a) is

$$A_x = \frac{\mu}{4\pi}\int_{v'} \frac{J_x}{R'}\, dv' \quad (\text{Wb/m}), \tag{5.64}$$

INTEL-1014
U.S. Patent 7,151,430

and similar solutions can be written for A_y in terms of J_y and A_z in terms of J_z. The three solutions can be combined into a vector equation of the form

$$\mathbf{A} = \frac{\mu}{4\pi} \int_{v'} \frac{\mathbf{J}}{R'} \, dv' \quad \text{(Wb/m)}. \tag{5.65}$$

In view of Eq. (5.23), if the current distribution is given in the form of a surface current density $\mathbf{J}_s$ over a surface S', then $\mathbf{J}\,dv'$ should be replaced with $\mathbf{J}_s\,ds'$ and v' should be replaced with S'; and, similarly, for a line distribution, $\mathbf{J}\,dv'$ should be replaced with $I\,d\mathbf{l}'$ and the integration should be performed over the associated line path l'.

In addition to the Biot–Savart law and Ampère's law, the vector magnetic potential provides a third approach for computing the magnetic field due to current-carrying conductors. For a specified current distribution, Eq. (5.65) can be used to find $\mathbf{A}$, and then Eq. (5.53) can be used to find $\mathbf{B}$. Except for simple current distributions with symmetrical geometries that lend themselves to the application of Ampère's law, the choice usually is between the approaches provided by the Biot–Savart law and the vector magnetic potential, and among those two the latter often is easier to apply because it is easier to perform the integration given by Eq. (5.65) than to perform the integration given by Eq. (5.22).

The *magnetic flux* Φ linking a surface S is defined as the total magnetic flux density passing through S, or

$$\Phi = \int_S \mathbf{B} \cdot d\mathbf{s} \quad \text{(Wb)}. \tag{5.66}$$

If we insert Eq. (5.53) into Eq. (5.66) and then invoke Stokes's theorem, we have

$$\Phi = \int_S (\nabla \times \mathbf{A}) \cdot d\mathbf{s} = \oint_C \mathbf{A} \cdot d\mathbf{l} \quad \text{(Wb)}, \tag{5.67}$$

where C is the contour bounding the surface S. Thus, Φ can be determined by either Eq. (5.66) or Eq. (5.67), whichever is easier to integrate for the specific problem under consideration.

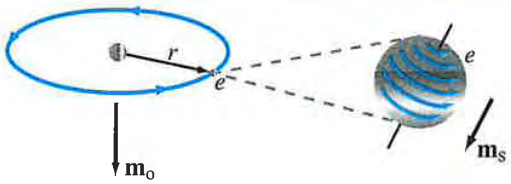
5-6 Magnetic Properties of Materials

According to our preceding discussions, because the pattern of the magnetic field generated by a current loop is similar to that exhibited by a permanent magnet, the loop is regarded as a magnetic dipole with a north pole and a south pole [see Section 5-2.2 and Fig. 5-13]. The magnetic moment $\mathbf{m}$ of a loop of area A has a magnitude $m = IA$, and the direction of $\mathbf{m}$ is normal to the plane of the loop in accordance with the right-hand rule. Magnetization in a material substance is associated with atomic current loops generated by two principal mechanisms: (1) orbital motions of the electrons around the nucleus and similar motions of the protons around each other in the nucleus and (2) electron spin. The magnetic moment of an electron is due to the combination of its orbital motion and its spinning motion about its own axis. As we will see later, the magnetic moment of the nucleus is much smaller than that of an electron, and therefore the total magnetic moment of an atom is dominated by the sum of the magnetic moments of its electrons. The magnetic behavior of a material is governed by the interaction of the magnetic dipole moments of its atoms with an external magnetic field. This behavior, which depends on the crystalline structure of the material, is used as a basis for classifying materials as *diamagnetic*, *paramagnetic*, or *ferromagnetic*. The atoms of a diamagnetic material have no permanent magnetic dipole moments. In contrast, both paramagnetic and ferromagnetic materials have atoms with permanent magnetic dipole moments, but, as will be explained later, the atoms of materials belonging to these two classes have very different organizational structures.

5-6.1 Orbital and Spin Magnetic Moments

To keep the following presentation simple, we will begin our discussion with a classical model of the atom, in which the electrons are assumed to move in circular motion about the nucleus, and we will then extend the results by incorporating the predictions provided by the

INTEL-1014
U.S. Patent 7,151,430



(a) Orbiting electron (b) Spinning electron

Figure 5-20: An electron generates (a) an orbital magnetic moment $\mathbf{m}_o$ as it rotates around the nucleus and (b) a spin magnetic moment $\mathbf{m}_s$, as it spins about its own axis.

more correct quantum-mechanical model of matter. An electron with charge of $-e$ moving with a constant velocity u in a circular orbit of radius r [Fig. 5-20(a)] completes one revolution in time $T = 2\pi r/u$. This circular motion of the electron constitutes a tiny current loop with current I given by

$$I = -\frac{e}{T} = -\frac{eu}{2\pi r}. \tag{5.68}$$

The magnitude of the associated ***orbital magnetic moment*** $\mathbf{m}_o$ is

$$m_o = IA = \left(-\frac{eu}{2\pi r}\right)(\pi r^2) = -\frac{eur}{2} = -\left(\frac{e}{2m_e}\right)L_e, \tag{5.69}$$

where $L_e = m_e ur$ is the angular momentum of the electron and m_e is its mass. According to quantum physics, the orbital angular momentum is quantized; specifically, L_e is always some integer multiple of $\hbar = h/2\pi$, where h is Planck's constant. That is, $L_e = 0, \hbar, 2\hbar, \ldots$. Consequently, the smallest nonzero magnitude of the orbital magnetic moment of an electron is

$$m_o = -\frac{e\hbar}{2m_e}. \tag{5.70}$$

Despite the fact that all substances contain electrons and the electrons exhibit magnetic dipole moments, most substances are effectively nonmagnetic. This is because, in the absence of an external magnetic field, the atoms of most materials are oriented *randomly*, as a result of which the net magnetic moment generated by their electrons is either zero or very small.

In addition to the magnetic moment produced by its orbital motion, an electron generates a ***spin magnetic moment*** $\mathbf{m}_s$ due to its spinning motion about its own axis [Fig. 5-20(b)]. The magnitude of $\mathbf{m}_s$ predicted by quantum theory is

$$m_s = -\frac{e\hbar}{2m_e}, \tag{5.71}$$

which is equal to the minimum orbital magnetic moment m_o. The electrons of an atom with an even number of electrons usually exist in pairs, with the members of a pair having opposite spin directions, thereby canceling each others' spin magnetic moments. If the number of electrons is odd, the atom will have a nonzero spin magnetic moment due to its unpaired electron.

According to Eq. (5.71), the spin magnetic moment of an electron is inversely proportional to the electron mass m_e. The nucleus of an atom also exhibits a spinning motion, but because its mass is much greater than that of an electron, its magnetic moment is on the order of 10^{-3} of that of an electron.

5-6.2 Magnetic Permeability

The ***magnetization vector*** $\mathbf{M}$ of a material is defined as the vector sum of the magnetic dipole moments of the atoms contained in a unit volume of the material. The magnetic flux density corresponding to $\mathbf{M}$ is $\mathbf{B}_m = \mu_0\mathbf{M}$. In the presence of an externally applied magnetic field $\mathbf{H}$, the total magnetic flux density in the material is

$$\mathbf{B} = \mu_0\mathbf{H} + \mu_0\mathbf{M} = \mu_0(\mathbf{H} + \mathbf{M}), \tag{5.72}$$

INTEL-1014
U.S. Patent 7,151,430

where the first term represents the contribution of the external field and the second term represents the contribution of the magnetization of the material. In general, a material becomes magnetized in response to the external field **H**. Hence, **M** can be expressed as

$$\mathbf{M} = \chi_m \mathbf{H}, \tag{5.73}$$

where χ_m is a dimensionless quantity called the ***magnetic susceptibility*** of the material. For diamagnetic and paramagnetic materials, χ_m is a constant at a given temperature, resulting in a linear relationship between **M** and **H**. This is not the case for ferromagnetic substances; the relationship between **M** and **H** not only is nonlinear, but also depends on the previous "history" of the material, as explained in the next section.

While keeping this fact in mind, let us combine Eqs. (5.72) and (5.73) to get

$$\mathbf{B} = \mu_0(\mathbf{H} + \chi_m \mathbf{H}) = \mu_0(1 + \chi_m)\mathbf{H}, \tag{5.74}$$

or

$$\mathbf{B} = \mu \mathbf{H}, \tag{5.75}$$

where μ, the ***magnetic permeability*** of the material, is given in terms of χ_m by

$$\mu = \mu_0(1 + \chi_m) \quad \text{(H/m)}. \tag{5.76}$$

Often it is convenient to define the magnetic properties of a material in terms of the ***relative permeability*** μ_r:

$$\mu_r = \frac{\mu}{\mu_0} = 1 + \chi_m, \tag{5.77}$$

where μ_0 is the permeability of free space. A material usually is classified as diamagnetic, paramagnetic, or ferromagnetic on the basis of the value of its χ_m, as shown in Table 5-2. Diamagnetic materials have negative susceptibilities and paramagnetic materials have positive susceptibilities. However, the absolute magnitude of χ_m is on the order of 10^{-5} for both classes of materials, which allows us to ignore χ_m relative to 1 in Eq. (5.77). *This gives $\mu_r \simeq 1$ or $\mu \simeq \mu_0$ for diamagnetic and paramagnetic substances, which include dielectric materials and most metals. In contrast, $|\mu_r| \gg 1$ for ferromagnetic materials; $|\mu_r|$ of purified iron, for example, is on the order of 2×10^5.* Ferromagnetic materials are discussed next.

EXERCISE 5.11 The magnetic vector **M** is the vector sum of the magnetic moments of all the atoms contained in a unit volume (1m^3). If a certain type of iron with 8.5×10^{28} atoms/m^3 contributes one electron per atom to align its spin magnetic moment along the direction of the applied field, find (a) the spin magnetic moment of a single electron, given that $m_e = 9.1 \times 10^{-31}$ (kg) and $\hbar = 1.06 \times 10^{-34}$ (J·s), and (b) the magnitude of **M**.

Ans. (a) $m_s = 9.27 \times 10^{-24}$ (A·m^2), (b) $M = 7.88 \times 10^5$ (A/m).

5-6.3 Magnetic Hysteresis of Ferromagnetic Materials

Ferromagnetic materials, which include iron, nickel, and cobalt, exhibit strong magnetic properties due to the fact that their magnetic moments tend to align readily along the direction of an external magnetic field. Moreover, such materials remain partially magnetized even after the removal of the external field. Because of this property, ferromagnetic materials are used in the fabrication of permanent magnets.

Common to all ferromagnetic materials is a characteristic feature described by ***magnetized domains***. A magnetized domain of a material is a microscopic region (on the order of 10^{-10} m^3) within which the magnetic moments of all its atoms (typically on the order of 10^{19} atoms) are aligned parallel to each other. This permanent alignment is attributed to strong coupling forces between

INTEL-1014
U.S. Patent 7,151,430

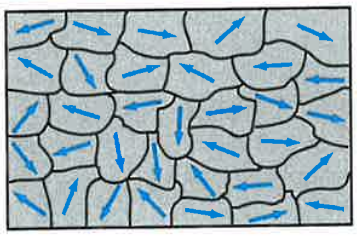
Table 5-2: Properties of magnetic materials.

	Diamagnetism	Paramagnetism	Ferromagnetism
Permanent magnetic dipole moment	No	Yes, but weak	Yes, and strong
Primary magnetization mechanism	Electron orbital magnetic moment	Electron spin magnetic moment	Magnetized domains
Direction of induced magnetic field (relative to external field)	Opposite	Same	Hysteresis [see Fig. 5-22]
Common substances	Bismuth, copper, diamond, gold, lead, mercury, silver, silicon	Aluminum, calcium, chromium, magnesium, niobium, platinum, tungsten	Iron, nickel, cobalt
Typical value of χ_m **Typical value of μ_r**	$\approx -10^{-5}$ ≈ 1	$\approx 10^{-5}$ ≈ 1	$\lvert\chi_m\rvert \gg 1$ and hysteretic $\lvert\mu_r\rvert \gg 1$ and hysteretic

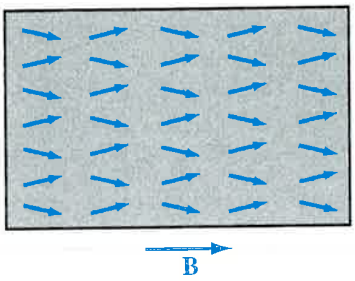
the magnetic dipole moments constituting an individual domain. In the absence of an external magnetic field, the domains take on random orientations relative to each other, as shown in Fig. 5-21(a), resulting in a net magnetization of zero. The ***domain walls*** forming the boundaries between adjacent domains consist of thin transition regions. When an unmagnetized sample of a ferromagnetic material is placed in an external magnetic field, the domains will align partially with the external field, as illustrated in Fig. 5-21(b). A quantitative understanding of how these domains form and how they behave under the influence of an external magnetic field requires a heavy dose of quantum mechanics, which is outside the scope of the present treatment. Hence, we will confine our discussion to a qualitative description of the magnetization process and its implications.

The magnetization behavior of a ferromagnetic material is described in terms of its B–H ***magnetization curve***, where H is the amplitude of the externally applied magnetic field, $\mathbf{H}$, and B is the amplitude of the total magnetic flux density $\mathbf{B}$ present within the material. According to Eq. (5.72), the flux $\mathbf{B}$ consists of a contribution $\mu_0\mathbf{H}$ due to the external field and a contribution $\mu_0\mathbf{M}$ due to the magnetization field induced in the material. Suppose that we start with an unmagnetized sample of iron, and let us assume that we have an experimental arrangement capable of measuring $\mathbf{B}$ and $\mathbf{H}$. The unmagnetized state is denoted by point O in Fig. 5-22. As we start to increase $\mathbf{H}$ continuously, $\mathbf{B}$ increases also, and the response follows the curve from point O to point A_1, at which nearly all the domains have become aligned with $\mathbf{H}$. Point A_1 represents a saturation condition. If we now start to decrease $\mathbf{H}$ from its value at point A_1 back to zero, the magnetization curve follows the path from A_1 to A_2. At point A_2, the external field $\mathbf{H}$ is zero, but the flux density $\mathbf{B}$ in the material is not zero. This value of $\mathbf{B}$ is called the ***residual flux density*** B_r. The iron material is now magnetized and can serve as a permanent magnet owing to the fact that a large fraction of its magnetization domains have remained aligned. Reversing the direction of $\mathbf{H}$ and increasing its intensity causes $\mathbf{B}$ to decrease from B_r at point A_2 to zero at point A_3, and if the

INTEL-1014
U.S. Patent 7,151,430



(a) Unmagnetized domains



(b) Magnetized domains

Figure 5-21: Comparison of (a) unmagnetized and (b) magnetized domains in a ferromagnetic material.

intensity of **H** is increased further (while maintaining its negative direction), the magnetization curve moves to the saturation condition at point A_4. Finally, as **H** is made to return to zero and is then increased again in the positive direction, the curve follows the path from A_4 to A_1. This process is called ***magnetic hysteresis***. The term hysteresis means "to lag behind." The ***hysteresis loop*** shows that the magnetization process in ferromagnetic materials depends not only on the external magnetic field **H**, but on the magnetic history of the material as well. The specific shape and extent of the hysteresis loop depend on the properties of the ferromagnetic material and on the peak-to-peak range over which **H** is made to vary. Materials characterized by wide hysteresis loops are called ***hard ferromagnetic materials*** [Fig. 5-23(a)]. These materials cannot be easily demagnetized by an external magnetic field because they have a large residual magnetization B_r. Hard ferromagnetic materials are used in the fabrication of permanent magnets for motors and generators. ***Soft ferromagnetic materials*** have narrow hysteresis loops [Fig. 5-23(b)], and hence they can be more easily magnetized and demagnetized. To demagnetize any ferromagnetic material, the material

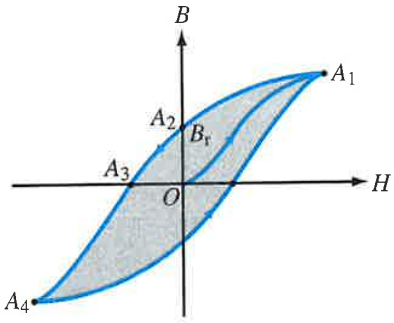
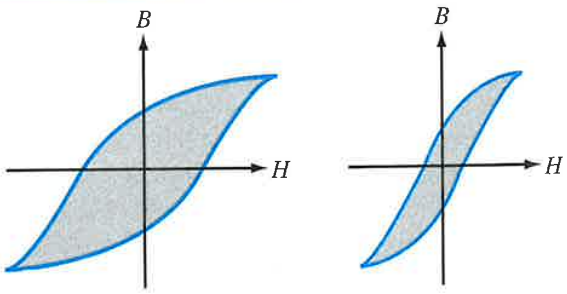


Figure 5-22: Typical hysteresis curve for a ferromagnetic material.



(a) Hard material (b) Soft material

Figure 5-23: Comparison of hysteresis curves for (a) a hard ferromagnetic material and (b) a soft ferromagnetic material.

INTEL-1014
U.S. Patent 7,151,430

is subjected to several hysteresis cycles while gradually decreasing the peak-to-peak range of the applied field.

REVIEW QUESTIONS

Q5.12 What are the three types of magnetic materials and what are typical values of their relative magnetic permeabilities?

Q5.13 What causes magnetic hysteresis in ferromagnetic materials?

Q5.14 What does the magnetization curve describe? What is the difference between the magnetization curves of hard and soft ferromagnetic materials?

5-7 Magnetic Boundary Conditions

In Section 4-9, we derived a set of boundary conditions that describes how, at the boundary between two dissimilar contiguous media, the electric field quantities **D** and **E** in the first medium are related to those in the second medium. We will now derive a similar set of boundary conditions for the magnetic field quantities **B** and **H**. By applying Gauss's law to a pill box that straddles the boundary, we determined that the difference between the normal components of the electric flux densities in the two media is equal to the surface charge density ρ_s. That is,

$$\oint_S \mathbf{D} \cdot d\mathbf{s} = Q \quad \Longrightarrow \quad \boxed{D_{1n} - D_{2n} = \rho_s.} \qquad (5.78)$$

By analogy, application of Gauss's law for magnetism, as expressed by Eq. (5.44), would lead to the conclusion that

$$\oint_S \mathbf{B} \cdot d\mathbf{s} = 0 \quad \Longrightarrow \quad \boxed{B_{1n} = B_{2n}.} \qquad (5.79)$$

This result states that *the normal component of* **B** *is continuous across the boundary between two adjacent media.* In view of the relations $\mathbf{B}_1 = \mu_1 \mathbf{H}_1$ and $\mathbf{B}_2 = \mu_2 \mathbf{H}_2$ for linear, isotropic media, the boundary condition for **H** corresponding to Eq. (5.79) is

$$\boxed{\mu_1 H_{1n} = \mu_2 H_{2n}.} \qquad (5.80)$$

Comparison of Eqs. (5.78) and (5.79) tells us that, *whereas the normal component of* **B** *is continuous across the boundary, the normal component of* **D** *may not be (unless* $\rho_s = 0$*).* A similar reversal applies to the tangential components of the electric and magnetic fields **E** and **H**: *whereas the tangential component of* **E** *is continuous across the boundary, the tangential component of* **H** *may not be (unless the surface current density* $\mathbf{J}_s = 0$*).* To obtain the boundary condition for the tangential component of **H**, we follow the same basic procedure that we used previously in Section 4-9 to establish the boundary condition for the tangential component of **E**. With reference to Fig. 5-24, if we apply Ampère's law [Eq. (5.47)] to a closed rectangular path with sides Δl and Δh, and then we let $\Delta h \to 0$, we end up with the result

$$\oint_C \mathbf{H} \cdot d\mathbf{l} = \int_a^b \mathbf{H}_2 \cdot d\mathbf{l} + \int_c^d \mathbf{H}_1 \cdot d\mathbf{l} = I, \qquad (5.81)$$

where $\mathbf{H}_1$ and $\mathbf{H}_2$ are the magnetic fields in media 1 and 2, respectively. According to Ampère's law, I is the net current crossing the surface of the loop in the direction specified by the right-hand rule (I is in the direction of the thumb when the fingers of the right hand extend in the direction of the loop C). For the directions of $\mathbf{H}_1$ and $\mathbf{H}_2$ and the direction of the integration contour C indicated in Fig. 5-24, the component of $\mathbf{H}_2$ tangential to the boundary, $\mathbf{H}_{2t}$, is parallel to and in the same direction as $d\mathbf{l}$ over segment ab, but the tangential component of $\mathbf{H}_1$ is antiparallel to $d\mathbf{l}$ over segment cd. Furthermore, as we let Δh of the loop approach zero, the surface of the loop approaches a thin line of length Δl. Hence, the

INTEL-1014
U.S. Patent 7,151,430

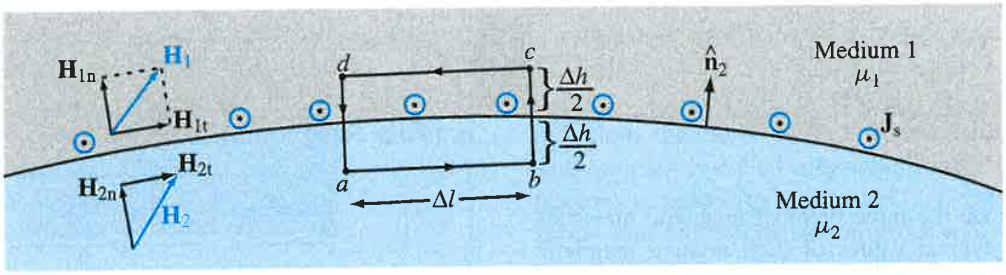


Figure 5-24: Boundary between medium 1 with μ_1 and medium 2 with μ_2.

total current flowing through this thin line is $I = J_s\,\Delta l$, where J_s is the magnitude of the normal component of the surface current density traversing the loop. In view of these considerations, Eq. (5.81) becomes

$$H_{2t}\,\Delta l - H_{1t}\,\Delta l = J_s\,\Delta l \qquad (5.82)$$

or

$$H_{2t} - H_{1t} = J_s \quad \text{(A/m)}. \qquad (5.83)$$

This result can be generalized to a vector form that incorporates the directional relationship defined by the right-hand rule,

$$\hat{\mathbf{n}}_2 \times (\mathbf{H}_1 - \mathbf{H}_2) = \mathbf{J}_s, \qquad (5.84)$$

where $\hat{\mathbf{n}}_2$ is the normal unit vector pointing away from medium 2 (Fig. 5-24). Surface currents can exist only on the surfaces of perfect conductors and superconductors. Hence, *at the interface between media with finite conductivities,* $\mathbf{J}_s = 0$ and

$$H_{1t} = H_{2t}. \qquad (5.85)$$

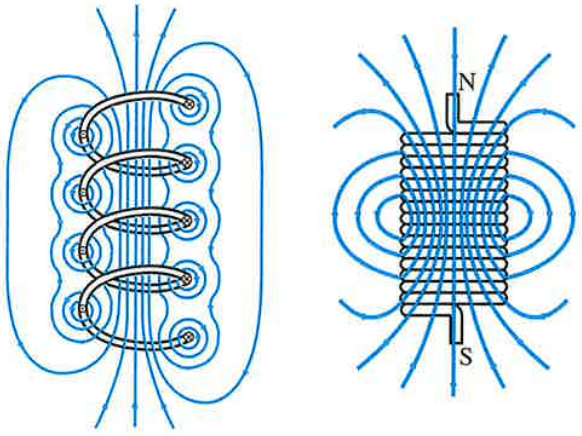
EXERCISE 5.12 With reference to Fig. 5-24, determine the angle between $\mathbf{H}_1$ and $\hat{\mathbf{n}}_2 = \hat{\mathbf{z}}$ if $\mathbf{H}_2 = (\hat{\mathbf{x}}3 + \hat{\mathbf{z}}2)$ (A/m), $\mu_{r_1} = 2$, and $\mu_{r_2} = 8$, and $\mathbf{J}_s = 0$.

Ans. $\theta = 20.6°$.

5-8 Inductance

An inductor is the magnetic analogue of an electrical capacitor. Just as a capacitor can store electric energy in the electric field present in the medium between its conducting surfaces, an inductor can store magnetic energy in the volume comprising the inductors. A typical example of an inductor is a coil consisting of multiple turns of wire wound in a helical geometry around a cylindrical core, as shown in Fig. 5-25(a). Such a structure is called a ***solenoid***. The core may be air filled or may contain a magnetic material with magnetic permeability μ. If the wire carries a current I and the turns are closely spaced, the solenoid can produce a relatively uniform magnetic field within its interior region, and its magnetic field pattern resembles that of a permanent magnet, as illustrated by the field lines in Fig. 5-25(b).

INTEL-1014
U.S. Patent 7,151,430



(a) Loosely wound solenoid (b) Tightly wound solenoid

Figure 5-25: Magnetic field lines of (a) a loosely wound solenoid and (b) a tightly wound solenoid.

5-8.1 Magnetic Field in a Solenoid

We precede our discussion of inductance by deriving an expression for the magnetic flux density **B** in the interior region of a tightly wound solenoid with n turns per unit length. Even though the turns are slightly helical in shape, we will treat them as circular loops, as shown in Fig. 5-26. The solenoid is of length l and radius a and carries a current I. Let us start by considering the magnetic flux density **B** at point P, located on the axis of the solenoid. In Example 5-4, we derived the following expression for the magnetic field **H** at a distance z along the axis of a circular loop of radius a:

$$\mathbf{H} = \hat{\mathbf{z}} \frac{I'a^2}{2(a^2 + z^2)^{3/2}}, \tag{5.86}$$

where I' is the current carried by the loop. If we treat an incremental length dz of the solenoid as an equivalent loop of $n\,dz$ turns and carrying a current $I' = In\,dz$, then the induced field at point P is

$$d\mathbf{B} = \mu\, d\mathbf{H} = \hat{\mathbf{z}} \frac{\mu n I a^2}{2(a^2 + z^2)^{3/2}}\, dz. \tag{5.87}$$

The total field **B** at P is obtained by integrating the contributions from the entire length of the solenoid. This is facilitated by expressing the variable z in terms of the angle θ. That is,

$$z = a \tan\theta, \tag{5.88a}$$

$$a^2 + z^2 = a^2 + a^2 \tan^2\theta = a^2 \sec^2\theta, \tag{5.88b}$$

$$dz = a \sec^2\theta\, d\theta. \tag{5.88c}$$

Upon substituting the last two expressions in Eq. (5.87) and integrating from θ_1 to θ_2, we have

$$\mathbf{B} = \hat{\mathbf{z}} \frac{\mu n I a^2}{2} \int_{\theta_1}^{\theta_2} \frac{a \sec^2\theta\, d\theta}{a^3 \sec^3\theta}$$

$$= \hat{\mathbf{z}} \frac{\mu n I}{2} (\sin\theta_2 - \sin\theta_1). \tag{5.89}$$

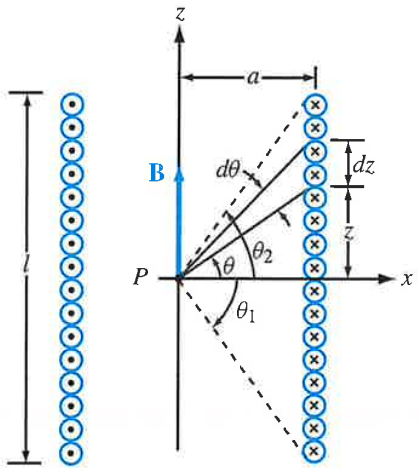


Figure 5-26: Solenoid cross section showing geometry for calculating **H** at a point P on the solenoid axis.

INTEL-1014
U.S. Patent 7,151,430

If the solenoid length l is much larger than its radius a, then $\theta_1 \simeq -90°$ and $\theta_2 \simeq 90°$, in which case Eq. (5.89) reduces to

$$\mathbf{B} \simeq \hat{\mathbf{z}}\mu nI = \frac{\hat{\mathbf{z}}\mu NI}{l} \quad \text{(long solenoid with } l/a \gg 1\text{)}, \tag{5.90}$$

where $N = nl$ is the total number of turns over the length l. Even though the expression given by Eq. (5.90) was derived for the field **B** at the midpoint of the solenoid, it is approximately valid at all points in the interior of the solenoid, except near the ends.

We now return to a discussion of inductance, which includes ***self-inductance***, representing the magnetic flux linkage of a coil or circuit with itself, and ***mutual inductance***, which involves the magnetic flux linkage in a circuit due to the magnetic field generated by a current in another circuit. Usually, when the term ***inductance*** is used, the intended reference is to self-inductance.

EXERCISE 5.13 Use Eq. (5.89) to obtain an expression for **B** at a point on the axis of a very long solenoid but situated at its end points. How does **B** at the end points compare to **B** at the midpoint of the solenoid?

Ans. $\mathbf{B} = \hat{\mathbf{z}}(\mu NI/2l)$ at the end points, which is half as large as **B** at the midpoint.

5-8.2 Self-inductance

From Eq. (5.66), the magnetic flux Φ linking a surface S is given by

$$\Phi = \int_S \mathbf{B} \cdot d\mathbf{s} \quad \text{(Wb)}. \tag{5.91}$$

In a solenoid with an approximately uniform magnetic field given by Eq. (5.90), the flux linking a single loop is

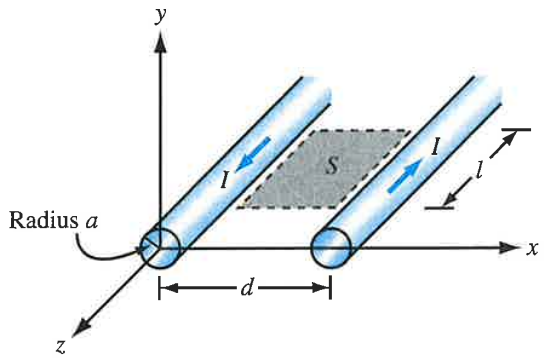
$$\Phi = \int_S \hat{\mathbf{z}} \left(\mu \frac{N}{l} I\right) \cdot \hat{\mathbf{z}}\, ds = \mu \frac{N}{l} IS, \tag{5.92}$$

where S is the cross-sectional area of the loop. ***Magnetic flux linkage*** Λ is defined as the total magnetic flux linking a given circuit or conducting structure. If the structure consists of a single conductor with multiple loops, as in the case of the solenoid, Λ is equal to the flux linking all loops of the structure. For a solenoid with N turns,

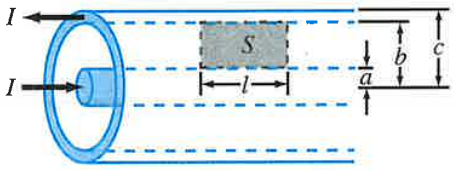
$$\Lambda = N\Phi = \mu \frac{N^2}{l} IS \quad \text{(Wb)}. \tag{5.93}$$

If, on the other hand, the structure consists of two *separate* conductors, as in the case of the parallel-wire and coaxial transmission lines shown in Fig. 5-27, the flux linkage Λ associated with a length l of either line refers to the flux Φ through the closed surface between the two conductors, as highlighted by the shaded areas in Fig. 5-27. In reality, there is also some magnetic flux that passes through the conductors themselves, but it may be ignored by assuming that the currents flow only on the surfaces of the conductors, in which case the magnetic fields inside the conductors are zero. This assumption is justified by the fact that our interest in calculating Λ is for the purpose of determining the inductance of a given structure, and inductance is of interest primarily in the a-c case (i.e., time-varying currents, voltages, and fields). As we will see later in Section 7-5, the current flowing in a conductor under a-c conditions is concentrated within a very thin layer on the skin of the conductor. For the parallel-wire transmission line, the currents flow on the outer surfaces of the wires, and for the coaxial line, the current flows on the outer surface of the inner conductor and on the inner surface of the outer conductor (the current-carrying surfaces are those adjacent to the electric and magnetic fields present in the region between the conductors).

INTEL-1014
U.S. Patent 7,151,430



(a) Parallel-wire transmission line



(b) Coaxial transmission line

Figure 5-27: To compute the inductance per unit length of a two-conductor transmission line, we need to determine the magnetic flux through the area S between the conductors.

The ***self-inductance*** of any conducting structure is defined as the ratio of the magnetic flux linkage Λ to the current I flowing through the structure:

$$L = \frac{\Lambda}{I} \quad \text{(H)}. \qquad (5.94)$$

The SI unit for inductance is the henry (H), which is equivalent to webers per ampere (Wb/A).

For a solenoid, use of Eq. (5.93) gives

$$L = \mu \frac{N^2}{l} S \quad \text{(solenoid)}, \qquad (5.95)$$

and for two-conductor configurations similar to those of Fig. 5-27,

$$L = \frac{\Lambda}{I} = \frac{\Phi}{I} = \frac{1}{I} \int_S \mathbf{B} \cdot d\mathbf{s}. \qquad (5.96)$$

Example 5-8 Inductance of a Coaxial Transmission Line

Develop an expression for the inductance per unit length of a coaxial transmission line. The conductors have radii a and b, as shown in Fig. 5-28, and the insulating material has a linear permeability μ.

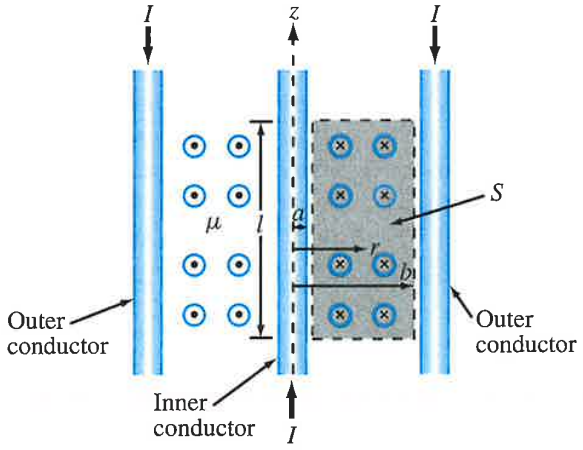


Figure 5-28: Cross-sectional view of coaxial transmission line (Example 5-8).

INTEL-1014
U.S. Patent 7,151,430

Solution: Due to the current I in the inner conductor, the magnetic field generated in the region with permeability μ between the two conductors is given by Eq. (5.30) as

$$\mathbf{B} = \hat{\boldsymbol{\phi}} \frac{\mu I}{2\pi r}, \tag{5.97}$$

where r is the radial distance from the axis of the coaxial line. Let us choose a transmission-line segment of length l as shown in Fig. 5-28. Over the planar surface S between the conductors, $\mathbf{B}$ is everywhere perpendicular to the surface. Hence, the flux through S is

$$\Phi = l \int_a^b B\, dr = l \int_a^b \frac{\mu I}{2\pi r}\, dr = \frac{\mu I l}{2\pi} \ln\left(\frac{b}{a}\right). \tag{5.98}$$

Using Eq. (5.96), the inductance per unit length of the coaxial transmission line is given by

$$L' = \frac{L}{l} = \frac{\Phi}{lI} = \frac{\mu}{2\pi} \ln\left(\frac{b}{a}\right). \quad \blacksquare \tag{5.99}$$

5-8.3 Mutual Inductance

Magnetic coupling between two different conducting structures is described in terms of the mutual inductance between them. For simplicity, let us assume that we have two closed loops with surfaces S_1 and S_2 and a current I_1 flowing through the first loop, as shown in Fig. 5-29. The magnetic field $\mathbf{B}_1$ generated by I_1 results in a flux Φ_{12} through loop 2, given by

$$\Phi_{12} = \int_{S_2} \mathbf{B}_1 \cdot d\mathbf{s}, \tag{5.100}$$

and if loop 2 consists of N_2 turns all coupled by $\mathbf{B}_1$ in exactly the same way, then the total magnetic flux linkage through loop 2 due to $\mathbf{B}_1$ is

$$\Lambda_{12} = N_2 \Phi_{12} = N_2 \int_{S_2} \mathbf{B}_1 \cdot d\mathbf{s}. \tag{5.101}$$

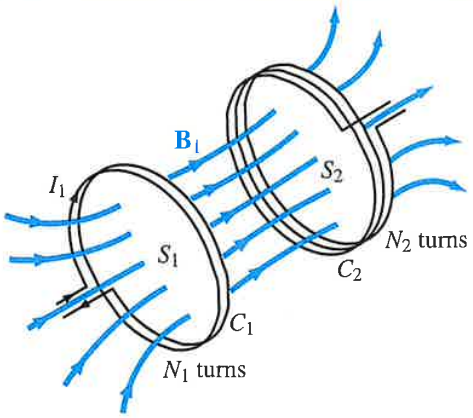


Figure 5-29: Magnetic field lines generated by current I_1 in loop 1 linking surface S_2 of loop 2.

The mutual inductance associated with this magnetic coupling is given by

$$L_{12} = \frac{\Lambda_{12}}{I_1} = \frac{N_2}{I_1} \int_{S_2} \mathbf{B}_1 \cdot d\mathbf{s} \quad \text{(H)}. \tag{5.102}$$

Mutual inductance is important in transformers wherein the windings of two or more circuits share a common magnetic core, as illustrated by the toroidal arrangement shown in Fig. 5-30.

REVIEW QUESTIONS

Q5.15 What is the magnetic field like in the interior of a long solenoid?

Q5.16 What is the difference between self-inductance and mutual inductance?

Q5.17 How is the inductance of a solenoid related to its number of turns N?

INTEL-1014
U.S. Patent 7,151,430

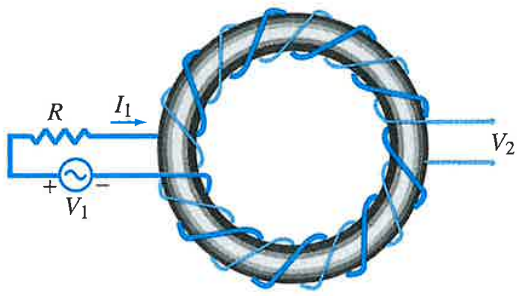


Figure 5-30: Toroidal coil with two windings used as a transformer.

5-9 Magnetic Energy

When we introduced electrostatic energy in Section 4-11, we did so by examining what happens to the energy expended in charging up a capacitor from zero voltage to some final voltage V. We will now use a similar analogy by considering an inductor with inductance L connected to a current source. Suppose that we were to increase the current i flowing through the inductor from zero to a final value I. From circuit theory, we know that the voltage v across the inductor is given by $v = L\,di/dt$. Power p is equal to the product of v and i, and the time integral of power is work, or energy. Hence, the total energy in joules (J) expended in building up the current in the inductor is

$$W_m = \int p\,dt = \int iv\,dt = L\int_0^I i\,di$$
$$= \tfrac{1}{2}LI^2 \quad \text{(J)}. \quad (5.103)$$

For reasons that will become apparent shortly, we call this the ***magnetic energy*** stored in the inductor.

Let us consider the solenoid inductor. Its inductance is given by Eq. (5.95) as $L = \mu N^2 S/l$, and the magnitude of the magnetic flux density in its interior is given from Eq. (5.90) by $B = \mu NI/l$. Equivalently, $I = Bl/(\mu N)$.

If we use these expressions for L and I in Eq. (5.103), we get

$$W_m = \frac{1}{2}LI^2 = \frac{1}{2}\left(\mu\frac{N^2}{l}S\right)\left(\frac{Bl}{\mu N}\right)^2$$
$$= \frac{1}{2}\frac{B^2}{\mu}(lS) = \frac{1}{2}\mu H^2 v, \quad (5.104)$$

where $v = lS$ is the volume of the interior of the solenoid and $H = B/\mu$. The ***magnetic energy density*** w_m is defined as the magnetic energy W_m per unit volume,

$$w_m = \frac{W_m}{v} = \frac{1}{2}\mu H^2 \quad (\text{J/m}^3). \quad (5.105)$$

Even though this expression was derived for a solenoid inductor, it is equally valid for any medium with magnetic field **H**. Furthermore, for any volume v containing a material with permeability μ (including free space with permeability μ_0), the total magnetic energy stored in the medium due to the presence of a magnetic field **H** is

$$W_m = \frac{1}{2}\int_v \mu H^2\,dv \quad \text{(J)}. \quad (5.106)$$

Example 5-9 **Magnetic Energy in a Coaxial Cable**

Derive an expression for the magnetic energy stored in a coaxial cable of length l and inner and outer radii a and b. The insulation material has permeability μ.

Solution: From Eq. (5.97), the magnitude of the magnetic field in the insulating material is given by

$$H = \frac{B}{\mu} = \frac{I}{2\pi r},$$

where r is the radial distance from the center of the inner conductor, as shown in Fig. 5-28. The magnetic energy stored in the coaxial cable is then given by

$$W_m = \frac{1}{2}\int_v \mu H^2\,dv = \frac{\mu I^2}{8\pi^2}\int_v \frac{1}{r^2}\,dv.$$

INTEL-1014
U.S. Patent 7,151,430

Since H is a function of r only, we choose $d\mathcal{V}$ to be a cylindrical shell of length l, radius r, and thickness dr along the radial direction. Thus, $d\mathcal{V} = 2\pi r l\, dr$ and

$$W_m = \frac{\mu I^2}{8\pi^2} \int_a^b \frac{1}{r^2} \cdot 2\pi r l\, dr$$
$$= \frac{\mu I^2 l}{4\pi} \ln\left(\frac{b}{a}\right) \quad \text{(J)}. \blacksquare$$

CHAPTER HIGHLIGHTS

- Magnetic force acting on a charged particle q moving with a velocity $\mathbf{u}$ in a region containing a magnetic flux density $\mathbf{B}$ is $\mathbf{F}_m = q\mathbf{u} \times \mathbf{B}$.
- The total electromagnetic force, known as the Lorentz force, acting on a moving charge in the presence of both electric and magnetic fields is $\mathbf{F} = q(\mathbf{E} + \mathbf{u} \times \mathbf{B})$.
- Magnetic forces acting on current loops can generate magnetic torques.
- The magnetic field intensity induced by a current element is defined by the Biot–Savart law.
- Gauss's law for magnetism states that the net magnetic flux flowing out of any closed surface is zero.
- Ampère's law states that the line integral of $\mathbf{H}$ over a closed contour is equal to the net current crossing the surface bounded by the contour.
- Vector magnetic potential $\mathbf{A}$ is related to $\mathbf{B}$ by $\mathbf{B} = \nabla \times \mathbf{A}$.
- Materials are classified as diamagnetic, paramagnetic, or ferromagnetic, depending on their crystalline structure and behavior under the influence of an external magnetic field.
- Diamagnetic and paramagnetic materials exhibit a linear behavior between $\mathbf{B}$ and $\mathbf{H}$, with $\mu \simeq \mu_0$ for both.
- Ferromagnetic materials exhibit a nonlinear hysteretic behavior between $\mathbf{B}$ and $\mathbf{H}$ and, for some, their μ may be as large as $10^5\mu_0$.
- At the boundary between two different media, the normal component of $\mathbf{B}$ is continuous, and the tangential components of $\mathbf{H}$ are related by $H_{2t} - H_{1t} = J_s$, where J_s is the surface current density flowing in a direction orthogonal to H_{1t} and H_{2t}.
- Inductance of a circuit is defined as the ratio of magnetic flux linking the circuit to the current flowing through it.
- Magnetic energy density is given by $w_m = \frac{1}{2}\mu H^2$.

GLOSSARY OF IMPORTANT TERMS

Provide definitions or explain the meaning of the following terms:

magnetic flux density $\mathbf{B}$
magnetic force $\mathbf{F}_m$
Lorentz force $\mathbf{F}$
moment arm $\mathbf{d}$
torque $\mathbf{T}$
magnetic moment $\mathbf{m}$
Biot–Savart law
current density (volume) $\mathbf{J}$
surface current density $\mathbf{J}_s$
magnetic dipole
Gauss's law for magnetism
Ampère's law
toroidal coil
vector Poisson's equation
magnetic flux Φ
orbital and spin magnetic moments
magnetization vector $\mathbf{M}$
magnetic susceptibility χ_m
diamagnetic, paramagnetic, ferromagnetic
magnetized domains
magnetization curve
magnetic hysteresis
hard and soft ferromagnetic materials
inductance (self- and mutual)

INTEL-1014
U.S. Patent 7,151,430

solenoid
magnetic energy W_m
magnetic energy density w_m

PROBLEMS

Section 5-1: Forces and Torques

5.1* An electron with a speed of 4×10^6 m/s is projected along the positive x-direction into a medium containing a uniform magnetic flux density $\mathbf{B} = (\hat{\mathbf{x}}2 - \hat{\mathbf{z}}3)$ T. Given that $e = 1.6 \times 10^{-19}$ C and the mass of an electron is $m_e = 9.1 \times 10^{-31}$ kg, determine the initial acceleration vector of the electron (at the moment it is projected into the medium).

5.2 When a particle with charge q and mass m is introduced into a medium with a uniform field $\mathbf{B}$ such that the initial velocity of the particle $\mathbf{u}$ is perpendicular to $\mathbf{B}$, as shown in Fig. 5-31, the magnetic force exerted on the particle causes it to move in a circle of radius a. By equating $\mathbf{F}_m$ to the centripetal force on the particle, determine a in terms of q, m, u, and $\mathbf{B}$.

5.3* The circuit shown in Fig. 5-32 uses two identical springs to support a 10-cm-long horizontal wire with a mass of 5 g. In the absence of a magnetic field, the weight of the wire causes the springs to stretch a distance of 0.2 cm each. When a uniform magnetic field is turned on in the region containing the horizontal wire, the springs are observed to stretch an additional 0.5 cm. What is the intensity of the magnetic flux density $\mathbf{B}$?

5.4 The rectangular loop shown in Fig. 5-33 consists of 20 closely wrapped turns and is hinged along the z-axis. The plane of the loop makes an angle of 30° with the y-axis, and the current in the windings is 0.5 A. What is the magnitude of the torque exerted on the loop in the presence of a uniform field $\mathbf{B} = \hat{\mathbf{y}}\,1.2$ T? When viewed from above, is the expected direction of rotation clockwise or counterclockwise?

*Answer(s) available in Appendix D.
Solution available in CD-ROM.

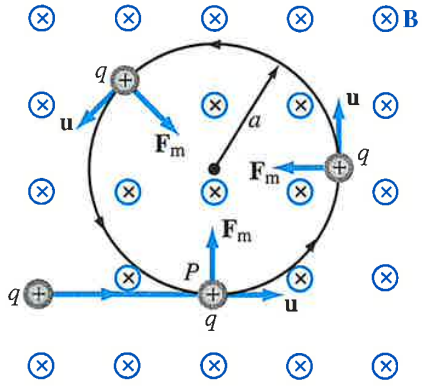


Figure 5-31: Particle of charge q projected with velocity $\mathbf{u}$ into a medium with a uniform field $\mathbf{B}$ perpendicular to $\mathbf{u}$ (Problem 5.2).

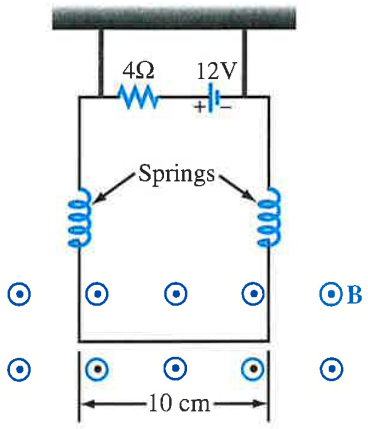


Figure 5-32: Configuration of Problem 5.3.

INTEL-1014
U.S. Patent 7,151,430

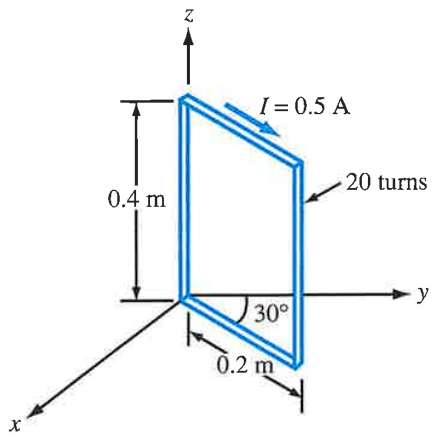


Figure 5-33: Hinged rectangular loop of Problem 5.4.

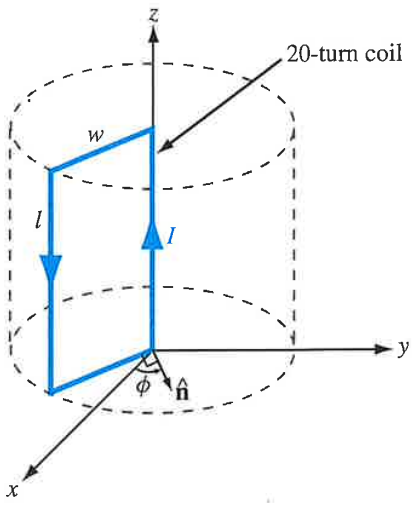


Figure 5-34: Rectangular loop of Problem 5.6.

5.5* In a cylindrical coordinate system, a 2-m-long straight wire carrying a current of 5 A in the positive z-direction is located at $r = 4$ cm, $\phi = \pi/2$, and $-1 \text{ m} \le z \le 1$ m.

(a) If $\mathbf{B} = \hat{\mathbf{r}}\, 0.2 \cos\phi$ (T), what is the magnetic force acting on the wire?

(b) How much work is required to rotate the wire once about the z-axis in the negative ϕ-direction (while maintaining $r = 4$ cm)?

(c) At what angle ϕ is the force a maximum?

5.6 A 20-turn rectangular coil with sides $l = 15$ cm and $w = 5$ cm is placed in the y–z plane as shown in Fig. 5-34.

(a) If the coil, which carries a current $I = 10$ A, is in the presence of a magnetic flux density

$$\mathbf{B} = 2 \times 10^{-2}(\hat{\mathbf{x}} + \hat{\mathbf{y}}2) \quad \text{(T)}$$

determine the torque acting on the coil.

(b) At what angle ϕ is the torque zero?

(c) At what angle ϕ is the torque maximum? Determine its value.

Section 5-2: Biot–Savart Law

5.7* An 8 cm × 12 cm rectangular loop of wire is situated in the x–y plane with the center of the loop at the origin and its long sides parallel to the x-axis. The loop has a current of 25 A flowing clockwise (when viewed from above). Determine the magnetic field at the center of the loop.

5.8 Use the approach outlined in Example 5-2 to develop an expression for the magnetic field $\mathbf{H}$ at an arbitrary point P due to the linear conductor defined by the geometry shown in Fig. 5-35. If the conductor extends between $z_1 = 3$ m and $z_2 = 7$ m and carries a current $I = 5$ A, find $\mathbf{H}$ at $P(2, \phi, 0)$.

5.9* The loop shown in Fig. 5-36 consists of radial lines and segments of circles whose centers are at point P. Determine the magnetic field $\mathbf{H}$ at P in terms of a, b, θ, and I.

INTEL-1014
U.S. Patent 7,151,430

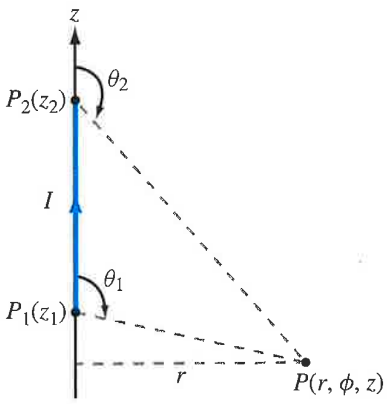


Figure 5-35: Current-carrying linear conductor of Problem 5.8.

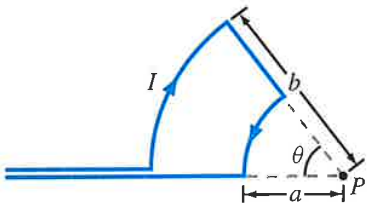


Figure 5-36: Configuration of Problem 5.9.

5.10 An infinitely long, thin conducting sheet defined over the space $0 \leq x \leq w$ and $-\infty \leq y \leq \infty$ is carrying a current with a uniform surface current density $\mathbf{J}_s = \hat{\mathbf{y}}5$ (A/m). Obtain an expression for the magnetic field at point $P(0, 0, z)$ in Cartesian coordinates.

5.11* An infinitely long wire carrying a 50-A current in the positive x-direction is placed along the x-axis in the vicinity of a 10-turn circular loop located in the x–y plane as shown in Fig. 5-37. If the magnetic field at the center of the loop is zero, what is the direction and magnitude of the current flowing in the loop?

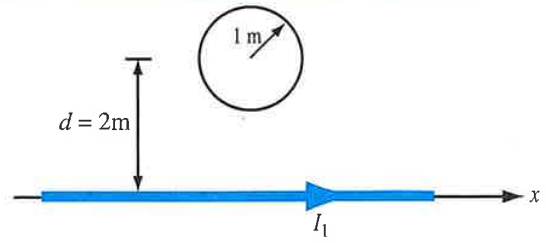


Figure 5-37: Circular loop next to a linear current (Problem 5.11).

5.12 Two infinitely long, parallel wires are carrying 6-A currents in opposite directions. Determine the magnetic flux density at point P in Fig. 5-38.

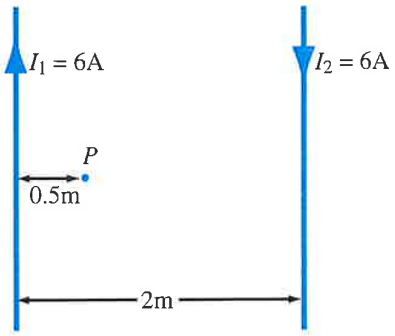


Figure 5-38: Arrangement for Problem 5.12.

5.13* A long, East-West–oriented power cable carrying an unknown current I is at a height of 8 m above the Earth's surface. If the magnetic flux density recorded by a magnetic-field meter placed at the surface is 12 μT when the current is flowing through the cable and 20 μT when the current is zero, what is the magnitude of I?

INTEL-1014
U.S. Patent 7,151,430

5.14 Two parallel, circular loops carrying a current of 20 A each are arranged as shown in Fig. 5-39. The first loop is situated in the x–y plane with its center at the origin, and the second loop's center is at $z = 2$ m. If the two loops have the same radius $a = 3$ m, determine the magnetic field at:

(a) $z = 0$

(b) $z = 1$ m

(c) $z = 2$ m

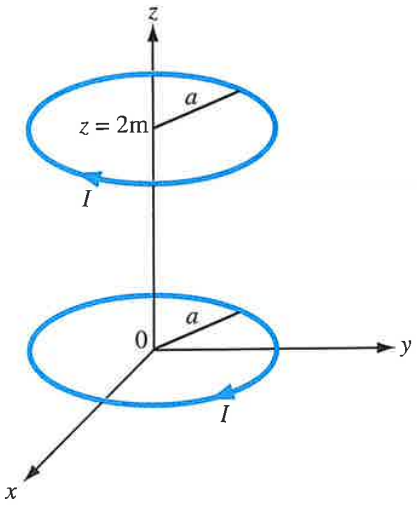


Figure 5-39: Parallel circular loops of Problem 5.14.

Section 5-3: Forces between Currents

5.15* The long, straight conductor shown in Fig. 5-40 lies in the plane of the rectangular loop at a distance $d = 0.1$ m. The loop has dimensions $a = 0.2$ m and $b = 0.5$ m, and the currents are $I_1 = 10$ A and $I_2 = 15$ A. Determine the net magnetic force acting on the loop.

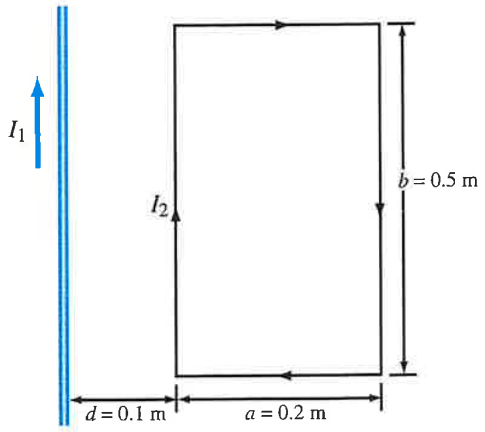


Figure 5-40: Current loop next to a conducting wire (Problem 5.15).

5.16 In the arrangement shown in Fig. 5-41, each of the two long, parallel conductors carries a current I, is supported by 8-cm-long strings, and has a mass per unit length of 0.3 g/cm. Due to the repulsive force acting on the conductors, the angle θ between the supporting strings is 10°. Determine the magnitude of I and the relative directions of the currents in the two conductors.

5.17* An infinitely long, thin conducting sheet of width w along the x-direction lies in the x–y plane and carries a current I in the $-y$-direction. Determine the following:

(a) The magnetic field at a point P midway between the edges of the sheet and at a height h above it. (Fig. 5-42)

(b) The force per unit length exerted on an infinitely long wire passing through point P and parallel to the sheet if the current through the wire is equal in magnitude but opposite in direction to that carried by the sheet.

INTEL-1014
U.S. Patent 7,151,430

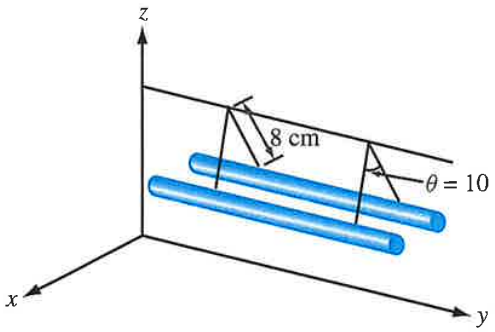


Figure 5-41: Parallel conductors supported by strings (Problem 5.16).

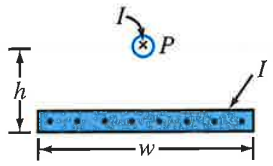


Figure 5-42: A linear current source above a current sheet (Problem 5.17).

5.18 Three long, parallel wires are arranged as shown in Fig. 5-43. Determine the force per unit length acting on the wire carrying I_3.

5.19* A square loop placed as shown in Fig. 5-44 has 2-m sides and carries a current $I_1 = 5$ A. If a straight, long conductor carrying a current $I_2 = 10$ A is introduced and placed just above the midpoints of two of the loop's sides, determine the net force acting on the loop.

Section 5-4: Gauss's Law for Magnetism and Ampère's Law

5.20 Current I flows along the positive z-direction in the inner conductor of a long coaxial cable and returns through the outer conductor. The inner conductor has

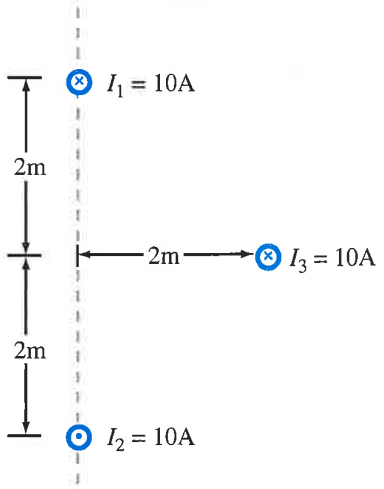


Figure 5-43: Three parallel wires of Problem 5.18.

radius a, and the inner and outer radii of the outer conductor are b and c, respectively.

(a) Determine the magnetic field in each of the following

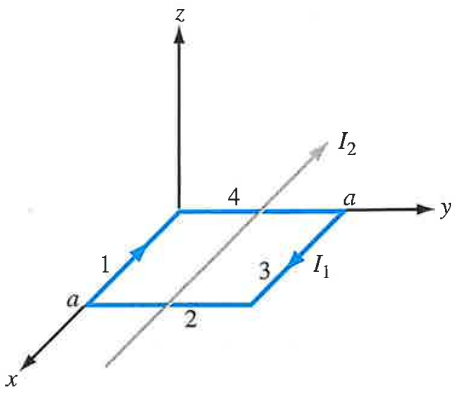


Figure 5-44: Long wire carrying current I_2, just above a square loop carrying I_1 (Problem 5.19).

INTEL-1014
U.S. Patent 7,151,430

regions: $0 \le r \le a$, $a \le r \le b$, $b \le r \le c$, and $r \ge c$.

(b) Plot the magnitude of $\mathbf{H}$ as a function of r over the range from $r = 0$ to $r = 10$ cm, given that $I = 10$ A, $a = 2$ cm, $b = 4$ cm, and $c = 5$ cm.

5.21* A long cylindrical conductor whose axis is coincident with the z-axis has a radius a and carries a current characterized by a current density $\mathbf{J} = \hat{\mathbf{z}} J_0/r$, where J_0 is a constant and r is the radial distance from the cylinder's axis. Obtain an expression for the magnetic field $\mathbf{H}$ for

(a) $0 \le r \le a$

(b) $r > a$

5.22 Repeat Problem 5.21 for a current density $\mathbf{J} = \hat{\mathbf{z}} J_0 e^{-r}$.

5.23* In a certain conducting region, the magnetic field is given in cylindrical coordinates by

$$\mathbf{H} = \hat{\boldsymbol{\phi}} \frac{4}{r}[1 - (1 + 2r)e^{-2r}]$$

Find the current density $\mathbf{J}$.

Section 5-5: Magnetic Potential

5.24 With reference to Fig. 5-10:

(a) Derive an expression for the vector magnetic potential $\mathbf{A}$ at a point P located at a distance r from the wire in the x–y plane.

(b) Derive $\mathbf{B}$ from $\mathbf{A}$. Show that your result is identical with the expression given by Eq. (5.29), which was derived by applying the Biot–Savart law.

5.25* In a given region of space, the vector magnetic potential is given by $\mathbf{A} = \hat{\mathbf{x}} 5 \cos \pi y + \hat{\mathbf{z}}(2 + \sin \pi x)$ (Wb/m).

(a) Determine $\mathbf{B}$.

(b) Use Eq. (5.66) to calculate the magnetic flux passing through a square loop with 0.25-m-long edges if the loop is in the x–y plane, its center is at the origin, and its edges are parallel to the x- and y-axes.

(c) Calculate Φ again using Eq. (5.67).

5.26 A uniform current density given by

$$\mathbf{J} = \hat{\mathbf{z}} J_0 \qquad (\text{A/m}^2)$$

gives rise to a vector magnetic potential

$$\mathbf{A} = -\hat{\mathbf{z}} \frac{\mu_0 J_0}{4}(x^2 + y^2) \qquad (\text{Wb/m})$$

(a) Apply the vector Poisson's equation to confirm the above statement.

(b) Use the expression for $\mathbf{A}$ to find $\mathbf{H}$.

(c) Use the expression for $\mathbf{J}$ in conjunction with Ampère's law to find $\mathbf{H}$. Compare your result with that obtained in part (b).

5.27* A thin current element extending between $z = -L/2$ and $z = L/2$ carries a current I along $+\hat{\mathbf{z}}$ through a circular cross-section of radius a.

(a) Find $\mathbf{A}$ at a point P located very far from the origin (assume R is so much larger than L that point P may be considered to be at approximately the same distance from every point along the current element).

(b) Determine the corresponding $\mathbf{H}$.

Section 5-6: Magnetic Properties of Materials

5.28 In the model of the hydrogen atom proposed by Bohr in 1913, the electron moves around the nucleus at a speed of 2×10^6 m/s in a circular orbit of radius 5×10^{-11} m. What is the magnitude of the magnetic moment generated by the electron's motion?

INTEL-1014
U.S. Patent 7,151,430

5.29* Iron contains 8.5×10^{28} atoms/m^3. At saturation, the alignment of the electrons' spin magnetic moments in iron can contribute 1.5 T to the total magnetic flux density **B**. If the spin magnetic moment of a single electron is 9.27×10^{-24} (A·m^2), how many electrons per atom contribute to the saturated field?

Section 5-7: Magnetic Boundary Conditions

5.30 The x–y plane separates two magnetic media with magnetic permeabilities μ_1 and μ_2, as shown in Fig. 5-45. If there is no surface current at the interface and the magnetic field in medium 1 is

$$\mathbf{H}_1 = \hat{\mathbf{x}}H_{1x} + \hat{\mathbf{y}}H_{1y} + \hat{\mathbf{z}}H_{1z}$$

find:

(a) $\mathbf{H}_2$

(b) θ_1 and θ_2

(c) Evaluate $\mathbf{H}_2$, θ_1, and θ_2 for $H_{1x} = 3$ (A/m), $H_{1y} = 0$, $H_{1z} = 4$ (A/m), $\mu_1 = \mu_0$, and $\mu_2 = 4\mu_0$

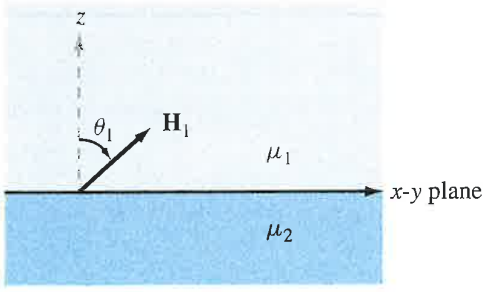


Figure 5-45: Adjacent magnetic media (Problem 5.30).

5.31* Given that a current sheet with surface current density $\mathbf{J}_s = \hat{\mathbf{x}}4$ (A/m) exists at $y = 0$, the interface between two magnetic media, and $\mathbf{H}_1 = \hat{\mathbf{z}}8$ (A/m) in medium 1 ($y > 0$), determine $\mathbf{H}_2$ in medium 2 ($y < 0$).

5.32 In Fig. 5-46, the plane defined by $x - y = 1$ separates medium 1 of permeability μ_1 from medium 2 of permeability μ_2. If no surface current exists on the boundary and

$$\mathbf{B}_1 = \hat{\mathbf{x}}2 + \hat{\mathbf{y}}3 \quad \text{(T)}$$

find $\mathbf{B}_2$ and then evaluate your result for $\mu_1 = 5\mu_2$.

Hint: Start by deriving the equation for the unit vector normal to the given plane.

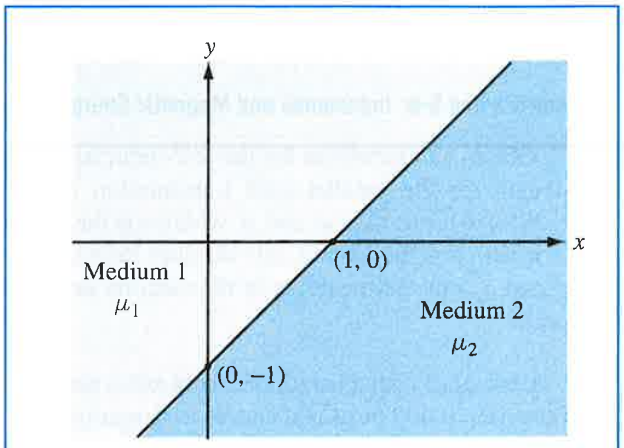


Figure 5-46: Magnetic media separated by the plane $x - y = 1$ (Problem 5.32).

5.33 The plane boundary defined by $z = 0$ separates air from a block of iron. If $\mathbf{B}_1 = \hat{\mathbf{x}}4 - \hat{\mathbf{y}}6 + \hat{\mathbf{z}}8$ in air ($z \geq 0$), find $\mathbf{B}_2$ in iron ($z \leq 0$), given that $\mu = 5000\mu_0$ for iron.

5.34 Show that if no surface current densities exist at the parallel interfaces shown in Fig. 5-47, the relationship between θ_4 and θ_1 is independent of μ_2.

INTEL-1014
U.S. Patent 7,151,430

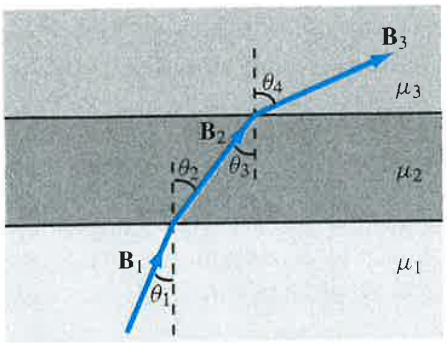


Figure 5-47: Three magnetic media with parallel interfaces (Problem 5.34).

Sections 5-8 and 5-9: Inductance and Magnetic Energy

5.35* Obtain an expression for the self-inductance per unit length for the parallel wire transmission line of Fig. 5-27(a) in terms of a, d, and μ, where a is the radius of the wires, d is the axis-to-axis distance between the wires, and μ is the permeability of the medium in which they reside.

5.36 A solenoid with a length of 20 cm and a radius of 5 cm consists of 400 turns and carries a current of 12 A. If $z = 0$ represents the midpoint of the solenoid, generate a plot for $|\mathbf{H}(z)|$ as a function of z along the axis of the solenoid for the range $-20\text{ cm} \leq z \leq 20\text{ cm}$ in 1-cm steps.

5.37* In terms of the d-c current I, how much magnetic energy is stored in the insulating medium of a 2-m-long, air-filled section of a coaxial transmission line, given that the radius of the inner conductor is 5 cm and the inner radius of the outer conductor is 10 cm?

5.38 The rectangular loop shown in Fig. 5-48 is coplanar with the long, straight wire carrying the current $I = 20$ A. Determine the magnetic flux through the loop.

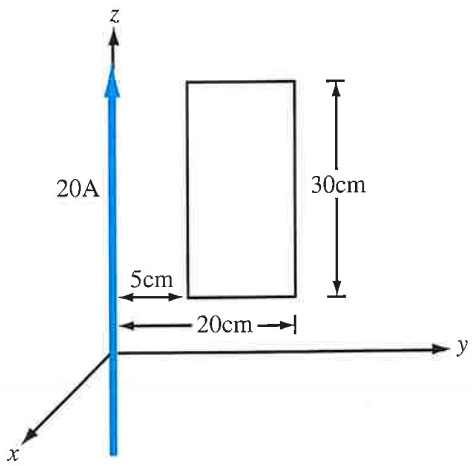
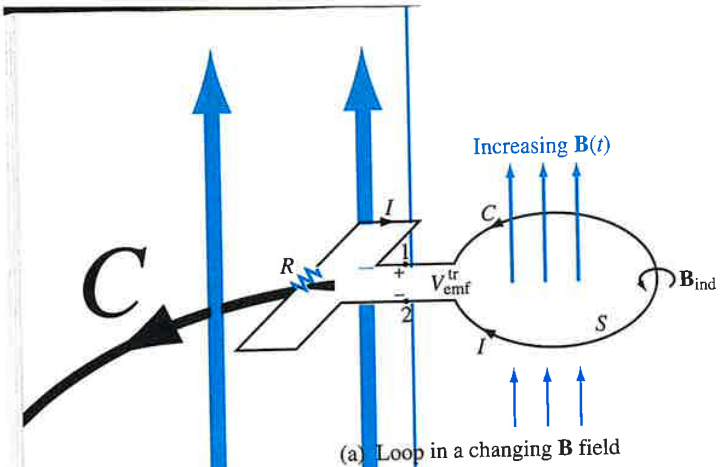


Figure 5-48: Loop and wire arrangement for Problem 5.38.

INTEL-1014
U.S. Patent 7,151,430



(a) Loop in a changing **B** field

CHAPTER 6

Maxwell's Equations for Time-Varying Fields

Dynamics Fields

6-1 Faraday's Law

6-2 Stationary Loop in a Time-Varying Magnetic Field

6-3 The Ideal Transformer

6-4 Moving Conductor in a Static Magnetic Field

6-5 The Electromagnetic Generator

6-6 Moving Conductor in a Time-Varying Magnetic Field

6-7 Displacement Current

6-8 Boundary Conditions for Electromagnetics

6-9 Charge—Current Continuity Relation

6-10 Free-Charge Dissipation in a Conductor

6-11 Electromagnetic Potentials

INTEL-1014
U.S. Patent 7,151,430

DYNAMIC FIELDS

Electric charges induce electric fields and electric currents induce magnetic fields. Those are the lessons we learned in the preceding two chapters. As long as the charge and current distributions remain constant in time, so will the fields that they induce. However, if the charge and current sources were to vary with time t, not only will the fields also vary with time, but much more happens. The electric and magnetic fields become interconnected, and the coupling between them produces electromagnetic waves capable of traveling through free space and in material media. Electromagnetic waves, which include light waves, x-rays, infrared waves, gamma rays, and radio waves [see Fig. 1-15], are an important part of our physical world, and their uses are manifested in many fields of science and technology.

To study time-varying electromagnetic phenomena, we need to use Maxwell's equations as an integrated unit. These equations, which were first introduced in the opening section of Chapter 4, are given in both differential and integral form in Table 6-1. Whereas in the static case ($\partial/\partial t = 0$) we were able to use the first pair of Maxwell's equations to study electrical phenomena in Chapter 4 and the second pair to study magnetic phenomena in Chapter 5, in the dynamic case we have to deal with the coupling that exists between the electric and magnetic fields, as expressed by the second and fourth equations in Table 6-1. The first equation represents Gauss's law, and it is equally valid for static and dynamic fields. The same is true for the third equation, $\nabla \cdot \mathbf{B} = 0$, which basically states that there are no such things as magnetic charges. The second and fourth equations, however, exhibit different meanings for static and dynamic fields. In the dynamic case, a time-varying magnetic field gives rise to an electric field (Faraday's law) and, conversely, a time-varying electric field gives rise to a magnetic field (Ampère's law).

Some of the results we will obtain in this and succeeding chapters might contradict statements made and conclusions reached in Chapter 4 and 5. This is because the earlier material pertains to the special case of steady currents and static charges. When $\partial/\partial t$ is set equal to zero, the results and expressions for the fields under dynamic conditions will reduce to those applicable under static conditions.

We begin this chapter with examinations of Faraday's and Ampère's laws and some of their practical applications. We will then combine Maxwell's equations to obtain relations among the charge and current sources, ρ_v and $\mathbf{J}$, the scalar and vector potentials, V and $\mathbf{A}$, and the electromagnetic fields, $\mathbf{E}$, $\mathbf{D}$, $\mathbf{H}$, and $\mathbf{B}$, for the time-varying case in general and for sinusoidal-time variations in particular.

6-1 Faraday's Law

The close connection between electricity and magnetism was established by Oersted, who demonstrated that a wire carrying an electric current exerts a force on a compass needle and that the needle always turns so as to point in the $\hat{\boldsymbol{\phi}}$-direction when the current is along the $\hat{\mathbf{z}}$-direction. The force acting on the compass needle is due to the magnetic field produced by the current in the wire. Following this discovery, Michael Faraday developed the following hypothesis: if a current can produce a magnetic field, then the converse should also be true: a magnetic field should produce a current in a wire. To prove his hypothesis, he conducted numerous experiments in his

INTEL-1014
U.S. Patent 7,151,430

Table 6-1: Maxwell's equations.

Reference	Differential Form	Integral Form	
Gauss's law	$\nabla \cdot \mathbf{D} = \rho_v$	$\oint_S \mathbf{D} \cdot d\mathbf{s} = Q$	(6.1)
Faraday's law	$\nabla \times \mathbf{E} = -\frac{\partial \mathbf{B}}{\partial t}$	$\oint_C \mathbf{E} \cdot d\mathbf{l} = -\int_S \frac{\partial \mathbf{B}}{\partial t} \cdot d\mathbf{s}$	(6.2)*
No magnetic charges (Gauss's law for magnetism)	$\nabla \cdot \mathbf{B} = 0$	$\oint_S \mathbf{B} \cdot d\mathbf{s} = 0$	(6.3)
Ampère's law	$\nabla \times \mathbf{H} = \mathbf{J} + \frac{\partial \mathbf{D}}{\partial t}$	$\oint_C \mathbf{H} \cdot d\mathbf{l} = \int_S \left(\mathbf{J} + \frac{\partial \mathbf{D}}{\partial t}\right) \cdot d\mathbf{s}$	(6.4)

*For a stationary surface S.

laboratory in London over a period of about 10 years, all aimed at making magnetic fields induce currents in wires. Similar work was being conducted by Joseph Henry in Albany, New York. Wires were placed next to permanent magnets of all different sizes, but no currents were detected in the wires. Current was passed through a wire while another wire was placed parallel to it, with the expectation that the magnetic field of the current-carrying wire would induce a current in the other wire, but again the result was negative. Eventually, these types of experiments led to the true answer, which both Faraday and Henry discovered independently at about the same time (1831). They discovered that indeed *magnetic fields can produce an electric current in a closed loop, but only if the magnetic flux linking the surface area of the loop changes with time.* The key to the induction process is *change*. To explain how the induction process works, let us consider the arrangement shown in Fig. 6-1. A square conducting loop connected to a galvanometer, which is a sensitive instrument used in the 1800s to detect the flow of current in a circuit, is placed next to a conducting coil connected to a battery. The current in the coil produces a magnetic field **B** whose lines pass through the loop as shown in Fig. 6-1. In Section 5-5, we defined the

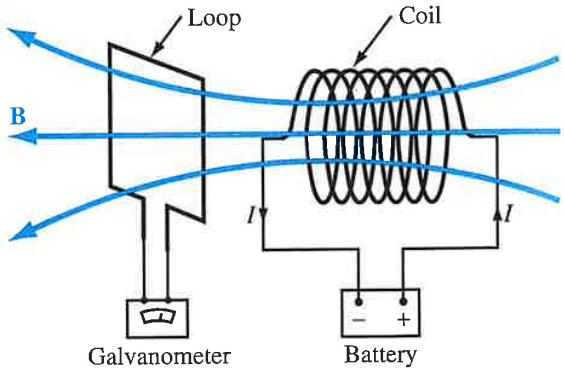


Figure 6-1: The galvanometer shows a deflection whenever the magnetic flux passing through the square loop changes with time.

INTEL-1014
U.S. Patent 7,151,430

magnetic flux Φ passing through a loop as the integral of the normal component of the magnetic flux density over the surface area of the loop, S, or

$$\Phi = \int_S \mathbf{B} \cdot d\mathbf{s} \quad \text{(Wb)}. \tag{6.5}$$

Under stationary conditions, the d-c current in the coil produces a constant magnetic field $\mathbf{B}$, which in turn produces a constant flux through the loop. When the flux is constant, no current is detected by the galvanometer. However, when the battery is disconnected, thereby interrupting the flow of current in the coil, the magnetic field drops to zero, and the consequent change in magnetic flux causes a momentary deflection of the galvanometer needle. When the battery is reconnected, the galvanometer again exhibits a momentary deflection, but in the opposite direction. Thus, current is induced in the loop when the magnetic flux changes, and the direction of the current depends on whether the flux is increasing (as when the battery is being connected) or decreasing (as when the battery is being disconnected). It was further discovered that current can also flow in the loop, while the battery is connected to the coil, if the loop is turned around suddenly or while moving it closer to or away from the coil. The physical movement of the loop changes the amount of flux linking its surface S, even though the field $\mathbf{B}$ due to the coil has not changed.

A galvanometer is the predecessor of the voltmeter and ammeter. When a galvanometer detects the flow of current through the coil, it means that a voltage has been induced across the galvanometer terminals. This voltage is called the ***electromotive force*** (emf), V_{emf}, and the process is called ***electromagnetic induction***. The emf induced in a closed conducting loop of N turns is given by

$$V_{\text{emf}} = -N\frac{d\Phi}{dt} = -N\frac{d}{dt}\int_S \mathbf{B} \cdot d\mathbf{s} \quad \text{(V)}. \tag{6.6}$$

Even though the results leading to Eq. (6.6) were also discovered independently by Henry, Eq. (6.6) is attributed to Faraday and is known as ***Faraday's law***. The significance of the negative sign in Eq. (6.6) will be explained in the next section.

We note that the derivative in Eq. (6.6) is a total time derivative that operates on the magnetic field $\mathbf{B}$, as well as the differential surface area $d\mathbf{s}$. Accordingly, an emf can be generated in a closed conducting loop under any of the following three conditions:

1. *A time-varying magnetic field linking a stationary loop;* the induced emf is then called the ***transformer emf***, $V_{\text{emf}}^{\text{tr}}$.
2. *A moving loop with a time-varying area (relative to the normal component of* $\mathbf{B}$*) in a static field* $\mathbf{B}$*;* the induced emf is then called the ***motional emf***, $V_{\text{emf}}^{\text{m}}$.
3. *A moving loop in a time-varying field* $\mathbf{B}$.

The total emf is given by

$$V_{\text{emf}} = V_{\text{emf}}^{\text{tr}} + V_{\text{emf}}^{\text{m}}, \tag{6.7}$$

with $V_{\text{emf}}^{\text{m}} = 0$ if the loop is stationary (case (1)) and $V_{\text{emf}}^{\text{tr}} = 0$ if $\mathbf{B}$ is static (case (2)). For case (3), neither term is zero. Each of the three cases will be examined separately in the following sections.

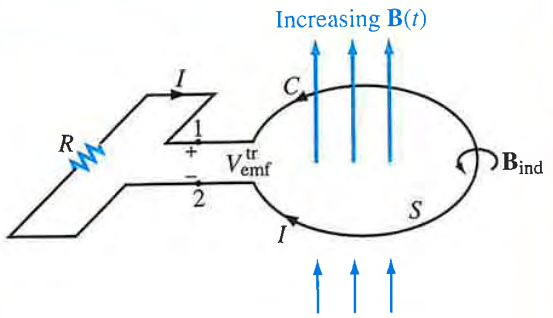
6-2 Stationary Loop in a Time-Varying Magnetic Field

The single-turn, conducting, circular loop with contour C and surface area S shown in Fig. 6-2(a) is in a time-varying magnetic field $\mathbf{B}(t)$. As was stated earlier, the emf induced when S is stationary and the field is time varying is called the ***transformer emf*** and is denoted $V_{\text{emf}}^{\text{tr}}$. Since the loop is stationary, d/dt in Eq. (6.6) now operates on $\mathbf{B}(t)$ only. Hence,

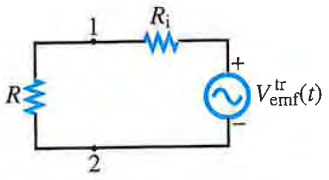
$$V_{\text{emf}}^{\text{tr}} = -N\int_S \frac{\partial \mathbf{B}}{\partial t} \cdot d\mathbf{s}, \tag{6.8}$$

where the full derivative d/dt has been moved inside the integral and changed into a partial derivative $\partial/\partial t$ to

INTEL-1014
U.S. Patent 7,151,430



(a) Loop in a changing **B** field



(b) Equivalent circuit

Figure 6-2: (a) Stationary circular loop in a changing magnetic field $\mathbf{B}(t)$, and (b) its equivalent circuit.

signify that it operates on **B** only. The transformer emf is the voltage difference that would appear across the small opening between terminals 1 and 2, even in the absence of the resistor R. That is, $V_{emf}^{tr} = V_{12}$, where V_{12} is the open-circuit voltage across the open ends of the loop. Under d-c conditions, $V_{emf}^{tr} = 0$. For the loop shown in Fig. 6-2(a) and the associated definition for V_{emf}^{tr} given by Eq. (6.8), the direction of $d\mathbf{s}$, the loop's differential surface normal, can be chosen to be either upward or downward. The two choices are associated with opposite designations of the polarities of terminals 1 and 2 in Fig. 6-2(a). The connection between the direction of $d\mathbf{s}$ and the polarity of V_{emf}^{tr} is governed by the following right-hand rule: if $d\mathbf{s}$ points along the thumb of the right hand, then the direction of the contour C indicated by the four fingers is such that it always passes across the opening from the positive terminal of V_{emf}^{tr} to the negative terminal.

If the loop has an internal resistance R_i, the circuit in Fig. 6-2(a) can be represented by the equivalent circuit shown in Fig. 6-2(b), in which case the current I flowing through the circuit is given by

$$I = \frac{V_{emf}^{tr}}{R + R_i}. \tag{6.9}$$

For good conductors, R_i usually is very small, and it may be ignored in comparison with practical values of R, except when $R = 0$ (loop is shorted across its ends).

The polarity of V_{emf}^{tr} and hence the direction of I is governed by ***Lenz's law***, which states that *the current in the loop is always in such a direction as to oppose the change of magnetic flux $\Phi(t)$ that produced it.* The current I induces a magnetic field of its own, $\mathbf{B}_{ind}$, with a corresponding flux Φ_{ind}. The direction of $\mathbf{B}_{ind}$ is governed by the right-hand rule; if I is in a clockwise direction, then $\mathbf{B}_{ind}$ points downward through S and, conversely, if I is in a counterclockwise direction, then $\mathbf{B}_{ind}$ points upward through S. If the original field $\mathbf{B}(t)$ is increasing, which means that $d\Phi/dt > 0$, then according to Lenz's law, I has to be in the direction shown in Fig. 6-2(a) in order for $\mathbf{B}_{ind}$ to be in opposition to $\mathbf{B}(t)$. Consequently, terminal 2 would be at a higher potential than terminal 1, and V_{emf}^{tr} would have a negative value. However, if $\mathbf{B}(t)$ were to remain in the same direction but to decrease in magnitude, then $d\Phi/dt$ would become negative, the current would have to reverse direction, and its induced field $\mathbf{B}_{ind}$ would be in the same direction as $\mathbf{B}(t)$ so as to oppose the change (decrease) of $\mathbf{B}(t)$. In that case, V_{emf}^{tr} would be positive. It is important to remember that $\mathbf{B}_{ind}$ serves to oppose the *change* in $\mathbf{B}(t)$, and not necessarily $\mathbf{B}(t)$ itself.

Despite the presence of the small opening between terminals 1 and 2 of the loop in Fig. 6-2(a), we shall treat the loop as a closed path with contour C. We do this in order to establish the link between **B** and the electric field **E** associated with the induced emf, V_{emf}^{tr}. Also, at any point along the loop, the field E is related to the

INTEL-1014
U.S. Patent 7,151,430

current I flowing through the loop. For contour C, $V_{\text{emf}}^{\text{tr}}$ is related to $\mathbf{E}$ by

$$V_{\text{emf}}^{\text{tr}} = \oint_C \mathbf{E} \cdot d\mathbf{l}. \tag{6.10}$$

For $N = 1$ (a loop with one turn), equating Eqs. (6.8) and (6.10) gives

$$\oint_C \mathbf{E} \cdot d\mathbf{l} = -\int_S \frac{\partial \mathbf{B}}{\partial t} \cdot d\mathbf{s}, \tag{6.11}$$

which is the integral form of Faraday's law given in Table 6-1. We should keep in mind that the direction of the contour C and the direction of $d\mathbf{s}$ are related by the right-hand rule.

By applying Stokes's theorem to the left-hand side of Eq. (6.11), we have

$$\int_S (\nabla \times \mathbf{E}) \cdot d\mathbf{s} = -\int_S \frac{\partial \mathbf{B}}{\partial t} \cdot d\mathbf{s}, \tag{6.12}$$

and in order for the two integrals to be equal, their integrands have to be equal, which gives

$$\nabla \times \mathbf{E} = -\frac{\partial \mathbf{B}}{\partial t} \quad \text{(Faraday's law).} \tag{6.13}$$

This differential form of Faraday's law states that a time-varying magnetic field induces an electric field $\mathbf{E}$ whose curl is equal to the negative of the time derivative of $\mathbf{B}$. Even though the derivation leading to Faraday's law started out by considering the field associated with a physical circuit, Eq. (6.13) applies at any point in space, whether or not a physical circuit exists at that point.

Example 6-1 Inductor in a Changing Magnetic Field

An inductor is formed by winding N turns of a thin conducting wire into a circular loop of radius a. The inductor loop is in the x–y plane with its center at the origin, and it is connected to a resistor R, as shown in Fig. 6-3. In the presence of a magnetic field given by $\mathbf{B} = B_0(\hat{\mathbf{y}}2 + \hat{\mathbf{z}}3) \sin \omega t$, where ω is the angular frequency, find

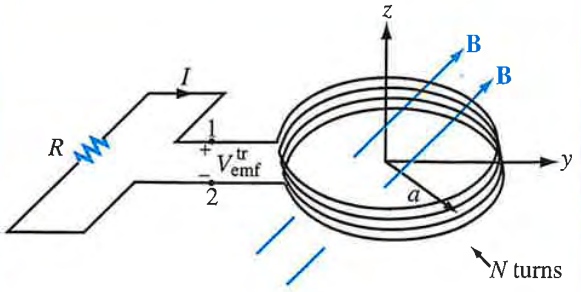


Figure 6-3: Circular loop with N turns in the x–y plane. The magnetic field is $\mathbf{B} = B_0(\hat{\mathbf{y}}2 + \hat{\mathbf{z}}3) \sin \omega t$ (Example 6-1).

(a) the magnetic flux linking a single turn of the inductor,
(b) the transformer emf, given that $N = 10$, $B_0 = 0.2$ T, $a = 10$ cm, and $\omega = 10^3$ rad/s,
(c) the polarity of $V_{\text{emf}}^{\text{tr}}$ at $t = 0$, and
(d) the induced current in the circuit for $R = 1$ kΩ (assume the wire resistance to be negligibly small).

Solution: (a) The magnetic flux linking each turn of the inductor is

$$\Phi = \int_S \mathbf{B} \cdot d\mathbf{s}$$
$$= \int_S [B_0(\hat{\mathbf{y}}2 + \hat{\mathbf{z}}3) \sin \omega t] \cdot \hat{\mathbf{z}}\, ds = 3\pi a^2 B_0 \sin \omega t.$$

(b) To find $V_{\text{emf}}^{\text{tr}}$, we can apply Eq. (6.8) or we can apply the general expression given by Eq. (6.6) directly. The latter approach gives

$$V_{\text{emf}}^{\text{tr}} = -N\frac{d\Phi}{dt}$$
$$= -\frac{d}{dt}(3\pi N a^2 B_0 \sin \omega t) = -3\pi N \omega a^2 B_0 \cos \omega t.$$

For $N = 10$, $a = 0.1$ m, $\omega = 10^3$ rad/s, and $B_0 = 0.2$ T,

$$V_{\text{emf}}^{\text{tr}} = -188.5 \cos 10^3 t \quad \text{(V)}.$$

INTEL-1014
U.S. Patent 7,151,430

(c) At $t = 0$, $d\Phi/dt > 0$ and $V_{emf}^{tr} = -188.5$ V. Since the flux is increasing, the current I must be in the direction shown in Fig. 6-3 in order to satisfy Lenz's law. Consequently, point 2 is at a higher potential than point 1 and

$$V_{emf}^{tr} = V_1 - V_2 = -188.5 \quad \text{(V)}.$$

(d) The current I is given by

$$I = \frac{V_2 - V_1}{R} = \frac{188.5}{10^3} \cos 10^3 t = 0.19 \cos 10^3 t \quad \text{(A)}.$$

■

EXERCISE 6.1 For the loop shown in Fig. 6-3, what is V_{emf}^{tr} if $\mathbf{B} = \hat{\mathbf{y}} B_0 \cos \omega t$? Explain.

Ans. $V_{emf}^{tr} = 0$ because $\mathbf{B}$ is orthogonal to the loop's surface normal $d\mathbf{s}$.

EXERCISE 6.2 Suppose that the loop of Example 6-1 is replaced with a 10-turn square loop centered at the origin and having 20-cm sides oriented parallel to the x- and y-axes. If $\mathbf{B} = \hat{\mathbf{z}} B_0 x^2 \cos 10^3 t$ and $B_0 = 100$ T, find the current in the circuit.

Ans. $I = -133 \sin 10^3 t$ (mA).

Example 6-2 Lenz's Law

Determine the voltages V_1 and V_2 across the 2-Ω and 4-Ω resistors shown in Fig. 6-4. The loop is located in the x–y plane, its area is 4 m^2, the magnetic flux density is $\mathbf{B} = -\hat{\mathbf{z}} 0.3t$ (T), and the internal resistance of the wire may be ignored.

Solution: The flux flowing through the loop is

$$\Phi = \int_S \mathbf{B} \cdot d\mathbf{s} = \int_S (-\hat{\mathbf{z}} 0.3t) \cdot \hat{\mathbf{z}}\, ds = -0.3t \times 4 = -1.2t \quad \text{(Wb)},$$

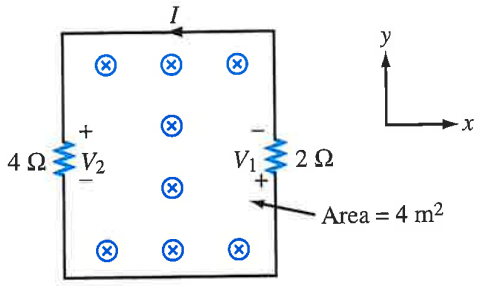


Figure 6-4: Circuit for Example 6-2.

and the corresponding transformer emf is

$$V_{emf}^{tr} = -\frac{d\Phi}{dt} = 1.2 \quad \text{(V)}.$$

Since the magnetic flux through the loop is along the $-z$-direction (into the page) and it is increasing in magnitude with time t, Lenz's law states that the induced current I should be in a direction such that the magnetic flux density $\mathbf{B}_{ind}$ induced by I counteracts the direction of change of Φ. Hence, I has to be in the direction shown in the circuit because the corresponding $\mathbf{B}_{ind}$ is along the $+z$-direction in the region inside the loop area. This, in turn, means that V_1 and V_2 are positive voltages.

The total voltage of 1.2 V is distributed across two resistors in series. Consequently,

$$I = \frac{V_{emf}^{tr}}{R_1 + R_2} = \frac{1.2}{2+4} = 0.2 \text{ A},$$

and

$$V_1 = I R_1 = 0.2 \times 2 = 0.4 \text{ V},$$
$$V_2 = I R_2 = 0.2 \times 4 = 0.8 \text{ V}. \quad ■$$

REVIEW QUESTIONS

Q6.1 Explain Faraday's law and the function of Lenz's law.

INTEL-1014
U.S. Patent 7,151,430

Q6.2 Under what circumstances is the net voltage around a closed loop equal to zero?

Q6.3 Suppose the magnetic flux density linking the loop of Fig. 6-4 (Example 6-2) is given by $\mathbf{B} = -\hat{\mathbf{z}}\,0.3e^{-t}$ (T). What would the direction of the current be, relative to that shown in Fig. 6-4, for $t \geq 0$? Explain.

6-3 The Ideal Transformer

The transformer shown in Fig. 6-5(a) consists of two coils wound around a common magnetic core. The coil of the primary circuit has N_1 turns and that of the secondary circuit has N_2 turns. The primary coil is connected to an a-c voltage source $V_1(t)$ and the secondary coil is connected to a load resistor R_L. In an ideal transformer the core has infinite permeability ($\mu = \infty$), and the magnetic flux is confined within the core. The directions of the currents flowing in the two coils, I_1 and I_2, are defined such that, when I_1 and I_2 are both positive, the flux generated by I_2 is opposite that generated by I_1. *The transformer gets its name from the fact that it is used to transform currents, voltages, and impedances between its primary and secondary circuits.*

On the primary side of the transformer, the voltage source V_1 generates a current I_1 in the primary coil, which establishes a flux Φ in the magnetic core. The flux Φ and the voltage V_1 are related by Faraday's law:

$$V_1 = -N_1 \frac{d\Phi}{dt}, \tag{6.14}$$

and, similarly, on the secondary side,

$$V_2 = -N_2 \frac{d\Phi}{dt}. \tag{6.15}$$

The combination of Eqs. (6.14) and (6.15) gives

$$\frac{V_1}{V_2} = \frac{N_1}{N_2}. \tag{6.16}$$

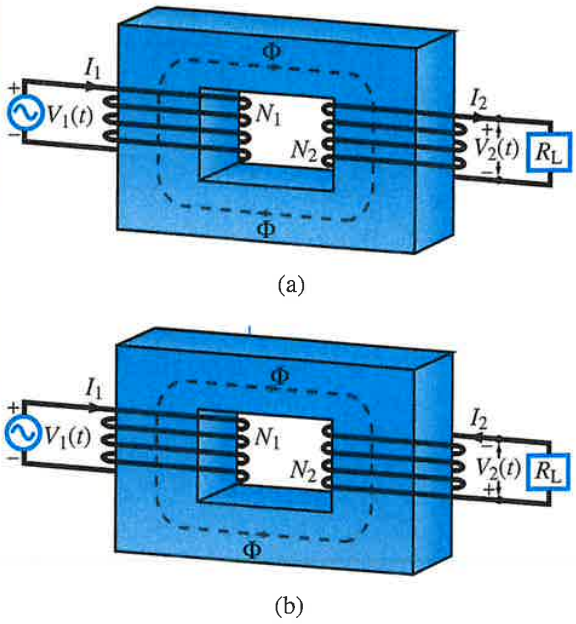


Figure 6-5: In a transformer, the directions of I_1 and I_2 are such that the flux Φ generated by one of them is opposite that generated by the other. The direction of the secondary winding in (b) is opposite that in (a), and so are the direction of I_2 and the polarity of V_2.

In an ideal lossless transformer, all the instantaneous power supplied by the source connected to the primary coil is delivered to the load on the secondary side. Thus, no power is lost in the core, and

$$P_1 = P_2. \tag{6.17}$$

Since $P_1 = I_1 V_1$ and $P_2 = I_2 V_2$, and in view of Eq. (6.16), we have

$$\frac{I_1}{I_2} = \frac{N_2}{N_1}. \tag{6.18}$$

INTEL-1014
U.S. Patent 7,151,430

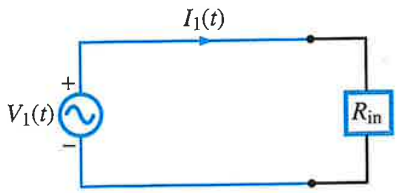


Figure 6-6: Equivalent circuit for the primary side of the transformer.

Thus, whereas the ratio of the voltages given by Eq. (6.16) is proportional to the corresponding turns ratio, the ratio of the currents is equal to the inverse of the turns ratio. If $N_1/N_2 = 0.1$, V_2 of the secondary circuit would be 10 times V_1 of the primary circuit, but I_2 would be only $I_1/10$.

The transformer shown in Fig. 6-5(b) is identical to that in Fig. 6-5(a) except for the direction of the windings of the secondary coil. Because of this change, the direction of I_2 and the polarity of V_2 in Fig. 6-5(b) are the reverse of those in Fig. 6-5(a).

The voltage and current in the secondary circuit in Fig. 6-5(a) are related by $V_2 = I_2 R_L$. To the input circuit, the transformer may be represented by an equivalent input resistance R_{in}, as shown in Fig. 6-6, defined as

$$R_{in} = \frac{V_1}{I_1}. \tag{6.19}$$

Use of Eqs. (6.16) and (6.18) gives

$$R_{in} = \frac{V_2}{I_2}\left(\frac{N_1}{N_2}\right)^2 = \left(\frac{N_1}{N_2}\right)^2 R_L. \tag{6.20}$$

When the load is an impedance Z_L and V_1 is a sinusoidal source, the input resistance representation can be extended to an equivalent input impedance Z_{in} given by

$$Z_{in} = \left(\frac{N_1}{N_2}\right)^2 Z_L. \tag{6.21}$$

6-4 Moving Conductor in a Static Magnetic Field

Consider a wire of length l moving across a static magnetic field $\mathbf{B} = \hat{\mathbf{z}}B_0$ at a constant velocity $\mathbf{u}$, as shown in Fig. 6-7. The conducting wire contains free electrons. From Eq. (5.3), the magnetic force $\mathbf{F}_m$ acting on any charged particle q moving with a velocity $\mathbf{u}$ in a magnetic field $\mathbf{B}$ is given by

$$\mathbf{F}_m = q(\mathbf{u} \times \mathbf{B}). \tag{6.22}$$

This magnetic force is equivalent to the electrical force that would be exerted on the particle by an electric field $\mathbf{E}_m$ given by

$$\mathbf{E}_m = \frac{\mathbf{F}_m}{q} = \mathbf{u} \times \mathbf{B}. \tag{6.23}$$

The field $\mathbf{E}_m$ generated by the motion of the charged particle is called a ***motional electric field***, and it is in a direction perpendicular to the plane containing $\mathbf{u}$ and $\mathbf{B}$. For the wire shown in Fig. 6-7, $\mathbf{E}_m$ is along $-\hat{\mathbf{y}}$. The magnetic force acting on the electrons in the wire causes them to move in the direction of $-\mathbf{E}_m$; that is, toward the end labeled 1 in Fig. 6-7. This in turn induces a

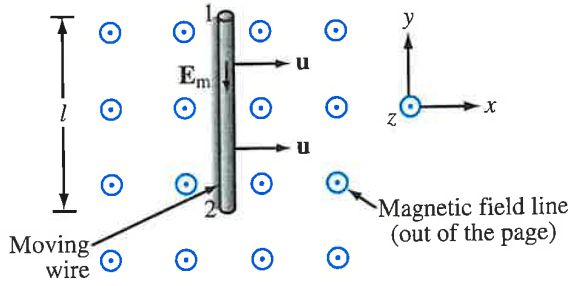


Figure 6-7: Conducting wire moving in a static magnetic field.

INTEL-1014
U.S. Patent 7,151,430

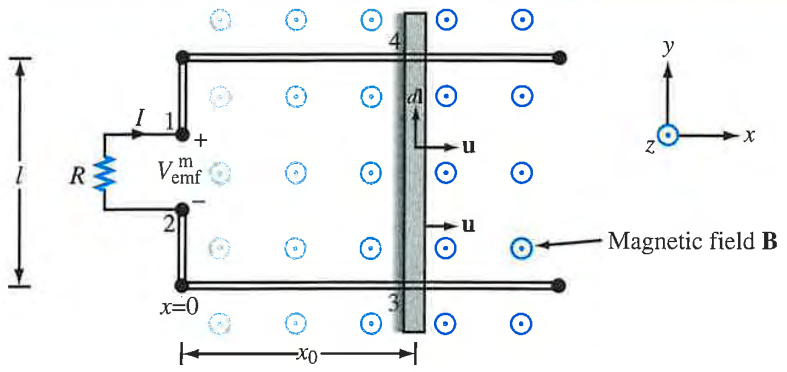


Figure 6-8: Sliding bar in a magnetic field that increases linearly with x; that is, $\mathbf{B} = \hat{\mathbf{z}}B_0x$ (Example 6-3).

voltage difference between ends 1 and 2, with end 2 being at the higher potential. The induced voltage is called a ***motional emf***, V_{emf}^{m}, and is defined as the line integral of $\mathbf{E}_m$ between ends 2 and 1 of the wire,

$$V_{emf}^{m} = V_{12} = \int_2^1 \mathbf{E}_m \cdot d\mathbf{l} = \int_2^1 (\mathbf{u} \times \mathbf{B}) \cdot d\mathbf{l}. \quad (6.24)$$

For the conducting wire, $\mathbf{u} \times \mathbf{B} = \hat{\mathbf{x}}u \times \hat{\mathbf{z}}B_0 = -\hat{\mathbf{y}}uB_0$ and $d\mathbf{l} = \hat{\mathbf{y}}\,dl$. Hence,

$$V_{emf}^{m} = V_{12} = -uB_0l. \quad (6.25)$$

In general, if any segment of a closed circuit with contour C moves with a velocity $\mathbf{u}$ across a static magnetic field $\mathbf{B}$, then the induced motional emf is given by

$$V_{emf}^{m} = \oint_C (\mathbf{u} \times \mathbf{B}) \cdot d\mathbf{l}. \quad (6.26)$$

Only those segments of the circuit that cross magnetic field lines contribute to V_{emf}^{m}.

Example 6-3 Sliding Bar

The rectangular loop shown in Fig. 6-8 has a constant width l, but its length x_0 increases with time as a conducting bar slides at a uniform velocity $\mathbf{u}$ in a static magnetic field $\mathbf{B} = \hat{\mathbf{z}}B_0x$. Note that $\mathbf{B}$ increases linearly with x. The bar starts from $x = 0$ at $t = 0$. Find the motional emf between terminals 1 and 2 and the current I flowing through the resistor R. Assume that the loop resistance $R_i \ll R$.

Solution: This problem can be solved by using the motional emf expression given by Eq. (6.26) or by applying the general formula of Faraday's law. We will show that the two approaches yield the same result.

The sliding bar, being the only part of the circuit that crosses the lines of the field $\mathbf{B}$, is the only part of contour 2341 that contributes to V_{emf}^{m}. Hence, at $x = x_0$,

$$V_{emf}^{m} = V_{12} = V_{43} = \int_3^4 (\mathbf{u} \times \mathbf{B}) \cdot d\mathbf{l}$$
$$= \int_3^4 (\hat{\mathbf{x}}u \times \hat{\mathbf{z}}B_0x_0) \cdot \hat{\mathbf{y}}\,dl = -uB_0x_0l.$$

The length of the loop is related to u by $x_0 = ut$. Hence,

$$V_{emf}^{m} = -B_0u^2lt \quad \text{(V)}. \quad (6.27)$$

Since $\mathbf{B}$ is static, $V_{emf}^{tr} = 0$ and $V_{emf} = V_{emf}^{m}$ only. To verify that the same result can be obtained by the general form of

INTEL-1014
U.S. Patent 7,151,430

Faraday's law, we start by finding the flux Φ through the surface of the loop. Thus,

$$\Phi = \int_S \mathbf{B} \cdot d\mathbf{s}$$
$$= \int_S (\hat{\mathbf{z}} B_0 x) \cdot \hat{\mathbf{z}}\, dx\, dy$$
$$= B_0 l \int_0^{x_0} x\, dx = \frac{B_0 l x_0^2}{2}. \qquad (6.28)$$

Substituting $x_0 = ut$ in Eq. (6.28) and then taking the negative derivative with respect to time gives

$$V_{\text{emf}} = -\frac{d\Phi}{dt} = -\frac{d}{dt}\left(\frac{B_0 l u^2 t^2}{2}\right)$$
$$= -B_0 u^2 l t \quad \text{(V)}, \qquad (6.29)$$

which is identical with Eq. (6.27). Since V_{12} is negative, the current $I = B_0 u^2 l t / R$ flows in the direction shown in Fig. 6-8. ■

Example 6-4 Moving Loop

The rectangular loop shown in Fig. 6-9 is situated in the x–y plane and moves away from the origin at a velocity $\mathbf{u} = \hat{\mathbf{y}}5$ (m/s) in a magnetic field given by

$$\mathbf{B}(y) = \hat{\mathbf{z}}\, 0.2 e^{-0.1y} \quad \text{(T)}.$$

If $R = 5\ \Omega$, find the current I at the instant that the loop sides are at $y_1 = 2$ m and $y_2 = 2.5$ m. The loop resistance may be ignored.

Solution: Since $\mathbf{u} \times \mathbf{B}$ is along $\hat{\mathbf{x}}$, voltages are induced across only the sides oriented along $\hat{\mathbf{x}}$, namely the side between points 1 and 2 and the side between points 3 and 4. Had $\mathbf{B}$ been uniform, the induced voltages would have been the same and the net voltage across the resistor would have been zero. In the present case, however, $\mathbf{B}$ decreases exponentially with y, thereby assuming a different value over side 1-2 than over side 3-4. Side 1-2 is at $y_1 = 2$ m, and the corresponding magnetic field is

$$\mathbf{B}(y_1) = \hat{\mathbf{z}}\, 0.2 e^{-0.1 y_1} = \hat{\mathbf{z}}\, 0.2 e^{-0.2} \quad \text{(T)}.$$

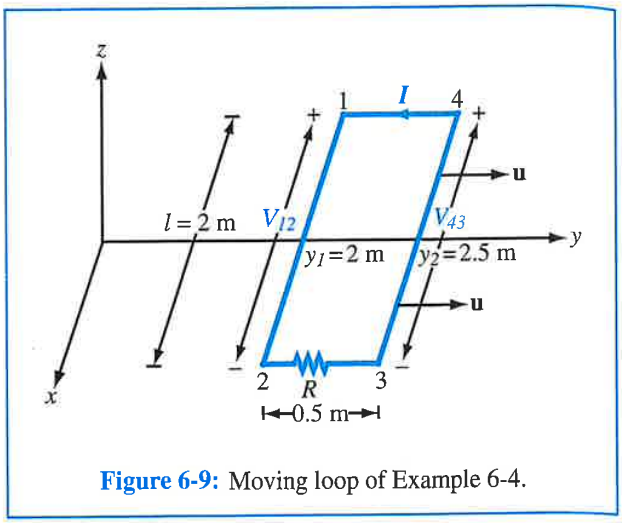


Figure 6-9: Moving loop of Example 6-4.

The induced voltage V_{12} is then given by

$$V_{12} = \int_2^1 [\mathbf{u} \times \mathbf{B}(y_1)] \cdot d\mathbf{l}$$
$$= \int_{l/2}^{-l/2} (\hat{\mathbf{y}}5 \times \hat{\mathbf{z}}\, 0.2 e^{-0.2}) \cdot \hat{\mathbf{x}}\, dx$$
$$= -e^{-0.2} l = -2e^{-0.2} = -1.637 \quad \text{(V)}.$$

Similarly,

$$V_{43} = -u\, B(y_2)\, l = -5 \times 0.2 e^{-0.25} \times 2$$
$$= -1.558 \quad \text{(V)}.$$

Consequently, the current is in the direction shown in the figure and its magnitude is

$$I = \frac{V_{43} - V_{12}}{R} = \frac{0.079}{5} = 15.8\ \text{(mA)}. \quad ■$$

Example 6-5 Moving Rod Next to a Wire

The wire shown in Fig. 6-10 is in free space and carries a current $I = 10$ A. A 30-cm-long metal rod moves at a constant velocity $\mathbf{u} = \hat{\mathbf{z}}5$ m/s. Find V_{12}.

INTEL-1014
U.S. Patent 7,151,430

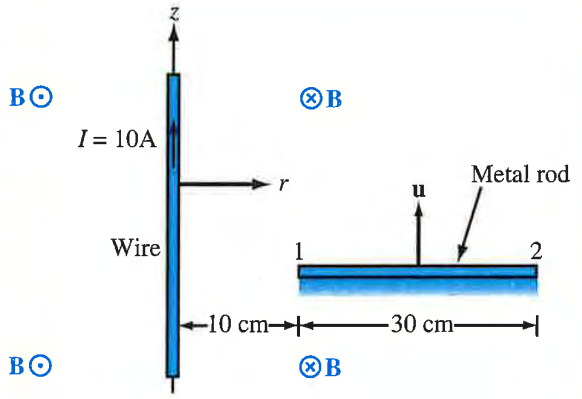


Figure 6-10: Moving rod of Example 6-5.

Solution: The current I induces a magnetic field

$$\mathbf{B} = \hat{\boldsymbol{\phi}} \frac{\mu_0 I}{2\pi r},$$

where r is the radial distance from the wire and the direction of $\hat{\boldsymbol{\phi}}$ is into the page at the metal rod side of the wire. The movement of the rod in the presence of the field $\mathbf{B}$ induces a motional emf given by

$$\begin{aligned} V_{12} &= \int_{40\text{ cm}}^{10\text{ cm}} (\mathbf{u} \times \mathbf{B}) \cdot d\mathbf{l} \\ &= \int_{40\text{ cm}}^{10\text{ cm}} \left(\hat{\mathbf{z}}5 \times \hat{\boldsymbol{\phi}} \frac{\mu_0 I}{2\pi r}\right) \cdot \hat{\mathbf{r}}\, dr \\ &= -\frac{5\mu_0 I}{2\pi} \int_{40\text{ cm}}^{10\text{ cm}} \frac{dr}{r} \\ &= -\frac{5 \times 4\pi \times 10^{-7} \times 10}{2\pi} \times \ln\left(\frac{10}{40}\right) = 13.9\ (\mu\text{V}). \blacksquare \end{aligned}$$

EXERCISE 6.3 For the moving loop of Fig. 6-9, find I at the instant that the loop sides are at $y_1 = 4$ m and $y_2 = 4.5$ m. Also, reverse the direction of motion such that $\mathbf{u} = -\hat{\mathbf{y}}5$ (m/s).

Ans. $I = -13$ (mA).

EXERCISE 6.4 Suppose that we turn the loop of Fig. 6-9 so that its surface is parallel to the x–z plane. What would I be in that case?

Ans. $I = 0$.

REVIEW QUESTIONS

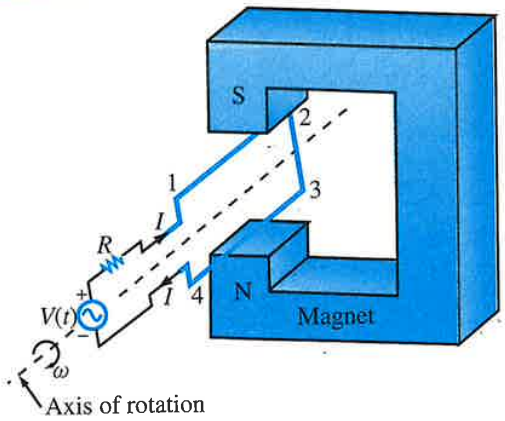
Q6.4 Suppose that no friction is involved in sliding the conducting bar of Fig. 6-8 and that the horizontal arms of the circuit are very long. Hence, if the bar is given an initial push, it should continue moving at a constant velocity, and its movement generates electrical energy in the form of an induced emf, indefinitely. Is this a valid argument? If not, why not? How can we generate electrical energy without having to supply an equal amount of energy by other means?

Q6.5 Is the current flowing in the rod of Fig. 6-10 a steady current? Examine the force on a charge q at ends 1 and 2 and compare.

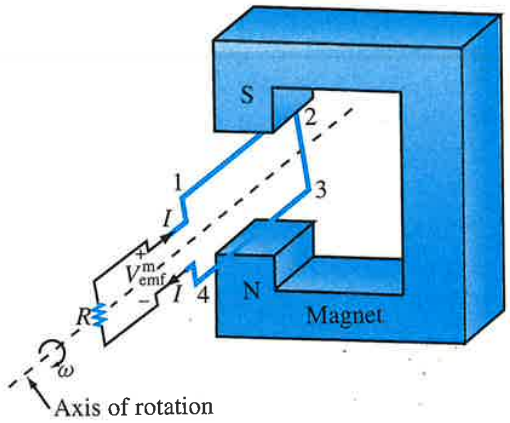
6-5 The Electromagnetic Generator

The electromagnetic generator is the converse of the electromagnetic motor. The principles of operation of both instruments may be explained with the help of Fig. 6-11. A permanent magnet is used to produce a static magnetic field $\mathbf{B}$ in the slot between the two poles of the magnet. When a current is passed through the conducting loop, as depicted in Fig. 6-11(a), the current flows in opposite directions in segments 1–2 and 3–4 of the loop. The induced magnetic forces on the two segments are also opposite, resulting in a torque that causes the loop to rotate about its axis. Thus, in a motor, electrical energy supplied by a voltage

INTEL-1014
U.S. Patent 7,151,430



(a) a-c motor



(b) a-c generator

Figure 6-11: Principles of the a-c motor and the a-c generator. In (a) the magnetic torque on the wires causes the loop to rotate, and in (b) the rotating loop generates an emf.

source is converted into mechanical energy in the form of a rotating loop, which can be coupled to pulleys, gears, or other movable objects.

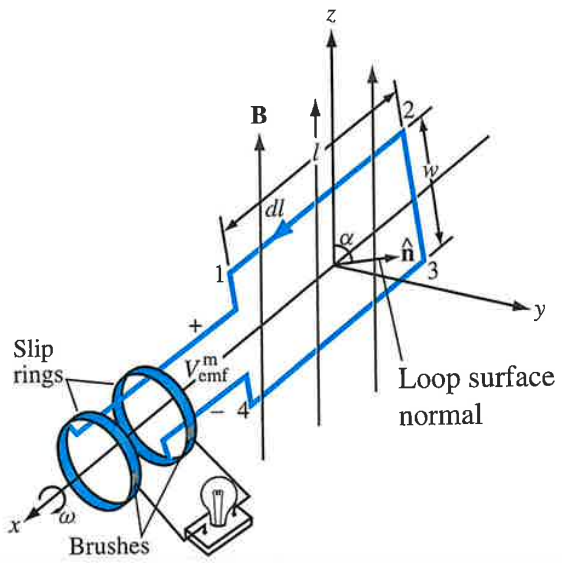


Figure 6-12: A loop rotating in a magnetic field induces an emf.

If, instead of passing a current through the loop to make it turn, the loop is made to rotate by an external force, the movement of the loop in the magnetic field will produce a motional emf, V_{emf}^{m}, as shown in Fig. 6-11(b). Hence, the motor has become a generator, and mechanical energy is being converted into electrical energy.

Let us examine the operation of the electromagnetic generator in more detail using the coordinate system shown in Fig. 6-12. The magnetic field is given by

$$\mathbf{B} = \hat{\mathbf{z}} B_0, \tag{6.30}$$

and the axis of rotation of the conducting loop is along the x-axis. Segments 1–2 and 3–4 of the loop are of length l each, and both cross the magnetic flux lines as the loop rotates. The other two segments are each of width w, and neither crosses the **B** lines when the loop rotates. Hence, only segments 1–2 and 3–4 contribute to the generation of the motional emf, V_{emf}^{m}.

INTEL-1014
U.S. Patent 7,151,430

As the loop rotates with an angular velocity ω about its own axis, segment 1–2 moves with a velocity $\mathbf{u}$ given by

$$\mathbf{u} = \hat{\mathbf{n}}\omega\frac{w}{2}, \tag{6.31}$$

where $\hat{\mathbf{n}}$, the surface normal to the loop, makes an angle α with the z-axis. Hence,

$$\hat{\mathbf{n}} \times \hat{\mathbf{z}} = \hat{\mathbf{x}}\sin\alpha. \tag{6.32}$$

Segment 3–4 moves with a velocity $-\mathbf{u}$. Application of Eq. (6.26), consistent with our choice of $\hat{\mathbf{n}}$, gives

$$\begin{aligned} V_{\text{emf}}^{\text{m}} = V_{14} &= \int_2^1 (\mathbf{u}\times\mathbf{B})\cdot d\mathbf{l} + \int_4^3 (\mathbf{u}\times\mathbf{B})\cdot d\mathbf{l} \\ &= \int_{-l/2}^{l/2}\left[\left(\hat{\mathbf{n}}\omega\frac{w}{2}\right)\times\hat{\mathbf{z}}B_0\right]\cdot\hat{\mathbf{x}}\,dx \\ &\quad + \int_{l/2}^{-l/2}\left[\left(-\hat{\mathbf{n}}\omega\frac{w}{2}\right)\times\hat{\mathbf{z}}B_0\right]\cdot\hat{\mathbf{x}}\,dx. \end{aligned} \tag{6.33}$$

Using Eq. (6.32) in Eq. (6.33), we obtain the result

$$V_{\text{emf}}^{\text{m}} = wl\omega B_0\sin\alpha = A\omega B_0\sin\alpha, \tag{6.34}$$

where $A = wl$ is the surface area of the loop. The angle α is related to ω by

$$\alpha = \omega t + C_0, \tag{6.35}$$

where C_0 is a constant determined by initial conditions. For example, if $\alpha = 0$ at $t = 0$, then $C_0 = 0$. In general,

$$V_{\text{emf}}^{\text{m}} = A\omega B_0\sin(\omega t + C_0) \quad \text{(V)}. \tag{6.36}$$

This result can also be obtained by applying the general form of Faraday's law given by Eq. (6.6). The flux linking the surface of the loop is

$$\begin{aligned} \Phi = \int_S \mathbf{B}\cdot d\mathbf{s} &= \int_S \hat{\mathbf{z}}B_0\cdot\hat{\mathbf{n}}\,ds \\ &= B_0 A\cos\alpha \\ &= B_0 A\cos(\omega t + C_0), \end{aligned} \tag{6.37}$$

and

$$\begin{aligned} V_{\text{emf}} = -\frac{d\Phi}{dt} &= -\frac{d}{dt}[B_0 A\cos(\omega t + C_0)] \\ &= A\omega B_0\sin(\omega t + C_0), \end{aligned} \tag{6.38}$$

which is identical with the result given by Eq. (6.36).

REVIEW QUESTIONS

Q6.6 Contrast the operation of an a-c motor with that of an a-c generator.

Q6.7 The rotating loop of Fig. 6-12 had a single turn. What would be the emf generated by a loop with 10 turns?

Q6.8 The magnetic flux linking the loop shown in Fig. 6-12 is a maximum when $\alpha = 0$ (loop in x–y plane), and yet according to Eq. (6.34), the induced emf is zero when $\alpha = 0$. Conversely, when $\alpha = 90°$, the flux linking the loop is zero, but $V_{\text{emf}}^{\text{m}}$ is at a maximum. Is this consistent with your expectations? Why?

6-6 Moving Conductor in a Time-Varying Magnetic Field

For the general case of a single-turn conducting loop moving in a time-varying magnetic field, the induced emf is the sum of a transformer component and a motional component. Thus, the sum of Eqs. (6.8) and (6.26) gives

$$\begin{aligned} V_{\text{emf}} &= V_{\text{emf}}^{\text{tr}} + V_{\text{emf}}^{\text{m}} \\ &= \oint_C \mathbf{E}\cdot d\mathbf{l} \\ &= -\int_S \frac{\partial\mathbf{B}}{\partial t}\cdot d\mathbf{s} + \oint_C (\mathbf{u}\times\mathbf{B})\cdot d\mathbf{l}. \end{aligned} \tag{6.39}$$

INTEL-1014
U.S. Patent 7,151,430

V_{emf} is also given by the general expression of Faraday's law:

$$V_{emf} = -\frac{d\Phi}{dt} = -\frac{d}{dt}\int_S \mathbf{B}\cdot d\mathbf{s}. \quad (6.40)$$

In fact, it can be shown mathematically that the right-hand side of Eq. (6.39) is equivalent to the right-hand side of Eq. (6.40). For a particular problem, the choice between using Eq. (6.39) or Eq. (6.40) is usually made on the basis of which is the easier to apply. If the loop consists of N turns, the terms on the right-hand sides of Eqs. (6.39) and (6.40) should be multiplied by N.

Example 6-6 Electromagnetic Generator

Find the induced voltage when the rotating loop of the electromagnetic generator of Section 6-5 is in a magnetic field $\mathbf{B} = \hat{\mathbf{z}}B_0 \cos\omega t$. Assume that $\alpha = 0$ at $t = 0$.

Solution: In this case the flux Φ is given by Eq. (6.37) with B_0 replaced with $B_0 \cos\omega t$. Thus,

$$\Phi = B_0 A \cos^2 \omega t,$$

and

$$\begin{aligned} V_{emf} &= -\frac{\partial \Phi}{\partial t} \\ &= -\frac{\partial}{\partial t}(B_0 A \cos^2 \omega t) \\ &= 2B_0 A\omega \cos\omega t \sin\omega t = B_0 A\omega \sin 2\omega t. \end{aligned}$$

■

6-7 Displacement Current

From Table 6-1, Ampère's law in differential form is given by

$$\nabla \times \mathbf{H} = \mathbf{J} + \frac{\partial \mathbf{D}}{\partial t} \quad \text{(Ampère's law)}. \quad (6.41)$$

If we take the surface integral of both sides of Eq. (6.41) over an arbitrary open surface S with contour C, we have

$$\int_S (\nabla \times \mathbf{H})\cdot d\mathbf{s} = \int_S \mathbf{J}\cdot d\mathbf{s} + \int_S \frac{\partial \mathbf{D}}{\partial t}\cdot d\mathbf{s}. \quad (6.42)$$

The surface integral of $\mathbf{J}$ is equal to the conduction current I_c flowing through S, and the surface integral of $\nabla \times \mathbf{H}$ can be converted into a line integral of $\mathbf{H}$ over the contour C by invoking Stokes's theorem. Hence,

$$\oint_C \mathbf{H}\cdot d\mathbf{l} = I_c + \int_S \frac{\partial \mathbf{D}}{\partial t}\cdot d\mathbf{s} \quad \text{(Ampère's law)}. \quad (6.43)$$

The second term on the right-hand side of Eq. (6.43) has to have the same unit (amperes) as the current I_c, and because it is proportional to the time derivative of the electric flux density $\mathbf{D}$ (which is also called the electric displacement), it is called the ***displacement current*** I_d. That is,

$$I_d \triangleq \int_S \mathbf{J}_d \cdot d\mathbf{s} = \int_S \frac{\partial \mathbf{D}}{\partial t}\cdot d\mathbf{s}, \quad (6.44)$$

where $\mathbf{J}_d = \partial \mathbf{D}/\partial t$ represents a ***displacement current density***. In view of Eq. (6.44),

$$\oint_C \mathbf{H}\cdot d\mathbf{l} = I_c + I_d = I, \quad (6.45)$$

where I is the total current. In electrostatics, $\partial \mathbf{D}/\partial t = 0$ and therefore $I_d = 0$ and $I = I_c$. The concept of displacement current was first introduced by James Clerk Maxwell in 1873 in his successful attempt to establish a

INTEL-1014
U.S. Patent 7,151,430

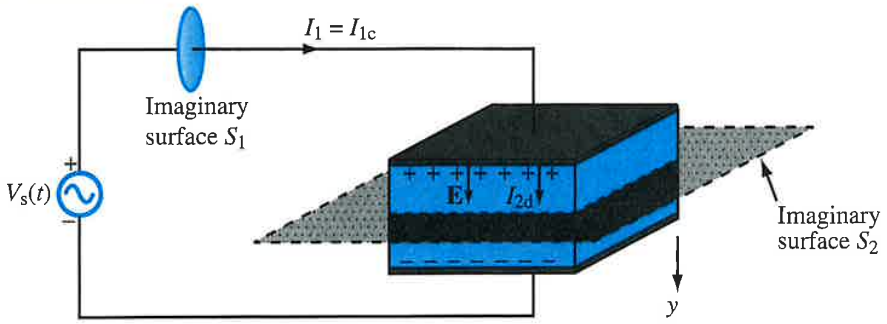


Figure 6-13: The displacement current I_{2d} in the insulating material of the capacitor is equal to the conducting current I_{1c} in the wire.

unified connection between electric and magnetic fields under time-varying conditions.

The parallel-plate capacitor is commonly used as a convenient example to illustrate the physical meaning of the displacement current I_d. The simple circuit shown in Fig. 6-13 consists of a capacitor and an a-c source with voltage $V_s(t)$ given by

$$V_s(t) = V_0 \cos \omega t \quad \text{(V)}. \tag{6.46}$$

According to Eq. (6.45), the total current flowing through any surface consists, in general, of a conduction current I_c and a displacement current I_d. Let us find I_c and I_d through each of the following two imaginary surfaces: (1) the cross section of the conducting wire, S_1, and (2) the cross section of the capacitor (surface S_2 in Fig. 6-13). We shall denote the conduction and displacement currents in the wire I_{1c} and I_{1d} and those through the capacitor I_{2c} and I_{2d}.

In a perfect conductor, $\mathbf{D} = \mathbf{E} = 0$; hence, Eq. (6.44) gives $I_{1d} = 0$ in the wire. As to I_{1c}, we know from circuit theory that it is related to the voltage across the capacitor V_c by

$$I_{1c} = C \frac{dV_c}{dt} = C \frac{d}{dt}(V_0 \cos \omega t) = -CV_0\omega \sin \omega t, \tag{6.47}$$

where we used the fact that $V_c = V_s(t)$. With $I_{1d} = 0$, the total current in the wire is simply $I_1 = I_{1c} = -CV_0\omega \sin \omega t$.

We now consider the currents flowing through surface S_2 in Fig. 6-13, which is an imaginary, open surface parallel to the capacitor plates and situated somewhere between them. The space between the two plates, each of which is of area A, is filled with a perfect dielectric material with permittivity ε. Since electrical charges cannot physically move through a dielectric medium, conduction cannot take place between the conducting plates of the capacitor, and therefore $I_{2c} = 0$. To determine I_{2d}, we need to apply Eq. (6.44). From Example 4-11, the electric field $\mathbf{E}$ in the dielectric spacing is related to the voltage V_c across the capacitor by

$$\mathbf{E} = \hat{\mathbf{y}} \frac{V_c}{d} = \hat{\mathbf{y}} \frac{V_0}{d} \cos \omega t, \tag{6.48}$$

where d is the spacing between the plates and $\hat{\mathbf{y}}$ is the direction from the higher-potential plate toward the lower-potential plate. The displacement current I_{2d} in the direction shown in Fig. 6-13 is obtained by applying

INTEL-1014
U.S. Patent 7,151,430

Eq. (6.44) with $d\mathbf{s} = \hat{\mathbf{y}}\, ds$:

$$I_{2d} = \int_S \frac{\partial \mathbf{D}}{\partial t} \cdot d\mathbf{s}$$
$$= \int_A \left[\frac{\partial}{\partial t}\left(\hat{\mathbf{y}}\frac{\varepsilon V_0}{d}\cos\omega t\right)\right] \cdot (\hat{\mathbf{y}}\, ds)$$
$$= -\frac{\varepsilon A}{d} V_0 \omega \sin\omega t = -C V_0 \omega \sin\omega t, \qquad (6.49)$$

where we used the relation $C = \varepsilon A/d$ for the capacitance of the parallel-plate capacitor. The expression for I_{2d} in the dielectric region between the conducting plates is identical with that given by Eq. (6.47) for the conduction current I_{1c} in the wire. The fact that these two currents are equal ensures the continuity of current flow through the circuit. *Even though the displacement current does not carry real charge, it nonetheless behaves like a real current.*

In the capacitor example, we treated the wire as a perfect conductor, and we assumed that the spacing between the capacitor plates is a perfect dielectric. If the wire has a finite conductivity σ_w, then $\mathbf{D}$ in the wire would not be zero, and therefore the current I_1 would consist of a conduction current I_{1c} as well as a displacement current I_{1d}; that is, $I_1 = I_{1c} + I_{1d}$. By the same token, if the dielectric spacing material has a nonzero conductivity σ_d, then charges would be able to flow between the two plates and I_{2c} would not be zero. In that case, the total current flowing through the capacitor would be $I_2 = I_{2c} + I_{2d}$, and it would be equal to the total current in the wire. That is, $I_1 = I_2$.

Example 6-7 Displacement Current Density

The conduction current flowing through a wire with conductivity $\sigma = 2 \times 10^7$ S/m and relative permittivity $\varepsilon_r = 1$ is given by $I_c = 2\sin\omega t$ (mA). If $\omega = 10^9$ rad/s, find the displacement current.

Solution: The conduction current $I_c = JA = \sigma EA$, where A is the cross section of the wire. Hence,

$$E = \frac{I_c}{\sigma A} = \frac{2 \times 10^{-3} \sin\omega t}{2 \times 10^7 A}$$
$$= \frac{1 \times 10^{-10}}{A}\sin\omega t \qquad \text{(V/m)}.$$

Application of Eq. (6.44), with $D = \varepsilon E$, leads to

$$I_d = J_d A$$
$$= \varepsilon A\, \partial E/\partial t$$
$$= \varepsilon A \frac{\partial}{\partial t}\left(\frac{1 \times 10^{-10}}{A}\sin\omega t\right)$$
$$= \varepsilon\omega \times 10^{-10}\cos\omega t = 0.885 \times 10^{-12}\cos\omega t \qquad \text{(A)},$$

where we used $\omega = 10^9$ rad/s and $\varepsilon = \varepsilon_0 = 8.85 \times 10^{-12}$ F/m. Note that I_c and I_d are in phase quadrature (90° phase shift between them). Also, I_d is about nine orders of magnitude smaller than I_c, which is why the displacement current usually is ignored in good conductors. ■

EXERCISE 6.5 A poor conductor is characterized by a conductivity $\sigma = 100$ (S/m) and permittivity $\varepsilon = 4\varepsilon_0$. At what angular frequency ω is the amplitude of the conduction current density $\mathbf{J}$ equal to the amplitude of the displacement current density $\mathbf{J}_d$?

Ans. $\omega = 2.82 \times 10^{12}$ (rad/s).

6-8 Boundary Conditions for Electromagnetics

In Chapters 4 and 5 we applied the integral form of Maxwell's equations under static conditions to obtain boundary conditions that the tangential and normal components of $\mathbf{E}$, $\mathbf{D}$, $\mathbf{B}$, and $\mathbf{H}$ must satisfy at the interface between two contiguous media. These conditions are given in

INTEL-1014
U.S. Patent 7,151,430

Table 6-2: Boundary conditions for the electric and magnetic fields.

Field Components	General Form	Medium 1 Dielectric	Medium 2 Dielectric	Medium 1 Dielectric	Medium 2 Conductor
Tangential E	$\hat{\mathbf{n}}_2 \times (\mathbf{E}_1 - \mathbf{E}_2) = 0$	$E_{1t} = E_{2t}$		$E_{1t} = E_{2t} = 0$	
Normal D	$\hat{\mathbf{n}}_2 \cdot (\mathbf{D}_1 - \mathbf{D}_2) = \rho_s$	$D_{1n} - D_{2n} = \rho_s$		$D_{1n} = \rho_s$	$D_{2n} = 0$
Tangential H	$\hat{\mathbf{n}}_2 \times (\mathbf{H}_1 - \mathbf{H}_2) = \mathbf{J}_s$	$H_{1t} = H_{2t}$		$H_{1t} = J_s$	$H_{2t} = 0$
Normal B	$\hat{\mathbf{n}}_2 \cdot (\mathbf{B}_1 - \mathbf{B}_2) = 0$	$B_{1n} = B_{2n}$		$B_{1n} = B_{2n} = 0$	

Notes: (1) ρ_s is the surface charge density at the boundary; (2) $\mathbf{J}_s$ is the surface current density at the boundary; (3) normal components of all fields are along $\hat{\mathbf{n}}_2$, the outward unit vector of medium 2; (4) $E_{1t} = E_{2t}$ implies that the tangential components are equal in magnitude and parallel in direction; (5) direction of $\mathbf{J}_s$ is orthogonal to $(\mathbf{H}_1 - \mathbf{H}_2)$.

Section 4-9 for **E** and **D** and in Section 5-7 for **B** and **H**. In the dynamic case, Maxwell's equations [Table 6-1] include two new terms, $\partial\mathbf{B}/\partial t$ in Faraday's law and $\partial\mathbf{D}/\partial t$ in Ampère's law. Nevertheless, *the boundary conditions derived previously for electrostatics and magnetostatics remain valid for time-varying fields as well.* This is because, if we were to apply the same procedures outlined in the above-referenced sections, we would find that the combination of the aforementioned terms vanish as the areas of the rectangular loops in Figs. 4-18 and 5-24 are made to approach zero.

For easy access, the combined set of electromagnetic boundary conditions is given in Table 6-2.

REVIEW QUESTIONS

Q6.9 When conduction current flows through a material, a certain number of charges enter the material on one end and an equal number leave on the other end. What's the situation like for the displacement current through a perfect dielectric?

Q6.10 Verify that the integral form of Ampère's law given by Eq. (6.43) leads to the boundary condition that the tangential component of **H** is continuous across the boundary between two dielectric media.

6-9 Charge–Current Continuity Relation

Under static conditions, the charge density ρ_v and the current density **J** at a given point in a material are totally independent of one another. This is not true in the time-varying case. To show the connection between ρ_v and **J**, we start by considering an arbitrary volume v bounded by a closed surface S, as shown in Fig. 6-14. The net positive charge contained in v is Q. Since, according to the law of conservation of electric charge [Section 1-2.2], charge can neither be created nor destroyed, the only way Q can increase is as a result of a net inward flux of positive charge into the volume v and, by the same token, for Q to decrease there has to be a net outward flux of charge from v. The inward and outward fluxes of charge constitute currents flowing across the surface S into and out of v, respectively. We define I as the *net current flowing across S out of v.* Accordingly, I is equal to the *negative* rate of change of Q:

$$I = -\frac{dQ}{dt} = -\frac{d}{dt}\int_v \rho_v \, dv, \tag{6.50}$$

INTEL-1014
U.S. Patent 7,151,430

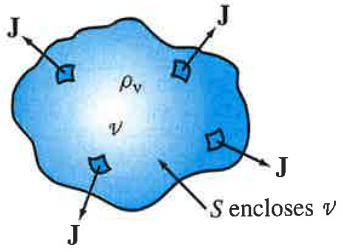


Figure 6-14: Total current flowing out of a volume v is equal to the flux of current density $\mathbf{J}$ through the surface S, which in turn is equal to the rate of decrease of the charge enclosed in v.

where ρ_v is the volume charge density in v. According to Eq. (4.12), the current I is also defined as the outward flux of the current density vector $\mathbf{J}$ through the surface S. Hence,

$$\oint_S \mathbf{J} \cdot d\mathbf{s} = -\frac{d}{dt} \int_v \rho_v \, dv. \tag{6.51}$$

By applying the divergence theorem given by Eq. (3.98), we can convert the surface integral of $\mathbf{J}$ into a volume integral of its divergence $\nabla \cdot \mathbf{J}$, which then gives

$$\oint_S \mathbf{J} \cdot d\mathbf{s} = \int_v \nabla \cdot \mathbf{J} \, dv = -\frac{d}{dt} \int_v \rho_v \, dv. \tag{6.52}$$

For a stationary volume v, the time derivative operates on ρ_v only. Hence, we can move it inside the integral and express it as a partial derivative of ρ_v:

$$\int_v \nabla \cdot \mathbf{J} \, dv = -\int_v \frac{\partial \rho_v}{\partial t} \, dv. \tag{6.53}$$

In order for the volume integrals on the two sides of Eq. (6.53) to be equal for any volume v, their integrands have to be equal at every point within v. Hence,

$$\nabla \cdot \mathbf{J} = -\frac{\partial \rho_v}{\partial t}, \tag{6.54}$$

which is known as the ***charge–current continuity relation*** or simply as the ***charge continuity equation***.

If the volume charge density within an elemental volume Δv (such as a small cylinder) is not a function of time (i.e., $\partial \rho_v / \partial t = 0$), it means that the net current flowing out of Δv is zero or, equivalently, that the current flowing into Δv is equal to the current flowing out of it. In this case, Eq. (6.54) becomes

$$\nabla \cdot \mathbf{J} = 0, \tag{6.55}$$

and its integral-form equivalent [from Eq. (6.51)] is

$$\oint_S \mathbf{J} \cdot d\mathbf{s} = 0 \quad \text{(Kirchhoff's current law)}. \tag{6.56}$$

Let us examine the meaning of Eq. (6.56) by considering a junction (or node) connecting two or more branches in an electric circuit. No matter how small, the junction has a volume v enclosed by a surface S. The junction shown in Fig. 6-15 has been drawn as a cube, and its dimensions have been artificially enlarged to facilitate the present discussion. The junction has six faces (surfaces), which collectively constitute the surface S associated with the closed-surface integration given by Eq. (6.56). For

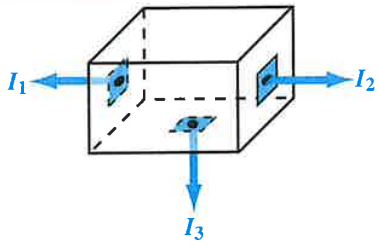


Figure 6-15: Kirchhoff's current law states that the algebraic sum of all the currents flowing out of a junction is zero.

INTEL-1014
U.S. Patent 7,151,430

each face, the integration represents the current flowing out through that face. Thus, Eq. (6.56) can be rewritten as

$$\sum_i I_i = 0 \qquad \text{(Kirchhoff's current law)}, \tag{6.57}$$

where I_i is the current flowing outward through the ith face. For the junction of Fig. 6-15, Eq. (6.57) translates into $(I_1 + I_2 + I_3) = 0$. In its general form, Eq. (6.57) is an expression of ***Kirchhoff's current law***, which states that in an electric circuit *the algebraic sum of all the currents flowing out of a junction is zero.*

6-10 Free-Charge Dissipation in a Conductor

We stated earlier that current flow in a conductor is realized by the movement of loosely attached electrons under the influence of an externally applied electric field. These electrons, however, *are not excess charges*; they are balanced by an equal amount of positive charge in the atoms' nuclei. In other words, the conductor material is electrically neutral, and the net charge density in the conductor is zero ($\rho_v = 0$). What happens then if an excess free charge q is introduced at some interior point in a conductor? The excess charge will give rise to an electric field, which will force the charges of the host material nearest to the excess charge to rearrange their locations, which in turn cause other charges to move, and the process will continue until neutrality is reestablished in the conductor material and a charge equal to q is supplied to the conductor's surface.

How fast does the excess charge dissipate? To answer this question, let us introduce a volume charge density ρ_{vo} at the interior of a conductor and then find out the rate at which it decays down to zero. From Eq. (6.54), the continuity equation is given by

$$\nabla \cdot \mathbf{J} = -\frac{\partial \rho_v}{\partial t}. \tag{6.58}$$

In a conductor, the point form of Ohm's law, given by Eq. (4.67), states that $\mathbf{J} = \sigma \mathbf{E}$. Hence,

$$\sigma \nabla \cdot \mathbf{E} = -\frac{\partial \rho_v}{\partial t}. \tag{6.59}$$

Next, we use Eq. (6.1), $\nabla \cdot \mathbf{E} = \rho_v/\varepsilon$, to obtain the partial differential equation

$$\frac{\partial \rho_v}{\partial t} + \frac{\sigma}{\varepsilon}\rho_v = 0. \tag{6.60}$$

Given that $\rho_v = \rho_{vo}$ at $t = 0$, the solution of Eq. (6.60) is

$$\rho_v(t) = \rho_{vo} e^{-(\sigma/\varepsilon)t} = \rho_{vo} e^{-t/\tau_r} \qquad (\text{C/m}^3), \tag{6.61}$$

where $\tau_r = \varepsilon/\sigma$ is called the ***relaxation time constant***. We see from Eq. (6.61) that the initial excess charge ρ_{vo} decays exponentially at a rate τ_r. At $t = \tau_r$, the initial charge ρ_{vo} will have decayed to $1/e \approx 37\%$ of its initial value, and at $t = 3\tau_r$, it will have decayed to $e^{-3} \approx 5\%$ of its initial value at $t = 0$. For copper, with $\varepsilon \simeq \varepsilon_0 = 8.854 \times 10^{-12}$ F/m and $\sigma = 5.8 \times 10^7$ S/m, $\tau_r = 1.53 \times 10^{-19}$ s. Thus, the charge dissipation process in a conductor is extremely fast. In contrast, the decay rate is very slow in a good insulator. For a material like mica with $\varepsilon = 6\varepsilon_0$ and $\sigma = 10^{-15}$ S/m, $\tau_r = 5.31 \times 10^4$ s, or approximately 14.8 hours.

REVIEW QUESTIONS

Q6.11 Explain how the charge continuity equation leads to Kirchhoff's current law.

Q6.12 How long is the relaxation time constant for charge dissipation in a perfect conductor? In a perfect dielectric?

EXERCISE 6.6 Determine (a) the relaxation time constant and (b) the time it takes for a charge density to decay to 1% of its initial value in quartz, given that $\varepsilon_r = 5$ and $\sigma = 10^{-17}$ S/m.

Ans. (a) $\tau_r = 51.2$ days, (b) 236 days.

INTEL-1014
U.S. Patent 7,151,430

6-11 Electromagnetic Potentials

Through our discussion of Faraday's and Ampère's laws, we examined two aspects of the interconnection that exists between the electric and magnetic fields when the fields are time varying. We will now examine the implications of this interconnection with regard to the electric scalar potential V and the vector magnetic potential $\mathbf{A}$.

For $\partial/\partial t = 0$, Faraday's law reduces to

$$\nabla \times \mathbf{E} = 0 \quad \text{(electrostatics)}, \tag{6.62}$$

which states that the electrostatic field $\mathbf{E}$ is conservative. According to the rules of vector calculus, if a vector field $\mathbf{E}$ is conservative, it can be expressed as the gradient of a scalar. Hence, in Chapter 4 we defined $\mathbf{E}$ as

$$\mathbf{E} = -\nabla V \quad \text{(electrostatics)}. \tag{6.63}$$

In the dynamic case, Faraday's law is given by

$$\nabla \times \mathbf{E} = -\frac{\partial \mathbf{B}}{\partial t}, \tag{6.64}$$

and in view of the relation $\mathbf{B} = \nabla \times \mathbf{A}$, Eq. (6.64) becomes

$$\nabla \times \mathbf{E} = -\frac{\partial}{\partial t}(\nabla \times \mathbf{A}), \tag{6.65}$$

which can be rewritten as

$$\nabla \times \left(\mathbf{E} + \frac{\partial \mathbf{A}}{\partial t}\right) = 0 \quad \text{(dynamic case)}. \tag{6.66}$$

Let us for the moment define

$$\mathbf{E}' = \mathbf{E} + \frac{\partial \mathbf{A}}{\partial t}, \tag{6.67}$$

in which case Eq. (6.66) becomes

$$\nabla \times \mathbf{E}' = 0. \tag{6.68}$$

Following the same logic that led to Eq. (6.63) from Eq. (6.62), we define

$$\mathbf{E}' = -\nabla V. \tag{6.69}$$

Upon substituting Eq. (6.67) for $\mathbf{E}'$ in Eq. (6.69) and then solving for $\mathbf{E}$, we have

$$\boxed{\mathbf{E} = -\nabla V - \frac{\partial \mathbf{A}}{\partial t} \quad \text{(dynamic case)}.} \tag{6.70}$$

Equation (6.70) reduces to Eq. (6.63) in the static case.

When the scalar potential V and the vector potential $\mathbf{A}$ are known, $\mathbf{E}$ can be obtained from Eq. (6.70), and $\mathbf{B}$ can be obtained from

$$\boxed{\mathbf{B} = \nabla \times \mathbf{A}.} \tag{6.71}$$

Next we examine the relations between the potentials, V and $\mathbf{A}$, and their sources, the charge and current distributions ρ_v and $\mathbf{J}$, in the time-varying case.

6-11.1 Retarded Potentials

Consider the situation depicted in Fig. 6-16. A charge distribution ρ_v exists over a volume v' centered at the origin of a coordinate system. The surrounding medium is a perfect dielectric with permittivity ε. From Eq. (4.48a), the electric potential $V(\mathbf{R})$ at an observation point in space specified by the position vector $\mathbf{R}$ is given by

$$V(\mathbf{R}) = \frac{1}{4\pi\varepsilon}\int_{v'} \frac{\rho_v(\mathbf{R}_i)}{R'}\, dv', \tag{6.72}$$

where $\mathbf{R}_i$ denotes the position vector of an elemental volume $\Delta v'$ containing charge density ρ_v, and $R' = |\mathbf{R} - \mathbf{R}_i|$ is the distance between $\Delta v'$ and the observation point. If

INTEL-1014
U.S. Patent 7,151,430

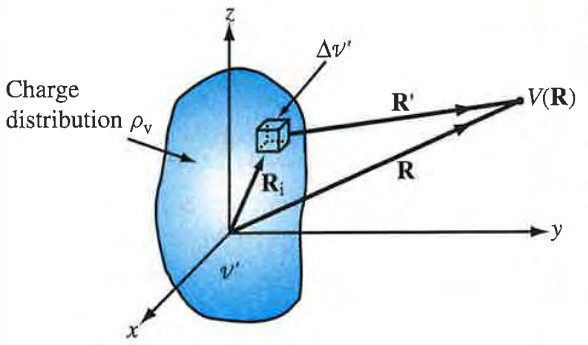


Figure 6-16: Electric potential $V(\mathbf{R})$ due to a charge distribution ρ_v over a volume v'.

the charge distribution is a time-varying function, we may be tempted to rewrite Eq. (6.72) for the dynamic case as

$$V(\mathbf{R}, t) = \frac{1}{4\pi\varepsilon} \int_{v'} \frac{\rho_v(\mathbf{R}_i, t)}{R'} \, dv', \qquad (6.73)$$

but such a form does not account for "reaction time." If V_1 is the potential due to a certain distribution ρ_{v1}, and if ρ_{v1} were to suddenly change to ρ_{v2}, it will take a finite amount of time before V_1 at distance R' changes to V_2. In other words, $V(\mathbf{R}, t)$ cannot change instantaneously. The delay time is equal to $t' = R'/u_p$, where u_p is the velocity of propagation in the medium between the charge distribution and the observation point. Thus, $V(\mathbf{R}, t)$ at time t corresponds to ρ_v at an earlier time, that is, $(t - t')$. Hence, Eq. (6.73) should be rewritten as

$$V(\mathbf{R}, t) = \frac{1}{4\pi\varepsilon} \int_{v'} \frac{\rho_v(\mathbf{R}_i, t - R'/u_p)}{R'} \, dv' \quad \text{(V)}, \qquad (6.74)$$

and $V(\mathbf{R}, t)$ is appropriately called the ***retarded scalar potential***. If the propagation medium is vacuum, u_p is equal to the velocity of light c.

Similarly, the ***retarded vector potential*** $\mathbf{A}(\mathbf{R}, t)$ is related to the distribution of current density $\mathbf{J}$ by

$$\mathbf{A}(\mathbf{R}, t) = \frac{\mu}{4\pi} \int_{v'} \frac{\mathbf{J}(\mathbf{R}_i, t - R'/u_p)}{R'} \, dv' \quad \text{(Wb/m)}. \qquad (6.75)$$

This expression is obtained by extending the expression for the magnetostatic vector potential $\mathbf{A}(\mathbf{R})$ given by Eq. (5.65) to the time-varying case.

6-11.2 Time-Harmonic Potentials

The expressions given by Eqs. (6.74) and (6.75) for the retarded scalar and vector potentials are valid under both static and dynamic conditions and for any type of time dependence that the source functions ρ_v and $\mathbf{J}$ may exhibit. In the dynamic case, ρ_v and $\mathbf{J}$ are linked to one another by the charge continuity relation given by Eq. (6.54). Hence, in general, both quantities will have the same functional dependence on time t and, by extension, so will the potentials V and $\mathbf{A}$ and the fields $\mathbf{E}$, $\mathbf{D}$, $\mathbf{B}$, and $\mathbf{H}$. Furthermore, because V and $\mathbf{A}$ are linearly dependent on ρ_v and $\mathbf{J}$, respectively, and also $\mathbf{E}$ and $\mathbf{B}$ are linearly dependent on V and $\mathbf{A}$, the relationships interconnecting all these quantities obey the rules of linear systems. When a system is linear, we can take advantage of sinusoidal-time functions to determine the response of the system due to a source with any type of time dependence. As was noted in Section 1-6, if the time dependence is described by a (nonsinusoidal) periodic time function, it can always be expanded into a Fourier series of sinusoidal components, and if the time function is nonperiodic, it can be represented by a Fourier integral. In either case, if the response of the linear system is known for the steady-state sinusoidal case, the principle of superposition can be used to determine the response for the specified time function. Thus, the sinusoidal response of the system constitutes a fundamental building block determining the response due to a source described by any function of time. The term

INTEL-1014
U.S. Patent 7,151,430

time harmonic is often used in this context as a synonym for "steady-state sinusoidal time dependence."

In this subsection, we will examine the time-harmonic responses of the retarded scalar and vector potentials. Suppose that $\rho_v(\mathbf{R}_i, t)$ is a sinusoidal-time function with angular frequency ω, given by

$$\rho_v(\mathbf{R}_i, t) = \rho_v(\mathbf{R}_i) \cos \omega t. \tag{6.76}$$

Phasor analysis, which was first introduced in Section 1-6 and then used extensively in Chapter 2 to study wave propagation on transmission lines, is a useful tool for solving time-harmonic problems. In phasor notation, $\rho_v(\mathbf{R}_i, t)$ is written in the form

$$\rho_v(\mathbf{R}_i, t) = \mathfrak{Re}\left[\tilde{\rho}_v(\mathbf{R}_i)\, e^{j\omega t}\right], \tag{6.77}$$

where $\tilde{\rho}_v(\mathbf{R}_i)$ is defined as the phasor function corresponding to the time function $\rho_v(\mathbf{R}_i, t)$. The phasor function is denoted with a tilde ($\sim$) over the letter for easy recognition. Comparison of Eqs. (6.76) and (6.77) shows that in the present case $\tilde{\rho}_v(\mathbf{R}_i) = \rho_v(\mathbf{R}_i)$.

Next, we express the retarded charge density $\rho_v(\mathbf{R}_i, t - R'/u_p)$ in phasor form by replacing t with $(t - R'/u_p)$ in Eq. (6.77):

$$\begin{aligned}\rho_v(\mathbf{R}_i, t - R'/u_p) &= \mathfrak{Re}\left[\tilde{\rho}_v(\mathbf{R}_i)\, e^{j\omega(t - R'/u_p)}\right] \\ &= \mathfrak{Re}\left[\tilde{\rho}_v(\mathbf{R}_i)\, e^{-j\omega R'/u_p} e^{j\omega t}\right] \\ &= \mathfrak{Re}\left[\tilde{\rho}_v(\mathbf{R}_i)\, e^{-jkR'} e^{j\omega t}\right] \end{aligned} \tag{6.78}$$

where

$$k = \frac{\omega}{u_p} \tag{6.79}$$

is called the ***wavenumber*** or phase constant of the propagation medium. (In general, the phase constant is denoted by the symbol "β", but for lossless dielectric media, it is commonly denoted by the symbol "k" and called the wavenumber.) Similarly, we define the phasor $\tilde{V}(\mathbf{R})$ of the time function $V(\mathbf{R}, t)$ according to

$$V(\mathbf{R}, t) = \mathfrak{Re}\left[\tilde{V}(\mathbf{R})\, e^{j\omega t}\right]. \tag{6.80}$$

Using Eqs. (6.78) and (6.80) in Eq. (6.74) gives

$$\mathfrak{Re}\left[\tilde{V}(\mathbf{R})\, e^{j\omega t}\right] = \mathfrak{Re}\left[\frac{1}{4\pi\varepsilon}\int_{v'} \frac{\tilde{\rho}_v(\mathbf{R}_i)\, e^{-jkR'}}{R'} e^{j\omega t}\, dv'\right]. \tag{6.81}$$

By equating the quantities inside the square brackets on the two sides of Eq. (6.81) and then deleting $e^{j\omega t}$ from both sides, we obtain the phasor-domain expression

$$\tilde{V}(\mathbf{R}) = \frac{1}{4\pi\varepsilon}\int_{v'} \frac{\tilde{\rho}_v(\mathbf{R}_i)\, e^{-jkR'}}{R'}\, dv' \quad \text{(V)}. \tag{6.82}$$

For any given charge distribution, Eq. (6.82) can be used to compute $\tilde{V}(\mathbf{R})$, and then the resultant expression can be used in Eq. (6.80) to find $V(\mathbf{R}, t)$. In like manner, the expression for $\mathbf{A}(\mathbf{R}, t)$ given by Eq. (6.75) can be transformed into

$$\mathbf{A}(\mathbf{R}, t) = \mathfrak{Re}\left[\tilde{\mathbf{A}}(\mathbf{R})\, e^{j\omega t}\right] \tag{6.83}$$

with

$$\tilde{\mathbf{A}}(\mathbf{R}) = \frac{\mu}{4\pi}\int_{v'} \frac{\tilde{\mathbf{J}}(\mathbf{R}_i)\, e^{-jkR'}}{R'}\, dv', \tag{6.84}$$

where $\tilde{\mathbf{J}}(\mathbf{R}_i)$ is the phasor function corresponding to $\mathbf{J}(\mathbf{R}_i, t)$.

The magnetic field phasor $\tilde{\mathbf{H}}$ corresponding to $\tilde{\mathbf{A}}$ is given by

$$\tilde{\mathbf{H}} = \frac{1}{\mu}\nabla \times \tilde{\mathbf{A}}. \tag{6.85}$$

Recalling that differentiation in the time domain is equivalent to multiplication by $j\omega$ in the phasor domain, in a

INTEL-1014
U.S. Patent 7,151,430

nonconducting medium ($\mathbf{J} = 0$), Ampère's law given by Eq. (6.4) becomes

$$\nabla \times \widetilde{\mathbf{H}} = j\omega\varepsilon\widetilde{\mathbf{E}} \quad \text{or} \quad \widetilde{\mathbf{E}} = \frac{1}{j\omega\varepsilon}\nabla \times \widetilde{\mathbf{H}}. \qquad (6.86)$$

Hence, given a time-harmonic current-density distribution with phasor $\widetilde{\mathbf{J}}$, Eqs. (6.84) to (6.86) can be used successively to determine both $\widetilde{\mathbf{E}}$ and $\widetilde{\mathbf{H}}$. The phasor vectors $\widetilde{\mathbf{E}}$ and $\widetilde{\mathbf{H}}$ also are related by the phasor form of Faraday's law:

$$\nabla \times \widetilde{\mathbf{E}} = -j\omega\mu\widetilde{\mathbf{H}} \quad \text{or} \quad \widetilde{\mathbf{H}} = -\frac{1}{j\omega\mu}\nabla \times \widetilde{\mathbf{E}}. \qquad (6.87)$$

Example 6-8

In a nonconducting medium with $\varepsilon = 16\varepsilon_0$ and $\mu = \mu_0$, the electric field intensity of an electromagnetic wave is given by

$$\mathbf{E}(z, t) = \hat{\mathbf{x}}\, 10 \sin(10^{10}t - kz) \quad \text{(V/m)}. \qquad (6.88)$$

Determine the associated magnetic field intensity $\mathbf{H}$ and find the value of k.

Solution: We begin by finding the phasor $\widetilde{\mathbf{E}}(z)$ of $\mathbf{E}(z, t)$. Since $\mathbf{E}(z, t)$ is given as a sine function and phasors are defined in this book with reference to the cosine function, we rewrite Eq. (6.88) as

$$\begin{aligned}\mathbf{E}(z, t) &= \hat{\mathbf{x}}\, 10 \cos(10^{10}t - kz - \pi/2) \quad \text{(V/m)} \\ &= \mathfrak{Re}\left[\widetilde{\mathbf{E}}(z)\, e^{j\omega t}\right], \qquad (6.89)\end{aligned}$$

with $\omega = 10^{10}$ (rad/s) and

$$\widetilde{\mathbf{E}}(z) = \hat{\mathbf{x}}\, 10 e^{-jkz} e^{-j\pi/2} = -\hat{\mathbf{x}} j 10 e^{-jkz}. \qquad (6.90)$$

To find both $\widetilde{\mathbf{H}}(z)$ and k, we will perform a "circle": we will use the given expression for $\widetilde{\mathbf{E}}(z)$ in Faraday's law to find $\widetilde{\mathbf{H}}(z)$; then we will use $\widetilde{\mathbf{H}}(z)$ in Ampère's law to find $\widetilde{\mathbf{E}}(z)$, which we will then compare with the original expression for $\widetilde{\mathbf{E}}(z)$; and the comparison will yield the value of k. Application of Eq. (6.87) gives

$$\begin{aligned}\widetilde{\mathbf{H}}(z) &= -\frac{1}{j\omega\mu}\nabla \times \widetilde{\mathbf{E}} \\ &= -\frac{1}{j\omega\mu}\begin{vmatrix} \hat{\mathbf{x}} & \hat{\mathbf{y}} & \hat{\mathbf{z}} \\ \partial/\partial x & \partial/\partial y & \partial/\partial z \\ -j10e^{-jkz} & 0 & 0 \end{vmatrix} \\ &= -\frac{1}{j\omega\mu}\left[\hat{\mathbf{y}}\frac{\partial}{\partial z}(-j10e^{-jkz})\right] \\ &= -\hat{\mathbf{y}} j\frac{10k}{\omega\mu}e^{-jkz}. \qquad (6.91)\end{aligned}$$

So far, we have used Eq. (6.90) for $\widetilde{\mathbf{E}}(z)$ to find $\widetilde{\mathbf{H}}(z)$, but k remains unknown. To find k, we use $\widetilde{\mathbf{H}}(z)$ in Eq. (6.86) to find $\widetilde{\mathbf{E}}(z)$:

$$\begin{aligned}\widetilde{\mathbf{E}}(z) &= \frac{1}{j\omega\varepsilon}\nabla \times \widetilde{\mathbf{H}} \\ &= \frac{1}{j\omega\varepsilon}\left[-\hat{\mathbf{x}}\frac{\partial}{\partial z}\left(-j\frac{10k}{\omega\mu}e^{-jkz}\right)\right] \\ &= -\hat{\mathbf{x}} j\frac{10k^2}{\omega^2\mu\varepsilon}e^{-jkz}. \qquad (6.92)\end{aligned}$$

Equating Eqs. (6.90) and (6.92) leads to

$$k^2 = \omega^2\mu\varepsilon,$$

or

$$\begin{aligned}k &= \omega\sqrt{\mu\varepsilon} \\ &= 4\omega\sqrt{\mu_0\varepsilon_0} \\ &= \frac{4\omega}{c} = \frac{4 \times 10^{10}}{3 \times 10^8} = 133 \quad \text{(rad/m)}. \qquad (6.93)\end{aligned}$$

INTEL-1014
U.S. Patent 7,151,430

With k known, the instantaneous magnetic field intensity is then given by

$$\begin{aligned}\mathbf{H}(z,t) &= \mathfrak{Re}\left[\widetilde{\mathbf{H}}(z)\, e^{j\omega t}\right] \\ &= \mathfrak{Re}\left[-\hat{\mathbf{y}}\, j\frac{10k}{\omega\mu}e^{-jkz}e^{j\omega t}\right] \\ &= \hat{\mathbf{y}}\, 0.11\sin(10^{10}t - 133z) \quad \text{(A/m)}. \quad (6.94)\end{aligned}$$

We note that k has the same expression as the phase constant of a lossless transmission line [Eq. (2.39)]. ■

EXERCISE 6.7 The magnetic field intensity of an electromagnetic wave propagating in a lossless medium with $\varepsilon = 9\varepsilon_0$ and $\mu = \mu_0$ is given by

$$\mathbf{H}(z,t) = \hat{\mathbf{x}}\, 0.3\cos(10^8 t - kz + \pi/4) \quad \text{(A/m)}.$$

Find $\mathbf{E}(z,t)$ and k.

Ans. $\mathbf{E}(z,t) = -\hat{\mathbf{y}}\, 37.7\cos(10^8 t - z + \pi/4)$ (V/m); $k = 1$ (rad/m).

CHAPTER HIGHLIGHTS

- Faraday's law states that a voltage is induced across the terminals of a loop if the magnetic flux linking its surface changes with time.
- In an ideal transformer, the ratios of the primary to secondary voltages, currents, and impedances are governed by the turns ratio.
- Displacement current accounts for the "apparent" flow of charges through a dielectric. In reality, charges of opposite polarity accumulate along the two ends of a dielectric, giving the appearance of current flow through it.
- Boundary conditions for the electromagnetic fields at the interface between two different media are the same for both static and dynamic conditions.
- The charge continuity equation is a mathematical statement of the law of conservation of electric charge.
- Excess charges in the interior of a good conductor dissipate very quickly; through a rearrangement process, the excess charge is transferred to the surface of the conductor.
- In the dynamic case, the electric field $\mathbf{E}$ is related to both the scalar electric potential V and the magnetic vector potential $\mathbf{A}$.
- The retarded scalar and vector potentials at a given observation point take into account the finite time required for propagation between their sources, the charge and current distributions, and the location of the observation point.

GLOSSARY OF IMPORTANT TERMS

Provide definitions or explain the meaning of the following terms:

Faraday's law
electromotive force V_{emf}
electromagnetic induction
transformer emf $V_{\text{emf}}^{\text{tr}}$
motional emf $V_{\text{emf}}^{\text{m}}$
Lenz's law
displacement current I_{d}
charge continuity equation
Kirchhoff's current law
charge dissipation
relaxation time constant
wavenumber k
retarded potential

INTEL-1014
U.S. Patent 7,151,430

PROBLEMS

Sections 6-1 to 6-6: Faraday's Law and its Applications

6.1* The switch in the bottom loop of Fig. 6-17 is closed at $t = 0$ and then opened at a later time t_1. What is the direction of the current I in the top loop (clockwise or counterclockwise) at each of these two times?

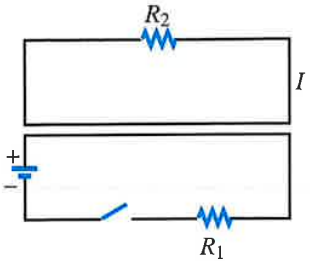


Figure 6-17: Loops of Problem 6.1.

6.2 The loop in Fig. 6-18 is in the x–y plane and $\mathbf{B} = \hat{\mathbf{z}} B_0 \sin \omega t$ with B_0 positive. What is the direction of I ($\hat{\boldsymbol{\phi}}$ or $-\hat{\boldsymbol{\phi}}$) at:

(a) $t = 0$

(b) $\omega t = \pi/4$

(c) $\omega t = \pi/2$

6.3* A coil consists of 100 turns of wire wrapped around a square frame of sides 0.25 m. The coil is centered at the origin with each of its sides parallel to the x- or y-axis. Find the induced emf across the open-circuited ends of the coil if the magnetic field is given by

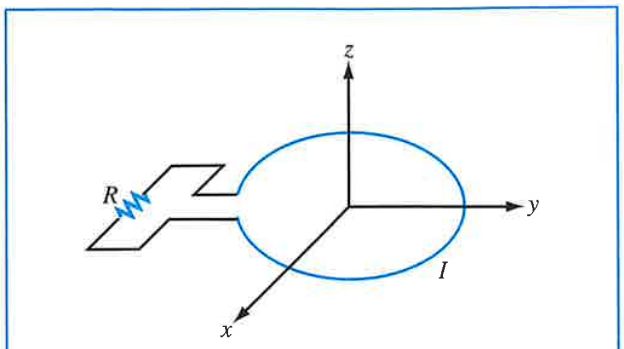


Figure 6-18: Loop of Problem 6.2.

(a) $\mathbf{B} = \hat{\mathbf{z}}\, 10e^{-2t}$ (T)

(b) $\mathbf{B} = \hat{\mathbf{z}}\, 10 \cos x \cos 10^3 t$ (T)

(c) $\mathbf{B} = \hat{\mathbf{z}}\, 10 \cos x \sin 2y \cos 10^3 t$ (T)

6.4 A stationary conducting loop with an internal resistance of 0.5 Ω is placed in a time-varying magnetic field. When the loop is closed, a current of 2.5 A flows through it. What will the current be if the loop is opened to create a small gap and a 2-Ω resistor is connected across its open ends?

6.5* A circular-loop TV antenna with 0.01-m^2 area is in the presence of a uniform-amplitude 300-MHz signal. When oriented for maximum response, the loop develops an emf with a peak value of 20 (mV). What is the peak magnitude of $\mathbf{B}$ of the incident wave?

6.6 The square loop shown in Fig. 6-19 is coplanar with a long, straight wire carrying a current

$$i(t) = 2.5 \cos 2\pi \times 10^4 t \quad \text{(A)}$$

*Answer(s) available in Appendix D.

Solution available in CD-ROM.

INTEL-1014
U.S. Patent 7,151,430

(a) Determine the emf induced across a small gap created in the loop.

(b) Determine the direction and magnitude of the current that would flow through a 4-Ω resistor connected across the gap. The loop has an internal resistance of 1 Ω.

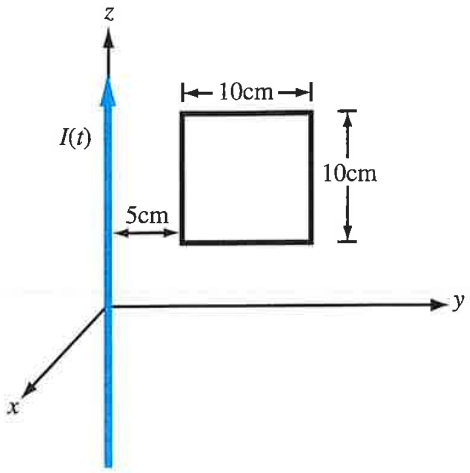


Figure 6-19: Loop coplanar with long wire (Problem 6.6).

6.7* The rectangular conducting loop shown in Fig. 6-20 rotates at 6,000 revolutions per minute in a uniform magnetic flux density given by

$$\mathbf{B} = \hat{\mathbf{y}}\, 50 \quad \text{(mT)}$$

Determine the current induced in the loop if its internal resistance is 0.5 Ω.

6.8 A rectangular conducting loop 5 cm × 10 cm with a small air gap in one of its sides is spinning at 7200 revolutions per minute. If the field **B** is normal to the loop

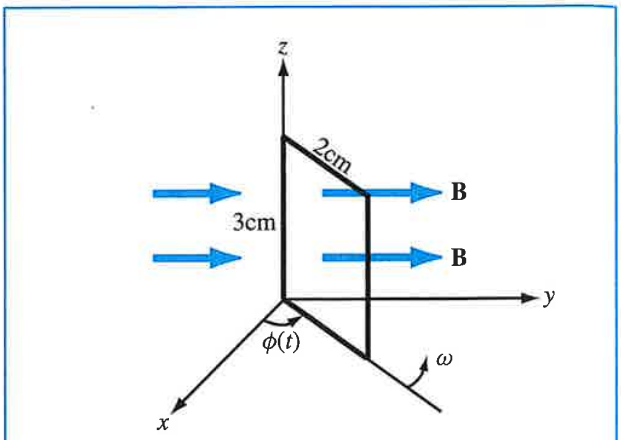


Figure 6-20: Rotating loop in a magnetic field (Problem 6.7).

axis and its magnitude is 5×10^{-6} T, what is the peak voltage induced across the air gap?

6.9* A 50-cm-long metal rod rotates about the z-axis at 180 revolutions per minute, with end 1 fixed at the origin as shown in Fig. 6-21. Determine the induced emf V_{12} if $\mathbf{B} = \hat{\mathbf{z}}\, 3 \times 10^{-4}$ T.

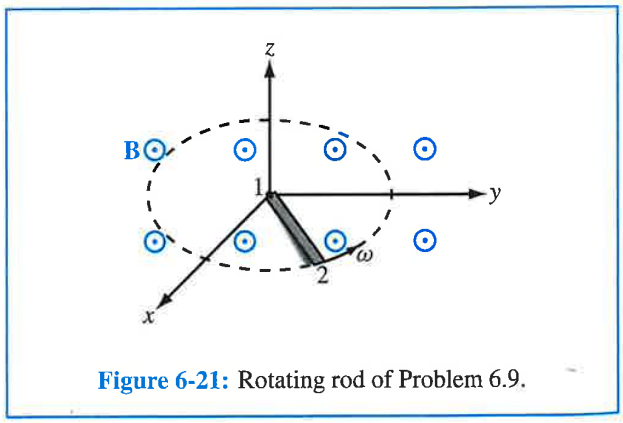


Figure 6-21: Rotating rod of Problem 6.9.

INTEL-1014
U.S. Patent 7,151,430

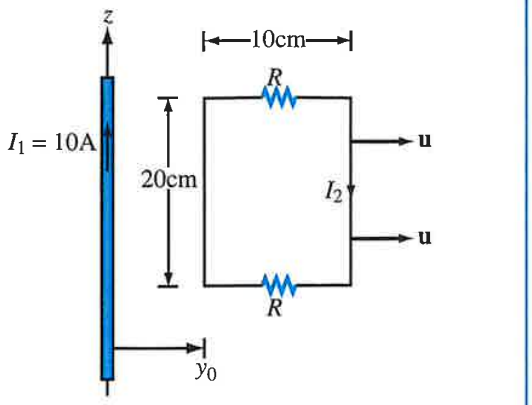


Figure 6-22: Moving loop of Problem 6.10.

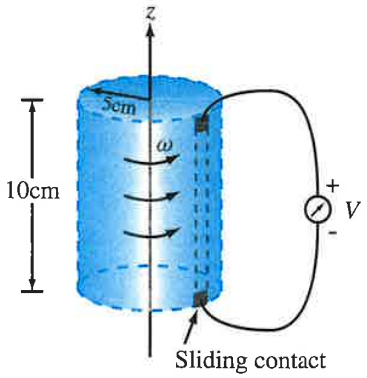


Figure 6-23: Rotating cylinder in a magnetic field (Problem 6.11).

6.10 The loop shown in Fig. 6-22 moves away from a wire carrying a current $I_1 = 10$ A at a constant velocity $\mathbf{u} = \hat{\mathbf{y}}5$ (m/s). If $R = 10\ \Omega$ and the direction of I_2 is as defined in the figure, find I_2 as a function of y_0, the distance between the wire and the loop. Ignore the internal resistance of the loop.

6.11* The conducting cylinder shown in Fig. 6-23 rotates about its axis at 1,200 revolutions per minute in a radial field given by

$$\mathbf{B} = \hat{\mathbf{r}}\,6 \qquad \text{(T)}$$

The cylinder, whose radius is 5 cm and height is 10 cm, has sliding contacts at its top and bottom connected to a voltmeter. Determine the induced voltage.

6.12 The electromagnetic generator shown in Fig. 6-12 is connected to an electric bulb with a resistance of 100 Ω. If the loop area is 0.1 m^2 and it rotates at 3,600 revolutions per minute in a uniform magnetic flux density $B_0 = 0.2$ T, determine the amplitude of the current generated in the light bulb.

6.13* The circular disk shown in Fig. 6-24 lies in the x–y plane and rotates with uniform angular velocity ω about the z-axis. The disk is of radius a and is present in a uniform magnetic flux density $\mathbf{B} = \hat{\mathbf{z}}B_0$. Obtain an expression for the emf induced at the rim relative to the center of the disk.

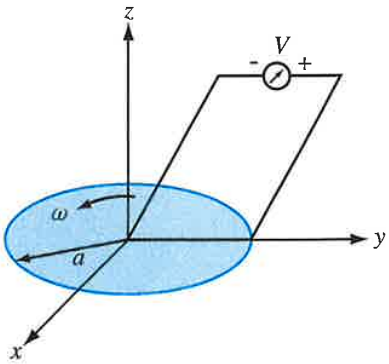


Figure 6-24: Rotating circular disk in a magnetic field (Problem 6.13).

INTEL-1014
U.S. Patent 7,151,430

Section 6-7: Displacement Current

6.14 The plates of a parallel-plate capacitor have areas of 10 cm^2 each and are separated by 1 cm. The capacitor is filled with a dielectric material with $\varepsilon = 4\varepsilon_0$, and the voltage across it is given by $V(t) = 20\cos 2\pi \times 10^6 t$ (V). Find the displacement current.

6.15* A coaxial capacitor of length $l = 6$ cm uses an insulating dielectric material with $\epsilon_r = 9$. The radii of the cylindrical conductors are 0.5 cm and 1 cm. If the voltage applied across the capacitor is

$$V(t) = 100\sin(120\pi t) \quad \text{(V)}$$

what is the displacement current?

6.16 The parallel-plate capacitor shown in Fig. 6-25 is filled with a lossy dielectric material of relative permittivity ϵ_r and conductivity σ. The separation between the plates is d and each plate is of area A. The capacitor is connected to a time-varying voltage source $V(t)$.

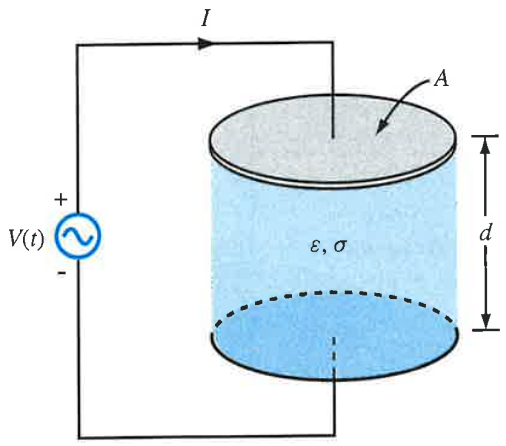


Figure 6-25: Parallel-plate capacitor containing a lossy dielectric material (Problem 6.16).

(a) Obtain an expression for I_c, the conduction current flowing between the plates inside the capacitor, in terms of the given quantities.

(b) Obtain an expression for I_d, the displacement current flowing inside the capacitor.

(c) Based on your expressions for parts (a) and (b), give an equivalent-circuit representation for the capacitor.

(d) Evaluate the values of the circuit elements for $A = 2$ cm^2, $d = 0.5$ cm, $\epsilon_r = 4$, $\sigma = 2.5$ (S/m), and $V(t) = 10\cos(3\pi \times 10^3 t)$ (V).

6.17 An electromagnetic wave propagating in seawater has an electric field with a time variation given by $\mathbf{E} = \hat{\mathbf{z}} E_0 \cos \omega t$. If the permittivity of water is $81\varepsilon_0$ and its conductivity is 4 (S/m), find the ratio of the magnitudes of the conduction current density to displacement current density at each of the following frequencies:

(a) 1 kHz

(b) 1 MHz

(c) 1 GHz

(d) 100 GHz

Sections 6-9 and 6-10: Continuity Equation and Charge Dissipation

6.18 At $t = 0$, charge density ρ_{v0} was introduced into the interior of a material with a relative permittivity $\varepsilon_r = 4$. If at $t = 1$ μs the charge density has dissipated down to $10^{-3}\rho_{v0}$, what is the conductivity of the material?

6.19* If the current density in a conducting medium is given by

$$\mathbf{J}(x, y, z; t) = (\hat{\mathbf{x}}z - \hat{\mathbf{y}}3y^2 + \hat{\mathbf{z}}2x)\cos \omega t$$

determine the corresponding charge distribution $\rho_v(x, y, z; t)$.

INTEL-1014
U.S. Patent 7,151,430

6.20 In a certain medium, the direction of current density $\mathbf{J}$ points in the radial direction in cylindrical coordinates and its magnitude is independent of both ϕ and z. Determine $\mathbf{J}$, given that the charge density in the medium is

$$\rho_v = \rho_0 r \cos \omega t \quad (\text{C/m}^3)$$

6.21 If we were to characterize how good a material is as an insulator by its resistance to dissipating charge, which of the following two materials is the better insulator?

Dry Soil: $\epsilon_r = 2.5, \quad \sigma = 10^{-4}$ (S/m)
Fresh Water: $\epsilon_r = 80, \quad \sigma = 10^{-3}$ (S/m)

Sections 6-11: Electromagnetic Potentials

6.22 The electric field of an electromagnetic wave propagating in air is given by

$$\mathbf{E}(z, t) = \hat{\mathbf{x}} 4 \cos(6 \times 10^8 t - 2z) + \hat{\mathbf{y}} 3 \sin(6 \times 10^8 t - 2z) \quad (\text{V/m})$$

Find the associated magnetic field $\mathbf{H}(z, t)$.

6.23* The magnetic field in a dielectric material with $\varepsilon = 4\varepsilon_0$, $\mu = \mu_0$, and $\sigma = 0$ is given by

$$\mathbf{H}(y, t) = \hat{\mathbf{x}} 5 \cos(2\pi \times 10^7 t + ky) \quad (\text{A/m})$$

Find k and the associated electric field $\mathbf{E}$.

6.24 Given an electric field

$$\mathbf{E} = \hat{\mathbf{x}} E_0 \sin ay \cos(\omega t - kz)$$

where E_0, a, ω, and k are constants, find $\mathbf{H}$.

6.25* The electric field radiated by a short dipole antenna is given in spherical coordinates by

$$\mathbf{E}(R, \theta; t) = \hat{\theta} \frac{2 \times 10^{-2}}{R} \sin\theta \cos(6\pi \times 10^8 t - 2\pi R) \quad (\text{V/m})$$

Find $\mathbf{H}(R, \theta; t)$.

6.26 A Hertzian dipole is a short conducting wire carrying an approximately constant current over its length l. If such a dipole is placed along the z-axis with its midpoint at the origin, and if the current flowing through it is $i(t) = I_0 \cos \omega t$, find the following:

(a) The retarded vector potential $\widetilde{\mathbf{A}}(R, \theta, \phi)$ at an observation point $Q(R, \theta, \phi)$ in a spherical coordinate system.
(b) The magnetic field phasor $\widetilde{\mathbf{H}}(R, \theta, \phi)$.

Assume l to be sufficiently small so that the observation point is approximately equidistant to all points on the dipole; that is, assume $R' \simeq R$.

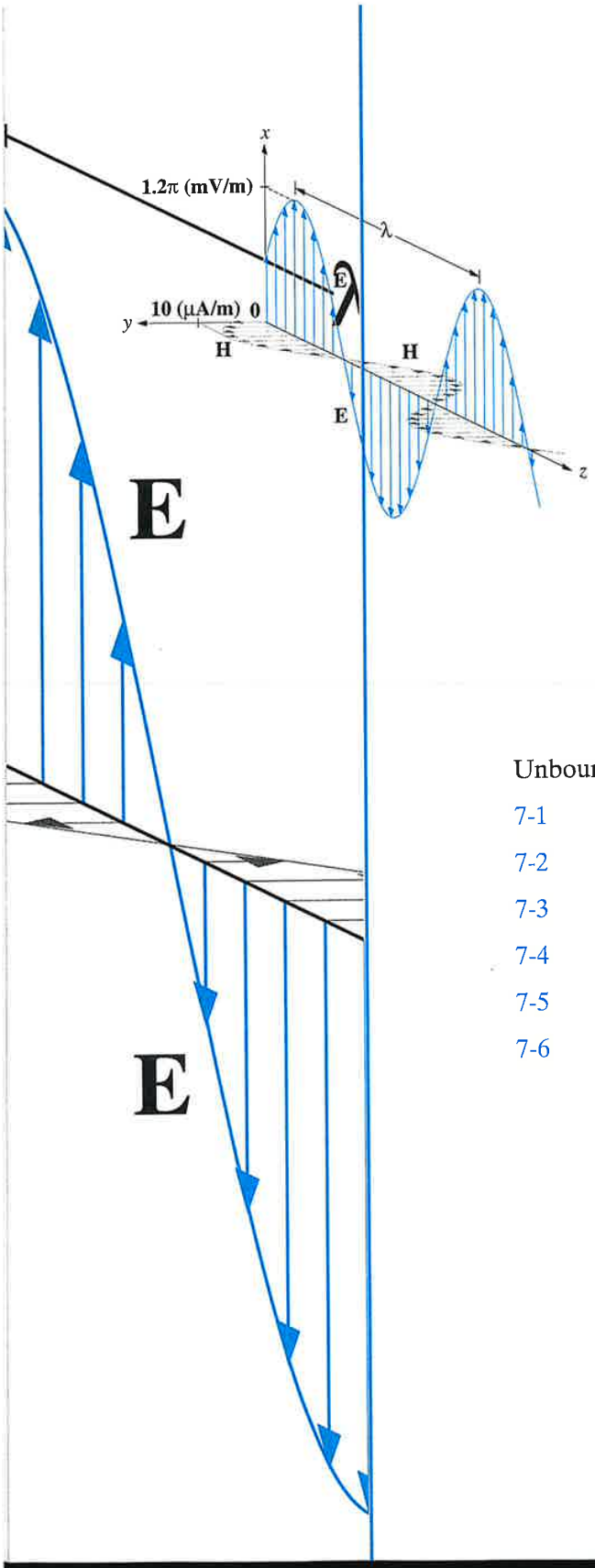
6.27 The magnetic field in a given dielectric medium is given by

$$\mathbf{H} = \hat{\mathbf{y}} 6 \cos 2z \sin(2 \times 10^7 t - 0.1x) \quad (\text{A/m})$$

where x and z are in meters. Determine:

(a) $\mathbf{E}$.
(b) The displacement current density $\mathbf{J}_d$.
(c) The charge density ρ_v.

INTEL-1014
U.S. Patent 7,151,430



CHAPTER 7

Plane-Wave Propagation

Unbounded EM Waves

7-1 Time-Harmonic Fields

7-2 Plane-Wave Propagation in Lossless Media

7-3 Wave Polarization

7-4 Plane-Wave Propagation in Lossy Media

7-5 Current Flow in a Good Conductor

7-6 Electromagnetic Power Density

INTEL-1014
U.S. Patent 7,151,430

UNBOUNDED EM WAVES

We established in Chapter 6 that a time-varying electric field $\mathbf{E}(t)$ produces a time-varying magnetic field $\mathbf{H}(t)$ and, conversely, a time-varying magnetic field produces an electric field. This cyclic pattern generates electromagnetic (EM) waves capable of propagating through free space and in material media. When its propagation is guided by a material structure, such as a transmission line, the EM wave is said to be traveling in a ***guided medium***. Earth's surface and ionosphere constitute parallel boundaries of a natural guiding structure for the propagation of short-wave radio transmissions in the HF band* (3 to 30 MHz); the ionosphere is a good reflector at these frequencies, thereby allowing the waves to zigzag between the two boundaries [Fig. 7-1]. EM waves also can travel in ***unbounded media***; light waves emitted by the sun and radio transmissions by antennas are typical examples.

When we discussed wave propagation on a transmission line in Chapter 2, we dealt with voltages and currents. For a transmission-line circuit such as that shown in Fig. 7-2, the a-c voltage source excites an incident wave that travels down the coaxial line toward the load, and unless the load is properly matched to the line, part (or all) of the incident wave is reflected back toward the generator. At any point z on the line, the instantaneous total voltage $v(z, t)$ is the sum of the incident and reflected waves, both of which vary sinusoidally with time. Associated with the voltage difference between the inner and outer conductors of the coaxial line is a radial electric field $\mathbf{E}$ that exists in the dielectric material between the conductors, and since $v(z, t)$ varies sinusoidally with time, so does $\mathbf{E}(z, t)$. Furthermore, the current flowing through the inner conductor induces an azimuthal magnetic field $\mathbf{H}(z, t)$ in the dielectric material surrounding it. These coupled fields, $\mathbf{E}(z, t)$ and $\mathbf{H}(z, t)$, constitute electromagnetic waves. Thus, we can model wave propagation on such a transmission line either in terms of the voltages across the line and the currents

*See Fig. 1-16.

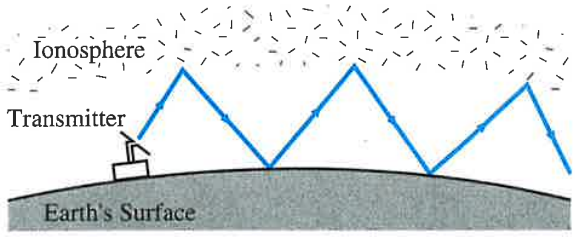


Figure 7-1: The atmospheric layer bounded by the ionosphere at the top and Earth's surface at the bottom forms a guiding structure for the propagation of radio waves in the HF band.

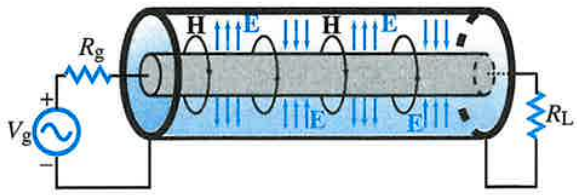


Figure 7-2: A guided electromagnetic wave traveling in a coaxial transmission line consists of time-varying electric and magnetic fields in the dielectric medium between the inner and outer conductors.

INTEL-1014
U.S. Patent 7,151,430

through its conductors or in terms of the electric and magnetic fields in the dielectric medium between the conductors.

In this chapter we focus our attention on wave propagation in unbounded media. We will consider both lossless and lossy media. Wave propagation in a ***lossless medium*** (perfect dielectric such as air) is similar to that on a lossless transmission line. In a ***lossy medium*** characterized by a nonzero conductivity, such as water, part of the power carried by the EM wave gets converted into heat, just like what happens to a wave propagating on a lossy transmission line.

When energy is emitted by a source, such as an antenna, it expands outwardly from the source in the form of ***spherical waves***, as depicted in Fig. 7-3(a). Even though the antenna may radiate more energy along some directions than along others, the spherical wave travels at the same speed in all directions and therefore expands at the same rate. To an observer very far away from the source, the ***wavefront*** of the spherical wave appears approximately *planar*, as if it were part of a ***uniform plane wave*** with uniform properties at all points in the plane tangent to the wavefront [Fig. 7-3(b)]. Plane-wave propagation can be accommodated by Cartesian coordinates, which are easier to work with mathematically than the spherical coordinates needed for describing the propagation of a spherical wave. Hence, even though strictly speaking a uniform plane wave cannot exist, we will nonetheless use it in this chapter to develop a physical understanding for wave propagation in lossless and lossy media, and then in Chapter 8 we will examine how waves, both planar and spherical, are reflected by and transmitted through boundaries between dissimilar media. The processes of radiation and reception of waves by antennas are treated in Chapter 9.

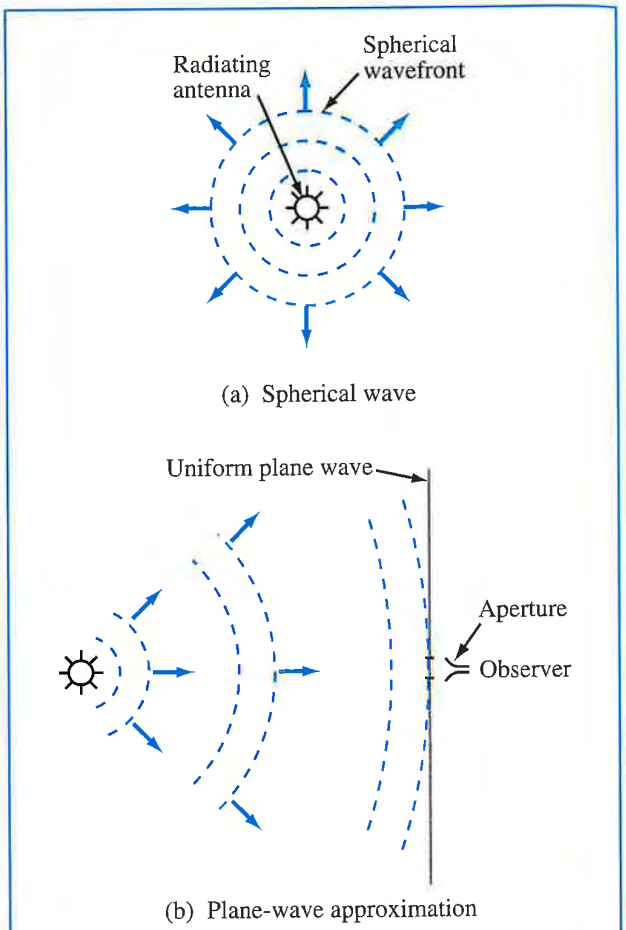


Figure 7-3: Waves radiated by an EM source, such as a light bulb or an antenna, have spherical wavefronts, as in (a); to a distant observer, however, the wavefront across the observer's aperture appears approximately planar, as in (b).

7-1 Time-Harmonic Fields

In the time-varying case, the electric and magnetic fields, **E**, **D**, **B**, and **H**, and their sources, the charge density ρ_v and current density **J**, are each, in general, a function of the spatial coordinates (x, y, z) and the time variable t. If their time variation is a sinusoidal function with an angular frequency ω, each of these quantities can be represented by a time-independent phasor that depends

INTEL-1014
U.S. Patent 7,151,430

on (x, y, z) only. Thus, the vector phasor $\widetilde{\mathbf{E}}(x, y, z)$ corresponding to the instantaneous field $\mathbf{E}(x, y, z; t)$ is defined according to

$$\mathbf{E}(x, y, z; t) = \Re\mathrm{e}\left[\widetilde{\mathbf{E}}(x, y, z)\, e^{j\omega t}\right], \tag{7.1}$$

and similar definitions apply to the other fields and to ρ_v and $\mathbf{J}$. For a linear, isotropic, and homogeneous medium characterized by electrical permittivity ε, magnetic permeability μ, and conductivity σ, and recalling that differentiation in the time domain corresponds to multiplication by $j\omega$ in the phasor domain, Maxwell's equations given by Eqs. (6.1) to (6.4) assume the following form in the phasor domain:

$$\nabla \cdot \widetilde{\mathbf{E}} = \tilde{\rho}_v/\varepsilon, \tag{7.2a}$$
$$\nabla \times \widetilde{\mathbf{E}} = -j\omega\mu\widetilde{\mathbf{H}}, \tag{7.2b}$$
$$\nabla \cdot \widetilde{\mathbf{H}} = 0, \tag{7.2c}$$
$$\nabla \times \widetilde{\mathbf{H}} = \widetilde{\mathbf{J}} + j\omega\varepsilon\widetilde{\mathbf{E}}, \tag{7.2d}$$

where we have used the relations $\mathbf{D} = \varepsilon\mathbf{E}$ and $\mathbf{B} = \mu\mathbf{H}$. This set of equations defines the starting point for the subject matter treated in this chapter.

7-1.1 Complex Permittivity

In a medium with conductivity σ, the current density $\mathbf{J}$ is related to $\mathbf{E}$ by $\mathbf{J} = \sigma\mathbf{E}$. Consequently, Eq. (7.2d) may be written as

$$\nabla \times \widetilde{\mathbf{H}} = \widetilde{\mathbf{J}} + j\omega\varepsilon\widetilde{\mathbf{E}} = (\sigma + j\omega\varepsilon)\widetilde{\mathbf{E}} = j\omega\left(\varepsilon - j\frac{\sigma}{\omega}\right)\widetilde{\mathbf{E}}. \tag{7.3}$$

By introducing the *complex permittivity* ε_c defined as

$$\varepsilon_c \triangleq \varepsilon - j\frac{\sigma}{\omega}, \tag{7.4}$$

Eq. (7.3) can be rewritten as

$$\nabla \times \widetilde{\mathbf{H}} = j\omega\varepsilon_c\widetilde{\mathbf{E}}. \tag{7.5}$$

The complex permittivity ε_c given by Eq. (7.4) is often written in terms of a real part ε' and an imaginary part ε''. Thus,

$$\varepsilon_c = \varepsilon - j\frac{\sigma}{\omega} \triangleq \varepsilon' - j\varepsilon'', \tag{7.6}$$

with

$$\varepsilon' = \varepsilon, \tag{7.7a}$$
$$\varepsilon'' = \frac{\sigma}{\omega}. \tag{7.7b}$$

For a lossless medium with $\sigma = 0$, it follows that $\varepsilon'' = 0$ and $\varepsilon_c = \varepsilon' = \varepsilon$.

7-1.2 Wave Equations for a Charge-Free Medium

A medium is said to be charge free if it contains no excess charges, that is, if $\rho_v = 0$. Upon replacing Eq. (7.2d) with Eq. (7.5) and setting $\rho_v = 0$ in Eq. (7.2a), Maxwell's equations for a charge-free medium become

$$\nabla \cdot \widetilde{\mathbf{E}} = 0, \tag{7.8a}$$
$$\nabla \times \widetilde{\mathbf{E}} = -j\omega\mu\widetilde{\mathbf{H}}, \tag{7.8b}$$
$$\nabla \cdot \widetilde{\mathbf{H}} = 0, \tag{7.8c}$$
$$\nabla \times \widetilde{\mathbf{H}} = j\omega\varepsilon_c\widetilde{\mathbf{E}}. \tag{7.8d}$$

To describe the propagation of an EM wave in a charge-free medium, we need to derive wave equations for $\widetilde{\mathbf{E}}$ and $\widetilde{\mathbf{H}}$ and then solve them to obtain explicit expressions for $\widetilde{\mathbf{E}}$ and $\widetilde{\mathbf{H}}$ as a function of the spatial variables (x, y, z). To this end, we start by taking the curl of both sides of Eq. (7.8b) to get

$$\nabla \times (\nabla \times \widetilde{\mathbf{E}}) = -j\omega\mu(\nabla \times \widetilde{\mathbf{H}}). \tag{7.9}$$

Upon substituting Eq. (7.8d) into Eq. (7.9) we have

$$\nabla \times (\nabla \times \widetilde{\mathbf{E}}) = -j\omega\mu(j\omega\varepsilon_c\widetilde{\mathbf{E}}) = \omega^2\mu\varepsilon_c\widetilde{\mathbf{E}}. \tag{7.10}$$

INTEL-1014
U.S. Patent 7,151,430

From Eq. (3.113), the curl of the curl of $\widetilde{\mathbf{E}}$ is given by

$$\nabla \times (\nabla \times \widetilde{\mathbf{E}}) = \nabla(\nabla \cdot \widetilde{\mathbf{E}}) - \nabla^2 \widetilde{\mathbf{E}}, \tag{7.11}$$

where $\nabla^2 \widetilde{\mathbf{E}}$ is the Laplacian of $\widetilde{\mathbf{E}}$ and is given in Cartesian coordinates by

$$\nabla^2 \widetilde{\mathbf{E}} = \left(\frac{\partial^2}{\partial x^2} + \frac{\partial^2}{\partial y^2} + \frac{\partial^2}{\partial z^2}\right) \widetilde{\mathbf{E}}. \tag{7.12}$$

In view of Eq. (7.8a), which states that $\nabla \cdot \widetilde{\mathbf{E}} = 0$, the use of Eq. (7.11) in Eq. (7.10) gives

$$\nabla^2 \widetilde{\mathbf{E}} + \omega^2 \mu \varepsilon_c \widetilde{\mathbf{E}} = 0, \tag{7.13}$$

which is called the ***homogeneous wave equation for*** $\widetilde{\mathbf{E}}$. Upon introducing the ***propagation constant*** γ defined such that

$$\gamma^2 \triangleq -\omega^2 \mu \varepsilon_c, \tag{7.14}$$

Eq. (7.13) can be rewritten as

$$\nabla^2 \widetilde{\mathbf{E}} - \gamma^2 \widetilde{\mathbf{E}} = 0. \tag{7.15}$$

In deriving Eq. (7.15), we started by taking the curl of both sides of Eq. (7.8b) and then we used Eq. (7.8d) to obtain an equation in $\widetilde{\mathbf{E}}$ only. If we reverse the process, that is, if we start by taking the curl of both sides of Eq. (7.8d) and then use Eq. (7.8b), we obtain the wave equation for $\widetilde{\mathbf{H}}$:

$$\nabla^2 \widetilde{\mathbf{H}} - \gamma^2 \widetilde{\mathbf{H}} = 0. \tag{7.16}$$

Since the wave equations for $\widetilde{\mathbf{E}}$ and $\widetilde{\mathbf{H}}$ are of the same form, their solutions will have the same form also.

7-2 Plane-Wave Propagation in Lossless Media

The propagation properties of an electromagnetic wave, such as its phase velocity u_p and wavelength λ, are governed by the angular frequency ω and the three constitutive parameters of the medium: ε, μ, and σ. If the medium is ***nonconducting*** ($\sigma = 0$), the wave does not suffer any attenuation as it travels through the medium, and hence the medium is said to be ***lossless***. From Eq. (7.4), $\varepsilon_c = \varepsilon$ in a lossless medium, in which case Eq. (7.14) becomes

$$\gamma^2 = -\omega^2 \mu \varepsilon. \tag{7.17}$$

When the medium is lossless, it is customary to introduce the ***wavenumber*** k defined by

$$k = \omega \sqrt{\mu \varepsilon}\,. \tag{7.18}$$

In view of Eq. (7.17), $\gamma^2 = -k^2$ and Eq. (7.15) becomes

$$\nabla^2 \widetilde{\mathbf{E}} + k^2 \widetilde{\mathbf{E}} = 0. \tag{7.19}$$

7-2.1 Uniform Plane Waves

For an electric field phasor given in Cartesian coordinates by

$$\widetilde{\mathbf{E}} = \hat{\mathbf{x}} \widetilde{E}_x + \hat{\mathbf{y}} \widetilde{E}_y + \hat{\mathbf{z}} \widetilde{E}_z, \tag{7.20}$$

substitution of Eq. (7.12) into Eq. (7.19) gives

$$\left(\frac{\partial^2}{\partial x^2} + \frac{\partial^2}{\partial y^2} + \frac{\partial^2}{\partial z^2}\right)(\hat{\mathbf{x}} \widetilde{E}_x + \hat{\mathbf{y}} \widetilde{E}_y + \hat{\mathbf{z}} \widetilde{E}_z) + k^2(\hat{\mathbf{x}} \widetilde{E}_x + \hat{\mathbf{y}} \widetilde{E}_y + \hat{\mathbf{z}} \widetilde{E}_z) = 0. \tag{7.21}$$

To satisfy Eq. (7.21), each vector component on the left-hand side of the equation has to equal zero. Hence,

$$\left(\frac{\partial^2}{\partial x^2} + \frac{\partial^2}{\partial y^2} + \frac{\partial^2}{\partial z^2} + k^2\right) \widetilde{E}_x = 0, \tag{7.22}$$

INTEL-1014
U.S. Patent 7,151,430

and similar expressions apply to $\widetilde{E}_y$ and $\widetilde{E}_z$.

A ***uniform plane wave*** is characterized by electric and magnetic fields that have uniform properties at all points across an infinite plane [see Fig. 7-3(b)]. If this is the x–y plane, then $\mathbf{E}$ and $\mathbf{H}$ do not vary with x and y. Hence, $\partial \widetilde{E}_x/\partial x = 0$ and $\partial \widetilde{E}_x/\partial y = 0$, in which case Eq. (7.22) reduces to

$$\frac{d^2\widetilde{E}_x}{dz^2} + k^2\widetilde{E}_x = 0, \tag{7.23}$$

and similar expressions apply to $\widetilde{E}_y$, $\widetilde{H}_x$, and $\widetilde{H}_y$. The remaining components of $\widetilde{\mathbf{E}}$ and $\widetilde{\mathbf{H}}$ are zero; that is, $\widetilde{E}_z = \widetilde{H}_z = 0$. To show that $\widetilde{E}_z = 0$, let us consider the z-component of Eq. (7.8d),

$$\hat{\mathbf{z}}\left(\frac{\partial \widetilde{H}_y}{\partial x} - \frac{\partial \widetilde{H}_x}{\partial y}\right) = \hat{\mathbf{z}}\, j\omega\varepsilon \widetilde{E}_z. \tag{7.24}$$

Since $\partial \widetilde{H}_y/\partial x = \partial \widetilde{H}_x/\partial y = 0$, it follows that $\widetilde{E}_z = 0$. A similar examination involving Eq. (7.8b) reveals that $\widetilde{H}_z = 0$. This means that *a plane wave has no electric- or magnetic-field components along its direction of propagation.*

For the phasor quantity $\widetilde{E}_x$, the general solution of the ordinary differential equation given by Eq. (7.23) is

$$\widetilde{E}_x(z) = \widetilde{E}_x^+(z) + \widetilde{E}_x^-(z) = E_{x0}^+ e^{-jkz} + E_{x0}^- e^{jkz}, \tag{7.25}$$

where E_{x0}^+ and E_{x0}^- are constants to be determined from boundary conditions. The solution given by Eq. (7.25) is similar in form to the solution for the phasor voltage $\widetilde{V}(z)$ given by Eq. (2.44a) for the lossless transmission line. The first term in Eq. (7.25), containing the negative exponential e^{-jkz}, represents a wave with amplitude E_{x0}^+ traveling in the $+z$-direction, and the second term (with e^{jkz}) represents a wave with amplitude E_{x0}^- traveling in the $-z$-direction. Let us assume for the time being that $\widetilde{\mathbf{E}}$ has only a component along x (i.e., $\widetilde{E}_y = 0$) and that $\widetilde{E}_x$ consists of a wave traveling in the $+z$-direction only (i.e., $E_{x0}^- = 0$). Hence,

$$\widetilde{\mathbf{E}}(z) = \hat{\mathbf{x}}\widetilde{E}_x^+(z) = \hat{\mathbf{x}}E_{x0}^+ e^{-jkz}. \tag{7.26}$$

With $\widetilde{E}_y = \widetilde{E}_z = 0$, we apply Eq. (7.8b) to find the magnetic field $\widetilde{\mathbf{H}}(z)$:

$$\nabla \times \widetilde{\mathbf{E}} = \begin{vmatrix} \hat{\mathbf{x}} & \hat{\mathbf{y}} & \hat{\mathbf{z}} \\ \dfrac{\partial}{\partial x} & \dfrac{\partial}{\partial y} & \dfrac{\partial}{\partial z} \\ \widetilde{E}_x^+(z) & 0 & 0 \end{vmatrix}$$

$$= -j\omega\mu(\hat{\mathbf{x}}\widetilde{H}_x + \hat{\mathbf{y}}\widetilde{H}_y + \hat{\mathbf{z}}\widetilde{H}_z). \tag{7.27}$$

For a plane wave traveling in the z-direction,

$$\partial E_x^+(z)/\partial x = \partial E_x^+(z)/\partial y = 0.$$

Hence, Eq. (7.27) gives

$$\widetilde{H}_x = 0, \tag{7.28a}$$

$$\widetilde{H}_y = \frac{1}{-j\omega\mu}\frac{\partial \widetilde{E}_x^+(z)}{\partial z}, \tag{7.28b}$$

$$\widetilde{H}_z = \frac{1}{-j\omega\mu}\frac{\partial E_x^+(z)}{\partial y} = 0. \tag{7.28c}$$

Use of Eq. (7.26) in Eq. (7.28b) gives

$$\widetilde{H}_y(z) = \frac{k}{\omega\mu}E_{x0}^+ e^{-jkz} = H_{y0}^+ e^{-jkz}, \tag{7.29}$$

where H_{y0}^+ is the amplitude of $\widetilde{H}_y(z)$ and is given by

$$H_{y0}^+ = \frac{k}{\omega\mu}E_{x0}^+. \tag{7.30}$$

For a wave traveling from the source toward the load on a transmission line, the amplitudes of its voltage and current phasors, V_0^+ and I_0^+, are related by the characteristic impedance of the line, Z_0. A similar connection exists between the electric and magnetic fields of an electromagnetic wave. The ***intrinsic impedance*** of a lossless medium is defined as

$$\eta \triangleq \frac{\omega\mu}{k} = \frac{\omega\mu}{\omega\sqrt{\mu\varepsilon}} = \sqrt{\frac{\mu}{\varepsilon}} \quad (\Omega), \tag{7.31}$$

INTEL-1014
U.S. Patent 7,151,430

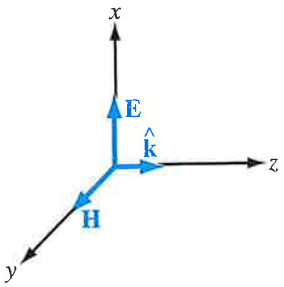


Figure 7-4: A transverse electromagnetic (TEM) wave propagating in the direction $\hat{\mathbf{k}} = \hat{\mathbf{z}}$. For all TEM waves, $\hat{\mathbf{k}}$ is parallel to $\mathbf{E} \times \mathbf{H}$.

where we used the expression for k given by Eq. (7.18). In view of Eq. (7.31), we can summarize our results as

$$\widetilde{\mathbf{E}}(z) = \hat{\mathbf{x}}\widetilde{E}_x^+(z) = \hat{\mathbf{x}}E_{x0}^+ e^{-jkz}, \qquad (7.32a)$$

$$\widetilde{\mathbf{H}}(z) = \hat{\mathbf{y}}\frac{\widetilde{E}_x^+(z)}{\eta} = \hat{\mathbf{y}}\frac{E_{x0}^+}{\eta}e^{-jkz}. \qquad (7.32b)$$

The electric and magnetic fields are perpendicular to each other, and both are perpendicular to the direction of wave travel (Fig. 7-4). These directional properties characterize a ***transverse electromagnetic (TEM)*** wave. Other examples of TEM waves include cylindrical waves traveling along coaxial transmission lines ($\mathbf{E}$ is along $\hat{\mathbf{r}}$, $\mathbf{H}$ is along $\hat{\boldsymbol{\phi}}$, and direction of travel is along $\hat{\mathbf{z}}$) and spherical waves radiated by antennas.

In the general case, E_{x0}^+ may be a complex quantity composed of a magnitude $|E_{x0}^+|$ and a phase angle ϕ^+. That is,

$$E_{x0}^+ = |E_{x0}^+|e^{j\phi^+}. \qquad (7.33)$$

The instantaneous electric and magnetic fields are then given by

$$\mathbf{E}(z,t) = \Re\mathrm{e}\left[\widetilde{\mathbf{E}}(z)\, e^{j\omega t}\right] = \hat{\mathbf{x}}|E_{x0}^+|\cos(\omega t - kz + \phi^+) \quad \text{(V/m)}, \qquad (7.34a)$$

$$\mathbf{H}(z,t) = \Re\mathrm{e}\left[\widetilde{\mathbf{H}}(z)\, e^{j\omega t}\right] = \hat{\mathbf{y}}\frac{|E_{x0}^+|}{\eta}\cos(\omega t - kz + \phi^+) \quad \text{(A/m)}. \qquad (7.34b)$$

Because $\mathbf{E}(z,t)$ and $\mathbf{H}(z,t)$ exhibit the same functional dependence on z and t, they are said to be ***in phase***; when the amplitude of one of them is a maximum, the amplitude of the other is a maximum also. This in-phase property is characteristic of waves propagating in lossless media. Their time variation is defined by the oscillation frequency $f = \omega/2\pi$, and their spatial variation is characterized by the wavelength λ. From the material on wave motion given in Section 1-3, we deduce that the ***phase velocity*** of the wave is given by

$$u_\mathrm{p} = \frac{\omega}{k} = \frac{\omega}{\omega\sqrt{\mu\varepsilon}} = \frac{1}{\sqrt{\mu\varepsilon}} \quad \text{(m/s)}, \qquad (7.35)$$

and the wavelength is

$$\lambda = \frac{2\pi}{k} = \frac{u_\mathrm{p}}{f} \quad \text{(m)}. \qquad (7.36)$$

If the medium is vacuum, $\varepsilon = \varepsilon_0$ and $\mu = \mu_0$, in which case the phase velocity u_p and the intrinsic impedance η given by Eq. (7.31) become

$$u_\mathrm{p} = c = \frac{1}{\sqrt{\mu_0\varepsilon_0}} = 3 \times 10^8 \quad \text{(m/s)}, \qquad (7.37)$$

$$\eta = \eta_0 \triangleq \sqrt{\frac{\mu_0}{\varepsilon_0}} = 377\ (\Omega) \approx 120\pi \quad (\Omega), \qquad (7.38)$$

where c is the velocity of light and η_0 is called the ***intrinsic impedance of free space***.

Example 7-1 **EM Plane Wave in Air**

This example is analogous to the "Sound Wave in Water" problem described by Example 1-1.

INTEL-1014
U.S. Patent 7,151,430

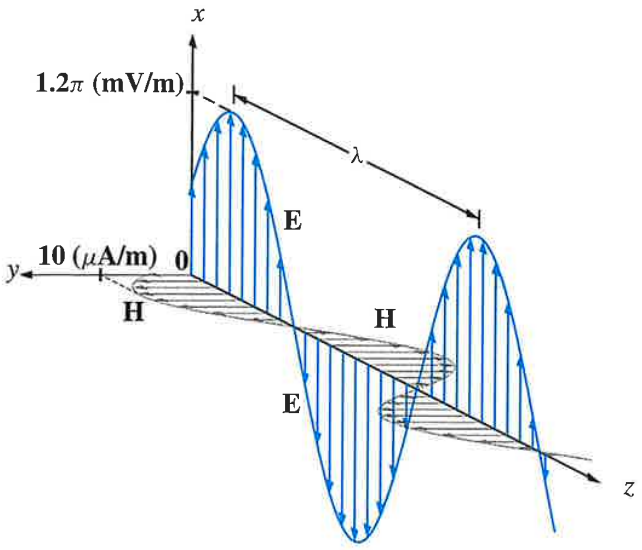


Figure 7-5: Spatial variations of **E** and **H** at $t = 0$ for the plane wave of Example 7-1.

The electric field of a 1-MHz plane wave traveling in the $+z$-direction in air points along the x-direction. If the peak value of E is 1.2π (mV/m) and E is maximum at $t = 0$ and $z = 50$ m, obtain expressions for $\mathbf{E}(z, t)$ and $\mathbf{H}(z, t)$, and then plot these variations as a function of z at $t = 0$.

Solution: At $f = 1$ MHz, the wavelength in air is given by

$$\lambda = \frac{c}{f} = \frac{3 \times 10^8}{1 \times 10^6} = 300 \text{ m},$$

and the corresponding wavenumber is $k = (2\pi/300)$ (rad/m). The general expression for an x-directed electric field traveling in the $+z$-direction is given by Eq. (7.34a) as

$$\mathbf{E}(z, t) = \hat{\mathbf{x}} |E_{x0}^+| \cos(\omega t - kz + \phi^+)$$
$$= \hat{\mathbf{x}}\, 1.2\pi \cos\left(2\pi \times 10^6 t - \frac{2\pi z}{300} + \phi^+\right) \text{ (mV/m)}.$$

The field $\mathbf{E}(z, t)$ is maximum when the argument of the cosine function equals zero or multiples of 2π. At $t = 0$ and $z = 50$ m, this condition is

$$-\frac{2\pi \times 50}{300} + \phi^+ = 0 \quad \text{or} \quad \phi^+ = \frac{\pi}{3}.$$

Hence,

$$\mathbf{E}(z, t) = \hat{\mathbf{x}}\, 1.2\pi \cos\left(2\pi \times 10^6 t - \frac{2\pi z}{300} + \frac{\pi}{3}\right) \text{ (mV/m)},$$

INTEL-1014
U.S. Patent 7,151,430

and from Eq. (7.34b) we have

$$\mathbf{H}(z,t) = \hat{\mathbf{y}}\frac{E(z,t)}{\eta_0}$$
$$= \hat{\mathbf{y}}\,10\cos\left(2\pi\times10^6 t - \frac{2\pi z}{300} + \frac{\pi}{3}\right) \quad (\mu\text{A/m}),$$

where we have used the approximation $\eta_0 \simeq 120\pi$ (Ω).

At $t = 0$,

$$\mathbf{E}(z,0) = \hat{\mathbf{x}}\,1.2\pi\cos\left(\frac{2\pi z}{300} - \frac{\pi}{3}\right) \quad (\text{mV/m}),$$

$$\mathbf{H}(z,0) = \hat{\mathbf{y}}\,10\cos\left(\frac{2\pi z}{300} - \frac{\pi}{3}\right) \quad (\mu\text{A/m}).$$

Plots of $\mathbf{E}(z,0)$ and $\mathbf{H}(z,0)$ are shown in Fig. 7-5 as a function of z. ■

7-2.2 General Relation between E and H

It can be shown that, for any uniform plane wave traveling in an arbitrary direction denoted by the unit vector $\hat{\mathbf{k}}$, the magnetic field phasor $\widetilde{\mathbf{H}}$ is interrelated to the electric field phasor $\widetilde{\mathbf{E}}$ by

$$\widetilde{\mathbf{H}} = \frac{1}{\eta}\hat{\mathbf{k}}\times\widetilde{\mathbf{E}}, \quad (7.39a)$$
$$\widetilde{\mathbf{E}} = -\eta\hat{\mathbf{k}}\times\widetilde{\mathbf{H}}. \quad (7.39b)$$

The cross product can be phrased in terms of the following right-hand rule: *when we rotate the four fingers of the right hand from the direction of* **E** *toward the direction of* **H**, *the thumb will point in the direction of wave travel,* $\hat{\mathbf{k}}$. The relations given by Eqs. (7.39a and b) are valid not only for lossless media, but for lossy media as well. As we will see later in Section 7-4, the expression for η of a lossy medium is different from that given by Eq. (7.31). As long as the expression used for η is appropriate for the medium in which the wave is traveling, the relations given by Eqs. (7.39a and b) always hold.

Let us apply Eq. (7.39a) to the wave given by Eq. (7.32a). The direction of propagation $\hat{\mathbf{k}} = \hat{\mathbf{z}}$ and $\widetilde{\mathbf{E}} = \hat{\mathbf{x}}\,\widetilde{E}_x^+(z)$. Hence,

$$\widetilde{\mathbf{H}} = \frac{1}{\eta}\hat{\mathbf{k}}\times\widetilde{\mathbf{E}} = \frac{1}{\eta}(\hat{\mathbf{z}}\times\hat{\mathbf{x}})\,\widetilde{E}_x^+(z) = \hat{\mathbf{y}}\frac{\widetilde{E}_x^+(z)}{\eta}, \quad (7.40)$$

which is the same as the result given by Eq. (7.32b). For a wave traveling in the $-z$-direction with an electric field given by

$$\widetilde{\mathbf{E}} = \hat{\mathbf{x}}\,\widetilde{E}_x^-(z) = \hat{\mathbf{x}}E_{x0}^- e^{jkz}, \quad (7.41)$$

application of Eq. (7.39a) gives

$$\widetilde{\mathbf{H}} = \frac{1}{\eta}(-\hat{\mathbf{z}}\times\hat{\mathbf{x}})\,\widetilde{E}_x^-(z) = -\hat{\mathbf{y}}\frac{\widetilde{E}_x^-(z)}{\eta} = -\hat{\mathbf{y}}\frac{E_{x0}^-}{\eta}e^{jkz}. \quad (7.42)$$

Hence, in this case, $\widetilde{\mathbf{H}}$ points in the negative y-direction.

In general, a uniform plane wave traveling in the $+z$-direction may have both x- and y-components, in which case $\widetilde{\mathbf{E}}$ is given by

$$\widetilde{\mathbf{E}} = \hat{\mathbf{x}}\,\widetilde{E}_x^+(z) + \hat{\mathbf{y}}\,\widetilde{E}_y^+(z), \quad (7.43a)$$

and the associated magnetic field is

$$\widetilde{\mathbf{H}} = \hat{\mathbf{x}}\,\widetilde{H}_x^+(z) + \hat{\mathbf{y}}\,\widetilde{H}_y^+(z). \quad (7.43b)$$

Application of Eq. (7.39a) gives

$$\widetilde{\mathbf{H}} = \frac{1}{\eta}\hat{\mathbf{z}}\times\widetilde{\mathbf{E}} = -\hat{\mathbf{x}}\frac{\widetilde{E}_y^+(z)}{\eta} + \hat{\mathbf{y}}\frac{\widetilde{E}_x^+(z)}{\eta}. \quad (7.44)$$

By equating Eq. (7.43b) to Eq. (7.44), we have

$$\widetilde{H}_x^+(z) = -\frac{\widetilde{E}_y^+(z)}{\eta}, \qquad \widetilde{H}_y^+ = \frac{\widetilde{E}_x^+(z)}{\eta}. \quad (7.45)$$

These results are illustrated in Fig. 7-6. The wave may be considered the sum of two waves, one with (E_x^+, H_y^+) components and another with (E_y^+, H_x^+) components. In general, a TEM wave may have an electric field in any direction in the plane orthogonal to the direction of wave travel, and the associated magnetic field is also in the same plane and its direction is dictated by Eq. (7.39a).

INTEL-1014
U.S. Patent 7,151,430

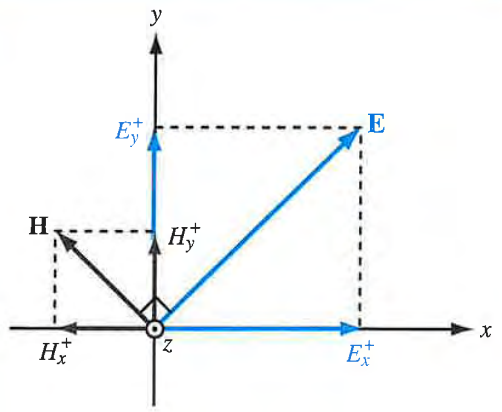


Figure 7-6: The wave (**E**, **H**) is equivalent to the sum of two waves, one with fields (E_x^+, H_y^+) and another with (E_y^+, H_x^+), with both traveling in the $+z$-direction.

REVIEW QUESTIONS

Q7.1 What is a uniform plane wave? Describe its properties, both physically and in mathematical terms. Under what conditions is it appropriate to treat a spherical wave as a plane wave?

Q7.2 Since $\widetilde{\mathbf{E}}$ and $\widetilde{\mathbf{H}}$ are governed by wave equations of the same form [Eqs. (7.15) and (7.16)], does it follow that $\widetilde{\mathbf{E}} = \widetilde{\mathbf{H}}$? Explain.

Q7.3 If a TEM wave is traveling in the $\hat{\mathbf{y}}$-direction, can its electric field have components along $\hat{\mathbf{x}}$, $\hat{\mathbf{y}}$, and $\hat{\mathbf{z}}$? Explain.

EXERCISE 7.1 A 10-MHz uniform plane wave is traveling in a nonmagnetic medium with $\mu = \mu_0$ and $\varepsilon_r = 9$. Find (a) the phase velocity, (b) the wavenumber, (c) the wavelength in the medium, and (d) the intrinsic impedance of the medium.

Ans. (a) $u_p = 1 \times 10^8$ m/s, (b) $k = 0.2\pi$ rad/m, (c) $\lambda = 10$ m, (d) $\eta = 125.67\ \Omega$.

EXERCISE 7.2 The electric field phasor of a uniform plane wave traveling in a lossless medium with an intrinsic impedance of 188.5 Ω is given by $\widetilde{\mathbf{E}} = \hat{\mathbf{z}}\, 10e^{-j4\pi y}$ (mV/m). Determine (a) the associated magnetic field phasor and (b) the instantaneous expression for $\mathbf{E}(y, t)$ if the medium is nonmagnetic ($\mu = \mu_0$).

Ans. (a) $\widetilde{\mathbf{H}} = \hat{\mathbf{x}}\, 53e^{-j4\pi y}$ (μA/m), (b) $\mathbf{E}(y, t) = \hat{\mathbf{z}}\, 10\cos(6\pi \times 10^8 t - 4\pi y)$ (mV/m).

EXERCISE 7.3 If the magnetic field phasor of a plane wave traveling in a medium with intrinsic impedance $\eta = 100\ \Omega$ is given by $\widetilde{\mathbf{H}} = (\hat{\mathbf{y}}\, 10 + \hat{\mathbf{z}}\, 20)e^{-j4x}$ (mA/m), find the associated electric field phasor.

Ans. $\widetilde{\mathbf{E}} = (-\hat{\mathbf{z}} + \hat{\mathbf{y}}\, 2)e^{-j4x}$ (V/m).

EXERCISE 7.4 Repeat Exercise 7.3 for a magnetic field given by $\widetilde{\mathbf{H}} = \hat{\mathbf{y}}(10e^{-j3x} - 20e^{j3x})$ (mA/m).

Ans. $\widetilde{\mathbf{E}} = -\hat{\mathbf{z}}(e^{-j3x} + 2e^{j3x})$ (V/m).

7-3 Wave Polarization

The ***polarization*** of a uniform plane wave *describes the shape and locus of the tip of the* **E** *vector (in the plane orthogonal to the direction of propagation) at a given point in space as a function of time.* In the most general case, the locus of **E** is an ellipse, and the wave is called ***elliptically polarized***. Under certain conditions, the ellipse may degenerate into a circle or a segment of a straight line, in which case the ***polarization state*** is then called ***circular*** or ***linear***, respectively.

As was shown in Section 7-2, the z-components of the electric and magnetic fields of a z-propagating plane wave are both zero. Hence, the electric field phasor $\widetilde{\mathbf{E}}(z)$ may consist of an x-component, $\widetilde{E}_x(z)$, and a y-component, $\widetilde{E}_y(z)$:

$$\widetilde{\mathbf{E}}(z) = \hat{\mathbf{x}}\widetilde{E}_x(z) + \hat{\mathbf{y}}\widetilde{E}_y(z), \qquad (7.46)$$

INTEL-1014
U.S. Patent 7,151,430

with

$$\widetilde{E}_x(z) = E_{x0}e^{-jkz}, \tag{7.47a}$$

$$\widetilde{E}_y(z) = E_{y0}e^{-jkz}, \tag{7.47b}$$

where E_{x0} and E_{y0} are the complex amplitudes of $\widetilde{E}_x(z)$ and $\widetilde{E}_y(z)$, respectively. For the sake of simplicity, the plus sign superscript has been suppressed throughout; the negative sign in e^{-jkz} is sufficient to remind us that the wave is traveling in the positive z-direction.

The two amplitudes E_{x0} and E_{y0} are, in general, complex quantities, with each characterized by a magnitude and a phase angle. The phase of a wave is defined relative to a reference condition, such as $z = 0$ and $t = 0$ or any other combination of z and t. *Wave polarization depends on the phase of E_{y0} relative to that of E_{x0}, but not on the absolute phases of E_{x0} and E_{y0}.* Hence, for convenience, we will choose the phase of E_{x0} as our reference (thereby assigning E_{x0} a phase angle of zero), and we will denote the phase of E_{y0}, relative to that of E_{x0}, as δ. Thus, δ is the *phase difference* between the y-component of $\widetilde{\mathbf{E}}$ and its x-component. Accordingly, we define E_{x0} and E_{y0} as

$$E_{x0} = a_x, \tag{7.48a}$$

$$E_{y0} = a_y e^{j\delta}, \tag{7.48b}$$

where $a_x = |E_{x0}|$ and $a_y = |E_{y0}|$ are the magnitudes of E_{x0} and E_{y0}, respectively. Thus, by definition, a_x and a_y may not assume negative values. Using Eqs. (7.48a) and (7.48b) in Eqs. (7.47a) and (7.47b), the total electric field phasor is then given by

$$\widetilde{\mathbf{E}}(z) = (\hat{\mathbf{x}}a_x + \hat{\mathbf{y}}a_y e^{j\delta})e^{-jkz}, \tag{7.49}$$

and the corresponding instantaneous field is

$$\begin{aligned}\mathbf{E}(z,t) &= \mathfrak{Re}\left[\widetilde{\mathbf{E}}(z)\, e^{j\omega t}\right] \\ &= \hat{\mathbf{x}}a_x \cos(\omega t - kz) \\ &\quad + \hat{\mathbf{y}}a_y \cos(\omega t - kz + \delta).\end{aligned} \tag{7.50}$$

When characterizing the behavior of an EM wave, two properties of particular interest are the intensity and direction of its electric field. The intensity of $\mathbf{E}(z,t)$ is given by its modulus $|\mathbf{E}(z,t)|$, namely

$$\begin{aligned}|\mathbf{E}(z,t)| &= [E_x^2(z,t) + E_y^2(z,t)]^{1/2} \\ &= [a_x^2 \cos^2(\omega t - kz) \\ &\quad + a_y^2 \cos^2(\omega t - kz + \delta)]^{1/2}.\end{aligned} \tag{7.51}$$

The electric field $\mathbf{E}(z,t)$ has components along the x- and y-directions. At a specific position z, the direction of $\mathbf{E}(z,t)$ is defined in the x–y plane (at that value of z) by the inclination angle ψ, defined with respect to the zero-phase reference component of $\mathbf{E}(z,t)$, which is the x-component in the present case. Thus,

$$\psi(z,t) \triangleq \tan^{-1}\left(\frac{E_y(z,t)}{E_x(z,t)}\right). \tag{7.52}$$

In the general case, both the intensity of $\mathbf{E}(z,t)$ and its direction are functions of z and t. Next, we examine some special cases.

7-3.1 Linear Polarization

The polarization state of a wave traveling in the z-direction is determined by tracing the tip of $\mathbf{E}(z,t)$ as a function of time in a plane orthogonal to the direction of wave travel. For convenience and without loss of generality, we usually choose the $z = 0$ plane. *A wave is said to be linearly polarized if $E_x(z,t)$ and $E_y(z,t)$ are **in phase** (i.e., $\delta = 0$) or **out of phase** ($\delta = \pi$).* This is because, at a specified value of z, say $z = 0$, the tip of $\mathbf{E}(0,t)$ traces a straight line in the x–y plane. At $z = 0$ and for $\delta = 0$ or π, Eq. (7.50) simplifies to

$$\mathbf{E}(0,t) = (\hat{\mathbf{x}}a_x + \hat{\mathbf{y}}a_y)\cos\omega t \quad \text{(in-phase)}, \tag{7.53a}$$

$$\mathbf{E}(0,t) = (\hat{\mathbf{x}}a_x - \hat{\mathbf{y}}a_y)\cos\omega t \quad \text{(out-of-phase)}. \tag{7.53b}$$

Let us examine the out-of-phase case. At $\omega t = 0$, $\mathbf{E}(0,0) = \hat{\mathbf{x}}a_x - \hat{\mathbf{y}}a_y$, which means that $\mathbf{E}$ extends from the origin in Fig. 7-7 to the point $(a_x, -a_y)$ in the fourth quadrant in the x–y plane. As t increases, the modulus

INTEL-1014
U.S. Patent 7,151,430

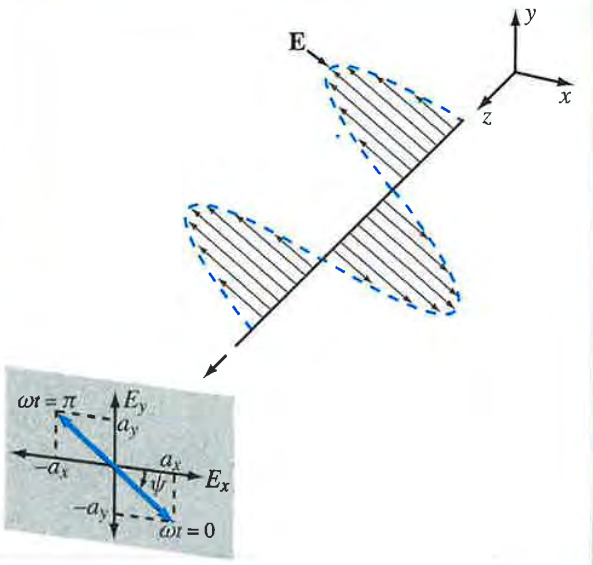


Figure 7-7: Linearly polarized wave traveling in the $+z$-direction (out of the page).

of $\mathbf{E}(0, t)$ varies as $\cos \omega t$:

$$|\mathbf{E}(0, t)| = [a_x^2 + a_y^2]^{1/2} \cos \omega t, \tag{7.54a}$$

and the inclination angle defined by Eq. (7.52) is given by

$$\psi = \tan^{-1}\left(\frac{-a_y}{a_x}\right) \quad \text{(out-of-phase)}, \tag{7.54b}$$

which is independent of both z and t. Thus, the length of the vector representing $\mathbf{E}(0, t)$ decreases to zero at $\omega t = \pi/2$, then reverses direction and increases in magnitude to $[a_x^2 + a_y^2]^{1/2}$ in the second quadrant of the x–y plane at $\omega t = \pi$. Since ψ is independent of both z and t, $\mathbf{E}(z, t)$ maintains a direction along the line making an angle ψ with the x-axis.

If $a_y = 0$, $\psi = 0°$ or $180°$, and the wave becomes x-polarized, and if $a_x = 0$, $\psi = 90°$ or $-90°$, and the wave becomes y-polarized.

7-3.2 Circular Polarization

We now consider the special case when the magnitudes of the x- and y-components of $\widetilde{\mathbf{E}}(z)$ are equal, and the phase difference $\delta = \pm\pi/2$. For reasons that will become evident shortly, the wave polarization is called ***left-hand circular*** when $\delta = \pi/2$, and it is called ***right-hand circular*** when $\delta = -\pi/2$.

Left-Hand Circular (LHC) Polarization

For $a_x = a_y = a$ and $\delta = \pi/2$, Eqs. (7.49) and (7.50) become

$$\begin{aligned}\widetilde{\mathbf{E}}(z) &= (\hat{\mathbf{x}}a + \hat{\mathbf{y}}ae^{j\pi/2})e^{-jkz} \\ &= a(\hat{\mathbf{x}} + j\hat{\mathbf{y}})e^{-jkz}, \end{aligned} \tag{7.55a}$$

$$\begin{aligned}\mathbf{E}(z, t) &= \Re\mathrm{e}\left[\widetilde{\mathbf{E}}(z)\, e^{j\omega t}\right] \\ &= \hat{\mathbf{x}}a\cos(\omega t - kz) + \hat{\mathbf{y}}a\cos(\omega t - kz + \pi/2) \\ &= \hat{\mathbf{x}}a\cos(\omega t - kz) - \hat{\mathbf{y}}a\sin(\omega t - kz). \end{aligned} \tag{7.55b}$$

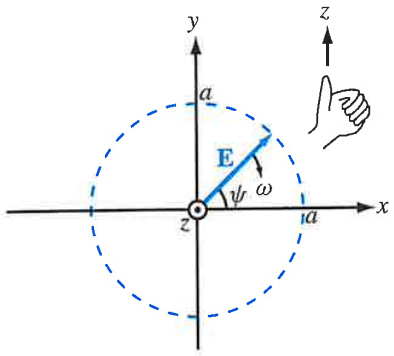
The corresponding modulus and inclination angle are given by

$$\begin{aligned}|\mathbf{E}(z, t)| &= \left[E_x^2(z, t) + E_y^2(z, t)\right]^{1/2} \\ &= [a^2\cos^2(\omega t - kz) + a^2\sin^2(\omega t - kz)]^{1/2} \\ &= a, \end{aligned} \tag{7.56a}$$

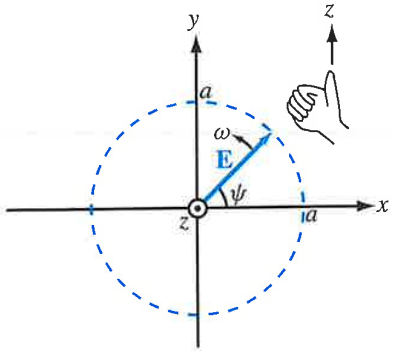
$$\begin{aligned}\psi(z, t) &= \tan^{-1}\left[\frac{E_y(z, t)}{E_x(z, t)}\right] \\ &= \tan^{-1}\left[\frac{-a\sin(\omega t - kz)}{a\cos(\omega t - kz)}\right] \\ &= -(\omega t - kz). \end{aligned} \tag{7.56b}$$

We observe that in this case the modulus of $\mathbf{E}$ is independent of both z and t, whereas ψ depends on both variables. These functional dependencies are the

INTEL-1014
U.S. Patent 7,151,430



(a) LHC polarization



(b) RHC polarization

Figure 7-8: Circularly polarized plane waves propagating in the $+z$-direction (out of the page).

converse of those applicable to the linear-polarization case.

At a fixed position z, say $z = 0$, Eq. (7.56b) gives $\psi = -\omega t$; the negative sign means that the inclination angle decreases with increasing time. As illustrated in Fig. 7-8(a), the tip of $\mathbf{E}(t)$ traces a circle in the x–y plane, and it rotates in a clockwise direction as a function of time (when viewing the wave approaching). Such a wave is called ***left-hand circularly polarized*** because, when the thumb of the left hand points along the direction of propagation of the wave (the z-direction in this case), the other four fingers point in the direction of rotation of $\mathbf{E}$.

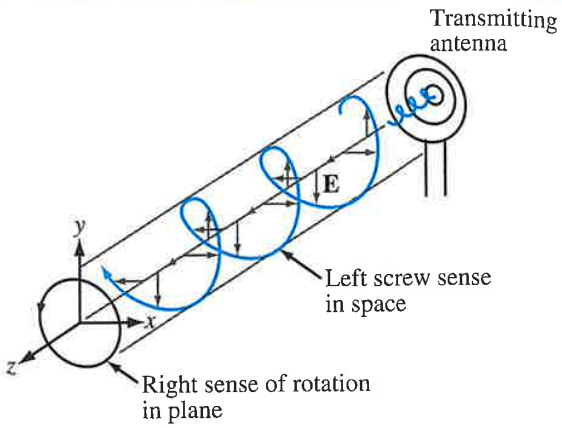


Figure 7-9: Right-hand circularly polarized wave radiated by a helical antenna.

Right-Hand Circular (RHC) Polarization

For $a_x = a_y = a$ and $\delta = -\pi/2$, we have

$$|\mathbf{E}(z,t)| = a, \qquad \psi = (\omega t - kz). \tag{7.57}$$

The trace of $\mathbf{E}$ as a function of t is shown in Fig. 7-8(b) for $z = 0$. For RHC polarization, the fingers of the right hand point in the direction of rotation of $\mathbf{E}$ when the thumb is along the propagation direction. Figure 7-9 depicts a right-hand circularly polarized wave radiated by a helical antenna. Note that *polarization handedness is defined in terms of the rotation of* $\mathbf{E}$ *as a function of time in a fixed plane orthogonal to the direction of propagation,* which is opposite of the direction of rotation of $\mathbf{E}$ as a function of distance at a fixed point in time.

Example 7-2 RHC Polarized Wave

An RHC polarized plane wave with electric field modulus of 3 (mV/m) is traveling in the $+y$-direction in

INTEL-1014
U.S. Patent 7,151,430

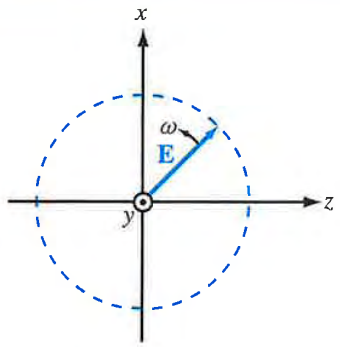


Figure 7-10: Right-hand circularly polarized wave of Example 7-2.

a dielectric medium with $\varepsilon = 4\varepsilon_0$, $\mu = \mu_0$, and $\sigma = 0$. If the wave frequency is 100 MHz, obtain expressions for $\mathbf{E}(y, t)$ and $\mathbf{H}(y, t)$.

Solution: Since the wave is traveling in the $+y$-direction, its field components must be along the x- and z-directions. The rotation of $\mathbf{E}(y, t)$ is depicted in Fig. 7-10, where $\hat{\mathbf{y}}$ is out of the page. By comparison with the RHC polarized wave shown in Fig. 7-8(b), we assign the z-component of $\widetilde{\mathbf{E}}(y)$ a phase angle of zero and the x-component a phase shift $\delta = -\pi/2$. Both components have a magnitude $a = 3$ (mV/m). Hence,

$$\begin{aligned}\widetilde{\mathbf{E}}(y) &= \hat{\mathbf{x}}\widetilde{E}_x + \hat{\mathbf{z}}\widetilde{E}_z \\ &= \hat{\mathbf{x}}ae^{-j\pi/2}e^{-jky} + \hat{\mathbf{z}}ae^{-jky} \\ &= (-\hat{\mathbf{x}}j + \hat{\mathbf{z}})3e^{-jky} \quad \text{(mV/m)},\end{aligned}$$

and application of (7.39a) gives

$$\begin{aligned}\widetilde{\mathbf{H}}(y) &= \frac{1}{\eta}\hat{\mathbf{y}} \times \widetilde{\mathbf{E}}(y) \\ &= \frac{1}{\eta}\hat{\mathbf{y}} \times (-\hat{\mathbf{x}}j + \hat{\mathbf{z}})3e^{-jky} \\ &= \frac{3}{\eta}(\hat{\mathbf{z}}j + \hat{\mathbf{x}})e^{-jky} \quad \text{(mA/m)}.\end{aligned}$$

With $\omega = 2\pi f = 2\pi \times 10^8$ (rad/s), the wavenumber k is

$$k = \frac{\omega\sqrt{\varepsilon_r}}{c} = \frac{2\pi \times 10^8\sqrt{4}}{3 \times 10^8} = \frac{4}{3}\pi \quad \text{(rad/m)},$$

and the intrinsic impedance η is given by

$$\eta = \frac{\eta_0}{\sqrt{\varepsilon_r}} \simeq \frac{120\pi}{\sqrt{4}} = 60\pi \quad (\Omega).$$

The instantaneous functions $\mathbf{E}(y, t)$ and $\mathbf{H}(y, t)$ are then given by

$$\begin{aligned}\mathbf{E}(y,t) &= \Re\mathrm{e}\left[\widetilde{\mathbf{E}}(y)\, e^{j\omega t}\right] \\ &= \Re\mathrm{e}\left[(-\hat{\mathbf{x}}j + \hat{\mathbf{z}})3e^{-jky}e^{j\omega t}\right] \\ &= 3[\hat{\mathbf{x}}\sin(\omega t - ky) + \hat{\mathbf{z}}\cos(\omega t - ky)] \quad \text{(mV/m)},\end{aligned}$$

$$\begin{aligned}\mathbf{H}(y,t) &= \Re\mathrm{e}\left[\widetilde{\mathbf{H}}(y)\, e^{j\omega t}\right] \\ &= \Re\mathrm{e}\left[\frac{3}{\eta}(\hat{\mathbf{z}}j + \hat{\mathbf{x}})e^{-jky}e^{j\omega t}\right] \\ &= \frac{1}{20\pi}[\hat{\mathbf{x}}\cos(\omega t - ky) - \hat{\mathbf{z}}\sin(\omega t - ky)] \quad \text{(mA/m)},\end{aligned}$$

with $\omega = 2\pi \times 10^8$ (rad/s) and $k = 4\pi/3$ (rad/m). ■

7-3.3 Elliptical Polarization

In the most general case, where $a_x \neq 0$, $a_y \neq 0$, and $\delta \neq 0$, the tip of $\mathbf{E}$ traces an ellipse in the x–y plane, and the wave is said to be elliptically polarized. The shape of the ellipse and its handedness (left-hand or right-hand rotation) are determined by the values of the ratio (a_y/a_x) and the polarization phase difference δ.

The polarization ellipse shown in Fig. 7-11 has a major axis a_ξ along the ξ-direction and a minor axis a_η along the η-direction. The *rotation angle* γ is defined as the angle between the major axis of the ellipse and a reference direction, chosen here to be the x-axis, with γ being bounded within the range $-\pi/2 \leq \gamma \leq \pi/2$. The shape

INTEL-1014
U.S. Patent 7,151,430

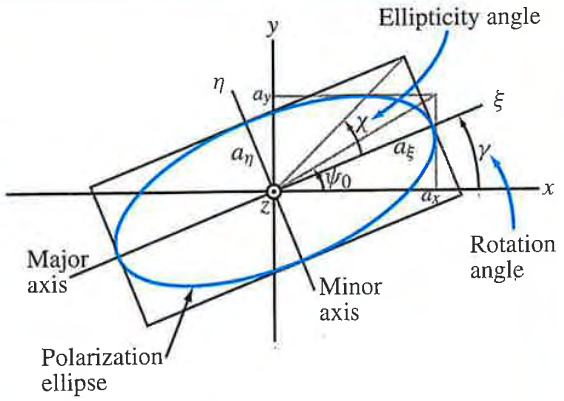


Figure 7-11: Polarization ellipse in the x–y plane, with the wave traveling in the z-direction (out of the page).

of the ellipse and its handedness are characterized by the ***ellipticity angle*** χ, defined as follows:

$$\tan\chi = \pm\frac{a_\eta}{a_\xi} = \pm\frac{1}{R}, \tag{7.58}$$

with the plus sign corresponding to left-handed rotation and the minus sign corresponding to right-handed rotation. The limits for χ are $-\pi/4 \le \chi \le \pi/4$. The quantity $R = a_\xi/a_\eta$ is called the ***axial ratio*** of the polarization ellipse, and it varies between 1 for circular polarization and ∞ for linear polarization. The polarization angles γ and χ are related to the wave parameters a_x, a_y, and δ by*

$$\tan 2\gamma = (\tan 2\psi_0)\cos\delta \quad (-\pi/2 \le \gamma \le \pi/2), \tag{7.59a}$$

$$\sin 2\chi = (\sin 2\psi_0)\sin\delta \quad (-\pi/4 \le \chi \le \pi/4), \tag{7.59b}$$

where ψ_0 is an auxiliary angle defined by

$$\tan\psi_0 = \frac{a_y}{a_x} \qquad \left(0 \le \psi_0 \le \frac{\pi}{2}\right). \tag{7.60}$$

*From M. Born and E. Wolf, *Principles of Optics*, New York: Macmillan, 1965, p. 27.

Sketches of the polarization ellipse are shown in Fig. 7-12 for various combinations of the angles (γ, χ). The ellipse reduces to a circle for $\chi = \pm 45°$ and to a line for $\chi = 0$. *Positive values of χ, corresponding to $\sin\delta > 0$, are associated with left-handed rotation, and negative values of χ, corresponding to $\sin\delta < 0$, are associated with right-handed rotation.*

Since the magnitudes a_x and a_y are, by definition, nonnegative numbers, the ratio a_y/a_x may vary between zero for an x-polarized linear polarization and ∞ for a y-polarized linear polarization. Consequently, the angle ψ_0 is limited to the range $0 \le \psi_0 \le 90°$. Application of Eq. (7.59a) leads to two possible solutions for the value of γ, both of which fall within the defined range from $-\pi/2$ to $\pi/2$. The correct choice is governed by the following rule:

$$\gamma > 0 \text{ if } \cos\delta > 0,$$
$$\gamma < 0 \text{ if } \cos\delta < 0.$$

In summary, the sign of the rotation angle γ is the same as the sign of $\cos\delta$ and the sign of the ellipticity angle χ is the same as the sign of $\sin\delta$.

Example 7-3 Polarization State

Determine the polarization state of a plane wave with electric field

$$\mathbf{E}(z,t) = \hat{\mathbf{x}}\,3\cos(\omega t - kz + 30°) - \hat{\mathbf{y}}\,4\sin(\omega t - kz + 45°) \quad \text{(mV/m)}.$$

Solution: We begin by converting the second term into a cosine reference,

$$\begin{aligned}\mathbf{E} &= \hat{\mathbf{x}}\,3\cos(\omega t - kz + 30°) - \hat{\mathbf{y}}\,4\cos(\omega t - kz + 45° - 90°)\\ &= \hat{\mathbf{x}}\,3\cos(\omega t - kz + 30°) - \hat{\mathbf{y}}\,4\cos(\omega t - kz - 45°).\end{aligned}$$

INTEL-1014
U.S. Patent 7,151,430

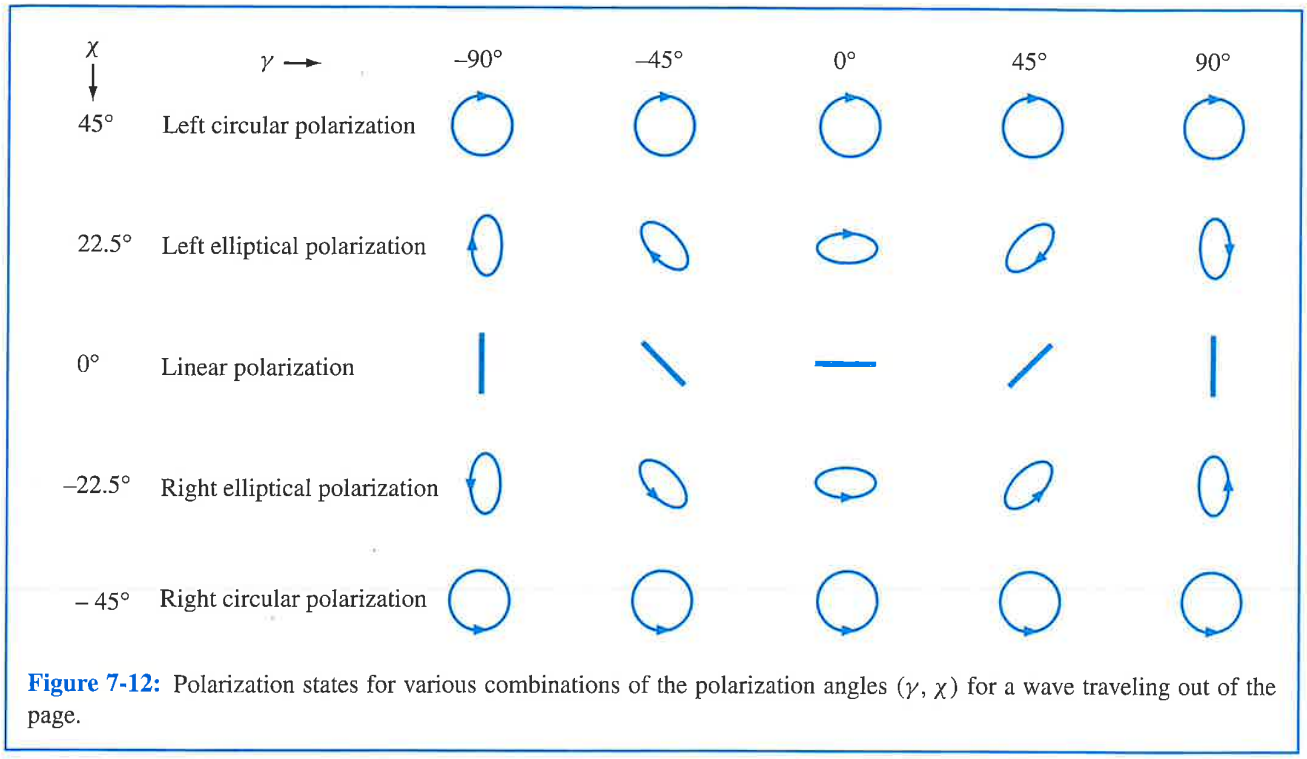


Figure 7-12: Polarization states for various combinations of the polarization angles (γ, χ) for a wave traveling out of the page.

The corresponding field phasor $\widetilde{\mathbf{E}}(z)$ is

$$\begin{aligned}\widetilde{\mathbf{E}}(z) &= \hat{\mathbf{x}}\,3e^{-jkz}e^{j30^\circ} - \hat{\mathbf{y}}\,4e^{-jkz}e^{-j45^\circ} \\ &= \hat{\mathbf{x}}\,3e^{-jkz}e^{j30^\circ} + \hat{\mathbf{y}}\,4e^{-jkz}e^{-j45^\circ}e^{j180^\circ} \\ &= \hat{\mathbf{x}}\,3e^{-jkz}e^{j30^\circ} + \hat{\mathbf{y}}\,4e^{-jkz}e^{j135^\circ},\end{aligned}$$

where we have replaced the negative sign of the second term with e^{j180° in order to have positive amplitudes for both terms, thereby allowing us to use the definitions given in Section 7-3.3. According to the expression for $\widetilde{\mathbf{E}}(z)$, the phase angles of the x- and y-components are $\delta_x = 30^\circ$ and $\delta_y = 135^\circ$, giving a phase difference $\delta = \delta_y - \delta_x = 135^\circ - 30^\circ = 105^\circ$. The auxiliary angle ψ_0 is obtained from

$$\psi_0 = \tan^{-1}\left(\frac{a_y}{a_x}\right) = \tan^{-1}\left(\frac{4}{3}\right) = 53.1^\circ.$$

From Eq. (7.59a),

$$\begin{aligned}\tan 2\gamma &= (\tan 2\psi_0)\cos\delta \\ &= \tan 106.2^\circ \cos 105^\circ \\ &= 0.89,\end{aligned}$$

which gives two solutions for γ, namely $\gamma = 20.8^\circ$ and $\gamma = -69.2^\circ$. Since $\cos\delta < 0$, the correct value of γ is -69.2°. From Eq. (7.59b),

$$\begin{aligned}\sin 2\chi &= (\sin 2\psi_0)\sin\delta \\ &= \sin 106.2^\circ \sin 105^\circ \\ &= 0.93 \quad \text{or} \quad \chi = 34.0^\circ.\end{aligned}$$

The magnitude of χ indicates that the wave is elliptically polarized and its positive polarity specifies its rotation as left handed. ■

INTEL-1014
U.S. Patent 7,151,430

REVIEW QUESTIONS

Q7.4 An elliptically polarized wave is characterized by amplitudes a_x and a_y and by the phase difference δ. If a_x and a_y are both nonzero, what should δ be in order for the polarization state to reduce to linear polarization?

Q7.5 Which of the following two descriptions defines an RHC polarized wave: A wave incident upon an observer is RHC polarized if its electric field appears to the observer to rotate in a counterclockwise direction (a) as a function of time in a fixed plane perpendicular to the direction of wave travel or (b) as a function of travel distance at a fixed time t?

EXERCISE 7.5 The electric field of a plane wave is given by

$$\mathbf{E}(z,t) = \hat{\mathbf{x}}\,3\cos(\omega t - kz) + \hat{\mathbf{y}}\,4\cos(\omega t - kz) \quad \text{(V/m)}.$$

Determine (a) the polarization state, (b) the modulus of $\mathbf{E}$, and (c) the inclination angle.

Ans. (a) Linear, (b) $|\mathbf{E}| = 5\cos(\omega t - kz)$ (V/m), (c) $\psi_0 = 53.1°$.

EXERCISE 7.6 If the electric field phasor of a TEM wave is given by $\widetilde{\mathbf{E}} = (\hat{\mathbf{y}} - \hat{\mathbf{z}}j)e^{-jkx}$, determine the polarization state.

Ans. RHC polarization.

7-4 Plane-Wave Propagation in Lossy Media

To examine wave propagation in a conducting medium, we return to the wave equation given by Eq. (7.15),

$$\nabla^2\widetilde{\mathbf{E}} - \gamma^2\widetilde{\mathbf{E}} = 0, \tag{7.61}$$

with

$$\gamma^2 = -\omega^2\mu\varepsilon_c = -\omega^2\mu(\varepsilon' - j\varepsilon''), \tag{7.62}$$

where $\varepsilon' = \varepsilon$ and $\varepsilon'' = \sigma/\omega$. Since γ is complex, we express it as

$$\gamma = \alpha + j\beta, \tag{7.63}$$

where α is the ***attenuation constant*** of the medium and β is its ***phase constant***. By replacing γ with $(\alpha + j\beta)$ in Eq. (7.62), we have

$$\begin{aligned}(\alpha + j\beta)^2 &= (\alpha^2 - \beta^2) + j2\alpha\beta \\ &= -\omega^2\mu\varepsilon' + j\omega^2\mu\varepsilon''.\end{aligned} \tag{7.64}$$

The rules of complex algebra require the real and imaginary parts on one side of an equation to be respectively equal to the real and imaginary parts on the other side. Hence,

$$\alpha^2 - \beta^2 = -\omega^2\mu\varepsilon', \tag{7.65a}$$

$$2\alpha\beta = \omega^2\mu\varepsilon''. \tag{7.65b}$$

Solving these two equations for α and β gives

$$\alpha = \omega\left\{\frac{\mu\varepsilon'}{2}\left[\sqrt{1+\left(\frac{\varepsilon''}{\varepsilon'}\right)^2} - 1\right]\right\}^{1/2} \quad \text{(Np/m)}, \tag{7.66a}$$

$$\beta = \omega\left\{\frac{\mu\varepsilon'}{2}\left[\sqrt{1+\left(\frac{\varepsilon''}{\varepsilon'}\right)^2} + 1\right]\right\}^{1/2} \quad \text{(rad/m)}. \tag{7.66b}$$

For a uniform plane wave with an electric field $\widetilde{\mathbf{E}} = \hat{\mathbf{x}}\,\widetilde{E}_x(z)$ traveling in the $+z$-direction, the wave equation given by Eq. (7.61) reduces to

$$\frac{d^2\widetilde{E}_x(z)}{dz^2} - \gamma^2\widetilde{E}_x(z) = 0. \tag{7.67}$$

INTEL-1014
U.S. Patent 7,151,430

The solution of this wave equation leads to

$$\widetilde{\mathbf{E}}(z) = \hat{\mathbf{x}}\widetilde{E}_x(z) = \hat{\mathbf{x}}E_{x0}e^{-\gamma z} = \hat{\mathbf{x}}E_{x0}e^{-\alpha z}e^{-j\beta z}. \quad (7.68)$$

The associated magnetic field $\widetilde{\mathbf{H}}$ can be determined either (1) by applying Eq. (7.2b): $\nabla \times \widetilde{\mathbf{E}} = -j\omega\mu\widetilde{\mathbf{H}}$, (2) by applying Eq. (7.39a): $\widetilde{\mathbf{H}} = (\hat{\mathbf{k}} \times \widetilde{\mathbf{E}})/\eta_c$, where η_c is the ***intrinsic impedance of the lossy medium***, or (3) by analogy with the lossless case. Any one of these approaches gives

$$\widetilde{\mathbf{H}}(z) = \hat{\mathbf{y}}\,\widetilde{H}_y(z) = \hat{\mathbf{y}}\frac{\widetilde{E}_x(z)}{\eta_c} = \hat{\mathbf{y}}\frac{E_{x0}}{\eta_c}e^{-\alpha z}e^{-j\beta z}, \quad (7.69)$$

where

$$\eta_c = \sqrt{\frac{\mu}{\varepsilon_c}} = \sqrt{\frac{\mu}{\varepsilon'}}\left(1 - j\frac{\varepsilon''}{\varepsilon'}\right)^{-1/2} \quad (\Omega). \quad (7.70)$$

We noted earlier that in a nonconducting medium, $\mathbf{E}(z, t)$ is in phase with $\mathbf{H}(z, t)$, but because η_c is a complex quantity in a conducting medium, the fields no longer have equal phase (as will be illustrated in Example 7-4).

From Eq. (7.68), the magnitude of $\widetilde{E}_x(z)$ is given by

$$|\widetilde{E}_x(z)| = |E_{x0}e^{-\alpha z}e^{-j\beta z}| = |E_{x0}|e^{-\alpha z}, \quad (7.71)$$

which decreases exponentially with z at a rate specified by the attenuation constant α. Since $\widetilde{H}_y = \widetilde{E}_x/\eta_c$, the magnitude of $\widetilde{H}_y$ also attenuates as $e^{-\alpha z}$. The attenuation process converts part of the energy carried by the electromagnetic wave into heat as a result of conduction in the medium. Through a distance $z = \delta_s$ such that

$$\delta_s = \frac{1}{\alpha} \quad (\text{m}), \quad (7.72)$$

the wave magnitude decreases by a factor of $e^{-1} \approx 0.37$ compared with its value at $z = 0$, as shown in Fig. 7-13. This distance δ_s, called the ***skin depth*** of the medium, characterizes how well an electromagnetic wave can penetrate into a conducting medium. In a perfect dielectric, $\sigma = 0$; hence, $\alpha = 0$ and therefore $\delta_s = \infty$. Thus, in free space, a plane wave can propagate with no loss in magnitude indefinitely. On the other extreme, if the medium is a perfect conductor with $\sigma = \infty$, use of $\varepsilon'' = \sigma/\omega$ in Eq. (7.66a) leads to $\alpha = \infty$ and hence $\delta_s = 0$. In a coaxial cable, if the outer conductor is designed to be several skin depths thick, it serves to prevent the energy inside the cable from leaking outward, as well as to shield against the penetration of outside electromagnetic energy into the cable.

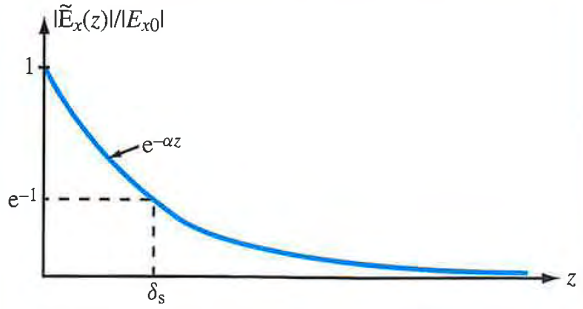


Figure 7-13: Attenuation of the magnitude of $\widetilde{E}_x(z)$ with distance z. The skin depth δ_s is the value of z at which $|\widetilde{E}_x(z)|/|E_{x0}| = e^{-1}$, or $z = \delta_s = 1/\alpha$.

The expressions given by Eqs. (7.66a), (7.66b), and (7.70) for α, β, and η_c are valid for any linear, isotropic, and homogeneous medium. If the medium is a perfect dielectric ($\sigma = 0$), these expressions reduce to the lossless case [Section 7-2], wherein $\alpha = 0$, $\beta = k = \omega\sqrt{\mu\varepsilon}$, and $\eta_c = \eta$. For a lossy medium, the ratio $\varepsilon''/\varepsilon' = \sigma/\omega\varepsilon$ appears in all these expressions and plays an important role in determining how lossy a medium is. When $\varepsilon''/\varepsilon' \ll 1$, the medium is called a ***low-loss dielectric***, and when $\varepsilon''/\varepsilon' \gg 1$, the medium is characterized as a ***good conductor***. In practice, the medium may be regarded as a low-loss dielectric if $\varepsilon''/\varepsilon' < 10^{-2}$, as a

INTEL-1014
U.S. Patent 7,151,430

good conductor if $\varepsilon''/\varepsilon' > 10^2$, and as a *quasi-conductor* if $10^{-2} \leq \varepsilon''/\varepsilon' \leq 10^2$.

7-4.1 Low-Loss Dielectric

From Eq. (7.62), the general expression for γ is given by

$$\gamma = j\omega\sqrt{\mu\varepsilon'}\left(1 - j\frac{\varepsilon''}{\varepsilon'}\right)^{1/2}. \tag{7.73}$$

For any quantity $|x| \ll 1$, the function $(1-x)^{1/2}$ can be approximated by the first two terms of its binomial series; that is, $(1-x)^{1/2} \simeq 1 - x/2$. By applying such an expansion to Eq. (7.73) for a low-loss dielectric with $x = j\varepsilon''/\varepsilon'$ and $\varepsilon''/\varepsilon' \ll 1$, we have

$$\gamma \cong j\omega\sqrt{\mu\varepsilon'}\left(1 - j\frac{\varepsilon''}{2\varepsilon'}\right). \tag{7.74}$$

The real and imaginary parts of Eq. (7.74) give

$$\alpha \cong \frac{\omega\varepsilon''}{2}\sqrt{\frac{\mu}{\varepsilon'}} = \frac{\sigma}{2}\sqrt{\frac{\mu}{\varepsilon}} \quad \text{(Np/m)}, \tag{7.75a}$$

$$\beta \cong \omega\sqrt{\mu\varepsilon'} = \omega\sqrt{\mu\varepsilon} \quad \text{(rad/m)}. \tag{7.75b}$$

We note that the expression for β is the same as that for the wavenumber k of a lossless medium. Applying the binomial approximation $(1-x)^{-1/2} \simeq (1 + x/2)$ to Eq. (7.70) leads to

$$\eta_c \cong \sqrt{\frac{\mu}{\varepsilon'}}\left(1 + j\frac{\varepsilon''}{2\varepsilon'}\right) = \sqrt{\frac{\mu}{\varepsilon}}\left(1 + j\frac{\sigma}{2\omega\varepsilon}\right). \tag{7.76a}$$

In practice, these approximate expressions for α, β, and η_c are used whenever $\varepsilon''/\varepsilon' = \sigma/\omega\varepsilon < 1/100$, in which case the second term in Eq. (7.76a) may be ignored. Thus,

$$\eta_c \cong \sqrt{\frac{\mu}{\varepsilon}}, \tag{7.76b}$$

which is the same as the expression given by Eq. (7.31) for the lossless case.

7-4.2 Good Conductor

We now examine the case of a good conductor characterized by $\varepsilon''/\varepsilon' > 100$. Under this condition, Eqs. (7.66a), (7.66b), and (7.70) can be approximated as

$$\alpha \cong \omega\sqrt{\frac{\mu\varepsilon''}{2}} = \omega\sqrt{\frac{\mu\sigma}{2\omega}} = \sqrt{\pi f\mu\sigma} \quad \text{(Np/m)}, \tag{7.77a}$$

$$\beta = \alpha \cong \sqrt{\pi f\mu\sigma} \quad \text{(rad/m)}, \tag{7.77b}$$

$$\eta_c \cong \sqrt{j\frac{\mu}{\varepsilon''}} = (1+j)\sqrt{\frac{\pi f\mu}{\sigma}} = (1+j)\frac{\alpha}{\sigma} \quad (\Omega). \tag{7.77c}$$

In Eq. (7.77c), we used the relation given by Eq. (1.53): $\sqrt{j} = (1+j)/\sqrt{2}$. For a perfect conductor with $\sigma = \infty$, these expressions give $\alpha = \beta = \infty$, and $\eta_c = 0$. A perfect conductor is equivalent to a short circuit.

Expressions for the propagation parameters in various types of media are summarized in Table 7-1 for easy reference.

Example 7-4 Plane Wave in Seawater

A uniform plane wave is traveling downward in the $+z$-direction in seawater, with the x–y plane denoting the sea surface and $z = 0$ denoting a point just below the surface. The constitutive parameters of seawater are $\varepsilon_r = 80$, $\mu_r = 1$, and $\sigma = 4$ S/m. If the magnetic field at $z = 0$ is given by $\mathbf{H}(0, t) = \hat{\mathbf{y}}\, 100\cos(2\pi \times 10^3 t + 15°)$ (mA/m),

(a) obtain expressions for $\mathbf{E}(z, t)$ and $\mathbf{H}(z, t)$, and

(b) determine the depth at which the amplitude of $\mathbf{E}$ is 1% of its value at $z = 0$.

Solution: (a) Since $\mathbf{H}$ is along $\hat{\mathbf{y}}$ and the propagation direction is $\hat{\mathbf{z}}$, $\mathbf{E}$ must be along $\hat{\mathbf{x}}$. Hence, the general expressions for the phasor fields are

$$\tilde{\mathbf{E}}(z) = \hat{\mathbf{x}}E_{x0}e^{-\alpha z}e^{-j\beta z}, \tag{7.78a}$$

$$\tilde{\mathbf{H}}(z) = \hat{\mathbf{y}}\frac{E_{x0}}{\eta_c}e^{-\alpha z}e^{-j\beta z}. \tag{7.78b}$$

INTEL-1014
U.S. Patent 7,151,430

Table 7-1: Expressions for α, β, η_c, u_p, and λ for various types of media.

	Any Medium	Lossless Medium ($\sigma = 0$)	Low-loss Medium ($\varepsilon''/\varepsilon' \ll 1$)	Good Conductor ($\varepsilon''/\varepsilon' \gg 1$)	Units
$\alpha =$	$\omega\left[\frac{\mu\varepsilon'}{2}\left[\sqrt{1+\left(\frac{\varepsilon''}{\varepsilon'}\right)^2}-1\right]\right]^{1/2}$	0	$\frac{\sigma}{2}\sqrt{\frac{\mu}{\varepsilon}}$	$\sqrt{\pi f\mu\sigma}$	(Np/m)
$\beta =$	$\omega\left[\frac{\mu\varepsilon'}{2}\left[\sqrt{1+\left(\frac{\varepsilon''}{\varepsilon'}\right)^2}+1\right]\right]^{1/2}$	$\omega\sqrt{\mu\varepsilon}$	$\omega\sqrt{\mu\varepsilon}$	$\sqrt{\pi f\mu\sigma}$	(rad/m)
$\eta_c =$	$\sqrt{\frac{\mu}{\varepsilon'}}\left(1-j\frac{\varepsilon''}{\varepsilon'}\right)^{-1/2}$	$\sqrt{\frac{\mu}{\varepsilon}}$	$\sqrt{\frac{\mu}{\varepsilon}}$	$(1+j)\frac{\alpha}{\sigma}$	(Ω)
$u_p =$	ω/β	$1/\sqrt{\mu\varepsilon}$	$1/\sqrt{\mu\varepsilon}$	$\sqrt{4\pi f/\mu\sigma}$	(m/s)
$\lambda =$	$2\pi/\beta = u_p/f$	u_p/f	u_p/f	u_p/f	(m)

Notes: $\varepsilon' = \varepsilon$; $\varepsilon'' = \sigma/\omega$; in free space, $\varepsilon = \varepsilon_0$, $\mu = \mu_0$; in practice, a material is considered a low-loss medium if $\varepsilon''/\varepsilon' = \sigma/\omega\varepsilon < 0.01$ and a good conducting medium if $\varepsilon''/\varepsilon' > 100$.

To determine α, β, and η_c for seawater, we begin by evaluating the ratio $\varepsilon''/\varepsilon'$. From the argument of the cosine function of $\mathbf{H}(0, t)$, we deduce that $\omega = 2\pi \times 10^3$ (rad/s), and therefore $f = 1$ kHz. Hence,

$$\frac{\varepsilon''}{\varepsilon'} = \frac{\sigma}{\omega\varepsilon} = \frac{\sigma}{\omega\varepsilon_r\varepsilon_0} = \frac{4}{2\pi \times 10^3 \times 80 \times (10^{-9}/36\pi)} = 9 \times 10^5.$$

Since $\varepsilon''/\varepsilon' \gg 1$, seawater is a good conductor at 1 kHz. This allows us to use the good-conductor expressions given in Table 7-1:

$$\alpha = \sqrt{\pi f\mu\sigma} = \sqrt{\pi \times 10^3 \times 4\pi \times 10^{-7} \times 4} = 0.126 \quad \text{(Np/m)}, \tag{7.79a}$$

$$\beta = \alpha = 0.126 \quad \text{(rad/m)}, \tag{7.79b}$$

$$\eta_c = (1+j)\frac{\alpha}{\sigma} = (\sqrt{2}\, e^{j\pi/4})\frac{0.126}{4} = 0.044e^{j\pi/4} \quad (\Omega). \tag{7.79c}$$

As no explicit information has been given about the electric field amplitude E_{x0}, we should assume it to be complex; that is, $E_{x0} = |E_{x0}|e^{j\phi_0}$. The wave's instantaneous electric and magnetic fields are then given by

$$\mathbf{E}(z, t) = \Re\mathfrak{e}\left[\hat{\mathbf{x}}|E_{x0}|e^{j\phi_0}e^{-\alpha z}e^{-j\beta z}e^{j\omega t}\right] = \hat{\mathbf{x}}|E_{x0}|e^{-0.126z}\cos(2\pi \times 10^3 t - 0.126z + \phi_0) \quad \text{(V/m)}, \tag{7.80a}$$

$$\mathbf{H}(z, t) = \Re\mathfrak{e}\left[\hat{\mathbf{y}}\frac{|E_{x0}|e^{j\phi_0}}{0.044e^{j\pi/4}}e^{-\alpha z}e^{-j\beta z}e^{j\omega t}\right] = \hat{\mathbf{y}}22.5|E_{x0}|e^{-0.126z}\cos(2\pi \times 10^3 t - 0.126z + \phi_0 - 45°) \quad \text{(A/m)}. \tag{7.80b}$$

INTEL-1014
U.S. Patent 7,151,430

At $z = 0$,

$$\mathbf{H}(0, t) = \hat{\mathbf{y}}\, 22.5|E_{x0}| \cos(2\pi \times 10^3 t + \phi_0 - 45°) \quad \text{(A/m)}. \tag{7.81}$$

By comparing Eq. (7.81) with the expression given in the problem statement,

$$\mathbf{H}(0, t) = \hat{\mathbf{y}}\, 100 \cos(2\pi \times 10^3 t + 15°) \quad \text{(mA/m)},$$

we deduce that

$$22.5|E_{x0}| = 100 \times 10^{-3}$$

or

$$|E_{x0}| = 4.44 \quad \text{(mV/m)},$$

and

$$\phi_0 - 45° = 15° \quad \text{or} \quad \phi_0 = 60°.$$

Hence, the final expressions for $\mathbf{E}(z, t)$ and $\mathbf{H}(z, t)$ are

$$\mathbf{E}(z, t) = \hat{\mathbf{x}}\, 4.44 e^{-0.126z} \cos(2\pi \times 10^3 t - 0.126z + 60°) \quad \text{(mV/m)}, \tag{7.82a}$$

$$\mathbf{H}(z, t) = \hat{\mathbf{y}}\, 100 e^{-0.126z} \cos(2\pi \times 10^3 t - 0.126z + 15°) \quad \text{(mA/m)}. \tag{7.82b}$$

(b) The depth at which the amplitude of $\mathbf{E}$ has decreased to 1% of its initial value at $z = 0$ is obtained from

$$0.01 = e^{-0.126z} \quad \text{or} \quad z = \frac{\ln(0.01)}{-0.126} = 36 \text{ m}. \quad \blacksquare$$

EXERCISE 7.7 The constitutive parameters of copper are $\mu = \mu_0 = 4\pi \times 10^{-7}$ (H/m), $\varepsilon = \varepsilon_0 \simeq (1/36\pi) \times 10^{-9}$ (F/m), and $\sigma = 5.8 \times 10^7$ (S/m). Assuming that these parameters are frequency independent, over what frequency range of the electromagnetic spectrum [see Fig. 1-15] is copper a good conductor?

Ans. $f < 1.04 \times 10^{16}$ Hz, which includes the radio spectrum, the infrared and visible regions, and part of the ultraviolet region.

EXERCISE 7.8 Over what frequency range may dry soil, with $\varepsilon_r = 3$, $\mu_r = 1$, and $\sigma = 10^{-4}$ (S/m), be regarded as a low-loss dielectric medium?

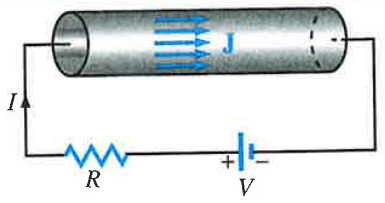
Ans. $f > 60$ MHz.

EXERCISE 7.9 For a wave traveling in a medium with a skin depth δ_s, what is the amplitude of $\mathbf{E}$ at a distance of $3\delta_s$ compared with its initial value?

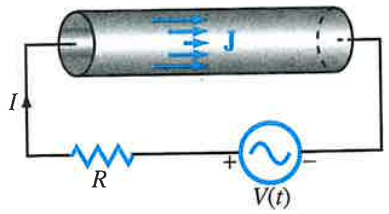
Ans. $e^{-3} \approx 0.05$ or 5%.

7-5 Current Flow in a Good Conductor

When a d-c voltage is connected across the ends of a conducting wire, the current flowing through the wire has a uniform current density $\mathbf{J}$ over the wire's cross section. That is, $\mathbf{J}$ has the same value along the axis of the wire as along its outer perimeter [Fig. 7-14(a)]. This is not true in the a-c case. As we will see shortly, the current density



(a) d-c case



(b) a-c case

Figure 7-14: Current density $\mathbf{J}$ in a conducting wire is (a) uniform across its cross section in the d-c case, but (b) in the a-c case, $\mathbf{J}$ is highest along the wire's perimeter.

INTEL-1014
U.S. Patent 7,151,430

in the time-varying case is maximum along the perimeter of the wire and decreases exponentially as a function of distance toward the axis of the wire [Fig. 7-14(b)]. In fact, at very high frequencies most of the current flows through a thin outer layer of the wire, and if the wire material is a perfect conductor, the current flows entirely along the surface of the wire.

Before we deal with the situation for a wire with circular cross section, let us consider the simpler geometry of a semi-infinite solid, as shown in Fig. 7-15(a). The conducting solid is infinite in depth and has a planar surface coincident with the x–y plane. If at $z = 0^-$ (just above the surface), an x-polarized EM field with $\widetilde{\mathbf{E}} = \hat{\mathbf{x}}E_0$ and $\widetilde{\mathbf{H}} = \hat{\mathbf{y}}E_0/\eta$ exists in the medium above the conductor, a similarly polarized EM field will be induced in the conducting medium and will constitute a plane wave that travels along the $+z$-direction. As a consequence of the boundary condition mandating that the tangential component of $\mathbf{E}$ be continuous across the boundary between any two contiguous media, at $z = 0^+$ (just below the boundary) the electric field of the wave is $\widetilde{\mathbf{E}}(0) = \hat{\mathbf{x}}E_0$. The fields of the EM wave at any depth z in the conductor are then given by

$$\widetilde{\mathbf{E}}(z) = \hat{\mathbf{x}}E_0 e^{-\alpha z} e^{-j\beta z}, \tag{7.83a}$$

$$\widetilde{\mathbf{H}}(z) = \hat{\mathbf{y}}\frac{E_0}{\eta_c} e^{-\alpha z} e^{-j\beta z}. \tag{7.83b}$$

From $\mathbf{J} = \sigma\mathbf{E}$, the current flows in the x-direction, and its density is

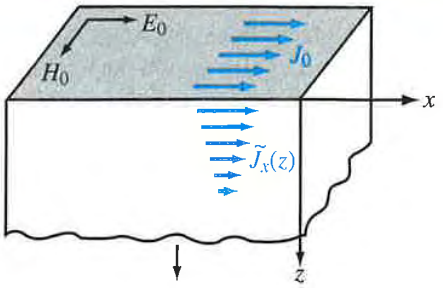
$$\widetilde{\mathbf{J}}(z) = \hat{\mathbf{x}}\,\widetilde{J}_x(z), \tag{7.84}$$

with

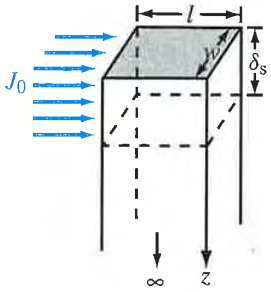
$$\widetilde{J}_x(z) = \sigma E_0 e^{-\alpha z} e^{-j\beta z} = J_0 e^{-\alpha z} e^{-j\beta z}, \tag{7.85}$$

where $J_0 = \sigma E_0$ is the magnitude of the current density at the surface. In terms of the skin depth $\delta_s = 1/\alpha$ defined by Eq. (7.72) and in view of Eq. (7.77b), which states that $\alpha = \beta$ for a good conductor, Eq. (7.85) can be written as

$$\widetilde{J}_x(z) = J_0 e^{-(1+j)z/\delta_s} \quad (\text{A/m}^2). \tag{7.86}$$



(a) Exponentially decaying $\widetilde{J}_x(z)$



(b) Equivalent J_0 over skin depth δ_s

Figure 7-15: Exponential decay of current density $\widetilde{J}_x(z)$ with z in a solid conductor. The total current flowing through (a) a section of width w extending between $z = 0$ and $z = \infty$ is equivalent to (b) a constant current density J_0 flowing through a section of depth δ_s.

The current flowing through a rectangular strip extending between zero and ∞ in the z-direction and of width w in the y-direction is

$$\widetilde{I} = w\int_0^\infty \widetilde{J}_x(z)\,dz$$

$$= w\int_0^\infty J_0 e^{-(1+j)z/\delta_s}\,dz = \frac{J_0 w\delta_s}{(1+j)} \quad \text{(A)}. \tag{7.87}$$

The numerator of Eq. (7.87) is equivalent to a uniform

INTEL-1014
U.S. Patent 7,151,430

current density J_0 flowing through a thin surface section of width w and depth δ_s. Because $\widetilde{J}_x(z)$ decreases exponentially with depth z, a conductor with a finite thickness d may be treated in practice as infinitely deep as long as d is several skin depths in extent. If $d = 3\delta_s$ [instead of ∞ in the integral of Eq. (7.87)], the error incurred in using the result on the right-hand side of Eq. (7.87) is less than 5%; and if $d = 5\delta_s$, the error is less than 1%.

The voltage across a length l at the surface [Fig. 7-15(b)] is given by

$$\widetilde{V} = E_0 l = \frac{J_0}{\sigma} l. \tag{7.88}$$

Hence, the impedance of a slab of width w, length l, and depth $d = \infty$ (or, in practice, $d > 5\delta_s$) is

$$Z = \frac{\widetilde{V}}{\widetilde{I}} = \frac{1+j}{\sigma\delta_s}\frac{l}{w} \quad (\Omega). \tag{7.89}$$

It is customary to represent Z as

$$Z = Z_s \frac{l}{w}, \tag{7.90}$$

where Z_s, which is called the ***internal*** or ***surface impedance*** of the conductor, is defined as the impedance Z for a unit length $l = 1$ m and a unit width $w = 1$ m. Thus,

$$Z_s = \frac{1+j}{\sigma\delta_s} \quad (\Omega). \tag{7.91}$$

Since the reactive part of Z_s is positive, Z_s can be defined as

$$Z_s = R_s + j\omega L_s$$

with

$$R_s = \frac{1}{\sigma\delta_s} = \sqrt{\frac{\pi f\mu}{\sigma}} \quad (\Omega), \tag{7.92a}$$

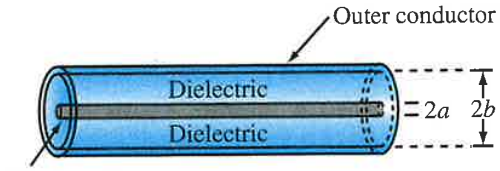
$$L_s = \frac{1}{\omega\sigma\delta_s} = \frac{1}{2}\sqrt{\frac{\mu}{\pi f\sigma}} \quad (\text{H}), \tag{7.92b}$$

where we used the relation $\delta_s = 1/\alpha \simeq 1/\sqrt{\pi f\mu\sigma}$ given by Eq. (7.77a). In terms of the ***surface resistance*** R_s, the ***a-c resistance*** of a slab of width w and length l is

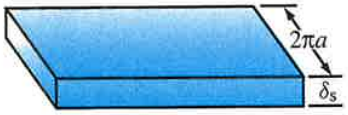
$$R = R_s \frac{l}{w} = \frac{l}{\sigma\delta_s w} \quad (\Omega). \tag{7.93}$$

The expression for the a-c resistance R is equivalent to the d-c resistance of a plane conductor of length l and cross section $A = \delta_s w$.

The results obtained for the planar conductor will now be extended to the coaxial cable shown in Fig. 7-16(a). If the conductors are made of copper with $\sigma = 5.8 \times 10^7$ S/m, the skin depth $\delta_s = 1/\sqrt{\pi f\mu\sigma} = 0.066$ mm at 1 MHz, and since δ_s varies as $1/\sqrt{f}$, it becomes smaller at higher frequencies. For the inner conductor, as long as its radius a is greater than $5\delta_s$, or 0.33 mm at 1 MHz, its "depth" may be regarded as semiinfinite, and a similar criterion applies to the thickness of the outer conductor. The current flowing



(a) Coaxial cable



(b) Equivalent inner conductor

Figure 7-16: The inner conductor of the coaxial cable in (a) is represented in (b) by a planar conductor of width $2\pi a$ and depth δ_s, as if its skin has been cut along its length on the bottom side and then unfurled into a planar geometry.

INTEL-1014
U.S. Patent 7,151,430

through the inner conductor is concentrated on its outer surface and is approximately equivalent to a uniform current flowing through a thin layer of depth δ_s and circumference $2\pi a$. This is equivalent to a planar conductor of width $w = 2\pi a$, as shown in Fig. 7-16(b). The corresponding resistance per unit length is obtained by setting $w = 2\pi a$ and dividing by l in Eq. (7.93):

$$R_1' = \frac{R}{l} = \frac{R_s}{2\pi a} \quad (\Omega/\text{m}). \tag{7.94}$$

Similarly, for the outer conductor, the current is concentrated within a thin layer on the inside surface of the conductor adjacent to the insulating medium between the two conductors, which is where the EM fields exist. The resistance per unit length for the outer conductor with radius b is

$$R_2' = \frac{R_s}{2\pi b} \quad (\Omega/\text{m}), \tag{7.95}$$

and the total a-c resistance per unit length is

$$R' = R_1' + R_2' = \frac{R_s}{2\pi}\left(\frac{1}{a} + \frac{1}{b}\right) \quad (\Omega/\text{m}). \tag{7.96}$$

This expression was used in Chapter 2 for characterizing the resistance per unit length of a coaxial transmission line.

REVIEW QUESTIONS

Q7.6 How does β of a low-loss dielectric medium compare to that of a lossless medium?

Q7.7 In a good conductor, does the phase of **H** lead or lag that of **E** and by how much?

Q7.8 Attenuation means that a wave loses energy as it propagates in a lossy medium. What happens to the lost energy?

Q7.9 Is a conducting medium dispersive or dispersionless? Explain.

Q7.10 Compare the flow of current through a wire in the d-c and a-c cases. Compare the corresponding d-c and a-c resistances of the wire.

7-6 Electromagnetic Power Density

This section deals with the flow of power carried by an electromagnetic wave. For any wave with an electric field **E** and magnetic field **H**, the *Poynting vector* **S** is defined as

$$\mathbf{S} = \mathbf{E} \times \mathbf{H} \quad (\text{W/m}^2). \tag{7.97}$$

The unit of **S** is (V/m) × (A/m) = (W/m^2), and the direction of **S** is along the propagation direction of the wave, $\hat{\mathbf{k}}$. Thus, **S** represents the power per unit area (power density) carried by the wave, and if the wave is incident upon an aperture of area A with outward surface unit vector $\hat{\mathbf{n}}$ as shown in Fig. 7-17, then the total power that flows through or is intercepted by the aperture is

$$P = \int_A \mathbf{S} \cdot \hat{\mathbf{n}} dA \quad (\text{W}). \tag{7.98}$$

For a uniform plane wave propagating in a direction $\hat{\mathbf{k}}$ that makes an angle θ with $\hat{\mathbf{n}}$, $P = SA\cos\theta$, where $S = |\mathbf{S}|$.

Except for the fact that the units of **S** are per unit area, Eq. (7.97) is the vector analogue of the scalar expression

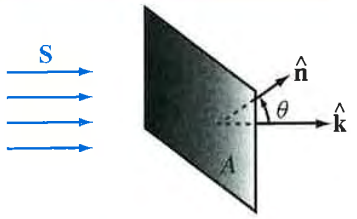


Figure 7-17: EM power flow through an aperture.

INTEL-1014
U.S. Patent 7,151,430

for the instantaneous power $P(z,t)$ flowing through a transmission line; that is,

$$P(z,t) = v(z,t)\, i(z,t), \tag{7.99}$$

where $v(z,t)$ and $i(z,t)$ are the instantaneous voltage and current on the line.

Since both $\mathbf{E}$ and $\mathbf{H}$ are functions of time, so is the Poynting vector $\mathbf{S}$. In practice, however, the quantity of greater interest is the ***average power density*** of the wave, $\mathbf{S}_{av}$, which is the time-average value of $\mathbf{S}$. For a transmission line excited by a time-harmonic (sinusoidal) source, we showed in Chapter 2 that the time-average power flowing toward the load can be computed by applying Eq. (2.87):

$$P_{av}(z) = \tfrac{1}{2}\,\mathrm{Re}\left[\widetilde{V}(z)\,\widetilde{I}^{*}(z)\right], \tag{7.100}$$

where $\widetilde{V}(z)$ and $\widetilde{I}(z)$ are the phasors corresponding to $v(z,t)$ and $i(z,t)$, respectively. The analogous expression for an electromagnetic wave is

$$\mathbf{S}_{av} = \tfrac{1}{2}\,\mathrm{Re}\left[\widetilde{\mathbf{E}} \times \widetilde{\mathbf{H}}^{*}\right] \quad (\mathrm{W/m^2}). \tag{7.101}$$

7-6.1 Plane Wave in a Lossless Medium

The general expression for the phasor electric field of a uniform plane wave with arbitrary polarization, traveling in the $+z$-direction, is given by

$$\begin{aligned}\widetilde{\mathbf{E}}(z) &= \hat{\mathbf{x}}\,\widetilde{E}_x(z) + \hat{\mathbf{y}}\,\widetilde{E}_y(z)\\ &= (\hat{\mathbf{x}}\,E_{x0} + \hat{\mathbf{y}}\,E_{y0})e^{-jkz},\end{aligned} \tag{7.102}$$

where, in the general case, E_{x0} and E_{y0} may be complex quantities. The magnitude of $\widetilde{\mathbf{E}}$ is

$$|\widetilde{\mathbf{E}}| = (\widetilde{\mathbf{E}} \cdot \widetilde{\mathbf{E}}^{*})^{1/2} = [|E_{x0}|^2 + |E_{y0}|^2]^{1/2}. \tag{7.103}$$

The phasor magnetic field associated with $\widetilde{\mathbf{E}}$ is obtained by applying Eq. (7.39a):

$$\widetilde{\mathbf{H}}(z) = \frac{1}{\eta}\hat{\mathbf{z}} \times \widetilde{\mathbf{E}} = \frac{1}{\eta}(-\hat{\mathbf{x}}E_{y0} + \hat{\mathbf{y}}E_{x0})e^{-jkz}. \tag{7.104}$$

The wave can be considered to be the sum of two waves, one with $(\widetilde{E}_x, \widetilde{H}_y)$ and another with $(\widetilde{E}_y, \widetilde{H}_x)$. Using Eqs. (7.102) and (7.104) in Eq. (7.101) leads to

$$\begin{aligned}\mathbf{S}_{av} &= \hat{\mathbf{z}}\frac{1}{2\eta}(|E_{x0}|^2 + |E_{y0}|^2)\\ &= \hat{\mathbf{z}}\frac{|\widetilde{\mathbf{E}}|^2}{2\eta} \quad (\mathrm{W/m^2}),\end{aligned} \tag{7.105}$$

which states that the power flow is in the z-direction and the average power density is equal to the sum of the average power densities of the $(\widetilde{E}_x, \widetilde{H}_y)$ wave and the $(\widetilde{E}_y, \widetilde{H}_x)$ wave. Note that, because $\mathbf{S}_{av}$ depends only on η and $|\widetilde{\mathbf{E}}|$, waves characterized by different polarizations carry the same amount of average power if their electric fields have the same magnitudes.

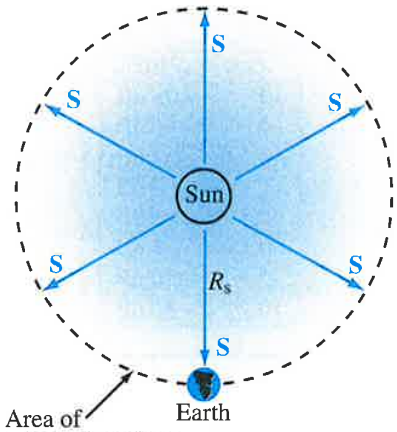
Example 7-5 Solar Power

If solar illumination is characterized by a power density of 1 kW/m^2 at Earth's surface, find (a) the total power radiated by the sun, (b) the total power intercepted by Earth, and (c) the electric field of the power density incident upon Earth's surface, assuming that all the solar illumination is at a single frequency. The radius of Earth's orbit around the sun, R_s, is approximately 1.5×10^8 km, and Earth's mean radius R_e is 6,380 km.

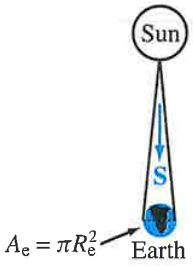
Solution: (a) Assuming that the sun radiates isotropically (equally in all directions), the total power it radiates is equal to $S_{av}\, A_{sph}$, where A_{sph} is the area of a spherical shell of radius R_s [Fig. 7-18(a)]. Thus,

$$\begin{aligned}P_{sun} = S_{av}(4\pi R_s^2) &= 1 \times 10^3 \times 4\pi \times (1.5 \times 10^{11})^2\\ &= 2.8 \times 10^{26}\ \mathrm{W}.\end{aligned}$$

INTEL-1014
U.S. Patent 7,151,430



(a) Radiated solar power



(b) Earth intercepted power

Figure 7-18: Solar radiation intercepted by (a) a spherical surface of radius R_s, and (b) Earth's surface (Example 7-5).

(b) With reference to Fig. 7-18(b), the power intercepted by Earth's cross section $A_e = \pi R_e^2$ is

$$P_{int} = S_{av}(\pi R_e^2) = 1 \times 10^3 \times \pi \times (6.38 \times 10^6)^2$$
$$= 1.28 \times 10^{17} \text{ W}.$$

(c) The power density S_{av} is related to the magnitude of the electric field $|E_0|$ by

$$S_{av} = \frac{|E_0|^2}{2\eta_0},$$

where $\eta_0 = 377$ (Ω) for air. Hence,

$$|E_0| = \sqrt{2\eta_0 S_{av}} = \sqrt{2 \times 377 \times 10^3}$$
$$= 870 \quad \text{(V/m)}. \blacksquare$$

7-6.2 Plane Wave in a Lossy Medium

The expressions given by Eqs. (7.68) and (7.69) characterize the electric and magnetic fields of a z-directed, x-polarized plane wave propagating in a lossy medium with a propagation constant $\gamma = \alpha + j\beta$. By extending these expressions to the more general case of a wave with components along both x and y, we have

$$\widetilde{\mathbf{E}}(z) = \hat{\mathbf{x}}\widetilde{E}_x(z) + \hat{\mathbf{y}}\widetilde{E}_y(z)$$
$$= (\hat{\mathbf{x}}E_{x0} + \hat{\mathbf{y}}E_{y0})e^{-\alpha z}e^{-j\beta z}, \qquad (7.106a)$$

$$\widetilde{\mathbf{H}}(z) = \frac{1}{\eta_c}(-\hat{\mathbf{x}}E_{y0} + \hat{\mathbf{y}}E_{x0})e^{-\alpha z}e^{-j\beta z}, \qquad (7.106b)$$

where η_c is the intrinsic impedance of the lossy medium. Application of Eq. (7.101) gives

$$\mathbf{S}_{av}(z) = \frac{1}{2}\Re\mathrm{e}\left[\widetilde{\mathbf{E}} \times \widetilde{\mathbf{H}}^*\right]$$
$$= \frac{\hat{\mathbf{z}}(|E_{x0}|^2 + |E_{y0}|^2)}{2}e^{-2\alpha z}\,\Re\mathrm{e}\left(\frac{1}{\eta_c^*}\right). \qquad (7.107)$$

By expressing η_c in polar form as

$$\eta_c = |\eta_c|e^{j\theta_\eta}, \qquad (7.108)$$

Eq. (7.107) can be rewritten as

$$\mathbf{S}_{av}(z) = \hat{\mathbf{z}}\frac{|E_0|^2}{2|\eta_c|}e^{-2\alpha z}\cos\theta_\eta \quad \text{(W/m}^2\text{)}, \qquad (7.109)$$

where $|E_0| = [|E_{x0}|^2 + |E_{y0}|^2]^{1/2}$ is the magnitude of $\widetilde{\mathbf{E}}(z)$ at $z = 0$. Whereas the fields $\widetilde{\mathbf{E}}(z)$ and $\widetilde{\mathbf{H}}(z)$ decay with z as $e^{-\alpha z}$, the power density $\mathbf{S}_{av}$ decreases as $e^{-2\alpha z}$. When a wave propagates through a distance $z = \delta_s = 1/\alpha$, the magnitudes of its electric and magnetic fields decrease to $e^{-1} \approx 37\%$ of their initial values, and its average power density decreases to $e^{-2} \approx 14\%$ of its initial value.

INTEL-1014
U.S. Patent 7,151,430

7-6.3 Decibel Scale for Power Ratios

The unit for power P is watts (W). In many engineering problems, the quantity of interest is the ratio of two power levels, P_1 and P_2, such as the incident and reflected powers on a transmission line, and often the ratio P_1/P_2 may vary over several orders of magnitude. The decibel (dB) scale is logarithmic, thereby providing a convenient representation of the power ratio, particularly when numerical values of P_1/P_2 are plotted against some variable of interest. If

$$G = \frac{P_1}{P_2}, \tag{7.110}$$

then

$$G\ [\text{dB}] \triangleq 10 \log G = 10 \log \left(\frac{P_1}{P_2}\right) \quad (\text{dB}). \tag{7.111}$$

Table 7-2 provides a comparison between some values of G and the corresponding values of G [dB]. Even though decibels are defined for power ratios, they can sometimes be used to represent other quantities. For example, if $P_1 = V_1^2/R$ is the power dissipated in a resistor R with voltage V_1 across it at time t_1, and $P_2 = V_2^2/R$ is the power dissipated in the same resistor at time t_2, then

$$\begin{aligned} G\ [\text{dB}] &= 10 \log \left(\frac{P_1}{P_2}\right) \\ &= 10 \log \left(\frac{V_1^2/R}{V_2^2/R}\right) \\ &= 20 \log \left(\frac{V_1}{V_2}\right) \\ &= 20 \log(g) \triangleq g\ [\text{dB}], \end{aligned} \tag{7.112}$$

where $g = V_1/V_2$ is the voltage ratio. *Note that for voltage (or current) ratios the scale factor is 20 rather than 10,* which results in G [dB] = g [dB].

Table 7-2: Power ratios in natural numbers and in decibels.

G	G [dB]
10^x	$10x$ dB
4	6 dB
2	3 dB
1	0 dB
0.5	−3 dB
0.25	−6 dB
0.1	−10 dB
10^{-3}	−30 dB

The ***attenuation rate***, representing the rate of decrease of the magnitude of $\mathbf{S}_{\text{av}}(z)$ as a function of propagation distance, is defined as

$$\begin{aligned} A &= 10 \log \left[\frac{S_{\text{av}}(z)}{S_{\text{av}}(0)}\right] \\ &= 10 \log(e^{-2\alpha z}) \\ &= -20\alpha z \log e \\ &= -8.68\alpha z = -\alpha\ [\text{dB/m}]\ z \quad (\text{dB}), \end{aligned} \tag{7.113}$$

where

$$\alpha\ [\text{dB/m}] \triangleq 8.68\alpha\ [\text{Np/m}]. \tag{7.114}$$

We also note that, since $\mathbf{S}_{\text{av}}(z)$ is directly proportional to $|\mathbf{E}(z)|^2$,

$$A = 10 \log \left[\frac{|E(z)|^2}{|E(0)|^2}\right] = 20 \log \left[\frac{|E(z)|}{|E(0)|}\right] \quad (\text{dB}). \tag{7.115}$$

Example 7-6 **Power Received by a Submarine Antenna**

A submarine at a depth of 200 m uses a wire antenna to receive signal transmissions at 1 kHz. Determine the power density incident upon the submarine antenna due to the EM wave of Example 7-4.

INTEL-1014
U.S. Patent 7,151,430

Solution: From Example 7-4, $|E_0| = |E_{x0}| = 4.44$ (mV/m), $\alpha = 0.126$ (Np/m), and $\eta_c = 0.044\angle 45°$ (Ω). Application of Eq. (7.109) gives

$$\begin{aligned}\mathbf{S}_{av}(z) &= \hat{\mathbf{z}}\frac{|E_0|^2}{2|\eta_c|}e^{-2\alpha z}\cos\theta_\eta \\ &= \hat{\mathbf{z}}\frac{(4.44\times10^{-3})^2}{2\times0.044}e^{-0.252z}\cos 45° \\ &= \hat{\mathbf{z}}\,0.16e^{-0.252z} \quad (\text{mW/m}^2).\end{aligned}$$

At $z = 200$ m, the incident power density is

$$\begin{aligned}\mathbf{S}_{av} &= \hat{\mathbf{z}}(0.16\times10^{-3}e^{-0.252\times200}) \\ &= 2.1\times10^{-26} \quad (\text{W/m}^2). \blacksquare\end{aligned}$$

EXERCISE 7.10 Convert the following values of the power ratio G from natural numbers to decibels: (a) 2.3, (b) 4×10^3, (c) 3×10^{-2}.

Ans. (a) 3.6 dB, (b) 36 dB, (c) -15.2 dB.

EXERCISE 7.11 Find the voltage ratio g in natural units corresponding to the following decibel values of the power ratio G: (a) 23 dB, (b) -14 dB, (c) -3.6 dB.

Ans. (a) 14.13, (b) 0.2, (c) 0.66.

CHAPTER HIGHLIGHTS

- A spherical wave radiated by a source becomes approximately a uniform plane wave at large distances from the source.
- The electric and magnetic fields of a transverse electromagnetic (TEM) wave are orthogonal to each other, and both are perpendicular to the direction of wave travel.
- The magnitudes of the electric and magnetic fields of a TEM wave are related by the intrinsic impedance of the medium.
- Wave polarization describes the shape and locus of the tip of the **E** vector at a given point in space as a function of time. The polarization state, which may be linear, circular, or elliptical, is governed by the ratio of the magnitudes of and the difference in phase between the two orthogonal components of the electric field vector.
- Media are classified as lossless, low-loss, quasi-conducting, or good conducting on the basis of the ratio $\varepsilon''/\varepsilon' = \sigma/\omega\varepsilon$.
- Unlike the d-c case, wherein the current flowing through a wire is distributed uniformly across its cross section, in the a-c case most of the current is concentrated along the outer perimeter of the wire.
- Power density carried by a plane EM wave traveling in an unbounded medium is akin to the power carried by the voltage/current wave on a transmission line.

GLOSSARY OF IMPORTANT TERMS

Provide definitions or explain the meaning of the following terms:

guided medium
unbounded media
spherical wave
uniform plane wave
complex permittivity ε_c
wavenumber k
TEM wave
intrinsic impedance η
wave polarization
elliptical polarization
circular polarization
linear polarization
LHC and RHC polarizations
attenuation constant α
phase constant β
skin depth δ_s
low-loss dielectric
quasi-conductor
good conductor

INTEL-1014
U.S. Patent 7,151,430

internal or surface impedance
surface resistance R_s
d-c and a-c resistances
Poynting vector $\mathbf{S}$
average power density $\mathbf{S}_{av}$

PROBLEMS

Section 7-2: Propagation in Lossless Media

7.1* The magnetic field of a wave propagating through a certain nonmagnetic material is given by

$$\mathbf{H} = \hat{\mathbf{z}}\, 50 \cos(10^9 t - 5y) \quad \text{(mA/m)}$$

Find the following:
(a) The direction of wave propagation.
(b) The phase velocity.
(c) The wavelength in the material.
(d) The relative permittivity of the material.
(e) The electric field phasor.

7.2 Write general expressions for the electric and magnetic fields of a 1-GHz sinusoidal plane wave traveling in the $+y$-direction in a lossless nonmagnetic medium with relative permittivity $\varepsilon_r = 9$. The electric field is polarized along the x-direction, its peak value is 3 V/m, and its intensity is 2 V/m at $t = 0$ and $y = 2$ cm.

7.3* The electric field phasor of a uniform plane wave is given by $\tilde{\mathbf{E}} = \hat{\mathbf{y}}\, 10e^{j0.2z}$ (V/m). If the phase velocity of the wave is 1.5×10^8 m/s and the relative permeability of the medium is $\mu_r = 2.4$, find the following:
(a) The wavelength.
(b) The frequency f of the wave.
(c) The relative permittivity of the medium.
(d) The magnetic field $\mathbf{H}(z, t)$.

*Answer(s) available in Appendix D.
Solution available in CD-ROM.

7.4 The electric field of a plane wave propagating in a nonmagnetic material is given by

$$\mathbf{E} = [\hat{\mathbf{y}}\, 3 \sin(2\pi \times 10^7 t - 0.4\pi x) + \hat{\mathbf{z}}\, 4 \cos(2\pi \times 10^7 t - 0.4\pi x)] \quad \text{(V/m)}$$

Determine:
(a) The wavelength.
(b) ε_r.
(c) $\mathbf{H}$.

7.5* A wave radiated by a source in air is incident upon a soil surface, whereupon a part of the wave is transmitted into the soil medium. If the wavelength of the wave is 30 cm in air and 15 cm in the soil medium, what is the soil's relative permittivity? Assume the soil to be a very low-loss medium.

7.6 The electric field of a plane wave propagating in a lossless, nonmagnetic, dielectric material with $\varepsilon_r = 2.56$ is given by

$$\mathbf{E} = \hat{\mathbf{y}}\, 20 \cos(8\pi \times 10^9 t - kz) \quad \text{(V/m)}$$

Determine:
(a) f, u_p, λ, k, and η.
(b) The magnetic field $\mathbf{H}$.

Section 7-3: Wave Polarization

7.7* An RHC-polarized wave with a modulus of 2 (V/m) is traveling in free space in the negative z-direction. Write the expression for the wave's electric field vector, given that the wavelength is 6 cm.

7.8 For a wave characterized by the electric field

$$\mathbf{E}(z, t) = \hat{\mathbf{x}} a_x \cos(\omega t - kz) + \hat{\mathbf{y}} a_y \cos(\omega t - kz + \delta)$$

identify the polarization state, determine the polarization angles (γ, χ), and sketch the locus of $\mathbf{E}(0, t)$ for each of the following cases:
(a) $a_x = 3$ V/m, $a_y = 4$ V/m, and $\delta = 0$
(b) $a_x = 3$ V/m, $a_y = 4$ V/m, and $\delta = 180°$
(c) $a_x = 3$ V/m, $a_y = 3$ V/m, and $\delta = 45°$
(d) $a_x = 3$ V/m, $a_y = 4$ V/m, and $\delta = -135°$

INTEL-1014
U.S. Patent 7,151,430

7.9* The electric field of a uniform plane wave propagating in free space is given by

$$\tilde{\mathbf{E}} = (\hat{\mathbf{x}} + j\hat{\mathbf{y}})20e^{-j\pi z/6} \quad \text{(V/m)}$$

Specify the modulus and direction of the electric field intensity at the $z = 0$ plane at $t = 0$, 5, and 10 ns.

7.10 A linearly polarized plane wave of the form $\tilde{\mathbf{E}} = \hat{\mathbf{x}}a_x e^{-jkz}$ can be expressed as the sum of an RHC polarized wave with magnitude a_R, and an LHC polarized wave with magnitude a_L. Prove this statement by finding expressions for a_R and a_L in terms of a_x.

7.11* The electric field of an elliptically polarized plane wave is given by

$$\mathbf{E}(z,t) = [-\hat{\mathbf{x}}\,10\sin(\omega t - kz - 60°) + \hat{\mathbf{y}}\,20\cos(\omega t - kz)] \quad \text{(V/m)}$$

Determine the following:
(a) The polarization angles (γ, χ).
(b) The direction of rotation.

7.12 Compare the polarization states of each of the following pairs of plane waves:
(a) Wave 1: $\mathbf{E}_1 = \hat{\mathbf{x}}2\cos(\omega t - kz) + \hat{\mathbf{y}}2\sin(\omega t - kz)$.
Wave 2: $\mathbf{E}_2 = \hat{\mathbf{x}}2\cos(\omega t + kz) + \hat{\mathbf{y}}2\sin(\omega t + kz)$.
(b) Wave 1: $\mathbf{E}_1 = \hat{\mathbf{x}}2\cos(\omega t - kz) - \hat{\mathbf{y}}2\sin(\omega t - kz)$.
Wave 2: $\mathbf{E}_2 = \hat{\mathbf{x}}2\cos(\omega t + kz) - \hat{\mathbf{y}}2\sin(\omega t + kz)$.

7.13 Plot the locus of $\mathbf{E}(0, t)$ for a plane wave with

$$\mathbf{E}(z,t) = \hat{\mathbf{x}}\sin(\omega t + kz) + \hat{\mathbf{y}}\,2\cos(\omega t + kz)$$

Determine the polarization state from your plot.

Sections 7-4: Propagation in a Lossy Medium

7.14 For each of the following combinations of parameters, determine if the material is a low-loss dielectric, a quasi-conductor, or a good conductor, and then calculate α, β, λ, u_p, and η_c:
(a) Glass with $\mu_r = 1$, $\varepsilon_r = 5$, and $\sigma = 10^{-12}$ S/m at 10 GHz.
(b) Animal tissue with $\mu_r = 1$, $\varepsilon_r = 12$, and $\sigma = 0.3$ S/m at 100 MHz.
(c) Wood with $\mu_r = 1$, $\varepsilon_r = 3$, and $\sigma = 10^{-4}$ S/m at 1 kHz.

7.15 Dry soil is characterized by $\varepsilon_r = 2.5$, $\mu_r = 1$, and $\sigma = 10^{-4}$ (S/m). At each of the following frequencies, determine if dry soil may be considered a good conductor, a quasi-conductor, or a low-loss dielectric, and then calculate α, β, λ, u_p, and η_c:
(a) 60 Hz
(b) 1 kHz
(c) 1 MHz
(d) 1 GHz

7.16 In a medium characterized by $\varepsilon_r = 9$, $\mu_r = 1$, and $\sigma = 0.1$ S/m, determine the phase angle by which the magnetic field leads the electric field at 100 MHz.

7.17 Generate a plot for the skin depth δ_s versus frequency for seawater for the range from 1 kHz to 10 GHz (use log–log scales). The constitutive parameters of seawater are $\mu_r = 1$, $\varepsilon_r = 80$, and $\sigma = 4$ S/m.

7.18 Ignoring reflection at the air–soil boundary, if the amplitude of a 2-GHz incident wave is 10 V/m at the surface of a wet soil medium, at what depth will it be down to 1 mV/m? Wet soil is characterized by $\mu_r = 1$, $\varepsilon_r = 16$, and $\sigma = 5 \times 10^{-4}$ S/m.

7.19* The skin depth of a certain nonmagnetic conducting material is 2 μm at 5 GHz. Determine the phase velocity in the material.

7.20 Based on wave attenuation and reflection measurements conducted at 1 MHz, it was determined that the intrinsic impedance of a certain medium is $28.1\angle 45°$ (Ω) and the skin depth is 5 m. Determine the following:

INTEL-1014
U.S. Patent 7,151,430

(a) The conductivity of the material.
(b) The wavelength in the medium.
(c) The phase velocity.

7.21* The electric field of a plane wave propagating in a nonmagnetic medium is given by

$$\mathbf{E} = \hat{\mathbf{z}}\, 25e^{-30x}\cos(2\pi \times 10^9 t - 40x) \quad \text{(V/m)}$$

Obtain the corresponding expression for $\mathbf{H}$.

Section 7-5: Current Flow in Conductors

7.22 In a nonmagnetic, lossy, dielectric medium, a 300-MHz plane wave is characterized by the magnetic field phasor

$$\tilde{\mathbf{H}} = (\hat{\mathbf{x}} - j4\hat{\mathbf{z}})e^{-2y}e^{-j9y} \quad \text{(A/m)}$$

Obtain time-domain expressions for the electric and magnetic field vectors.

7.23* A rectangular copper block is 30 cm in height (along z). In response to a wave incident upon the block from above, a current is induced in the block in the positive x-direction. Determine the ratio of the a-c resistance of the block to its d-c resistance at 1 kHz. The relevant properties of copper are given in Appendix B.

7.24 The inner and outer conductors of a coaxial cable have radii of 0.5 cm and 1 cm, respectively. The conductors are made of copper with $\varepsilon_r = 1$, $\mu_r = 1$, and $\sigma = 5.8 \times 10^7$ S/m, and the outer conductor is 0.1 cm thick. At 10 MHz:
(a) Are the conductors thick enough to be considered infinitely thick as far as the flow of current through them is concerned?
(b) Determine the surface resistance R_s.
(c) Determine the a-c resistance per unit length of the cable.

Section 7-6: EM Power Density

7.25* The magnetic field of a plane wave traveling in air is given by $\mathbf{H} = \hat{\mathbf{x}}\, 25\sin(2\pi \times 10^7 t - ky)$ (mA/m). Determine the average power density carried by the wave.

7.26 A wave traveling in a nonmagnetic medium with $\varepsilon_r = 9$ is characterized by an electric field given by

$$\mathbf{E} = [\hat{\mathbf{y}}\, 3\cos(\pi \times 10^7 t + kx) - \hat{\mathbf{z}}\, 2\cos(\pi \times 10^7 t + kx)] \quad \text{(V/m)}$$

Determine the direction of wave travel and average power density carried by the wave.

7.27* The electric-field phasor of a uniform plane wave traveling downward in water is given by

$$\tilde{\mathbf{E}} = \hat{\mathbf{x}}\, 10e^{-0.2z}e^{-j0.2z} \quad \text{(V/m)}$$

where $\hat{\mathbf{z}}$ is the downward direction and $z = 0$ is the water surface. If $\sigma = 4$ S/m,
(a) Obtain an expression for the average power density.
(b) Determine the attenuation rate.
(c) Determine the depth at which the power density has been reduced by 40 dB.

7.28 The amplitudes of an elliptically polarized plane wave traveling in a lossless, nonmagnetic medium with $\varepsilon_r = 4$ are $H_{y0} = 6$ (mA/m) and $H_{z0} = 8$ (mA/m). Determine the average power flowing through an aperture in the y–z plane if its area is 20 m^2.

7.29* A wave traveling in a lossless, nonmagnetic medium has an electric field amplitude of 24.56 V/m and an average power density of 4 W/m^2. Determine the phase velocity of the wave.

7.30 At microwave frequencies, the power density considered safe for human exposure is 1 (mW/cm^2). A radar radiates a wave with an electric field amplitude E that decays with distance as $E(R) = (3,000/R)$ (V/m), where R is the distance in meters. What is the radius of the unsafe region?

INTEL-1014
U.S. Patent 7,151,430

7.31 Consider the imaginary rectangular box shown in Fig. 7-19.

(a) Determine the net power flux $P(t)$ entering the box due to a plane wave in air given by

$$\mathbf{E} = \hat{\mathbf{x}} E_0 \cos(\omega t - ky) \quad \text{(V/m)}$$

(b) Determine the net time-average power entering the box.

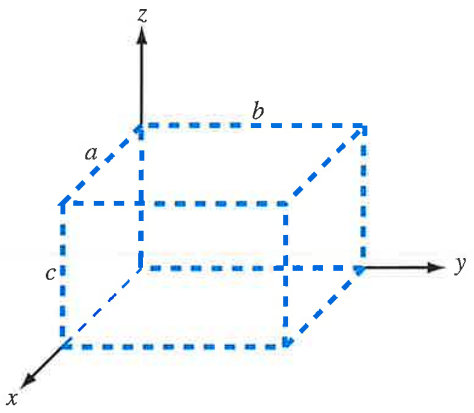


Figure 7-19: Imaginary rectangular box of Problems 7.31 and 7.32.

7.32 Repeat Problem 7.31 for a wave traveling in a lossy medium in which

$$\mathbf{E} = \hat{\mathbf{x}}\, 100 e^{-30y} \cos(2\pi \times 10^9 t - 40y) \quad \text{(V/m)}$$

$$\mathbf{H} = -\hat{\mathbf{z}}\, 0.64 e^{-30y} \cos(2\pi \times 10^9 t - 40y - 36.85°) \quad \text{(A/m)}$$

The box has dimensions $A = 1$ cm, $b = 2$ cm, and $c = 0.5$ cm.

7.33 Given a wave with

$$\mathbf{E} = \hat{\mathbf{x}} E_0 \cos(\omega t - kz)$$

calculate:

(a) The time-average electric energy density

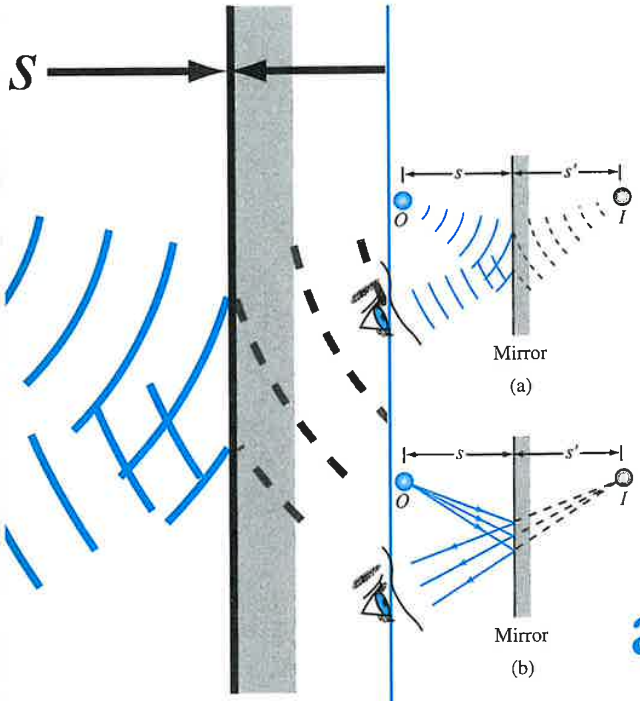
$$(w_e)_{av} = \frac{1}{T}\int_0^T w_e\, dt = \frac{1}{2T}\int_0^T \varepsilon E^2\, dt$$

(b) The time-average magnetic energy density

$$(w_m)_{av} = \frac{1}{T}\int_0^T w_m\, dt = \frac{1}{2T}\int_0^T \mu H^2\, dt$$

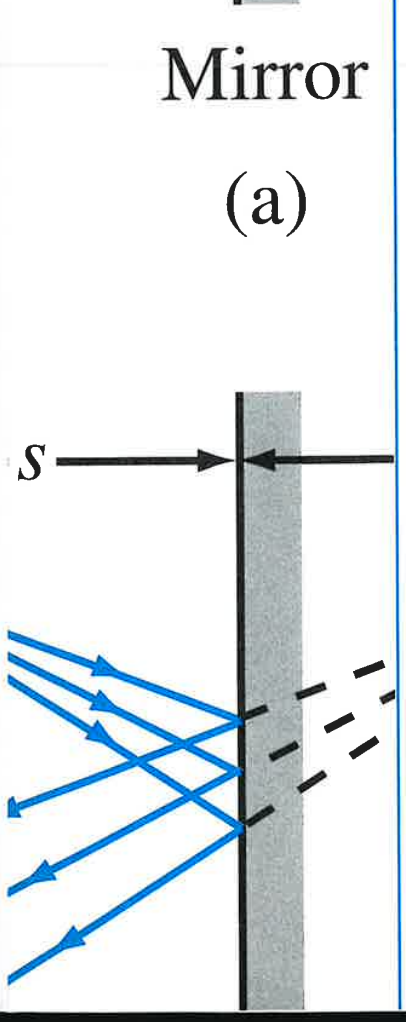
(c) Show that $(w_e)_{av} = (w_m)_{av}$.

INTEL-1014
U.S. Patent 7,151,430



CHAPTER 8

Wave Reflection and Transmission, and Geometric Optics



EM Waves at Boundaries

8-1 Wave Reflection and Transmission at Normal Incidence

8-2 Snell's Laws

8-3 Fiber Optics

8-4 Wave Reflection and Transmission at Oblique Incidence

8-5 Reflectivity and Transmissivity

8-6 Geometric Optics

8-7 Images Formed by Mirrors

8-8 Imaged Formed by Spherical Lenses

INTEL-1014
U.S. Patent 7,151,430

EM WAVES AT BOUNDARIES

The sketch in Fig. 8-1 depicts the propagation path that a signal travels between a shipboard transmitter and a receiver on a submerged submarine. Let us use this communication system to examine the wave-related processes that take place along the signal path. Starting with the transmitter (denoted Tx for short in Fig. 8-1), the signal travels along a transmission line to the antenna. The relationship between the transmitter (generator) output power, P_t, and the power supplied to the antenna is governed by the transmission-line equations given in Chapter 2. If the transmission line is approximately lossless and if it is properly matched to the transmitter antenna, then all of P_t is delivered to the antenna. The next wave-related process is that of radiation; that is, converting the guided wave provided to the antenna by the transmission line into a spherical wave radiated outward into space. The radiation process is the subject of Chapter 9. From point 1, denoting the location of the shipboard antenna, to point 2, denoting the point of incidence of the wave onto the water's surface, the signal is governed by the equations characterizing wave propagation in a lossless medium, which we covered in Chapter 7. As the wave impinges upon the air–water boundary, a part of it gets reflected by the surface and another part gets transmitted across the boundary into the water medium. The transmitted part undergoes refraction, wherein the direction of wave travel moves closer toward the vertical. The reflection and transmission processes are treated in this chapter. Wave travel from point 3, representing a point just below the water surface, to point 4, denoting the location of the submarine antenna, is subject to the laws of wave propagation in a lossy medium, which also were treated in Chapter 7. The final step involves intercepting the wave incident upon the receiver antenna and converting its power into a received power, P_{rec}, for delivery via a transmission line to the receiver. The receiving properties of antennas are covered in Chapter 9. In summary, then, each wave-related aspect of the transmission process depicted in Fig. 8-1, starting with the transmitter and ending up with the receiver, is treated in some section or chapter in this book.

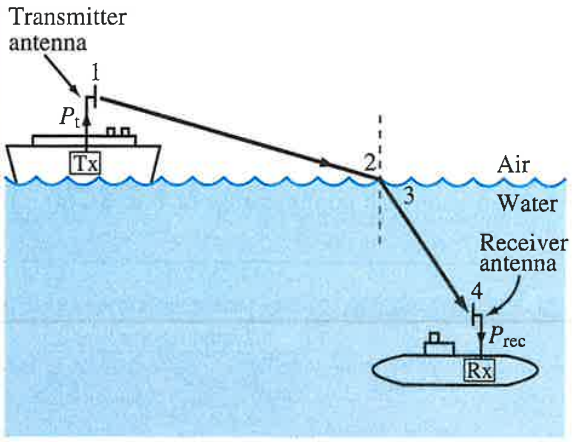


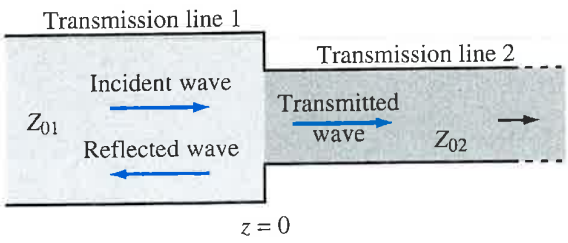
Figure 8-1: Signal path between a shipboard transmitter (Tx) and a submarine receiver (Rx).

This chapter begins with examinations of the reflection and transmission properties of plane waves incident upon planar boundaries and concludes with sections on geometric optics, in which we discuss the imaging properties of mirrors and lenses. The in-between topics include discussions of power relations, and fiber optics.

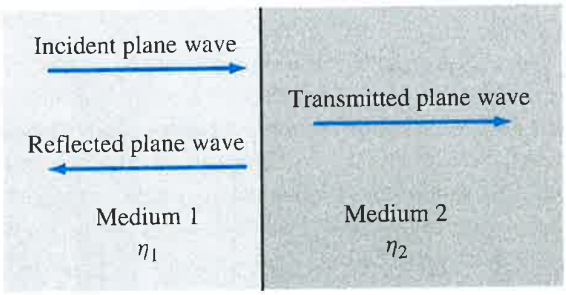
INTEL-1014
U.S. Patent 7,151,430

8-1 Wave Reflection and Transmission at Normal Incidence

We know from Chapter 2 that when a guided wave traveling along a transmission line encounters an impedance discontinuity, such as that shown in Fig. 8-2(a) at the boundary between two lines with different characteristic impedances, the incident wave is partly reflected back toward the source and partly transmitted across the boundary into the second line. A similar process applies to a uniform plane wave propagating in an ***unbounded*** medium when it encounters a boundary. In fact, the situation depicted in Fig. 8-2(b) is exactly analogous to the transmission-line configuration of Fig. 8-2(a). The boundary conditions governing the relationships between the electric and magnetic fields of the incident, reflected, and transmitted waves in Fig. 8-2(b) are similar to those we developed in Chapter 2 for the voltages and currents of the corresponding waves on the transmission line.



(a) Boundary between transmission lines



(b) Boundary between different media

Figure 8-2: Discontinuity between two different transmission lines is analogous to that between two dissimilar media.

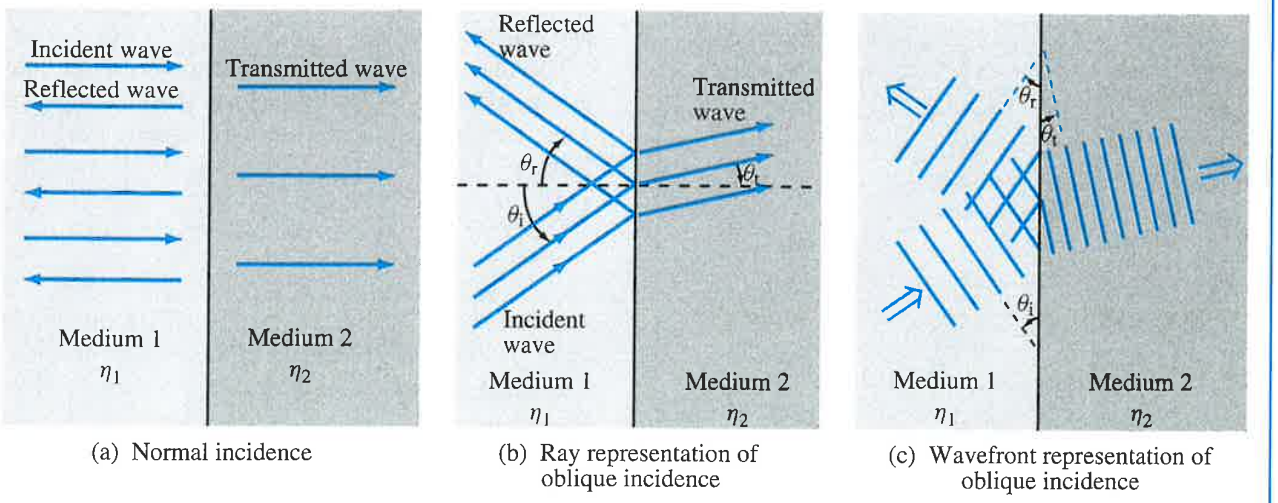
For convenience, we divide our treatment of wave reflection by and transmission through planar boundaries into two parts: in this section we confine our discussion to the normal-incidence case depicted in Fig. 8-3(a), and in Sections 8-2 to 8-4 we will examine the more general oblique-incidence situation depicted in Fig. 8-3(b). We will show the basis for the analogy between the transmission-line and plane-wave configurations so that we may use transmission-line equivalent models for solving plane-wave problems.

Before we proceed with our treatment, however, we should explain the relationship between rays and wavefronts, as both will be used to represent the propagation of electromagnetic waves. A ***ray*** is a line drawn to represent the direction of flow of electromagnetic energy carried by the wave, and therefore it is parallel to the propagation unit vector $\hat{\mathbf{k}}$ and orthogonal to the ***wavefront***. The ray representation of wave incidence, reflection, and transmission shown in Fig. 8-3(b) is equivalent to the wavefront representation depicted in Fig. 8-3(c). The two representations are complimentary; the ray representation is easier to use in graphical illustrations, whereas the wavefront representation provides greater physical insight when examining what happens to a wave when it encounters a discontinuous boundary. Both representations will be used in our forthcoming discussions.

8-1.1 Boundary between Lossless Media

The planar boundary located at $z = 0$ in Fig. 8-4(a) separates two lossless, homogeneous, dielectric media. Medium 1, defined for $z \leq 0$, is characterized by (ε_1, μ_1), and medium 2, defined for $z \geq 0$, is characterized by (ε_2, μ_2). In medium 1, an incident x-polarized plane wave with fields $(\mathbf{E}^i, \mathbf{H}^i)$ is traveling in direction

INTEL-1014
U.S. Patent 7,151,430



(a) Normal incidence (b) Ray representation of oblique incidence (c) Wavefront representation of oblique incidence

Figure 8-3: Ray representation of wave reflection and transmission at (a) normal incidence and (b) oblique incidence, and (c) wavefront representation of oblique incidence.

$\hat{\mathbf{k}}_i = \hat{\mathbf{z}}$ toward medium 2. Reflection and transmission at the discontinuous boundary result in a reflected wave ($\mathbf{E}^r, \mathbf{H}^r$) with $\hat{\mathbf{k}}_r = -\hat{\mathbf{z}}$ in medium 1 and a transmitted wave ($\mathbf{E}^t, \mathbf{H}^t$) with $\hat{\mathbf{k}}_t = \hat{\mathbf{z}}$ in medium 2. On the basis of the formulations developed in Sections 7-2 and 7-3 for characterizing the fields of a TEM wave, the three waves can be described in phasor form by:

Incident Wave

$$\widetilde{\mathbf{E}}^i(z) = \hat{\mathbf{x}} E_0^i e^{-jk_1 z}, \tag{8.1a}$$

$$\widetilde{\mathbf{H}}^i(z) = \hat{\mathbf{z}} \times \frac{\widetilde{\mathbf{E}}^i(z)}{\eta_1} = \hat{\mathbf{y}} \frac{E_0^i}{\eta_1} e^{-jk_1 z}. \tag{8.1b}$$

Reflected Wave

$$\widetilde{\mathbf{E}}^r(z) = \hat{\mathbf{x}} E_0^r e^{jk_1 z}, \tag{8.2a}$$

$$\widetilde{\mathbf{H}}^r(z) = (-\hat{\mathbf{z}}) \times \frac{\widetilde{\mathbf{E}}^r(z)}{\eta_1} = -\hat{\mathbf{y}} \frac{E_0^r}{\eta_1} e^{jk_1 z}. \tag{8.2b}$$

Transmitted Wave

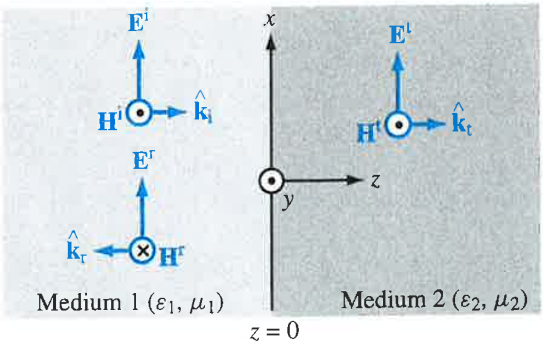
$$\widetilde{\mathbf{E}}^t(z) = \hat{\mathbf{x}} E_0^t e^{-jk_2 z}, \tag{8.3a}$$

$$\widetilde{\mathbf{H}}^t(z) = \hat{\mathbf{z}} \times \frac{\widetilde{\mathbf{E}}^t(z)}{\eta_2} = \hat{\mathbf{y}} \frac{E_0^t}{\eta_2} e^{-jk_2 z}. \tag{8.3b}$$

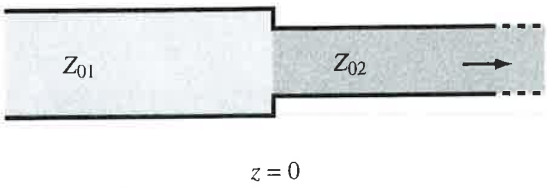
The quantities E_0^i, E_0^r, and E_0^t are, respectively, the amplitudes of the incident, reflected, and transmitted electric fields, all specified at $t = 0$ and $z = 0$ (the boundary between the two media). The wavenumber and intrinsic impedance of medium 1 are $k_1 = \omega\sqrt{\mu_1\varepsilon_1}$ and $\eta_1 = \sqrt{\mu_1/\varepsilon_1}$ and, similarly, $k_2 = \omega\sqrt{\mu_2\varepsilon_2}$ and $\eta_2 = \sqrt{\mu_2/\varepsilon_2}$ for medium 2.

The amplitude E_0^i is related to the source responsible for generating the incident wave, and therefore it is assumed to be a known quantity. Our goal is to relate E_0^r and E_0^t each to E_0^i. We do so by applying boundary conditions for $\widetilde{\mathbf{E}}$ and $\widetilde{\mathbf{H}}$ at $z = 0$. According to Table 6-2, the tangential component of $\mathbf{E}$ is always continuous across a boundary between two contiguous media, and in the

INTEL-1014
U.S. Patent 7,151,430



(a) Boundary between dielectric media



(b) Transmission-line analogue

Figure 8-4: The two dielectric media separated by the x–y plane in (a) can be represented by the transmission-line analogue in (b).

absence of current sources at the boundary, the tangential component of **H** also is continuous across the boundary. In the present case, both **E** and **H** of the normally incident wave are tangential to the boundary. Consequently, since no free charges or currents exist at the boundary, the fields of the reflected and transmitted waves will have tangential components only. In Fig. 8-4(a) and correspondingly in Eqs. (8.2a) and (8.3a), we arbitrarily chose the directions of $\widetilde{\mathbf{E}}^{\mathrm{r}}$ and $\widetilde{\mathbf{E}}^{\mathrm{t}}$ to coincide with the direction of $\widetilde{\mathbf{E}}^{\mathrm{i}}$ along the positive x-direction. Their true directions, relative to the assumed directions, will be determined by the polarities of the amplitudes E_0^{r} and E_0^{t}. As we will see shortly, both the magnitudes and polarities of these two amplitudes are governed by the values of the intrinsic impedances of the two media, η_1 and η_2.

The total electric field $\widetilde{\mathbf{E}}_1(z)$ in medium 1 is the sum of the electric fields of the incident and reflected waves, and a similar statement applies to the magnetic field $\widetilde{\mathbf{H}}_1(z)$. Hence,

Medium 1

$$\begin{aligned}\widetilde{\mathbf{E}}_1(z) &= \widetilde{\mathbf{E}}^{\mathrm{i}}(z) + \widetilde{\mathbf{E}}^{\mathrm{r}}(z)\\ &= \hat{\mathbf{x}}(E_0^{\mathrm{i}} e^{-jk_1 z} + E_0^{\mathrm{r}} e^{jk_1 z}), \qquad (8.4a)\\ \widetilde{\mathbf{H}}_1(z) &= \widetilde{\mathbf{H}}^{\mathrm{i}}(z) + \widetilde{\mathbf{H}}^{\mathrm{r}}(z)\\ &= \hat{\mathbf{y}}\frac{1}{\eta_1}(E_0^{\mathrm{i}} e^{-jk_1 z} - E_0^{\mathrm{r}} e^{jk_1 z}). \qquad (8.4b)\end{aligned}$$

With only the transmitted wave present in medium 2, the fields are

Medium 2

$$\widetilde{\mathbf{E}}_2(z) = \widetilde{\mathbf{E}}^{\mathrm{t}}(z) = \hat{\mathbf{x}} E_0^{\mathrm{t}} e^{-jk_2 z}, \qquad (8.5a)$$

$$\widetilde{\mathbf{H}}_2(z) = \widetilde{\mathbf{H}}^{\mathrm{t}}(z) = \hat{\mathbf{y}}\frac{E_0^{\mathrm{t}}}{\eta_2} e^{-jk_2 z}. \qquad (8.5b)$$

At the boundary ($z = 0$), the tangential components of the electric and magnetic fields are continuous. Hence,

$$\widetilde{\mathbf{E}}_1(0) = \widetilde{\mathbf{E}}_2(0) \quad \text{or} \quad E_0^{\mathrm{i}} + E_0^{\mathrm{r}} = E_0^{\mathrm{t}}, \qquad (8.6a)$$

$$\widetilde{\mathbf{H}}_1(0) = \widetilde{\mathbf{H}}_2(0) \quad \text{or} \quad \frac{E_0^{\mathrm{i}}}{\eta_1} - \frac{E_0^{\mathrm{r}}}{\eta_1} = \frac{E_0^{\mathrm{t}}}{\eta_2}. \qquad (8.6b)$$

Simultaneous solutions for E_0^{r} and E_0^{t} in terms of E_0^{i} give

$$E_0^{\mathrm{r}} = \left(\frac{\eta_2 - \eta_1}{\eta_2 + \eta_1}\right) E_0^{\mathrm{i}} = \Gamma E_0^{\mathrm{i}}, \qquad (8.7a)$$

$$E_0^{\mathrm{t}} = \left(\frac{2\eta_2}{\eta_2 + \eta_1}\right) E_0^{\mathrm{i}} = \tau E_0^{\mathrm{i}}, \qquad (8.7b)$$

INTEL-1014
U.S. Patent 7,151,430

where

$$\Gamma = \frac{E_0^r}{E_0^i} = \frac{\eta_2 - \eta_1}{\eta_2 + \eta_1} \quad \text{(normal incidence)}, \tag{8.8a}$$

$$\tau = \frac{E_0^t}{E_0^i} = \frac{2\eta_2}{\eta_2 + \eta_1} \quad \text{(normal incidence)}. \tag{8.8b}$$

The quantities Γ and τ are called the ***reflection coefficient*** and ***transmission coefficient***, respectively. For lossless dielectric media, η_1 and η_2 are real quantities; consequently, both Γ and τ are real also. As we will see in Section 8-1.4, the expressions given by Eqs. (8.8a) and (8.8b) are equally applicable when the media are conductive, but in that case η_1 and η_2 may be complex, and hence Γ and τ may be complex as well. From Eqs. (8.8a) and (8.8b), it can be easily shown that Γ and τ are interrelated by the simple formula

$$\tau = 1 + \Gamma \quad \text{(normal incidence)}. \tag{8.9}$$

For nonmagnetic media,

$$\eta_1 = \frac{\eta_0}{\sqrt{\varepsilon_{r_1}}},$$

$$\eta_2 = \frac{\eta_0}{\sqrt{\varepsilon_{r_2}}},$$

where η_0 is the intrinsic impedance of free space, in which case Eq. (8.8a) may be rewritten as

$$\Gamma = \frac{\sqrt{\varepsilon_{r_1}} - \sqrt{\varepsilon_{r_2}}}{\sqrt{\varepsilon_{r_1}} + \sqrt{\varepsilon_{r_2}}} \quad \text{(nonmagnetic media)}. \tag{8.10}$$

8-1.2 Transmission-Line Analogue

The transmission-line configuration shown in Fig. 8-4(b) consists of a lossless transmission line with characteristic impedance Z_{01}, connected at $z = 0$ to an infinitely long lossless transmission line with characteristic impedance Z_{02}. The input impedance of an infinitely long line is equal to its characteristic impedance. Hence, at $z = 0$, the voltage reflection coefficient (looking toward the boundary from the vantage point of the first line) is

$$\Gamma = \frac{Z_{02} - Z_{01}}{Z_{02} + Z_{01}},$$

which is identical in form to Eq. (8.8a). To show the basis for the analogy between the plane-wave and transmission-line situations, the expressions for the two cases are given in Table 8-1. Comparison of the two columns shows that there is a one-to-one correspondence between the transmission-line parameters ($\widetilde{V}$, $\widetilde{I}$, β, Z_0) and the plane-wave parameters ($\widetilde{\mathbf{E}}$, $\widetilde{\mathbf{H}}$, k, η). This correspondence allows us to use the techniques we developed in Chapter 2, including the Smith-chart method for calculating impedance transformations, to solve plane-wave propagation problems.

Simultaneous presence of incident and reflected waves in a medium, such as medium 1 in Fig. 8-4(a), gives rise to a standing-wave pattern. By analogy with the transmission-line case, the ***standing-wave ratio*** in medium 1 is given by

$$S = \frac{|\widetilde{E}_1|_{\max}}{|\widetilde{E}_1|_{\min}} = \frac{1 + |\Gamma|}{1 - |\Gamma|}. \tag{8.15}$$

If the two media have equal impedances ($\eta_1 = \eta_2$), then $\Gamma = 0$ and $S = 1$, and if medium 2 is a perfect conductor with $\eta_2 = 0$ (which is equivalent to a short-circuited transmission line), then $\Gamma = -1$ and $S = \infty$. The distances from the boundary to where the magnitude of the electric field intensity in medium 1 is at a maximum, denoted $l_{\max}$, are described by the same expression as

INTEL-1014
U.S. Patent 7,151,430

Table 8-1: Analogy between plane-wave equations for normal incidence and transmission-line equations, both under lossless conditions.

Plane Wave [Fig. 8-4(a)]	Transmission Line [Fig. 8-4(b)]
$\widetilde{\mathbf{E}}_1(z) = \hat{\mathbf{x}} E_0^{\mathrm{i}}(e^{-jk_1 z} + \Gamma e^{jk_1 z})$ (8.11a)	$\widetilde{V}_1(z) = V_0^+(e^{-j\beta_1 z} + \Gamma e^{j\beta_1 z})$ (8.11b)
$\widetilde{\mathbf{H}}_1(z) = \hat{\mathbf{y}} \dfrac{E_0^{\mathrm{i}}}{\eta_1}(e^{-jk_1 z} - \Gamma e^{jk_1 z})$ (8.12a)	$\widetilde{I}_1(z) = \dfrac{V_0^+}{Z_{01}}(e^{-j\beta_1 z} - \Gamma e^{j\beta_1 z})$ (8.12b)
$\widetilde{\mathbf{E}}_2(z) = \hat{\mathbf{x}} \tau E_0^{\mathrm{i}} e^{-jk_2 z}$ (8.13a)	$\widetilde{V}_2(z) = \tau V_0^+ e^{-j\beta_2 z}$ (8.13b)
$\widetilde{\mathbf{H}}_2(z) = \hat{\mathbf{y}} \tau \dfrac{E_0^{\mathrm{i}}}{\eta_2} e^{-jk_2 z}$ (8.14a)	$\widetilde{I}_2(z) = \tau \dfrac{V_0^+}{Z_{02}} e^{-j\beta_2 z}$ (8.14b)
$\Gamma = (\eta_2 - \eta_1)/(\eta_2 + \eta_1)$	$\Gamma = (Z_{02} - Z_{01})/(Z_{02} + Z_{01})$
$\tau = 1 + \Gamma$	$\tau = 1 + \Gamma$
$k_1 = \omega\sqrt{\mu_1 \varepsilon_1}$, $k_2 = \omega\sqrt{\mu_2 \varepsilon_2}$	$\beta_1 = \omega\sqrt{\mu_1 \varepsilon_1}$, $\beta_2 = \omega\sqrt{\mu_2 \varepsilon_2}$
$\eta_1 = \sqrt{\mu_1/\varepsilon_1}$, $\eta_2 = \sqrt{\mu_2/\varepsilon_2}$	Z_{01} and Z_{02} depend on transmission-line parameters

that given by Eq. (2.56) for the voltage maxima on a transmission line:

$$-z = l_{\max} = \frac{\theta_{\mathrm{r}} + 2n\pi}{2k_1} = \frac{\theta_{\mathrm{r}}\lambda_1}{4\pi} + \frac{n\lambda_1}{2}, \quad \begin{cases} n = 1, 2, \ldots, & \text{if } \theta_{\mathrm{r}} < 0, \\ n = 0, 1, 2, \ldots, & \text{if } \theta_{\mathrm{r}} \geq 0, \end{cases} \tag{8.16}$$

where $\lambda_1 = 2\pi/k_1$ and θ_{r} is the phase angle of Γ (i.e., $\Gamma = |\Gamma| e^{j\theta_{\mathrm{r}}}$, and θ_{r} is bounded in the range $-\pi < \theta_{\mathrm{r}} \leq \pi$). The spacing between adjacent maxima is $\lambda_1/2$, and the spacing between a maximum and the nearest minimum is $\lambda_1/4$. The electric-field minima occur at

$$l_{\min} = \begin{cases} l_{\max} + \lambda_1/4, & \text{if } l_{\max} < \lambda_1/4, \\ l_{\max} - \lambda_1/4, & \text{if } l_{\max} \geq \lambda_1/4. \end{cases} \tag{8.17}$$

The expressions for $l_{\max}$ and $l_{\min}$ are valid provided that the medium containing the standing-wave pattern is either lossless or a low-loss dielectric, but no restrictions are imposed on the nature of the reflecting medium.

8-1.3 Power Flow in Lossless Media

Medium 1 of Fig. 8-4(a) contains an incident wave and a reflected wave, which together produce the electric and magnetic fields $\widetilde{\mathbf{E}}_1(z)$ and $\widetilde{\mathbf{H}}_1(z)$ given by Eqs. (8.11a) and (8.12a) of Table 8-1. Using Eq. (7.101), the net average power density flowing in medium 1 is

$$\begin{aligned} \mathbf{S}_{\mathrm{av}_1}(z) &= \tfrac{1}{2}\mathrm{Re}[\widetilde{\mathbf{E}}_1(z) \times \widetilde{\mathbf{H}}_1^*(z)] \\ &= \tfrac{1}{2}\mathrm{Re}\left[\hat{\mathbf{x}} E_0^{\mathrm{i}}(e^{-jk_1 z} + \Gamma e^{jk_1 z}) \right. \\ &\quad \left. \times \hat{\mathbf{y}} \frac{E_0^{\mathrm{i}*}}{\eta_1}(e^{jk_1 z} - \Gamma^* e^{-jk_1 z})\right] \\ &= \hat{\mathbf{z}} \frac{|E_0^{\mathrm{i}}|^2}{2\eta_1}(1 - |\Gamma|^2), \end{aligned} \tag{8.18}$$

INTEL-1014
U.S. Patent 7,151,430

which is analogous to Eq. (2.86) for the lossless transmission-line case. The first term in Eq. (8.18) represents the average power density of the incident wave, and the second term (proportional to $|\Gamma|^2$) represents the average power density of the reflected wave. Thus,

$$\mathbf{S}_{\text{av}_1} = \mathbf{S}^{\text{i}}_{\text{av}} + \mathbf{S}^{\text{r}}_{\text{av}}, \tag{8.19a}$$

with

$$\mathbf{S}^{\text{i}}_{\text{av}} = \hat{\mathbf{z}}\,\frac{|E^{\text{i}}_0|^2}{2\eta_1}, \tag{8.19b}$$

$$\mathbf{S}^{\text{r}}_{\text{av}} = -\hat{\mathbf{z}}|\Gamma|^2\frac{|E^{\text{i}}_0|^2}{2\eta_1} = -|\Gamma|^2\mathbf{S}^{\text{i}}_{\text{av}}. \tag{8.19c}$$

Even though Γ is purely real when both media are lossless dielectrics, we chose to treat it as complex, thereby providing in Eq. (8.19c) an expression that is also valid when medium 2 is conducting.

The average power density of the transmitted wave in medium 2 is

$$\begin{aligned}\mathbf{S}_{\text{av}_2}(z) &= \tfrac{1}{2}\mathcal{R}\text{e}[\widetilde{\mathbf{E}}_2(z)\times\widetilde{\mathbf{H}}^*_2(z)]\\ &= \tfrac{1}{2}\mathcal{R}\text{e}\left[\hat{\mathbf{x}}\tau E^{\text{i}}_0 e^{-jk_2z}\times\hat{\mathbf{y}}\tau^*\frac{E^{\text{i}*}_0}{\eta_2}e^{jk_2z}\right]\\ &= \hat{\mathbf{z}}|\tau|^2\frac{|E^{\text{i}}_0|^2}{2\eta_2}.\end{aligned} \tag{8.20}$$

This expression is applicable when both media are lossless, as well as when medium 1 is conducting and only medium 2 is lossless.

Through the use of Eqs. (8.8a) and (8.8b), it can be easily shown that for lossless media (for which Γ and τ are real)

$$\frac{\tau^2}{\eta_2} = \frac{1-\Gamma^2}{\eta_1} \quad \text{(lossless media)}, \tag{8.21}$$

which leads to

$$\mathbf{S}_{\text{av}_1} = \mathbf{S}_{\text{av}_2}.$$

This result is as expected from considerations of power conservation.

Example 8-1 Radar Radome Design

A 10-GHz aircraft radar uses a narrow-beam scanning antenna mounted on a gimbal behind a dielectric radome, as shown in Fig. 8-5. Even though the radome shape is far from planar, it is approximately planar over the narrow extent of the radar beam. If the radome material is a lossless dielectric with $\mu_r = 1$ and $\varepsilon_r = 9$, choose its thickness d such that the radome appears transparent to the radar beam. Mechanical integrity requires d to be greater than 2.3 cm.

Solution: The propagation problem is shown in Fig. 8-6(a) at an expanded scale. The incident wave is approximated as a plane wave propagating in medium 1 (air) with intrinsic impedance η_0, the radome (medium 2) is of thickness d and intrinsic impedance η_r, and medium 3 is semi-infinite with intrinsic impedance η_0. Figure 8-6(b) is an equivalent transmission-line model with $z = 0$ selected to coincide with the outside surface of the radome, and the load impedance $Z_L = \eta_0$ represents the input impedance of the semi-infinite medium.

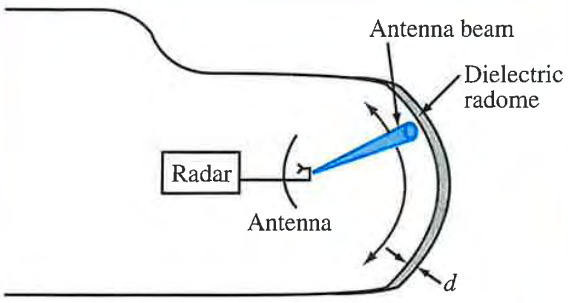


Figure 8-5: Antenna beam "looking" through an aircraft radome of thickness d (Example 8-1).

INTEL-1014
U.S. Patent 7,151,430

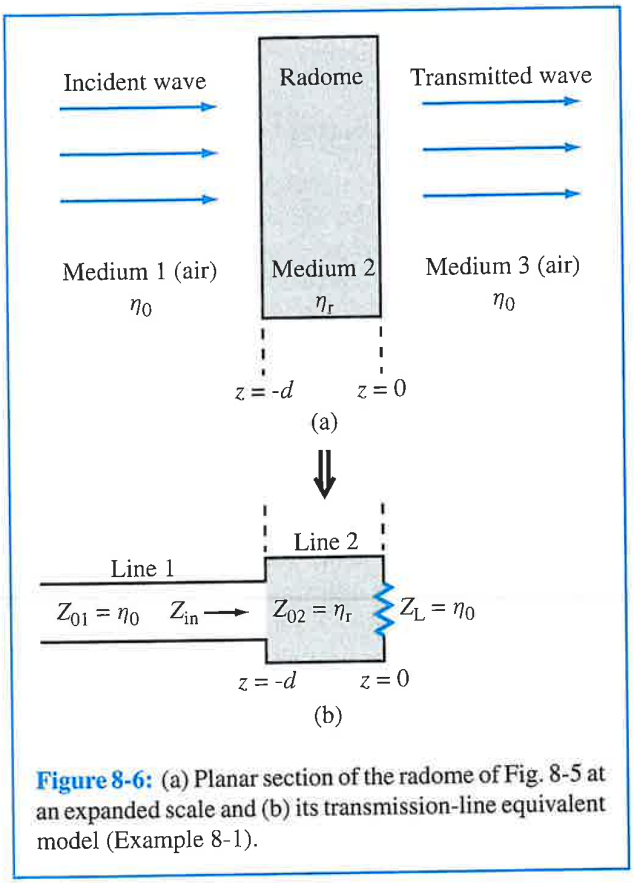


Figure 8-6: (a) Planar section of the radome of Fig. 8-5 at an expanded scale and (b) its transmission-line equivalent model (Example 8-1).

Requiring the radome to "appear" transparent to the incident wave simply means that the reflection coefficient must be zero at $z = -d$, thereby achieving total transmission of the incident power into medium 3. Since $Z_L = \eta_0$ in Fig. 8-6(b), no reflection will take place at $z = -d$ if $Z_{in} = \eta_0$, which can be realized by choosing $d = n\lambda_2/2$ [see Section 2-7.4], where λ_2 is the wavelength in medium 2 and n is a positive integer. At 10 GHz, the wavelength in air is $\lambda_0 = c/f = 3$ cm, and in the radome material

$$\lambda_2 = \frac{\lambda_0}{\sqrt{\varepsilon_r}} = \frac{3 \text{ cm}}{3} = 1 \text{ cm}.$$

Hence, if we choose $d = 5\lambda_2/2 = 2.5$ cm, we will satisfy both the no-reflection and the mechanical integrity requirements. ■

Example 8-2 **Yellow Light Incident upon a Glass Surface**

A beam of yellow light with wavelength of 0.6 μm is normally incident in air upon a glass surface. If the surface is situated in the plane $z = 0$ and the relative permittivity of glass is 2.25, determine:

(a) the locations of the electric field maxima in medium 1 (air),
(b) the standing-wave ratio, and
(c) the fraction of the incident power transmitted into the glass medium.

Solution: (a) We begin by determining the value of η_1, η_2, and Γ:

$$\eta_1 = \sqrt{\frac{\mu_1}{\varepsilon_1}} = \sqrt{\frac{\mu_0}{\varepsilon_0}} \simeq 120\pi \ (\Omega),$$

$$\eta_2 = \sqrt{\frac{\mu_2}{\varepsilon_2}} = \sqrt{\frac{\mu_0}{\varepsilon_0}} \cdot \frac{1}{\sqrt{\varepsilon_r}} \simeq \frac{120\pi}{\sqrt{2.25}} = 80\pi \ (\Omega),$$

$$\Gamma = \frac{\eta_2 - \eta_1}{\eta_2 + \eta_1} = \frac{80\pi - 120\pi}{80\pi + 120\pi} = -0.2.$$

Hence, $|\Gamma| = 0.2$ and $\theta_r = \pi$. From Eq. (8.16), the electric-field magnitude is a maximum at

$$l_{max} = \frac{\theta_r \lambda_1}{4\pi} + n\frac{\lambda_1}{2}$$
$$= \frac{\lambda_1}{4} + n\frac{\lambda_1}{2} \qquad (n = 0, 1, 2, \ldots)$$

with $\lambda_1 = 0.6$ μm.

(b)

$$S = \frac{1 + |\Gamma|}{1 - |\Gamma|} = \frac{1 + 0.2}{1 - 0.2} = 1.5.$$

(c) The fraction of the incident power transmitted into the glass medium is equal to the ratio of the transmitted

INTEL-1014
U.S. Patent 7,151,430

power density, given by Eq. (8.20), to the incident power density, $S_{av}^{i} = |E_0^i|^2/2\eta_1$:

$$\frac{S_{av_2}}{S_{av}^{i}} = \tau^2 \frac{|E_0^i|^2}{2\eta_2} \Bigg/ \left[\frac{|E_0^i|^2}{2\eta_1}\right] = \tau^2 \frac{\eta_1}{\eta_2}.$$

In view of Eq. (8.21),

$$\frac{S_{av_2}}{S_{av}^{i}} = 1 - |\Gamma|^2 = 1 - (0.2)^2 = 0.96, \text{ or } 96\%. \blacksquare$$

8-1.4 Boundary between Lossy Media

In Section 8-1.1 we considered a plane wave in a lossless medium incident normally on a planar boundary of another lossless medium. We will now generalize our expressions to lossy media. In a medium with constitutive parameters $(\varepsilon, \mu, \sigma)$, the propagation parameters of interest are the propagation constant $\gamma = \alpha + j\beta$ and the complex intrinsic impedance η_c. The general expressions for α, β, and η_c are given by Eqs. (7.66a), (7.66b), and (7.70), respectively, and approximate expressions are given in Table 7-1 for the special cases of low-loss media and good conducting media. If medium 1 is characterized by $(\varepsilon_1, \mu_1, \sigma_1)$ and medium 2 by $(\varepsilon_2, \mu_2, \sigma_2)$, as shown in Fig. 8-7, the expressions for the electric and magnetic fields in media 1 and 2 can be obtained from Eqs. (8.11a) through (8.14a) of Table 8-1 by replacing jk with γ and η with η_c everywhere. Thus,

Medium 1

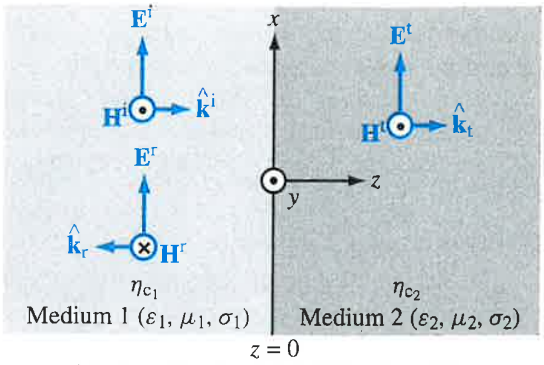
$$\widetilde{\mathbf{E}}_1(z) = \hat{\mathbf{x}} E_0^i (e^{-\gamma_1 z} + \Gamma e^{\gamma_1 z}), \tag{8.22a}$$

$$\widetilde{\mathbf{H}}_1(z) = \hat{\mathbf{y}} \frac{E_0^i}{\eta_{c_1}} (e^{-\gamma_1 z} - \Gamma e^{\gamma_1 z}), \tag{8.22b}$$

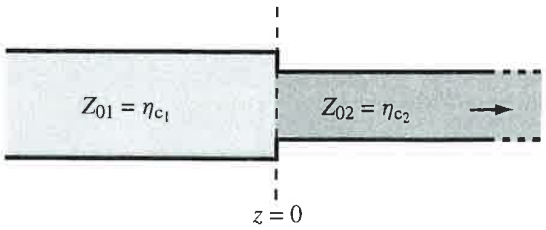
Medium 2

$$\widetilde{\mathbf{E}}_2(z) = \hat{\mathbf{x}} \tau E_0^i e^{-\gamma_2 z}, \tag{8.23a}$$

$$\widetilde{\mathbf{H}}_2(z) = \hat{\mathbf{y}} \tau \frac{E_0^i}{\eta_{c_2}} e^{-\gamma_2 z}, \tag{8.23b}$$



(a) Boundary between dielectric media



(b) Transmission-line analogue

Figure 8-7: Normal incidence at a planar boundary between two lossy media.

where $\gamma_1 = \alpha_1 + j\beta_1$, $\gamma_2 = \alpha_2 + j\beta_2$, and

$$\Gamma = \frac{\eta_{c_2} - \eta_{c_1}}{\eta_{c_2} + \eta_{c_1}}, \tag{8.24a}$$

$$\tau = 1 + \Gamma = \frac{2\eta_{c_2}}{\eta_{c_2} + \eta_{c_1}}. \tag{8.24b}$$

Because η_{c_1} and η_{c_2} are, in general, complex, Γ and τ may be complex as well.

Example 8-3 Normal Incidence on a Metal Surface

A 1-GHz x-polarized TEM wave traveling in the $+z$-direction is incident in air upon a metal surface coincident

INTEL-1014
U.S. Patent 7,151,430

with the x–y plane at $z = 0$. If the amplitude of the electric field of the incident wave is 12 (mV/m) and the metal surface is made of copper with $\mu_r = 1$, $\varepsilon_r = 1$, and $\sigma = 5.8 \times 10^7$ (S/m), obtain expressions for the instantaneous electric and magnetic fields in the air medium. Assume the metal surface to be several skin depths deep.

Solution: In medium 1 (air), $\alpha = 0$,

$$\beta = k_1 = \frac{\omega}{c} = \frac{2\pi \times 10^9}{3 \times 10^8} = \frac{20\pi}{3} \quad \text{(rad/m)},$$

$$\eta_1 = \eta_0 = 377\ (\Omega), \qquad \lambda = \frac{2\pi}{k_1} = 0.3\ \text{m}.$$

At $f = 1$ GHz, copper is an excellent conductor because

$$\frac{\varepsilon''}{\varepsilon'} = \frac{\sigma}{\omega \varepsilon_r \varepsilon_0} = \frac{5.8 \times 10^7}{2\pi \times 10^9 \times (10^{-9}/36\pi)} = 1 \times 10^9 \gg 1.$$

Use of Eq. (7.77c) gives

$$\begin{aligned} \eta_{c_2} &= (1+j)\sqrt{\frac{\pi f \mu}{\sigma}} \\ &= (1+j)\left[\frac{\pi \times 10^9 \times 4\pi \times 10^{-7}}{5.8 \times 10^7}\right]^{1/2} \\ &= 8.25(1+j) \quad (\text{m}\Omega). \end{aligned}$$

Since η_{c_2} is so small compared to $\eta_0 = 377\ (\Omega)$ for air, the copper surface acts, in effect, like a short circuit. Hence,

$$\Gamma = \frac{\eta_{c_2} - \eta_0}{\eta_{c_2} + \eta_0} \simeq -1.$$

Upon setting $\Gamma = -1$ in Eqs. (8.11a) and (8.12a) of Table 8-1, we have

$$\begin{aligned} \widetilde{\mathbf{E}}_1(z) &= \hat{\mathbf{x}} E_0^i (e^{-jk_1 z} - e^{jk_1 z}) \\ &= -\hat{\mathbf{x}} j 2 E_0^i \sin k_1 z, \end{aligned} \tag{8.25a}$$

$$\begin{aligned} \widetilde{\mathbf{H}}_1(z) &= \hat{\mathbf{y}} \frac{E_0^i}{\eta_1} (e^{-jk_1 z} + e^{jk_1 z}) \\ &= \hat{\mathbf{y}} 2 \frac{E_0^i}{\eta_1} \cos k_1 z. \end{aligned} \tag{8.25b}$$

With $E_0^i = 12$ (mV/m), the instantaneous fields corresponding to these phasors are

$$\begin{aligned} \mathbf{E}_1(z,t) &= \Re\mathrm{e}[\widetilde{\mathbf{E}}_1(z)\, e^{j\omega t}] \\ &= \hat{\mathbf{x}} 2 E_0^i \sin k_1 z \sin \omega t \\ &= \hat{\mathbf{x}} 24 \sin(20\pi z/3) \sin(2\pi \times 10^9 t) \quad \text{(mV/m)}, \\ \mathbf{H}_1(z,t) &= \Re\mathrm{e}[\widetilde{\mathbf{H}}_1(z)\, e^{j\omega t}] \\ &= \hat{\mathbf{y}} 2 \frac{E_0^i}{\eta_1} \cos k_1 z \cos \omega t \\ &= \hat{\mathbf{y}} 64 \cos(20\pi z/3) \cos(2\pi \times 10^9 t) \quad (\mu\text{A/m}). \end{aligned}$$

Plots of the magnitude of $\mathbf{E}_1(z,t)$ and $\mathbf{H}_1(z,t)$ are shown in Fig. 8-8 as a function of negative z at various values of ωt. The standing-wave patterns exhibit a repetition period of $\lambda/2$, and E and H are in phase quadrature (90° phase shift) in both space and time. This behavior is identical with that of the standing-wave patterns for voltage and current on a shorted transmission line. ■

REVIEW QUESTIONS

Q8.1 What boundary conditions were used in the derivations of the expressions for Γ and τ?

Q8.2 In the radar radome design of Example 8-1, all the incident energy in medium 1 ends up getting transmitted into medium 3, and vice versa. Does this imply that no reflections take place within medium 2? Explain.

Q8.3 Explain on the basis of boundary conditions why it is necessary that $\Gamma = -1$ at the boundary between a dielectric and a perfect conductor.

EXERCISE 8.1 To eliminate wave reflections, a dielectric slab of thickness d and relative permittivity ε_{r_2} is to be inserted between two semi-infinite media with relative permittivities $\varepsilon_{r_1} = 1$ and $\varepsilon_{r_3} = 16$. Use the quarter-wave

INTEL-1014
U.S. Patent 7,151,430

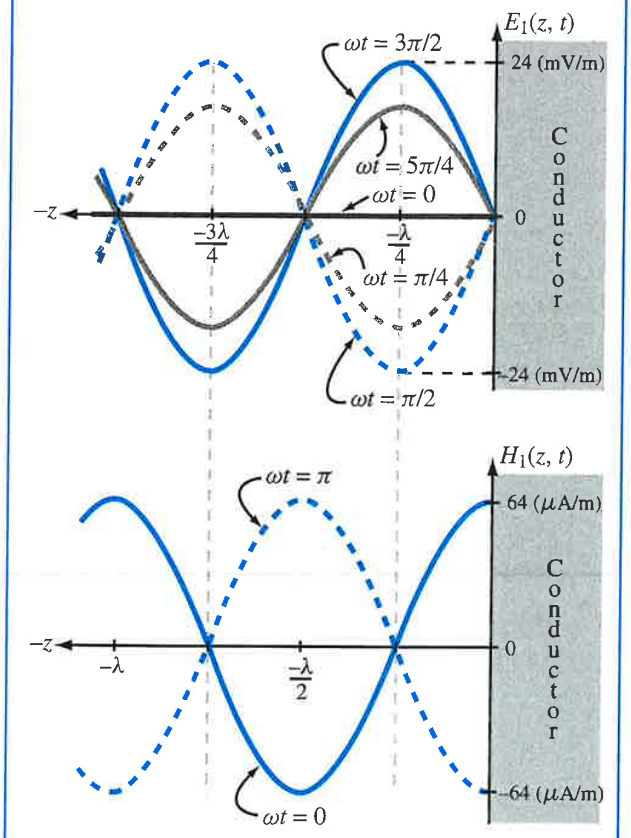


Figure 8-8: Standing-wave patterns for fields $E_1(z, t)$ and $H_1(z, t)$ of Example 8-3.

transformer technique to select d and ε_{r_2} for normally incident waves at 3 GHz.

Ans. $\varepsilon_{r_2} = 4$ and $d = (1.25 + 2.5n)$ (cm), with $n = 0, 1, 2, \ldots$.

EXERCISE 8.2 Express the normal-incidence reflection coefficient at the boundary between two nonmagnetic, conducting media in terms of their complex permittivities.

Ans. For incidence in medium 1 $(\varepsilon_1, \mu_0, \sigma_1)$ onto medium 2 $(\varepsilon_2, \mu_0, \sigma_2)$,

$$\Gamma = \frac{\sqrt{\varepsilon_{c_1}} - \sqrt{\varepsilon_{c_2}}}{\sqrt{\varepsilon_{c_1}} + \sqrt{\varepsilon_{c_2}}},$$

with $\varepsilon_{c_1} = (\varepsilon_1 - j\sigma_1/\omega)$ and $\varepsilon_{c_2} = (\varepsilon_2 - j\sigma_2/\omega)$.

EXERCISE 8.3 Obtain expressions for the average power densities in media 1 and 2 for the fields described by Eqs. (8.22a) through (8.23b), assuming medium 1 is slightly lossy with η_{c_1} approximately real.

Ans.

$$\mathbf{S}_{av_1} = \hat{\mathbf{z}} \frac{|E_0^i|^2}{2\eta_{c_1}} \left(e^{-2\alpha_1 z} - |\Gamma|^2 e^{2\alpha_1 z}\right),$$

$$\mathbf{S}_{av_2} = \hat{\mathbf{z}} |\tau|^2 \frac{|E_0^i|^2}{2} e^{-2\alpha_2 z} \mathfrak{Re}\left(\frac{1}{\eta_{c_2}^*}\right).$$

8-2 Snell's Laws

In the preceding sections we examined the reflection and transmission properties of plane waves when incident normally upon a planar interface between two different media. We now consider the oblique-incidence case depicted in Fig. 8-9. The $z = 0$ plane is the boundary between two dielectric media characterized by (ε_1, μ_1) for medium 1 and (ε_2, μ_2) for medium 2. The two lines with direction $\hat{\mathbf{k}}_i$ represent rays drawn normal to the wavefront of the incident wave and, similarly, those along $\hat{\mathbf{k}}_r$ and $\hat{\mathbf{k}}_t$ represent the reflected and transmitted waves, respectively. Defined with respect to the normal to the boundary (the z-axis), the ***angles of incidence***, ***reflection***, and ***transmission*** (or ***refraction***) are, respectively, θ_i, θ_r, and θ_t. These three angles are interrelated by ***Snell's laws***, which we will derive by considering the propagation of the wavefronts of the three waves. The incident wave intersects the boundary at O and O'. The constant-phase wavefront of the incident wave is $A_i O$, and the wavefronts of the reflected and transmitted waves are

INTEL-1014
U.S. Patent 7,151,430

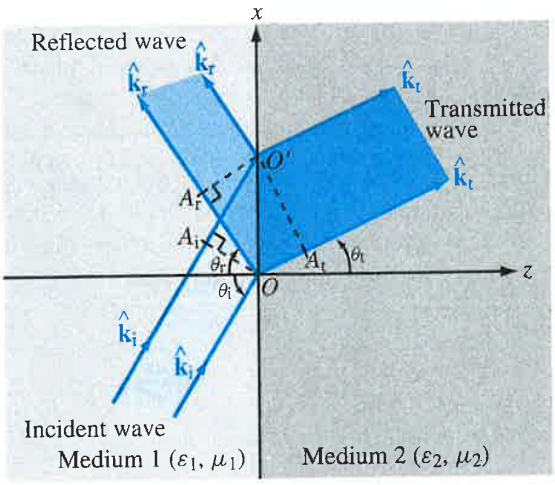


Figure 8-9: Wave reflection and refraction at a planar boundary between different media.

$A_r O'$ and $A_t O'$, as shown in Fig. 8-9. The incident and reflected waves propagate in medium 1 with the same phase velocity $u_{p_1} = 1/\sqrt{\mu_1 \varepsilon_1}$, and the transmitted wave in medium 2 propagates with a velocity $u_{p_2} = 1/\sqrt{\mu_2 \varepsilon_2}$. The time it takes the incident wave to travel from A_i to O' is the same as the time it takes the reflected wave to travel from O to A_r and also the time it takes the transmitted wave to travel from O to A_t. Since time is equal to distance divided by velocity, it follows that

$$\frac{\overline{A_i O'}}{u_{p_1}} = \frac{\overline{O A_r}}{u_{p_1}} = \frac{\overline{O A_t}}{u_{p_2}}. \tag{8.26}$$

From the geometries of the three right triangles in Fig. 8-9, we deduce that

$$\overline{A_i O'} = \overline{O O'} \sin\theta_i, \tag{8.27a}$$

$$\overline{O A_r} = \overline{O O'} \sin\theta_r, \tag{8.27b}$$

$$\overline{O A_t} = \overline{O O'} \sin\theta_t. \tag{8.27c}$$

Use of these expressions in Eq. (8.26) leads to

$$\theta_i = \theta_r \quad \text{(Snell's law of reflection)}, \tag{8.28a}$$

$$\frac{\sin\theta_t}{\sin\theta_i} = \frac{u_{p_2}}{u_{p_1}} = \sqrt{\frac{\mu_1 \varepsilon_1}{\mu_2 \varepsilon_2}} \quad \text{(Snell's law of refraction)}. \tag{8.28b}$$

Snell's law of reflection states that the angle of reflection is equal to the angle of incidence, and ***Snell's law of refraction*** provides a relation between $\sin\theta_t$ and $\sin\theta_i$ in terms of the ratio of the phase velocities.

The ***index of refraction*** of a medium, n, is defined as the ratio of the phase velocity in free space (i.e., the speed of light c) to the phase velocity in the medium. Thus,

$$n = \frac{c}{u_p} = \sqrt{\frac{\mu \varepsilon}{\mu_0 \varepsilon_0}} = \sqrt{\mu_r \varepsilon_r}. \tag{8.29}$$

In view of Eq. (8.29), Eq. (8.28b) may be rewritten as

$$\frac{\sin\theta_t}{\sin\theta_i} = \frac{n_1}{n_2} = \sqrt{\frac{\mu_{r_1} \varepsilon_{r_1}}{\mu_{r_2} \varepsilon_{r_2}}}. \tag{8.30}$$

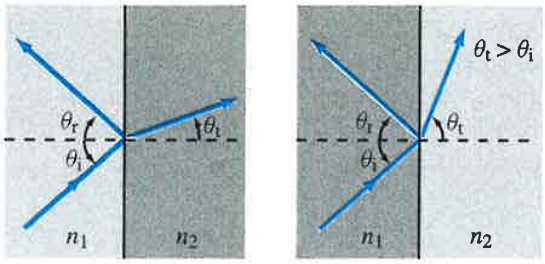
For nonmagnetic materials, $\mu_{r_1} = \mu_{r_2} = 1$, in which case

$$\frac{\sin\theta_t}{\sin\theta_i} = \frac{n_1}{n_2} = \sqrt{\frac{\varepsilon_{r_1}}{\varepsilon_{r_2}}} = \frac{\eta_2}{\eta_1} \quad (\text{for } \mu_1 = \mu_2), \tag{8.31}$$

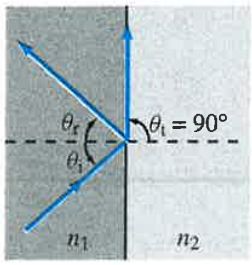
where $\eta = \sqrt{\mu/\varepsilon}$ is the intrinsic impedance of a dielectric medium. Usually, materials with higher densities have higher permittivities. Air, with $\mu_r = \varepsilon_r = 1$, has an index of refraction $n_0 = 1$. Since for nonmagnetic materials $n = \sqrt{\varepsilon_r}$, *a material is often referred to as more dense than a second material if the index of refraction of the first material is greater than that of the second.*

At normal incidence ($\theta_i = 0$), Eq. (8.31) gives $\theta_t = 0$, as expected, and at oblique incidence $\theta_t < \theta_i$ when $n_2 > n_1$ and $\theta_t > \theta_i$ when $n_2 < n_1$. That is, *if the wave*

INTEL-1014
U.S. Patent 7,151,430



(a) $n_1 < n_2$ (b) $n_1 > n_2$



(c) $n_1 > n_2$ and $\theta_i = \theta_c$

Figure 8-10: Snell's laws state that $\theta_r = \theta_i$ and $\sin\theta_t = (n_1/n_2)\sin\theta_i$. Refraction is (a) inward if $n_1 < n_2$ and (b) outward if $n_1 > n_2$; and (c) the refraction angle is 90° if $n_1 > n_2$ and θ_i is equal to or greater than the critical angle $\theta_c = \sin^{-1}(n_2/n_1)$.

in medium 1 is incident on a more dense medium, as in Fig. 8-10(a), the transmitted wave refracts inwardly toward the z-axis, and the opposite is true if the wave is incident on a less dense medium [Fig. 8-10(b)]. A case of particular interest is when $\theta_t = \pi/2$, as shown in Fig. 8-10(c); in this case, the refracted wave flows along the surface and no energy is transmitted into medium 2. The value of the angle of incidence θ_i corresponding to $\theta_t = \pi/2$ is called the ***critical angle*** θ_c and is obtained from Eq. (8.30) as

$$\sin\theta_c = \frac{n_2}{n_1}\sin\theta_t\Big|_{\theta_t=\pi/2} = \frac{n_2}{n_1} \tag{8.32a}$$

$$= \sqrt{\frac{\varepsilon_{r_2}}{\varepsilon_{r_1}}} \quad (\text{for } \mu_1 = \mu_2). \tag{8.32b}$$

If θ_i exceeds θ_c, the incident wave is totally reflected, and the refracted wave becomes a nonuniform ***surface wave*** that travels along the boundary between the two media. This wave behavior is called ***total internal reflection***.

Example 8-4 Light Beam Passing through a Slab

A dielectric slab with index of refraction n_2 is surrounded by a medium with index of refraction n_1, as shown in Fig. 8-11. If $\theta_i < \theta_c$, show that the emerging beam is parallel to the incident beam.

Solution: At the slab's upper surface, Snell's law gives

$$\sin\theta_2 = \frac{n_1}{n_2}\sin\theta_1 \tag{8.33}$$

and, similarly, at the slab's lower surface,

$$\sin\theta_3 = \frac{n_2}{n_3}\sin\theta_2 = \frac{n_2}{n_1}\sin\theta_2. \tag{8.34}$$

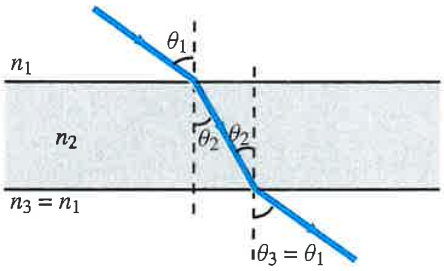


Figure 8-11: The exit angle θ_3 is equal to the incidence angle θ_1 if the dielectric slab has parallel boundaries and is surrounded by the same index of refraction on both sides (Example 8-4).

INTEL-1014
U.S. Patent 7,151,430

Substituting Eq. (8.33) into Eq. (8.34) gives

$$\sin\theta_3 = \left(\frac{n_2}{n_1}\right)\left(\frac{n_1}{n_2}\right)\sin\theta_1 = \sin\theta_1.$$

Hence, $\theta_3 = \theta_1$. The slab displaces the beam's position, but the beam's direction remains unchanged. ■

EXERCISE 8.4 In the visible part of the electromagnetic spectrum, the index of refraction of water is 1.33. What is the critical angle for light waves generated by an upward-looking underwater light source?

Ans. $\theta_c = 48.8°$.

EXERCISE 8.5 If the light source of Exercise 8.4 is situated at a depth of 1 m below the water surface and if its beam is isotropic (radiates in all directions), how large a circle would it illuminate when observed from above?

Ans. Circle's diameter = 2.28 m.

8-3 Fiber Optics

By successive total internal reflections, as indicated in Fig. 8-12(a), light can be guided through thin dielectric rods made of glass or transparent plastic, known as ***optical fibers***. Because the light is confined to traveling within the rod, the only loss in power is due to reflections at the sending and receiving ends of the fiber and absorption by the fiber material (because it is not a perfect dielectric). Fiber optics is useful for the transmission of wide-bandwidth signals and in a wide range of imaging applications.

An optical fiber usually consists of a cylindrical ***fiber core*** with an index of refraction n_f, surrounded by another cylinder of lower index of refraction, n_c, called a ***cladding***, as shown in Fig. 8-12(b). The cladding layer serves to optically isolate the fiber from adjacent fibers when a large number of fibers are packed in close proximity, thereby avoiding the leakage of light from one fiber to another. To satisfy the condition of total internal reflection, the incident angle θ_3 in the fiber core must be equal to or greater than the critical angle θ_c for a wave in the fiber medium (with n_f) incident upon the cladding medium (with n_c). From Eq. (8.32a), we have

$$\sin\theta_c = \frac{n_c}{n_f}. \tag{8.35}$$

To meet the total-reflection requirement that $\theta_3 \geq \theta_c$, it is then necessary that $\sin\theta_3 \geq n_c/n_f$. The angle θ_2 is the complement of angle θ_3, and $\cos\theta_2 = \sin\theta_3$. Hence, the necessary condition may be written as

$$\cos\theta_2 \geq \frac{n_c}{n_f}. \tag{8.36}$$

Moreover, θ_2 is related to the incidence angle on the face of the fiber, θ_i, by Snell's law:

$$\sin\theta_2 = \frac{n_0}{n_f}\sin\theta_i, \tag{8.37}$$

where n_0 is the index of refraction of the medium surrounding the fiber ($n_0 = 1$ for air and $n_0 = 1.33$ if the fiber is in water), or

$$\cos\theta_2 = \left[1 - \left(\frac{n_0}{n_f}\right)^2 \sin^2\theta_i\right]^{1/2}. \tag{8.38}$$

Using Eq. (8.38) in the left-hand side of Eq. (8.36) and then solving for $\sin\theta_i$ gives

$$\sin\theta_i \leq \frac{1}{n_0}(n_f^2 - n_c^2)^{1/2}. \tag{8.39}$$

The ***acceptance angle*** θ_a is defined as the maximum value of θ_i for which the condition of total internal reflection remains satisfied:

$$\sin\theta_a = \frac{1}{n_0}(n_f^2 - n_c^2)^{1/2}. \tag{8.40}$$

INTEL-1014
U.S. Patent 7,151,430

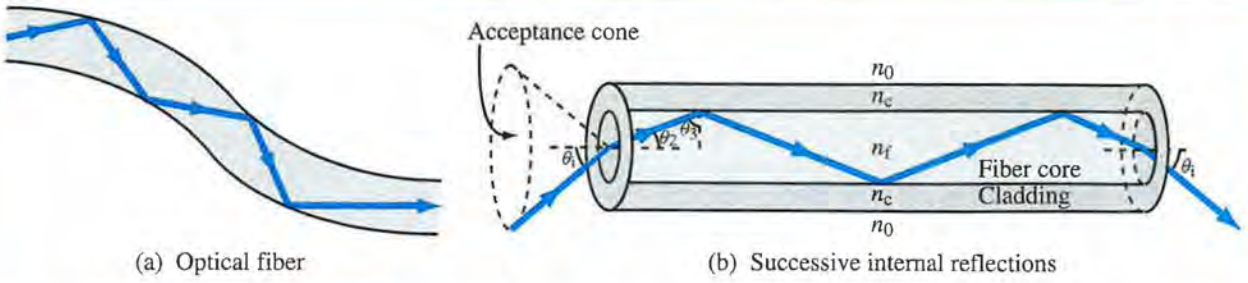


Figure 8-12: Waves can be guided along optical fibers as long as the reflection angles exceed the critical angle for total internal reflection.

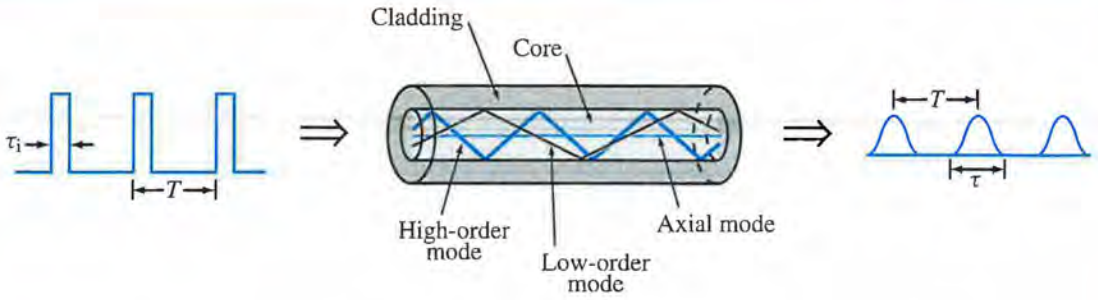


Figure 8-13: Distortion of rectangular pulses caused by modal dispersion in optical fibers.

The angle θ_a is equal to half the angle of the acceptance cone of the fiber. Any ray of light incident upon the face of the core fiber at an incidence angle within the acceptance cone can propagate down the core. This means that there can be a larger number of ray paths, called ***modes***, by which light energy can travel in the core. Higher-angle rays travel longer paths than rays that propagate along the axis of the fiber, as illustrated by the three modes shown in Fig. 8-13. Consequently, different modes have different transit times between the two ends of the fiber. This property of optical fibers is called ***modal dispersion*** and has the undesirable effect of changing the shape of pulses used for the transmission of digital data. When a rectangular pulse of light incident upon the face of the fiber gets broken up into many modes and the different modes do not arrive at the other end of the fiber at the same time, the pulse shape gets distorted, both in shape and length. In the example shown in Fig. 8-13, the narrow rectangular pulses at the input side of the optical fiber are of width τ_i separated by a time duration T. After propagating through the fiber core, modal dispersion causes the pulses to look more like spread-out sine waves with spread-out width τ. If the output pulses spread out so much that $\tau > T$, the output signals will smear out, making it impossible to read the transmitted message. Hence, to ensure that the

INTEL-1014
U.S. Patent 7,151,430

transmitted pulses remain distinguishable at the output side of the fiber, it is necessary that τ be shorter than T. As a safety margin, it is common practice to require that $T \geq 2\tau$.

The spread-out width τ is equal to the time delay Δt between the arrival of the slowest ray and the fastest ray. The slowest ray is the one traveling the longest distance and corresponds to the ray incident upon the input face of the fiber at the acceptance angle θ_a. From the geometry of Fig. 8-12(b) and Eq. (8.36), this ray corresponds to $\cos\theta_2 = n_c/n_f$. For an optical fiber of length l, the length of the path traveled by such a ray is

$$l_{max} = \frac{l}{\cos\theta_2} = l\frac{n_f}{n_c}, \tag{8.41}$$

and its travel time in the fiber at the velocity $u_p = c/n_f$ is

$$t_{max} = \frac{l_{max}}{u_p} = \frac{ln_f^2}{cn_c}. \tag{8.42}$$

The minimum time of travel is realized by the axial ray and is given by

$$t_{min} = \frac{l}{u_p} = \frac{l}{c}n_f. \tag{8.43}$$

The total time delay is therefore

$$\tau = \Delta t = t_{max} - t_{min} = \frac{ln_f}{c}\left(\frac{n_f}{n_c} - 1\right) \quad \text{(s)}. \tag{8.44}$$

As we stated before, to retrieve the desired information from the transmitted signals, it is advisable that T, the interpulse period of the input train of pulses, be no shorter than 2τ. This, in turn, means that the data rate (in bits per second), or equivalently the number of pulses per second, that can be transmitted through the fiber is limited to

$$f_p = \frac{1}{T} = \frac{1}{2\tau} = \frac{cn_c}{2ln_f(n_f - n_c)} \quad \text{(bits/s)}. \tag{8.45}$$

Example 8-5 Transmission Data Rate on Optical Fibers

A 1-km-long optical fiber (in air) is made of a fiber core with an index of refraction of 1.52 and a cladding with an index of refraction of 1.49. Determine

(a) the acceptance angle θ_a, and

(b) the maximum usable data rate that can be transmitted through the fiber.

Solution: (a) From Eq. (8.40),

$$\sin\theta_a = \frac{1}{n_0}(n_f^2 - n_c^2)^{1/2} = [(1.52)^2 - (1.49)^2]^{1/2} = 0.3,$$

which corresponds to $\theta_a = 17.5°$.

(b) From Eq. (8.45),

$$f_p = \frac{cn_c}{2ln_f(n_f - n_c)} = \frac{3 \times 10^8 \times 1.49}{2 \times 10^3 \times 1.52(1.52 - 1.49)} = 4.9 \text{ (Mb/s)}. \blacksquare$$

EXERCISE 8.6 If the index of refraction of the cladding material in Example 8-5 is increased to 1.50, what would be the new maximum usable data rate?

Ans. 7.4 (Mb/s).

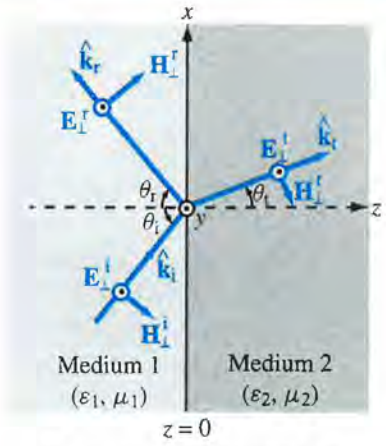
8-4 Wave Reflection and Transmission at Oblique Incidence

For normal incidence, the reflection coefficient Γ and transmission coefficient τ of a boundary between two different media is independent of the polarization of the incident wave, because the electric and magnetic fields of a normally incident plane wave are both always tangential to the boundary regardless of the wave polarization. This is not the case for oblique incidence at an angle

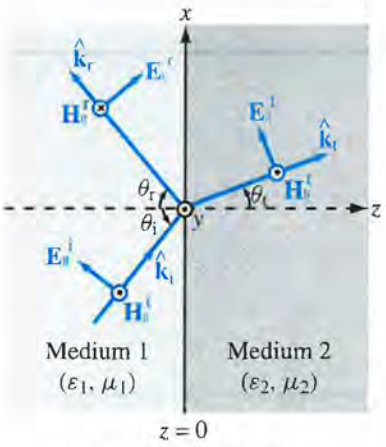
INTEL-1014
U.S. Patent 7,151,430

$\theta_i \neq 0$. A wave with any specified polarization may be described as the superposition of two orthogonally polarized waves, one with its electric field parallel to the plane of incidence—and it is called ***parallel polarization***—and another with its electric field perpendicular to the plane of incidence—and it is called ***perpendicular polarization***. ***The plane of incidence*** *is defined as the plane containing the normal to the boundary and the direction of propagation of the incident wave.* These two polarization configurations are shown in Fig. 8-14, in which the plane of incidence is coincident with the x–z plane. Polarization with $\mathbf{E}$ perpendicular to the plane of incidence is also called ***transverse electric*** (TE) polarization because $\mathbf{E}$ is perpendicular to the plane of incidence, and that with $\mathbf{E}$ parallel to the plane of incidence is called ***transverse magnetic*** (TM) polarization because in this case it is the magnetic field that is perpendicular to the plane of incidence.

Instead of solving the reflection and transmission problems for the general case of a wave with an arbitrary polarization, it is more convenient in practice to first decompose the incident wave $(\mathbf{E}^i, \mathbf{H}^i)$ into a perpendicularly polarized component $(\mathbf{E}^i_\perp, \mathbf{H}^i_\perp)$ and a parallel polarized component $(\mathbf{E}^i_\parallel, \mathbf{H}^i_\parallel)$, and then after determining the reflected waves $(\mathbf{E}^r_\perp, \mathbf{H}^r_\perp)$ and $(\mathbf{E}^r_\parallel, \mathbf{H}^r_\parallel)$ due to the two incident components, the reflected waves can be added together to give the total reflected wave corresponding to the original incident wave. A similar process applies to the transmitted wave.



(a) Perpendicular polarization



(b) Parallel polarization

Figure 8-14: The plane of incidence is the plane containing the direction of wave travel, $\hat{\mathbf{k}}$, and the surface normal to the boundary, which in the present case is the plane of the paper. A wave is (a) perpendicularly polarized when its $\mathbf{E}$ is perpendicular to the plane of incidence and (b) parallel polarized when its $\mathbf{E}$ lies in the plane of incidence.

8-4.1 Perpendicular Polarization

In Fig. 8-15, we show a perpendicularly polarized incident plane wave propagating along the x_i-direction in dielectric medium 1. The electric field phasor $\widetilde{\mathbf{E}}^i_\perp$ points along the y-direction, and the associated magnetic field phasor $\widetilde{\mathbf{H}}^i_\perp$ is along the y_i-axis. The directions of $\widetilde{\mathbf{E}}^i_\perp$ and $\widetilde{\mathbf{H}}^i_\perp$ satisfy the condition that $\widetilde{\mathbf{E}}^i_\perp \times \widetilde{\mathbf{H}}^i_\perp$ points along the propagation direction, $\hat{\mathbf{x}}_i$. The expressions for such a

INTEL-1014
U.S. Patent 7,151,430

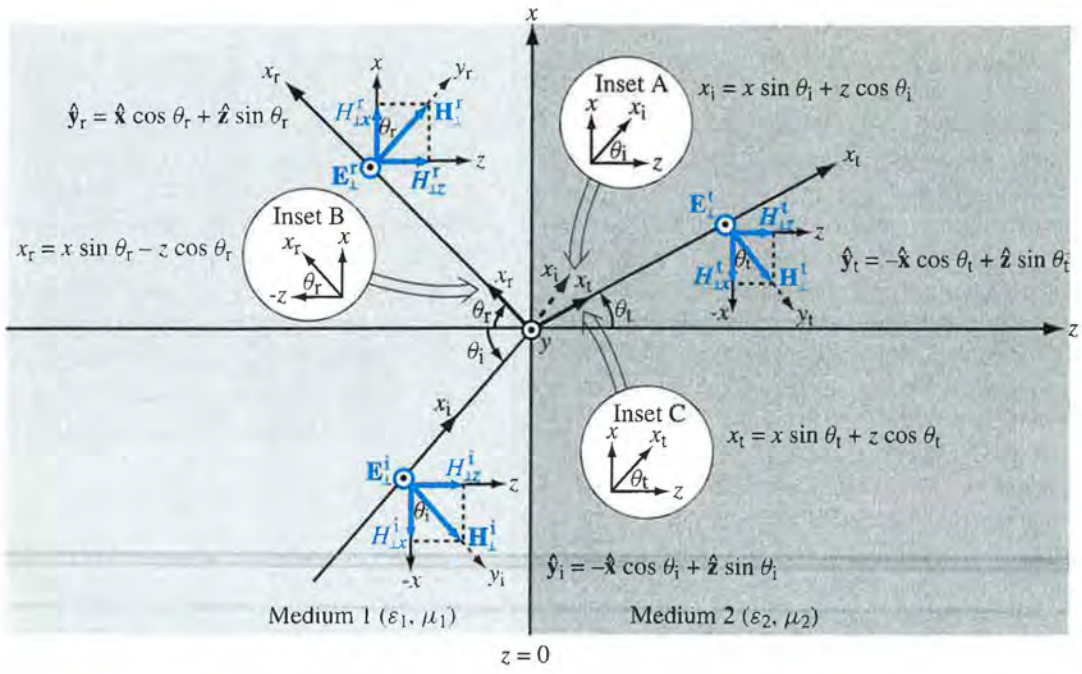


Figure 8-15: Perpendicularly polarized plane wave incident at an angle θ_i upon a planar boundary.

plane wave are given by

$$\widetilde{\mathbf{E}}^i_\perp = \hat{\mathbf{y}} E^i_{\perp 0} e^{-jk_1 x_i}, \tag{8.46a}$$

$$\widetilde{\mathbf{H}}^i_\perp = \hat{\mathbf{y}}_i \frac{E^i_{\perp 0}}{\eta_1} e^{-jk_1 x_i}, \tag{8.46b}$$

where $E^i_{\perp 0}$ is the amplitude of the electric field phasor at $x_i = 0$, $k_1 = \omega\sqrt{\mu_1 \varepsilon_1}$ is the wavenumber, and $\eta_1 = \sqrt{\mu_1/\varepsilon_1}$ is the intrinsic impedance, both for medium 1. From Fig. 8-15, the distance x_i and the unit vector $\hat{\mathbf{y}}_i$ may be expressed in terms of the (x, y, z) global coordinate system as follows:

$$x_i = x \sin\theta_i + z \cos\theta_i, \tag{8.47a}$$

$$\hat{\mathbf{y}}_i = -\hat{\mathbf{x}} \cos\theta_i + \hat{\mathbf{z}} \sin\theta_i. \tag{8.47b}$$

Substituting Eqs. (8.47a) and (8.47b) into Eqs. (8.46a) and (8.46b) gives:

Incident Wave

$$\widetilde{\mathbf{E}}^i_\perp = \hat{\mathbf{y}} E^i_{\perp 0} e^{-jk_1(x \sin\theta_i + z \cos\theta_i)}, \tag{8.48a}$$

$$\widetilde{\mathbf{H}}^i_\perp = (-\hat{\mathbf{x}} \cos\theta_i + \hat{\mathbf{z}} \sin\theta_i) \times \frac{E^i_{\perp 0}}{\eta_1} e^{-jk_1(x \sin\theta_i + z \cos\theta_i)}. \tag{8.48b}$$

With the aid of the directional relationships given in Fig. 8-15 for the reflected and transmitted waves, the fields are given by:

INTEL-1014
U.S. Patent 7,151,430

Reflected Wave

$$\begin{aligned}\widetilde{\mathbf{E}}^{\mathrm{r}}_{\perp} &= \hat{\mathbf{y}} E^{\mathrm{r}}_{\perp 0} e^{-jk_1 x_{\mathrm{r}}} \\ &= \hat{\mathbf{y}} E^{\mathrm{r}}_{\perp 0} e^{-jk_1(x\sin\theta_{\mathrm{r}} - z\cos\theta_{\mathrm{r}})}, \end{aligned} \tag{8.49a}$$

$$\begin{aligned}\widetilde{\mathbf{H}}^{\mathrm{r}}_{\perp} &= \hat{\mathbf{y}}_{\mathrm{r}} \frac{E^{\mathrm{r}}_{\perp 0}}{\eta_1} e^{-jk_1 x_{\mathrm{r}}} \\ &= (\hat{\mathbf{x}}\cos\theta_{\mathrm{r}} + \hat{\mathbf{z}}\sin\theta_{\mathrm{r}}) \\ &\quad \times \frac{E^{\mathrm{r}}_{\perp 0}}{\eta_1} e^{-jk_1(x\sin\theta_{\mathrm{r}} - z\cos\theta_{\mathrm{r}})}, \end{aligned} \tag{8.49b}$$

Transmitted Wave

$$\begin{aligned}\widetilde{\mathbf{E}}^{\mathrm{t}}_{\perp} &= \hat{\mathbf{y}} E^{\mathrm{t}}_{\perp 0} e^{-jk_2 x_{\mathrm{t}}} \\ &= \hat{\mathbf{y}} E^{\mathrm{t}}_{\perp 0} e^{-jk_2(x\sin\theta_{\mathrm{t}} + z\cos\theta_{\mathrm{t}})}, \end{aligned} \tag{8.49c}$$

$$\begin{aligned}\widetilde{\mathbf{H}}^{\mathrm{t}}_{\perp} &= \hat{\mathbf{y}}_{\mathrm{t}} \frac{E^{\mathrm{t}}_{\perp 0}}{\eta_2} e^{-jk_2 x_{\mathrm{t}}} \\ &= (-\hat{\mathbf{x}}\cos\theta_{\mathrm{t}} + \hat{\mathbf{z}}\sin\theta_{\mathrm{t}}) \\ &\quad \times \frac{E^{\mathrm{t}}_{\perp 0}}{\eta_2} e^{-jk_2(x\sin\theta_{\mathrm{t}} + z\cos\theta_{\mathrm{t}})}, \end{aligned} \tag{8.49d}$$

where θ_{r} and θ_{t} are the reflection and transmission angles shown in Fig. 8-15 and k_2 and η_2 are the wavenumber and intrinsic impedance of medium 2. Our goal is to characterize the reflected and transmitted fields in terms of the parameters of the incident wave, which include the incidence angle θ_{i} and the amplitude $E^{\mathrm{i}}_{\perp 0}$. The four expressions given by Eqs. (8.49a) through (8.49d) contain four unknown quantities: $E^{\mathrm{r}}_{\perp 0}$, $E^{\mathrm{t}}_{\perp 0}$, θ_{r}, and θ_{t}. Angles θ_{r} and θ_{t} can be related to θ_{i} by Snell's laws, Eqs. (8.28a) and (8.28b), but we choose to keep them as unknowns for the time being, because we intend to show that Snell's laws can also be derived by applying the fields' boundary conditions at $z = 0$. The total electric field in medium 1 is the sum of the incident and reflected electric fields: $\widetilde{\mathbf{E}}^{1}_{\perp} = \widetilde{\mathbf{E}}^{\mathrm{i}}_{\perp} + \widetilde{\mathbf{E}}^{\mathrm{r}}_{\perp}$; and the same is true for the total magnetic field in medium 1: $\widetilde{\mathbf{H}}^{1}_{\perp} = \widetilde{\mathbf{H}}^{\mathrm{i}}_{\perp} + \widetilde{\mathbf{H}}^{\mathrm{r}}_{\perp}$. Boundary conditions state that the tangential components of $\widetilde{\mathbf{E}}$ and $\widetilde{\mathbf{H}}$ must each be continuous across the boundary between the two media. Field components tangential to the boundary are those along $\hat{\mathbf{x}}$ and $\hat{\mathbf{y}}$. Since the electric fields in media 1 and 2 have $\hat{\mathbf{y}}$-components only, the boundary condition for $\widetilde{\mathbf{E}}$ is

$$(\widetilde{E}^{\mathrm{i}}_{\perp y} + \widetilde{E}^{\mathrm{r}}_{\perp y})\big|_{z=0} = \widetilde{E}^{\mathrm{t}}_{\perp y}\big|_{z=0}. \tag{8.50}$$

Upon using Eqs. (8.48a), (8.49a), and (8.49c) in Eq. (8.50) and then setting $z = 0$, we have

$$E^{\mathrm{i}}_{\perp 0} e^{-jk_1 x\sin\theta_{\mathrm{i}}} + E^{\mathrm{r}}_{\perp 0} e^{-jk_1 x\sin\theta_{\mathrm{r}}} = E^{\mathrm{t}}_{\perp 0} e^{-jk_2 x\sin\theta_{\mathrm{t}}}. \tag{8.51}$$

The boundary condition for the tangential component of the magnetic field (i.e., the x-component) is

$$(\widetilde{H}^{\mathrm{i}}_{\perp x} + \widetilde{H}^{\mathrm{r}}_{\perp x})\big|_{z=0} = \widetilde{H}^{\mathrm{t}}_{\perp x}\big|_{z=0}, \tag{8.52}$$

or

$$-\frac{E^{\mathrm{i}}_{\perp 0}}{\eta_1}\cos\theta_{\mathrm{i}}\, e^{-jk_1 x\sin\theta_{\mathrm{i}}} + \frac{E^{\mathrm{r}}_{\perp 0}}{\eta_1}\cos\theta_{\mathrm{r}}\, e^{-jk_1 x\sin\theta_{\mathrm{r}}} = -\frac{E^{\mathrm{t}}_{\perp 0}}{\eta_2}\cos\theta_{\mathrm{t}}\, e^{-jk_2 x\sin\theta_{\mathrm{t}}}. \tag{8.53}$$

To satisfy Eqs. (8.51) and (8.53) for all possible values of x (all along the boundary), it follows that all three exponential arguments must be equal. That is,

$$k_1\sin\theta_{\mathrm{i}} = k_1\sin\theta_{\mathrm{r}} = k_2\sin\theta_{\mathrm{t}}, \tag{8.54}$$

which is known as the ***phase-matching condition***. The first equality in Eq. (8.54) leads to

$$\theta_{\mathrm{r}} = \theta_{\mathrm{i}} \quad \text{(Snell's law of reflection)}, \tag{8.55}$$

and the second equality leads to

$$\frac{\sin\theta_{\mathrm{t}}}{\sin\theta_{\mathrm{i}}} = \frac{k_1}{k_2} = \frac{\omega\sqrt{\mu_1\varepsilon_1}}{\omega\sqrt{\mu_2\varepsilon_2}} = \frac{n_1}{n_2} \quad \text{(Snell's law of refraction)}. \tag{8.56}$$

The results expressed by Eqs. (8.55) and (8.56) are identical with those derived previously in Section 8-2

INTEL-1014
U.S. Patent 7,151,430

through consideration of the ray path traversed by the incident, reflected, and transmitted wavefronts.

In view of Eq. (8.54), the boundary conditions given by Eqs. (8.51) and (8.53) reduce to

$$E^{i}_{\perp 0} + E^{r}_{\perp 0} = E^{t}_{\perp 0}, \tag{8.57a}$$

$$\frac{\cos\theta_i}{\eta_1}(-E^{i}_{\perp 0} + E^{r}_{\perp 0}) = -\frac{\cos\theta_t}{\eta_2} E^{t}_{\perp 0}. \tag{8.57b}$$

These two equations can be solved simultaneously to yield the following expressions for the reflection and transmission coefficients in the perpendicular polarization case:

$$\Gamma_\perp = \frac{E^{r}_{\perp 0}}{E^{i}_{\perp 0}} = \frac{\eta_2 \cos\theta_i - \eta_1 \cos\theta_t}{\eta_2 \cos\theta_i + \eta_1 \cos\theta_t}, \tag{8.58a}$$

$$\tau_\perp = \frac{E^{t}_{\perp 0}}{E^{i}_{\perp 0}} = \frac{2\eta_2 \cos\theta_i}{\eta_2 \cos\theta_i + \eta_1 \cos\theta_t}. \tag{8.58b}$$

These two coefficients, which formally are known as the ***Fresnel reflection and transmission coefficients for perpendicular polarization***, are related by

$$\tau_\perp = 1 + \Gamma_\perp. \tag{8.59}$$

If medium 2 is a perfect conductor ($\eta_2 = 0$), Eqs. (8.58a) and (8.58b) reduce to $\Gamma_\perp = -1$ and $\tau_\perp = 0$, respectively, which means that the incident wave is totally reflected by the conducting medium.

For nonmagnetic dielectrics with $\mu_1 = \mu_2 = \mu_0$ and with the help of Eq. (8.56), the expression for $\Gamma_\perp$ can be written as

$$\Gamma_\perp = \frac{\cos\theta_i - \sqrt{(\varepsilon_2/\varepsilon_1) - \sin^2\theta_i}}{\cos\theta_i + \sqrt{(\varepsilon_2/\varepsilon_1) - \sin^2\theta_i}} \quad (\text{for } \mu_1 = \mu_2). \tag{8.60}$$

Since $(\varepsilon_2/\varepsilon_1) = (n_2/n_1)^2$, this expression can also be written in terms of the indices of refraction n_1 and n_2.

Example 8-6 Wave Incident Obliquely on a Soil Surface

Using the coordinate system of Fig. 8-15, a plane wave radiated by a distant antenna is incident in air upon a plane soil surface at $z = 0$. The electric field of the incident wave is given by

$$\mathbf{E}^i = \hat{\mathbf{y}} 100 \cos(\omega t - \pi x - 1.73\pi z) \quad (\text{V/m}), \tag{8.61}$$

and the soil medium may be assumed to be a lossless dielectric with a relative permittivity of 4.

(a) Determine k_1, k_2, and the incidence angle θ_i.
(b) Obtain expressions for the total electric fields in air and in the soil medium.
(c) Determine the average power density carried by the wave traveling in the soil medium.

Solution: (a) We begin by converting Eq. (8.61) into phasor form, akin to the expression given by Eq. (8.46a):

$$\begin{aligned}\widetilde{\mathbf{E}}^i &= \hat{\mathbf{y}} 100 e^{-j\pi x - j1.73\pi z} \\ &= \hat{\mathbf{y}} 100 e^{-jk_1 x_i} \quad (\text{V/m}),\end{aligned} \tag{8.62}$$

where x_i is the axis along which the wave is traveling, and

$$k_1 x_i = \pi x + 1.73\pi z. \tag{8.63}$$

Using Eq. (8.47a), we have

$$k_1 x_i = k_1 x \sin\theta_i + k_1 z \cos\theta_i. \tag{8.64}$$

Hence,

$$k_1 \sin\theta_i = \pi,$$
$$k_1 \cos\theta_i = 1.73\pi,$$

which together give

$$k_1 = \sqrt{\pi^2 + (1.73\pi)^2} = 2\pi \quad (\text{rad/m}),$$
$$\theta_i = \tan^{-1}\left(\frac{\pi}{1.73\pi}\right) = 30°.$$

INTEL-1014
U.S. Patent 7,151,430

The wavelength in medium 1 (air) is

$$\lambda_1 = \frac{2\pi}{k_1} = 1 \text{ m},$$

and the wavelength in medium 2 (soil) is

$$\lambda_2 = \frac{\lambda_1}{\sqrt{\varepsilon_{r_2}}} = \frac{1}{\sqrt{4}} = 0.5 \text{ m}.$$

The corresponding wave number in medium 2 is

$$k_2 = \frac{2\pi}{\lambda_2} = 4\pi \quad \text{(rad/m)}.$$

Since $\widetilde{\mathbf{E}}^{\mathrm{i}}$ is along $\hat{\mathbf{y}}$, it is perpendicularly polarized ($\hat{\mathbf{y}}$ is perpendicular to the plane of incidence containing the surface normal $\hat{\mathbf{z}}$ and the propagation direction $\hat{\mathbf{x}}_{\mathrm{i}}$).

(b) Corresponding to $\theta_{\mathrm{i}} = 30°$, the transmission angle θ_{t} is obtained with the help of Eq. (8.56):

$$\sin\theta_{\mathrm{t}} = \frac{k_1}{k_2}\sin\theta_{\mathrm{i}} = \frac{2\pi}{4\pi}\sin 30° = 0.25$$

or

$$\theta_{\mathrm{t}} = 14.5°.$$

With $\varepsilon_1 = \varepsilon_0$ and $\varepsilon_2 = \varepsilon_{r_2}\varepsilon_0 = 4\varepsilon_0$, the reflection and transmission coefficients for perpendicular polarization are determined with the help of Eqs. (8.59) and (8.60),

$$\Gamma_\perp = \frac{\cos\theta_{\mathrm{i}} - \sqrt{(\varepsilon_2/\varepsilon_1) - \sin^2\theta_{\mathrm{i}}}}{\cos\theta_{\mathrm{i}} + \sqrt{(\varepsilon_2/\varepsilon_1) - \sin^2\theta_{\mathrm{i}}}} = -0.38,$$

$$\tau_\perp = 1 + \Gamma_\perp = 0.62.$$

Using Eqs. (8.48a) and (8.49a) with $E^{\mathrm{i}}_{\perp 0} = 100$ V/m and $\theta_{\mathrm{i}} = \theta_{\mathrm{r}}$, the total electric field phasor in medium 1 is

$$\begin{aligned}\widetilde{\mathbf{E}}^{1}_{\perp} &= \widetilde{\mathbf{E}}^{\mathrm{i}}_{\perp} + \widetilde{\mathbf{E}}^{\mathrm{r}}_{\perp} \\ &= \hat{\mathbf{y}}E^{\mathrm{i}}_{\perp 0}e^{-jk_1(x\sin\theta_{\mathrm{i}} + z\cos\theta_{\mathrm{i}})} \\ &\quad + \hat{\mathbf{y}}\Gamma E^{\mathrm{i}}_{\perp 0}e^{-jk_1(x\sin\theta_{\mathrm{i}} - z\cos\theta_{\mathrm{i}})} \\ &= \hat{\mathbf{y}}100e^{-j(\pi x + 1.73\pi z)} - \hat{\mathbf{y}}38e^{-j(\pi x - 1.73\pi z)},\end{aligned}$$

and the corresponding instantaneous electric field in medium 1 is

$$\begin{aligned}\mathbf{E}^{1}_{\perp}(x,z,t) &= \mathrm{Re}\left[\widetilde{\mathbf{E}}^{1}_{\perp}e^{j\omega t}\right] \\ &= \hat{\mathbf{y}}[100\cos(\omega t - \pi x - 1.73\pi z) \\ &\quad - 38\cos(\omega t - \pi x + 1.73\pi z)] \quad \text{(V/m)}.\end{aligned}$$

In medium 2, using Eq. (8.49c) with $E^{\mathrm{t}}_{\perp 0} = \tau_\perp E^{\mathrm{i}}_{\perp 0}$ gives

$$\begin{aligned}\widetilde{\mathbf{E}}^{\mathrm{t}}_{\perp} &= \hat{\mathbf{y}}\tau E^{\mathrm{i}}_{\perp 0}e^{-jk_2(x\sin\theta_{\mathrm{t}} + z\cos\theta_{\mathrm{t}})} \\ &= \hat{\mathbf{y}}62e^{-j(\pi x + 3.87\pi z)}\end{aligned}$$

and, correspondingly,

$$\begin{aligned}\mathbf{E}^{\mathrm{t}}_{\perp}(x,z,t) &= \mathrm{Re}\left[\widetilde{\mathbf{E}}^{\mathrm{t}}_{\perp}e^{j\omega t}\right] \\ &= \hat{\mathbf{y}}62\cos(\omega t - \pi x - 3.87\pi z) \quad \text{(V/m)}.\end{aligned}$$

(c) In medium 2, $\eta_2 = \eta_0/\sqrt{\varepsilon_{r_2}} \simeq 120\pi/\sqrt{4} = 60\pi$ (Ω), and the average power density carried by the wave is

$$S^{\mathrm{t}}_{\mathrm{av}} = \frac{|E^{\mathrm{t}}_{\perp 0}|^2}{2\eta_2} = \frac{(62)^2}{2\times 60\pi} = 10.2 \quad \text{(W/m}^2\text{)}. \blacksquare$$

8-4.2 Parallel Polarization

If we interchange **E** and **H** of the perpendicular polarization situation, while keeping in mind the requirement that relates the directions of **E** and **H** to the direction of propagation for each of the incident, reflected, and transmitted waves, we end up with the geometry shown in Fig. 8-16 for parallel polarization. Now the electric fields lie in the plane of incidence, and the associated magnetic fields are perpendicular to the plane of incidence. With reference to the directions indicated in Fig. 8-16, the fields of the incident, reflected, and transmitted waves are given by

INTEL-1014
U.S. Patent 7,151,430

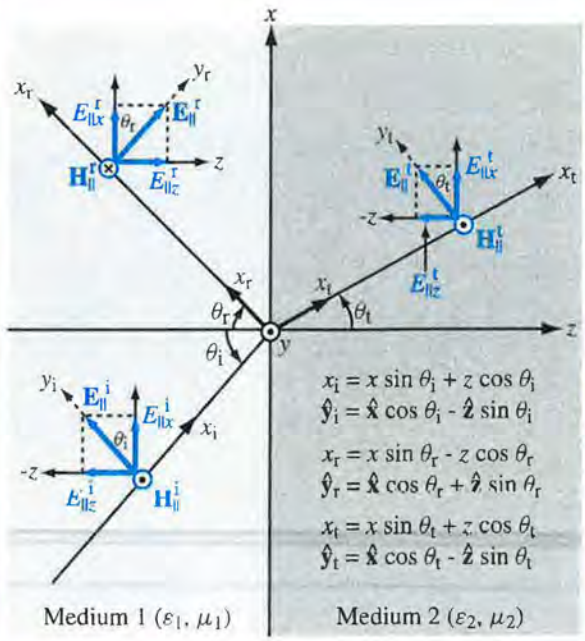


Figure 8-16: Parallel polarized plane wave incident at an angle θ_i upon a planar boundary.

Incident Wave

$$\widetilde{\mathbf{E}}^i_\parallel = \hat{\mathbf{y}}_i E^i_{\parallel 0} e^{-jk_1 x_i}$$
$$= (\hat{\mathbf{x}} \cos\theta_i - \hat{\mathbf{z}} \sin\theta_i) E^i_{\parallel 0} e^{-jk_1(x \sin\theta_i + z\cos\theta_i)}, \quad (8.65a)$$

$$\widetilde{\mathbf{H}}^i_\parallel = \hat{\mathbf{y}} \frac{E^i_{\parallel 0}}{\eta_1} e^{-jk_1 x_i} = \hat{\mathbf{y}} \frac{E^i_{\parallel 0}}{\eta_1} e^{-jk_1(x\sin\theta_i + z\cos\theta_i)}, \quad (8.65b)$$

Reflected Wave

$$\widetilde{\mathbf{E}}^r_\parallel = \hat{\mathbf{y}}_r E^r_{\parallel 0} e^{-jk_1 x_r}$$
$$= (\hat{\mathbf{x}} \cos\theta_r + \hat{\mathbf{z}} \sin\theta_r) E^r_{\parallel 0} e^{-jk_1(x\sin\theta_r - z\cos\theta_r)}, \quad (8.65c)$$

$$\widetilde{\mathbf{H}}^r_\parallel = -\hat{\mathbf{y}} \frac{E^r_{\parallel 0}}{\eta_1} e^{-jk_1 x_r}$$
$$= -\hat{\mathbf{y}} \frac{E^r_{\parallel 0}}{\eta_1} e^{-jk_1(x\sin\theta_r - z\cos\theta_r)}, \quad (8.65d)$$

Transmitted Wave

$$\widetilde{\mathbf{E}}^t_\parallel = \hat{\mathbf{y}}_t E^t_{\parallel 0} e^{-jk_2 x_t}$$
$$= (\hat{\mathbf{x}} \cos\theta_t - \hat{\mathbf{z}} \sin\theta_t) E^t_{\parallel 0} e^{-jk_2(x\sin\theta_t + z\cos\theta_t)}, \quad (8.65e)$$

$$\widetilde{\mathbf{H}}^t_\parallel = \hat{\mathbf{y}} \frac{E^t_{\parallel 0}}{\eta_2} e^{-jk_2 x_t} = \hat{\mathbf{y}} \frac{E^t_{\parallel 0}}{\eta_2} e^{-jk_2(x\sin\theta_t + z\cos\theta_t)}. \quad (8.65f)$$

By matching the tangential components of $\widetilde{\mathbf{E}}$ and $\widetilde{\mathbf{H}}$ in the two media at $z = 0$, as we did previously in the perpendicular-polarization case, we again obtain the relations defining Snell's laws, as well as the following expressions for the ***Fresnel reflection and transmission coefficients for parallel polarization***:

$$\Gamma_\parallel = \frac{E^r_{\parallel 0}}{E^i_{\parallel 0}} = \frac{\eta_2 \cos\theta_t - \eta_1 \cos\theta_i}{\eta_2 \cos\theta_t + \eta_1 \cos\theta_i}, \quad (8.66a)$$

$$\tau_\parallel = \frac{E^t_{\parallel 0}}{E^i_{\parallel 0}} = \frac{2\eta_2 \cos\theta_i}{\eta_2 \cos\theta_t + \eta_1 \cos\theta_i}. \quad (8.66b)$$

The preceding expressions can be shown to yield the relation

$$\tau_\parallel = (1 + \Gamma_\parallel) \frac{\cos\theta_i}{\cos\theta_t}. \quad (8.67)$$

We noted earlier in connection with the perpendicular-polarization case that, when the second medium is a perfect conductor with $\eta_2 = 0$, the incident wave gets totally reflected by the boundary. The same is true for parallel polarization; setting $\eta_2 = 0$ in Eqs. (8.66a) and (8.66b) gives $\Gamma_\parallel = -1$ and $\tau_\parallel = 0$.

For nonmagnetic materials, Eq. (8.66a) becomes

$$\Gamma_\parallel = \frac{-(\varepsilon_2/\varepsilon_1)\cos\theta_i + \sqrt{(\varepsilon_2/\varepsilon_1) - \sin^2\theta_i}}{(\varepsilon_2/\varepsilon_1)\cos\theta_i + \sqrt{(\varepsilon_2/\varepsilon_1) - \sin^2\theta_i}} \quad (\text{for } \mu_1 = \mu_2). \quad (8.68)$$

INTEL-1014
U.S. Patent 7,151,430

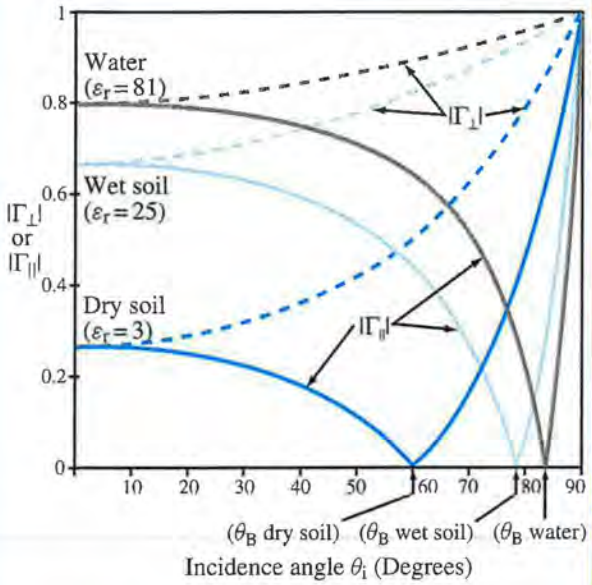


Figure 8-17: Plots for $|\Gamma_\perp|$ and $|\Gamma_\parallel|$ as a function of θ_i for a dry soil surface, a wet-soil surface, and a water surface. For each surface, $|\Gamma_\parallel| = 0$ at the Brewster angle.

To illustrate the angular variations of the magnitudes of $\Gamma_\perp$ and $\Gamma_\parallel$, in Fig. 8-17 we show plots for waves incident in air onto three different types of dielectric surfaces: dry soil ($\varepsilon_r = 3$), wet soil ($\varepsilon_r = 25$), and water ($\varepsilon_r = 81$). For each of the surfaces, (1) $\Gamma_\perp = \Gamma_\parallel$ at normal incidence ($\theta_i = 0$), as expected, (2) $|\Gamma_\perp| = |\Gamma_\parallel| = 1$ at *grazing* incidence ($\theta_i = 90°$), and (3) $\Gamma_\parallel$ goes to zero at an angle labeled the ***Brewster angle*** in Fig. 8-17. For nonmagnetic materials, the Brewster angle exists only for parallel polarization, and its value depends on the ratio $(\varepsilon_2/\varepsilon_1)$, as we will see shortly. *At the Brewster angle, the parallel-polarized component of the incident wave is totally transmitted into medium 2.*

8-4.3 Brewster Angle

The Brewster angle θ_B is defined as the incidence angle θ_i at which the Fresnel reflection coefficient $\Gamma = 0$.

Perpendicular Polarization

For perpendicular polarization, the Brewster angle $\theta_{B\perp}$ can be obtained by setting the numerator of the expression for $\Gamma_\perp$, given by Eq. (8.58a), equal to zero or, equivalently, when

$$\eta_2 \cos\theta_i = \eta_1 \cos\theta_t. \tag{8.69}$$

After (1) squaring both sides of Eq. (8.69), (2) using Eq. (8.56), (3) solving for θ_i, and then denoting θ_i as $\theta_{B\perp}$, we have

$$\sin\theta_{B\perp} = \sqrt{\frac{1-(\mu_1\varepsilon_2/\mu_2\varepsilon_1)}{1-(\mu_1/\mu_2)^2}}. \tag{8.70}$$

Because the denominator of Eq. (8.70) goes to zero when $\mu_1 = \mu_2$, *$\theta_{B\perp}$ does not exist for nonmagnetic materials.*

Parallel Polarization

The value of θ_i, denoted $\theta_{B\parallel}$, at which $\Gamma_\parallel = 0$ can be found by setting the numerator of Eq. (8.66a) equal to zero. The result is identical with Eq. (8.70), but with μ and ε interchanged. That is,

$$\sin\theta_{B\parallel} = \sqrt{\frac{1-(\varepsilon_1\mu_2/\varepsilon_2\mu_1)}{1-(\varepsilon_1/\varepsilon_2)^2}}. \tag{8.71}$$

For nonmagnetic materials,

$$\theta_{B\parallel} = \sin^{-1}\sqrt{\frac{1}{1+(\varepsilon_1/\varepsilon_2)}} = \tan^{-1}\sqrt{\frac{\varepsilon_2}{\varepsilon_1}} \quad (\text{for } \mu_1 = \mu_2). \tag{8.72}$$

The Brewster angle is also called the ***polarizing angle***. This is because, if a wave composed of both perpendicular and parallel polarization components is incident upon a nonmagnetic surface at the Brewster angle $\theta_{B\parallel}$, the parallel polarized component is totally transmitted

INTEL-1014
U.S. Patent 7,151,430

into the second medium, and only the perpendicularly polarized component is reflected by the surface. Natural light, including sunlight and light generated by most manufactured sources, is considered unpolarized because the direction of the electric field of the light waves varies randomly in angle over the plane perpendicular to the direction of propagation. Thus, on average half of the intensity of natural light is perpendicularly polarized and the other half is parallel polarized. When unpolarized light is incident upon a surface at the Brewster angle, the reflected wave is strictly perpendicularly polarized. Hence, the reflection process acts as a polarizer.

REVIEW QUESTIONS

Q8.4 Can total internal reflection take place for a wave incident in medium 1 (with n_1) onto medium 2 (with n_2) when $n_2 > n_1$?

Q8.5 What is the difference between the boundary conditions applied in Section 8-1.1 for normal incidence and those applied in Section 8-4.1 for oblique incidence with perpendicular polarization?

Q8.6 Why is the Brewster angle also called the polarizing angle?

Q8.7 At the boundary, the vector sum of the tangential components of the incident and reflected electric fields has to be equal to the tangential component of the transmitted electric field. For $\varepsilon_{r_1} = 1$ and $\varepsilon_{r_2} = 16$, determine the Brewster angle and then verify the validity of the preceding statement by sketching to scale the tangential components of the three electric fields at the Brewster angle.

EXERCISE 8.7 A wave in air is incident upon the flat boundary of a soil medium with $\varepsilon_r = 4$ and $\mu_r = 1$ at $\theta_i = 50°$. Determine $\Gamma_\perp$, $\tau_\perp$, $\Gamma_\parallel$, and $\tau_\parallel$,

Ans. $\Gamma_\perp = -0.48, \tau_\perp = 0.52, \Gamma_\parallel = -0.16, \tau_\parallel = 0.58.$

EXERCISE 8.8 Determine the Brewster angle for the boundary of Exercise 8.7.

Ans. $\theta_B = 63.4°$.

EXERCISE 8.9 Show that the incident, reflected, and transmitted electric and magnetic fields given by Eqs. (8.65a) through (8.65f) all have the same exponential phase function along the x-direction.

Ans. With the help of Eqs. (8.55) and (8.56), all six fields are shown to vary as $e^{-jk_1 x \sin\theta_i}$.

8-5 Reflectivity and Transmissivity

The reflection and transmission coefficients represent the ratios of the reflected and transmitted electric field amplitudes to the amplitude of the incident wave. We now examine power ratios, and we start the process by considering the perpendicular polarization case. Figure 8-18 shows a circular beam of electromagnetic energy incident upon the boundary between two contiguous, lossless media. The area of the spot illuminated by the beam is A, and the incident, reflected, and transmitted beams have electric-field amplitudes $E^i_{\perp 0}$, $E^r_{\perp 0}$, and $E^t_{\perp 0}$, respectively. The average power densities carried by the incident, reflected, and transmitted beams are

$$S^i_\perp = \frac{|E^i_{\perp 0}|^2}{2\eta_1}, \tag{8.73a}$$

$$S^r_\perp = \frac{|E^r_{\perp 0}|^2}{2\eta_1}, \tag{8.73b}$$

$$S^t_\perp = \frac{|E^t_{\perp 0}|^2}{2\eta_2}, \tag{8.73c}$$

where η_1 and η_2 are the intrinsic impedances of media 1 and 2, respectively. The cross-sectional areas of the

INTEL-1014
U.S. Patent 7,151,430

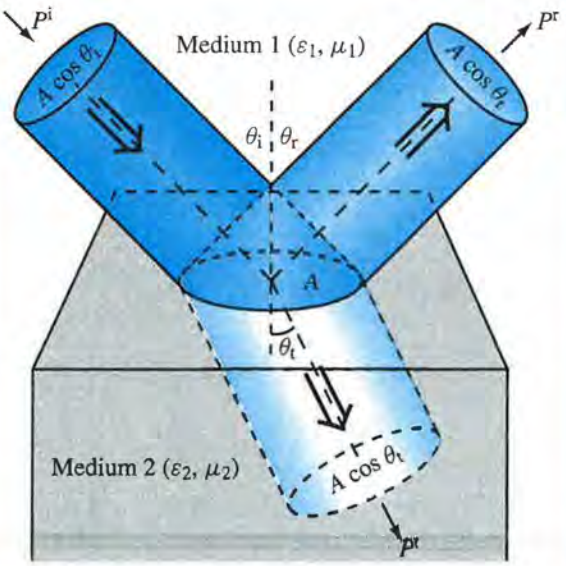


Figure 8-18: Reflection and transmission of an incident circular beam illuminating a spot of size A on the interface.

incident, reflected, and transmitted beams are

$$A_i = A\cos\theta_i, \tag{8.74a}$$

$$A_r = A\cos\theta_r, \tag{8.74b}$$

$$A_t = A\cos\theta_t, \tag{8.74c}$$

and the corresponding average powers carried by the beams are

$$P_\perp^i = S_\perp^i A_i = \frac{|E_{\perp 0}^i|^2}{2\eta_1} A\cos\theta_i, \tag{8.75a}$$

$$P_\perp^r = S_\perp^r A_r = \frac{|E_{\perp 0}^r|^2}{2\eta_1} A\cos\theta_r, \tag{8.75b}$$

$$P_\perp^t = S_\perp^t A_t = \frac{|E_{\perp 0}^t|^2}{2\eta_2} A\cos\theta_t. \tag{8.75c}$$

The ***reflectivity*** R (also called ***reflectance*** in optics) is defined as the ratio of the reflected power to the incident power. The reflectivity for perpendicular polarization is then

$$R_\perp = \frac{P_\perp^r}{P_\perp^i} = \frac{|E_{\perp 0}^r|^2 \cos\theta_r}{|E_{\perp 0}^i|^2 \cos\theta_i} = \left|\frac{E_{\perp 0}^r}{E_{\perp 0}^i}\right|^2, \tag{8.76}$$

where we used the fact that $\theta_r = \theta_i$, in accordance with Snell's law of reflection. The ratio of the reflected to incident electric field amplitudes, $|E_{\perp 0}^r / E_{\perp 0}^i|$, is simply equal to the magnitude of the reflection coefficient $\Gamma_\perp$. Hence,

$$\boxed{R_\perp = |\Gamma_\perp|^2,} \tag{8.77}$$

and, similarly, for parallel polarization

$$\boxed{R_\parallel = \frac{P_\parallel^r}{P_\parallel^i} = |\Gamma_\parallel|^2.} \tag{8.78}$$

The ***transmissivity*** T (or ***transmittance*** in optics) is defined as the ratio of the transmitted power to incident power:

$$T_\perp = \frac{P_\perp^t}{P_\perp^i} = \frac{|E_{\perp 0}^t|^2}{|E_{\perp 0}^i|^2} \frac{\eta_1}{\eta_2} \frac{A\cos\theta_t}{A\cos\theta_i}$$

$$= |\tau_\perp|^2 \left(\frac{\eta_1 \cos\theta_t}{\eta_2 \cos\theta_i}\right), \tag{8.79a}$$

$$T_\parallel = \frac{P_\parallel^t}{P_\parallel^i} = |\tau_\parallel|^2 \left(\frac{\eta_1 \cos\theta_t}{\eta_2 \cos\theta_i}\right). \tag{8.79b}$$

The incident, reflected, and transmitted waves do not have to obey any such laws as conservation of electric field, conservation of magnetic field, or conservation of power density, but they do have to obey the law of conservation of power. In fact, in many cases the transmitted electric field is larger than the incident electric field.

INTEL-1014
U.S. Patent 7,151,430

Table 8-2: Expressions for Γ, τ, R, and T for wave incidence from a medium with intrinsic impedance η_1 onto a medium with intrinsic impedance η_2. Angles θ_i and θ_t are the angles of incidence and transmission, respectively.

Property	Normal Incidence $\theta_i = \theta_t = 0$	Perpendicular Polarization	Parallel Polarization
Reflection coefficient	$\Gamma = \dfrac{\eta_2 - \eta_1}{\eta_2 + \eta_1}$	$\Gamma_\perp = \dfrac{\eta_2 \cos\theta_i - \eta_1 \cos\theta_t}{\eta_2 \cos\theta_i + \eta_1 \cos\theta_t}$	$\Gamma_\parallel = \dfrac{\eta_2 \cos\theta_t - \eta_1 \cos\theta_i}{\eta_2 \cos\theta_t + \eta_1 \cos\theta_i}$
Transmission coefficient	$\tau = \dfrac{2\eta_2}{\eta_2 + \eta_1}$	$\tau_\perp = \dfrac{2\eta_2 \cos\theta_i}{\eta_2 \cos\theta_i + \eta_1 \cos\theta_t}$	$\tau_\parallel = \dfrac{2\eta_2 \cos\theta_i}{\eta_2 \cos\theta_t + \eta_1 \cos\theta_i}$
Relation of Γ to τ	$\tau = 1 + \Gamma$	$\tau_\perp = 1 + \Gamma_\perp$	$\tau_\parallel = (1 + \Gamma_\parallel)\dfrac{\cos\theta_i}{\cos\theta_t}$
Reflectivity	$R = \lvert\Gamma\rvert^2$	$R_\perp = \lvert\Gamma_\perp\rvert^2$	$R_\parallel = \lvert\Gamma_\parallel\rvert^2$
Transmissivity	$T = \lvert\tau\rvert^2\left(\dfrac{\eta_1}{\eta_2}\right)$	$T_\perp = \lvert\tau_\perp\rvert^2 \dfrac{\eta_1 \cos\theta_t}{\eta_2 \cos\theta_i}$	$T_\parallel = \lvert\tau_\parallel\rvert^2 \dfrac{\eta_1 \cos\theta_t}{\eta_2 \cos\theta_i}$
Relation of R to T	$T = 1 - R$	$T_\perp = 1 - R_\perp$	$T_\parallel = 1 - R_\parallel$

Notes: (1) $\sin\theta_t = \sqrt{\mu_1\varepsilon_1/\mu_2\varepsilon_2}\sin\theta_i$; (2) $\eta_1 = \sqrt{\mu_1/\varepsilon_1}$; (3) $\eta_2 = \sqrt{\mu_2/\varepsilon_2}$; (4) for nonmagnetic media, $\eta_2/\eta_1 = n_1/n_2$.

Conservation of power requires that the incident power be equal to the sum of the reflected and transmitted powers. That is, for perpendicular polarization, for example,

$$P_\perp^i = P_\perp^r + P_\perp^t, \tag{8.80}$$

or

$$\frac{|E_{\perp 0}^i|^2}{2\eta_1} A\cos\theta_i = \frac{|E_{\perp 0}^r|^2}{2\eta_1} A\cos\theta_r + \frac{|E_{\perp 0}^t|^2}{2\eta_2} A\cos\theta_t. \tag{8.81}$$

Use of Eqs. (8.76), (8.79a), and (8.79b) leads to

$$R_\perp + T_\perp = 1, \tag{8.82a}$$

$$R_\parallel + T_\parallel = 1, \tag{8.82b}$$

or

$$|\Gamma_\perp|^2 + |\tau_\perp|^2\left(\frac{\eta_1\cos\theta_t}{\eta_2\cos\theta_i}\right) = 1, \tag{8.83a}$$

$$|\Gamma_\parallel|^2 + |\tau_\parallel|^2\left(\frac{\eta_1\cos\theta_t}{\eta_2\cos\theta_i}\right) = 1. \tag{8.83b}$$

Figure 8-19 shows plots for $(R_\parallel, T_\parallel)$ as a function of θ_i for an air–glass interface. Note that the sum of $R_\parallel$ and $T_\parallel$ is always equal to 1, as mandated by Eq. (8.82b). We also note that, at the Brewster angle θ_B, $R_\parallel = 0$ and $T_\parallel = 1$.

Table 8-2 provides a summary of the general expressions for Γ, τ, R, and T for both normal incidence and oblique incidence.

INTEL-1014
U.S. Patent 7,151,430

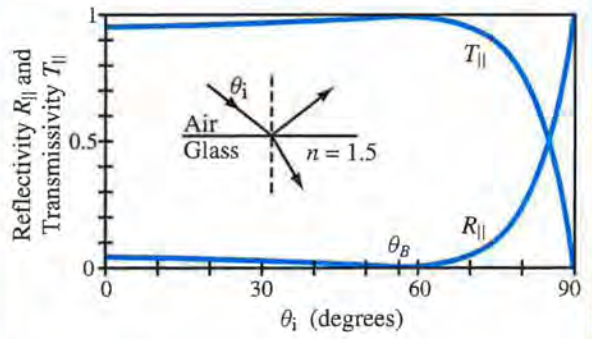


Figure 8-19: Angular plots for $(R_\parallel, T_\parallel)$ for an air–glass interface.

Example 8-7 Beam of Light

A 5-W beam of light with circular cross section is incident in air upon a plane boundary of a dielectric medium with an index of refraction of 5. If the angle of incidence is 60° and the incident wave is parallel polarized, determine the transmission angle and the powers contained in the reflected and transmitted beams.

Solution: From Eq. (8.56),

$$\sin\theta_t = \frac{n_1}{n_2}\sin\theta_i = \frac{1}{5}\sin 60° = 0.17$$

or

$$\theta_t = 10°.$$

With $\varepsilon_2/\varepsilon_1 = n_2^2/n_1^2 = (5)^2 = 25$, the reflection coefficients for parallel polarization can be computed by applying Eq. (8.68) as follows:

$$\Gamma_\parallel = \frac{-(\varepsilon_2/\varepsilon_1)\cos\theta_i + \sqrt{(\varepsilon_2/\varepsilon_1) - \sin^2\theta_i}}{(\varepsilon_2/\varepsilon_1)\cos\theta_i + \sqrt{(\varepsilon_2/\varepsilon_1) - \sin^2\theta_i}}$$

$$= \frac{-25\cos 60° + \sqrt{25 - \sin^2 60°}}{25\cos 60° + \sqrt{25 - \sin^2 60°}} = -0.435.$$

The reflected and transmitted powers are then

$$P_\parallel^r = P_\parallel^i|\Gamma_\parallel|^2 = 5(0.435)^2 = 0.95 \text{ W},$$

$$P_\parallel^t = P_\parallel^i - P_\parallel^r = 5 - 0.95 = 4.05 \text{ W}. \blacksquare$$

8-6 Geometric Optics

In the foregoing material, we examined the reflection and refraction behavior of *uniform, plane* electromagnetic waves when incident upon *planar* boundaries between dissimilar materials. In practice, wave interaction with matter may involve waves that are neither uniform nor plane. Also, the objects that the waves interact with may be of any shape and size. How then do we put the results we obtained in the preceding sections to use when dealing with practical situations? The answer depends in large part on the size of the object and the degree of curvature of its surfaces relative to the wavelength of the incident wave. We have available to us two fundamental approaches for describing wave interaction with matter; these are the physical-optics method and the geometric-optics method. In ***physical optics***, also known as ***wave optics***, a wave is characterized mathematically by all its attributes: its amplitude, phase factor, and polarization vector. In contrast, in ***geometric optics***, otherwise known as ***ray optics***, a wave is represented by a ray denoting the direction of travel of the wave's energy. Neither the phase nor the polarization of the wave is accounted for explicitly in geometric optics. Thus, geometric optics is a ray approximation of physical optics. Although it is mathematically superior and its formulation is traceable back to Maxwell's equations, the physical-optics method is mathematically more complicated to apply than the geometric-optics method, and therefore physical optics is used whenever geometric optics is inapplicable or when a greater degree of accuracy is desired than that used in geometric optics. *In general, the geometric-optics method provides fairly accurate results whenever the size of the object illuminated by an electromagnetic wave is much larger than the wavelength* λ. There is also the

INTEL-1014
U.S. Patent 7,151,430

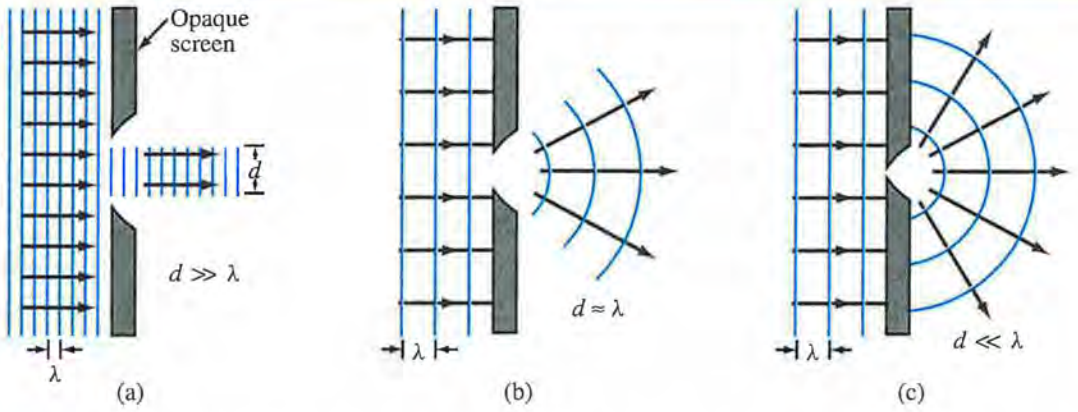


Figure 8-20: A plane wave of wavelength λ incident upon an opaque screen with opening of diameter d. The wave emerging from the opening (a) maintains its original direction if $d \gg \lambda$, (b) gets diffracted by the opening when $d \approx \lambda$, and (c) behaves like a spherical wave emanating from a point source when $d \ll \lambda$.

additional secondary requirement that the curvatures of the object's surfaces be relatively smooth relative to λ.

By treating waves as rays of energy, geometric optics does not account for the relative phases of multiple waves arriving at a given point in space. Consequently, ***interference effects*** due to phase addition and subtraction cannot be predicted on the basis of geometric optics. Another wave phenomenon ignored by geometric optics is ***diffraction***, which is the deviation of wave propagation from the straight-line representation used in geometric optics. Diffraction accounts for the "bending" of waves around the edges of objects. To explain what we mean by diffraction, let us consider the three situations depicted in Fig. 8-20. In part (a), a plane wave is incident upon an opaque barrier with a circular opening whose diameter d is very large relative to the wavelength λ. Apart from some small edge effects, the wave emerging from the opening continues to move in a straight line. This situation adheres to the condition of geometric optics, that the dimensions of reflecting boundaries (in a transparent medium) or, conversely, the dimensions of openings in opaque boundaries be much larger than λ. The situations in Fig. 8-20(b) and (c) are for openings with diameters comparable with and smaller than λ, respectively. In both cases, the incident wave is said to be ***diffracted*** by the opening; as a consequence, the emerging wave is no longer a plane wave. To account for wave interference and diffraction, it is necessary to use the physical-optics representation of electromagnetic waves. We should note that the term "optics" in the names "geometric optics" and "physical optics" is historically based and does not imply that these methods are limited to optical systems; the methods are applicable across the entire electromagnetic spectrum.

The next two sections are intended to provide an overview of geometric optics, with particular emphasis on how mirrors and lenses are used as imaging devices.

8-7 Images Formed by Mirrors

Mirrors are used throughout the electromagnetic spectrum, including the x-ray, ultraviolet, visible, infrared,

INTEL-1014
U.S. Patent 7,151,430

and radio regions. A mirror is usually made by coating a dielectric substrate, such as glass, with a thin layer of silver or aluminum. A perfect mirror is a perfectly conducting surface with a reflectivity of 1, and it is analogous to a short circuit at the end of a transmission line. In this section, we will examine how images are formed by both plane mirrors and spherical mirrors.

8-7.1 Images Formed by Plane Mirrors

The point source at point O in Fig. 8-21 is at a distance s, called the ***object distance***, in front of a plane mirror.

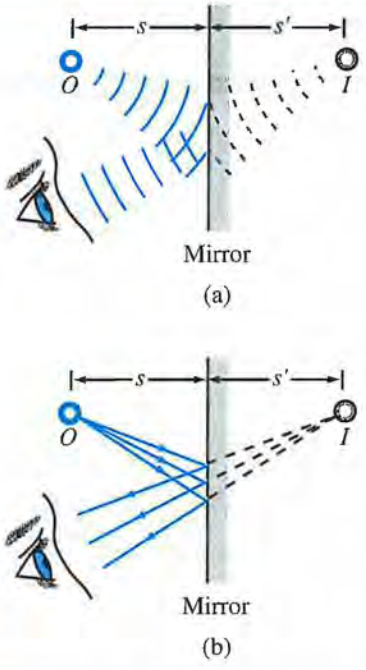


Figure 8-21: The image-formation process due to reflection from a plane mirror may be represented (a) in terms of spherical wavefronts or (b) in terms of rays of light emanating from the source at point O.

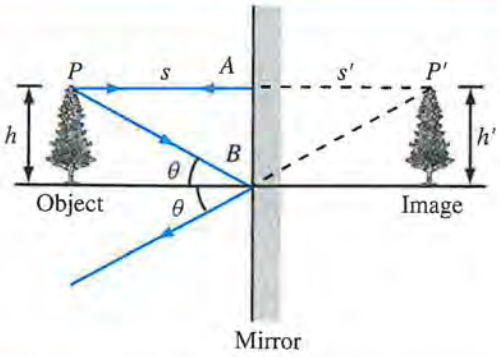


Figure 8-22: Image location and orientation are determined by ray optics and Snell's law of reflection.

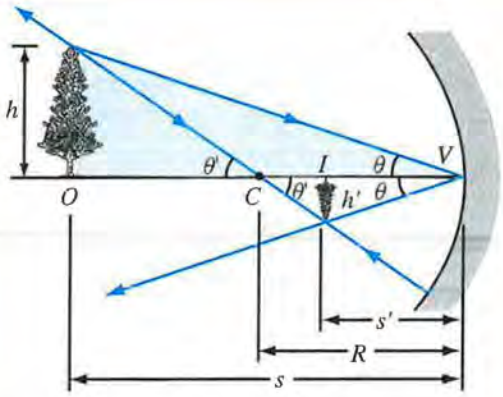
The source radiates spherical waves, which may be represented by wavefronts, as shown in Fig. 8-21(a), or, equivalently, the waves may be represented by light rays, as in Fig. 8-21(b). To a viewer at the location shown in the figure, the reflected rays appear to come from point I located a distance s', called the ***image distance***, behind the mirror. The image is called a ***real image*** if the rays of reflected light actually pass through the image point, and it is called a ***virtual image*** if the rays do not actually pass through the image point but appear to diverge from that point. The image formed by the plane mirror in this case is a virtual image.

By considering a self-luminous or externally illuminated object to consist of a large number of point sources, the point-source imaging process can be extended to generate the image of the object shown in Fig. 8-22. To determine where an image is formed, it is necessary to follow at least two rays of light as they are reflected by the mirror. Point P', the image of point P, is at the intersection of the horizontal ray to the mirror, which reflects back on itself, and the oblique ray that reflects at point B on the mirror. Because triangles PAB and $P'AB$ are congruent, $s = s'$ and $h = h'$.

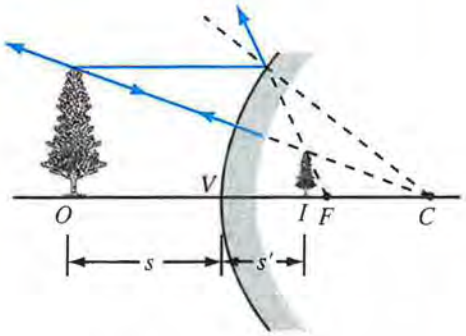
INTEL-1014
U.S. Patent 7,151,430

8-7.2 Images Formed by Spherical Mirrors

A spherical mirror is a segment of a sphere painted or covered with a highly reflective material. It is called a ***concave*** mirror when the rays of light are reflected by its inner surface, as in Fig. 8-23(a), and it is called a ***convex*** mirror when the reflection takes place at its outer surface, as in Fig. 8-23(b). The center of the sphere (of which the spherical mirror is a part) is called the ***center of curvature*** and is denoted by point C, and the radius R is called the ***radius of curvature***. The ***principal axis*** of the mirror is the line connecting point C to point V, the center (or vertex) of the spherical segment. In Fig. 8-23(a), the object of height h and located at object distance s is imaged as an inverted real image of height h' at image distance s'. From the large triangle with included angle θ, we have $\tan\theta = h/s$, and the small triangle with angle θ gives $\tan\theta = -h'/s'$, where the negative sign signifies that the image is inverted because h' is negative. The ***lateral magnification*** of the mirror is defined as the ratio of h' to h:



(a) Concave mirror



(b) Convex mirror

Figure 8-23: Image formation by (a) a concave mirror and (b) a convex mirror.

$$M = \frac{h'}{h} = \frac{s'}{s}. \qquad (8.84)$$

From the two similar triangles involving the angles θ',

$$\tan\theta' = \frac{h}{s-R} = -\frac{h'}{R-s'}. \qquad (8.85)$$

Upon combining Eqs. (8.84) and (8.85), we obtain the ***mirror equation***

$$\frac{1}{s} + \frac{1}{s'} = \frac{2}{R}. \qquad (8.86)$$

When the object is very far away from the mirror compared to R, we can regard it as being at infinity, in which case $1/s \simeq 0$ and $s' \simeq R/2$. Thus, the image point is halfway between the center of curvature C and the center of the mirror V, as shown in Fig. 8-24. In this case, the image point is called the ***focal point*** F, and the image distance is called the ***focal length*** of the mirror, f. That is,

$$f = \frac{R}{2}, \qquad (8.87)$$

INTEL-1014
U.S. Patent 7,151,430

Table 8-3: Sign convention for spherical mirrors.

Quantity	Sign	Condition
s	+	if object is in front side of mirror (real object)
s	−	if object is in back side of mirror (virtual object)
s'	+	if image is in front side of mirror (real image)
s'	−	if image is in back side of mirror (virtual image)
f and R	+	if C is in front side of mirror (concave)
f and R	−	if C is in back side of mirror (convex)

Notes: (1) The front side of a mirror is defined as the side from which the light approaches the mirror, regardless of the mirror's shape. (2) An object cannot be virtual in single-mirror reflection, but its image, if virtual, can become a virtual object for reflections by additional mirrors.

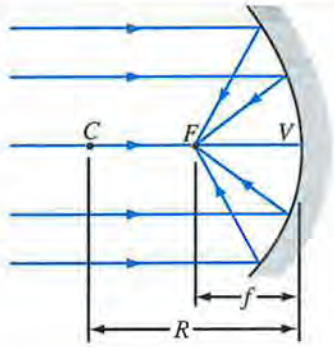


Figure 8-24: A source point at infinity is imaged at the focal point F of the mirror. The focal length $f = R/2$.

and the mirror equation can be rewritten in terms of f as

$$\frac{1}{s} + \frac{1}{s'} = \frac{1}{f}. \quad (8.88)$$

An object at infinity is imaged at the focal point and, conversely, an object at the focal point is imaged at infinity.

Equations (8.84) and (8.88) can be used for both concave and convex mirrors, as long as we adhere to the sign convention given in Table 8-3. The sign convention refers to two regions: (1) the ***front side*** of the mirror, which is the region in which the light rays actually exist, and (2) the ***back side***, which is the region where virtual images of real objects are formed. For both mirrors in Figs. 8-23(a) and (b), the front sides are the sides to the left of the mirrors. Note that f is positive for concave mirrors and negative for convex mirrors.

The magnification and orientation (erect or inverted) of the image depend on the type of mirror (concave or convex) and the location of the object relative to the mirror center. A summary of these properties is provided in Table 8-4 for various object locations.

Example 8-8 Image Formed by a Concave Mirror

A flower is placed at a distance of 20 cm in front of a concave mirror with a 15-cm focal length. Locate and describe the image.

Solution: Inserting $s = 20$ cm and $f = 15$ cm in Eq. (8.88) gives

$$\frac{1}{20} + \frac{1}{s'} = \frac{1}{15},$$

INTEL-1014
U.S. Patent 7,151,430

Table 8-4: Images of real objects formed by spherical mirrors.[a]

Concave				
Object	**Image**			
Location	Type	Location	Orientation	Relative size
$2f < s < \infty$	Real	$2f > s' > f$	Inverted	Minified
$s = 2f$	Real	$s' = 2f$	Inverted	Same size
$f < s < 2f$	Real	$\infty > s' > 2f$	Inverted	Magnified
$s = f$		$s' = \infty$		
$s < f$	Virtual	$\lvert s' \rvert > s$	Erect	Magnified
Convex				
Object	**Image**			
Location	Type	Location	Orientation	Relative size
Anywhere	Virtual	$\lvert s' \rvert < \lvert f \rvert$, $s > \lvert s' \rvert$	Erect	Minified

[a]Adapted from E. Hecht, *Optics*, second edition, Addison-Wesley Publishing Co., 1990.

which leads to $s' = 60$ cm. According to Eq. (8.84), the lateral magnification is

$$M = -\frac{s'}{s} = -\frac{60}{15} = -4.$$

The magnitude of M means that the image is magnified by a factor of 4, and the negative sign means that the image is inverted. ■

8-8 Images Formed by Spherical Lenses

Lenses are commonly used to form images in optical instruments, such as cameras, telescopes, and microscopes, but their use also extends to nonimaging applications and to many parts of the electromagnetic spectrum. A lens is characterized in terms of three features: its size, shape, and index of refraction. For the present treatment, we will limit our discussion to *thin* lenses with spherical or planar surfaces, such as those shown in Fig. 8-25. For each lens, the signs of the radii of curvature R_1 and R_2 of its two surfaces are governed by the sign convention discussed later and summarized in Table 8-5. Convex lenses, which also are called ***converging*** or ***positive lenses***, are thicker

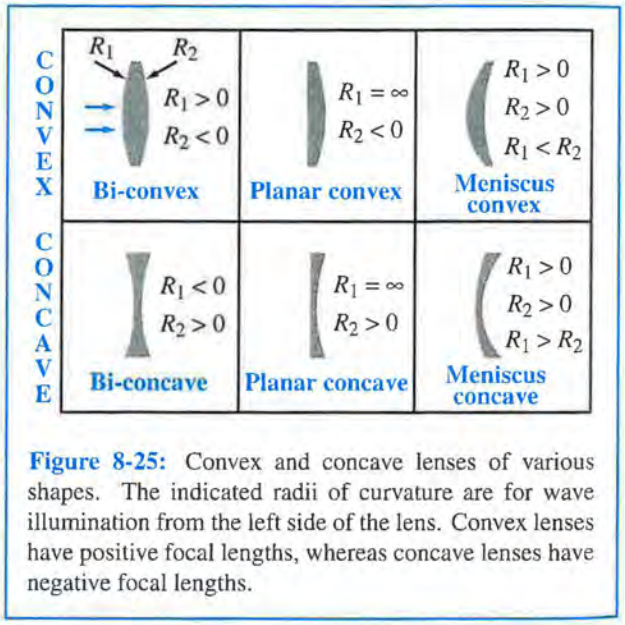


Figure 8-25: Convex and concave lenses of various shapes. The indicated radii of curvature are for wave illumination from the left side of the lens. Convex lenses have positive focal lengths, whereas concave lenses have negative focal lengths.

INTEL-1014
U.S. Patent 7,151,430

Table 8-5: Sign convention for spherical refracting surfaces and thin lenses.

Quantity	Sign	Condition
s	+	if object is in front side of surface (real object)
s	−	if object is in back side of surface (virtual object)
s'	+	if image is in back side of surface (real image)
s'	−	if image is in front side of surface (virtual image)
R	+	if C is in back side of surface
R	−	if C is in front side of surface
f	+	convex lens
f	−	concave lens

Notes: (1) The front side of a surface is defined as the side from which the light approaches the surface. (2) An object cannot be virtual with refraction by a single surface, but its image, if virtual, can become a virtual object for refraction by another surface.

at the center than at the ends. In contrast, concave lenses, otherwise known as ***diverging*** or ***negative lenses***, are narrower at the center than at the ends.

The imaging process performed by a lens involves refraction at both of its surfaces. As an initial step toward understanding the process, we begin by considering the refraction at a spherical boundary between a medium with index of refraction n_1 and a second medium with index of refraction n_2, as shown in Fig. 8-26. Spherical waves radiated by a point source at point O are represented by rays emanating radially from the source in the direction of energy flow. When a ray reaches a point on the spherical boundary, it reflects and refracts in accordance with Snell's laws as if the surface is part of an infinite plane tangent to the surface at that point. Of the total energy arriving at point I, the bulk of it is due to rays incident upon the central region of the lens. Rays originating at the source and refracting at points within the central region of the spherical surface are called ***paraxial rays***. These rays form an image of the source at a single point, called the image point. The imaging process can be demonstrated by considering any one of these paraxial rays. One such ray is the ray at angle ϕ relative to the horizontal in

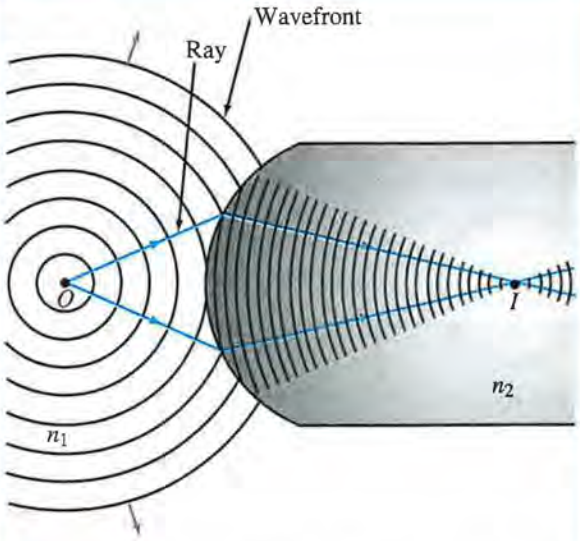


Figure 8-26: Spherical waves radiated by a source at O are refracted by the spherical boundary of medium 2 (with $n_2 > n_1$).

INTEL-1014
U.S. Patent 7,151,430

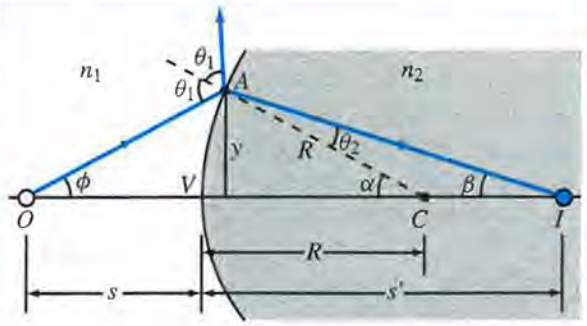


Figure 8-27: Ray refraction at a spherical boundary.

Fig. 8-27. At point A, Snell's law of refraction gives

$$n_1 \sin\theta_1 = n_2 \sin\theta_2, \tag{8.89}$$

where θ_1 is the angle between $\overline{OA}$ and the normal to the spherical surface at point A, which originates at C, the center of curvature of the spherical surface. Over the central region of the spherical surface, angles θ_1 and θ_2 are sufficiently small to allow use of the approximations $\sin\theta_1 \simeq \theta_1$ and $\sin\theta_2 \simeq \theta_2$. Hence, Eq. (8.89) may be rewritten as

$$n_1\theta_1 \simeq n_2\theta_2. \tag{8.90}$$

From the geometry of triangles OAC and AIC, we know that the exterior angle θ_1 is equal to the sum of angles ϕ and α and, similarly, angle α is equal to the sum of angles θ_2 and β. Thus,

$$\theta_1 = \phi + \alpha, \tag{8.91a}$$

$$\alpha = \theta_2 + \beta. \tag{8.91b}$$

Upon using these relations to replace θ_1 and θ_2 in Eq. (8.90), we have

$$n_1\phi + n_2\beta = (n_2 - n_1)\alpha. \tag{8.92}$$

The paraxial approximation noted earlier can again be invoked to allow us to use the approximation $\tan\theta \simeq \theta$ for angles ϕ, α, and β. Hence,

$$\phi \simeq \tan\phi = \frac{y}{s}, \tag{8.93a}$$

$$\alpha \simeq \tan\alpha = \frac{y}{R}, \tag{8.93b}$$

$$\beta \simeq \tan\beta = \frac{y}{s'}, \tag{8.93c}$$

where s and s' are the source (or object) and image distances and R is the radius of curvature of the spherical surface. Upon substituting these relations in Eq. (8.92) and dividing all terms by y, we have

$$\frac{n_1}{s} + \frac{n_2}{s'} = \frac{n_2 - n_1}{R} \quad \text{(single spherical boundary)}. \tag{8.94}$$

Since for a fixed source distance s, the image s' is independent of the angle ϕ that the ray makes with the axis, all paraxial rays focus at the image point I.

In contrast to mirrors, where real images are formed on the same side as the object, with a refracting surface, real images are formed on the side opposite the one from which the source of energy originates. The sign convention for spherical refracting surfaces is given in Table 8-5, which will also be used for thin lenses later.

We will now extend our results to a lens with two spherical surfaces of radii of curvature R_1 and R_2, as in Fig. 8-28. The lens has an index of refraction n_l and is surrounded by a medium with index of refraction n_m. The imaging process can be analyzed in two different ways, which we shall call the actual imaging process and the equivalent imaging process. If we have an object or source at point O in Fig. 8-28, the rays emanating from it will refract at the first surface of the lens, propagate to the second surface, and then refract again at the second surface. All paraxial rays end up intersecting at the image point I. Although this is what actually happens, it is not

INTEL-1014
U.S. Patent 7,151,430

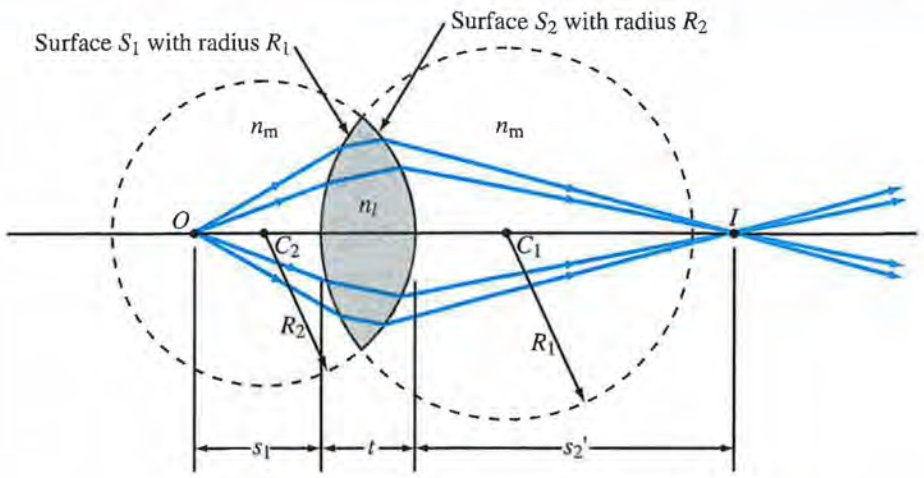


Figure 8-28: Image formation by a thin lens.

immediately obvious why the rays do intersect at point I or how to easily relate the image distance s_2' to the object distance s_1.

These questions can be addressed by using an equivalent imaging process that divides the refractive effects of the two surfaces of the lens into two sequential steps. Considering the first surface alone and treating it as if it were the boundary between the medium containing the object and an extended medium of index of refraction n_l (i.e., the same as the boundary we treated earlier in Fig. 8-27), the object located at point O in Fig. 8-29 produces an image I_1, located a distance s_1' from surface S_1. Because of the particular choice we made for the location of the object in Fig. 8-29, the image I_1 is virtual. The relationship governing the distances s_1 and s_1' is obtained from Eq. (8.94) upon replacing n_1 with n_m and n_2 with n_l:

$$\frac{n_m}{s_1} + \frac{n_l}{s_1'} = \frac{n_l - n_m}{R_1}, \tag{8.95}$$

where R_1 is the radius of curvature of surface S_1. We now repeat the process with respect to surface S_2 by treating

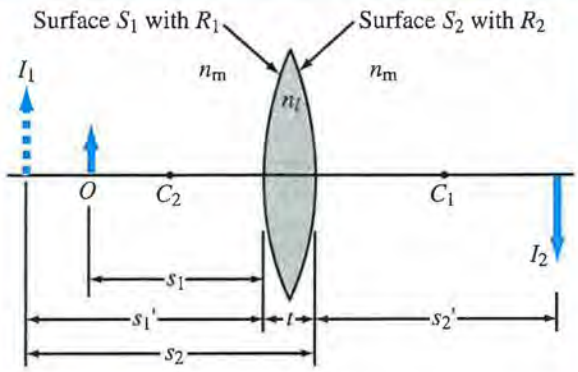


Figure 8-29: Image I_2 of object O can be determined by first locating image I_1 formed by surface S_1 of the lens and then using I_1 as the object for surface S_2.

the image I_1 as a virtual object at a distance s_2 from surface S_2. In this case, we regard S_2 as the boundary between a medium with index of refraction n_l to its

INTEL-1014
U.S. Patent 7,151,430

left (and containing its object I_1) and a medium with index of refraction n_m to its right. Hence, we need to reverse the assignments of n_l and n_m when using Eq. (8.94). Accordingly, for surface S_2, the final image I_2 at distance s_2' is related to s_2 by

$$\frac{n_l}{s_2} + \frac{n_m}{s_2'} = \frac{n_m - n_l}{R_2}. \tag{8.96}$$

As far as surface S_2 is concerned, its object I_1 is in its front side (the side containing the rays coming from I_1). Hence, by our sign convention, the distance s_2 must be positive; that is, $s_2 = |s_2|$. When we apply the sign convention to s_1', the image distance due to surface S_1, we find that s_1' must be negative because the image was formed on the same side as the object O. Hence, $s_1' = -|s_1'|$. From Fig. 8-29,

$$|s_2| = |s_1'| + t, \tag{8.97}$$

where t is the thickness of the lens. In view of the fact that s_1' is negative and s_2 is positive, it follows that

$$s_2 = -s_1' + t. \tag{8.98}$$

Upon using Eq. (8.98) in Eq. (8.96) and then adding Eqs. (8.95) and (8.96), we have

$$\frac{n_m}{s_1} + \frac{n_m}{s_2'} = (n_l - n_m)\left(\frac{1}{R_1} - \frac{1}{R_2}\right) + \frac{n_l t}{s_1'(s_1' - t)}. \tag{8.99}$$

For a thin lens with thickness t sufficiently small as to allow us to ignore the last term, we obtain the ***thin-lens equation*** given by

$$\frac{n_m}{s_1} + \frac{n_m}{s_2'} = (n_l - n_m)\left(\frac{1}{R_1} - \frac{1}{R_2}\right). \tag{8.100}$$

We note that, by our sign convention, $R_1 > 0$ and $R_2 < 0$ for the bi-convex lens we used in Fig. 8-29. The radii of curvature for lenses with various combinations of concave, convex, and planar surfaces are given in Fig. 8-25.

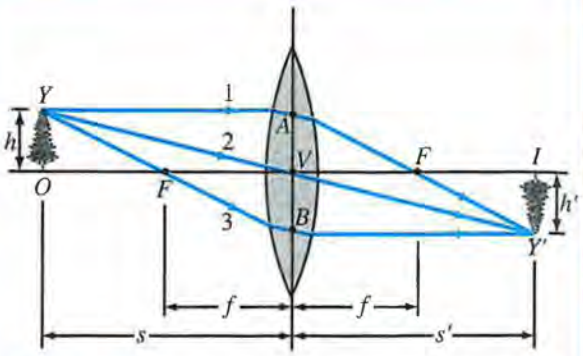


Figure 8-30: Rotation between object and image for a thin lens.

If the surrounding medium is air ($n_m = 1$), Eq. (8.100) reduces to the ***lensmaker's formula***:

$$\frac{1}{s} + \frac{1}{s'} = (n-1)\left(\frac{1}{R_1} - \frac{1}{R_2}\right) \quad \text{(thin lens)}, \tag{8.101}$$

where we have omitted the subscripts on s_1 and s_2' and n_l in Eq. (8.100). Since t is negligibly small, we now refer to s and s' as the object and image distances, respectively, and we measure them from the lens center, as shown in Fig. 8-30.

In Section 8-7.2, we defined the focal length f of a reflecting mirror as the image distance when the object is moved out to infinity. Applying the same definition for the lens leads to

$$\frac{1}{f} = (n-1)\left(\frac{1}{R_1} - \frac{1}{R_2}\right), \tag{8.102}$$

in which case Eq. (8.101) can be rewritten as

$$\frac{1}{s} + \frac{1}{s'} = \frac{1}{f} \quad \text{(Gaussian lens formula)}. \tag{8.103}$$

INTEL-1014
U.S. Patent 7,151,430

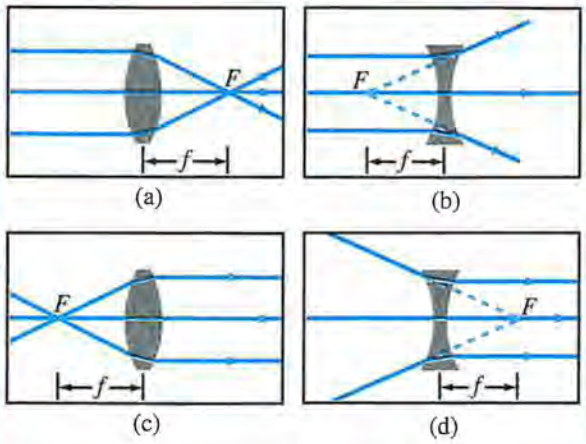


Figure 8-31: An object at infinity is imaged at the focal point, as in (a) and (b), and if the object is at the focal point, as in (c) and (d), it is imaged at infinity.

which is known as the ***Gaussian lens formula*** and is identical in form to Eq. (8.88) for mirrors. The sign convention for thin lenses is the same as that outlined in Table 8-5 for spherical refracting surfaces. *Convex lenses have positive focal lengths, and concave lenses have negative focal lengths.* According to Eq. (8.103), if the object is at infinity ($s = \infty$), then $s' = f$; this means that rays coming from infinity (and therefore parallel to the optic axis) are refracted by the lens and intersect at the focal point F, as in Fig. 8-31(a) for the positive-focal-length convex lens and in Fig. 8-31(b) for the negative-focal-length concave lens. The convex lens is a converging lens, whereas the concave lens is a diverging lens.

The Gaussian lens formula of Eq. (8.103) also states that if the object is at the focal point ($s = f$) then $s' = \infty$; the corresponding ray representation is illustrated in Figs. 8-31(c) and (d). These two properties will prove useful in locating the image of an object and in relating the size of the image to that of the object. In Fig. 8-30, the object at location O is of height h and its tip is denoted by point Y. The image at location I is inverted, it has a height h' (which is negative in this case), and its tip is at point Y'. Point Y' is at the intersection of rays 1, 2, and 3. Ray 1 arrives at the lens in a direction parallel to the optic axis, whereupon it is refracted by the lens and emerges in a direction that passes through the focal point F. (In the case of a diverging lens, ray 1 would appear to come from the focal point to the left of the lens.) Ray 3, drawn from point Y through the focal point F to the left of the lens, is refracted by the lens and emerges in a direction parallel to the optic axis. A third useful property of thin lenses pertains to the ray drawn through the center of the lens. Such a ray, labeled 2 in Fig. 8-30, emerges from the lens undeviated, meaning that points Y and Y' are joined by a straight line that passes through the center of the lens.

For rays emanating from an object to the left of the lens, the ray properties of thin lenses may be summarized as follows:

(1) For a converging lens, the ray arriving at the lens in a direction parallel to the optic axis, such as ray 1 in Fig. 8-30, gets diffracted by the lens and emerges in a direction that passes through the focal point F to the right of the lens. In the case of a diverging lens, the refracted ray would appear to come from the focal point to the left of the lens, as shown in Fig. 8-31(b).

(2) For both converging and diverging lenses, the ray directed toward the center of the lens, such as ray 2 in Fig. 8-30, emerges from the lens undeviated in direction.

(3) For a converging lens, the ray arriving at the lens through the focal point to the left of the lens, such as ray 3 in Fig. 8-30, gets refracted by the lens and emerges in a direction parallel to the optic axis. For a diverging lens, the ray traveling in the direction of the focal point to the right of the lens, such as the rays shown in Fig. 8-31(d), gets diffracted by the lens and appears to come from the left side of the lens along a direction parallel to the optic axis.

The ***lateral magnification*** of a thin lens is defined as the ratio of the image height h' to the object height h.

INTEL-1014
U.S. Patent 7,151,430

Table 8-6: Images of real objects formed by thin lenses.[a]

Convex				
Object	**Image**			
Location	Type	Location	Orientation	Relative size
$2f < s < \infty$	Real	$2f > s' > f$	Inverted	Minified
$s = 2f$	Real	$s' = 2f$	Inverted	Same size
$f < s < 2f$	Real	$\infty > s' > 2f$	Inverted	Magnified
$s = f$		$s' = \infty$		
$s < f$	Virtual	$\lvert s' \rvert > s$	Erect	Magnified
Concave				
Object	**Image**			
Location	Type	Location	Orientation	Relative size
Anywhere	Virtual	$\lvert s' \rvert < \lvert f \rvert$, $s > \lvert s' \rvert$	Erect	Minified

[a]Adapted from E. Hecht, *Optics*, second edition, Addison-Wesley Publishing Co., 1990.

From Fig. 8-30,

$$M = \frac{h'}{h} = -\frac{s'}{s}. \quad (8.104)$$

For the example shown in Fig. 8-30, M is negative because h' is negative. By our sign convention, both s and s' are positive. Hence, in order for M to be positive (image is erect), s' has to be negative (assuming that the object is real with positive s), which corresponds to a virtual image. Thus, *a lens can generate a real inverted image to the right of the lens or an erect virtual image to its left.* Image properties are summarized in Table 8-6 for both convex and concave lenses.

The image-construction process is extendible to imaging systems consisting of multiple lenses. In a two-lens system, for example, the image of an object formed by the first lens serves as the object for the second lens.

Example 8-9 Image Formed by a Bi-convex Lens

A 5-cm-tall pencil is placed at a distance of 25 cm in front of a bi-convex lens with radii of curvature of 50 cm and 12.5 cm. If the index of refraction of the lens is 1.5, determine the location of the image and describe its properties.

Solution: A bi-convex lens has a positive focal length f, corresponding to radii $R_1 > 0$ and $R_2 < 0$ [see Fig. 8-25]. We can choose $R_1 = 50$ cm and $R_2 = -12.5$ cm or $R_1 = 12.5$ cm and $R_2 = -50$ cm. Either choice gives the same value for f when applied to Eq. (8.102). The first choice gives

$$\frac{1}{f} = (1.5 - 1)\left(\frac{1}{0.5} - \frac{1}{-0.125}\right),$$

from which we determine that $f = 0.2$ m. From Eq. (8.103),

$$\frac{1}{0.25} + \frac{1}{s'} = \frac{1}{0.2},$$

INTEL-1014
U.S. Patent 7,151,430

which gives $s' = 1$ m.

The lateral magnification is

$$M = \frac{h'}{h} = -\frac{s'}{s} = -\frac{1}{0.25} = -4.$$

Hence, the pencil's image is inverted (M is negative), and its height $h' = -4 \times 5$ cm $= -20$ cm. ■

REVIEW QUESTIONS

Q8.8 Under what conditions is geometric optics applicable?

Q8.9 What are paraxial rays and what approximation do they allow us to make?

Q8.10 What is the thin-lens approximation?

EXERCISE 8.10 Show that for a plane refracting surface Eq. (8.94) reduces to $s' = -(n_2/n_1)s$.

EXERCISE 8.11 Calculate the focal length of a planar concave lens with a radius of curvature of 10 cm and an index of refraction of 1.5.

Ans. $f = -20$ cm.

CHAPTER HIGHLIGHTS

- The relations describing the reflection and transmission behavior of a plane EM wave at the boundary between two different media are the consequence of satisfying the conditions of continuity of the tangential components of **E** and **H** across the boundary.
- Snell's laws state that $\theta_i = \theta_r$ and

$$\sin\theta_t = (n_1/n_2)\sin\theta_i.$$

  For media such that $n_2 < n_1$, the incident wave is reflected totally by the boundary when $\theta_i \geq \theta_c$, where θ_c is the critical angle given by $\theta_c = \sin^{-1}(n_2/n_1)$.
- By successive multiple reflections, light can be guided through optical fibers. The maximum data rate of digital pulses that can be transmitted along optical fibers is dictated by modal dispersion.
- At the Brewster angle for a given polarization, the incident wave is transmitted totally across the boundary. For nonmagnetic materials, the Brewster angle exists for parallel polarization only.
- Any plane wave incident on a plane boundary can be synthesized as the sum of a perpendicularly polarized wave and a parallel polarized wave.
- Transmission-line equivalent models can be used to characterize wave propagation, reflection by, and transmission through boundaries between different media.
- In geometric optics, waves are represented by rays that travel in straight lines. Geometric optics, which can be used for constructing images formed by mirrors and lenses, is valid as long as the objects with which the waves interact are much larger in size than the wavelength and their surfaces are relatively smooth relative to λ.

GLOSSARY OF IMPORTANT TERMS

Provide definitions or explain the meaning of the following terms:

rays
wavefront
reflection coefficient Γ
transmission coefficient τ
standing-wave ratio S
Snell's laws

INTEL-1014
U.S. Patent 7,151,430

angles of incidence, reflection, and transmission
refraction angle
index of refraction n
dense medium
surface wave
critical angle θ_c
total internal reflection
acceptance angle θ_a
modal dispersion
parallel polarization
perpendicular polarization
plane of incidence
transverse electric (TE) polarization
transverse magnetic (TM) polarization
phase-matching condition
Brewster angle θ_B
polarizing angle
grazing incidence
reflectivity (reflectance) R
transmissivity (transmittance) T
physical optics (wave optics)
geometric optics (ray optics)
interference effects
diffraction
object and image distances
real and virtual images
center and radius of curvature
principal axis of mirror or lens
lateral magnification M
convex and concave surfaces
mirror equation
focal length of mirror or lens, f
focal point of mirror or lens, F
front and back sides of mirror or lens
paraxial rays
thin-lens equation
lensmaker's formula
Gaussian lens formula

PROBLEMS

Section 8-1: Reflection and Transmission at Normal Incidence

8.1* A plane wave in air with an electric field amplitude of 10 V/m is incident normally upon the surface of a lossless, nonmagnetic medium with $\varepsilon_r = 25$. Determine the following:

(a) The reflection and transmission coefficients.
(b) The standing-wave ratio in the air medium.
(c) The average power densities of the incident, reflected, and transmitted waves.

8.2 A plane wave traveling in medium 1 with $\epsilon_{r1} = 2.25$ is normally incident upon medium 2 with $\epsilon_{r2} = 4$. Both media are made of nonmagnetic, non-conducting materials. If the electric field of the incident wave is given by

$$\mathbf{E}^i = \hat{\mathbf{y}} 4 \cos(6\pi \times 10^9 t - 30\pi x) \quad \text{(V/m)}$$

(a) Obtain time-domain expressions for the electric and magnetic fields in each of the two media.
(b) Determine the average power densities of the incident, reflected and transmitted waves.

8.3 A plane wave traveling in a medium with $\varepsilon_{r_1} = 9$ is normally incident upon a second medium with $\varepsilon_{r_2} = 4$. Both media are made of nonmagnetic, non-conducting materials. If the magnetic field of the incident plane wave is given by

$$\mathbf{H}^i = \hat{\mathbf{z}} 2 \cos(2\pi \times 10^9 t - ky) \quad \text{(A/m)}$$

(a) Obtain time-domain expressions for the electric and magnetic fields in each of the two media.
(b) Determine the average power densities of the incident, reflected, and transmitted waves.

*Answer(s) available in Appendix D.
Solution available in CD-ROM.

INTEL-1014
U.S. Patent 7,151,430

8.4 A 200-MHz, left-hand circularly polarized plane wave with an electric field modulus of 10 V/m is normally incident in air upon a dielectric medium with $\varepsilon_r = 4$, and occupies the region defined by $z \geq 0$.

(a) Write an expression for the electric field phasor of the incident wave, given that the field is a positive maximum at $z = 0$ and $t = 0$.

(b) Calculate the reflection and transmission coefficients.

(c) Write expressions for the electric field phasors of the reflected wave, the transmitted wave, and the total field in the region $z \leq 0$.

(d) Determine the percentages of the incident average power reflected by the boundary and transmitted into the second medium.

8.5* Repeat Problem 8.4, but replace the dielectric medium with a poor conductor characterized by $\varepsilon_r = 2.25$, $\mu_r = 1$, and $\sigma = 10^{-4}$ S/m.

8.6 A 50-MHz plane wave with electric field amplitude of 30 V/m is normally incident in air onto a semi-infinite, perfect dielectric medium with $\varepsilon_r = 36$. Determine the following:

(a) Γ

(b) The average power densities of the incident and reflected waves.

(c) The distance in the air medium from the boundary to the nearest minimum of the electric field intensity, $|\mathbf{E}|$.

8.7* What is the maximum amplitude of the total electric field in the air medium of Problem 8.6, and at what nearest distance from the boundary does it occur?

8.8 Repeat Problem 8.6, but replace the dielectric medium with a conductor with $\varepsilon_r = 1$, $\mu_r = 1$, and $\sigma = 2.78 \times 10^{-3}$ S/m.

8.9* The three regions shown in Fig. 8-32 contain perfect dielectrics. For a wave in medium 1, incident normally upon the boundary at $z = -d$, what combination of ε_{r_2} and d produces no reflection? Express your answers in terms of ε_{r_1}, ε_{r_3} and the oscillation frequency of the wave, f.

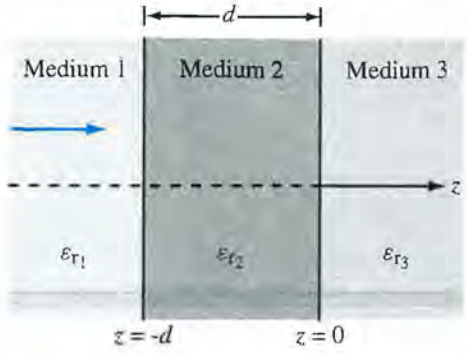


Figure 8-32: Dielectric layers for Problems 8.9 to 8.11.

8.10 For the configuration shown in Fig. 8-32, use transmission-line equations (or the Smith chart) to calculate the input impedance at $z = -d$ for $\varepsilon_{r_1} = 1$, $\varepsilon_{r_2} = 9$, $\varepsilon_{r_3} = 4$, $d = 1.2$ m, and $f = 50$ MHz. Also determine the fraction of the incident average power density reflected by the structure. Assume all media are lossless and nonmagnetic.

8.11* Repeat Problem 8.10, but interchange ε_{r_1} and ε_{r_3}.

8.12 Orange light of wavelength 0.61 μm in air enters a block of glass with $\varepsilon_r = 2.25$. What color would it appear to a sensor embedded in the glass? The wavelength ranges of colors are violet (0.39 to 0.45 μm), blue (0.45 to 0.49 μm), green (0.49 to 0.58 μm), yellow (0.58 to 0.60 μm), orange (0.60 to 0.62 μm), and red (0.62 to 0.78 μm).

INTEL-1014
U.S. Patent 7,151,430

8.13* A plane wave of unknown frequency is normally incident in air upon the surface of a perfect conductor. Using an electric-field meter, it was determined that the total electric field in the air medium is always zero when measured at a distance of 2.5 m from the conductor surface. Moreover, no such nulls were observed at distances closer to the conductor. What is the frequency of the incident wave?

8.14 Consider a thin film of soap in air under illumination by yellow light with $\lambda = 0.6\ \mu$m in vacuum. If the film is treated as a planar dielectric slab with $\varepsilon_r = 1.72$, surrounded on both sides by air, what film thickness would produce strong reflection of the yellow light at normal incidence?

8.15* A 5-MHz plane wave with electric field amplitude of 20 (V/m) is normally incident in air onto the plane surface of a semi-infinite conducting material with $\varepsilon_r = 4$, $\mu_r = 1$, and $\sigma = 100$ (S/m). Determine the average power dissipated (lost) per unit cross-sectional area in a 2-mm penetration of the conducting medium.

8.16 A 0.5-MHz antenna carried by an airplane flying over the ocean surface generates a wave that approaches the water surface in the form of a normally incident plane wave with an electric-field amplitude of 3,000 (V/m). Seawater is characterized by $\varepsilon_r = 72$, $\mu_r = 1$, and $\sigma = 4$ (S/m). The plane is trying to communicate a message to a submarine submerged at a depth d below the water surface. If the submarine's receiver requires a minimum signal amplitude of 0.1 (μV/m), what is the maximum depth d to which successful communication is still possible?

Sections 8-2 and 8-3: Snell's Laws and Fiber Optics

8.17* A light ray is incident on a prism in air at an angle θ as shown in Fig. 8-33. The ray is refracted at the first surface and again at the second surface. In terms of the apex angle ϕ of the prism and its index of refraction n, determine the smallest value of θ for which the ray will emerge from the other side. Find this minimum θ for $n = 1.5$ and $\phi = 60°$.

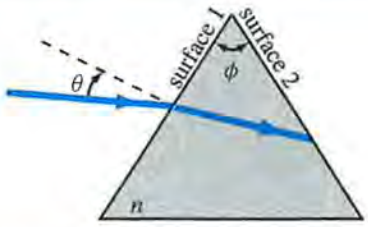


Figure 8-33: Prism of Problem 8.17.

8.18 For some types of glass, the index of refraction varies with wavelength. A prism made of a material with

$$n = 1.71 - \frac{4}{30}\lambda_0, \qquad (\lambda_0 \text{ in } \mu\text{m})$$

where λ_0 is the wavelength in vacuum, was used to disperse white light as shown in Fig. 8-34. The white light is incident at an angle of 50°, the wavelength λ_0 of red light is 0.7 μm, and that of violet light is 0.4 μm. Determine the angular dispersion in degrees.

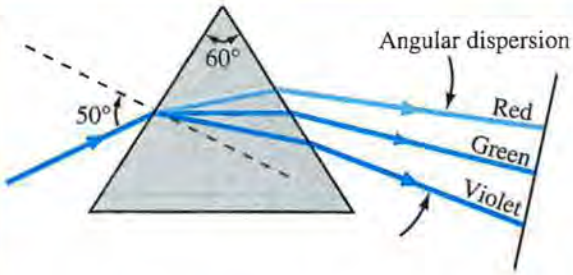


Figure 8-34: Prism of Problem 8.18.

8.19* The two prisms in Fig. 8-35 are made of glass with $n = 1.52$. What fraction of the power density carried by the ray incident upon the top prism emerges from the bottom prism? Neglect multiple internal reflections.

INTEL-1014
U.S. Patent 7,151,430

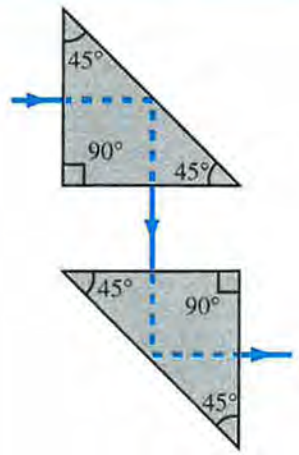


Figure 8-35: Periscope prisms of Problem 8.19.

8.20 A light ray incident at 45° passes through two dielectric materials with the indices of refraction and thicknesses given in Fig. 8-36. If the ray strikes the surface of the first dielectric at a height of 2 cm, at what height will it strike the screen?

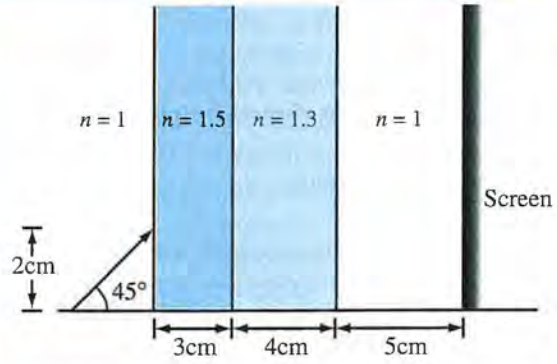


Figure 8-36: Light incident on a screen through a multi-layered dielectric (Problem 8.20).

8.21 Figure 8-37 depicts a beaker containing a block of glass on the bottom and water over it. The glass block contains a small air bubble at an unknown depth below the water surface. When viewed from above at an angle of 60°, the air bubble appears at a depth of 6.81 cm. What is the true depth of the air bubble?

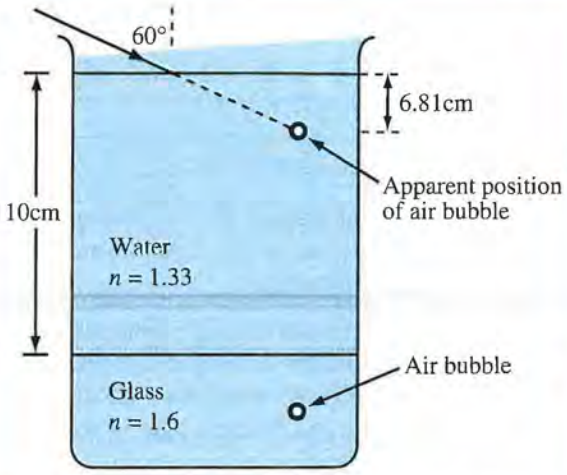


Figure 8-37: Apparent position of the air bubble in Problem 8.21.

8.22 A glass semicylinder with $n = 1.5$ is positioned such that its flat face is horizontal, as shown in Fig. 8-38, and its horizontal surface supports a drop of oil, as also shown. When light is directed radially toward the oil, total internal reflection occurs if θ exceeds 60°. What is the index of refraction of the oil?

8.23 A penny lies at the bottom of a water fountain at a depth of 30 cm. Determine the diameter of a piece of paper which, if placed to float on the surface of the water directly above the penny, would totally obscure the penny from view. Treat the penny as a point and assume that $n = 1.33$ for water.

INTEL-1014
U.S. Patent 7,151,430

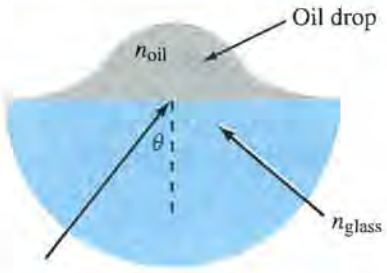


Figure 8-38: Oil drop on the flat surface of a glass semicylinder (Problem 8.22).

8.24 Suppose that the optical fiber of Example 8-5 is submerged in water (with $n = 1.33$) instead of air. Determine θ_a and f_p in that case.

8.25* Equation (8.45) was derived for the case where the light incident upon the sending end of the optical fiber extends over the entire acceptance cone shown in Fig. 8-12(b). Suppose the incident light is constrained to a narrower range extending between normal incidence and θ', where $\theta' < \theta_a$.

(a) Obtain an expression for the maximum data rate f_p in terms of θ'.

(b) Evaluate f_p for the fiber of Example 8-5 when $\theta' = 3°$.

Sections 8-4 and 8-5: Reflection and Transmission at Oblique Incidence

8.26 A plane wave in air with

$$\widetilde{\mathbf{E}}^i = \hat{\mathbf{y}}\, 10e^{-j(3x+4z)} \quad \text{(V/m)}$$

is incident upon the planar surface of a dielectric material, with $\varepsilon_r = 4$, occupying the half-space $z \geq 0$. Determine:

(a) The polarization of the incident wave.

(b) The angle of incidence.

(c) The time-domain expressions for the reflected electric and magnetic fields.

(d) The time-domain expressions for the transmitted electric and magnetic fields.

(e) The average power density carried by the wave in the dielectric medium.

8.27 Repeat Problem 8.26 for a wave in air with

$$\widetilde{\mathbf{H}}^i = \hat{\mathbf{y}}\, 2 \times 10^{-2} e^{-j(8x+6z)} \quad \text{(A/m)}$$

incident upon the planar boundary of a dielectric medium ($z \geq 0$) with $\varepsilon_r = 9$.

8.28 Natural light is randomly polarized, which means that, on average, half the light energy is polarized along any given direction (in the plane orthogonal to the direction of propagation) and the other half of the energy is polarized along the direction orthogonal to the first polarization direction. Hence, when treating natural light incident upon a planar boundary, we can consider half of its energy to be in the form of parallel-polarized waves and the other half as perpendicularly polarized waves. Determine the fraction of the incident power reflected by the planar surface of a piece of glass with $n = 1.5$ when illuminated by natural light at 70°.

8.29* A parallel-polarized plane wave is incident from air onto a dielectric medium with $\varepsilon_r = 9$ at the Brewster angle. What is the refraction angle?

8.30 A perpendicularly polarized wave in air is obliquely incident upon a planar glass–air interface at an incidence angle of 30°. The wave frequency is 600 THz (1 THz = 10^{12} Hz), which corresponds to green light, and the index of refraction of the glass is 1.6. If the electric field amplitude of the incident wave is 50 V/m, determine the following:

(a) The reflection and transmission coefficients.

(b) The instantaneous expressions for **E** and **H** in the glass medium.

8.31 Show that the reflection coefficient $\Gamma_\perp$ can be written in the following form:

$$\Gamma_\perp = \frac{\sin(\theta_t - \theta_i)}{\sin(\theta_t + \theta_i)}$$

INTEL-1014
U.S. Patent 7,151,430

8.32 Show that for nonmagnetic media, the reflection coefficient $\Gamma_{\parallel}$ can be written in the following form:

$$\Gamma_{\parallel} = \frac{\tan(\theta_t - \theta_i)}{\tan(\theta_t + \theta_i)}$$

8.33* A parallel-polarized beam of light with an electric field amplitude of 20 (V/m) is incident in air on polystyrene with $\mu_r = 1$ and $\varepsilon_r = 2.6$. If the incidence angle at the air–polystyrene planar boundary is 50°, determine the following:

(a) The reflectivity and transmissivity.

(b) The power carried by the incident, reflected, and transmitted beams if the spot on the boundary illuminated by the incident beam is 1 m^2 in area.

Sections 8-6 to 8-8: Geometric Optics

8.34 A man is 2 m tall. How long should a mirror be, when placed in front of him at a distance d, for him to have a full-length view of his reflected image? Does the answer depend on d?

8.35* A gas flame is 2 m from a screen, as shown in Fig. 8-39. A concave mirror is used to produce a real image of the flame on the screen, magnified four times. Determine s and the focal length of the mirror.

8.36 A dentist uses a concave mirror with a radius of curvature of 6 cm to view a filling in a tooth. If the mirror is placed 2 cm from the tooth, by how many times will the image of the filling be magnified?

8.37* A flower is 20 cm from a concave spherical mirror. If the image of the flower is formed at a distance of 80 cm from the mirror, determine the following:

(a) The mirror's radius of curvature.

(b) The lateral magnification.

8.38 A candle in air is placed at a distance of 25 cm to the left of a glass medium with a concave spherical boundary characterized by a radius of curvature of 50 cm. If the index of refraction of glass is 1.5, determine the location of the candle's image.

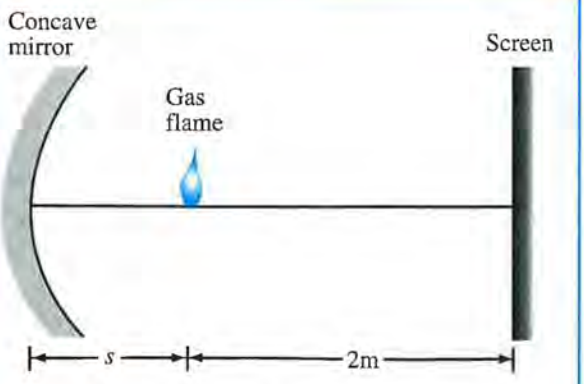


Figure 8-39: Imaging configuration of Problem 8.35.

8.39* A thin bi-convex lens with an index of refraction of 1.6 has radii of curvature of 20 cm and 30 cm. Determine the location, magnification, and orientation of an object placed 20 cm from the lens.

8.40 Repeat Problem 8.39 for an object placed 50 cm from a planar-concave lens with a radius of curvature of 15 cm.

8.41 The curved face of a planar convex lens has a radius of curvature of 3 cm and the index of refraction of the lens material is 1.5. Determine the focal length of the lens when:

(a) The planar surface of the lens faces the light.

(b) The convex surface of the lens faces the light.

8.42 An image formed by a convex lens was observed to move by a distance of 1 cm when the object was moved from far away (essentially at infinity) to only 42 cm from the lens. What is the focal length of the lens?

8.43* Equation (8.102) defines the focal length of a thin lens in air.

(a) Derive an expression for f for the general case of a thin lens with index of refraction n_l immersed in a medium with index of refraction n_m.

INTEL-1014
U.S. Patent 7,151,430

(b) Determine the focal length of a bi-concave lens with radii of curvature of 10 cm and 15 cm and an index of refraction of 1.5 when placed (i) in air, and (ii) in water (with an index of refraction of 1.33).

8.44 A positive lens is used to image an object placed 50 cm in front of it on a screen located 1 m behind the lens. What is the focal length of the lens?

8.45* An imaging system consists of two thin positive lenses with focal lengths of 15 cm for the first lens and 5 cm for the second. If the two lenses are separated by a distance of 50 cm, locate the image of an object placed 25 cm in front of the first lens, relative to the location of the second lens.

8.46 Two thin lenses with focal lengths f_1 and f_2 are placed in contact with each other, as shown in Fig. 8-40. Show that F, the focal length of the combination, is given by

$$\frac{1}{F} = \frac{1}{f_1} + \frac{1}{f_2}$$

8.47* Two thin lenses of focal lengths $f_1 = 5$ cm and $f_2 = -10$ cm are separated by a distance of 5 cm, as shown in Fig. 8-41. Determine the location of the object.

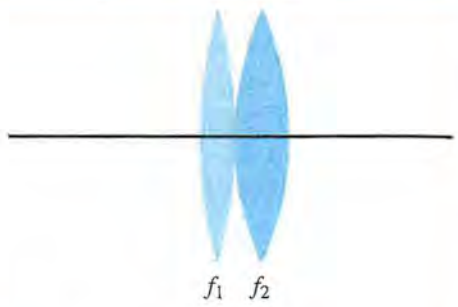


Figure 8-40: Two lenses in contact. The lenses are so thin that they may be considered to be at the same location (Problem 8.46).

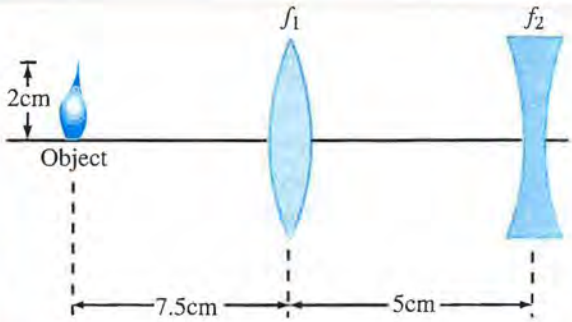
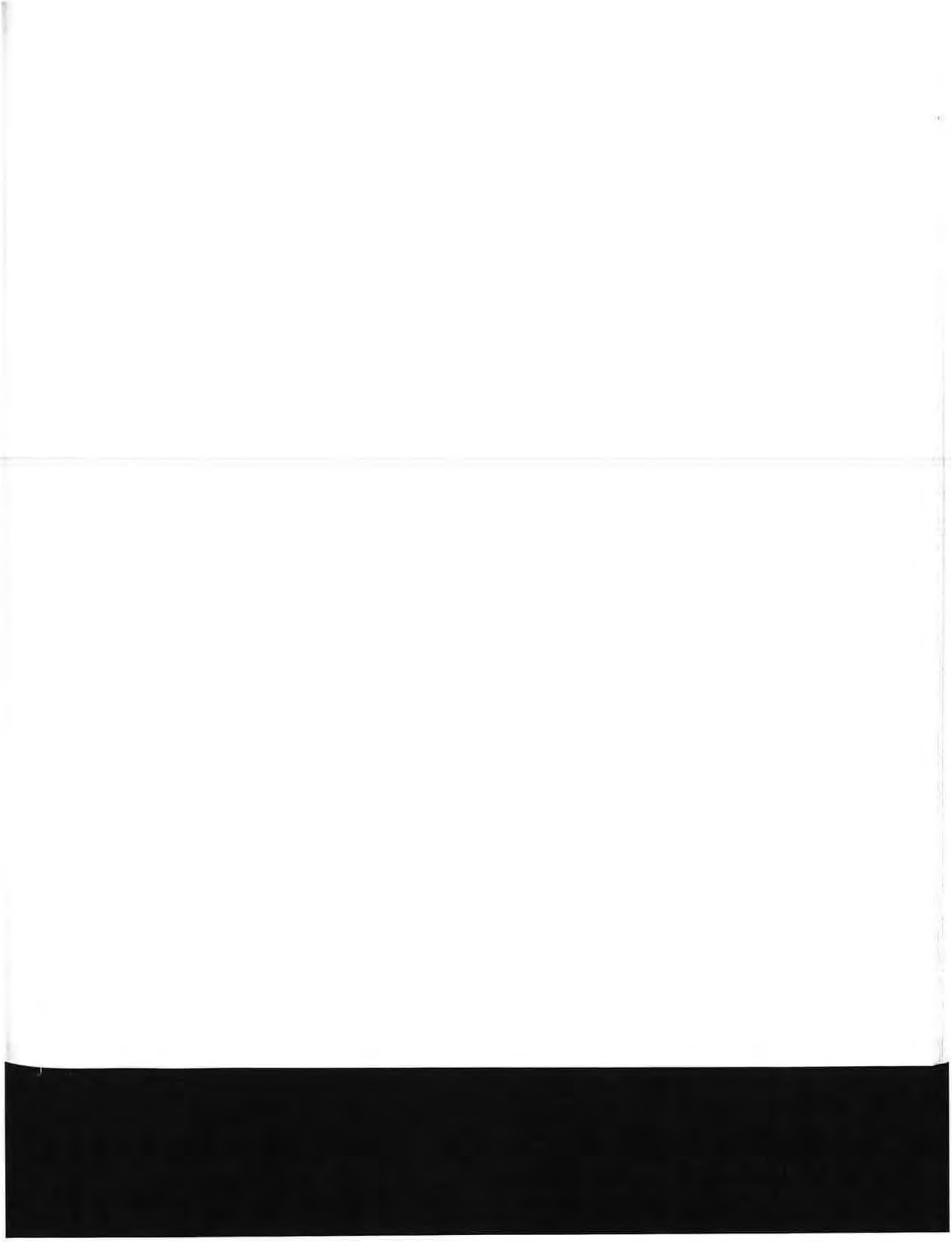
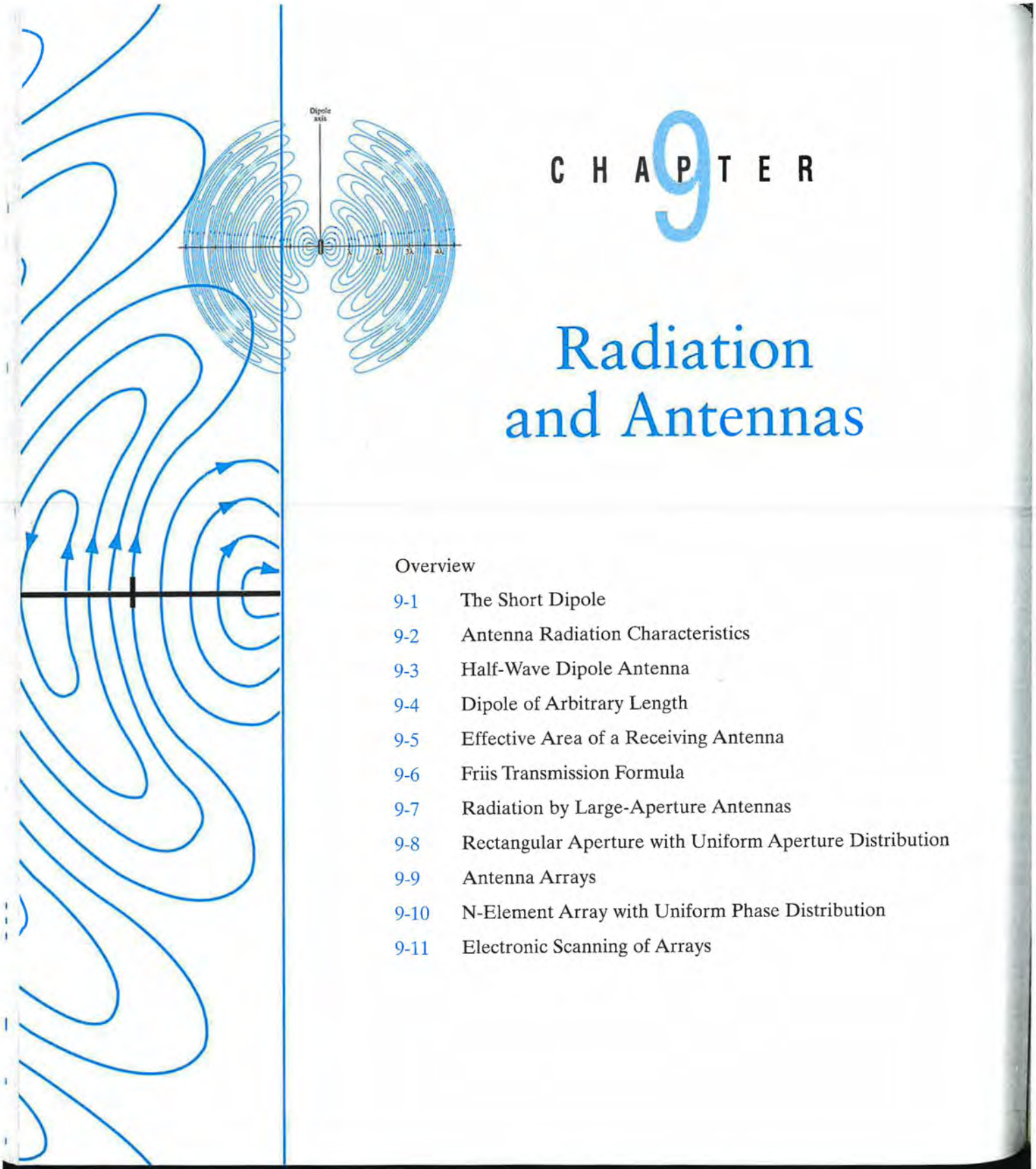


Figure 8-41: Imaging configuration of Problem 8.47.

INTEL-1014
U.S. Patent 7,151,430





CHAPTER 9

Radiation and Antennas

Overview

9-1 The Short Dipole

9-2 Antenna Radiation Characteristics

9-3 Half-Wave Dipole Antenna

9-4 Dipole of Arbitrary Length

9-5 Effective Area of a Receiving Antenna

9-6 Friis Transmission Formula

9-7 Radiation by Large-Aperture Antennas

9-8 Rectangular Aperture with Uniform Aperture Distribution

9-9 Antenna Arrays

9-10 N-Element Array with Uniform Phase Distribution

9-11 Electronic Scanning of Arrays

INTEL-1014
U.S. Patent 7,151,430

OVERVIEW

An *antenna* may be defined as a transducer between a guided wave propagating in a transmission line and an electromagnetic wave propagating in an unbounded medium (usually free space), or vice versa. Figure 9-1 shows how a wave is launched by a hornlike antenna, with the horn acting as a transition between the waveguide and free space. Although any conducting or dielectric structure can serve this function, an antenna is designed to radiate or receive electromagnetic energy with directional and polarization properties suitable for the intended application. Also, to minimize reflection at the transmission line–antenna juncture, it is important to know the impedance of the antenna and to match it to the transmission line.

Antennas are made in various shapes and sizes [Fig. 9-2] and are used in radio and television broadcasting and reception, radio-wave communication systems, cellular telephones, radar systems, and anticollision automobile sensors, among many other applications. The radiation and impedance properties of an antenna are governed by its shape and size and the material of which it is made. The dimensions of an antenna are usually measured in units of the wavelength of the wave it is launching or receiving; a 1-m-long dipole antenna operating at a wavelength of 2 m exhibits the same properties as a 1-cm-long dipole operating at $\lambda = 2$ cm. Hence, in most of our discussions in this chapter, we will refer to antenna dimensions in wavelength units.

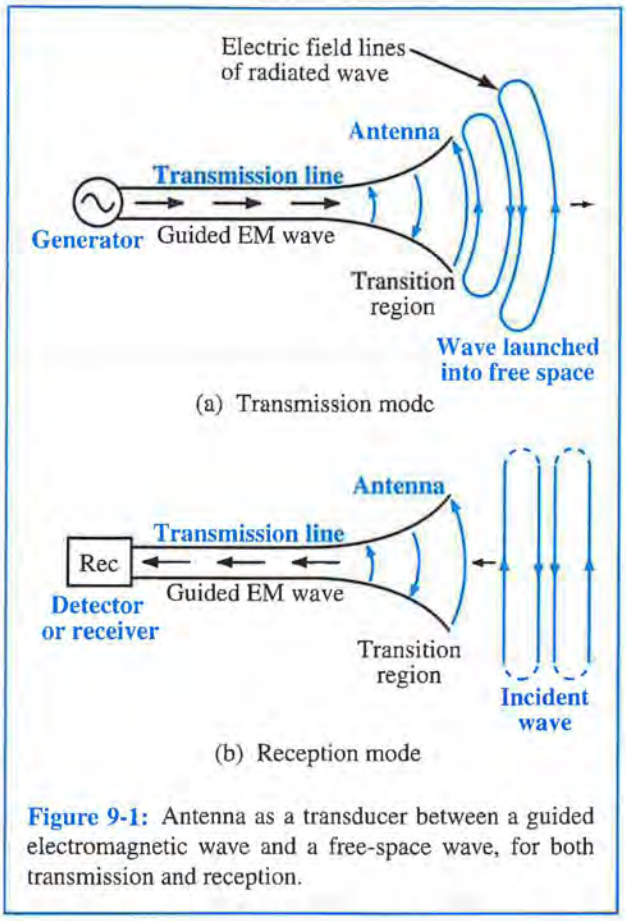


Figure 9-1: Antenna as a transducer between a guided electromagnetic wave and a free-space wave, for both transmission and reception.

Reciprocity

The directional function characterizing the *relative* distribution of power radiated by an antenna is known as the ***antenna radiation pattern***, or simply ***the antenna pattern***. An *isotropic* antenna is a hypothetical antenna that radiates equally in all directions, and it is often used as a reference radiator when describing the radiation properties of real antennas. Most antennas are *recip-*

INTEL-1014
U.S. Patent 7,151,430

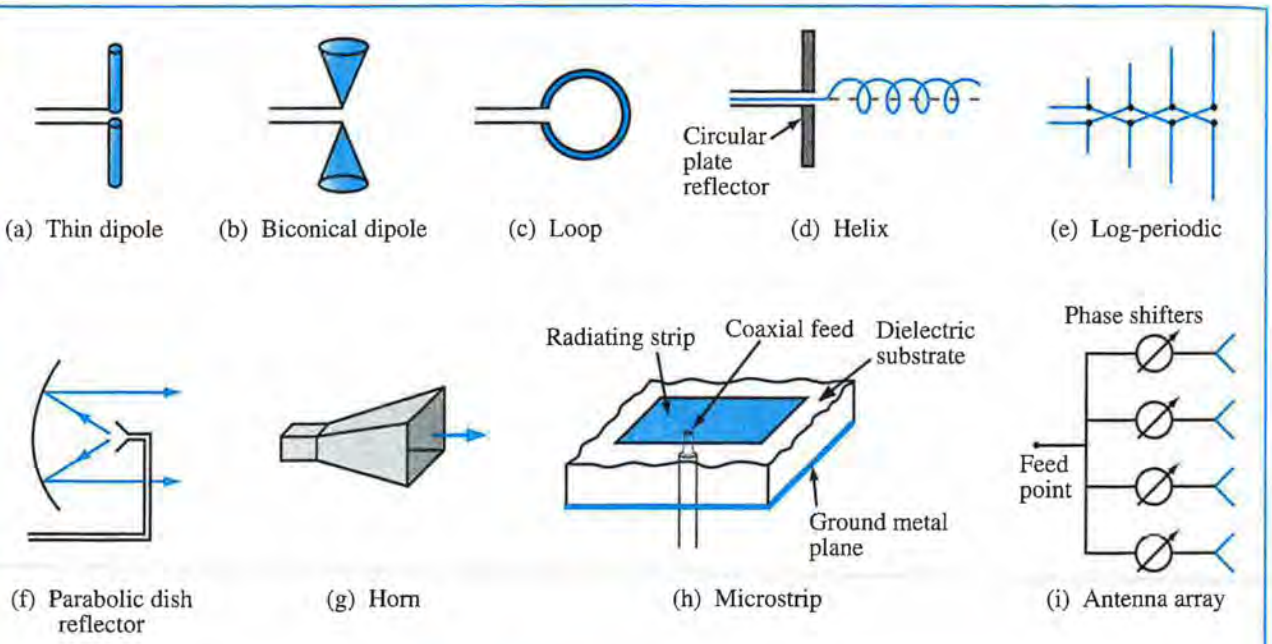


Figure 9-2: Various types of antennas.

rocal devices, exhibiting the same radiation pattern for transmission as for reception. Reciprocity means that, if in the transmission mode a given antenna transmits in direction A 100 times the power it transmits in direction B, then when used in the reception mode it will be 100 times more sensitive to electromagnetic radiation incident from direction A than B. All the antennas shown in Fig. 9-2 obey the reciprocity law, but not all antennas are reciprocal devices. Reciprocity may not hold for some solid-state antennas composed of nonlinear semiconductors or ferrite materials. Such nonreciprocal antennas are beyond the scope of this chapter, and hence reciprocity will be assumed throughout. The reciprocity property is very convenient because it allows us to compute the radiation pattern of an antenna in the transmission mode, even when the antenna is intended to operate as a receiver.

Antenna performance consists of two aspects: its radiation properties and its impedance. The radiation properties include its directional radiation pattern and the associated polarization state of the radiated wave when the antenna is used in the transmission mode. This polarization state is called ***antenna polarization***. Being a reciprocal device, an antenna, when operating in the receiving mode, can extract from an incident wave only that component of the wave whose electric field is parallel to that of the antenna polarization direction. The second aspect, the ***antenna impedance***, pertains to the transfer of power from a generator to the antenna when the antenna is used as a transmitter and, conversely, the transfer of power from the antenna to a load when the antenna is used as a receiver, as will be discussed later in Section 9-5. It should be noted that throughout our discussions in this chapter it will be assumed that

INTEL-1014
U.S. Patent 7,151,430

the antenna is properly matched to the transmission line connected to its terminals, thereby avoiding reflections and their associated problems.

Radiation Sources

Radiation sources fall into two groups: currents and aperture fields. The dipole and loop antennas [Fig. 9-2(a) and (c)] are examples of current sources; the time-varying currents flowing in the conducting wires give rise to the radiated electromagnetic field. A horn antenna [Fig. 9-2(g)] is an example of the second group because the electric and magnetic fields across the horn's aperture serve as the sources of the radiated field. The aperture fields are themselves induced by time-varying currents on the surfaces of the horn's walls, and therefore ultimately all radiation is due to time-varying currents. The choice of currents or apertures as the sources is merely a computational convenience dictated by the structure of the antenna. We will examine the basic methodology used for computing the radiation pattern for each of these two types of sources.

Far-Field Region

The wave radiated by a point source is spherical in shape, with the wavefront expanding outward at a rate equal to the phase velocity u_p (or the velocity of light c if the medium is free space). If R, the distance between the transmitting antenna and the receiving antenna, is sufficiently large that the wavefront across the receiving aperture may be considered a plane wave [Fig. 9-3], the receiving aperture is said to be in the ***far-field*** (or ***far-zone***) region of the transmitting point source. This region is of particular significance because, for most applications, the observation region of interest is indeed in the far-field region of the antenna. The far-field plane-wave approximation allows the use of certain mathematical approximations that simplify the computation of the radiated field and, conversely, provide convenient techniques for synthesizing the appropriate antenna structure that would give rise to the desired far-field antenna pattern.

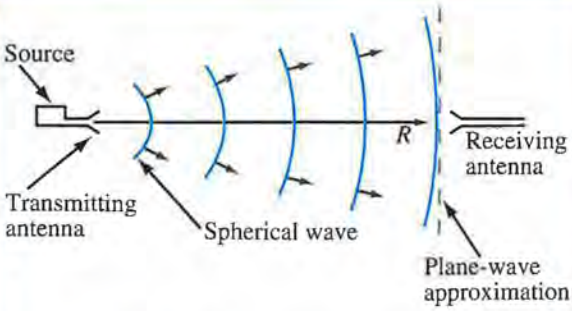


Figure 9-3: Far-field plane-wave approximation.

Antenna Arrays

When several antennas are connected together, the combination is called an ***antenna array*** [Fig. 9-2(i)], and the array as a whole behaves as if it were a single antenna. By controlling the magnitude and phase of the signal feeding each antenna individually, it is possible to *shape the radiation pattern* of the array and to *steer the direction of the beam electronically.* These topics are treated in Sections 9-9 to 9-11.

9-1 The Short Dipole

By regarding a linear antenna as consisting of a series of a large number of infinitesimally short conducting elements, each of which is so short that current may be considered uniform over its length, the field of the entire antenna may be obtained by integrating the fields from all these differential antennas, with the proper magnitudes and phases taken into account. We shall first examine the radiation properties of such a differential antenna, known as a ***short dipole***, and then in Section 9-3 we will extend the results to compute the fields radiated by a half-wave

INTEL-1014
U.S. Patent 7,151,430

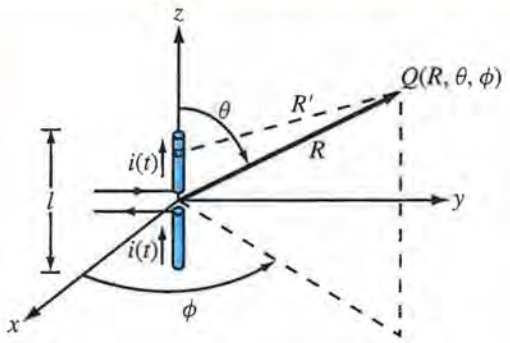


Figure 9-4: Short dipole placed at the origin of a spherical coordinate system.

dipole, which is commonly used as a standard antenna for many applications.

A short dipole, also called a ***Hertzian dipole***, is a thin, linear conductor whose length l is very short compared with the wavelength λ; to satisfy the uniform-current assumption, l should not exceed $\lambda/50$. The wire, which is oriented along the z-direction as shown in Fig. 9-4, carries a sinusoidally varying current given by

$$i(t) = I_0 \cos \omega t = \Re e[I_0 e^{j\omega t}] \quad \text{(A)}, \tag{9.1}$$

where I_0 is the current amplitude. From Eq. (9.1), the phasor current $\tilde{I} = I_0$. Even though the current has to go to zero at the two ends of the dipole, we shall treat it as constant across its entire length.

The customary approach for finding the electric and magnetic fields at a point Q in space [Fig. 9-4] due to radiation by a current source is through the retarded vector potential $\mathbf{A}$. From Eq. (6.84), the phasor retarded vector potential $\tilde{\mathbf{A}}(R)$ at a distance vector $\mathbf{R}$ from a volume v' containing a phasor current distribution $\tilde{\mathbf{J}}$ is given by

$$\tilde{\mathbf{A}}(\mathbf{R}) = \frac{\mu_0}{4\pi} \int_{v'} \frac{\tilde{\mathbf{J}} e^{-jkR'}}{R'} \, dv', \tag{9.2}$$

where μ_0 is the magnetic permeability of free space (because the observation point is in air) and $k = \omega/c = 2\pi/\lambda$ is the wavenumber. For the dipole, the current density is simply $\tilde{\mathbf{J}} = \hat{\mathbf{z}}(I_0/s)$, where s is the cross-sectional area of the dipole wire, $dv' = s\, dz$, and the limits of integration are from $z = -l/2$ to $z = l/2$. In Fig. 9-4, the distance R' between the observation point and a given point along the dipole is not the same as the distance to its center, R, but because we are dealing with a very short dipole, we can set $R' \simeq R$. Hence,

$$\begin{aligned} \tilde{\mathbf{A}} &= \frac{\mu_0}{4\pi} \frac{e^{-jkR}}{R} \int_{-l/2}^{l/2} \hat{\mathbf{z}} I_0 \, dz \\ &= \hat{\mathbf{z}} \frac{\mu_0}{4\pi} I_0 l \left(\frac{e^{-jkR}}{R} \right), \end{aligned} \tag{9.3}$$

The function (e^{-jkR}/R), called the ***spherical propagation factor***, accounts for the $1/R$ decay of the magnitude with distance as well as for the phase change represented by e^{-jkR}. The direction of $\tilde{\mathbf{A}}$ is dictated by the direction of flow of the current (z-direction).

Because our objective is to characterize the directional character of the radiated power at a fixed distance R from the antenna, the spherical coordinate system shown in Fig. 9-5 is deemed appropriate for the presentation of antenna pattern plots, with the variables R, θ, and ϕ referred to as the ***range***, ***zenith angle***, and ***azimuth angle***, respectively. To this end, we need to write $\tilde{\mathbf{A}}$ in terms of its spherical coordinate components, which is realized [with the help of Eq. (3.65c)] by expressing $\hat{\mathbf{z}}$ in terms of the unit vectors of the spherical coordinate system:

$$\hat{\mathbf{z}} = \hat{\mathbf{R}} \cos\theta - \hat{\boldsymbol{\theta}} \sin\theta. \tag{9.4}$$

Upon substituting Eq. (9.4) into Eq. (9.3), we have

$$\begin{aligned} \tilde{\mathbf{A}} &= (\hat{\mathbf{R}} \cos\theta - \hat{\boldsymbol{\theta}} \sin\theta) \frac{\mu_0 I_0 l}{4\pi} \left(\frac{e^{-jkR}}{R} \right) \\ &= \hat{\mathbf{R}} \tilde{A}_R + \hat{\boldsymbol{\theta}} \tilde{A}_\theta + \hat{\boldsymbol{\phi}} \tilde{A}_\phi, \end{aligned} \tag{9.5}$$

INTEL-1014
U.S. Patent 7,151,430

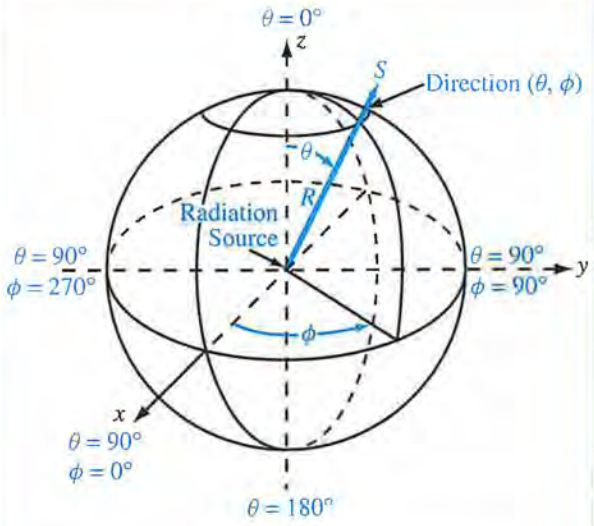


Figure 9-5: Spherical coordinate system.

with

$$\widetilde{A}_R = \frac{\mu_0 I_0 l}{4\pi}\cos\theta\left(\frac{e^{-jkR}}{R}\right), \tag{9.6a}$$

$$\widetilde{A}_\theta = -\frac{\mu_0 I_0 l}{4\pi}\sin\theta\left(\frac{e^{-jkR}}{R}\right), \tag{9.6b}$$

$$\widetilde{A}_\phi = 0.$$

With the spherical coordinate components of $\widetilde{\mathbf{A}}$ known, the next step is straightforward; we simply apply the free-space relationships given by Eqs. (6.85) and (6.86),

$$\widetilde{\mathbf{H}} = \frac{1}{\mu_0}\nabla \times \widetilde{\mathbf{A}}, \tag{9.7a}$$

$$\widetilde{\mathbf{E}} = \frac{1}{j\omega\varepsilon_0}\nabla \times \widetilde{\mathbf{H}}, \tag{9.7b}$$

to obtain the expressions

$$\widetilde{H}_\phi = \frac{I_0 l k^2}{4\pi}e^{-jkR}\left[\frac{j}{kR} + \frac{1}{(kR)^2}\right]\sin\theta \tag{9.8a}$$

$$\widetilde{E}_R = \frac{2I_0 l k^2}{4\pi}\eta_0 e^{-jkR}\left[\frac{1}{(kR)^2} - \frac{j}{(kR)^3}\right]\cos\theta \tag{9.8b}$$

$$\widetilde{E}_\theta = \frac{I_0 l k^2}{4\pi}\eta_0 e^{-jkR}\left[\frac{j}{kR} + \frac{1}{(kR)^2} - \frac{j}{(kR)^3}\right]\sin\theta, \tag{9.8c}$$

where $\eta_0 = \sqrt{\mu_0/\varepsilon_0} \cong 120\pi$ (Ω) is the intrinsic impedance of free space. The remaining components ($\widetilde{H}_R$, $\widetilde{H}_\theta$, and $\widetilde{E}_\phi$) are everywhere zero. Figure 9-6 depicts the electric field lines of the wave radiated by the short dipole.

9-1.1 Far-Field Approximation

As was stated earlier, in most antenna applications, we are primarily interested in the radiation pattern of the antenna at great distances from the source. For the electrical dipole, this corresponds to distances R such that $R \gg \lambda$ or, equivalently, $kR = 2\pi R/\lambda \gg 1$. This condition allows us to neglect the terms varying as $1/(kR)^2$ and $1/(kR)^3$ in Eqs. (9.8a) to (9.8c) in favor of the terms varying as $1/kR$, which yields the far-field expressions

$$\widetilde{E}_\theta = \frac{j I_0 l k \eta_0}{4\pi}\left(\frac{e^{-jkR}}{R}\right)\sin\theta \quad \text{(V/m)}, \tag{9.9a}$$

$$\widetilde{H}_\phi = \frac{\widetilde{E}_\theta}{\eta_0} \quad \text{(A/m)}, \tag{9.9b}$$

and $\widetilde{E}_R$ is negligible. At the observation point Q [Fig. 9-4], the wave now appears to be similar to a uniform plane wave with its electric and magnetic fields in time phase, related by the intrinsic impedance of the medium

INTEL-1014
U.S. Patent 7,151,430

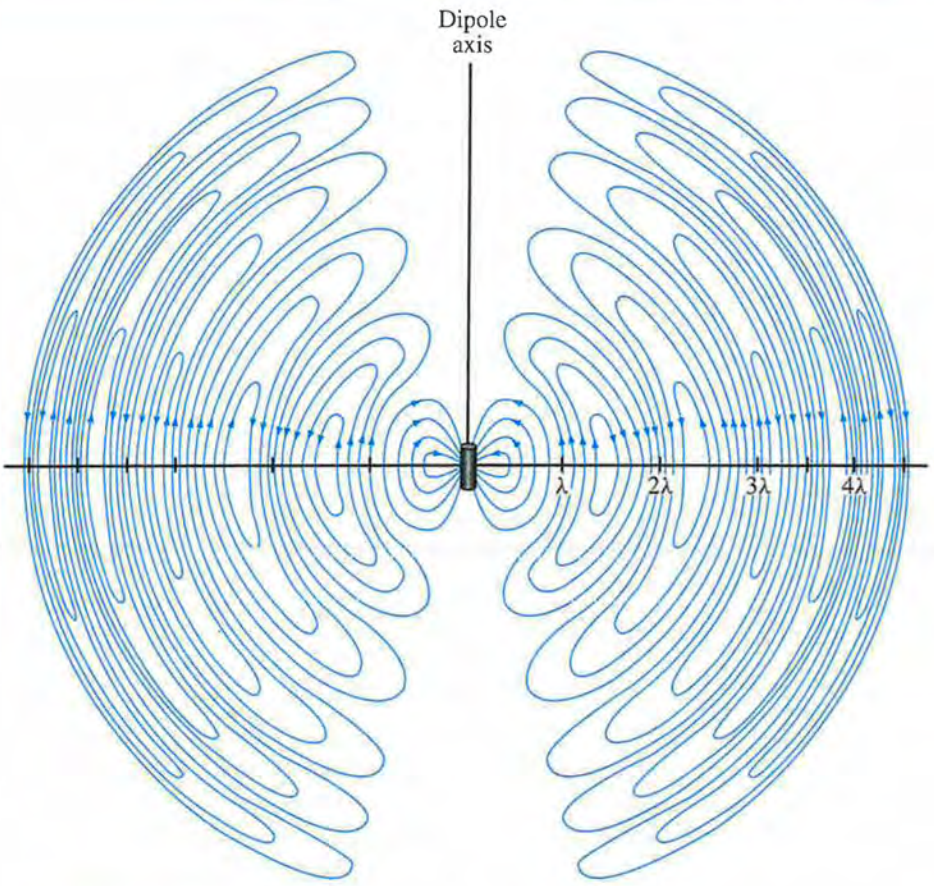


Figure 9-6: Electric field lines surrounding an oscillating dipole at a given instant.

η_0, and orthogonal to each other and to the direction of propagation ($\hat{\mathbf{R}}$). Both fields are proportional to $\sin\theta$ and independent of ϕ (which is as expected from symmetry considerations).

9-1.2 Power Density

Given $\widetilde{\mathbf{E}}$ and $\widetilde{\mathbf{H}}$ in phasor form, the *time-average Poynting vector* of the radiated wave, which is also called the *power density*, can be obtained by applying Eq. (7.101), that is,

$$\mathbf{S}_{\text{av}} = \tfrac{1}{2}\mathfrak{Re}\left(\widetilde{\mathbf{E}} \times \widetilde{\mathbf{H}}^*\right) \quad (\text{W/m}^2). \tag{9.10}$$

For the short dipole, use of Eqs. (9.9a) and (9.9b) gives

$$\mathbf{S}_{\text{av}} = \hat{\mathbf{R}}\, S(R, \theta), \tag{9.11}$$

INTEL-1014
U.S. Patent 7,151,430

with

$$S(R,\theta) = \left(\frac{\eta_0 k^2 I_0^2 l^2}{32\pi^2 R^2}\right)\sin^2\theta = S_0 \sin^2\theta \quad (\text{W/m}^2). \quad (9.12)$$

The directional pattern of any antenna is described in terms of the ***normalized radiation intensity*** $F(\theta,\phi)$, defined as the ratio of the power density $S(R,\theta,\phi)$ to $S_{\max}$, the maximum value of $S(R,\theta,\phi)$, at a specified range R:

$$F(\theta,\phi) = \frac{S(R,\theta,\phi)}{S_{\max}} \quad (\text{dimensionless}). \quad (9.13)$$

For the Hertzian dipole, the $\sin^2\theta$ dependence in Eq. (9.12) indicates that the radiation is maximum in the broadside direction ($\theta = \pi/2$), corresponding to the azimuth plane, and is given by

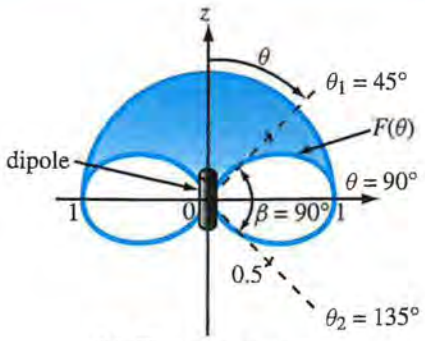
$$S_{\max} = S_0 = \frac{\eta_0 k^2 I_0^2 l^2}{32\pi^2 R^2} = \frac{15\pi I_0^2}{R^2}\left(\frac{l}{\lambda}\right)^2 \quad (\text{W/m}^2), \quad (9.14)$$

where use was made of the relations $k = 2\pi/\lambda$ and $\eta_0 \simeq 120\pi$. We observe that $S_{\max}$ is directly proportional to I_0^2 and to l^2 (with l measured in wavelengths), and it decreases with distance as $1/R^2$.

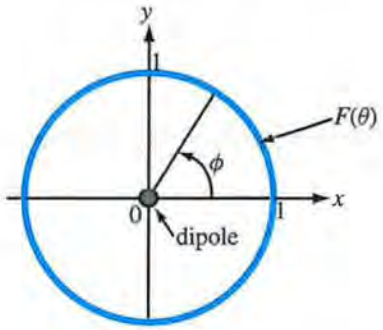
From the definition of the normalized radiation intensity given by Eq. (9.13), it follows that

$$F(\theta,\phi) = F(\theta) = \sin^2\theta. \quad (9.15)$$

Plots of $F(\theta)$ are shown in Fig. 9-7 in both the elevation plane (also called the θ-plane) and the azimuth plane (ϕ-plane). No energy is radiated by the dipole along the direction of the dipole axis and maximum radiation ($F = 1$) occurs in the broadside direction. Since $F(\theta)$ is independent of ϕ, the pattern is doughnut-shaped in θ–ϕ space.



(a) Elevation pattern



(b) Azimuth pattern

Figure 9-7: Radiation patterns of a short dipole.

REVIEW QUESTIONS

Q9.1 When is an antenna a reciprocal device?

Q9.2 What is the radiated wave like in the far-field region of the antenna?

Q9.3 How short should the length of a wire antenna be so that it may be considered a Hertzian dipole? What is the underlying assumption about the current flowing through the wire?

INTEL-1014
U.S. Patent 7,151,430

Q9.4 Outline the basic steps used in order to relate the current in the wire to the radiated power density.

EXERCISE 9.1 A 1-m-long dipole is excited by a 5-MHz current with an amplitude of 5 A. At a distance of 2 km, what is the power density radiated by the antenna along its broadside direction?

Ans. $S_0 = 8.2 \times 10^{-8}$ W/m^2.

9-2 Antenna Radiation Characteristics

An ***antenna pattern*** describes the far-field directional properties of an antenna when measured at a fixed distance from the antenna. In general, the antenna pattern is a three-dimensional plot that displays the strength of the radiated field or power density as a function of direction, with direction being specified by the zenith angle θ and the azimuth angle ϕ. By virtue of the reciprocity theorem, *a receiving antenna has the same directional antenna pattern as the pattern that it exhibits when operated in the transmission mode.*

Consider a transmitting antenna placed at the origin of the observation sphere shown in Fig. 9-8. The differential power radiated by the antenna through an elemental area dA is

$$dP_{\text{rad}} = \mathbf{S}_{\text{av}} \cdot d\mathbf{A} = \mathbf{S}_{\text{av}} \cdot \hat{\mathbf{R}}\, dA = S\, dA \quad \text{(W)}, \tag{9.16}$$

where S is the radial component of the time-average Poynting vector $\mathbf{S}_{\text{av}}$. In the far-field region of any antenna, $\mathbf{S}_{\text{av}}$ is always in the radial direction. In a spherical coordinate system,

$$dA = R^2 \sin\theta\, d\theta\, d\phi, \tag{9.17}$$

and the ***solid angle*** $d\Omega$ associated with dA, defined as the subtended area divided by R^2, is given by

$$d\Omega = \frac{dA}{R^2} = \sin\theta\, d\theta\, d\phi \quad \text{(sr)}. \tag{9.18}$$

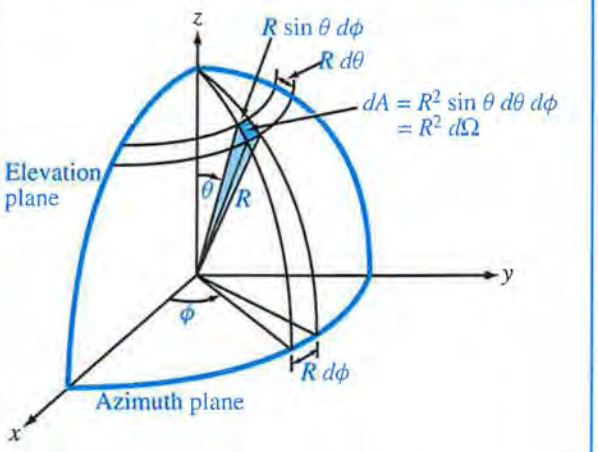


Figure 9-8: Definition of solid angle $d\Omega = \sin\theta\, d\theta\, d\phi$.

Note that, whereas a planar angle is measured in radians and the angular measure of a complete circle is 2π (rad), a solid angle is measured in ***steradians*** (sr), and the angular measure for a spherical surface is $\Omega = (4\pi R^2)/R^2 = 4\pi$ (sr). The solid angle of a hemisphere is 2π (sr).

Using the relation $dA = R^2\, d\Omega$, dP_{rad} can be rewritten as

$$dP_{\text{rad}} = R^2\, S(R, \theta, \phi)\, d\Omega. \tag{9.19}$$

The total power radiated by an antenna through a spherical surface at a fixed distance R is obtained by integrating Eq. (9.19):

$$\begin{aligned} P_{\text{rad}} &= R^2 \int_{\phi=0}^{2\pi} \int_{\theta=0}^{\pi} S(R, \theta, \phi) \sin\theta\, d\theta\, d\phi \\ &= R^2 S_{\max} \int_{\phi=0}^{2\pi} \int_{\theta=0}^{\pi} F(\theta, \phi) \sin\theta\, d\theta\, d\phi \\ &= R^2 S_{\max} \iint_{4\pi} F(\theta, \phi)\, d\Omega \quad \text{(W)}, \end{aligned} \tag{9.20}$$

INTEL-1014
U.S. Patent 7,151,430

where $F(\theta, \phi)$ is the normalized radiation intensity defined by Eq. (9.13). The 4π symbol under the integral sign is used as an abbreviation for the indicated limits on θ and ϕ. Formally, P_{rad} is called the ***total radiated power***.

9-2.1 Antenna Pattern

Each specific combination of the zenith angle θ and the azimuth angle ϕ denotes a specific direction in the spherical coordinate system of Fig. 9-8. The normalized radiation intensity $F(\theta, \phi)$ characterizes the directional pattern of the energy radiated by an antenna, and a plot of $F(\theta, \phi)$ as a function of both θ and ϕ constitutes a three-dimensional pattern, an example of which is shown in Fig. 9-9.

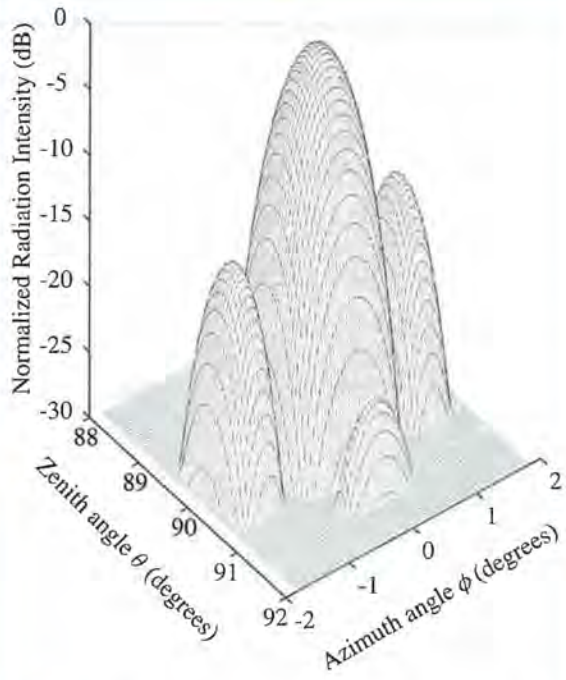


Figure 9-9: Three-dimensional pattern of a narrow-beam antenna.

Often, it is of interest to characterize the variation of $F(\theta, \phi)$ in the form of two-dimensional plots in specific planes in the spherical coordinate system. The two planes most commonly specified for this purpose are the elevation and azimuth planes. The ***elevation plane***, also called the θ plane, is the plane corresponding to a constant value of ϕ. For example, $\phi = 0$ defines the x–z plane and $\phi = 90°$ defines the y–z plane, both of which are elevation planes (Fig. 9-8). A plot of $F(\theta, \phi)$ versus θ in either of these planes constitutes a two-dimensional pattern in the elevation plane. This is not to imply, however, that the elevation-plane pattern is necessarily the same in all elevation planes. The ***azimuth plane***, also called the ϕ plane, is specified by $\theta = 90°$ and corresponds to the x–y plane. The elevation and azimuth planes are often called the two ***principal planes*** of the spherical coordinate system.

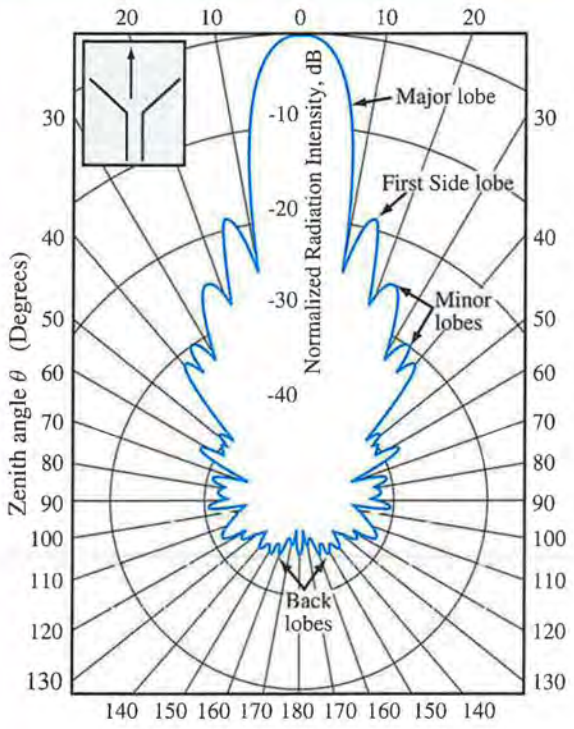
Some antennas exhibit highly directive patterns with narrow beams, in which case it is found convenient to plot the antenna pattern on a decibel scale by expressing F in decibels:

$$F \text{ (dB)} = 10 \log F.$$

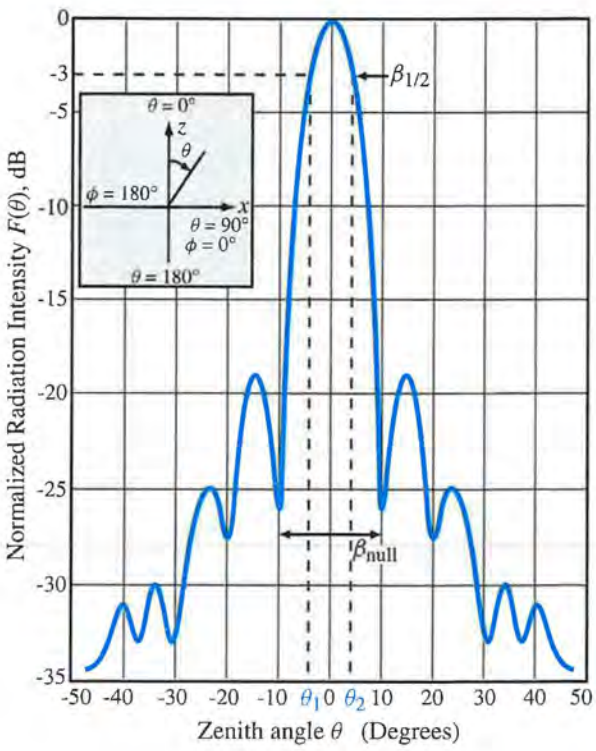
As an example, the antenna pattern shown in Fig. 9-10(a) is plotted on a decibel scale in polar coordinates, with intensity as the radial variable. This format permits a convenient visual interpretation of the directional distribution of the ***radiation lobes***. Another format commonly used for inspecting the pattern of a narrow-beam antenna is the rectangular display shown in Fig. 9-10(b), which permits the pattern to be easily expanded by changing the scale of the horizontal axis. These plots represent the variation in only one plane in the observation sphere, the $\phi = 0$ plane. Unless the pattern is symmetrical in ϕ, additional patterns are required to define the variation of $F(\theta, \phi)$ with θ and ϕ.

Strictly speaking, the polar angle θ is always positive, being defined over the range from 0° (z-direction) to 180° ($-z$-direction), and yet the θ-axis in Fig. 9-10(b) is shown to have both positive and negative values. This

INTEL-1014
U.S. Patent 7,151,430



(a) Polar Diagram



(b) Rectangular Plot

Figure 9-10: Representative plots of the normalized radiation pattern of a microwave antenna in (a) polar form and (b) rectangular form.

is not a contradiction, but rather a different form of plotting antenna patterns. The right-hand half of the plot represents the variation of F (dB) with θ as θ is increased in a clockwise direction in the x–z plane [see inset in Fig. 9-10(b)], corresponding to $\phi = 0$, whereas the left-hand half of the plot represents the variation of F (dB) with θ as θ is increased in a counterclockwise direction at $\phi = 180°$. Thus, a negative θ value simply denotes that the direction (θ, ϕ) is in the left-hand half of the x–z plane.

The pattern shown in Fig. 9-10(a) indicates that the antenna is fairly directive, since most of the energy is radiated through a narrow range called the ***main lobe***. In addition to the main lobe, the pattern exhibits several ***side lobes*** and ***back lobes*** as well. For most applications, these extra lobes are considered undesirable because they

INTEL-1014
U.S. Patent 7,151,430

represent wasted energy for transmitting antennas and potential interference directions for receiving antennas.

9-2.2 Beam Dimensions

For an antenna with a single main lobe, the ***pattern solid angle*** Ω_p describes the equivalent width of the main lobe of the antenna pattern [Fig. 9-11]. It is defined as the integral of the normalized radiation intensity $F(\theta, \phi)$ over a sphere:

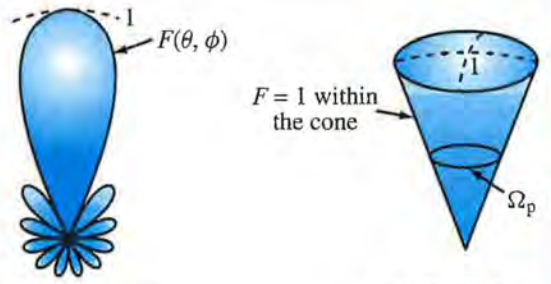
$$\Omega_p = \iint_{4\pi} F(\theta, \phi)\, d\Omega \quad \text{(sr)}. \tag{9.21}$$

For an isotropic antenna with $F(\theta, \phi) = 1$ in all directions, $\Omega_p = 4\pi$ (sr).

The pattern solid angle characterizes the directional properties of the three-dimensional radiation pattern. To characterize the width of the main lobe in a given plane, the term used is ***beamwidth***. The ***half-power beamwidth***, or simply the beamwidth β, is defined as the angular width of the main lobe between the two angles at which the magnitude of $F(\theta, \phi)$ is equal to half of its peak value (or -3 dB on a decibel scale). For example, for the pattern displayed in Fig. 9-10(b), β is given by

$$\beta = \theta_2 - \theta_1, \tag{9.22}$$

where θ_1 and θ_2 are the ***half-power angles*** at which $F(\theta, 0) = 0.5$ (with θ_2 denoting the larger value and θ_1 denoting the smaller one, as shown in the figure). If the pattern is symmetrical and the peak value of $F(\theta, \phi)$ is at $\theta = 0$, then $\beta = 2\theta_2$. For the short-dipole pattern shown earlier in Fig. 9-7(a), $F(\theta)$ is maximum at $\theta = 90°$, θ_2 is at 135°, and θ_1 is at 45°. In this case, $\beta = 135° - 45° = 90°$. The beamwidth β is also known as the ***3-dB beamwidth***. In addition to the half-power beamwidth, other beam dimensions may be of interest for certain applications, such as the ***null beamwidth*** β_{null}, which is the width of the spacing between the first nulls on the two sides of the peak [Fig. 9-10(b)].



(a) Actual pattern (b) Equivalent solid angle

Figure 9-11: The pattern solid angle Ω_p defines an equivalent cone over which all the radiation of the actual antenna is concentrated with equal intensity equal to the maximum of the actual pattern.

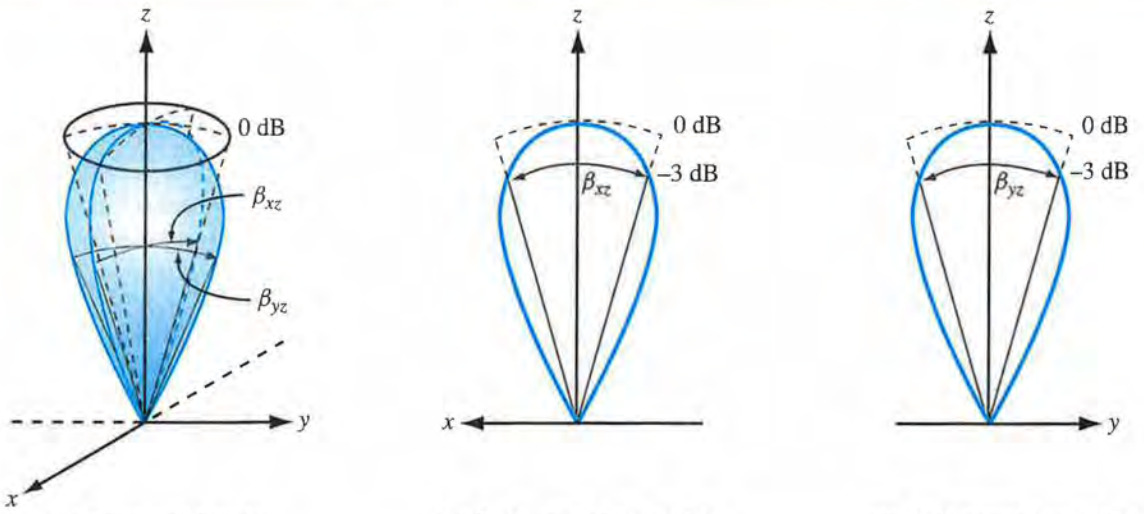
9-2.3 Antenna Directivity

The ***directivity*** D of an antenna is defined as the ratio of its maximum normalized radiation intensity, F_{max} (which by definition is equal to 1), to the average value of $F(\theta, \phi)$ over 4π space:

$$D = \frac{F_{max}}{F_{av}} = \frac{1}{\frac{1}{4\pi}\iint_{4\pi} F(\theta, \phi)\, d\Omega} = \frac{4\pi}{\Omega_p} \quad \text{(dimensionless)}, \tag{9.23}$$

where Ω_p is the pattern solid angle defined by Eq. (9.21). Thus, the narrower Ω_p of an antenna pattern is, the greater is the antenna directivity. For an isotropic antenna, $\Omega_p = 4\pi$; hence, its directivity $D_{iso} = 1$.

INTEL-1014
U.S. Patent 7,151,430



(a) Beam solid angle

(b) Half-power beamwidth in x-z plane

(c) Half-power beamwidth in y-z plane

Figure 9-12: The solid angle of a unidirectional radiation pattern is approximately equal to the product of the half-power beamwidths in the two principal planes; that is, $\Omega_p \simeq \beta_{xz}\beta_{yz}$.

By using Eq. (9.20) in Eq. (9.23), D can be expressed as

$$D = \frac{4\pi R^2 S_{max}}{P_{rad}} = \frac{S_{max}}{S_{av}}, \qquad (9.24)$$

where $S_{av} = P_{rad}/(4\pi R^2)$ is the average value of the radiated power density and is equal to the total power radiated by the antenna, P_{rad}, divided by the surface area of a sphere of radius R. Since $S_{av} = S_{iso}$, where S_{iso} is the power density radiated by an isotropic antenna, D represents the ratio of the maximum power density radiated by the antenna under consideration to the power density radiated by an isotropic antenna, both measured at the same range R and excited by the same amount of input power. Usually, D is expressed in decibels:* $D\,(\text{dB}) = 10 \log D$.

For an antenna with a single main lobe pointing in the z-direction as shown in Fig. 9-12, Ω_p may be approximated as the product of the half-power beamwidths β_{xz} and β_{yz} (in radians):

$$\Omega_p \simeq \beta_{xz}\beta_{yz}, \qquad (9.25)$$

and therefore

$$D = \frac{4\pi}{\Omega_p} \simeq \frac{4\pi}{\beta_{xz}\beta_{yz}}. \qquad (9.26)$$

*A note of caution: even though we often express certain dimensionless quantities in decibels, we should always convert their decibel values to natural values before using them in the relations given in this chapter.

INTEL-1014
U.S. Patent 7,151,430

Although approximate, this relation provides a useful method for estimating the antenna directivity from measurements of the beamwidths in the two orthogonal planes whose intersection is the axis of the main lobe.

Example 9-1 Antenna Radiation Properties

Determine (a) the direction of maximum radiation, (b) pattern solid angle, (c) directivity, and (d) half-power beamwidth in the y–z plane for an antenna that radiates into only the upper hemisphere and its normalized radiation intensity is given by $F(\theta, \phi) = \cos^2\theta$.

Solution: Mathematically, the statement that the antenna radiates along directions covering only the upper hemisphere can be written as

$$F(\theta, \phi) = F(\theta) = \begin{cases} \cos^2\theta, & \text{for } 0 \le \theta \le \pi/2 \\ & \text{and } 0 \le \phi \le 2\pi, \\ 0, & \text{elsewhere.} \end{cases}$$

(a) The function $F(\theta) = \cos^2\theta$ is independent of ϕ and is maximum when $\theta = 0°$. A polar plot of $F(\theta)$ is shown in Fig. 9-13.

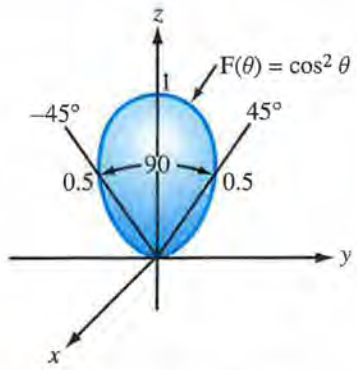


Figure 9-13: Polar plot of $F(\theta) = \cos^2\theta$.

(b) From Eq. (9.21), the pattern solid angle Ω_p is given by

$$\begin{aligned} \Omega_p &= \iint_{4\pi} F(\theta, \phi)\, d\Omega \\ &= \int_{\phi=0}^{2\pi} \left[\int_{\theta=0}^{\pi/2} \cos^2\theta \sin\theta\, d\theta \right] d\phi \\ &= \int_{\phi=0}^{2\pi} \left[-\frac{\cos^3\theta}{3} \right]_0^{\pi/2} d\phi \\ &= \int_0^{2\pi} \frac{1}{3}\, d\phi = \frac{2\pi}{3} \quad \text{(sr)}. \end{aligned}$$

(c) Application of Eq. (9.23) gives

$$D = \frac{4\pi}{\Omega_p} = 4\pi \left(\frac{3}{2\pi} \right) = 6,$$

which corresponds to D (dB) $= 10 \log 6 = 7.78$ dB.

(d) The half-power beamwidth β is obtained by setting $F(\theta) = 0.5$. That is,

$$F(\theta) = \cos^2\theta = 0.5,$$

which gives the half-power angles $\theta_1 = -45°$ and $\theta_2 = 45°$. Hence,

$$\beta = \theta_2 - \theta_1 = 90°. \quad \blacksquare$$

Example 9-2 Directivity of a Hertzian Dipole

Calculate the directivity of a Hertzian dipole.

Solution: Application of Eq. (9.23) with $F(\theta) = \sin^2\theta$ [from Eq. (9.15)] gives

$$\begin{aligned} D &= \frac{4\pi}{\displaystyle\iint_{4\pi} F(\theta, \phi) \sin\theta\, d\theta\, d\phi} \\ &= \frac{4\pi}{\displaystyle\int_{\phi=0}^{2\pi} \int_{\theta=0}^{\pi} \sin^3\theta\, d\theta\, d\phi} = \frac{4\pi}{8\pi/3} = 1.5 \end{aligned}$$

or, equivalently, 1.76 dB. $\blacksquare$

INTEL-1014
U.S. Patent 7,151,430

9-2.4 Antenna Gain

Of the total power P_t (transmitter power) supplied to the antenna, a part, P_{rad}, is radiated out into space, and the remainder, P_{loss}, is dissipated as heat loss in the antenna structure. The ***radiation efficiency*** ξ is defined as the ratio of P_{rad} to P_t:

$$\xi = \frac{P_{rad}}{P_t} \quad \text{(dimensionless)}. \tag{9.27}$$

The ***gain*** of an antenna is defined as

$$G = \frac{4\pi R^2 S_{max}}{P_t}, \tag{9.28}$$

which is similar in form to the expression given by Eq. (9.24) for the directivity D except that it is referred to the input power supplied to the antenna, P_t, rather than to the radiated power P_{rad}. In view of Eq. (9.27),

$$G = \xi D \quad \text{(dimensionless)}. \tag{9.29}$$

The gain accounts for ohmic losses in the antenna material, whereas the directivity does not. For a lossless antenna, $\xi = 1$.

9-2.5 Radiation Resistance

To the transmission line connected to its terminal, an antenna is merely an impedance. If the transmission line is matched to the antenna impedance, part of P_t, the power supplied by the generator, is radiated out into space, and the remainder is dissipated as heat in the antenna. The resistance part of the antenna impedance may be defined as consisting of a ***radiation resistance*** R_{rad} and a ***loss resistance*** R_{loss}. The corresponding time-average radiated power P_{rad} and dissipated power P_{loss} are

$$P_{rad} = \frac{1}{2} I_0^2 R_{rad}, \tag{9.30a}$$

$$P_{loss} = \frac{1}{2} I_0^2 R_{loss}, \tag{9.30b}$$

where I_0 is the amplitude of the sinusoidal current exciting the antenna. As defined earlier, the radiation efficiency is the ratio of P_{rad} to P_t,

$$\xi = \frac{P_{rad}}{P_t} = \frac{P_{rad}}{P_{rad} + P_{loss}} = \frac{R_{rad}}{R_{rad} + R_{loss}}. \tag{9.31}$$

The radiation resistance R_{rad} can be calculated by integrating the far-field power density over a sphere to obtain P_{rad} and then equating the result to Eq. (9.30a).

Example 9-3 Radiation Resistance and Efficiency of a Hertzian Dipole

A 4-cm-long center-fed dipole is used as an antenna at 75 MHz. The antenna wire is made of copper and has a radius $a = 0.4$ mm. From Eqs. (7.92a) and (7.94), the loss resistance of a circular wire of length l is given by

$$R_{loss} = \frac{l}{2\pi a}\sqrt{\frac{\pi f \mu_c}{\sigma_c}}, \tag{9.32}$$

where μ_c and σ_c are the magnetic permeability and conductivity of the wire, respectively. Calculate the radiation resistance and the radiation efficiency of the dipole antenna.

Solution: At 75 MHz,

$$\lambda = \frac{c}{f} = \frac{3 \times 10^8}{7.5 \times 10^7} = 4 \text{ m}.$$

The length to wavelength ratio is $l/\lambda = 4$ cm/4 m = 10^{-2}. Hence, this is a short dipole. From Eq. (9.24), P_{rad} is given by

$$P_{rad} = \frac{4\pi R^2}{D} S_{max}. \tag{9.33}$$

INTEL-1014
U.S. Patent 7,151,430

For the Hertzian dipole, S_{max} is given by Eq. (9.14), and from Example 9-2 we established that $D = 1.5$. Hence,

$$P_{rad} = \frac{4\pi R^2}{1.5} \times \frac{15\pi I_0^2}{R^2}\left(\frac{l}{\lambda}\right)^2 = 40\pi^2 I_0^2 \left(\frac{l}{\lambda}\right)^2. \quad (9.34)$$

Equating this result to Eq. (9.30a) and then solving for the radiation resistance R_{rad} gives

$$R_{rad} = 80\pi^2 (l/\lambda)^2 \quad (\Omega). \quad (9.35)$$

For $l/\lambda = 10^{-2}$, $R_{rad} = 0.08\ \Omega$.

Next, we will find the loss resistance R_{loss}. For copper, Appendix B gives $\mu_c \simeq \mu_0 = 4\pi \times 10^{-7}$ H/m and $\sigma_c = 5.8 \times 10^7$ S/m. Hence,

$$R_{loss} = \frac{l}{2\pi a}\sqrt{\frac{\pi f \mu_c}{\sigma_c}} = \frac{4\times 10^{-2}}{2\pi \times 4\times 10^{-4}}\left[\frac{\pi \times 75\times 10^6 \times 4\pi \times 10^{-7}}{5.8\times 10^7}\right]^{1/2} = 0.036\ \Omega,$$

and therefore the radiation efficiency is

$$\xi = \frac{R_{rad}}{R_{rad} + R_{loss}} = \frac{0.08}{0.08 + 0.036} = 0.69,$$

or 69% efficient. ■

REVIEW QUESTIONS

Q9.5 What does the pattern solid angle represent?

Q9.6 What is the magnitude of the directivity of an isotropic antenna?

Q9.7 What physical and material properties affect the radiation efficiency of a fixed-length Hertzian dipole antenna?

EXERCISE 9.2 An antenna has a conical radiation pattern with a normalized radiation intensity $F(\theta) = 1$ for θ between 0° and 45° and zero intensity for θ between 45° and 180°. The pattern is independent of the azimuth angle ϕ. Find (a) the pattern solid angle and (b) the directivity.

Ans. (a) $\Omega_p = 1.84$ sr, (b) $D = 6.83$ or, equivalently, 8.3 dB.

EXERCISE 9.3 The maximum power density radiated by a short dipole at a distance of 1 km is 60 (nW/m^2). If $I_0 = 10$ A, find the radiation resistance.

Ans. $R_{rad} = 10\ m\Omega$.

9-3 Half-Wave Dipole Antenna

In Section 9-1 we developed expressions for the electric and magnetic fields radiated by a short dipole of length much shorter than λ. We shall now use these expressions as building blocks to obtain expressions for the fields radiated by a half-wave dipole antenna, so named because its length $l = \lambda/2$. As shown in Fig. 9-14, the half-wave dipole consists of a thin wire fed at its center by a generator connected to the antenna terminals via a transmission line. The current flowing through the wire has a symmetrical distribution with respect to the center of the dipole, and the current has to be zero at the ends. Mathematically, $i(t)$ is given by

$$i(t) = I_0 \cos\omega t \cos kz = \mathfrak{Re}\left[I_0 \cos kz\, e^{j\omega t}\right], \quad (9.36)$$

whose current phasor is

$$\tilde{I}(z) = I_0 \cos kz, \qquad \frac{-\lambda}{4} \le z \le \frac{\lambda}{4}, \quad (9.37)$$

and $k = 2\pi/\lambda$. Equation (9.9a) gives an expression for $\tilde{E}_\theta$, the far field (at distance R) radiated by a short dipole of length l when excited by a current I_0. Let us adapt that expression to an infinitesimal dipole segment

INTEL-1014
U.S. Patent 7,151,430

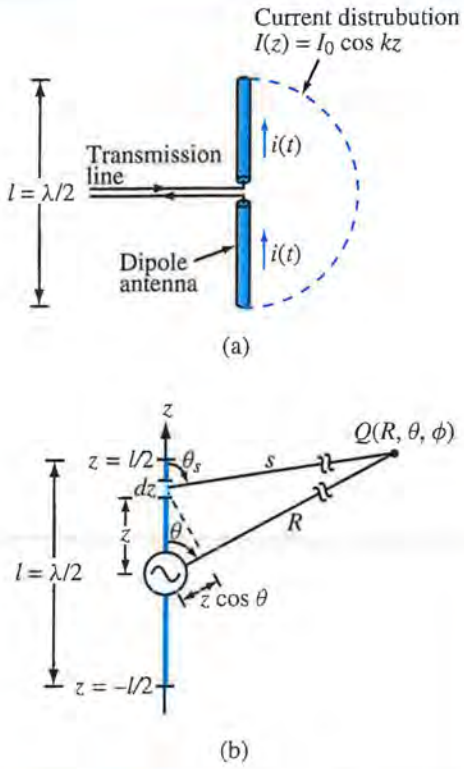


Figure 9-14: Center-fed half-wave dipole.

of length dz, excited by a current $\widetilde{I}(z)$ and located at a distance s from the observation point [Fig. 9-14(b)]. Thus,

$$d\widetilde{E}_\theta(z) = \frac{jk\eta_0}{4\pi}\widetilde{I}(z)\,dz\left(\frac{e^{-jks}}{s}\right)\sin\theta_s, \qquad (9.38a)$$

and the associated magnetic field is

$$d\widetilde{H}_\phi(z) = \frac{d\widetilde{E}_\theta(z)}{\eta_0}. \qquad (9.38b)$$

The far field due to radiation by the entire antenna is obtained by integrating the fields from all the Hertzian dipoles making up the antenna:

$$\widetilde{E}_\theta = \int_{z=-\lambda/4}^{\lambda/4} d\widetilde{E}_\theta. \qquad (9.39)$$

Before we calculate this integral, we shall make the following two approximations. The first approximation relates to the magnitude part of the spherical propagation factor, $1/s$. In Fig. 9-14(b), the distance s between the current element and the observation point Q is considered so large in comparison to the length of the dipole that the difference between s and R may be neglected in terms of its effect on $1/s$. Hence, we may set $1/s \simeq 1/R$, and by the same argument we set $\theta_s \simeq \theta$. The error Δ between s and R is a maximum when the observation point is along the z-axis and it is equal to $\lambda/4$ (corresponding to half of the antenna length). If $R \gg \lambda$, this error will have an insignificant effect on $1/s$. For the phase factor e^{-jks}, such an error in distance corresponds to an error in phase of $k\Delta = (2\pi/\lambda)(\lambda/4) = \pi/2$. As a rule of thumb, a phase error greater than $\pi/8$ is considered unacceptable because it may lead to a significant error in the computed value of the field $\widetilde{E}_\theta$. Hence, the approximation $s \simeq R$ is too crude for the phase factor and cannot be used. A more tolerable option is to use the parallel-ray approximation given by

$$s \simeq R - z\cos\theta, \qquad (9.40)$$

as illustrated in Fig. 9-14(b).

Substituting Eq. (9.40) for s in the phase factor of Eq. (9.38a) and replacing s with R and θ_s with θ elsewhere in the expression, we have

$$d\widetilde{E}_\theta = \frac{jk\eta_0}{4\pi}\widetilde{I}(z)\,dz\left(\frac{e^{-jkR}}{R}\right)\sin\theta\, e^{jkz\cos\theta}. \qquad (9.41)$$

After (1) inserting Eq. (9.41) into Eq. (9.39), (2) using the expression for $\widetilde{I}(z)$ given by Eq. (9.37), and (3)

INTEL-1014
U.S. Patent 7,151,430

carrying out the integration, the following expressions are obtained:

$$\widetilde{E}_\theta = j\,60 I_0 \left[\frac{\cos[(\pi/2)\cos\theta]}{\sin\theta}\right]\left(\frac{e^{-jkR}}{R}\right), \quad (9.42a)$$

$$\widetilde{H}_\phi = \frac{\widetilde{E}_\theta}{\eta_0}, \quad (9.42b)$$

and the corresponding time-average power density is

$$S(R,\theta) = \frac{|\widetilde{E}_\theta|^2}{2\eta_0} = \frac{15 I_0^2}{\pi R^2}\left[\frac{\cos^2[(\pi/2)\cos\theta]}{\sin^2\theta}\right], = S_0\left[\frac{\cos^2[(\pi/2)\cos\theta]}{\sin^2\theta}\right] \quad (\text{W/m}^2). \quad (9.43)$$

Examination of Eq. (9.43) reveals that $S(R,\theta)$ is maximum at $\theta = \pi/2$, and its value is

$$S_{\max} = S_0 = \frac{15 I_0^2}{(\pi R^2)}.$$

Hence, the normalized radiation intensity is

$$F(\theta) = \frac{S(R,\theta)}{S_0} = \left[\frac{\cos[(\pi/2)\cos\theta]}{\sin\theta}\right]^2. \quad (9.44)$$

The radiation pattern of the half-wave dipole exhibits roughly the same doughnutlike shape shown earlier in Fig. 9-7 for the short dipole. Its directivity is slightly larger (1.64 compared to 1.5 for the short dipole), but its radiation resistance is 73 Ω (as will be shown later in Section 9-3.2), which is orders of magnitude larger than that of a short dipole.

9-3.1 Directivity of $\lambda/2$ Dipole

To evaluate both the directivity D and the radiation resistance R_{rad} of the half-wave dipole, we first need to calculate the total radiated power P_{rad} by applying Eq. (9.20):

$$P_{\text{rad}} = R^2 \iint_{4\pi} S(R,\theta)\, d\Omega = \frac{15 I_0^2}{\pi}\int_0^{2\pi}\int_0^{\pi}\left[\frac{\cos[(\pi/2)\cos\theta]}{\sin\theta}\right]^2 \sin\theta\, d\theta\, d\phi. \quad (9.45)$$

The integration over ϕ is equal to 2π, and numerical evaluation of the integration over θ gives the value 1.22. Consequently,

$$P_{\text{rad}} = 36.6\, I_0^2 \quad (\text{W}). \quad (9.46)$$

From Eq. (9.43), we found that $S_{\max} = 15 I_0^2/(\pi R^2)$. Using this in Eq. (9.24) gives the following result for the directivity D of the half-wave dipole:

$$D = \frac{4\pi R^2 S_{\max}}{P_{\text{rad}}} = \frac{4\pi R^2}{36.6 I_0^2}\left(\frac{15 I_0^2}{\pi R^2}\right) = 1.64 \quad (9.47)$$

or, equivalently, 2.15 dB.

9-3.2 Radiation Resistance of $\lambda/2$ Dipole

Using Eq. (9.30a) to relate the radiation resistance R_{rad} to the total radiated power P_{rad}, we have

$$R_{\text{rad}} = \frac{2P_{\text{rad}}}{I_0^2} = \frac{2 \times 36.6 I_0^2}{I_0^2} \simeq 73\ \Omega. \quad (9.48)$$

As was noted earlier in Example 9-3, because the radiation resistance of a short dipole is comparable in magnitude to that of its loss resistance R_{loss}, its radiation efficiency ξ is quite small. For the 4-cm-long dipole of Example 9-3, $R_{\text{rad}} = 0.08\ \Omega$ (at 75 MHz) and $R_{\text{loss}} = 0.036\ \Omega$. If we keep the frequency the same and increase the length of the dipole to 2 m ($\lambda = 4$ m

INTEL-1014
U.S. Patent 7,151,430

at $f = 75$ MHz), R_{rad} becomes 73 Ω and R_{loss} increases to 1.8 Ω. The radiation efficiency increases from 69% for the short dipole to 98% for the half-wave dipole. More significant is the fact that it is practically impossible to match a transmission line to an antenna with a resistance on the order of 0.1 Ω, while it is quite easy to do so when $R_{rad} = 73$ Ω.

Another interesting feature of the half-wave dipole pertains to its reactance. As seen by a transmission line, an antenna may be represented by an ***input impedance*** connected to the line at the antenna terminals. The input impedance Z_{in} consists of a real part R_{in} and an imaginary part X_{in}:

$$Z_{in} = R_{in} + jX_{in}, \tag{9.49}$$

where R_{in} is the sum of the radiation resistance R_{rad} and the loss resistance R_{loss},

$$R_{in} = R_{rad} + R_{loss}. \tag{9.50}$$

For the half-wave dipole, R_{loss} is much smaller than R_{rad} and can be ignored. Hence,

$$Z_{in} \cong R_{rad} + jX_{in}. \tag{9.51}$$

Deriving an expression for X_{in} for the half-wave dipole is fairly complicated and beyond the scope of this book. However, it is significant to note that X_{in} is a strong function of l/λ, and it decreases from 42 Ω at $l/\lambda = 0.5$ down to zero at $l/\lambda = 0.48$, whereas R_{rad} remains approximately unchanged. Hence, by reducing the length of the half-wave dipole by 4%, Z_{in} becomes purely real and equal to 73 Ω, thereby making it possible to match the dipole to a 75-Ω transmission line without resorting to the use of a matching network.

9-3.3 Quarter-Wave Monopole Antenna

When placed over a conducting ground plane, a quarter-wave monopole antenna excited by a source at its base [Fig. 9-15(a)] exhibits the same radiation pattern in the region above the ground plane as a half-wave dipole in free space. This is because, from image theory [Section 4-12], the conducting plane can be replaced with the image of the $\lambda/4$ monopole, as illustrated in Fig. 9-15(b). Thus, the $\lambda/4$ monopole will radiate an electric field identical to that given by Eq. (9.42a), and its normalized radiation intensity is given by Eq. (9.44);

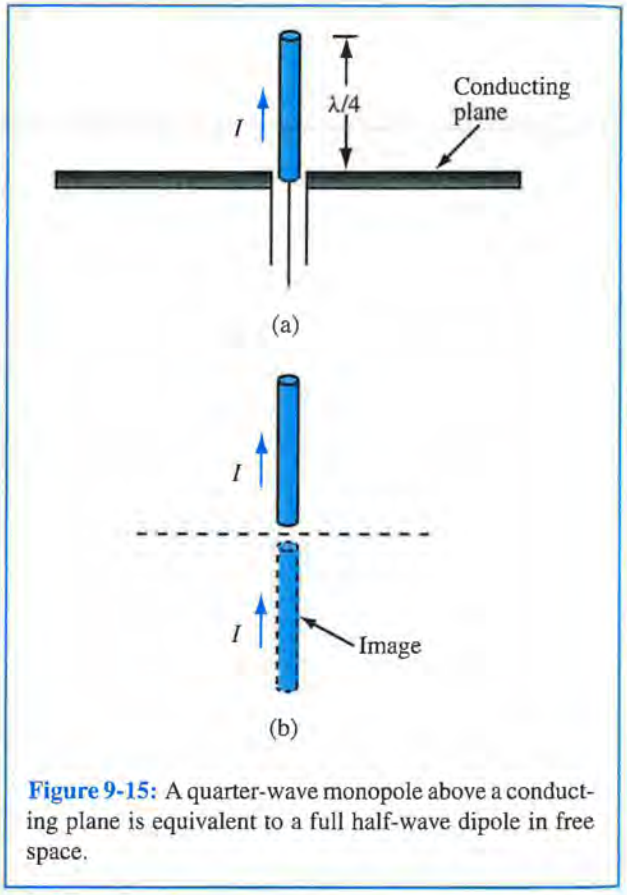


Figure 9-15: A quarter-wave monopole above a conducting plane is equivalent to a full half-wave dipole in free space.

INTEL-1014
U.S. Patent 7,151,430

but the radiation is limited to the upper half-space defined by $0 \le \theta \le \pi/2$. Hence, a monopole radiates only half as much power as the dipole. Consequently, for a $\lambda/4$ monopole, $P_{rad} = 18.3 I_0^2$ and its radiation resistance is $R_{rad} = 36.5\ \Omega$.

The approach used for the quarter-wave monopole is also valid for any vertical wire antenna placed above a conducting plane, including a Hertzian monopole.

REVIEW QUESTIONS

Q9.8 What is the physical length of a half-wave dipole operating at (a) 1 MHz (in the AM broadcast band), (b) 100 MHz (FM broadcast band), and (c) 10 GHz (microwave band)?

Q9.9 How does the radiation pattern of a half-wave dipole compare with that of a Hertzian dipole? How do their directivities, radiation resistances, and radiation efficiencies compare?

Q9.10 How does the radiation efficiency of a quarter-wave monopole compare with that of a half-wave dipole, assuming that both are made of the same material and have the same cross section?

EXERCISE 9.4 For the half-wave dipole antenna, evaluate $F(\theta)$ versus θ in order to determine the half-power beamwidth in the elevation plane (the plane containing the dipole axis).

Ans. $\beta = 78°$.

EXERCISE 9.5 If the maximum power density radiated by a half-wave dipole is 50 (μW/m^2) at a range of 1 km, what is the current amplitude I_0?

Ans. $I_0 = 3.24$ A.

9-4 Dipole of Arbitrary Length

So far, we have examined the radiation properties of the short Hertzian dipole and of the half-wave dipole. We will now consider the more general case of a linear dipole of any arbitrary length l, relative to λ. For a center-fed dipole, as depicted in Fig. 9-16, the currents flowing through its two halves are symmetrical and must go to zero at its ends. Hence, the current phasor $\tilde{I}(z)$ can be expressed as a sine function with an argument that goes to zero at $z = \pm l/2$:

$$\tilde{I}(z) = \begin{cases} I_0 \sin[k(l/2 - z)], & \text{for } 0 \le z \le l/2, \\ I_0 \sin[k(l/2 + z)], & \text{for } -l/2 \le z < 0, \end{cases} \tag{9.52}$$

where I_0 is the current amplitude. The procedure for calculating the electric and magnetic fields and the

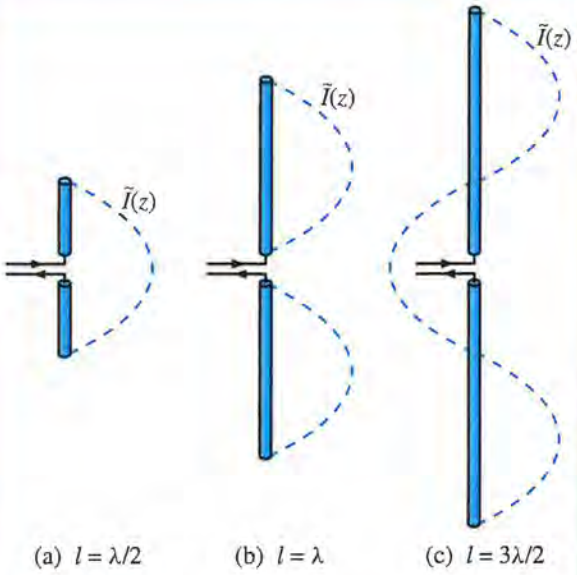


Figure 9-16: Current distribution for three center-fed dipoles.

INTEL-1014
U.S. Patent 7,151,430

associated power density of the wave radiated by such an antenna is basically the same as that used previously in connection with the half-wave dipole antenna. The only difference is the current distribution $\widetilde{I}(z)$. If we insert the expression for $\widetilde{I}(z)$ given by Eq. (9.52) in Eq. (9.41), we obtain the following expression for the differential electric field $d\widetilde{E}_\theta$ of the wave radiated by an elemental length dz at location z along the dipole:

$$d\widetilde{E}_\theta = \frac{jk\eta_0 I_0}{4\pi}\left(\frac{e^{-jkR}}{R}\right)\sin\theta\, e^{jkz\cos\theta}\, dz \times \begin{cases} \sin[k(l/2-z)], & \text{for } 0 \le z \le l/2, \\ \sin[k(l/2+z)], & \text{for } -l/2 \le z < 0. \end{cases} \tag{9.53}$$

The total field radiated by the dipole is

$$\begin{aligned}\widetilde{E}_\theta &= \int_{-l/2}^{l/2} d\widetilde{E}_\theta \\ &= \int_0^{l/2} d\widetilde{E}_\theta + \int_{-l/2}^{0} d\widetilde{E}_\theta \\ &= \frac{jk\eta_0 I_0}{4\pi}\left(\frac{e^{-jkR}}{R}\right)\sin\theta \\ &\quad \times \left[\int_0^{l/2} e^{jkz\cos\theta}\sin[k(l/2-z)]\,dz + \int_{-l/2}^{0} e^{jkz\cos\theta}\sin[k(l/2+z)]\,dz\right].\end{aligned} \tag{9.54}$$

If we apply Euler's identity to express $e^{jkz\cos\theta}$ as $[\cos(kz\cos\theta)+j\sin(kz\cos\theta)]$, we can integrate the two integrals and obtain the result

$$\widetilde{E}_\theta = j60I_0\left(\frac{e^{-jkR}}{R}\right) \times \left[\frac{\cos\left(\frac{kl}{2}\cos\theta\right)-\cos\left(\frac{kl}{2}\right)}{\sin\theta}\right]. \tag{9.55}$$

The corresponding time-average power density radiated by the dipole antenna is given by

$$\begin{aligned}S(\theta) &= \frac{|\widetilde{E}_\theta|^2}{2\eta_0} \\ &= \frac{15I_0^2}{\pi R^2}\left[\frac{\cos\left(\frac{\pi l}{\lambda}\cos\theta\right)-\cos\left(\frac{\pi l}{\lambda}\right)}{\sin\theta}\right]^2,\end{aligned} \tag{9.56}$$

where we have used the relations $\eta_0 \simeq 120\pi\ (\Omega)$ and $k = 2\pi/\lambda$. For $l = \lambda/2$, Eq. (9.56) reduces to the expression given by Eq. (9.43) for the half-wave dipole. Plots of the normalized radiation intensity, $F(\theta) = S(R,\theta)/S_{\max}$, are shown in Fig. 9-17 for dipoles with lengths of $\lambda/2$, λ, and $3\lambda/2$. The dipoles with $l = \lambda/2$ and $l = \lambda$ have similar radiation patterns with maxima along $\theta = 90°$, but the half-power beamwidth of the wavelength-long dipole is narrower than that of the half-wave dipole, and $S_{\max} = 60I_0^2/(\pi R^2)$ for the wavelength-long dipole, which is four times that for the half-wave dipole. The pattern of the dipole with length $l = 3\lambda/2$ exhibits a multiple lobe structure, and its direction of maximum radiation is not along $\theta = 90°$.

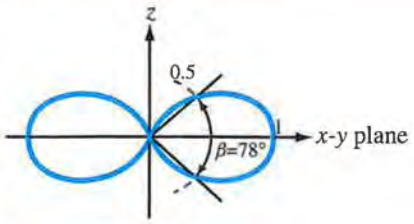
9-5 Effective Area of a Receiving Antenna

So far, we have examined the radiation characteristics of antennas by treating them as radiators of the energy supplied by a source. Now we shall consider the reverse process, that is, how a receiving antenna extracts energy from an incident wave and delivers it to a load. The ability of an antenna to capture energy from an incident wave of power density S_i (W/m^2) and to convert it into an *intercepted power* P_{int} (W) for delivery to a matched load is characterized by the *effective area* A_e:

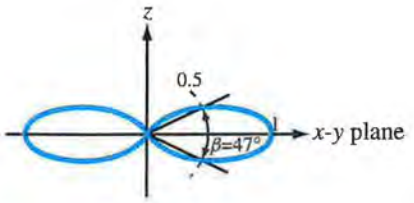
$$A_e = \frac{P_{int}}{S_i} \quad (\text{m}^2). \tag{9.57}$$

Other commonly used names for A_e include *effective aperture* and *receiving cross section*. The antenna

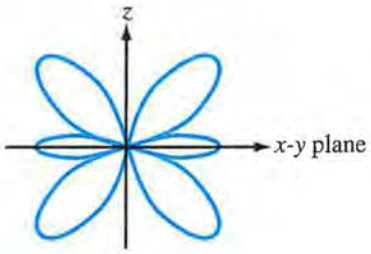
INTEL-1014
U.S. Patent 7,151,430



(a) $l = \lambda/2$

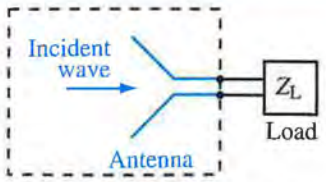


(b) $l = \lambda$

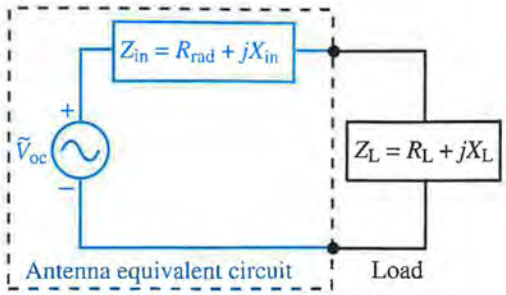


(c) $l = 3\lambda/2$

Figure 9-17: Radiation patterns of dipoles with lengths of $\lambda/2$, λ, and $3\lambda/2$.



(a) Receiving antenna



(b) Equivalent circuit

Figure 9-18: Receiving antenna represented by an equivalent circuit.

receiving process may be modeled in the form of a Thévenin equivalent circuit as shown in Fig. 9-18, where $\tilde{V}_{oc}$ is the open-circuit voltage phasor induced in the receiving antenna by the incident wave, Z_{in} is the antenna impedance, and Z_L is the impedance of the load for which the received power is intended. In general, both Z_{in} and Z_L are complex:

$$Z_{in} = R_{rad} + jX_{in}, \tag{9.58a}$$

$$Z_L = R_L + jX_L, \tag{9.58b}$$

where R_{rad} denotes the radiation resistance of the antenna, and it is assumed that the antenna loss resistance is much smaller than R_{rad} and can be ignored. As we will see later in Example 9-4, for maximum power transfer, the load impedance must be chosen such that $Z_L = Z_{in}^*$, or $R_L = R_{rad}$ and $X_L = -X_{in}$, in which case the circuit reduces to a source $\tilde{V}_{oc}$ connected across a resistance equal to $2R_{rad}$. Since $\tilde{V}_{oc}$ is a sinusoidal voltage phasor, the time-average power delivered to the load is

$$P_L = \frac{1}{2}|\tilde{I}_L|^2 R_{rad} = \frac{1}{2}\left[\frac{|\tilde{V}_{oc}|}{2R_{rad}}\right]^2 R_{rad} = \frac{|\tilde{V}_{oc}|^2}{8R_{rad}}, \tag{9.59}$$

INTEL-1014
U.S. Patent 7,151,430

where $\widetilde{I}_L = \widetilde{V}_{oc}/(2R_{rad})$ is the phasor current flowing through the circuit. Since the antenna is lossless, all the intercepted power P_{int} ends up in the load resistance R_L. Hence,

$$P_{int} = P_L = \frac{|\widetilde{V}_{oc}|^2}{8R_{rad}}. \tag{9.60}$$

For an incident wave with electric field $\widetilde{E}_i$ parallel to the antenna polarization direction, the power density carried by the wave is

$$S_i = \frac{|\widetilde{E}_i|^2}{2\eta_0} = \frac{|\widetilde{E}_i|^2}{240\pi}. \tag{9.61}$$

The ratio of the results provided by Eqs. (9.60) and (9.61) gives

$$A_e = \frac{P_{int}}{S_i} = \frac{30\pi|\widetilde{V}_{oc}|^2}{R_{rad}|\widetilde{E}_i|^2}. \tag{9.62}$$

The open-circuit voltage $\widetilde{V}_{oc}$ induced in the receiving antenna is due to the incident field $\widetilde{E}_i$, but the relation between them depends on the specific antenna under consideration. By way of illustration, let us consider the case of the short-dipole antenna of Section 9-1. Because the length l of the short dipole is small compared to λ, the current induced by the incident field will be uniform across its length, and the open-circuit voltage will simply be $\widetilde{V}_{oc} = \widetilde{E}_i l$. Noting that $R_{rad} = 80\pi^2(l/\lambda)^2$ for the short dipole [see Eq. (9.35)] and using $\widetilde{V}_{oc} = \widetilde{E}_i l$, Eq. (9.62) simplifies to

$$A_e = \frac{3\lambda^2}{8\pi} \quad (m^2) \quad \text{(short dipole)}. \tag{9.63}$$

In Example 9-2 it was shown that for the short dipole the directivity $D = 1.5$. In terms of D, Eq. (9.63) can be rewritten in the form

$$A_e = \frac{\lambda^2 D}{4\pi} \quad (m^2) \quad \text{(any antenna)}. \tag{9.64}$$

Despite the fact that the relation between A_e and D given by Eq. (9.64) was derived for a short dipole, it can be shown that it is also valid *for any antenna* under matched-impedance conditions.

Example 9-4 Maximum Power Transfer

The circuit shown in Fig. 9-18(b) consists of a generator comprised of a voltage phasor $\widetilde{V}_{oc}$ and an internal impedance Z_{in} connected to a load Z_L. If

$$Z_{in} = R_{rad} + jX_{in},$$
$$Z_L = R_L + jX_L,$$

what values of R_L and X_L yield the maximum transfer of power from the generator into the load?

Solution: The current phasor flowing through the circuit is

$$\widetilde{I}_L = \frac{\widetilde{V}_{oc}}{Z_{in} + Z_L} = \frac{\widetilde{V}_{oc}}{(R_{rad} + R_L) + j(X_{in} + X_L)}, \tag{9.65}$$

and the time-average power dissipated in the load resistance R_L is

$$P_L = \tfrac{1}{2}|\widetilde{I}_L|^2 R_L = \tfrac{1}{2}|\widetilde{V}_{oc}|^2 \frac{R_L}{(R_{rad} + R_L)^2 + (X_{in} + X_L)^2}. \tag{9.66}$$

Our task is to specify the load parameters, R_L and X_L, that maximize P_L. This is achieved by differentiating the expression for P_L with respect to R_L, equating it to zero, and then repeating the process with respect to X_L. The first of these two steps gives

$$\frac{\partial P_L}{\partial R_L} = \tfrac{1}{2}|\widetilde{V}_{oc}|^2 \left[\frac{1}{(R_{rad} + R_L)^2 + (X_{in} + X_L)^2} + \frac{-2R_L(R_{rad} + R_L)}{\left[(R_{rad} + R_L)^2 + (X_{in} + X_L)^2\right]^2}\right] = 0,$$

INTEL-1014
U.S. Patent 7,151,430

which yields the result

$$(X_{in} + X_L)^2 - R_L^2 + R_{rad}^2 = 0. \quad (9.67)$$

Application of the second step gives

$$\frac{\partial P_L}{\partial X_L} = \tfrac{1}{2}|\widetilde{V}_{oc}|^2 \left[\frac{-2R_L(X_{in} + X_L)}{[(R_{rad} + R_L)^2 + (X_{in} + X_L)^2]^2}\right] = 0,$$

which yields a second condition,

$$R_L(X_{in} + X_L) = 0. \quad (9.68)$$

To satisfy this result, we have to choose either $R_L = 0$, which is not an acceptable result because it means that $P_L = 0$, or

$$\boxed{X_L = -X_{in}.} \quad (9.69a)$$

Using Eq. (9.69a) in Eq. (9.67) gives

$$\boxed{R_L = R_{rad}.} \quad (9.69b)$$

These two results can be combined into

$$\boxed{Z_L = Z_{in}^*,} \quad (9.70)$$

where Z_{in}^* is the complex conjugate of Z_{in}. Thus, *for maximum power transfer, the load impedance should be equal to the complex conjugate of the generator impedance.* ■

EXERCISE 9.6 The effective area of an antenna is 9 m^2. What is its directivity in decibels at 3 GHz?

Ans. $D = 40.53$ dB.

EXERCISE 9.7 At 100 MHz, the pattern solid angle of an antenna is 1.3 sr. Find (a) the antenna directivity D and (b) its effective area A_e.

Ans. (a) $D = 9.67$, (b) $A_e = 6.92$ m^2.

9-6 Friis Transmission Formula

The two antennas shown in Fig. 9-19 are part of a free-space communication link, with the separation between the antennas, R, being large enough for each antenna to be in the far-field region of the other. The transmitting and receiving antennas have effective areas A_t and A_r and radiation efficiencies ξ_t and ξ_r, respectively. Our objective is to find a relationship between P_t, the transmitter power supplied to the transmitting antenna, and P_{rec}, the power delivered to the receiver by the receiving antenna. As always, we assume that both antennas are impedance matched to their respective transmission lines. Initially, we shall consider the case where the two antennas are oriented such that the peak of the radiation pattern of each antenna points in the direction of the other.

Let us start by treating the transmitting antenna as a lossless isotropic radiator. In this case, the power density incident upon the receiving antenna at a distance R from an isotropic transmitting antenna is simply equal to the transmitter power P_t divided by the surface area of a sphere of radius R:

$$S_{iso} = \frac{P_t}{4\pi R^2}. \quad (9.71)$$

The real transmitting antenna is neither lossless nor isotropic. Hence, the power density S_r due to the real

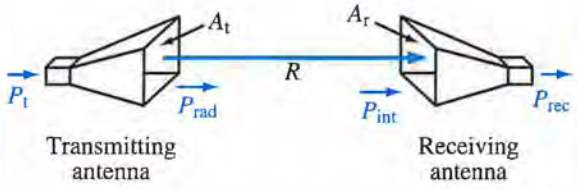


Figure 9-19: Transmitter–receiver configuration.

INTEL-1014
U.S. Patent 7,151,430

antenna is given by

$$S_r = G_t S_{iso} = \xi_t D_t S_{iso} = \frac{\xi_t D_t P_t}{4\pi R^2}, \qquad (9.72)$$

where, through the gain $G_t = \xi_t D_t$, ξ_t accounts for the fact that only part of the power P_t supplied to the antenna actually is radiated out into space, and D_t accounts for the directivity of the transmitting antenna (in the direction of the receiving antenna). Using Eq. (9.64), Eq. (9.72) can be expressed in terms of the effective area A_t of the transmitting antenna:

$$S_r = \frac{\xi_t A_t P_t}{\lambda^2 R^2}. \qquad (9.73)$$

On the receiving-antenna side, the power intercepted by the receiving antenna is equal to the product of the incident power density S_r and the effective area A_r:

$$P_{int} = S_r A_r = \frac{\xi_t A_t A_r P_t}{\lambda^2 R^2}. \qquad (9.74)$$

The received power P_{rec} delivered to the receiver is equal to the intercepted power P_{int} multiplied by the radiation efficiency of the receiving antenna, ξ_r. Thus, $P_{rec} = \xi_r P_{int}$, which leads to the result

$$\frac{P_{rec}}{P_t} = \frac{\xi_t \xi_r A_t A_r}{\lambda^2 R^2} = G_t G_r \left(\frac{\lambda}{4\pi R}\right)^2. \qquad (9.75)$$

This relation is known as the ***Friis transmission formula***, and P_{rec}/P_t is sometimes called the ***power transfer ratio***. In deriving the form of the Friis formula involving the gains G_t and G_r of the transmitting and receiving antennas, we used the fact that $\xi_t A_t = \xi_t D_t \lambda^2/4\pi = G_t \lambda^2/4\pi$, and similar relations apply to the receiving antenna.

If the two antennas are not oriented in the direction of maximum power transfer, Eq. (9.75) can be rewritten in the general form

$$\frac{P_{rec}}{P_t} = G_t G_r \left(\frac{\lambda}{4\pi R}\right)^2 F_t(\theta_t, \phi_t)\, F_r(\theta_r, \phi_r), \qquad (9.76)$$

where $F_t(\theta_t, \phi_t)$ is the normalized radiation intensity of the transmitting antenna, evaluated at the direction (θ_t, ϕ_t) corresponding to the direction of the receiving antenna (as seen by the antenna pattern of the transmitting antenna), and a similar definition applies to $F_r(\theta_r, \phi_r)$ for the receiving antenna.

Example 9-5 Satellite Communication System

A 6-GHz direct-broadcast TV satellite system transmits 100 W through a 2-m-diameter parabolic dish antenna from a distance of approximately 40,000 km above Earth's surface. Each TV channel occupies a bandwidth of 5 MHz. Due to electromagnetic noise picked up by the antenna as well as noise generated by the receiver electronics, a ground home receiving TV station has a noise level given by

$$P_n = K T_{sys} B \quad \text{(W)}, \qquad (9.77)$$

where T_{sys} [measured in kelvins (K)] is a figure of merit, called the ***system noise temperature***, that characterizes the noise performance of the receiver–antenna combination, K is Boltzmann's constant [1.38×10^{-23} (J/K)], and B is the receiver bandwidth in Hz.

The ***signal-to-noise ratio*** S_n (which should not be confused with the power density S) is defined as the ratio of P_{rec}, the signal power received from the transmitter, to P_n:

$$S_n = P_{rec}/P_n \quad \text{(dimensionless)}. \qquad (9.78)$$

For a receiver with $T_{sys} = 580$ K, what minimum diameter of a parabolic dish receiving antenna is required for high-quality TV reception with $S_n = 40$ dB? The satellite and ground receiving antennas may be assumed lossless, and their effective areas may be assumed equal to their physical apertures.

Solution: The following quantities are given:

$$P_t = 100 \text{ W}, \quad f = 6 \text{ GHz} = 6 \times 10^9 \text{ Hz}, \quad S_n = 10^4,$$

Transmit antenna diameter $d_t = 2$ m,

INTEL-1014
U.S. Patent 7,151,430

$$T_{sys} = 580 \text{ K},$$
$$R = 40,000 \text{ km} = 4 \times 10^7 \text{ m},$$
$$B = 5 \text{ MHz} = 5 \times 10^6 \text{ Hz}.$$

The wavelength $\lambda = c/f = 5 \times 10^{-2}$ m, and the area of the transmitting satellite antenna is $A_t = (\pi d_t^2/4) = \pi$ (m^2). From Eq. (9.77), the receiver noise power is

$$P_n = KT_{sys}B = 1.38 \times 10^{-23} \times 580 \times 5 \times 10^6$$
$$= 4 \times 10^{-14} \text{ W}.$$

Using Eq. (9.75) for lossless antennas ($\xi_t = \xi_r = 1$), the received signal power is

$$P_{rec} = \frac{P_t A_t A_r}{\lambda^2 R^2} = \frac{100\pi A_r}{(5 \times 10^{-2})^2 (4 \times 10^7)^2}$$
$$= 7.85 \times 10^{-11} A_r.$$

The area of the receiving antenna, A_r, can now be determined by equating the ratio P_{rec}/P_n to $S_n = 10^4$:

$$10^4 = \frac{7.85 \times 10^{-11} A_r}{4 \times 10^{-14}},$$

which yields the value $A_r = 5.1$ m^2. The required minimum diameter is $d_r = \sqrt{4A_r/\pi} = 2.55$ m. ■

REVIEW QUESTIONS

Q9.11 For an a-c generator connected to a load, what is the condition for maximum transfer of power from the generator to the load?

Q9.12 If the two antennas of a communication system have constant radiation efficiencies and effective areas, how does the power transfer ratio vary with λ? Explain in terms of how the antenna beams vary with λ.

EXERCISE 9.8 Suppose that the operating frequency of the communication system described in Example 9-5 were to be doubled to 12 GHz. What would then be the minimum required diameter of a home receiving TV antenna?

Ans. $d_r = 1.27$ m.

EXERCISE 9.9 A 3-GHz microwave link consists of two identical antennas each with a gain of 30 dB. If the transmitter output power is 1 kW and the two antennas are 10 km apart, find the received power.

Ans. $P_{rec} = 6.33 \times 10^{-4}$ W.

EXERCISE 9.10 The effective area of a parabolic dish antenna is approximately equal to its physical aperture. If the directivity of a dish antenna is 30 dB at 10 GHz, what is its effective area? If the frequency is increased to 30 GHz, what will be its new directivity?

Ans. $A_e = 0.07$ m^2, $D = 39.54$ dB.

9-7 Radiation by Large-Aperture Antennas

For wire antennas, the sources of radiation are the infinitesimal current elements comprising the current distribution along the wire, and the total radiated field at a given point in space is equal to the sum, or integral, of the fields radiated by all the elements. A parallel arrangement applies to aperture antennas, except that now the source of radiation is the electric-field distribution across the aperture. Consider the horn antenna shown in Fig. 9-20, which is connected to a source through a coaxial transmission line, with the outer conductor of the coaxial line being connected to the metal body of the horn and the inside conductor made to protrude, through a small hole, partially into the throat end of the horn. The protruding conductor acts as a monopole antenna, generating waves that radiate outwardly toward

INTEL-1014
U.S. Patent 7,151,430

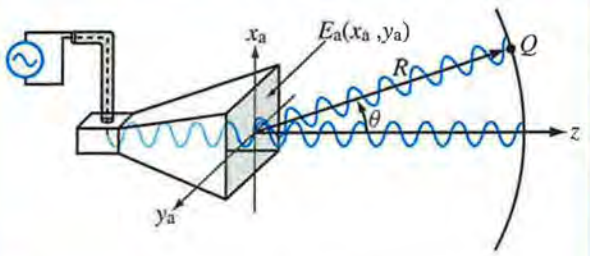
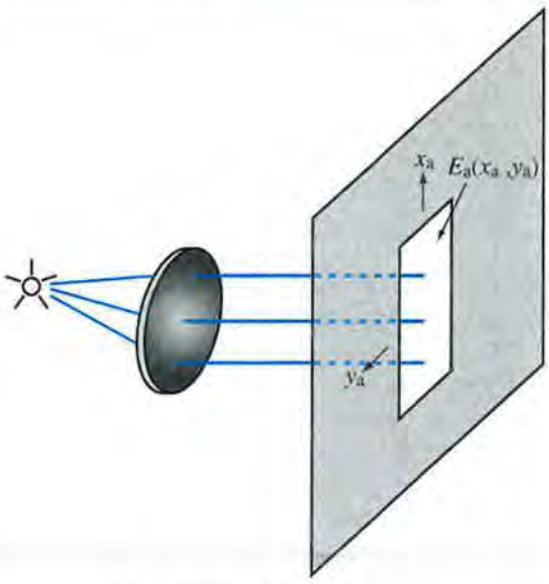


Figure 9-20: A horn antenna with aperture field distribution $E_a(x_a, y_a)$.

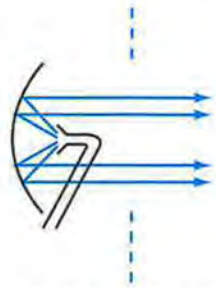
the horn's aperture. The electric field of the energy arriving at the aperture, which may vary as a function of x_a and y_a over the horn's aperture, is called the electric-field aperture distribution, $E_a(x_a, y_a)$. Inside the horn, wave propagation is guided by the horn's geometry; but as the wave transitions from a guided wave into an unbounded wave, every point of its wavefront serves as a source of spherical secondary wavelets. The aperture may then be represented as a distribution of isotropic radiators, each with an intensity proportional to the electric field $E_a(x_a, y_a)$ at its location (x_a, y_a). At a distant point Q, the combination of all the waves arriving from all of these radiators constitutes the total wave that would be observed by a receiver placed at that point.

The radiation process described for the horn antenna is equally applicable to any aperture upon which an electromagnetic wave is incident. For example, if a light source is used to illuminate an opening in an opaque screen through a collimating lens, as shown in Fig. 9-21(a), the opening becomes a source of secondary spherical wavelets, much like the aperture of the horn antenna. In the case of the parabolic reflector shown in Fig. 9-21(b), it can be described in terms of an imaginary aperture representing the electric-field distribution across a plane in front of the reflector.

Two types of mathematical formulations are available for computing the electromagnetic fields of waves radiated by apertures. The first type is a ***scalar formulation*** based on Kirchhoff's work and is used commonly in optical diffraction problems and for large-aperture



(a) Opening in an opaque screen



(b) Parabolic reflector antenna

Figure 9-21: Radiation by apertures: (a) an opening in an opaque screen illuminated by a light source through a collimating lens and (b) a parabolic dish reflector illuminated by a small horn antenna.

INTEL-1014
U.S. Patent 7,151,430

antennas. The second type is a ***vector formulation*** based on Maxwell's equations. Although theoretically superior, the vector approach generally is more difficult to apply. Hence, it is used mostly in connection with antenna apertures whose dimensions are comparable to or smaller than a wavelength, because in this case the scalar approach is inapplicable.

In this section, we shall limit our presentation to the scalar diffraction approach, in part because of its inherent simplicity and also because it is applicable to a wide range of practical applications. *The key requirement for the validity of the scalar formulation is that the antenna aperture be at least several wavelengths long along each of its principal dimensions.* A distinctive feature of such an antenna is its high directivity and correspondingly narrow beam, which makes it attractive for radar and free-space microwave communication systems. The frequency range commonly used for these applications is the 1- to 30-GHz microwave band. Because the corresponding wavelength range is 30 to 1 cm, respectively, it is quite practical to construct and use antennas (in this frequency range) with aperture dimensions that are many wavelengths in size.

The x_a–y_a plane in Fig. 9-22, denoted plane A, contains an aperture with an electric field distribution $E_a(x_a, y_a)$, usually called the ***aperture illumination***. For the sake of convenience, the opening has been chosen to be rectangular in shape, with dimensions l_x along x_a and l_y along y_a, even though the formulation we are about to discuss is general enough to accommodate any two-dimensional aperture distribution, including those associated with circular and elliptical apertures. At a distance z from the aperture plane A in Fig. 9-22, we have an observation plane O with axes (x, y). The two planes have parallel axes and are separated by a distance z that is sufficiently large so that any point Q in the observation plane is in the far-field region of the aperture. To satisfy the far-field condition, it is necessary that

$$R \geq 2d^2/\lambda, \qquad (9.79)$$

where d is the longest linear dimension of the radiating aperture.

The position of observation point Q is specified by the range R between the center of the aperture and point Q and by the angles θ and ϕ shown in Fig. 9-22, which together define the direction of the observation point relative to the coordinate system of the aperture. The electric field phasor of the wave incident upon point Q is denoted $\widetilde{E}(R, \theta, \phi)$. Kirchhoff's scalar diffraction theory provides the following relationship between the radiated field $\widetilde{E}(R, \theta, \phi)$ and the aperture illumination $\widetilde{E}_a(x_a, y_a)$:

$$\widetilde{E}(R, \theta, \phi) = \frac{j}{\lambda}\left(\frac{e^{-jkR}}{R}\right)\widetilde{h}(\theta, \phi), \qquad (9.80)$$

where

$$\widetilde{h}(\theta, \phi) = \iint_{-\infty}^{\infty} \widetilde{E}_a(x_a, y_a) \cdot \exp\left[jk \sin\theta (x_a \cos\phi + y_a \sin\phi)\right] dx_a\, dy_a. \qquad (9.81)$$

We shall refer to $\widetilde{h}(\theta, \phi)$ as the ***form factor*** of $\widetilde{E}(R, \theta, \phi)$. Its integral is written with infinite limits, with the understanding that $\widetilde{E}_a(x_a, y_a)$ is identically zero outside the aperture. The spherical propagation factor (e^{-jkR}/R) accounts for wave propagation between the center of the aperture and the observation point, and $\widetilde{h}(\theta, \phi)$ represents an integration of the exciting field $\widetilde{E}_a(x_a, y_a)$ over the extent of the aperture, taking into account [through the exponential function in Eq. (9.81)] the approximate deviation in distance between R and s, where s is the distance to any point (x_a, y_a) in the aperture plane [see Fig. 9-22]. *The polarization direction of the radiated field $\widetilde{E}(R, \theta, \phi)$ is the same as that of the aperture field*

INTEL-1014
U.S. Patent 7,151,430

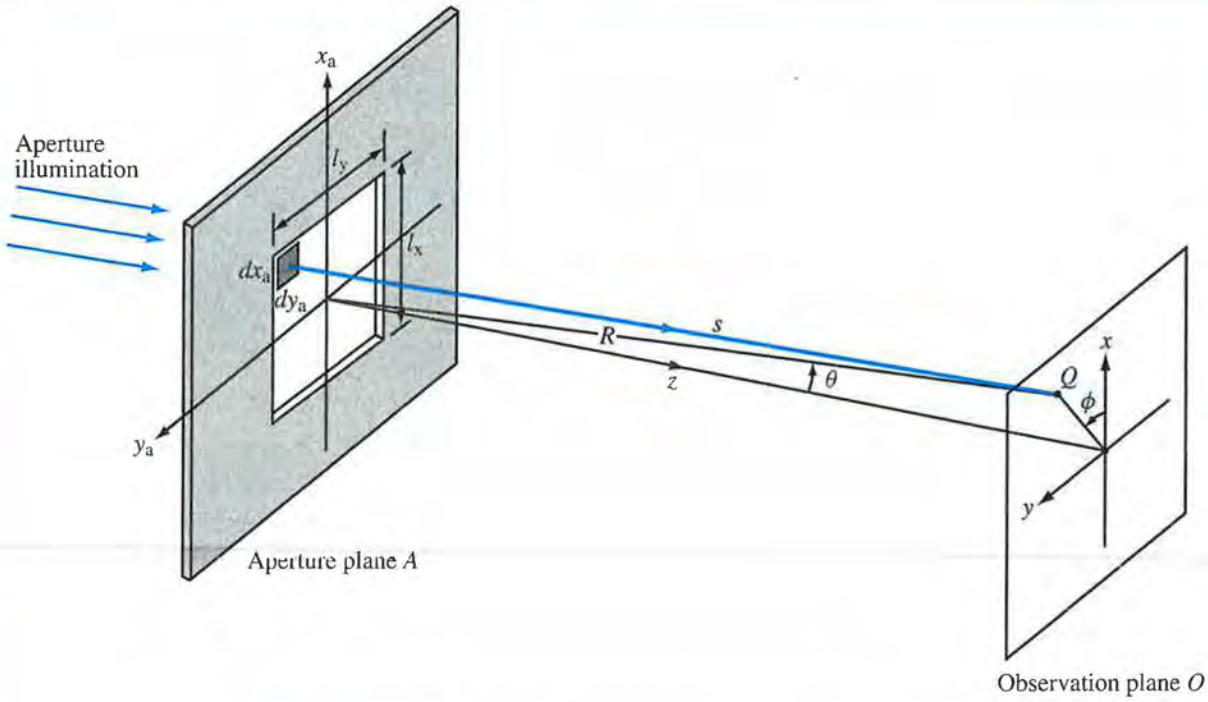


Figure 9-22: Radiation by an aperture in the x_a–y_a plane at $z = 0$.

$\widetilde{E}_a(x_a, y_a)$, and the power density of the radiated wave is given by

$$S(R, \theta, \phi) = \frac{|\widetilde{E}(R, \theta, \phi)|^2}{2\eta_0} = \frac{|\widetilde{h}(\theta, \phi)|^2}{2\eta_0 \lambda^2 R^2}. \quad (9.82)$$

9-8 Rectangular Aperture with Uniform Aperture Distribution

By way of illustrating the scalar diffraction technique, let us consider a rectangular aperture of height l_x and width l_y, both at least a few wavelengths long. The aperture is excited by a uniform field distribution given by

$$\widetilde{E}_a(x_a, y_a) = \begin{cases} E_0, & \text{for } -l_x/2 \le x_a \le l_x/2 \\ & \text{and } -l_y/2 \le y_a \le l_y/2, \\ 0, & \text{otherwise.} \end{cases} \quad (9.83)$$

To keep the mathematics simple, let us confine our examination to the radiation pattern at a fixed range R in the x–z plane, corresponding to $\phi = 0$. In this case, Eq. (9.81) simplifies to

$$\widetilde{h}(\theta) = \int_{y_a=-l_y/2}^{l_y/2} \int_{x_a=-l_x/2}^{l_x/2} E_0 \exp[jkx_a \sin\theta]\, dx_a\, dy_a. \quad (9.84)$$

INTEL-1014
U.S. Patent 7,151,430

In preparation for performing the integration in Eq. (9.84), we introduce the intermediate variable u defined as

$$u = k \sin\theta = \frac{2\pi \sin\theta}{\lambda}, \tag{9.85}$$

in which case Eq. (9.84) becomes

$$\begin{aligned}\widetilde{h}(\theta) &= E_0 \int_{-l_x/2}^{l_x/2} e^{jux_a}\, dx_a \cdot \int_{-l_y/2}^{l_y/2} dy_a \\ &= E_0 \left[\frac{e^{jul_x/2} - e^{-jul_x/2}}{ju}\right] \cdot l_y \\ &= \frac{2E_0 l_y}{u}\left[\frac{e^{jul_x/2} - e^{-jul_x/2}}{2j}\right] \\ &= \frac{2E_0 l_y}{u} \sin(ul_x/2).\end{aligned} \tag{9.86}$$

Upon replacing u with its defining expression, we have

$$\begin{aligned}\widetilde{h}(\theta) &= \frac{2E_0 l_y}{\left(\frac{2\pi}{\lambda}\sin\theta\right)} \sin(\pi l_x \sin\theta/\lambda) \\ &= E_0 l_x l_y \frac{\sin(\pi l_x \sin\theta/\lambda)}{\pi l_x \sin\theta/\lambda} \\ &= E_0 A_p \operatorname{sinc}(\pi l_x \sin\theta/\lambda),\end{aligned} \tag{9.87}$$

where $A_p = l_x l_y$ is the physical area of the aperture and where we have used the standard definition of the sinc function, which, for any argument t, is defined as

$$\operatorname{sinc} t = \frac{\sin t}{t}. \tag{9.88}$$

Using Eq. (9.82), we obtain the following expression for the power density of the radiated wave at the observation point:

$$S(R,\theta) = S_0 \operatorname{sinc}^2(\pi l_x \sin\theta/\lambda) \quad (x\text{–}z \text{ plane}), \tag{9.89}$$

where $S_0 = E_0^2 A_p^2/(2\eta_0 \lambda^2 R^2)$. The sinc function is at a maximum when its argument is equal to zero and its value is equal to unity. This occurs when $\theta = 0$. Thus, at a fixed range R, $S_{max} = S(\theta = 0) = S_0$. The normalized radiation intensity is then given by

$$\begin{aligned}F(\theta) &= \frac{S(R,\theta)}{S_{max}} \\ &= \operatorname{sinc}^2(\pi l_x \sin\theta/\lambda) \\ &= \operatorname{sinc}^2(\pi\gamma) \quad (x\text{–}z \text{ plane}),\end{aligned} \tag{9.90}$$

and it is plotted (on a decibel scale) in Fig. 9-23 as a function of the intermediate variable $\gamma = (l_x/\lambda)\sin\theta$. The pattern exhibits nulls at nonzero integer values of γ.

9-8.1 Beamwidth

The normalized radiation intensity $F(\theta)$ is symmetrical in the x–z plane, and its maximum is along the boresight direction ($\theta = 0$, in this case). Its half-power beamwidth $\beta_{xz} = \theta_2 - \theta_1$, where θ_1 and θ_2 are the values of θ at which $F(\theta, 0) = 0.5$ (or -3 dB on a decibel scale), as shown in Fig. 9-23. Since the pattern is symmetrical with respect to $\theta = 0$, $\theta_1 = -\theta_2$ and $\beta_{xz} = 2\theta_2$. The angle θ_2 can be obtained from a solution of

$$F(\theta_2) = \operatorname{sinc}^2(\pi l_x \sin\theta/\lambda) = 0.5. \tag{9.91}$$

From tabulated values of the sinc function, it is found that Eq. (9.91) yields the result

$$\frac{\pi l_x}{\lambda}\sin\theta_2 = 1.39, \tag{9.92}$$

or

$$\sin\theta_2 = 0.44\frac{\lambda}{l_x}. \tag{9.93}$$

Because $\lambda/l_x \ll 1$ (a fundamental condition of scalar diffraction theory is that the aperture dimensions be much

INTEL-1014
U.S. Patent 7,151,430

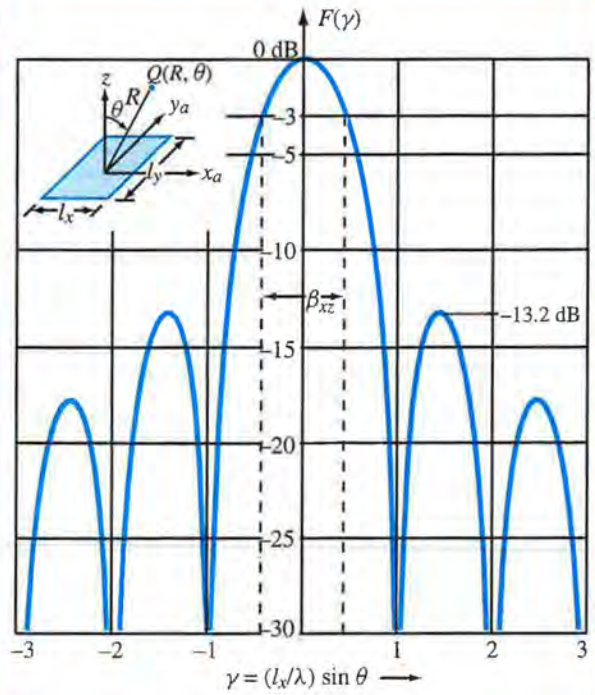


Figure 9-23: Normalized radiation pattern of a uniformly illuminated rectangular aperture in the x–z plane ($\phi = 0$).

larger than the wavelength λ), θ_2 is a small angle, in which case we can use the approximation $\sin\theta_2 \simeq \theta_2$. Hence,

$$\beta_{xz} = 2\theta_2 \simeq 2\sin\theta_2 = 0.88\frac{\lambda}{l_x} \quad \text{(rad)}. \qquad (9.94a)$$

A similar solution for the y–z plane ($\phi = \pi/2$) gives

$$\beta_{yz} = 0.88\frac{\lambda}{l_y} \quad \text{(rad)}. \qquad (9.94b)$$

It is worth noting that the uniform aperture distribution ($\widetilde{E}_a = E_0$ across the aperture) gives a far-field pattern with the narrowest possible beamwidth. The first sidelobe level is 13.2 dB below the peak value [see Fig. 9-23], which is equivalent to 4.8% of the peak value. If the intended application calls for a pattern with a lower sidelobe level (to avoid interference with signals from sources along directions outside the main beam of the antenna pattern), this can be accomplished by using a ***tapered aperture distribution***, one that is a maximum at the center of the aperture and decreases toward the edges. A tapered distribution provides a pattern with lower side lobes, but the main lobe becomes wider. The steeper the taper, the lower are the side lobes and the wider is the main lobe. In general, the beamwidth in a given plane, say the x–z plane, is given by

$$\beta_{xz} = k_x\frac{\lambda}{l_x}, \qquad (9.95)$$

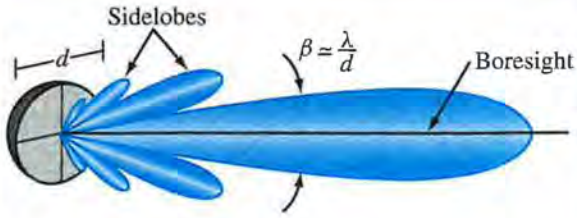
where k_x is a constant related to the steepness of the taper. For a uniform distribution with no taper, $k_x = 0.88$, and for a highly tapered distribution, $k_x \simeq 2$. In the typical case, $k_x \simeq 1$.

To illustrate the relationship between the antenna dimensions and the corresponding beam shape, we show in Fig. 9-24 the radiation patterns of a circular reflector and a cylindrical reflector. The circular reflector has a circularly symmetric pattern, whereas the pattern of the cylindrical reflector has a narrow beam in the azimuth plane corresponding to its long dimension and a wide beam in the elevation plane corresponding to its narrow dimension. For a circularly symmetric antenna pattern, the beamwidth β is related to the diameter d by the approximate relation $\beta \simeq \lambda/d$.

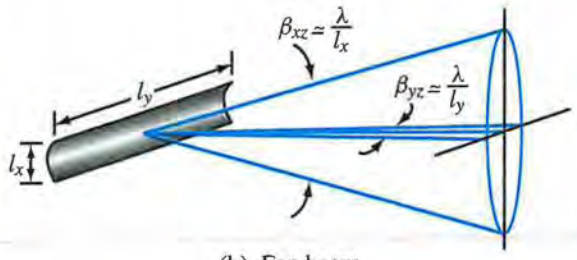
9-8.2 Directivity and Effective Area

In Section 9-2.3, we derived an approximate expression [Eq. (9.26)] for the antenna directivity D in terms of the half-power beamwidths β_{xz} and β_{yz} for antennas

INTEL-1014
U.S. Patent 7,151,430



(a) Pencil beam



(b) Fan beam

Figure 9-24: Radiation patterns of (a) a circular reflector and (b) a cylindrical reflector (side lobes not shown).

characterized by a single major lobe whose boresight is along the z-direction:

$$D \simeq \frac{4\pi}{\beta_{xz}\beta_{yz}} . \tag{9.96}$$

If we use the approximate relations $\beta_{xz} \simeq \lambda/l_x$ and $\beta_{yz} \simeq \lambda/l_y$, we have

$$D \simeq \frac{4\pi l_x l_y}{\lambda^2} = \frac{4\pi A_p}{\lambda^2} . \tag{9.97}$$

For any antenna, its directivity is related to its effective area A_e by Eq. (9.64):

$$D = \frac{4\pi A_e}{\lambda^2} . \tag{9.98}$$

Hence, *for aperture antennas, their effective apertures are approximately equal to their physical apertures;* that is, $A_e \simeq A_p$.

EXERCISE 9.11 Verify that Eq. (9.92) is a solution of Eq. (9.91) by calculating $\text{sinc}^2 t$ for $t = 1.39$.

EXERCISE 9.12 With its boresight direction along z, a square aperture was observed to have half-power beamwidths of 3° in both the x–z and y–z planes. Determine its directivity in decibels.

Ans. $D = 4{,}583.66 = 36.61$ dB.

EXERCISE 9.13 What condition must be satisfied in order to use scalar diffraction to compute the field radiated by an aperture antenna? Can we use it to compute the directional pattern of the eye's pupil ($d \cong 0.2$ cm) in the visible part of the spectrum ($\lambda = 0.35$ to 0.7 μm)? What would the beamwidth of the eye's directional pattern be at $\lambda = 0.5$ μm if we assume that the pupil is uniformly illuminated?

Ans. $\beta = 0.88\ \lambda/d = 2.2 \times 10^{-4}$ rad $= 0.76'$ (arc minute, with $60' = 1°$).

9-9 Antenna Arrays

AM broadcast services operate in the 535- to 1605-kHz band. The antennas they use are basically vertical dipoles mounted along tall towers. The antennas range in height from $\lambda/6$ to $5\lambda/8$, depending on the operating characteristics desired and other considerations. Their physical heights vary from 46 m (150 ft) to 274 m (900 ft); the wavelength at 1 MHz, approximately in the middle of the AM band, is 300 m. Because the field radiated by a single dipole is uniform in the horizontal plane (as discussed in Sections 9-1 and 9-3), it is necessary to use more than one antenna tower to direct the horizontal antenna pattern along directions of interest (such as a city)

INTEL-1014
U.S. Patent 7,151,430

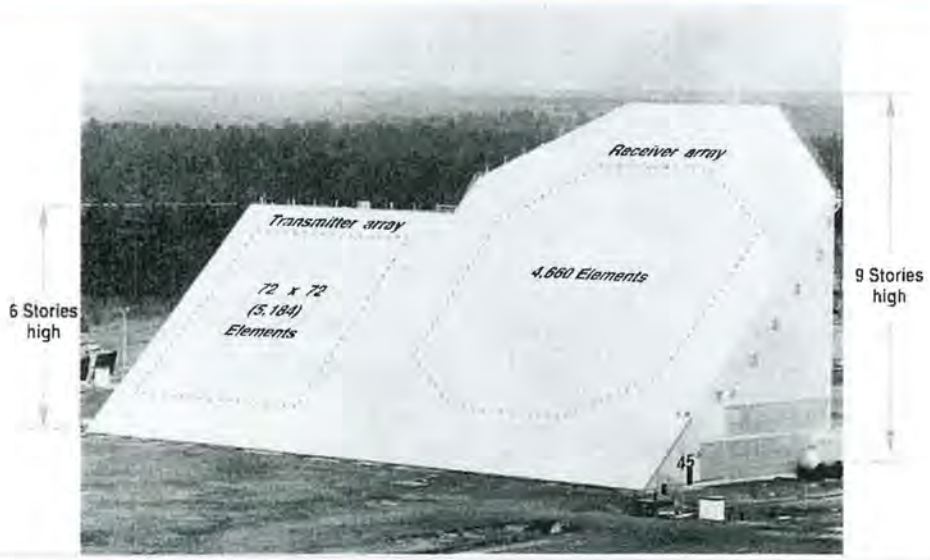


Figure 9-25: The AN/FPS-85 Phased Array Radar Facility in the Florida panhandle, near the city of Freeport. A several-mile no-fly zone surrounds the radar installation as a safety concern for electroexplosive devices, such as ejection seats and munitions, carried on military aircraft.

and to minimize it along directions of low population density or a direction corresponding to an area serviced by another station operating at the same frequency (to avoid undesirable interference effects). When two or more antennas are used together, the combination is called an ***antenna array***.

The AM broadcast antenna array is only one application example of antenna arrays; they are used extensively in numerous communication systems and radar applications as well. Antenna arrays provide the antenna designer the flexibility to obtain high directivity, narrow beams, low side lobes, steerable beams, and shaped antenna patterns. Figure 9-25 shows a photograph of a very large radar system consisting of a transmitter array composed of 5,184 individual dipole antenna elements and a receiver array composed of 4,660 elements. The radar system, part of the Space Surveillance Network operated by the U.S. Air Force, operates at 442 MHz and transmits a combined peak power of 30 MW!

Although an array need not consist of similar radiating elements, most arrays usually use identical elements, such as dipoles, slots, horn antennas, or parabolic dishes, excited by the same type of current or field distribution. The antenna elements comprising an array may be arranged in various configurations, but the most common are the linear one-dimensional configuration, wherein the elements are arranged along a straight line, and the two-dimensional lattice configuration, wherein the elements

INTEL-1014
U.S. Patent 7,151,430

form a rectangular grid. The desired shape of the far-field radiation pattern of the array can be synthesized by controlling the relative amplitudes of the array elements. Also, through the use of electronically controlled solid-state phase shifters, the beam direction of the antenna array can be steered electronically by controlling the relative phases of the array elements. This flexibility of the array antenna has led to numerous applications, including ***electronic steering*** and ***multiple-beam generation***.

The purpose of this and the next two sections is to introduce the reader to the basic principles of array theory and to the design techniques used in shaping the antenna pattern and steering the main lobe. The presentation will be confined to the one-dimensional linear array with equal spacing between adjacent elements.

A linear array of N identical radiators is arranged along the z-axis as shown in Fig. 9-26. The radiators are fed by a common oscillator through a branching network. In each branch, an attenuator (or amplifier) and phase shifter are inserted in series to control the amplitude and phase of the signal feeding the antenna element in that branch.

In the far-field region of any radiating element, the phasor electric-field intensity $\widetilde{E}_e(R, \theta, \phi)$ may be expressed as a product of two functions, the spherical propagation factor e^{-jkR}/R, which accounts for the dependence on the range R, and $\widetilde{f}_e(\theta, \phi)$, which accounts for the directional dependence of the element's electric field. Thus, for an isolated element, the radiated field is

$$\widetilde{E}_e(R, \theta, \phi) = \frac{e^{-jkR}}{R} \widetilde{f}_e(\theta, \phi), \qquad (9.99)$$

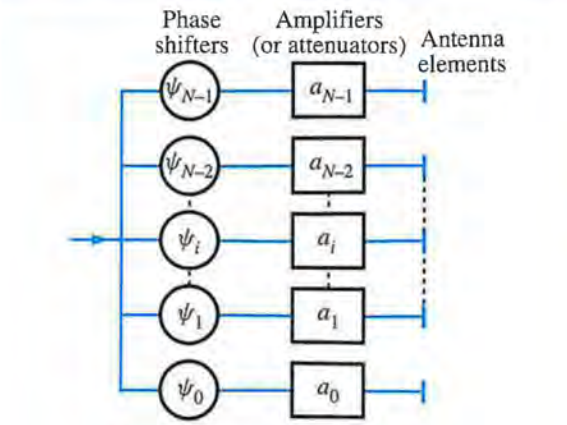
and the corresponding power density S_e is

$$S_e(R, \theta, \phi) = \frac{1}{2\eta_0} |\widetilde{E}_e(R, \theta, \phi)|^2 = \frac{1}{2\eta_0 R^2} |\widetilde{f}_e(\theta, \phi)|^2. \qquad (9.100)$$

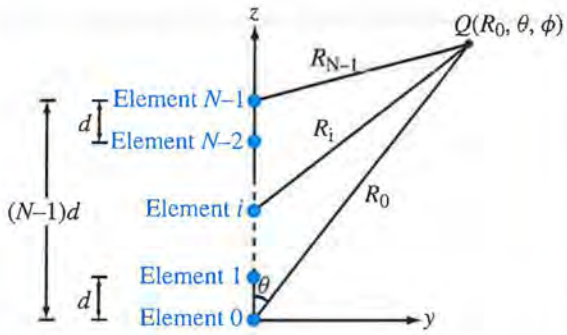
With regard to the elements in the array shown in Fig. 9-26(b), the far-zone field due to element i at range R_i from the observation point Q may then be written in the form

$$\widetilde{E}_i(R_i, \theta, \phi) = A_i \frac{e^{-jkR_i}}{R_i} \widetilde{f}_e(\theta, \phi), \qquad (9.101)$$

where $A_i = a_i e^{j\psi_i}$ is a ***complex feeding coefficient*** representing the amplitude a_i and phase ψ_i of the excitation



(a) Array elements with individual amplitude and phase control



(b) Array geometry relative to observation point

Figure 9-26: Linear-array configuration and geometry.

INTEL-1014
U.S. Patent 7,151,430

giving rise to $\widetilde{E}_i$, relative to a reference excitation. In practice, the excitation of one of the elements is used as reference. Note that R_i and A_i may be different for the different elements in the array, but $\widetilde{f}_e(\theta, \phi)$ is the same for all the elements since they are assumed to be identical and hence exhibit identical directional patterns.

The total field at the observation point $Q(R_0, \theta, \phi)$ is the sum of the fields due to the N elements:

$$\widetilde{E}(R_0, \theta, \phi) = \sum_{i=0}^{N-1} \widetilde{E}_i(R_i, \theta, \phi)$$

$$= \left[\sum_{i=0}^{N-1} A_i \frac{e^{-jkR_i}}{R_i}\right] \widetilde{f}_e(\theta, \phi), \quad (9.102)$$

where R_0 denotes the range of Q from the center of the coordinate system, chosen to be at the location of the zeroth element. To satisfy the far-field condition given by Eq. (9.79) for an array of length $l = (N-1)d$, where d is the interelement spacing, the range R_0 should be sufficiently large that

$$R_0 \geq \frac{2l^2}{\lambda} = \frac{2(N-1)^2 d^2}{\lambda}. \quad (9.103)$$

This condition allows us to ignore differences in the distances from Q to the individual elements as far as the magnitude of the radiated field is concerned. Thus, we can set $R_i = R_0$ in the denominator in Eq. (9.102) for all i. With regard to the phase part of the propagation factor, we can use the parallel-ray approximation given by

$$R_i \simeq R_0 - z_i \cos\theta = R_0 - id\cos\theta, \quad (9.104)$$

where $z_i = id$ is the distance between the ith element and the zeroth element [Fig. 9-27]. Employing these two approximations in Eq. (9.102) leads to

$$\widetilde{E}(R_0, \theta, \phi) = \widetilde{f}_e(\theta, \phi) \left(\frac{e^{-jkR_0}}{R_0}\right) \times \left[\sum_{i=0}^{N-1} A_i e^{jikd\cos\theta}\right], \quad (9.105)$$

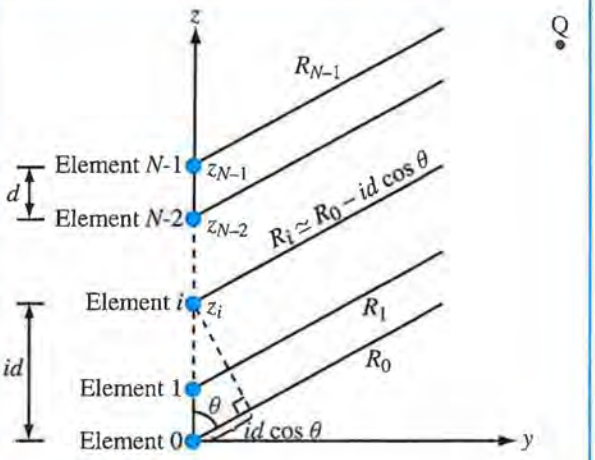


Figure 9-27: The rays between the elements and a faraway observation point are approximately parallel lines. Hence, the distance $R_i \simeq R_0 - id\cos\theta$.

and the corresponding array-antenna power density is given by

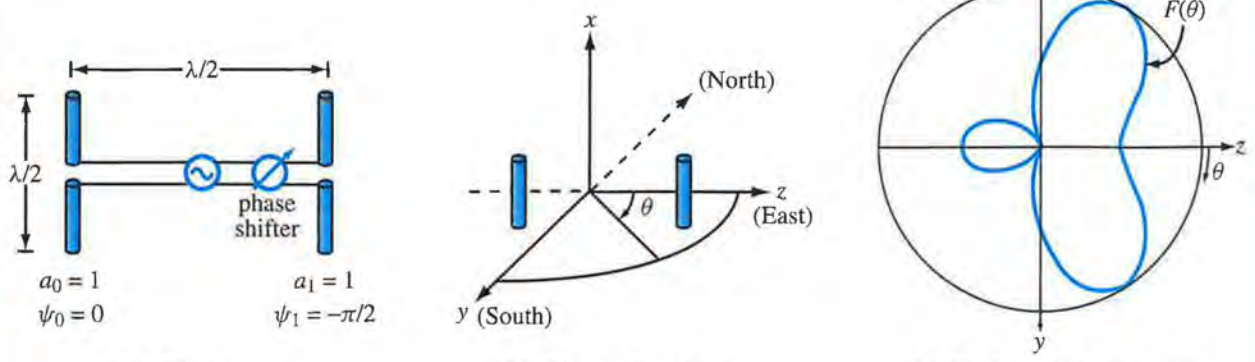
$$S(R_0, \theta, \phi) = \frac{1}{2\eta_0}|\widetilde{E}(R_0, \theta, \phi)|^2$$

$$= \frac{1}{2\eta_0 R_0^2}|\widetilde{f}_e(\theta, \phi)|^2 \left|\sum_{i=0}^{N-1} A_i e^{jikd\cos\theta}\right|^2$$

$$= S_e(R_0, \theta, \phi) \left|\sum_{i=0}^{N-1} A_i e^{jikd\cos\theta}\right|^2, \quad (9.106)$$

where use has been made of Eq. (9.100). This expression is a product of two factors. The first factor, $S_e(R_0, \theta, \phi)$, is the power density of the energy radiated by an individual element, and the second, usually called the ***array factor***, is a function of the positions of the individual elements and their feeding coefficients, but not a function of the specific type of radiators used. *The array factor represents the far-field radiation intensity of the*

INTEL-1014
U.S. Patent 7,151,430



(a) Dipole array (b) Observation plane (c) Horizontal-plane pattern

Figure 9-28: Two half-wave dipole array of Example 9-6.

N elements, had the elements been isotropic radiators. Denoting the array factor by

$$F_a(\theta) = \left| \sum_{i=0}^{N-1} A_i e^{jikd\cos\theta} \right|^2, \qquad (9.107)$$

the power density of the antenna array is then written as

$$S(R_0, \theta, \phi) = S_e(R_0, \theta, \phi)\, F_a(\theta). \qquad (9.108)$$

This equation is called the ***pattern multiplication principle***. It allows us to find the far-field power density of the antenna array by first computing the far-field power pattern with the array elements replaced with isotropic radiators, which yields the array factor $F_a(\theta)$, and then multiplying the result by $S_e(R_0, \theta, \phi)$, the power density for a single element (which should be the same for all the elements).

The feeding coefficient A_i is, in general, a complex amplitude consisting of an amplitude factor a_i and a phase factor ψ_i:

$$A_i = a_i e^{j\psi_i}. \qquad (9.109)$$

Insertion of Eq. (9.109) into Eq. (9.107) leads to

$$F_a(\theta) = \left| \sum_{i=0}^{N-1} a_i e^{j\psi_i} e^{jikd\cos\theta} \right|^2. \qquad (9.110)$$

The array factor is governed by two input functions: the ***array amplitude distribution*** given by the a_i's and the ***array phase distribution*** given by the ψ_i's. The amplitude distribution serves to control the shape of the array radiation pattern, while the phase distribution can be used to steer its direction.

Example 9-6 Array of Two Vertical Dipoles

An AM radio station uses two vertically oriented half-wave dipoles separated by a distance of $\lambda/2$, as shown in Fig. 9-28(a). The vector from the location of the first dipole to the location of the second dipole points toward the east. The two dipoles are fed with equal-amplitude excitations, and the dipole farther east is excited with a phase shift of $-\pi/2$ relative to the other one. Find and plot the antenna pattern of the antenna array in the horizontal plane.

INTEL-1014
U.S. Patent 7,151,430

Solution: The array factor given by Eq. (9.110) was derived for radiators arranged along the z-axis. To keep the coordinate system the same, we choose the easterly direction to be the z-axis as shown in Fig. 9-28(b), and we place the first dipole at $z = -\lambda/4$ and the second at $z = \lambda/4$. A half-wave dipole radiates uniformly in the plane perpendicular to its axis, which in this case is the horizontal plane. Hence, $S_e = S_0$ for all angles θ in Fig. 9-28(b), where S_0 is the maximum value of the power density radiated by each dipole individually. Consequently, the power density radiated by the two-dipole array is

$$S(R, \theta) = S_0 F_a(\theta).$$

For two elements separated by $d = \lambda/2$ and excited with equal amplitudes ($a_0 = a_1 = 1$) and with phase angles $\psi_0 = 0$ and $\psi_1 = -\pi/2$, Eq. (9.110) gives

$$\begin{aligned} F_a(\theta) &= \left| \sum_{i=0}^{1} a_i e^{j\psi_i} e^{jikd\cos\theta} \right|^2 \\ &= |1 + e^{-j\pi/2} e^{j(2\pi/\lambda)(\lambda/2)\cos\theta}|^2 \\ &= \left|1 + e^{j(\pi\cos\theta - \pi/2)}\right|^2. \end{aligned}$$

A function of the form $|1 + e^{jx}|^2$ can be evaluated by factoring out $e^{jx/2}$ from both terms:

$$\begin{aligned} |1 + e^{jx}|^2 &= |e^{jx/2}(e^{-jx/2} + e^{jx/2})|^2 \\ &= |e^{jx/2}|^2 \, |e^{-jx/2} + e^{jx/2}|^2 \\ &= |e^{jx/2}|^2 \left| 2\frac{[e^{-jx/2} + e^{jx/2}]}{2} \right|^2. \end{aligned}$$

The absolute value of $e^{jx/2}$ is equal to 1, and we recognize the function inside the square bracket as $\cos(x/2)$. Hence,

$$|1 + e^{jx}|^2 = 4\cos^2\left(\frac{x}{2}\right).$$

Applying this result to the expression for $F_a(\theta)$, we have

$$F_a(\theta) = 4\cos^2\left(\frac{\pi}{2}\cos\theta - \frac{\pi}{4}\right).$$

The power density radiated by the array is then

$$S(R, \theta) = S_0 F_a(\theta) = 4S_0 \cos^2\left(\frac{\pi}{2}\cos\theta - \frac{\pi}{4}\right).$$

This function has a maximum value $S_{max} = 4S_0$, and it occurs when the argument of the cosine function is equal to zero. Thus,

$$\frac{\pi}{2}\cos\theta - \frac{\pi}{4} = 0,$$

which leads to the solution: $\theta = 60°$. Upon normalizing $S(R, \theta)$ by its maximum value, we obtain the normalized radiation intensity given by

$$F(\theta) = \frac{S(R, \theta)}{S_{max}} = \cos^2\left(\frac{\pi}{2}\cos\theta - \frac{\pi}{4}\right).$$

The pattern of $F(\theta)$ is shown in Fig. 9-28(c). ■

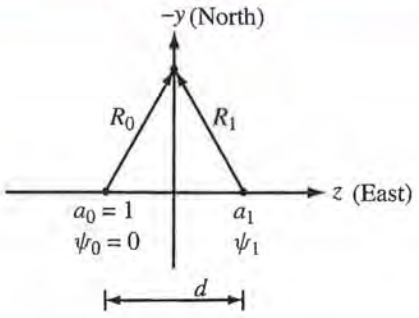
Example 9-7 Pattern Synthesis

In Example 9-6, we were given the array parameters a_0, a_1, ψ_0, ψ_1, and d, and we were then asked to determine the pattern of the two-element dipole array. We will now consider the reverse process; we will be given specifications on the desired pattern, and we are then asked to specify the array parameters to meet those specifications.

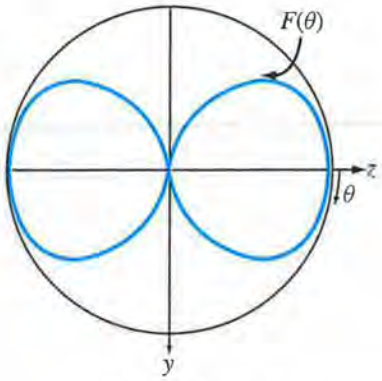
Given two vertical dipoles, as depicted in Fig. 9-28(b), specify the array parameters such that the array exhibits maximum radiation toward the east and no radiation toward the north or south.

Solution: From Example 9-6, we established that because each dipole radiates equally along all directions in the y–z plane, the radiation pattern of the two-dipole array in that plane is governed solely by the array factor $F_a(\theta)$. The shape of the pattern of the array factor depends on three parameters: the amplitude ratio a_1/a_0, the phase difference $\psi_1 - \psi_0$, and the spacing d

INTEL-1014
U.S. Patent 7,151,430



(a) Array arrangement



(b) Array pattern

Figure 9-29: (a) Two vertical dipoles separated by a distance d along the z-axis; (b) normalized array pattern in the y–z plane for $a_0 = a_1 = 1$, $\psi_1 = \psi_0 = -\pi$, and $d = \lambda/2$.

[Fig. 9-29(a)]. For convenience, we choose $a_0 = 1$ and $\psi_0 = 0$. Accordingly, Eq. (9.107) gives

$$F_a(\theta) = \left| \sum_{i=0}^{1} a_i e^{j\psi_i} e^{jikd\cos\theta} \right|^2$$
$$= |1 + a_1 e^{j\psi_1} e^{j(2\pi d/\lambda)\cos\theta}|^2.$$

Let us now consider the given specification requiring that F_a be equal to zero when $\theta = 90°$ (north and south directions in Fig. 9-29(a)). For any observation point on the y-axis, the ranges R_0 and R_1 shown in Fig. 9-29(a) are equal, which means that the propagation phases associated with the time travel of the waves radiated by the two dipoles to that point are identical. Hence, to satisfy the stated condition, we need to choose $a_1 = a_0$ and $\psi_1 = \pm\pi$. With these choices, the signals radiated by the two dipoles will have equal amplitudes and opposite phases, thereby interfering destructively. This conclusion can be ascertained by evaluating the array factor at $\theta = 90°$, with $a_0 = a_1 = 1$ and $\psi_1 = \pm\pi$:

$$F_a(\theta = 90°) = |1 + 1e^{\pm j\pi}|^2 = |1 - 1| = 0.$$

The two values of ψ_1, π and $-\pi$, lead to the same solution for the spacing d when we consider the specification that the array radiation pattern should have a maximum toward the east, corresponding to $\theta = 0°$. Let us choose $\psi_1 = -\pi$ and examine the array factor at $\theta = 0°$:

$$F_a(\theta = 0) = |1 + e^{-j\pi} e^{j2\pi d/\lambda}|^2$$
$$= |1 + e^{j(-\pi + 2\pi d/\lambda)}|^2.$$

For $F_a(\theta = 0)$ to be a maximum, we require the phase angle of the second term to be zero or a multiple of 2π:

$$-\pi + \frac{2\pi d}{\lambda} = 2n\pi,$$

or

$$d = (2n+1)\frac{\lambda}{2}, \qquad n = 0, 1, 2, \ldots$$

In summary, the two-dipole array will meet the given specifications if $a_0 = a_1$, $\psi_1 - \psi_0 = -\pi$, and $d = (2n+1)\lambda/2$.

INTEL-1014
U.S. Patent 7,151,430

For $d = \lambda/2$, the array factor at any angle θ is given by

$$\begin{aligned} F_a(\theta) &= |1 + e^{-j\pi} e^{j\pi\cos\theta}|^2 \\ &= |1 - e^{j\pi\cos\theta}|^2 \\ &= \left| 2je^{-j(\pi/2)\cos\theta} \left[\frac{e^{j(\pi/2)\cos\theta} - e^{-j(\pi/2)\cos\theta}}{2j} \right] \right|^2 \\ &= 4\sin^2\left(\frac{\pi}{2}\cos\theta\right). \end{aligned}$$

The array factor has a maximum value of 4, which is the maximum level attainable from a two-element array with unit amplitudes. The directions along which $F_a(\theta)$ is a maximum are those corresponding to $\theta = 0$ (east) and $\theta = 180°$ (west), as shown in Fig. 9-29(b). ■

EXERCISE 9.14 Derive an expression for the array factor of a two-element array excited in phase with $a_0 = 1$ and $a_1 = 3$. The elements are positioned along the z-axis and are separated by $\lambda/2$.

Ans. $F_a(\theta) = [10 + 6\cos(\pi\cos\theta)]$.

EXERCISE 9.15 An equally spaced N-element array arranged along the z-axis is fed with equal amplitudes and phases; that is, $A_i = 1$ for $i = 0, 1, \ldots, N-1$. What is the magnitude of the array factor in the broadside direction?

Ans. $F_a(\theta = 90°) = N^2$.

9-10 N-Element Array with Uniform Phase Distribution

We now consider an array of N elements with equal spacing d and equal-phase excitations; that is, $\psi_i = \psi_0$ for $i = 1, 2, \ldots, N-1$. Such an array of in-phase elements is sometimes referred to as a ***broadside array*** because the main beam of the radiation pattern of its array factor is always in the direction broadside to the array axis. From Eq. (9.110), its array factor is given by

$$\begin{aligned} F_a(\theta) &= \left| e^{j\psi_0} \sum_{i=0}^{N-1} a_i e^{jikd\cos\theta} \right|^2 \\ &= |e^{j\psi_0}|^2 \left| \sum_{i=0}^{N-1} a_i e^{jikd\cos\theta} \right|^2 \\ &= \left| \sum_{i=0}^{N-1} a_i e^{jikd\cos\theta} \right|^2. \end{aligned} \tag{9.111}$$

The phase difference between the fields radiated by adjacent elements is

$$\gamma = kd\cos\theta = \frac{2\pi d}{\lambda}\cos\theta. \tag{9.112}$$

In terms of γ, Eq. (9.111) takes the compact form

$$F_a(\gamma) = \left| \sum_{i=0}^{N-1} a_i e^{ji\gamma} \right|^2 \quad \text{(uniform phase)}. \tag{9.113}$$

For a uniform amplitude distribution with $a_i = 1$ for $i = 0, 1, \ldots, N-1$, Eq. (9.113) becomes

$$F_a(\gamma) = |1 + e^{j\gamma} + e^{j2\gamma} + \cdots + e^{j(N-1)\gamma}|^2. \tag{9.114}$$

This geometric series can be rewritten in a more compact form by applying the following procedure. First, we define

$$F_a(\gamma) = |f_a(\gamma)|^2, \tag{9.115}$$

with

$$f_a(\gamma) = [1 + e^{j\gamma} + e^{j2\gamma} + \cdots + e^{j(N-1)\gamma}]. \tag{9.116}$$

Next, we multiply $f_a(\gamma)$ by $e^{j\gamma}$ to obtain

$$f_a(\gamma)\, e^{j\gamma} = (e^{j\gamma} + e^{j2\gamma} + \cdots + e^{jN\gamma}). \tag{9.117}$$

INTEL-1014
U.S. Patent 7,151,430

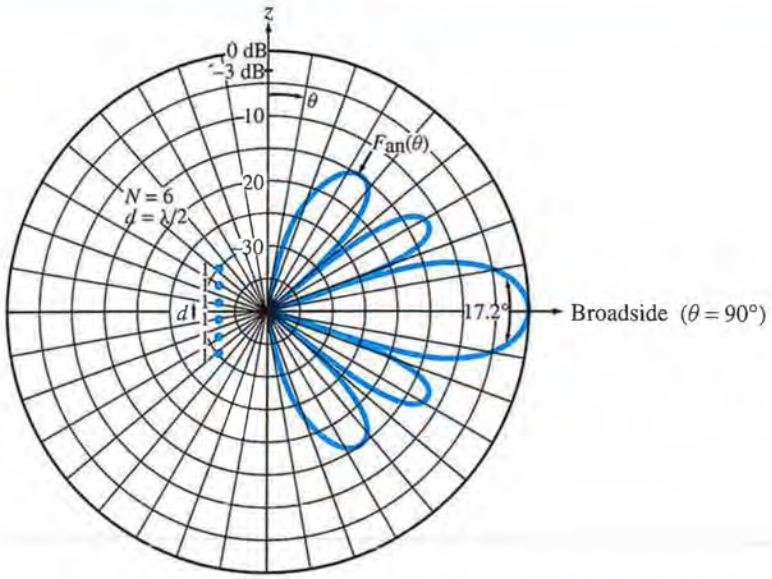


Figure 9-30: Normalized array pattern of a uniformly excited six-element array with interelement spacing $d = \lambda/2$.

Subtracting Eq. (9.117) from Eq. (9.116) gives

$$f_a(\gamma)\,(1 - e^{j\gamma}) = 1 - e^{jN\gamma}, \tag{9.118}$$

which, in turn, gives

$$\begin{aligned} f_a(\gamma) &= \frac{1 - e^{jN\gamma}}{1 - e^{j\gamma}} \\ &= \frac{e^{jN\gamma/2}}{e^{j\gamma/2}} \frac{(e^{-jN\gamma/2} - e^{jN\gamma/2})}{(e^{-j\gamma/2} - e^{j\gamma/2})} \\ &= e^{j(N-1)\gamma/2} \frac{\sin(N\gamma/2)}{\sin(\gamma/2)}. \end{aligned} \tag{9.119}$$

After multiplying $f_a(\gamma)$ by its complex conjugate, we obtain the result:

$$F_a(\gamma) = \frac{\sin^2(N\gamma/2)}{\sin^2(\gamma/2)} \quad \text{(uniform amplitude and phase).} \tag{9.120}$$

The maximum value of $F_a(\gamma)$ can be shown to occur at $\gamma = 0$ (or $\theta = \pi/2$) and is equal to N^2, which is easy to verify by evaluating Eq. (9.114) for $\gamma = 0$. Hence, the normalized array factor is given by

$$\begin{aligned} F_{an}(\gamma) = \frac{F_a(\gamma)}{F_{a,max}} &= \frac{\sin^2(N\gamma/2)}{N^2 \sin^2(\gamma/2)} \\ &= \frac{\sin^2\left[\dfrac{N\pi d}{\lambda}\cos\theta\right]}{N^2 \sin^2\left[\dfrac{\pi d}{\lambda}\cos\theta\right]}. \end{aligned} \tag{9.121}$$

A polar plot of $F_{an}(\theta)$ with $N = 6$ is shown in Fig. 9-30 for $d = \lambda/2$. The reader is reminded that this is a plot of the radiation pattern of the array factor alone; the pattern for the antenna array is equal to the product of this pattern and that of a single element, as discussed earlier in connection with the pattern multiplication principle.

INTEL-1014
U.S. Patent 7,151,430

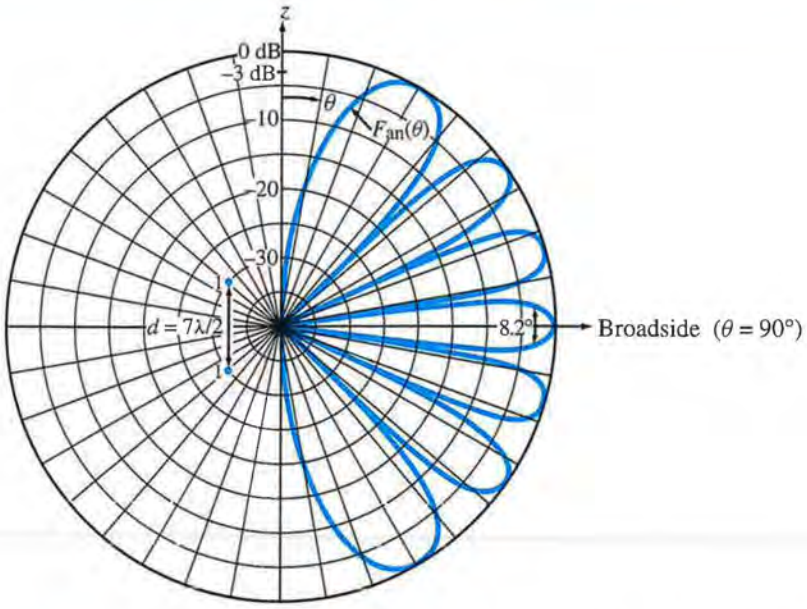


Figure 9-31: Normalized array pattern of a two-element array with spacing $d = 7\lambda/2$.

Example 9-8 Multiple-Beam Array

Obtain an expression for the array factor of a two-element array with equal excitation and a separation $d = 7\lambda/2$, and then plot the array pattern.

Solution: The array factor for a two-element array ($N = 2$) with equal excitation ($a_0 = a_1 = 1$) is given by

$$\begin{aligned} F_a(\gamma) &= \left| \sum_{i=0}^{1} a_i e^{ji\gamma} \right|^2 \\ &= |1 + e^{j\gamma}|^2, \\ &= |e^{j\gamma/2}(e^{-j\gamma/2} + e^{j\gamma/2})|^2 \\ &= |e^{j\gamma/2}|^2 \, |e^{-j\gamma/2} + e^{j\gamma/2}|^2 \\ &= 4\cos^2(\gamma/2), \end{aligned}$$

where $\gamma = (2\pi d/\lambda)\cos\theta$. The normalized array pattern, shown in Fig. 9-31, consists of seven beams, all with the same peak value, but not the same angular width. The number of beams in the angular range between $\theta = 0$ and $\theta = \pi$ is equal to the separation between the array elements, d, measured in units of $\lambda/2$. ■

9-11 Electronic Scanning of Arrays

The discussion in the preceding section was concerned with uniform-phase arrays, for which the phases of the feeding coefficients, ψ_0 to ψ_{N-1}, are all equal. In this section, we examine the use of phase delay between adjacent elements as a tool for ***electronically steering*** the direction of the array-antenna beam from broadside at $\theta = 90°$ to any desired angle θ_0. In addition to

INTEL-1014
U.S. Patent 7,151,430

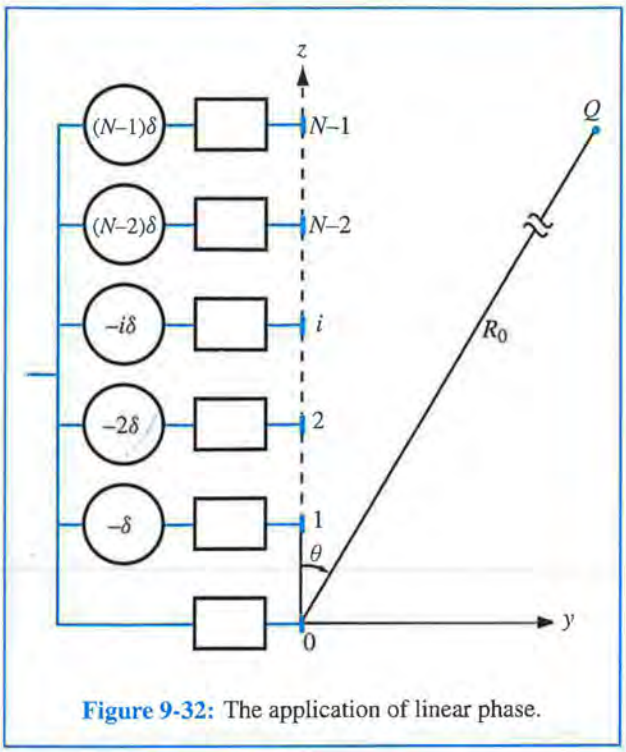


Figure 9-32: The application of linear phase.

eliminating the need to mechanically steer an antenna to change its beam's direction, electronic steering allows beam scanning at very fast rates.

Electronic steering is achieved by applying linearly progressive phase delays from element to element across the array, as shown in Fig. 9-32. Relative to the phase of the zeroth element, the phase of the ith element is

$$\psi_i = -i\delta, \tag{9.122}$$

where δ is the ***incremental phase delay*** between adjacent elements. Use of Eq. (9.122) in Eq. (9.110) leads to

$$F_a(\theta) = \left| \sum_{i=0}^{N-1} a_i e^{-ji\delta} e^{jikd\cos\theta} \right|^2$$

$$= \left| \sum_{i=0}^{N-1} a_i e^{ji(kd\cos\theta - \delta)} \right|^2$$

$$= \left| \sum_{i=0}^{N-1} a_i e^{ji\gamma'} \right|^2 \triangleq F_a(\gamma'), \tag{9.123}$$

where

$$\gamma' = kd\cos\theta - \delta. \tag{9.124}$$

For reasons that will become clear later, let us define the phase shift δ in terms of an angle θ_0, which we shall call the ***scan angle***, as follows:

$$\delta = kd\cos\theta_0. \tag{9.125}$$

In this case, γ' becomes

$$\gamma' = kd(\cos\theta - \cos\theta_0). \tag{9.126}$$

The array factor given by Eq. (9.123) has the same functional form as the array factor developed earlier for the case of the uniform-phase array [see Eq. (9.113)], except that γ is replaced with γ'. Hence, *for any amplitude distribution across the array, the array factor of an array excited by a linear-phase distribution may be obtained from the expression developed for the array assuming a uniform-phase distribution simply by replacing γ with γ'.* For an amplitude distribution symmetrical with respect to the array center, the array factor $F_a(\gamma')$ is maximum when its argument $\gamma' = 0$. When the phase is uniform ($\delta = 0$), this condition corresponds to the direction $\theta = 90°$, which is why the uniform-phase case is called a broadside array. According to Eq. (9.126), in the more general case of a linearly phased array, $\gamma' = 0$ corresponds to $\theta = \theta_0$. Thus, by applying linear phase across the array, the array pattern is shifted along the $\cos\theta$-axis by an amount $\cos\theta_0$, and the direction of maximum radiation is ***steered*** from the broadside direction ($\theta = 90°$) to the direction $\theta = \theta_0$. To steer the beam all the way to the ***end-fire*** direction ($\theta = 0$), the incremental phase shift δ should be equal to kd radians.

INTEL-1014
U.S. Patent 7,151,430

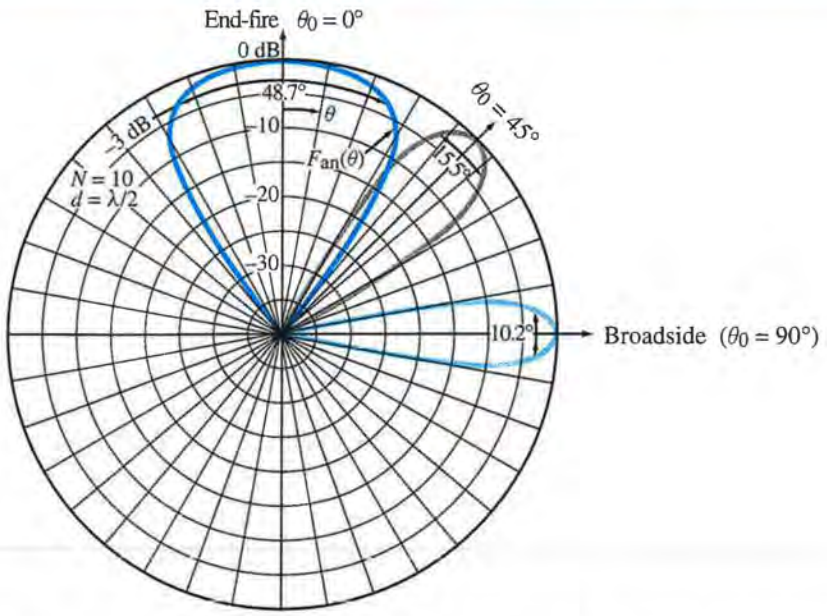


Figure 9-33: Normalized array pattern of a 10-element array with $\lambda/2$ spacing between adjacent elements. All elements are excited with equal amplitude. Through the application of linear phase across the array, the main beam can be steered from the broadside direction ($\theta_0 = 90°$) to any scan angle θ_0. Equiphase excitation corresponds to $\theta_0 = 90°$.

9-11.1 Uniform-Amplitude Excitation

To illustrate the process with an example, let us consider the case of the N-element array excited by a uniform-amplitude distribution. Its normalized array factor is given by Eq. (9.121). Upon replacing γ with γ', we have

$$F_{an}(\gamma') = \frac{\sin^2(N\gamma'/2)}{N^2 \sin^2(\gamma'/2)}, \tag{9.127}$$

with γ' defined by Eq. (9.126). The expression given by Eq. (9.127) now characterizes the array factor of an array excited with equal amplitudes ($a_i = 1$ for $i = 0, 1, \ldots, N-1$) and with incremental phases ($\psi_i = -i\delta$).

For $N = 10$ and $d = \lambda/2$, plots of the main lobe of $F_{an}(\theta)$ are shown in Fig. 9-33 for $\theta_0 = 0°$, 45°, and 90°. We note that the half-power beamwidth increases as the array beam is steered from broadside to end fire.

9-11.2 Array Feeding

According to the foregoing discussion, to steer the antenna beam to an angle θ_0, two conditions must be satisfied: (1) the phase distribution must be linear across the array, and (2) the magnitude of the incremental phase delay δ must satisfy Eq. (9.125). The combination of these two conditions provides the necessary translation of the phase front from $\theta = 90°$ (broadside) to $\theta = \theta_0$. This can be accomplished

INTEL-1014
U.S. Patent 7,151,430

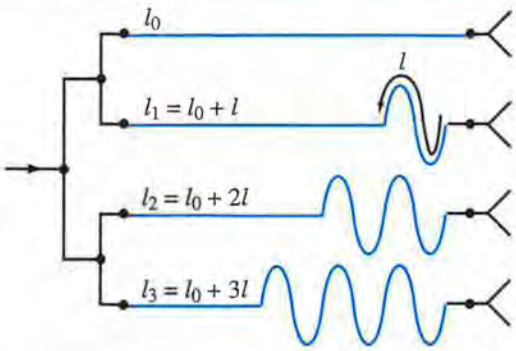


Figure 9-34: An example of a feeding arrangement for frequency-scanned arrays.

by controlling the excitation of each radiating element individually through the use of electronically controlled phase shifters. Alternatively, a technique known as ***frequency scanning*** can be used to provide control of the phases of all the elements simultaneously. Figure 9-34 shows an example of a simple feeding arrangement employed in frequency scanning arrays. A common feed point is connected to the radiating elements through transmission lines of varying lengths. Relative to the zeroth element, the path between the common feed point and a radiating element is longer by l for the first element, by $2l$ for the second, and by $3l$ for the third. Thus, the path length for the ith element is

$$l_i = il + l_0, \tag{9.128}$$

where l_0 is the path length of the zeroth element. Wave propagation at a frequency f on a transmission line of length l_i is characterized by a phase factor $e^{-j\beta l_i}$, where $\beta = 2\pi f/u_p$ is the phase constant of the line and u_p is its propagation velocity. Hence, the *incremental* phase delay of the ith element, relative to the phase of the zeroth element, is

$$\psi_i(f) = -\beta(l_i - l_0) = -\frac{2\pi}{u_p} f(l_i - l_0)$$
$$= -\frac{2\pi i}{u_p} fl. \tag{9.129}$$

Suppose that at a given reference frequency f_0 we choose the incremental length l such that

$$l = \frac{n_0 u_p}{f_0}, \tag{9.130}$$

where n_0 is a *specific* positive integer. In this case, the phase delay $\psi_1(f_0)$ becomes

$$\psi_1(f_0) = -2\pi\left(\frac{f_0 l}{u_p}\right) = -2n_0\pi \tag{9.131}$$

and, similarly, $\psi_2(f_0) = -4n_0\pi$ and $\psi_3(f_0) = -6n_0\pi$. That is, at f_0 all the elements will have equal phase (within multiples of 2π) and the array radiates in the broadside direction. If f is changed to $f_0 + \Delta f$, the new phase shift of the first element relative to the zeroth element is

$$\psi_1(f_0 + \Delta f) = -\frac{2\pi}{u_p}(f_0 + \Delta f)l$$
$$= -\frac{2\pi f_0 l}{u_p} - \left(\frac{2\pi l}{u_p}\right)\Delta f$$
$$= -2n_0\pi - 2n_0\pi\left(\frac{\Delta f}{f_0}\right)$$
$$= -2n_0\pi - \delta, \tag{9.132}$$

where use was made of Eq. (9.130) and δ is defined as

$$\delta = 2n_0\pi\left(\frac{\Delta f}{f_0}\right). \tag{9.133}$$

INTEL-1014
U.S. Patent 7,151,430

Similarly, $\psi_2(f_0+\Delta f) = 2\psi_1$ and $\psi_3(f_0+\Delta f) = 3\psi_1$. Ignoring the factor of 2π and its multiples (since they exercise no influence on the relative phases of the radiated fields), we see that the incremental phase shifts are directly proportional to the fractional frequency deviation $(\Delta f/f_0)$. Thus, in an array with N elements, controlling Δf provides a direct control of δ, which in turn controls the scan angle θ_0 according to Eq. (9.125). Equating Eq. (9.125) to Eq. (9.133) and then solving for $\cos\theta_0$ leads to

$$\cos\theta_0 = \frac{2n_0\pi}{kd}\left(\frac{\Delta f}{f_0}\right). \tag{9.134}$$

As f is changed from f_0 to $f_0 + \Delta f$, $k = 2\pi/\lambda = 2\pi f/c$ also changes with frequency. However, if $\Delta f/f_0$ is small, we may treat k as a constant equal to $2\pi f_0/c$; the error in $\cos\theta_0$ resulting from the use of this approximation in Eq. (9.134) is on the order of $\Delta f/f_0$.

Example 9-9 Electronic Steering

Design a steerable six-element array with the following specifications:

1. All elements are excited with equal amplitudes.
2. At $f_0 = 10$ GHz, the array radiates in the broadside direction, and the interelement spacing $d = \lambda_0/2$, where $\lambda_0 = c/f_0 = 3$ cm.
3. The array pattern is to be electronically steerable in the elevation plane over the angular range extending between $\theta_0 = 30°$ and $\theta_0 = 150°$.
4. The antenna array is fed by a voltage-controlled oscillator whose frequency can be varied over the range from 9.5 to 10.5 GHz.
5. The array uses a feeding arrangement of the type shown in Fig. 9-34, and the transmission lines have a phase velocity $u_p = 0.8c$.

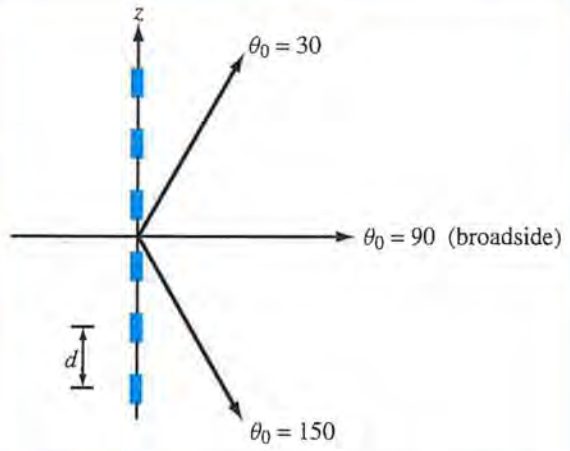


Figure 9-35: Steerable six-element array (Example 9-9).

Solution: The array is to be steerable from $\theta_0 = 30°$ to $\theta_0 = 150°$ (Fig. 9-35). For $\theta_0 = 30°$ and $kd = (2\pi/\lambda_0)(\lambda_0/2) = \pi$, Eq. (9.134) gives

$$\frac{1}{2} = 2n_0\left(\frac{\Delta f}{f_0}\right). \tag{9.135}$$

We are given that $f_0 = 10$ GHz and the oscillator frequency can be varied between $(f_0 - 0.5$ GHz) and $(f_0 + 0.5$ GHz). Thus, $\Delta f_{max} = 0.5$ GHz. To satisfy Eq. (9.135), we need to choose n_0 such that Δf is as close as possible to, but not larger than, Δf_{max}. Solving Eq. (9.135) for n_0 with $\Delta f = \Delta f_{max}$ gives

$$n_0 = \frac{f_0}{4\,\Delta f_{max}} = \frac{10\text{ GHz}}{4 \times 0.5\text{ GHz}} = 5.$$

Since n_0 is an integer, we do not need to modify its value; otherwise, we would have had to round it upward to the next whole-integer value.

Application of Eq. (9.130) specifies the magnitude of the incremental length l:

$$l = \frac{n_0 u_p}{f_0} = \frac{5 \times 0.8 \times 3 \times 10^8}{10^{10}} = 0.12\text{ m} = 12\text{ cm}.$$

INTEL-1014
U.S. Patent 7,151,430

In summary, with $N = 6$ and $kd = \pi$, Eq. (9.127) gives the following expression for the normalized array pattern:

$$F_{an}(\gamma') = \frac{\sin^2(3\gamma')}{36\sin^2(\gamma'/2)},$$

where, according to Eq. (9.126),

$$\gamma' = kd(\cos\theta - \cos\theta_0) = \pi(\cos\theta - \cos\theta_0),$$

and, from Eq. (9.134),

$$\cos\theta_0 = \frac{2n_0\pi}{kd}\left(\frac{\Delta f}{f_0}\right) = 10\left(\frac{f - 10\text{ GHz}}{10\text{ GHz}}\right). \quad (9.136)$$

The shape of the array pattern is similar to that shown in Fig. 9-30, and its main-beam direction is along $\theta = \theta_0$. For $f = f_0 = 10$ GHz, $\theta_0 = 90°$ (broadside direction); for $f = 10.5$ GHz, $\theta_0 = 30°$; and for $f = 9.5$ GHz, $\theta_0 = 150°$. For any other value of θ_0 between 30° and 150°, Eq. (9.136) provides the means for calculating the required value of the oscillator frequency f. ■

REVIEW QUESTIONS

Q9.13 Why are antenna arrays useful? Give examples of typical applications.

Q9.14 Explain how the pattern multiplication principle is used to compute the radiation pattern of an antenna array.

Q9.15 For a linear array, what roles do the array amplitudes and phases play?

Q9.16 Explain how electronic beam steering is accomplished.

Q9.17 Why is frequency scanning an attractive technique for steering the beam of an antenna array?

CHAPTER HIGHLIGHTS

- An antenna is a transducer between a guided wave propagating on a transmission line and an EM wave propagating in an unbounded medium, or vice versa.
- Except for some solid-state antennas composed of non-linear semiconductors or ferrite materials, antennas are reciprocal devices; they exhibit the same radiation patterns for transmission as for reception.
- In the far-field region of an antenna, the radiated energy is approximately a plane wave.
- The electric field radiated by current antennas, such as wires, is equal to the sum of the electric fields radiated by all the Hertzian dipoles making up the antenna.
- The radiation resistance R_{rad} of a half-wave dipole is 73 Ω, which can be easily matched to a transmission line.
- The directional properties of an antenna are described by its radiation pattern, directivity, pattern solid angle, and half-power beamwidth.
- The Friis transmission formula relates the power received by an antenna due to that transmitted by another antenna at a specified distance away.
- The far-zone electric field radiated by a large aperture (measured in wavelengths) is related to the field distribution across the aperture by Kirchhoff's scalar diffraction theory. A uniform aperture distribution produces a far-field pattern with the narrowest possible beamwidth.
- By controlling the amplitudes and phases of the individual elements of an antenna array, it is possible to shape the antenna pattern and to steer the direction of the beam electronically.
- The pattern of an array of identical elements is equal to the product of the array factor and the antenna pattern of an individual antenna element.

INTEL-1014
U.S. Patent 7,151,430

GLOSSARY OF IMPORTANT TERMS

Provide definitions or explain the meaning of the following terms:

antenna
isotropic antenna
radiation pattern
antenna impedance
far-field (or far-zone) region
short dipole (Hertzian dipole)
spherical propagation factor
power density $\mathbf{S}(\theta, \phi)$
broadside direction
solid angle
radiation intensity (normalized) F
elevation and azimuth planes
radiation lobes
pattern solid angle Ω_p
beamwidth β
antenna directivity D
antenna gain G
radiation efficiency ξ
radiation resistance R_{rad}
loss resistance R_{loss}
effective area (effective aperture) A_e
Friis transmission formula
system noise temperature T_{sys}
signal-to-noise ratio S_n
aperture distribution
antenna array
electronic steering
feeding coefficient
pattern multiplication principle
array factor $F_a(\theta, \phi)$
end-fire direction
frequency scanning

PROBLEMS

Sections 9-1 and 9-2: Short Dipole and Antenna Radiation Characteristics

9.1* A center-fed Hertzian dipole is excited by a current $I_0 = 10$ A. If the dipole is $\lambda/50$ in length, determine the maximum radiated power density at a distance of 1 km.

9.2 A 1-m-long dipole is excited by a 1-MHz current with an amplitude of 12 A. What is the average power density radiated by the dipole at a distance of 5 km in a direction that is 30° from the dipole axis?

9.3* Determine the following:
(a) The direction of maximum radiation.
(b) Directivity.
(c) Beam solid angle.
(d) Half-power beamwidth in the x–z plane.
for an antenna whose normalized radiation intensity is given by

$$F(\theta, \phi) = \begin{cases} 1, & \text{for } 0 \le \theta \le 60^\circ \text{and } 0 \le \phi \le 2\pi \\ 0, & \text{elsewhere.} \end{cases}$$

Suggestion: Sketch the pattern prior to calculating the desired quantities.

9.4 Repeat Problem 9.3 for an antenna with

$$F(\theta, \phi) = \begin{cases} \sin^2\theta \cos^2\phi & \text{for } 0 \le \theta \le \pi \\ & \text{and } -\pi/2 \le \phi \le \pi/2 \\ 0 & \text{elsewhere} \end{cases}$$

9.5* A 2-m-long center-fed dipole antenna operates in the AM broadcast band at 1 MHz. The dipole is made of copper wire with a radius of 1 mm.
(a) Determine the radiation efficiency of the antenna.
(b) What is the antenna gain in decibels?
(c) What antenna current is required so that the antenna will radiate 20 W, and how much power will the generator have to supply to the antenna?

*Answer(s) available in Appendix D.
Solution available in CD-ROM.

INTEL-1014
U.S. Patent 7,151,430

9.6 Repeat Problem 9.5 for a 20-cm-long antenna operating at 5 MHz.

9.7* An antenna with a pattern solid angle of 1.5 (sr) radiates 30 W of power. At a range of 1 km, what is the maximum power density radiated by the antenna?

9.8 An antenna with a radiation efficiency of 90% has a directivity of 6.7 dB. What is its gain in decibels?

9.9* The radiation pattern of a circular parabolic-reflector antenna consists of a circular major lobe with a half-power beamwidth of 2° and a few minor lobes. Ignoring the minor lobes, obtain an estimate for the antenna directivity in dB.

9.10 The normalized radiation intensity of a certain antenna is given by

$$F(\theta) = \exp(-20\theta^2) \qquad \text{for } 0 \le \theta \le \pi$$

where θ is in radians. Determine:
(a) The half-power beamwidth.
(b) The pattern solid angle.
(c) The antenna directivity.

Sections 9-3 and 9-4: Dipole Antennas

9.11* Repeat Problem 9.5 for a 1-m-long half-wave dipole that operates in the FM/TV broadcast band at 150 MHz.

9.12 Assuming the loss resistance of a half-wave dipole antenna to be negligibly small and ignoring the reactance component of its antenna impedance, calculate the standing-wave ratio on a 60-Ω transmission line connected to the dipole antenna.

9.13* For a short dipole with length l such that $l \ll \lambda$, instead of treating the current $\tilde{I}(z)$ as constant along the dipole, as was done in Section 9-1, a more realistic approximation that ensures that the current goes to zero at the ends is to describe $\tilde{I}(z)$ by the triangular function

$$\tilde{I}(z) = \begin{cases} I_0(1 - 2z/l), & \text{for } 0 \le z \le l/2 \\ I_0(1 + 2z/l), & \text{for } -l/2 \le z \le 0 \end{cases}$$

as shown in Fig. 9-36. Use this current distribution to determine the following:
(a) The far-field $\tilde{\mathbf{E}}(R, \theta, \phi)$.
(b) The power density $S(R, \theta, \phi)$.
(c) The directivity D.
(d) The radiation resistance R_{rad}.

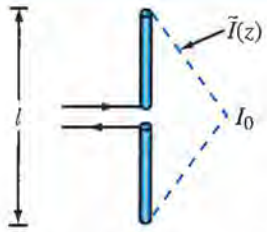


Figure 9-36: Triangular current distribution on a short dipole (Problem 9.13).

9.14 For a dipole antenna of length $l = 3\lambda/2$,
(a) Determine the directions of maximum radiation.
(b) Obtain an expression for S_{max}.
(c) Generate a plot of the normalized radiation pattern $F(\theta)$.
(d) Compare your pattern with that shown in Fig. 9-17(c).

9.15 Repeat parts (a)–(c) of Problem 9.14 for a dipole of length $l = 3\lambda/4$.

9.16 Repeat parts (a)–(c) of Problem 9.14 for a dipole of length $l = \lambda$.

INTEL-1014
U.S. Patent 7,151,430

9.17* A car antenna is a vertical monopole over a conducting surface. Repeat Problem 9.5 for a 1-m-long car antenna operating at 1 MHz. The antenna wire is made of aluminum with $\mu_c = \mu_0$ and $\sigma_c = 3.5 \times 10^7$ S/m, and its diameter is 1 cm.

Sections 9-5 and 9-6: Effective Area and Friis Formula

9.18 Determine the effective area of a half-wave dipole antenna at 100 MHz, and compare it to its physical cross-section if the wire diameter is 1 cm.

9.19* A 3-GHz line-of-sight microwave communication link consists of two lossless parabolic dish antennas, each 1 m in diameter. If the receive antenna requires 1 nW of receive power for good reception and the distance between the antennas is 40 km, how much power should be transmitted?

9.20 A half-wave dipole TV broadcast antenna transmits 1 kW at 50 MHz. What is the power received by a home television antenna with 13-dB gain if located at a distance of 30 km?

9.21* A 150-MHz communication link consists of two vertical half-wave dipole antennas separated by 2 km. The antennas are lossless, the signal occupies a bandwidth of 3 MHz, the system noise temperature of the receiver is 600 K, and the desired signal-to-noise ratio is 20 dB. What transmitter power is required?

9.22 Consider the communication system shown in Fig. 9-37, with all components properly matched. If $P_t = 10$ W and $f = 6$ GHz:

(a) What is the power density at the receiving antenna (assuming proper alignment of antennas)?

(b) What is the received power?

(c) If $T_{sys} = 1,000$ K and the receiver bandwidth is 10 MHz, what is the signal-to-noise ratio in decibels?

Sections 9-7 and 9-8: Radiation by Apertures

9.23* A uniformly illuminated aperture is of length $l_x = 20\lambda$. Determine the beamwidth between first nulls in the x–z plane.

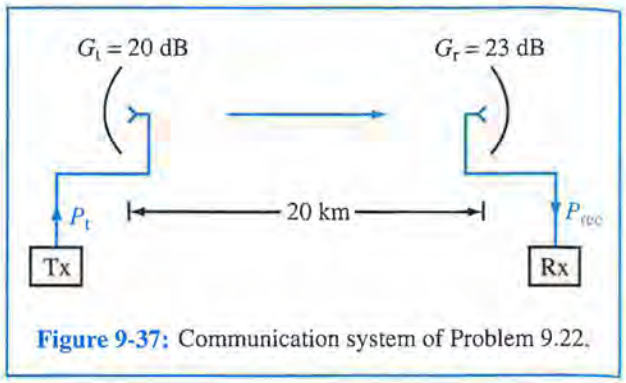


Figure 9-37: Communication system of Problem 9.22.

9.24 The 10-dB beamwidth is the beam size between the angles at which $F(\theta)$ is 10 dB below its peak value. Determine the 10-dB beamwidth in the x–z plane for a uniformly illuminated aperture with length $l_x = 10\lambda$.

9.25* A uniformly illuminated rectangular aperture situated in the x–y plane is 3 m high (along x) and 1 m wide (along y). If $f = 10$ GHz, determine the following:

(a) The beamwidths of the radiation pattern in the elevation plane (x–z plane) and the azimuth plane (y–z plane).

(b) The antenna directivity D in decibels.

9.26 An antenna with a circular aperture has a circular beam with a beamwidth of 1.5° at 20 GHz.

(a) What is the antenna directivity in dB?

(b) If the antenna area is doubled, what will be the new directivity and new beamwidth?

(c) If the aperture is kept the same as in (a), but the frequency is doubled to 40 GHz, what will the directivity and beamwidth become then?

9.27* A 94-GHz automobile collision-avoidance radar uses a rectangular-aperture antenna placed above the car's bumper. If the antenna is 1 m in length and 10 cm in height, determine the following:

(a) Its elevation and azimuth beamwidths.

(b) The horizontal extent of the beam at a distance of 300 m.

INTEL-1014
U.S. Patent 7,151,430

9.28 A microwave telescope consisting of a very sensitive receiver connected to a 100-m parabolic-dish antenna is used to measure the energy radiated by astronomical objects at 10 GHz. If the antenna beam is directed toward the moon and the moon extends over a planar angle of 0.5° from Earth, what fraction of the moon's cross-section will be occupied by the beam?

Sections 9-9 and 9-11: Antenna Arrays

9.29* A two-element array consisting of two isotropic antennas separated by a distance d along the z-axis is placed in a coordinate system whose z-axis points eastward and whose x-axis points toward the zenith. If a_0 and a_1 are the amplitudes of the excitations of the antennas at $z = 0$ and at $z = d$, respectively, and if δ is the phase of the excitation of the antenna at $z = d$ relative to that of the other antenna, find the array factor and plot the pattern in the x–z plane for the following:

(a) $a_0 = a_1 = 1$, $\delta = \pi/4$, and $d = \lambda/2$
(b) $a_0 = 1$, $a_1 = 2$, $\delta = 0$, and $d = \lambda$
(c) $a_0 = a_1 = 1$, $\delta = -\pi/2$, and $d = \lambda/2$
(d) $a_0 = 1$, $a_1 = 2$, $\delta = \pi/4$, and $d = \lambda/2$
(e) $a_0 = 1$, $a_1 = 2$, $\delta = \pi/2$, and $d = \lambda/4$

9.30 If the antennas in part (a) of Problem 9.29 are parallel, vertical, Hertzian dipoles with axes along the x-direction, determine the normalized radiation intensity in the x–z plane and plot it.

9.31* Consider the two-element dipole array of Fig. 9-29(a). If the two dipoles are excited with identical feeding coefficients ($a_0 = a_1 = 1$ and $\psi_0 = \psi_1 = 0$), choose (d/λ) such that the array factor has a maximum at $\theta = 45°$.

9.32 Choose (d/λ) so that the array pattern of the array of Problem 9.31 has a null, rather than a maximum, at $\theta = 45°$.

9.33* Find and plot the normalized array factor and determine the half-power beamwidth for a five-element linear array excited with equal phase and a uniform amplitude distribution. The interelement spacing is $3\lambda/4$.

9.34 A three-element linear array of isotropic sources aligned along the z-axis has an interelement spacing of $\lambda/4$ (Fig. 9-38). The amplitude excitation of the center element is twice that of the bottom and top elements, and the phases are $-\pi/2$ for the bottom element and $\pi/2$ for the top element, relative to that of the center element. Determine the array factor and plot it in the elevation plane.

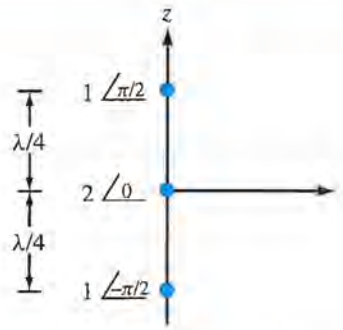


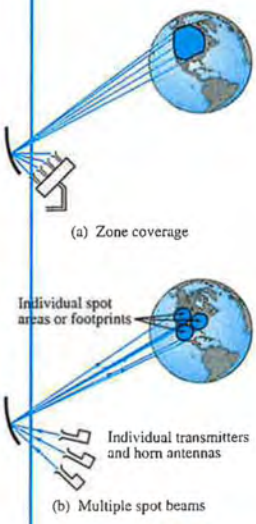
Figure 9-38: Three-element array of Problem 9.34.

9.35* An eight-element linear array with $\lambda/2$ spacing is excited with equal amplitudes. To steer the main beam to a direction 60° below the broadside direction, what should be the incremental phase delay between adjacent elements? Also, give the expression for the array factor and plot the pattern.

9.36 A linear array arranged along the z-axis consists of 12 equally spaced elements with $d = \lambda/2$. Choose an appropriate incremental phase delay δ so as to steer the main beam to a direction 30° above the broadside direction. Provide an expression for the array factor of the steered antenna and plot the pattern. From the pattern, estimate the beamwidth.

INTEL-1014
U.S. Patent 7,151,430





CHAPTER 10

Satellite Communication Systems and Radar Sensors



Application Examples

10-1 Satellite Communication Systems
10-2 Satellite Transponders
10-3 Communication-Link Power Budget
10-4 Antenna Beams
10-5 Radar Sensors
10-6 Target Detection
10-7 Doppler Radar
10-8 Monopulse Radar

INTEL-1014
U.S. Patent 7,151,430

APPLICATION EXAMPLES

This concluding chapter presents overviews of the principles of operation of satellite communication systems and radar sensors, with emphasis on electromagnetic-related topics.

10-1 Satellite Communication Systems

Today's world is connected by a vast communication network that provides a wide array of voice, data, and video services to both fixed and mobile terminals [Fig. 10-1]. The viability and effectiveness of the network are attributed in large measure to the use of orbiting satellite systems that function as relay stations with wide area coverage of Earth's surface. From a geostationary orbit position at 35,786 km above the equator, a satellite can view over one-third of Earth's surface and can connect any pair of points within its coverage [Fig. 10-2]. The history of communication satellite engineering dates back to the late 1950s when the U.S. navy used the moon as a passive reflector to relay low-data-rate communications between Washington, D.C., and Hawaii. The first major development

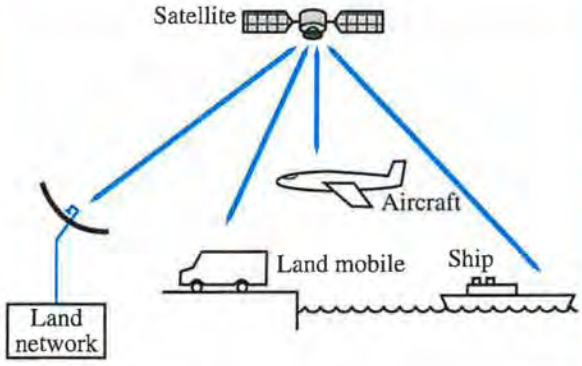
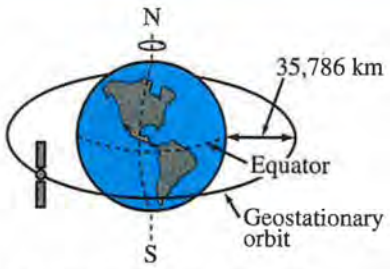
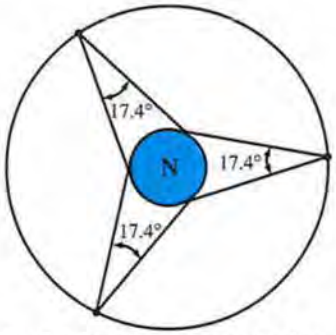


Figure 10-1: Elements of a satellite communication network.



(a) Geostationary satellite orbit



(b) Worldwide coverage by three satellites spaced 120° apart

Figure 10-2: Orbits of geostationary satellites.

INTEL-1014
U.S. Patent 7,151,430

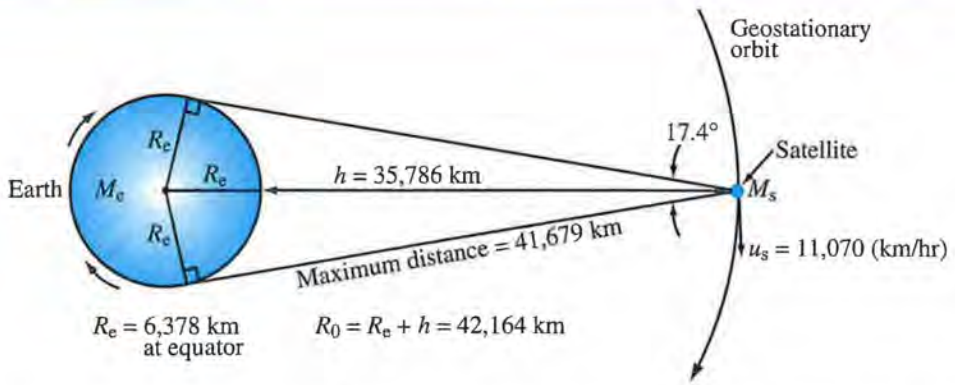


Figure 10-3: Satellite of mass m_s in orbit around Earth. For the orbit to be geostationary, the distance R_0 between the satellite and Earth's center should be 42,164 km. At the equator, this corresponds to an altitude of 35,786 km above Earth's surface.

involving artificial Earth satellites took place in October 1957 when the Soviet Union launched ***Sputnik I*** and used it for 21 days to transmit (one-way) telemetry information. This was followed by another telemetry satellite, ***Explorer I***, which was launched by the United States in January 1958, and in December of that year the satellite ***Score*** was launched and used to broadcast President Eisenhower's Christmas message, marking the first instance of two-way voice communication via an artificial satellite.

These achievements were followed by a flurry of space activity, leading to the development of operational communication satellites by many countries for both commercial and governmental services. This section provides an overview of the satellite communications link, including transmitter–receiver power calculations, propagation aspects, frequency allocations, and antenna design considerations.

A satellite is said to be in a ***geostationary orbit*** around Earth when it is in a circular orbit in a plane identical with Earth's equatorial plane and at such an altitude that the orbital period is identical with Earth's rotational period. A satellite of mass M_s in circular orbit around Earth [Fig. 10-3] is subject to two forces, a gravitational force F_g and a repelling centrifugal force F_c. The magnitudes of these two forces are given by

$$F_g = \frac{GM_sM_e}{R_0^2}, \tag{10.1}$$

$$F_c = \frac{M_s u_s^2}{R_0} = M_s\omega^2 R_0, \tag{10.2}$$

where $G = 6.67 \times 10^{-11}$ (N·m^2/kg^2) is the universal gravitational constant, $M_e = 5.98 \times 10^{24}$ kg is Earth's mass, R_0 is the distance between the satellite and the center of Earth, and u_s is the satellite velocity. For a rotating object, $u_s = \omega R_0$, where ω is its angular velocity. In order for the satellite to remain in orbit, the two opposing forces acting upon it have to be equal in magnitude, or

$$G\frac{M_sM_e}{R_0^2} = M_s\omega^2 R_0, \tag{10.3}$$

which yields a solution for R_0 given by

$$R_0 = \left[\frac{GM_e}{\omega^2}\right]^{1/3}. \tag{10.4}$$

INTEL-1014
U.S. Patent 7,151,430

To remain stationary with respect to Earth's surface, the satellite's angular velocity has to be the same as that of Earth's own angular velocity around its own axis. Thus,

$$\omega = \frac{2\pi}{T}, \tag{10.5}$$

where T is the period of one sidereal day in seconds. A sidereal day, which takes into account Earth's rotation around the sun, is equal to 23 hours, 56 minutes, and 4.1 seconds. Using Eq. (10.5) in Eq. (10.4) gives

$$R_0 = \left(\frac{GM_eT^2}{4\pi^2}\right)^{1/3}. \tag{10.6}$$

and upon using the numerical values for T, M_e, and G, we obtain the result $R_0 = 42,164$ km. Subtracting 6,378 km for Earth's mean radius at the equator gives an altitude of $h = 35,786$ km above Earth's surface.

From a geostationary orbit, Earth subtends an angle of 17.4°, covering an arc of about 18,000 km along the equator, which corresponds to a longitude angle of about 160°. With three equally spaced satellites in geostationary orbit over Earth's equator, complete global coverage of the entire equatorial plane can be achieved, with significant overlap between the beams of the three satellites. As far as coverage toward the poles, a global beam can reach Earth stations up to 81° of latitude on either side of the equator.

Not all satellite communication systems use spacecraft that are in geostationary orbits; because of transmitter power limitations or other considerations, it is sometimes necessary to operate from much lower altitudes, in which case the satellite is placed in a *highly elliptical orbit* (to satisfy Kepler's law) such that for part of the orbit (near its perigee) it is at a range of only a few hundred kilometers from Earth's surface. Whereas only three geostationary satellites are needed to provide global coverage of Earth's surface, a much larger number is needed when the satellites used are in highly elliptical orbits.

10-2 Satellite Transponders

A communication satellite functions as a distant repeater that receives *uplink* signals from Earth stations, processes the signals, and then retransmits them on the *downlink* to their intended Earth destinations. The International Telecommunication Union has allocated specific bands for satellite communications [Table 10-1]. Of these, the bands used by the majority of U.S. commercial satellites for domestic communications are the *4/6 GHz band* (3.7- to 4.2-GHz downlink and 5.925- to 6.425-GHz uplink) and the *12/14 GHz band* (11.7- to 12.2-GHz downlink and 14.0- to 14.5-GHz uplink). Each uplink and downlink segment has been allocated 500 MHz of bandwidth. By using different frequency bands for Earth-to-satellite uplink segment and for the satellite-to-Earth downlink segments, the same antennas can be used for both functions while simultaneously guarding against interference between the two signals. The downlink segment commonly uses a lower-frequency carrier than the uplink segment, because lower frequencies suffer lower attenuation by Earth's atmosphere, and thus eases the requirement on satellite output power.

We shall use the 4/6 GHz band as a model to facilitate discussion of the satellite-repeater operation, while keeping in mind that the functional structure of the repeater is basically the same regardless of which specific satellite communication band is used.

Figure 10-4 shows a generalized block diagram of a 12-channel repeater as implemented in a typical communications satellite. The path of each channel from the point of its reception by the antenna, followed by its transfer through the repeater up to the point of its retransmission through the antenna, is called a *transponder*. The available 500-MHz bandwidth is allocated to 12 channels (transponders) of 36-MHz bandwidth per channel and 4-MHz separation between channels. The basic functions of each transponder are isolation of neighboring radio frequency (RF) channels, frequency translation,

INTEL-1014
U.S. Patent 7,151,430

Table 10-1: Communications satellite frequency allocations.

Use	Downlink Frequency (MHz)	Uplink Frequency (MHz)
	Fixed Service	
Commercial (C-band)	3,700–4,200	5,925–6,425
Military (X-band)	7,250–7,750	7,900–8,400
Commercial (K-band)		
Domestic (USA)	11,700–12,200	14,000–14,500
International	10,950–11,200	27,500–31,000
	Mobile Service	
Maritime	1,535–1,542.5	1,635–1,644
Aeronautical	1,543.5–1,558.8	1,645–1,660
	Broadcast Service	
	2,500–2,535	2,655–2,690
	11,700–12,750	
	Telemetry, Tracking, and Command	
	137–138, 401–402, 1,525–1,540	

and amplification. With ***frequency-division multiple access*** (FDMA)—one of the schemes commonly used for information transmission—each transponder can accommodate thousands of individual telephone channels within its 36 MHz of bandwidth (telephone speech signals require a minimum bandwidth of 3 kHz, and the nominal frequency spacing usually used is 4 kHz per telephone channel), several TV channels (each requiring a bandwidth of 6 MHz), millions of bits of digital data, or combinations of all three.

When the same antenna is used for both transmission and reception, a ***duplexer*** is used to perform the signal separation. Many types of duplexers are available, but among the simplest to understand is the circulator shown in Fig. 10-5. A ***circulator*** is a three-port device that uses a ferrite material placed in a magnetic field induced by a permanent magnet to achieve power flow from ports 1 to 2, 2 to 3, and 3 to 1, but not in the reverse directions. With the antenna connected to port 1, the received signal is channeled only to port 2; with port 2 being properly matched to the band-pass filter, no part of the received signal will be reflected from port 2 to 3; and with the transmitted signal connected to port 3, the circulator channels it to port 1 for transmission by the antenna.

Following the duplexer shown in Fig. 10-4, the received signal passes through a receiver band-pass filter that ensures isolation of the received signal from the transmitted signal. The receiver filter covers the bandwidth from 5.925 to 6.425 GHz, which encompasses the cumulative bandwidths of all 12 channels; the first received channel extends from 5,927 to 5,963 MHz, the second one from 5,967 to 6,003 MHz, and so on until the twelfth channel, which covers the range from 6,367 to 6,403 MHz. The next subsystem along the received signal path is the

INTEL-1014
U.S. Patent 7,151,430

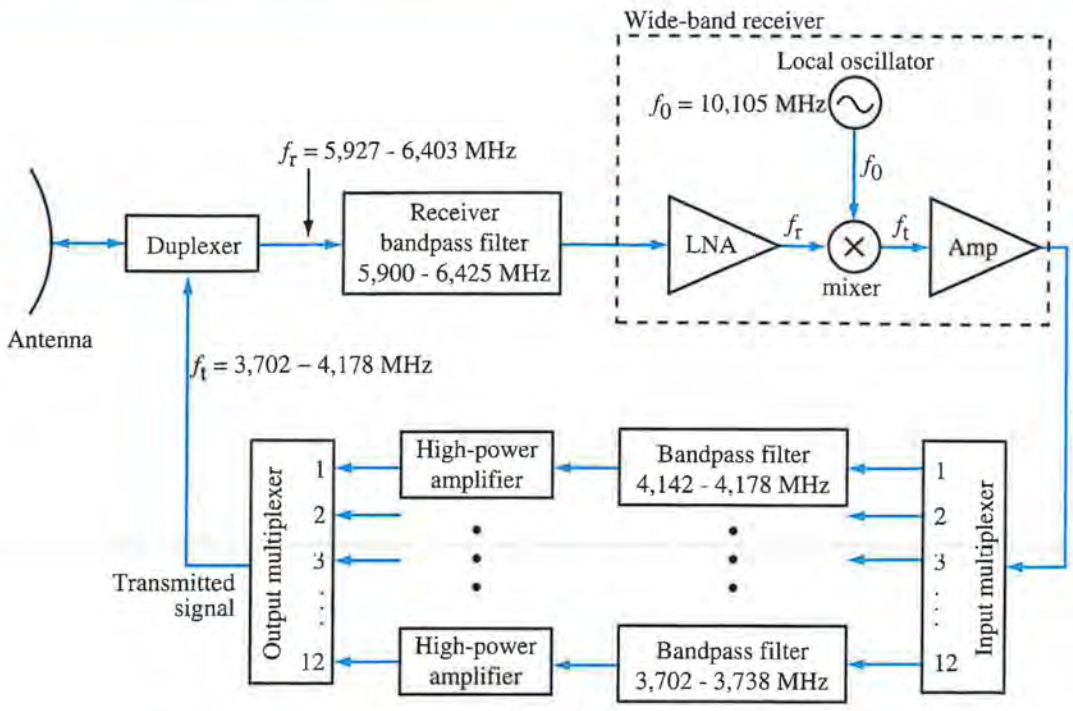


Figure 10-4: Elements of a 12-channel (transponder) communications system.

wideband receiver, which consists of three elements: a low-noise wideband amplifier, a frequency translator, and an output amplifier. The frequency translator consists of a stable local oscillator that generates a signal at a frequency $f_0 = 10,105$ MHz, connected to a nonlinear microwave mixer. The mixer serves to convert the frequency f_r of the received signal (which covers the range from 5,927 to 6,403 MHz) to a lower-frequency signal $f_t = f_0 - f_r$. Thus, the lower end of the received signal frequency gets converted from 5,927 to 4,178 MHz and the upper end gets converted from 6,403 to 3,702 MHz. This translation results in 12 channels with new frequency ranges, but their signals carry the same information (modulation) that was present in the received signals. In principle, the receiver output signal can now be further amplified and then channeled to the antenna through the duplexer for transmission back to Earth. Instead, the receiver output signal is separated into the 12 transponder channels through a ***multiplexer*** followed by a bank of narrow band-pass filters, each covering the bandwidth of one transponder channel. Each of the 12 channels is amplified by its own ***high-power amplifier*** (HPA), and then the 12 channels are combined by another multiplexer that feeds the combined spectrum into the duplexer. This channel separation and recombination process is used as a safety measure against losing all 12 channels should a high-power amplifier experience degradation in performance or total failure.

INTEL-1014
U.S. Patent 7,151,430

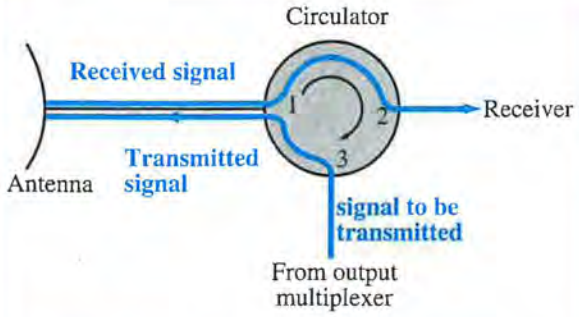


Figure 10-5: Basic operation of a ferrite circulator.

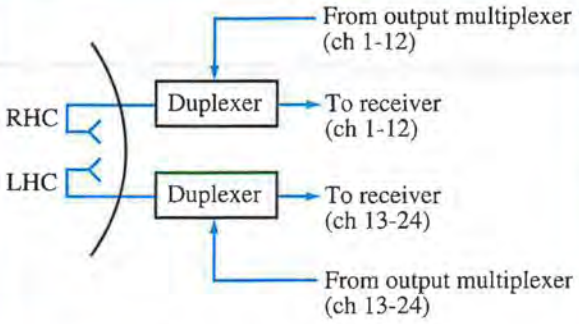


Figure 10-6: Polarization diversity is used to increase the number of channels from 12 to 24.

The information carrying capacity of a satellite repeater can be doubled from 12 to 24 channels over the same 500-MHz bandwidth by using ***polarization diversity***. Instead of transmitting one channel of information over channel 1 (5,927 to 5,963 MHz), for example, the ground station transmits to the satellite two signals carrying different information and covering the same frequency band, but with different antenna polarization configurations, such as right-hand circular (RHC) and left-hand circular (LHC) polarizations. The satellite antenna is equipped with a feed arrangement that can receive each of the two circular polarization signals individually with negligible interference between them. Two duplexers are used in this case, one connected to the RHC polarization feed and another connected to the LHC polarization feed, as illustrated in Fig. 10-6.

10-3 Communication-Link Power Budget

The uplink and downlink segments of a satellite communication link [Fig. 10-7] are each governed by the ***Friis transmission formula*** [Section 9-6], which states that the power P_r received by an antenna with gain G_r due to the transmission of power P_t by an antenna with gain G_t at a range R is given by

$$P_r = P_t G_t G_r \left(\frac{\lambda}{4\pi R}\right)^2. \qquad (10.7)$$

The expression given by Eq. (10.7) applies to a lossless medium, such as free space. To account for attenuation

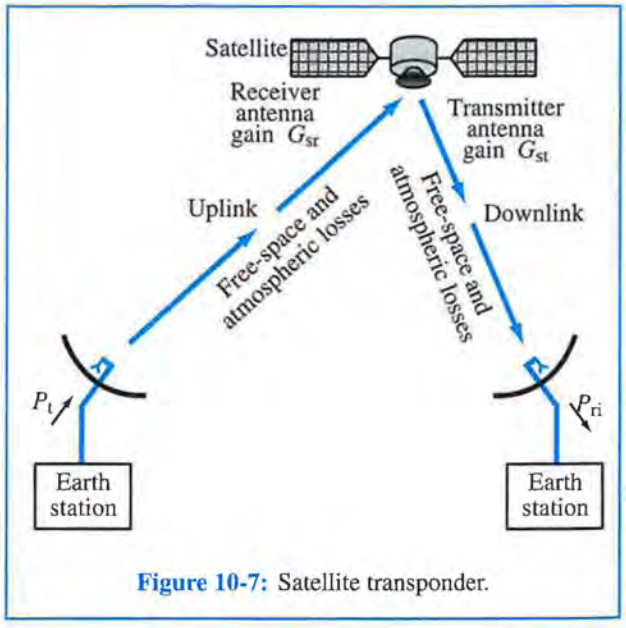


Figure 10-7: Satellite transponder.

INTEL-1014
U.S. Patent 7,151,430

by clouds and rain in Earth's atmosphere (when present along the propagation path), as well as absorption by certain atmospheric gases (primarily oxygen and water vapor), we should rewrite Eq. (10.7) in the following form:

$$P_{ri} = \Upsilon(\theta)\, P_r = \Upsilon(\theta)\, P_t G_t G_r \left(\frac{\lambda}{4\pi R}\right)^2, \qquad (10.8)$$

where now P_{ri} represents the input power at the receiver with atmospheric losses taken into account, and $\Upsilon(\theta)$ is the one-way ***transmissivity*** of the atmosphere at zenith angle θ. In addition to its dependence on θ, $\Upsilon(\theta)$ is a function of the microwave frequency of the communication link and the rain-rate conditions along the propagation path. At frequencies below 10 GHz, which include the 4/6 GHz band allocated for satellite communications, absorption by atmospheric gases is very small, and cloud and rain attenuation is also relatively small. Consequently, the magnitude of $\Upsilon(\theta)$ is typically on the order of 0.5 to 1 for most conditions. A transmissivity of 0.5 means that twice as much power needs to be transmitted (compared with the free-space case) in order to receive a specified power level. Among the various sources of atmospheric attenuation, the most serious is rainfall, and its attenuation coefficient increases rapidly with increasing frequency. Consequently, atmospheric attenuation assumes greater importance with regard to transmitter power requirements as the communication-system frequency is increased toward higher bands in the microwave region.

The noise appearing at the receiver output, P_{no}, consists of three contributions: (1) noise internally generated by the receiver electronics, (2) noise picked up by the antenna due to external sources, including emission by the atmosphere, and (3) noise due to thermal emission by the antenna material. The combination of all noise sources can be represented by an equivalent ***system noise temperature***, T_{sys}, defined such that

$$P_{no} = G_{rec} K T_{sys} B, \qquad (10.9)$$

where K is Boltzmann's constant, G_{rec} is the receiver power gain, and B is its bandwidth. This output noise level is the same as would appear at the output of a noise-free receiver with input noise level

$$P_{ni} = \frac{P_{no}}{G_{rec}} = K T_{sys} B. \qquad (10.10)$$

The ***signal-to-noise ratio*** is defined as the ratio of the signal power to the noise power *at the input of an equivalent noise-free receiver*. Hence,

$$S_n = \frac{P_{ri}}{P_{ni}} = \frac{\Upsilon(\theta)\, P_t G_t G_r}{K T_{sys} B} \left(\frac{\lambda}{4\pi R}\right)^2. \qquad (10.11)$$

The performance of a communication system is governed by two sets of factors. The first set encompasses the signal-processing techniques used to encode, modulate, combine, and transmit the signal at the transmitter end and to receive, separate, demodulate, and decode the signal at the receiver end. The second set of factors is the gains and losses in the communication link, and they are represented by the signal-to-noise ratio, S_n. For a given set of signal-processing techniques, S_n determines the quality of the received signal, such as the bit error rate in digital data transmission and sound and picture quality in audio and video transmissions. Very high quality signal transmission requires very high values of S_n; in broadcast-quality television by satellite, some systems are designed to provide values of S_n exceeding 50 dB (or a factor of 10^5).

The performance of a satellite link depends on the composite performance of the uplink and downlink segments. If either segment performs poorly, the composite performance will be poor, regardless of how good the performance of the other segment is. It is for this reason that system-power calculations are performed for each segment separately.

INTEL-1014
U.S. Patent 7,151,430

10-4 Antenna Beams

Whereas most Earth-station antennas must provide highly directive beams to avoid interference effects, the satellite antenna system is designed to produce beams tailored to match the areas served by the satellite. For global coverage, beamwidths of 17.4° are required. In contrast, for transmission to and reception from a small area, beamwidths on the order of 1° or less may be needed [Fig. 10-8]. An antenna with a beamwidth β of 1° would produce a spot beam on Earth covering an area approximately 630 km in diameter.

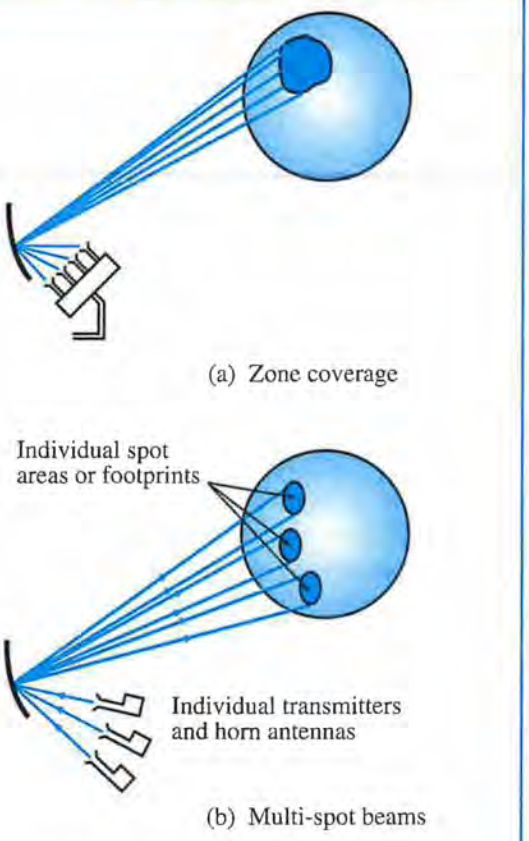


Figure 10-8: Spot and multi-beam satellite antenna systems for coverage of defined areas on Earth's surface.)

Beam size has a direct connection to antenna gain and, in turn, to transmitter power requirements. Antenna gain G is related to the directivity D by $G = \xi D$, where ξ is the radiation efficiency, and D is related to the beamwidth β by the approximate expression given by Eq. (9.26). For a circular beam,

$$G = \xi \frac{4\pi}{\beta^2}, \tag{10.12}$$

where β is in radians. For a lossless antenna ($\xi = 1$), a global beam with $\beta = 17.4°$ (= 0.3 rad) corresponds to a gain $G = 136$, or 21.3 dB. A narrow 1° beam, on the other hand, corresponds to an antenna gain of 41,253, or 46.2 dB.

To accommodate the various communication functions associated with satellite systems, four main types of antennas are used*:

1. Dipoles and helices at VHF and UHF for telemetry, tracking, and command functions;
2. Horns and relatively small parabolic dishes (with diameters on the order of a few centimeters) for producing wide-angled beams for global coverage;
3. Parabolic dishes fed by one or more horns to provide a beam for zone coverage [Fig. 10-8(a)] or multiple spot beams [Fig. 10-8(b)];
4. Antenna arrays consisting of many individual radiating elements for producing multi-spot beams and also for beam steering and scanning.

REVIEW QUESTIONS

Q10.1 What are the advantages and disadvantages of elliptical satellite orbits in comparison to the geostationary orbit?

*R. G. Meadows and A. J. Parsons, *Satellite Communications*, Hutchinson Publishers, London, 1989.

INTEL-1014
U.S. Patent 7,151,430

Q10.2 Why do satellite communication systems use different frequencies for the uplink and downlink segments? Which segment uses the higher frequency and why?

Q10.3 How does the use of antenna polarization increase the number of channels carried by the communication system?

Q10.4 What are the sources of noise that contribute to the total system noise temperature of a receiver?

10-5 Radar Sensors

The term *radar* is a contracted form of the phrase ***radio detection and ranging***, which conveys some, but not all, the features of a modern radar system. Historically, radar systems were first developed and used at *radio* frequencies, including the microwave band, but we now also have light radars, or ***lidars***, that operate at optical wavelengths. Over the years, the name radar has lost its original meaning and has come to signify any *active* electromagnetic sensor that uses its own source to illuminate a region of space and then measure the echoes generated by reflecting objects contained in the illuminated region. In addition to detecting the presence of a reflecting object and determining its *range* by measuring the time delay of short-duration pulses transmitted by the radar, a radar is also capable of specifying the *position* (*direction*) of the target and its radial velocity. Measurement of the ***radial velocity*** of a moving object, which is the component of the object's velocity vector along the direction from the object to the radar, is realized by measuring the ***Doppler frequency shift*** produced by the moving object, which is equal to the difference between the frequencies of the transmitted and received signals. Also, the strength and shape of the reflected pulse carry information about the shape and material properties of the reflecting object.

Radar is used for a wide variety of civilian and military applications, including air traffic control, aircraft navigation, law enforcement, control and guidance of weapon systems, remote sensing of Earth's environment, weather observations, astronomy, and collision avoidance for automobiles. The frequency bands used for the various types of radar applications extend from the megahertz region to frequencies as high as 225 GHz.

10-5.1 Basic Operation of a Radar System

The block diagram shown in Fig. 10-9 contains the basic functional elements of a pulse radar system. The ***synchronizer–modulator*** unit serves to synchronize the operation of the transmitter and the ***videoprocessor–display unit*** by generating a train of direct current (d-c) narrow-duration, evenly spaced pulses. These pulses, which are supplied to both the transmitter and the videoprocessor–display unit, specify the times at which radar pulses are transmitted. The transmitter contains a high-power radio-frequency (RF) oscillator with an on/off control voltage actuated by the pulses supplied by the synchronizer–modulator unit. Hence, the transmitter generates pulses of RF energy equal in duration and spacing to the d-c pulses generated by the synchronizer–modulator unit. Each pulse generated by the transmitter is supplied to the antenna through a ***duplexer***, which allows the antenna to be shared between the transmitter and the receiver. The duplexer, which often is called the ***transmitter/receiver*** (T/R) switch, connects the transmitter to the antenna for the duration of the pulse, and then connects the antenna to the receiver for the remaining period until the start of a new pulse. Some duplexers, however, are passive devices that perform the sharing and isolation functions continuously. The circulator shown in Fig. 10-5 is an example of a passive duplexer. After transmission by the antenna, a portion of the transmitted signal is intercepted by a reflecting object (often called a ***target***) and is reradiated in many directions. The energy reradiated by the target back toward the radar is collected by the antenna and delivered to the receiver, which processes the signal to detect the presence of the target and to extract information on its location and relative velocity. The receiver converts the reflected RF

INTEL-1014
U.S. Patent 7,151,430

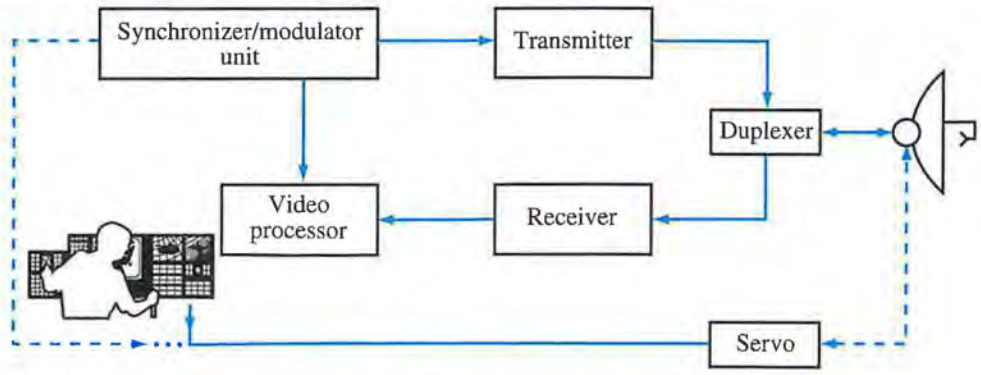


Figure 10-9: Basic block diagram of a radar system.

signals into lower-frequency video-frequency signals and supplies them to the videoprocessor–display unit, which displays the extracted information in a format suitable for the intended application. The servo unit positions the orientation of the antenna beam in response to control signals provided by either an operator, a control unit with preset functions, or a control unit commanded by another system. The control unit of an air traffic control radar, for example, commands the servo to rotate the antenna in azimuth continuously. In contrast, the radar antenna placed in the nose of an aircraft is made to scan back and forth over only a specified angular range.

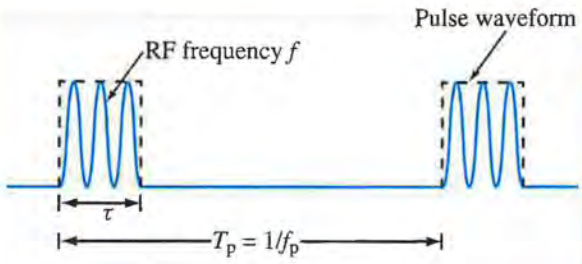


Figure 10-10: A pulse radar transmits a continuous train of RF pulses at a repetition frequency f_p.

10-5.2 Unambiguous Range

The collective features of the energy transmitted by a radar are called the ***signal waveform***. For a pulse radar, these features include (1) the carrier frequency f, (2) the ***pulse length*** τ, (3) the ***pulse repetition frequency*** f_p (number of pulses per second), or equivalently the ***interpulse period*** $T_p = 1/f_p$, and (4) the modulation (if any) within the pulses. Three of these features are illustrated in Fig. 10-10. Modulation, which refers to control of the amplitude, frequency, or phase of the signal, is beyond the level of the present treatment and therefore will not be considered.

The range to the target is determined by measuring the time delay T taken by the pulse to travel to the target and back. For a target at range R,

$$T = \frac{2R}{c}, \tag{10.13}$$

where $c = 3 \times 10^8$ m/s is the speed of light, and the factor 2 accounts for the two-way propagation. The maximum target range that a radar can measure

INTEL-1014
U.S. Patent 7,151,430

unambiguously, called the ***unambiguous range*** R_u, is determined by the interpulse period T_p and is given by

$$R_u = \frac{cT_p}{2} = \frac{c}{2f_p}. \tag{10.14}$$

The range R_u corresponds to the maximum range that a target can have such that its echo is received before the transmission of the next pulse. If T_p is too short, an echo signal due to a given pulse might arrive after the transmission of the next pulse, in which case the target would appear to be at a much shorter range than it actually is.

According to Eq. (10.14), if a radar is to be used to detect targets that are as far away as 100 km, for example, then f_p should be less than 1.5 kHz, and the higher the pulse repetition frequency (PRF), the shorter is the unambiguous range R_u. Consideration of R_u alone suggests selecting a low PRF, but other considerations suggest selecting a very high PRF. As we will see later in Section 10-6, the signal-to-noise ratio of the radar receiver is directly proportional to f_p, and hence it would be advantageous to select the PRF to be as high as possible. Moreover, in addition to determining the maximum unambiguous range R_u, the PRF also determines the maximum Doppler frequency (and hence the target's maximum radial velocity) that the radar can measure unambiguously. If the requirements on maximum range and velocity cannot be met by the same PRF, then some compromise may be necessary. Alternatively, it is possible to use a ***multiple-PRF*** radar system that transmits a few pulses at one PRF followed by another series of pulses at another PRF, and then the two sets of received pulses are processed together to remove the ambiguities that would have been present with either PRF alone.

10-5.3 Range and Angular Resolutions

Consider a radar observing two targets located at ranges R_1 and R_2, as shown in Fig. 10-11. Let $t = 0$ denote the time corresponding to the start of the transmitted pulse. The pulse length is τ. The return due to target 1 will arrive at $T_1 = 2R_1/c$ and will have a length τ (assuming that the pulse length in space is much greater than the radial extent of the target). Similarly, the return due to target 2 will arrive at $T_2 = 2R_2/c$. The two targets will be resolvable as distinct targets as long as $T_2 \geq T_1 + \tau$ or, equivalently,

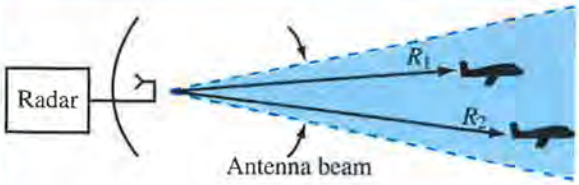


Figure 10-11: Radar beam viewing two targets at ranges R_1 and R_2.

$$\frac{2R_2}{c} \geq \frac{2R_1}{c} + \tau. \tag{10.15}$$

The ***range resolution*** of the radar, ΔR, is defined as the minimum spacing between two targets necessary to avoid overlap between the echoes from the two targets. From Eq. (10.15), this occurs when

$$\Delta R = R_2 - R_1 = c\tau/2. \tag{10.16}$$

Some radars are capable of transmitting pulses as short as 1 ns in duration or even shorter. For $\tau = 1$ ns, $\Delta R = 15$ cm.

The basic angular resolution of a radar system is determined by its antenna beamwidth β, as shown in

INTEL-1014
U.S. Patent 7,151,430

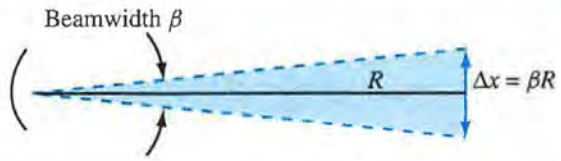


Figure 10-12: The azimuth resolution Δx at a range R is equal to βR.

Fig. 10-12. The corresponding ***azimuth resolution*** Δx at a range R is given by

$$\Delta x = \beta R, \tag{10.17}$$

where β is in radians. In some cases, special techniques are used to improve the angular resolution down to a fraction of the beamwidth β. One example is the monopulse tracking radar described in Section 10-8.

10-6 Target Detection

Target detection by radar is governed by two factors: (1) the ***signal energy*** received by the radar receiver due to reflection of part of the transmitted energy by the target, and (2) the ***noise energy*** generated by the receiver. Figure 10-13, which depicts the output of a radar receiver as a function of time, shows the signals due to the targets displayed against the noise contributed by external sources as well as by the devices making up the receiver. The random variations exhibited by the noise may at times make it difficult to distinguish the signal reflected by the target from a noise spike. In Fig. 10-13, the mean noise-power level at the receiver output is denoted by $P_{no} = G_{rec}P_{ni}$, where G_{rec} is the receiver gain and P_{ni} is the noise level referred to the receiver's input terminals. The power levels P_{r_1} and P_{r_2} represent the echoes of the two targets observed by the radar. Because of the random nature of the noise, it is necessary to set a threshold level, $P_{r_{min}}$, for detection. For the threshold level 1 indicated in Fig. 10-13, the radar will detect the presence of both targets, but it will also

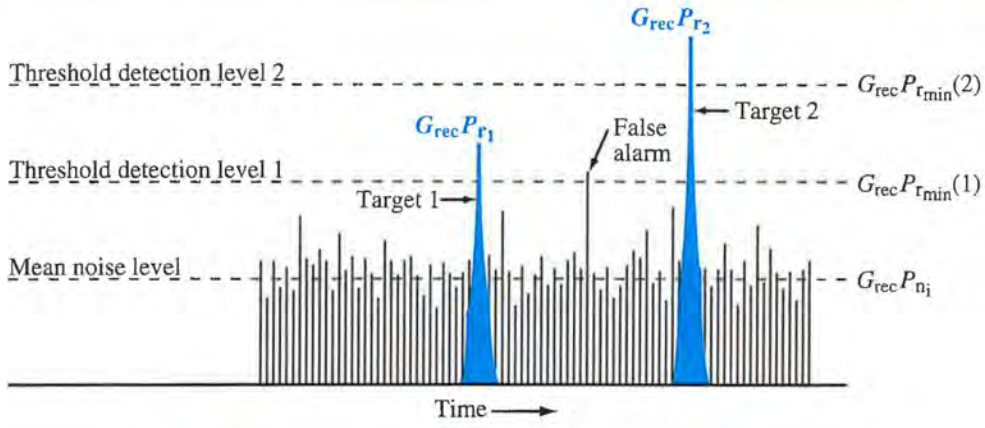


Figure 10-13: The output of a radar receiver as a function of time.

INTEL-1014
U.S. Patent 7,151,430

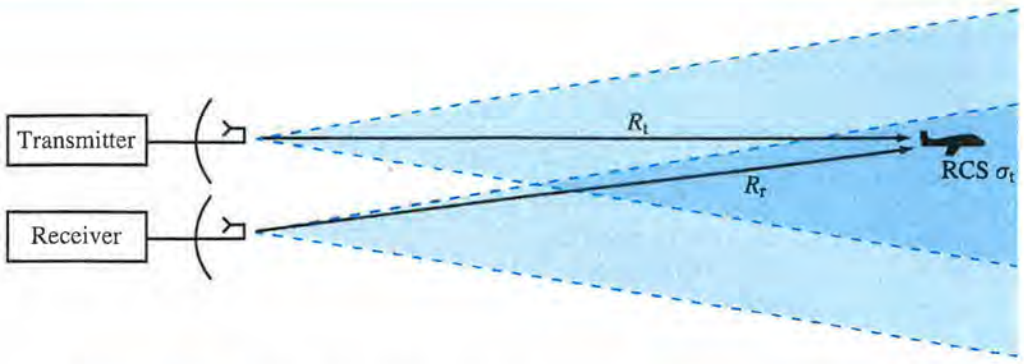


Figure 10-14: Bistatic radar system viewing a target with radar cross section (RCS) σ_t.

detect a ***false alarm***. The chance of this occurring is called the ***false-alarm probability***. On the other hand, if the threshold level is raised to level 2 to avoid the false alarm, the radar will not detect the presence of the first target. Correct detection of targets is called the ***detection probability***. The setting of the threshold signal level relative to the mean noise level is thus made on the basis of a compromise that considers both probabilities.

To keep the noise level at a minimum, the receiver is designed such that its bandwidth B is barely wide enough to pass most of the energy contained in the received pulse. Such a design, called a ***matched-filter design***, requires that B be equal to the reciprocal of the pulse length τ (i.e., $B = 1/\tau$). Hence, for a matched-filter receiver, Eq. (10.10) becomes

$$P_{ni} = KT_{sys}B = \frac{KT_{sys}}{\tau}. \tag{10.18}$$

The signal power received by the radar, P_r, is related to the transmitted power level, P_t, through the radar equation. We will first derive the radar equation for the general case of a ***bistatic radar*** configuration in which the transmitter and receiver are not necessarily at the same location, and then we will specialize the results to the ***monostatic radar*** case wherein the transmitter and receiver are colocated. In Fig. 10-14, the target is at a range R_t from the transmitter and at a range R_r from the receiver. The power density illuminating the target is given by

$$S_t = \frac{P_t}{4\pi R_t^2} G_t \quad (\text{W/m}^2), \tag{10.19}$$

where $(P_t/4\pi R_t^2)$ represents the power density that would have been radiated by an isotropic radiator, and G_t is the gain of the transmitting antenna in the direction of the target. The target is characterized by a ***radar cross section*** (RCS) σ_t (m^2), defined such that the power intercepted and then reradiated by the target is

$$P_{rer} = S_t\sigma_t = \frac{P_tG_t\sigma_t}{4\pi R_t^2} \quad (\text{W}). \tag{10.20}$$

This reradiated power spreads out over a spherical surface, resulting in a power density S_r incident upon the receiving radar antenna and given by

$$S_r = \frac{P_{rer}}{4\pi R_r^2} = \frac{P_tG_t\sigma_t}{(4\pi R_tR_r)^2} \quad (\text{W/m}^2). \tag{10.21}$$

INTEL-1014
U.S. Patent 7,151,430

With an effective area A_r and radiation efficiency ξ_r, the receiving radar antenna intercepts and delivers (to the receiver) power P_r given by

$$P_r = \xi_r A_r S_r = \frac{P_t G_t \xi_r A_r \sigma_t}{(4\pi R_t R_r)^2} = \frac{P_t G_t G_r \lambda^2 \sigma_t}{(4\pi)^3 R_t^2 R_r^2}, \quad (10.22)$$

where we have used Eqs. (9.29) and (9.64) to relate the effective area of the receive antenna, A_r, to its gain G_r. For a monostatic antenna that uses the same antenna for the transmit and receive functions, $G_t = G_r \triangleq G$ and $R_t = R_r \triangleq R$. Hence,

$$P_r = \frac{P_t G^2 \lambda^2 \sigma_t}{(4\pi)^3 R^4}. \quad (10.23)$$

Unlike the one-way communication system for which the dependence on R is as $1/R^2$, the range dependence given by the above ***radar equation*** goes as $1/R^4$, which in effect is the product of two one-way propagation processes.

The detection process may be based on the echo from a single pulse or on the addition (integration) of the echoes from several pulses. We will consider only the single-pulse case here. A target is said to be detectable if its echo signal power P_r exceeds $P_{r_{min}}$, the ***threshold detection level*** indicated in Fig. 10-13. The ***maximum detectable range*** R_{max} is the range beyond which the target cannot be detected, and it corresponds to the range at which $P_r = P_{r_{min}}$ in Eq. (10.23). Thus,

$$R_{max} = \left[\frac{P_t G^2 \lambda^2 \sigma_t}{(4\pi)^3 P_{r_{min}}}\right]^{1/4}. \quad (10.24)$$

The signal-to-noise ratio is equal to the ratio of the received signal power P_r to the mean input noise power P_{ni} given by Eq. (10.18):

$$S_n = \frac{P_r}{P_{ni}} = \frac{P_r \tau}{K T_{sys}}, \quad (10.25)$$

and the ***minimum signal-to-noise ratio*** S_{min} corresponds to when $P_r = P_{r_{min}}$:

$$S_{min} = \frac{P_{r_{min}} \tau}{K T_{sys}}. \quad (10.26)$$

Use of Eq. (10.26) in Eq. (10.24) gives

$$R_{max} = \left[\frac{P_t \tau G^2 \lambda^2 \sigma_t}{(4\pi)^3 K T_{sys} S_{min}}\right]^{1/4}. \quad (10.27)$$

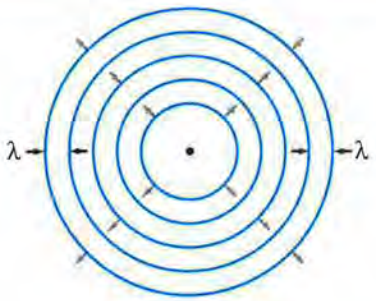
The product $P_t \tau$ is equal to the energy of the transmitted pulse. Hence, according to Eq. (10.27), *it is the energy of the transmitted pulse rather than the transmitter power level alone that determines the maximum detectable range.* A high-power narrow pulse and an equal-energy, low-power long pulse will yield the same radar performance as far as maximum detectable range is concerned. However, the range-resolution capability of the long pulse is much poorer than that of the short pulse [see Eq. (10.16)].

The maximum detectable range R_{max} can also be increased by improving the signal-to-noise ratio. This can be accomplished by integrating the echoes from multiple pulses in order to increase the total amount of energy received from the target. The number of pulses available for integration over a specified integration time is proportional to the PRF. Hence, from the standpoint of maximizing target detection, it is advantageous to use as high a PRF as allowed by other considerations.

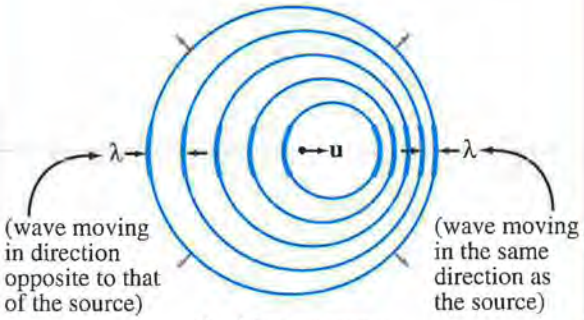
10-7 Doppler Radar

The Doppler effect is a shift in the frequency of a wave caused by the motion of the transmitting source, the reflecting object, or the receiving system. As illustrated in Fig. 10-15, a wave radiated by a stationary isotropic point source forms equally spaced concentric circles as a function of time travel from the source. In contrast, a wave radiated by a moving source is compressed in the

INTEL-1014
U.S. Patent 7,151,430



(a) Stationary source



(b) Moving source

Figure 10-15: A wave radiated from a point source when (a) stationary and (b) moving. The wave is compressed in the direction of motion, spread out in the opposite direction, and unaffected in the direction normal to motion.

direction of motion and is spread out in the opposite direction. Compressing a wave shortens its wavelength, which is equivalent to increasing its frequency. Conversely, spreading it out decreases its frequency. The change in frequency is called the ***Doppler frequency shift*** f_d. That is, if f_t is the frequency of the wave radiated by the moving source, then the frequency f_r of the wave that would be observed by a stationary receiver is

$$f_r = f_t + f_d. \tag{10.28}$$

The magnitude and sign of f_d depend on the direction of the velocity vector relative to the direction of the range vector connecting the source to the receiver.

Consider a source transmitting an electromagnetic wave with frequency f_t as shown in Fig. 10-16. At a distance R from the source, the electric field of the radiated wave is given by

$$E(R) = E_0 e^{j(\omega_t t - kR)} = E_0 e^{j\phi}, \tag{10.29}$$

where E_0 is the wave's magnitude, $\omega_t = 2\pi f_t$, and $k = 2\pi/\lambda_t$, where λ_t is the wavelength of the transmitted wave. The magnitude depends on the distance R and the gain of the source antenna, but it is not of concern as far as the Doppler effect is concerned. The quantity

$$\phi = \omega_t t - kR = 2\pi f_t t - \frac{2\pi}{\lambda_t} R \tag{10.30}$$

is the phase of the radiated wave relative to its phase at $R = 0$ and to a reference time $t = 0$. If the source is moving toward the receiver, as in Fig. 10-16, (or vice versa) at a radial velocity u_r, then

$$R = R_0 - u_r t, \tag{10.31}$$

where R_0 is the distance between the source and the receiver at $t = 0$. Hence,

$$\phi = 2\pi f_t t - \frac{2\pi}{\lambda_t}(R_0 - u_r t). \tag{10.32}$$

This is the phase of the signal detected by the receiver. The frequency of a wave is by definition equal to the time derivative of the phase ϕ divided by 2π. Thus,

$$f_r = \frac{1}{2\pi}\frac{d\phi}{dt} = f_t + \frac{u_r}{\lambda_t}. \tag{10.33}$$

Comparison of Eq. (10.33) with Eq. (10.28) leads to $f_d = u_r/\lambda_t$. For radar, the Doppler shift happens twice, once for the wave from the radar to the target and again

INTEL-1014
U.S. Patent 7,151,430

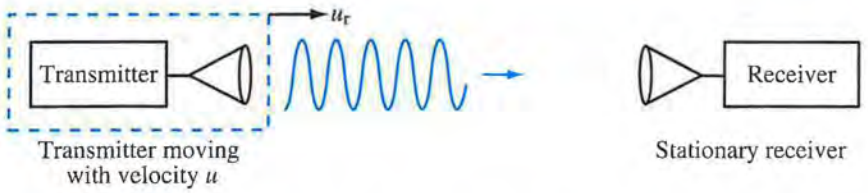


Figure 10-16: Transmitter with radial velocity u_r approaching a stationary receiver.

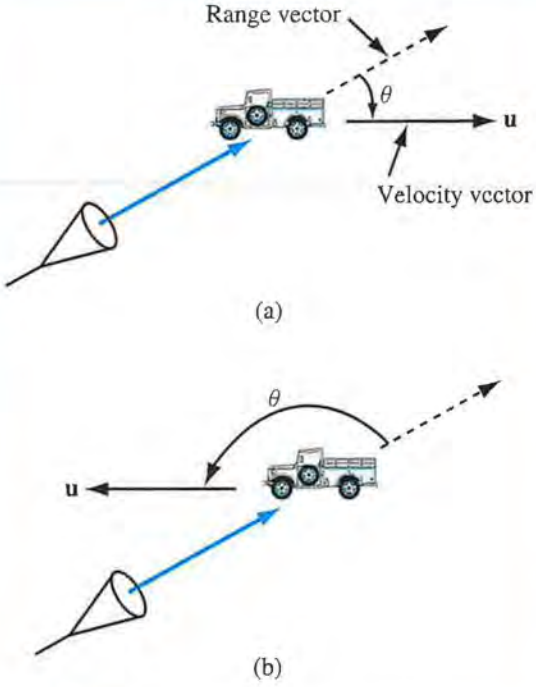


Figure 10-17: The Doppler frequency shift is negative for a receding target ($0 \le \theta \le 90°$), as in (a), and positive for an approaching target ($90° \le \theta \le 180°$), as in (b).

for the wave reflected by the target back to the radar. Hence, $f_d = 2u_r/\lambda_t$. The dependence of f_d on direction is given by the dot product of the velocity and range unit vectors, which leads to

$$f_d = -2\frac{u_r}{\lambda_t} = -\frac{2u}{\lambda_t}\cos\theta, \qquad (10.34)$$

where u_r is the radial velocity component of u and θ is the angle between the range vector and the velocity vector as shown in Fig. 10-17, with the direction of the range vector defined *from* the radar *to* the target. For a receding target (relative to the radar), $0 \le \theta \le 90°$, and for an approaching target, $90 \le \theta \le 180°$.

10-8 Monopulse Radar

On the basis of information extracted from the echo due to a single pulse, a ***monopulse radar*** can track the direction of a target with an angular accuracy equal to a fraction of its antenna beamwidth. To track a target in both elevation and azimuth, a monopulse radar uses an antenna such as a parabolic dish, with four separate small feeds at its focal point, as illustrated by the horns shown in Fig. 10-18. Monopulse systems are of two types; the first is called ***amplitude-comparison monopulse*** because the tracking information is extracted from the amplitudes of the echoes received by the four horns, and the second type is called ***phase-comparison monopulse*** because it relies on the phases of the received signals instead. We shall limit our present discussion to the amplitude-comparison scheme.

INTEL-1014
U.S. Patent 7,151,430

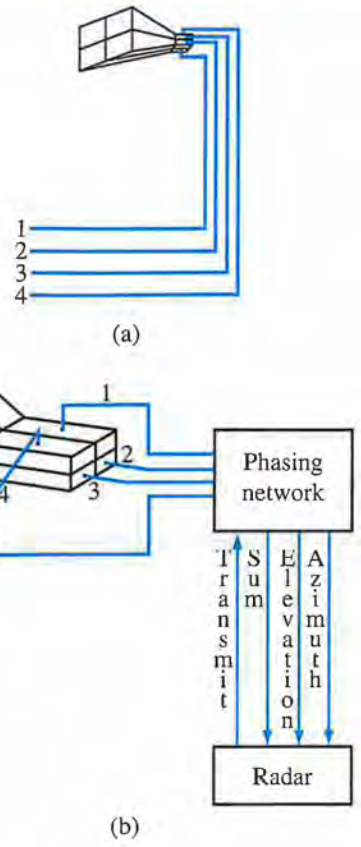


Figure 10-18: Antenna feeding arrangement for an amplitude-comparison monopulse radar: (a) feed horns and (b) connection to phasing network.

Individually, each horn would produce its own beam, with the four beams pointing in slightly different directions. Figure 10-19 shows the beams of two adjacent horns. The basic principle of the amplitude-comparison monopulse is to measure the amplitudes of the echo signals received through the two beams and then to apply the difference between them to repoint the antenna boresight direction toward the target. Using

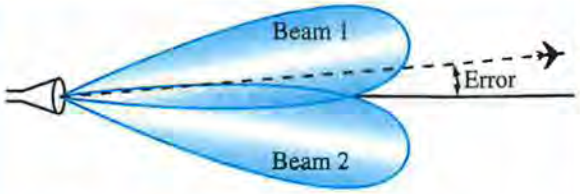


Figure 10-19: A target observed by two overlapping beams of a monopulse radar.

computer-controlled phase shifters, the ***phasing network*** shown in Fig. 10-18 can combine the signal delivered to the four-element horn array by the transmitter or by the echo signals received by them in different ways. Upon transmission, the network excites all four feeds in phase, thereby producing a single main beam called the ***sum beam***. The phasing network uses special microwave devices that allow it to provide the desired functionality during both the transmit and receive modes. Its equivalent functionality is described by the circuits shown in Fig. 10-20. During the receive period, the phasing network uses power dividers, power combiners, and phase shifters so as to generate three different output channels. One of these is the sum channel, corresponding to adding all four horns in phase, and its radiation pattern is depicted in Fig. 10-21(a). The second channel, called the ***elevation-difference channel***, is obtained by first adding the outputs of the top-right and top-left horns [Fig. 10-20(b)], then adding the outputs of the bottom-right and bottom-left horns, and then subtracting the second sum from the first. The subtraction process is accomplished by adding a 180° phase shifter in the path of the second sum before adding it to the first sum. The beam pattern of the elevation-difference channel is shown in Fig. 10-21(b). The third channel (not shown in Fig. 10-20) is the ***azimuth-difference channel***, and it is accomplished through a similar process that generates a beam corresponding to the difference between the

INTEL-1014
U.S. Patent 7,151,430

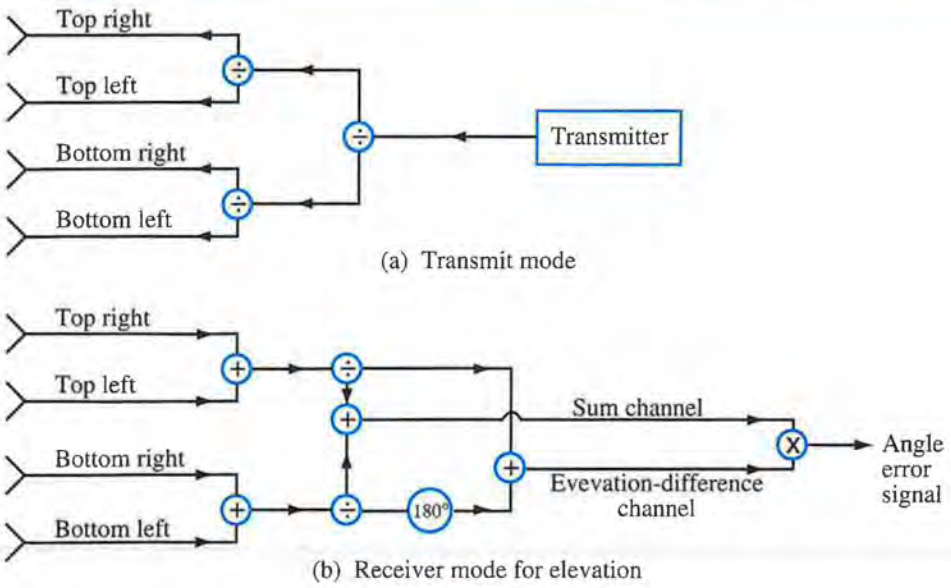


Figure 10-20: Functionality of the phasing network in (a) the transmit mode and (b) the receive mode for the elevation-difference channel.

sum of the two right horns and the sum of the two left horns. If the observed target is centered between the two elevation beams, the receiver echoes will have the same strength for both beams, thereby producing a zero output from the elevation-difference channel. If it is not, the amplitude of the elevation-difference channel will be proportional to the angular deviation of the target from the boresight direction, and its sign will denote the direction of the deviation. In practice, the output of the difference channel is multiplied by the output of the sum channel to increase the strength of the difference signal and to provide a phase reference for extracting the sign of the angle error. This product, called the ***angle error signal***, is displayed in Fig. 10-21(c) as a function of the angle error. The error signal activates a servo-control system to reposition the antenna direction. By applying a similar procedure along the azimuth direction using the product of the azimuth-difference channel and the sum channel, a monopulse radar provides automatic tracking in both directions. The range to the target is obtained by measuring the round-trip delay of the signal.

REVIEW QUESTIONS

Q10.5 How is the PRF related to unambiguous range?

Q10.6 Explain how the false-alarm probability and the detection probability are related to the noise level of the receiver.

Q10.7 In terms of the geometry shown in Fig. 10-17, when is the Doppler shift a maximum?

Q10.8 What is the principle of the monopulse radar?

INTEL-1014
U.S. Patent 7,151,430

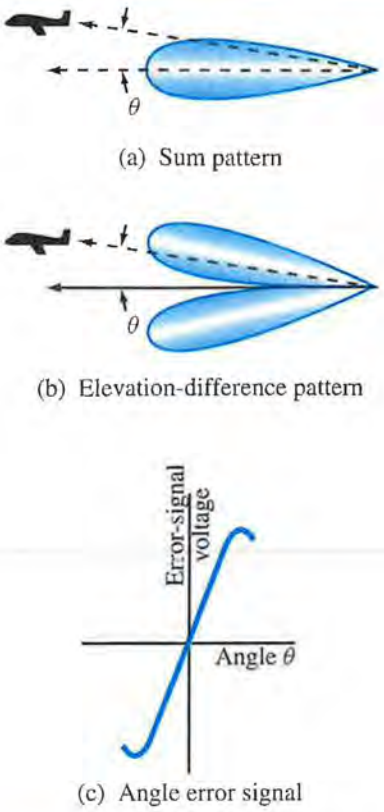


Figure 10-21: Monopulse antenna (a) sum pattern, (b) elevation-difference pattern, and (c) angle error signal.

CHAPTER HIGHLIGHTS

- Three equally spaced satellites in geostationary orbit can provide coverage of most of Earth's surface.
- The use of polarization diversity makes it possible to double the number of channels per unit bandwidth carried by a satellite repeater.
- A satellite antenna system is designed to produce beams tailored to match the areas served by the satellite. Antenna arrays are particularly suitable for this purpose.
- A radar is an electromagnetic sensor that illuminates a region of space and then measures the echoes due to reflecting objects. From the echoes, information can be extracted about the range of a target, its radial velocity, direction of motion, and other characteristics.
- Due to the random nature of the receiver noise, target detection is a statistical process characterized by false-alarm and detection probabilities.
- A moving object produces a Doppler frequency shift that is proportional to the radial velocity of the object relative to the radar and inversely proportional to λ.
- A monopulse radar uses multiple beams to track the direction of a target, with an angular accuracy equal to a fraction of its antenna beam.

GLOSSARY OF IMPORTANT TERMS

Provide definitions or explain the meaning of the following terms:

geostationary orbit
uplink and downlink
transponder
duplexer
circulator
multiplexer
polarization diversity
atmospheric transmissivity Υ
radial velocity u_r
Doppler frequency shift f_d
pulse length τ
pulse repetition frequency (PRF) f_p
interpulse period T_p
unambiguous range R_u
range resolution
azimuth resolution
false-alarm probability
detection probability
matched filter

INTEL-1014
U.S. Patent 7,151,430

bistatic radar
monostatic radar
radar cross section σ_t
threshold detection level
maximum detectable range R_{max}
monopulse radar
sum and difference channels

PROBLEMS

Sections 10-1 to 10-4: Satellite Communication Systems

10.1* A remote sensing satellite is in circular orbit around Earth at an altitude of 1,000 km above Earth's surface. What is its orbital period?

10.2 A transponder with a bandwidth of 500 MHz uses polarization diversity. If the bandwidth allocated to transmit a single telephone channel is 4 kHz, how many telephone channels can be carried by the transponder?

10.3* Repeat Problem 10.2 for TV channels, each requiring a bandwidth of 6 MHz.

10.4 A geostationary satellite is at a distance of 40,000 km from a ground receiving station. The satellite transmitting antenna is a circular aperture with a 1-m diameter, and the ground station uses a parabolic dish antenna with an effective diameter of 30 cm. If the satellite transmits 1 kW of power at 12 GHz and the ground receiver is characterized by a system noise temperature of 1,000 K, what would be the signal-to-noise ratio of a received TV signal with a bandwidth of 6 MHz? The antennas and the atmosphere may be assumed lossless.

Sections 10-5 to 10-8: Radar Sensors

10.5* A collision avoidance automotive radar is designed to detect the presence of vehicles up to a range of 1 km. What is the maximum usable PRF?

10.6 A 10-GHz weather radar uses a 30-cm-diameter lossless antenna. At a distance of 1 km, what are the dimensions of the volume resolvable by the radar if the pulse length is 1 μs?

10.7* A radar system is characterized by the following parameters: $P_t = 1$ kW, $\tau = 0.1$ μs, $G = 30$ dB, $\lambda = 3$ cm, and $T_{sys} = 1,500$ K. The radar cross section of a car is typically 10 m^2. How far away can the car be and remain detectable by the radar with a minimum signal-to-noise ratio of 13 dB?

10.8 A 3-cm-wavelength radar is located at the origin of an x–y coordinate system. A car located at $x = 100$ m and $y = 200$ m is heading east (x-direction) at a speed of 120 km/hr. What is the Doppler frequency measured by the radar?

*Answer(s) available in Appendix D.
Solution available in CD-ROM.

INTEL-1014
U.S. Patent 7,151,430

APPENDIX A: SYMBOLS, QUANTITIES, AND UNITS

Symbol	Quantity	SI Unit	Abbreviation
A	Magnetic potential (vector)	weber/meter	Wb/m
B	Susceptance	siemens	S
B	Magnetic flux density	tesla or weber/meter^2	T or W/m^2
C	Capacitance	farad	F
D	Directivity (antenna)	(dimensionless)	—
E	Electric-field intensity	volt/meter	V/m
D	Electric flux density	coulomb/meter^2	C/m^2
F	Radiation intensity (normalized)	(dimensionless)	—
F	Force	newton	N
f	Focal length	meter	m
f	Frequency	hertz	Hz
G	Conductance	siemens	S
G	Gain (power)	(dimensionless)	—
H	Magnetic field intensity	ampere/meter	A/m
I	Current	ampere	A
J	Current density (volume)	ampere/meter^2	A/m^2
$\mathbf{J}_s$	Current density (surface)	ampere/meter	A/m
k	Wavenumber	radian/meter	rad/m
L	Inductance	henry	H
l	Length	meter	m
M, m	Mass	kilogram	kg
M	Magnetization vector	ampere/meter	A/m
m	Magnetic dipole moment	ampere-meter^2	A·m^2
n	Index of refraction	(dimensionless)	—
P	Power	watt	W
P	Electric polarization vector	coulomb/meter^2	C/m^2
p	Pressure	newton/meter^2	N/m^2
p	Electric dipole moment	coulomb-meter	C·m
Q, q	Charge	coulomb	C
R	Reflectivity (reflectance)	(dimensionless)	—
R	Resistance	ohm	Ω
S	Standing-wave ratio	(dimensionless)	—
S	Poynting vector	watt/meter^2	W/m^2
$\mathbf{S}_{av}$	Power density	watt/meter^2	W/m^2
T	Temperature	kelvin	K

INTEL-1014
U.S. Patent 7,151,430

Symbol	Quantity	SI Unit	Abbreviation
T	Torque	newton-meter	N·m
T	Transmissivity (transmittance)	(dimensionless)	—
t	Time	second	s
$\mathbf{u}$	Velocity	meter/second	m/s
V	Electric potential	volt	V
V	Voltage	volt	V
V_{emf}	Electromotive force (emf)	volt	V
W	Energy (work)	joule	J
w	Energy density	joule/meter^3	J/m^3
X	Reactance	ohm	Ω
Y	Admittance	siemens	S
Z	Impedance	ohm	Ω
α	Attenuation constant	neper/meter	Np/m
β	Phase constant	radian/meter	rad/m
Γ	Reflection coefficient	(dimensionless)	—
γ	Propagation constant	meter^{-1}	m^{-1}
δ_s	Skin depth	meter	m
ε, ε_0	Permittivity	farad/meter	F/m
ε_r	Relative permittivity	(dimensionless)	—
η	Impedance	ohm	Ω
λ	Wavelength	meter	m
μ, μ_0	Permeability	henry/meter	H/m
μ_r	Relative permeability	(dimensionless)	—
μ_e, μ_h	Mobility (electron, hole)	meter^2/volt·second	m^2/V·s
ρ_l	Charge density (linear)	coulomb/meter	C/m
ρ_s	Charge density (surface)	coulomb/meter^2	C/m^2
ρ_v	Charge density (volume)	coulomb/meter^3	C/m^3
σ	Conductivity	siemens/meter	S/m
σ_t	Radar cross section	meter^2	m^2
τ	Transmission coefficient	(dimensionless)	—
τ	Pulse length	seconds	s
Φ	Magnetic flux	weber	Wb
ψ	Gravitational field	newton/kilogram	N/kg
χ_e	Electric susceptibility	(dimensionless)	—
χ_m	Magnetic susceptibility	(dimensionless)	—
Ω	Solid angle	steradian	sr
ω	Angular frequency	radian/second	rad/s

INTEL-1014
U.S. Patent 7,151,430

APPENDIX B: MATERIAL CONSTANTS OF SOME COMMON MATERIALS

Table B-1: RELATIVE PERMITTIVITY ε_r OF COMMON MATERIALS[a]

$\varepsilon = \varepsilon_r \varepsilon_0$ and $\varepsilon_0 = 8.854 \times 10^{-12}$ F/m.

Material	Relative Permittivity, ε_r	Material	Relative Permittivity, ε_r
Vacuum	1	Dry soil	2.5–3.5
Air (at sea level)	1.0006	Plexiglass	3.4
Styrofoam	1.03	Glass	4.5–10
Teflon	2.1	Quartz	3.8–5
Petroleum oil	2.1	Bakelite	5
Wood (dry)	1.5–4	Porcelain	5.7
Paraffin	2.2	Formica	6
Polyethylene	2.25	Mica	5.4–6
Polystyrene	2.6	Ammonia	22
Paper	2–4	Seawater	72–80
Rubber	2.2–4.1	Distilled water	81

[a]These are low-frequency values at room temperature (20° C).

Note: For most metals, $\varepsilon_r \simeq 1$.

Table B-2: CONDUCTIVITY σ OF SOME COMMON MATERIALS[a]

Material	Conductivity, σ (S/m)	Material	Conductivity, σ (S/m)
Conductors		*Semiconductors*	
Silver	6.2×10^7	Pure germanium	2.2
Copper	5.8×10^7	Pure silicon	4.4×10^{-4}
Gold	4.1×10^7	*Insulators*	
Aluminum	3.5×10^7	Wet soil	$\sim 10^{-2}$
Tungsten	1.8×10^7	Fresh water	$\sim 10^{-3}$
Zinc	1.7×10^7	Distilled water	$\sim 10^{-4}$
Brass	1.5×10^7	Dry soil	$\sim 10^{-4}$
Iron	10^7	Glass	10^{-12}
Bronze	10^7	Hard rubber	10^{-15}
Tin	9×10^6	Paraffin	10^{-15}
Lead	5×10^6	Mica	10^{-15}
Mercury	10^6	Fused quartz	10^{-17}
Carbon	3×10^4	Wax	10^{-17}
Seawater	4		
Animal body (average)	0.3 (poor cond.)		

[a]These are low-frequency values at room temperature (20° C).

INTEL-1014
U.S. Patent 7,151,430

Table B-3: RELATIVE PERMEABILITY μ_r OF SOME COMMON MATERIALS[a]

$\mu = \mu_r\mu_0$ and $\mu_0 = 4\pi \times 10^{-7}$ H/m.

Material	Relative Permeability, μ_r
Diamagnetic	
Bismuth	$0.99983 \simeq 1$
Gold	$0.99996 \simeq 1$
Mercury	$0.99997 \simeq 1$
Silver	$0.99998 \simeq 1$
Copper	$0.99999 \simeq 1$
Water	$0.99999 \simeq 1$
Paramagnetic	
Air	$1.000004 \simeq 1$
Aluminum	$1.00002 \simeq 1$
Tungsten	$1.00008 \simeq 1$
Titanium	$1.0002 \simeq 1$
Platinum	$1.0003 \simeq 1$
Ferromagnetic (nonlinear)	
Cobalt	250
Nickel	600
Mild steel	2,000
Iron (pure)	4,000–5,000
Silicon iron	7,000
Mumetal	$\sim 100,000$
Purified iron	$\sim 200,000$

[a]These are typical values; actual values depend on material variety.

Note: Except for ferromagnetic materials, $\mu_r \simeq 1$ for all dielectrics and conductors.

INTEL-1014
U.S. Patent 7,151,430

APPENDIX C: MATHEMATICAL FORMULAS

Trigonometric Relations

$$\sin(x \pm y) = \sin x \cos y \pm \cos x \sin y$$

$$\cos(x \pm y) = \cos x \cos y \mp \sin x \sin y$$

$$2 \sin x \sin y = \cos(x - y) - \cos(x + y)$$

$$2 \sin x \cos y = \sin(x + y) + \sin(x - y)$$

$$2 \cos x \cos y = \cos(x + y) + \cos(x - y)$$

$$\sin 2x = 2 \sin x \cos x$$

$$\cos 2x = 1 - 2 \sin^2 x$$

$$\sin x + \sin y = 2 \sin\left(\frac{x+y}{2}\right) \cos\left(\frac{x-y}{2}\right)$$

$$\sin x - \sin y = 2 \cos\left(\frac{x+y}{2}\right) \sin\left(\frac{x-y}{2}\right)$$

$$\cos x + \cos y = 2 \cos\left(\frac{x+y}{2}\right) \cos\left(\frac{x-y}{2}\right)$$

$$\cos x - \cos y = -2 \sin\left(\frac{x+y}{2}\right) \sin\left(\frac{x-y}{2}\right)$$

$$\cos(x \pm 90°) = \mp \sin x$$

$$\cos(-x) = \cos x$$

$$\sin(x \pm 90°) = \pm \cos x$$

$$\sin(-x) = -\sin x$$

$$e^{jx} = \cos x + j \sin x \qquad \text{(Euler's identity)}$$

$$\sin x = \frac{e^{jx} - e^{-jx}}{2j}$$

$$\cos x = \frac{e^{jx} + e^{-jx}}{2}$$

Approximations for Small Quantities

For $|x| \ll 1$,

$$(1 \pm x)^n \simeq 1 \pm nx$$

$$(1 \pm x)^2 \simeq 1 \pm 2x$$

$$\sqrt{1 \pm x} \simeq 1 \pm \frac{x}{2}$$

$$\frac{1}{\sqrt{1 \pm x}} \simeq 1 \mp \frac{x}{2}$$

$$e^x = 1 + x + \frac{x^2}{2!} + \cdots \simeq 1 + x$$

$$\ln(1 + x) \simeq x$$

$$\sin x = x - \frac{x^3}{3!} + \frac{x^5}{5!} + \cdots \simeq x$$

$$\cos x = 1 - \frac{x^2}{2!} + \frac{x^4}{4!} + \cdots \simeq 1 - \frac{x^2}{2}$$

$$\lim_{x \to 0} \frac{\sin x}{x} = 1$$

INTEL-1014
U.S. Patent 7,151,430

[redacted]

APPENDIX D: ANSWERS TO ODD-NUMBERED PROBLEMS

Chapter 1

1.1 $p(x,t) = 24\cos(8\pi \times 10^3 t - 24.24\pi x + 42°)$ (N/m^2)

1.3 $\lambda = 12.5$ cm

1.5 $u_p = 0.83$ (m/s); $\lambda = 10.47$ m

1.7 (a) $y_1(x,t)$ is traveling in positive x-direction, while $y_2(x,t)$ is traveling in negative x-direction.
(b) $x = (\pi/60 + 2n\pi/30)$ cm; $|y_s|_{max} = 1.9$
(c) $x = n\pi/30$; $|y_s|_{min} = 0$

1.9 $T = 1.5$ s; $u_p = 0.56$ m/s; $\lambda = 0.84$ m

1.11 $y_2(t)$ lags $y_1(t)$ by 60°.

1.13 $\alpha = 5 \times 10^{-3}$ (Np/m)

1.15 (a) $z_1 = 3.6e^{-j33.7°}$; $z_2 = 4.5e^{j153.4°}$
(b) $|z_1| = 3.60$
(c) $z_1 z_2 = 16.2e^{j119.7°}$
(d) $z_1/z_2 = 0.80e^{-j187.1°}$
(e) $z_1^3 = 46.66e^{-j101.1°}$

1.17 (a) $t = 3.16\,e^{j18.43°}$; $s = 5.10\,e^{j78.69°}$
(b) $t = 2.83\,e^{-j45°}$; $s = 2.83\,e^{j45°}$
(c) $t = 5.2$; $s = 3\,e^{j90°}$
(d) $t = 0$; $s = 6\,e^{j30°}$

1.19 $\ln(z) = 1.61 - j0.93$

1.21 $v_c(t) = 8.5\cos(2\pi \times 10^3 t - 62.1°)$ V

1.23 (a) $v(t) = 3\cos(\omega t - 2\pi/3)$ V
(b) $v(t) = 6\cos(\omega t + 3\pi/4)$ V
(c) $i(t) = 5\cos(\omega t + 53.1°)$ A
(d) $i(t) = 3.61\cos(\omega t + 146.31°)$ A
(e) $i(t) = -\sin\omega t$ A
(f) $i(t) = 2\cos(\omega t + 3\pi/4)$ A

Chapter 2

2.1 (a) $l/\lambda = 6.67 \times 10^{-6}$; transmission line may be ignored.
(b) $l/\lambda = 0.01$; borderline.
(c) $l/\lambda = 0.2$; transmission line effects should be included.
(d) $l/\lambda = 0.33$; transmission line effects should be included.

2.3 $R' = 1.0$ (Ω/m); $L' = 167$ (nH/m); $G' = 0$; $C' = 172$ (pF/m)

2.5 $\alpha = 0.14$ Np/m; $\beta = 31.5$ rad/m; $Z_0 = (27.7 + j0.098)$ Ω; $u_p = 2 \times 10^8$ m/s

2.7 $R' = 2$ (Ω/m); $L' = 200$ (nH/m); $G' = 800$ (μS/m); $C' = 80$ (pF/m); $\lambda = 1$ m

2.9 $R' = 0.8$ Ω/m; $L' = 38.2$ nH/m; $G' = 0.5$ mS/m; $C' = 23.9$ pF/m

2.11 (a) $b = 3.5$ mm
(b) $u_p = 1.98 \times 10^8$ m/s

2.13 $Z_L = (90 - j120)$ Ω

2.15 $Z_0 = 55.9$ Ω

2.17 $Z_{in} = (60 + j20)$ Ω

2.21 (a) $\Gamma = 0.62e^{-j29.7°}$
(b) $Z_{in} = (12.5 - j12.7)$ Ω
(c) $\tilde{V}_i = 1.40e^{-j34.0°}$ (V); $\tilde{I}_i = 78.4e^{-j11.5°}$ (mA)

2.23 (a) $Z_{in_1} = (35.20 - j8.62)$ Ω
(b) $Z'_L = (17.6 - j4.31)$ Ω
(c) $Z_{in} = (107.57 - j56.7)$ Ω

2.25 $l = \lambda/4 + n\lambda/2$

2.27 $Z_{in} = 240$ Ω

2.29 $l = 0.29\lambda$

2.31 (a) $Z_{in} = (41.25 - j16.35)$ Ω

INTEL-1014
U.S. Patent 7,151,430

(b) $\widetilde{I}_i = 1.08\,e^{j10.16°}$ A; $\widetilde{V}_i = 47.86\,e^{-j11.46°}$ V
(c) $P_{in} = 24$ W
(d) $\widetilde{V}_L = 60e^{-j54°}$ V; $\widetilde{I}_L = 0.8\,e^{-j54°}$ A; $P_L = P_{in} = 24$ W
(e) $P_{Z_g} = 29.15$ W; $P_g = 53.15$ W

2.33 $P_{av}^{i} = 10.0$ mW; $P_{av}^{r} = -1.1$ mW; $P_{av}^{t} = 8.9$ mW

2.35 (a) $\Gamma = 0.5$
(b) $\Gamma = 0.62\angle -29.7°$
(c) $\Gamma = 1.0\angle -53.1°$
(d) $\Gamma = 1.0\angle 180°$

2.37 $Z_{01} = 40\ \Omega$; $Z_{02} = 250\ \Omega$

2.39 (a) $Z_{in} = -j154\ \Omega$
(b) $0.074\lambda + (n\lambda/2)$, $n = 0, 1, 2, \ldots$

2.41 (a) $Z_L + j95\ \Omega$
(b) $l = 0.246\lambda$

2.43 $Z_L = (41 - j19.5)\ \Omega$

2.45 $Z_{in} = (95 - j70)\ \Omega$

2.47 First solution: Stub at $d = 0.199\lambda$ from antenna and stub length $l = 0.125\lambda$. Second solution: $d = 0.375\lambda$ from antenna and stub length $l = 0.375\lambda$.

2.49 $Z_{in} = 100\ \Omega$

2.53 $V_g = 19.2$ V; $R_g = 30\ \Omega$; $l = 525$ m

Chapter 3

3.1 $\hat{\mathbf{a}} = 0.45 + \hat{\mathbf{z}}0.89$

3.3 Area $= 9$

3.5 (a) $A = \sqrt{14}$; $\hat{\mathbf{a}}_A = (\hat{\mathbf{x}} + \hat{\mathbf{y}}2 - \hat{\mathbf{z}}3)/\sqrt{14}$
(b) $-12/5$
(c) $\theta_{AC} = 15.8°$
(d) $\mathbf{A} \times \mathbf{C} = \hat{\mathbf{x}} + \hat{\mathbf{y}}4 + \hat{\mathbf{z}}3$
(e) $\mathbf{A} \cdot (\mathbf{B} \times \mathbf{C}) = 13$
(f) $\mathbf{A} \times (\mathbf{B} \times \mathbf{C}) = \hat{\mathbf{x}}54 - \hat{\mathbf{y}}57 - \hat{\mathbf{z}}20$
(g) $\hat{\mathbf{x}} \times \mathbf{B} = -\hat{\mathbf{z}}4$
(h) $(\mathbf{A} \times \hat{\mathbf{y}}) \cdot \hat{\mathbf{z}} = 1$

3.7 $\dfrac{\mathbf{A}(1,-1,2)}{|\mathbf{A}(1,-1,2)|} = -\hat{\mathbf{x}}0.17 - \hat{\mathbf{y}}0.70 + \hat{\mathbf{z}}0.70$

3.9 $\hat{\mathbf{a}} = -(+\hat{\mathbf{y}}\,y + \hat{\mathbf{z}}2)/(5 + y^2)^{1/2}$

3.11 $\hat{\mathbf{a}} = (2 + \hat{\mathbf{z}}4)/\sqrt{20}$

3.13 $\mathbf{A} = 0.8 + \hat{\mathbf{y}}1.6$

3.15 $= 0.37 + \hat{\mathbf{y}}0.56 + \hat{\mathbf{z}}0.74$

3.19 (a) $P_1 = (2.24, 63.4°, 0)$ in cylindrical; $P_1 = (2.24, 90°, 63.4°)$ in spherical
(b) $P_2 = (0, 0°, 3)$ in cylindrical; $P_2 = (3, 0°, 0°)$ in spherical
(c) $P_3 = (1.41, 45°, 2)$ in cylindrical; $P_3 = (2.45, 35.3°, 45°)$ in spherical
(d) $P_4 = (4.24, 135°, -3)$ in cylindrical; $P_4 = (5.2, 125.3°, 135°)$ in spherical

3.21 (a) $P_1(0, 0, 5)$
(b) $P_2(0, \pi, 5)$
(c) $P_3(3, \pi, 0)$

3.23 (a) $V = 21\pi/2$
(b) $V = 125\pi/3$

3.25 (a) $\mathbf{E}_n = -\hat{\mathbf{r}}\,4$
(b) $\mathbf{E}_t = \hat{\mathbf{z}}\,4$

3.27 (a) $\theta_{AB} = 90°$
(b) $\pm(\hat{\mathbf{r}}\,0.487 + \hat{\boldsymbol{\phi}}\,0.228 + \hat{\mathbf{z}}\,0.843)$

3.29 (a) $d = \sqrt{2}$
(b) $d = 2.67$
(c) $d = 5$

3.31 (a) $\mathbf{A}(P_1) = \hat{\mathbf{R}}2.856 - \hat{\boldsymbol{\theta}}2.888 + \hat{\boldsymbol{\phi}}2.123$
(b) $\mathbf{B}(P_2) = -\hat{\mathbf{R}}0.896 + \hat{\boldsymbol{\theta}}0.449 - \hat{\boldsymbol{\phi}}5$
(c) $\mathbf{C}(P_3) = \hat{\mathbf{R}}0.854 + \hat{\boldsymbol{\theta}}0.146 - \hat{\boldsymbol{\phi}}0.707$
(d) $\mathbf{D}(P_4) = \hat{\mathbf{R}}3.67 - \hat{\boldsymbol{\theta}}1.73 - \hat{\boldsymbol{\phi}}0.707$

3.33 $T(z) = 10 + (1 - e^{-2z})/2$

3.35 $dV/dl = -3/\sqrt{5}$

3.37 $dU/dl = -3.125 \times 10^{-2}$

3.39 (a) $\oint \mathbf{E} \cdot d\mathbf{s} = -8/3$
(b) $\iiint \nabla \cdot \mathbf{E}\, dv = -8/3$

3.41 (a) $\oint \mathbf{D} \cdot d\mathbf{s} = 150\pi$

INTEL-1014
U.S. Patent 7,151,430

(b) $\iiint \nabla \cdot \mathbf{D}\, dv = 150\pi$

3.43 (a) $\oint E \cdot d\mathbf{l} = -1$

(b) $\iint \nabla \times \mathbf{E} \cdot d\mathbf{s} = -1$

3.45 (a) $\oint_C \mathbf{B} \cdot d\mathbf{l} = 8$

(b) $\int_S (\nabla \times \mathbf{B}) \cdot d\mathbf{s} = 8$

3.48 (a) **A** is solenoidal, but not conservative.
(b) **B** is conservative, but not solenoidal.
(c) **C** is neither solenoidal nor conservative.
(d) **D** is conservative, but not solenoidal.
(e) **E** is conservative, but not solenoidal.
(f) **F** is conservative and solenoidal.
(g) **G** is neither conservative nor solenoidal.
(h) **H** is conservative, but not solenoidal.

Chapter 4

4.1 $Q = 2.62$ (mC)

4.3 $Q = 0.173$ C

4.5 (a) $Q = 0$
(b) $Q = \pi a^2 \rho_{s0}/2$
(c) $Q = 2\pi\rho_{s0}[1 - e^{-a}(1 + a)]$
(d) $Q = \pi\rho_{s0}[1 - e^{-a}(1 + a)]$

4.7 $I = 1,570.8$ A

4.9 $\mathbf{E} = \hat{\mathbf{z}}\, 25.61$ kV/m

4.11 $q_2 = -63.13$ (μC)

4.13 $\mathbf{E}(0, 0, z) = \dfrac{706(-\hat{\mathbf{r}}0.02 + \hat{\mathbf{z}}z)}{(4 \times 10^{-4} + z^2)^{3/2}}$ (V/m)

(a) $\mathbf{E}(0, 0, 0) = -\hat{\mathbf{r}}1.76$ (MV/m)
(b) $\mathbf{E}(0, 0, 5\text{ cm}) = -\hat{\mathbf{r}}90.4 + \hat{\mathbf{z}}226$ (kV/m)
(c) $\mathbf{E}(0, 0, -5\text{ cm}) = -\hat{\mathbf{r}}90.4 - \hat{\mathbf{z}}226$ (kV/m)

4.15 $\mathbf{E} = \hat{\mathbf{z}}\,(\rho_{s0}h/2\varepsilon_0)[\sqrt{a^2 + h^2} + h^2/\sqrt{a^2 + h^2} - 2h]$

4.17 $\mathbf{E} = 0$

4.21 (a) $\rho_v = y^2 z^3$
(b) $Q = 64/3$ (C)
(c) $Q = 64/3$ (C)

4.23 $Q = 4\pi\rho_0 a^3$ (C)

4.25 $\mathbf{D} = \hat{\mathbf{r}}\,\rho_{v0}(r^2 - 1)/2r$, for $1 \le r \le 3$ m
$\mathbf{D} = \hat{\mathbf{r}}\,4\rho_{v0}/r$, for $r \ge 3$ m

4.29 (b) $\mathbf{E} = \hat{\mathbf{z}}(\rho_l a/2\varepsilon_0)[z/(a^2 + z^2)^{3/2}]$ (V/m)

4.31 $V(b) = (\rho_l/4\pi\varepsilon)$
$\times \ln[(l + \sqrt{l^2 + 4b^2})/(-l + \sqrt{l^2 + 4b^2})]$ (V)

4.35 $V_{AB} = -78.06$ V

4.37 (a) $\sigma = 4.32 \times 10^{-4}$ (S/m)
(b) $I = 542.9$ (nA)
(c) $\mathbf{u}_e = -13\mathbf{E}/|\mathbf{E}|$ (m/s); $\mathbf{u}_h = 5\mathbf{E}/|\mathbf{E}|$ (m/s)
(d) $R = 9.21$ (MΩ)
(e) $P = 2.7(\mu$W)

4.41 $R = 2.1$ (mΩ)

4.43 $\theta = 42°$

4.45 $\mathbf{E}_1 = \hat{\mathbf{R}}6\cos\theta - \hat{\boldsymbol{\theta}}3\sin\theta$ (V/m);
$\mathbf{D}_1 = \varepsilon_0(\hat{\mathbf{R}}18\cos\theta - \hat{\boldsymbol{\theta}}9\sin\theta)$ (C/m^2)

4.47 $\theta_1 = 71.6°$; $\theta_2 = 78.7°$; $\theta_3 = 81.9°$; $\theta_4 = 45°$

4.49 (a) $|E|$ is maximum at $r = a$.
(b) Breakdown voltage for the capacitor is $V = 1.39$ (MV).

4.51 $W_e = 4.62 \times 10^{-9}$ (J)

4.53 (a) $C = 3.1$ pF
(b) $C = 0.5$ pF
(c) $C = 0.31$ pF

Chapter 5

5.1 $\mathbf{a} = -\hat{\mathbf{y}}2.1 \times 10^{18}$ (m/s^2)

5.3 $|\mathbf{B}| = 410$ (mT)

5.5 (a) $\mathbf{F} = -1.41$ N
(b) $W = 0$
(c) $\phi = 0$

5.7 $\mathbf{B} = -\hat{\mathbf{z}}0.3$ (mT)

INTEL-1014
U.S. Patent 7,151,430

5.9 $\mathbf{H} = \hat{\mathbf{z}}\dfrac{I\theta(b-a)}{4\pi ab}$, with $\hat{\mathbf{z}}$ being out of the page

5.11 $I_2 = 0.8$ A; direction is clockwise, as seen from above.

5.13 $I = 320$ A

5.15 $\mathbf{F} = -\hat{\mathbf{x}}0.1$ (mN), where $\hat{\mathbf{x}}$ is the direction away from the wire, in the plane of the loop. Thus, the force is pulling the loop toward the wire.

5.17 (a) $\mathbf{H}(0, 0, h) = -\hat{\mathbf{x}}\dfrac{I}{\pi w}\tan^{-1}\left(\dfrac{w}{2h}\right)$ (A/m)

(b) $\mathbf{F}'_{\mathrm{m}} = \hat{\mathbf{z}}\dfrac{I^2\mu_0}{\pi w}\tan^{-1}\left(\dfrac{w}{2h}\right)$ (N)
Force is repulsive.

5.19 $\mathbf{F} = \hat{\mathbf{y}}\,4 \times 10^{-5}$ N

5.21 (a) $\mathbf{H}_1 = \hat{\boldsymbol{\phi}}J_0$ for $0 \le r \le a$
(b) $\mathbf{H}_2 = \hat{\boldsymbol{\phi}}J_0(a/r)$ for $r \ge a$

5.23 $\mathbf{J} = \hat{\mathbf{z}}\,16e^{-2r}$ A/m^2

5.25 (a) $\mathbf{B} = \hat{\mathbf{z}}5\pi \sin \pi y - \hat{\mathbf{y}}\pi \cos \pi x$ (T)
(b) $\Phi = 0$
(c) $\Phi = 0$

5.27 (a) $\mathbf{A} = \mu_0 IL/(4\pi R)$
(b) $\mathbf{H} = (IL/4\pi)[(-y + \hat{\mathbf{y}}\,x)/(x^2 + y^2 + z^2)^{3/2}]$

5.29 $n_{\mathrm{e}} = 1.5$ electrons/atom

5.31 $\mathbf{H}_2 = \hat{\mathbf{z}}\,4$

5.35 $L = (\mu l/\pi)\ln[(d-a)/a]$ (H)

5.37 $W_{\mathrm{m}} = 139I^2$ (nJ)

Chapter 6

6.1 At $t = 0$, current in top loop is momentarily clockwise. At $t = t_1$, current in top loop is momentarily counterclockwise.

6.3 (a) $V_{\mathrm{emf}} = 125e^{-2t}$ (V)
(b) $V_{\mathrm{emf}} = 62.3 \sin 10^3 t$ (kV)
(c) $V_{\mathrm{emf}} = 0$

6.5 $B_0 = 1.06$ (nT)

6.7 $I_{\mathrm{ind}} = 37.7 \sin(200\pi t)$ mA

6.9 $V_{12} = -707$ (μV)

6.11 $V_{12} = -3.77$ V

6.13 $V = \omega B_0 a^2/2$

6.15 $I = 1.63 \cos(120\pi t)$ (μA)

6.19 $\rho_{\mathrm{v}} = (6y/\omega)\sin \omega t + C_0$, where C_0 is a constant of integration.

6.23 $k = (4\pi/30)$ rad/m; $\widetilde{\mathbf{E}} = -\hat{\mathbf{z}}941e^{j4\pi y/30}$ (V/m)

6.25 $\mathbf{H} = \hat{\boldsymbol{\phi}}\frac{53}{R}\sin\theta \cos(6\pi \times 10^8 t - 2\pi R)$ (μA/m)

Chapter 7

7.1 (a) Positive y-direction
(b) $u_{\mathrm{p}} = 2 \times 10^8$ m/s
(c) $\lambda = 1.26$ m
(d) $\varepsilon_{\mathrm{r}} = 2.25$
(e) $\widetilde{\mathbf{E}} = -\hat{\mathbf{x}}12.57e^{-j5y}$ (V/m)

7.3 (a) $\lambda = 31.42$ m
(b) $f = 4.77$ MHz
(c) $\varepsilon_{\mathrm{r}} = 1.67$
(d) $\mathbf{H}(z, t) = \hat{\mathbf{x}}22.13 \cos(9.54\pi \times 10^6 t + 0.2z)$ (mA/m)

7.5 $\varepsilon_{\mathrm{r}} = 4$

7.7 $\mathbf{E} = \sqrt{2}\cos(\pi \times 10^{10}t + 104.72\,z) - \sqrt{2}\sin(\pi \times 10^{10}t + 104.72\,z)$ (V/m)

7.9 $|\mathbf{E}| = 20$; $\psi(t = 0) = 0$; $\psi(t = 5\text{ ns}) = -45°$; $\psi(t = 10\text{ ns}) = -90°$

7.11 (a) $\gamma = 65.5°$ and $\chi = -11.79°$
(b) Right-hand elliptically polarized

7.19 $u_{\mathrm{p}} = 6.28 \times 10^4$ (m/s)

7.21 $\mathbf{H} = -\hat{\mathbf{y}}\,0.16\,e^{-30x}\cos(2\pi \times 10^9 t - 40x - 36.85°)$ (A/m)

7.23 $(R_{\mathrm{ac}}/R_{\mathrm{dc}}) = 143.55$

7.25 $\mathbf{S}_{\mathrm{av}} = \hat{\mathbf{y}}0.12$ (W/m^2)

INTEL-1014
U.S. Patent 7,151,430

7.27 (a) $\mathbf{S}_{av} = \hat{\mathbf{z}}500e^{-0.4z}$ (W/m^2)
(b) $A = -1.74z$ (dB)
(c) $z = 23.03$ m

7.29 $u_p = 6 \times 10^7$ (m/s)

Chapter 8

8.1 (a) $\Gamma = -0.67$; $\tau = 0.33$
(b) $S = 5$
(c) $S_{av}^{i} = 0.13$ (W/m^2); $S_{av}^{r} = 0.06$ (W/m^2); $S_{av}^{t} = 0.07$ (W/m^2)

8.5 (a) $\widetilde{\mathbf{E}}^{i} = 10(\hat{\mathbf{x}} + j\hat{\mathbf{y}})e^{-j4\pi z/3}$ (V/m)
(b) $\Gamma = -0.2$; $\tau = 0.8$
(c) $\widetilde{\mathbf{E}}^{r} = -2(\hat{\mathbf{x}} + j\hat{\mathbf{y}})e^{j4\pi z/3}$ (V/m); $\widetilde{\mathbf{E}}^{t} = 8(\hat{\mathbf{x}} + j\hat{\mathbf{y}})e^{-1.26\times10^{-2}z}e^{-j2\pi z}$ (V/m); $\widetilde{\mathbf{E}}_1 - 10(\hat{\mathbf{x}} + j\hat{\mathbf{y}})[e^{-j4\pi z/3} - 0.2e^{j4\pi z/3}]$ (V/m)
(d) % of reflected power = 4%; % of transmitted power = 96%

8.7 $|\widetilde{\mathbf{E}}_1|_{max} = 51.3$ (V/m); $l_{max} = 1.5$ m

8.9 $\varepsilon_{r_2} = \sqrt{\varepsilon_{r_1}\varepsilon_{r_3}}$; $d = c/[4f(\varepsilon_{r_1}\varepsilon_{r_3})^{1/4}]$

8.11 $Z_{in} \simeq (100 - j127)\ \Omega$; reflected fraction of incident power = 0.24

8.13 $f = 60$ MHz

8.15 $P' = 4.04 \times 10^{-4}$ W/m^2

8.17 $\theta_{min} = 27.92°$

8.19 $\dfrac{S^t}{S^i} = 0.835$

8.21 $d = 15$ cm

8.23 $d = 68.42$ cm

8.25 $f_p = 166.33$ (Mb/s)

8.29 $\theta_t = 18.44°$

8.33 (a) $R = 6.4 \times 10^{-3}$; $T = 0.9936$
(b) $P^i = 0.34$ W; $P^r = 2.2 \times 10^{-3}$ W; $P^t = 0.338$ W

8.35 $s = 0.5$ m; $f = 0.4$ m

8.37 (a) $R = 32$ cm
(b) $M = -4$

8.39 $s' = -25$ cm; $M = 1.25$; image is virtual and erect.

8.43 (a) $\dfrac{1}{f} = \left(\dfrac{n_l - n_m}{n_m}\right)\left(\dfrac{1}{R_1} - \dfrac{1}{R_2}\right)$
(b) $f = -60$ cm in air; $f = -235$ cm in water.

8.45 $s_2' = 8.34$ cm

8.47 $s_2' = \infty$

Chapter 9

9.1 $S_{max} = 1.9$ (μW/m^2)

9.3 (a) Direction of maximum radiation is a circular cone 120° wide, centered around the $+z$-axis.
(b) $D = 4 = 6$ dB
(c) $\Omega_p = \pi$ (sr) $= 3.14$ (sr)
(d) $\beta = 120°$

9.5 (a) $\xi = 29.7\%$
(b) $G = 0.44 = -3.5$ dB
(c) $I_0 = 33.8$ A; $P_t = 67.3$ W

9.7 $S_{max} = 2 \times 10^{-5}$ (W/m^2)

9.9 $D = 40.13$ dB

9.11 (a) $\xi = 99.3\%$
(b) $G = 1.63 = 2.1$ dB
(c) $I_0 = 0.74$ A; $P_t = 20.1$ W

9.13 (a) $\widetilde{\mathbf{E}}(R, \theta, \phi) = \hat{\boldsymbol{\theta}}\widetilde{E}_\theta = \hat{\boldsymbol{\theta}}\, j\dfrac{I_0 lk\eta_0}{8\pi}\left(\dfrac{e^{-jkR}}{R}\right)\sin\theta$ (V/m)
(b) $S(R, \theta) = \left(\dfrac{\eta_0 k^2 I_0^2 l^2}{128\pi^2 R^2}\right)\sin^2\theta$ (W/m^2)
(c) $D = 1.5$
(d) $R_{rad} = 20\pi^2(l/\lambda)^2$ (Ω)

9.17 (a) $\xi = 62\%$
(b) $G = 0.93 = -0.3$ dB
(c) $I_0 = 47.5$ A; $P_t = 32.3$ W

9.19 $P_t = 25.9$ (mW)

9.21 $P_t = 0.15$ (mW)

9.23 $\beta_{null} = 5.73°$

9.25 (a) $\beta_{xz} = 0.5°$; $\beta_{yz} = 1.5°$

INTEL-1014
U.S. Patent 7,151,430

(b) $D = 5.41 \times 10^4 = 47.3$ dB

9.27 **(a)** $\beta_e = 1.8°$; $\beta_a = 0.18°$
(b) $\Delta y = \beta_a R = 0.96$ m

9.29 **(a)** $F_a(\theta) = 4\cos^2\left[\frac{\pi}{8}(4\cos\theta + 1)\right]$
(b) $F_a(\theta) = 5 + 4\cos(2\pi\cos\theta)$
(c) $F_a(\theta) = 4\cos^2(\frac{\pi}{2}\cos\theta - \frac{\pi}{4})$
(d) $F_a(\theta) = 5 + 4\cos(\pi\cos\theta + \frac{\pi}{4})$
(e) $F_a(\theta) = 5 - 4\sin(\frac{\pi}{2}\cos\theta)$

9.31 $d/\lambda = 1.414$

9.33 $F_{an}(\theta) = \dfrac{\sin^2[(15\pi/4)\cos\theta]}{25\sin^2[(3\pi/4)\cos\theta]}$; $\beta = 13.5°$

9.35 $\delta = -2.72$ (rad) $= -155.9°$

Chapter 10

10.1 $T = 105.08$ minutes

10.3 166 channels

10.5 $(f_p)_{max} = 150$ kHz

10.7 $R_{max} = 5.75$ km

INTEL-1014
U.S. Patent 7,151,430

BIBLIOGRAPHY

The following list of books, arranged by topic, provides references for further reading.

Electromagnetics

Balanis, C.A., *Advanced Engineering Electromagnetics,* John Wiley & Sons, New York, 1989.

Cheng, D.K., *Fundamentals of Engineering Electromagnetics,* Addison Wesley, Reading, Reading, MA, 1993.

Crowley, J.M., *Fundamentals of Applied Electrostatics,* John Wiley & Sons, New York, 1986.

DuBroff, R.E., S.V. Marshall, and G.G. Skitek, *Electromagnetic Concepts and Applications,* 4th ed., Prentice Hall, Upper Saddle River, New Jersey, 1996.

Hayt, W.H., Jr., *Engineering Electromagnetics,* 5th ed., McGraw-Hill, New York, 1989.

Iskander, M.F., *Electromagnetic Fields & Waves*, Prentice Hall, Upper Saddle River, NJ, 1992.

Johnk, C.T.A., *Engineering Electromagnetic Fields and Waves,* 2nd ed., John Wiley & Sons, New York, 1988.

King, R.W.P. and S. Prasad, *Fundamental Electromagnetic Theory and Applications,* Prentice Hall, Englewood Cliffs, New Jersey, 1986.

Kong, J.A., *Electromagnetic Wave Theory*, 2nd ed., John Wiley & Sons, New York, 1990.

Kraus, J.D., *Electromagnetics,* 4th ed., McGraw-Hill, New York, 1992.

Neff, H.P., Jr., *Introductory Electromagnetics*, JohnWiley & Sons, New York, 1991.

Parton, J.E, S.J.T. Owens, and M.S. Raven, *Applied Electromagnetics,* 2nd ed., Macmillan, London, 1986.

Paul, C.R. and S.A. Nasar, *Introduction to Electromagnetic Fields,* McGraw-Hill, New York, 1987.

Ramo, S., J.R. Whinnery, and T. Van Duzer, *Fields and Waves in Communication Electronics,* 3rd ed., John Wiley & Sons, New York, 1994.

Rao, N.N., *Elements of Engineering Electromagnetics*, 2nd ed., Prentice Hall, Upper Saddle River, New Jersey, 1987.

Shen, L.C. and J.A. Kong, *Applied Electromagnetism,* 2nd ed., PWS Engineering, Boston, Mass., 1987.

Taylor, D.M. and P.E. Secker, *Industrial Electrostatics: Fundamentals and Measurements,* John Wiley & Sons, New York, 1994.

Wait, J.R., *Electromagnetic Theory,* Harper & Row, New York, 1985.

Antennas and Radiowave Propagation

Balanis, C.A., *Antenna Theory: Analysis and Design,* Harper & Row, New York, 1982.

Collin, R.E., *Antennas and Radiowave Propagation,* McGraw-Hill, New York, 1985.

Ishimaru, A., *Electromagnetic Wave Propagation, Radiation, and Scattering,* Prentice Hall, Upper Saddle River, New Jersey, 1991.

Kraus, J.D.,*Antennas,* 2nd ed., McGraw-Hill, New York, 1988.

Sander, K.F. and G.A.L. Reed, *Transmission and Propagation of Electromagnetic Waves,* 2nd ed., Cambridge University Press, Cambridge, England, 1986.

Stutzman, W.L. and G.A. Thiele, *Antenna Theory and Design*, John Wiley & Sons, New York, 1981.

Optical Engineering

Bohren, C.F. and D.R. Huffman, *Absorption and Scattering of Light by Small Particles*, John Wiley & Sons, New York, 1983.

Born, M. and E. Wolf, *Principles of Optics*, 6th ed., Pergamon Press, New York, 1980.

Cho, Z.H., J.P. Jones, and M. Singh, *Foundations of Medical Imaging,* John Wiley & Sons, New York, 1993.

INTEL-1014
U.S. Patent 7,151,430

Hecht, E., *Optics,* 2nd ed., Addison-Wesley, Reading, Mass., 1990.

Keiser, G., *Optical Fiber Communications,* 2nd ed., McGraw-Hill, New York, 1991.

Lee, D.L., *Electromagnetic Principles of Integrated Optics,* John Wiley & Sons, New York, 1986.

Smith, W.J., *Modern Optical Engineering: The Design of Optical Systems,* McGraw-Hill, New York, 1991.

Walker, B.H., *Optical Engineering Fundamentals*, McGraw-Hill, New York, 1994.

Microwave Engineering

Freeman, J.C., *Fundamentals of Microwave Transmission Lines,* John Wiley & Sons, New York, 1996.

Pozar, D.M., *Microwave Engineering,* Addison-Wesley, Reading, Mass., 1990.

Richharia, M., *Satellite Communication Systems Design Principles,* McGraw-Hill, New York, 1995.

Scott, A.W., *Understanding Microwaves,* John Wiley & Sons, New York, 1993.

Sinnema, W., *Electronic Transmission Technology,* 2nd ed., Prentice Hall, Englewood Cliffs, New Jersey, 1988.

Skolnik, M.I., *Introduction to Radar Systems,* 2nd ed., McGraw-Hill, New York, 1980.

Stimson, G.W., *Introduction to Airborne Radar,* Hughes Aircraft Company, El Segundo, California, 1983.

INTEL-1014
U.S. Patent 7,151,430

INDEX

Admittance, 75
Air line, 43, 45
Ampere's circuital law, 202, 232
Amperian contour, 203
Angle
  azimuth, 109, 344
  Brewster, 315
  critical, 305
  incidence, 303
  polarizing, 315
  reflection, 303
  refraction, 303
  scan, 381, 384
  zenith, 113, 344
Anisotropic medium, 162
Antenna arrays, 342, 371
  broadside, 378
  endfire, 381
  frequency scanned, 383
  linear, 373
  phased, 381
Antenna properties
  beam width, 351
  directivity, 351
  effective area, 360
  gain, 354
  input impedance, 361
  pattern, 341, 348
  polarization, 342
  radiation efficiency, 354
  radiation resistance, 354
Antenna types
  electric dipole, 342
  half-wave dipole, 355–358
  horn, 342
  isotropic, 341
  linear dipole, 359
  loop, 342
  multiple beam, 373
  parabolic dish, 342
  quarter-wave monopole, 358
  satellite, 4, 364, 398
  short (Hertzian) dipole, 343
Aperture illumination, 367
Approximations, 415
Array factor, 374
  multiple-beam array, 380
  phased array, 381
  two-vertical dipoles, 375
  uniform array, 378
Array feeding, 382
Atmospheric opacity, 20
Atom, 8, 156, 161
Attenuation constant, 276
  good conductor, 278, 279
  lossless line, 47
  low-loss dielectric, 278, 279
  transmission line, 45
Attenuation factor, 17
Average power density, 284, 346
Axial ratio, 274
Azimuth angle, 109, 244
Azimuth resolution, 401

Band designations, 21
Base vectors
  Cartesian coordinates, 102
  cylindrical coordinates, 109
  spherical coordinates, 113
Beamwidth, 351
  half-wave dipole, 361
  rectangular aperture, 369
  short dipole, 347, 351
  wavelength-long dipole, 361
Biot-Savart law, 10, 205
Boltzmann's constant, *See* inside front cover
Bounce diagram, 88
Boundary conditions
  between a dielectric and a perfect conductor, 166
  between two dielectric media, 166



INTEL-1014
U.S. Patent 7,151,430

Boundary conditions *(cont.)*
current density, 168
electromagnetic fields, 246–247
electrostatic fields, 164
magnetostatic fields, 213
Breakdown voltage, 163
Brewster angle, 315
Broadcast service, 394
Broadside array, 378

Capacitance, 169
cylindrical capacitor, 171
parallel-plate capacitor, 170
Capacitance per unit length
coaxial line, 41 42, 171
parallel-plate line, 41
two-wire line, 41
Cartesian coordinates, 109
Characteristic impedance, 45, 49
Charge-continuity equation, 248
Charge density
line, 140
surface, 140
volume, 140
Charge dissipation, 249
Charge, electric
conservation property, 8
electron, 7
Circular polarization, 271
Circulation of a vector field
Circulator, 3, 394, 396
Coaxial cable, 3
capacitance, 41, 42, 171
conductance, 41, 42, 160
electrostatic field, 171
inductance, 41, 42, 218
magnetic field, 217
resistance, 41, 42, 283
Communication satellite, *See* Satellite.
Complex conjugate, 23
Complex feeding coefficient, 373
Complex number, 22
Complex permittivity, 269
Concave lens, 324, 325
Concave mirror, 322
Conductance, 159
Conductance per unit length, 159
coaxial line, 41, 42, 160
parallel-plate line, 41, 42
two-wire line, 41, 42
Conduction current, 142
Conduction current density, 157
Conductivity, 11, 157
materials, 156, 413
Conductors, 156
charges on, 167
good, 277
Conservative (or irrotational) field, 129, 152
Constitutive parameters, 11, 156
Convection current, 142
Converging lens, 324
Convex lens, 324
Convex mirror, 322
Coordinate systems
Cartesian, 109, 110
cylindrical, 109, 110
spherical, 110, 113
transformations between, 115–119
Coulomb, Charles Augustin de, 7
Coulomb's law, 7, 143
Critical angle, 305
Cross product, 105
Curl operator, 127–129, *See also* inside back cover
Current
conduction, 142
convection, 142
displacement, 244
Current density
conduction, 157
convection, 142
surface, 196
volume, 196
Cylindrical coordinates, 109

Decibel scale, 286
Del operator, 120
Depth of penetration, 277
Detection
maximum range, 404
probability, 403
threshold level, 404
Diamagnetism, 211
Dielectric breakdown, 163
Dielectric constant, 9, 143

INTEL-1014
U.S. Patent 7,151,430

Dielectric strength, 163
Dielectrics, 156, 163, 413
Dipole
  electric, 154
  half-wave, 355
  linear, 359
  magnetic, 199
Diffraction, 320
Dipole moment
  electric, 154
  magnetic, 194
Directional derivative, 121
Directivity, 351
  aperture antenna, 371
  half-wave dipole, 357
  Hertzian dipole, 353
Disk of charge, 147
Dispersion, 37
  optical fibers, 307
Dispersive medium, 48
Displacement current, 244, 246
Distance vector,
  Cartesian coordinates, 104, 119
  cylindrical coordinates, 112, 119
  spherical coordinates, 119
Distortionless line, 93 (Problem 2.6)
Divergence, 123–125, *See also* inside back cover
Divergence theorem, 123
Divergenceless field, 125
Diverging lens, 325
Domain wall, 211
Doppler frequency shift, 399, 405
Dot product, 104
Downlink, 4, 393, 394
Duplexer, 394

Earth's
  atmospheric opacity, 20
  mass, 392
  period, 393
  radius, 392, 393
Effective area
  any antenna, 362
  aperture antenna, 371
  short dipole, 362
Effective aperture, *See* Effective area
EHF, 21
Electric charge
  conservation of, 8
  electron, 7
Electric dipole, 9, 154
Electric dipole antenna, 342, 359
  half-wave dipole, 354–357
  quarter-wave monopole, 357
  short (Hertzian) dipole, 343
Electric dipole moment, 154
Electric displacement, 244
Electric field intensity
  charge distribution, 146
  circular disk of charge, 147
  electric dipole, 154
  infinite line of charge, 150
  point charges, 8, 144, 149
  ring of charge, 146
Electric flux density, 9
Electric force, 7, 173
Electric permittivity, *See* permittivity
Electric potential, scalar, 151
  retarded, 251
Electric susceptibility, 162
Electromagnetic
  fields, 231
  force, 6, 188
  generator, 241, 244
  induction, 233
  operator, 241, 244
  potentials, 250
  spectrum, 19–22
Electromotive force, 233
  motional, 233
  transformer, 233
Electron
  charge of, 7
  drift velocity, 156
  mobility, 157
Electronic steering, 373, 380, 384
Electrostatic energy, 172
Electrostatics, 11, 12, 139
ELF, 20, 21
Elliptical polarization, 273
Ellipticity angle, 274
EM, 19
Endfire direction, 381

INTEL-1014
U.S. Patent 7,151,430

Energy
  electric, 172
  magnetic, 219
Equipotential medium, 157
Euler's identity, 22
Explorer I, 392

False-alarm probability, 403
Far-field (or far-zone) region, 343
  aperture antennas, 367
  short dipole, 344
Faraday, Michael, 231
Faraday's law, 231, 232, 235
Feeding coefficient, 373
Ferromagnetism, 211
Field, 6
  conservative, 129, 152
  divergenceless, 125
  electrostatic, 11, 139
  irrotational, 129, 152
  magnetostatic, 11, 187
  solenoidal, 214
Flux
  density, 123
  lines, 123
  linkage, 216
Focal length
  mirror, 322
  thin lens, 328
Forces
  centrifugal, 392
  electric, 7, 173
  electromagnetic, (Lorentz), 188
  gravitational, 6, 392
  magnetic, 187
Form factor, of radiated field, 367
Free space
  constants of, *See* inside front cover
  intrinsic impedance of, 266
  permeability of, 10
  permittivity of, 7
  velocity of light in, 11
Frequency, 16
Frequency-division multiple access (FDMA), 393
Frequency scanning, 383
Fresnel reflection coefficient, 312
Fresnel transmission coefficient, 312
Friis transmission formula, 363
Fringing Fields, 170

Gausss law, 148, 232
Gauss's law for magnetism, 201, 232
Gaussian lens formula, 328
Gaussian surface, 148
Geometric optics, 319
Geostationary orbit, 392
Gradient operator, 120–122, *See also* inside back cover
Gravitational
  field, 6
  force, 6, 392
Grazing incidence, 315

Henry, Joseph, 232
Hertzian dipole, 344
  directivity, 353
  effective area of, 362
  electromagnetic fields, 345
  radiation pattern, 347
  radiation resistance, 354
HF, 20, 21
Hole drift velocity, 157
Hole mobility, 157
Homogeneous, 11, 156, 162
Hysteresis, 212

Image distance, 321
Image method, 173
Impedance
  characteristic, 45, 49
  input, 55
  intrinsic, 265
  load, 48
  matching network, 80
  open-circuited line, 60
  shorted line, 58
  surface (or internal), 282
Incidence
  angle of, 303
  plane of, 309
Index of refraction, 304
Inductance, 214
Inductance per unit length
  coaxial line, 41, 42, 218
  long solenoid, 215

INTEL-1014
U.S. Patent 7,151,430

parallel-plate line, 41, 42
two-wire line, 41, 42
Insulator, 156
Internal impedance, 282
International system of units, 4
Interpulse period, 400
Intrinsic impedance
free space, 266
good conductor, 278–279
low-loss dielectric, 278–279
medium, 265, 277
Irrotational (or conservation) field , 129, 152
Isotropic, 156, 162

Joule's law, 160

Kirchhoff's current law, 248
Kirchhoff's voltage law, 152

Laplace's equation, 155
Laplacian operator, 130–131, *See also* inside back cover
Lateral magnification
spherical mirror, 322
thin lens, 330
Left-hand circular (LHC) polarization, 271
Lenses, 324–331
Lensmaker's formulae, 328
Lenz's law, 234, 236
LF, 20, 21
Lidar, 399
Line of charge, 140, 150
Linear medium, 162
Linear polarization, 269
Load impedance, 48
Lorentz force, 188
Lossless medium, 14, 262
Lossless transmission line, 47
Lossy medium, 17, 262

Magnet, bar, 10, 200
Magnetic dipole, 199
Magnetic dipole moment, 194
Magnetic energy, 219
Magnetic field intensity, 11, 195
circular loop, 199
current distributions, 196
current element, 195
infinite current sheet, 205
linear conductor, 196, 204
magnetic dipole, 199
pie-shaped loop, 198
solenoid, 215
toroidal coil, 205
Magnetic flux, 208, 233
Magnetic flux density, 10, 187
Magnetic flux linkage, 216
Magnetic force, 187
between conductors, 200
conductor, 189
relation of torque to, 192
semicircular conductor, 191
Magnetic hysteresis, 212
Magnetic materials, 211
Magnetic permeability, *See* permeability
Magnetic potential, vector, 206
Magnetic susceptibility, 210
Magnetic torque, 192
Magnetite, 9
Magnetization curve, 211
hard ferromagnetics, 212
soft ferromagnetics, 212
Magnetization vector, 209
Magnetized domains, 210
Magnetostatics, 11, 12, 139, 187
Main lobe of antenna pattern, 350
Maxwell, James Clerk, 139
Maxwell's equations
differential form, 139, 232
integral form, 232
source-free, 263
time-harmonic, 263
Medium
anisotropic, 162
guided, 261
homogeneous, 11, 156, 162
isotropic, 156, 162,
linear, 162
lossless, 14, 262
lossy, 17, 262
unbounded, 261, 294
MF, 20, 21
Microstrip lines, 37, 38
Microwave band, 21, 22

INTEL-1014
U.S. Patent 7,151,430

Mirror
  plane, 321
  concave, 322
  convex, 322
  equation, 322
  focal length, 322
  spherical, 322
Mixer, 3
Mobile service, 394
Mobility
  electrons, 157
  holes, 157
Monopulse radar, 406
Motional emf, 233, 239
Multiple-beam antenna, 3, 373
Multiplexer, 395
Mutual inductance, 218

Negative lens, 325
Neper, 17
Noise temperature, 364
Nonmagnetic, 11
Nonpolar materials, 161
Nuclear force, 5

Object distance, 321
Oersted, Hans, 10
Ohm's law, 157
Open-circuited line, 60
Optical fibers, 3, 38, 306
  acceptance angle, 306
  cladding, 306
  dispersion in, 307
  fiber core, 306
  modes in, 307
Orbital magnetic moment, 209
Orthogonal coordinate systems, 108

Parallel polarization, 309, 313–315
Paramagnetism, 211
Paraxial rays, 325
Pattern multiplication principle, 375
Pattern solid angle, 351
Perfect conductor, 11, 42
Perfect dielectric, 11, 42
Period, 14
Periscope, 335

Permeability, 11, 12, 209
  common materials, 414
  free space, 10, 12
  relative, 210
Permittivity, 9, 12, 143
  air, 9
  common materials, 163, 413
  complex, 263
  free space, 7, 12, 143
  relative, 9, 143
Perpendicular polarization, 209–213
Phase, 14
  lag, 16
  lead, 16
Phase constant, 16, 276
  good conductor, 278–279
  lossless line, 47
  low-loss dielectric, 278–279
  transmission line, 45
Phase delay, 381
Phase matching condition, 311
Phase velocity, 15, 16, 36, 49
  good conductor, 279
  lossless line, 47, 49
  lossless medium, 266
  low-loss dielectric, 279
Phased array, 381
Phasor representation, 5, 25
Physical optics, 319
Plane mirror, 321
Plane of incidence, 309
Plane wave, 262
  polarization of, 269
  propagation, 264
Point charges, 8, 144, 149
Poisson's equation for electric potential, 155
Poisson's equation for magnetic potential, 207
Polar materials, 162
Polarization field, 161, 162
Polarization of materials, 9
Polarization state, 269, 275
  circular, 271–273
  diversity, 396
  elliptical, 273
  left hand circular, 271
  linear, 270
  parallel, 309

INTEL-1014
U.S. Patent 7,151,430

perpendicular, 209–213
right hand circular, 272
Polarizing angle, 315
Position vector, 103
Cartesian coordinates, 103
cylindrical coordinates, 110
spherical coordinates, 110, 113
Positive lens, 324
Potential
retarded, 251
scalar electric, 151
vector magnetic, 206
Power density, 284, 346
Power on transmission line,
instantaneous, 64
time average, 65
Power transfer, maximum, 362
Power transfer, ratio, 364
Poynting vector, 283
Prefixes, multiple and submultiple, 5, *See also* inside of front cover
Principal axis, 322
Principal planes, 349
Principle of superposition, 8
Prism, 334
Propagation constant, 264
good conductor, 278–279
low-loss dielectric, 278–279
transmission line, 45, 49
distortionless, 93 (Problem 2.6)
lossless, 47, 49
Propagation velocity, *See* Phase velocity
Proton, charge of, 7
Pulse length, 400
Pulse repetition frequency (PRF), 400

Quarter-wave monopole, 358
Quarter-wave transformer, 62

Radar, 399
azimuth resolution, 401
bistatic, 403
cross section, 403
Doppler, 404
false-alarm and detection probabilities, 403
monopulse, 406
monostatic, 403
PRF, 401
range resolution, 401
target detection, 402
unambiguous range, 401
Radar cross section, 403
Radar equation, 404
Radial distance, 109
Radiation
efficiency, 354
intensity, 347
lobes, 349
pattern, 341, 348
resistance, 354
half-wave dipole, 357
Hertzian dipole, 357
quarter-wave monopole, 360
Radius of curvature, 322
Radome, 299
Range coordinate, 113, 344
Range resolution, 401
Ray, 294
Ray optics, 319
Real image, 321
Receiving antenna, 361
Rectangular aperture, 368
Rectangular coordinates, 109
Reflection
angle of, 303
Snell's law of, 304
Reflection coefficient
normal incidence, 297
parallel polarization, 314, 318
perpendicular polarization, 312, 318
voltage, 50
Reflectivity (reflectance), 317
Refraction
angle of, 303
index of, 304
Snell's law of, 304
Refractive index, 304
Relaxation time constant, 249
Resistance, 158
Resistance per unit length
coaxial line, 41–42, 283
parallel-plate line, 41
two-wire line, 41

INTEL-1014
U.S. Patent 7,151,430

Retarded potential
  scalar, 253–254
  vector, 253–254
Right-hand circular (RHC) polarization, 272
Right-hand rule,
  Ampere's law, 203
  magnetic torque, 194
  relation between **E** and **H**, 268
  vector (cross) product, 106
Ring of charge, 146
Rotation angle, 273

Satellite
  communication, 3, 364, 391
    antenna beams, 398
    Explorer I, 392
    Score, 392
    Sputnik I, 392
  geostationary, 392
  telemetry and tracking, 394
  transponder, 393
Scalar, 101
  gradient of, 120
  product, 104
  triple product, 107
Scalar formulation, 366
Scan angle, 381, 384
Score, 392
Seawater, 278, 413
Self inductance, 216
Semiconductors, 156
SHF, 21
Short-circuited line, 58
SI units, 4
Sidelobes of antenna pattern, 350
Sidereal day, 393
Sign convention
  spherical mirrors, 323
  thin lenses, 325
Signal-to-noise ratio, 364, 397, 404
Single-stub matching, 80
Skin depth, 277
Slotted line, 54
Smith chart, 66
  angle of reflection coefficient, 70
  SWR circle on, 71
  unit circle, 66
  wavelengths toward generator (WTG), 71
  wavelengths toward load (WTL), 71
Snell's law
  reflection, 304, 311
  refraction, 304, 311
Solenoidal, 214
Solid angle, 348
Spectrum of electromagnetic waves, 20
Spherical coordinates, 113
Spherical mirror, 322
Spherical propagation factor, 344
Spin magnetic moment, 209
Sputnik I, 392
Standing-wave, 46, 51
  pattern, 52
  ratio circle on Smith chart, 71
  ratio (SWR), 54, 71, 297
Stokes's theorem, 129
Striplines, 37, 38
Stub tuner, 80
Superconductors, 156
Surface impedance, 282
Susceptance, 75
Susceptibility, magnetic, 210
System noise temperature, 364, 397

Tai, C.T., 126
Telegraphers equations, 38, 44
Tesla, Nikola, 10
Thévenin circuit, 361
Thin-lens equation, 328
Time-harmonic electromagnetics, 251
Toroid (or torus), 205
Torque, magnetic, 192
Total internal reflection, 305
Transformer emf, 233
Transformers,
  ideal, 237
  quarter-wave, 62
Transmission coefficient
  normal incidence, 297
  parallel polarization, 314, 318
  perpendicular polarization, 312, 318
Transmission line, 3, 38, 41
  attenuation constant of, 45, 49
  characteristic impedance of, 45, 49
  circuit elements, 59

INTEL-1014
U.S. Patent 7,151,430

coaxial, 3, 38, 41, 49
distortionless, 93 (Problem 2.6)
half-wave sections of, 62
impedance matching of, 62, 80
infinite, 96 (Problem 2.33)
input impedance of, 55
microstrip line, 38
open-circuited, 60
parallel-plate, 38, 41, 49
phase constant of, 45, 49
power flow on, 64
propagation constant of, 45, 49
short-circuited, 58
strip line, 38
transient response on, 84
two-wire, 38, 41, 49
voltage maximum on, 53
voltage minimum on, 54
Transmission-line parameters, 39–42
Transmissivity (transmittance), 317
Transponder, 393
Transverse electric (TE) wave, 309
Transverse electromagnetic (TEM), 37, 266
Transverse magnetic (TM) wave, 309
Trigonometric relations, 415

UHF, 21
Unambiguous range, 401
Uniform aperture distribution, 368
Uniform plane wave, 265
Unit vector, 101
Units,
derived quantities, 411, 412
fundamental, 5
SI system, 4
Universal constants, *See* inside front cover
Uplink, 4, 393, 394

Vector, 101
addition and subtraction, 103
multiplication, 104
product, 105
Vector formulation, 367
Vector identities, *See* inside back cover
Vector potential, magnetic, 206
retarded, 251
Velocity
light in free space, 11
phase, 15, 16, 36, 49
radial, 399, 405
VHF, 20, 21
Virtual image, 321
Visible light, 19, 333 (Problem 8.12)
VLF, 20,21
Voltage
breakdown, 163
electrostatic, 151
induced, 233
maximum, 53
minimum, 54
reflection coefficient, 50

Wave
circularly polarized, 271
continuous harmonic, 12
cylindrical, 12, 13
electromagnetic, 266
elliptically polarized, 273
lossless media, 266
lossy media, 276
interference, 30 (Problem 1.7), 52
linearly polarized, 270
one-dimensional, 12
sound, 18
spherical, 12, 13, 262
standing, 46, 51
three-dimensional, 12, 13
transient, 12
transverse electric (TE), 309
transverse electromagnetic (TEM), 37, 266
transverse magnetic (TM), 309
two-dimensional, 12, 13
uniform plane, 262
Wave equation, 43, 264
Wave optics, 319
Wavefront, 294
Wavelength, 14
Wavenumber, 16, 252, 264
Weak interaction force, 5
WTG (wavelengths toward generator), 71
WTL (wavelengths toward load), 71

Zenith angle, 113, 344

INTEL-1014
U.S. Patent 7,151,430

GRADIENT, DIVERGENCE, CURL, & LAPLACIAN OPERATORS

CARTESIAN (RECTANGULAR) COORDINATES (x, y, z)

$$\nabla V = \hat{\mathbf{x}}\frac{\partial V}{\partial x} + \hat{\mathbf{y}}\frac{\partial V}{\partial y} + \hat{\mathbf{z}}\frac{\partial V}{\partial z}$$

$$\nabla \cdot \mathbf{A} = \frac{\partial A_x}{\partial x} + \frac{\partial A_y}{\partial y} + \frac{\partial A_z}{\partial z}$$

$$\nabla \times \mathbf{A} = \begin{vmatrix} \hat{\mathbf{x}} & \hat{\mathbf{y}} & \hat{\mathbf{z}} \\ \frac{\partial}{\partial x} & \frac{\partial}{\partial y} & \frac{\partial}{\partial z} \\ A_x & A_y & A_z \end{vmatrix} = \hat{\mathbf{x}}\left(\frac{\partial A_z}{\partial y} - \frac{\partial A_y}{\partial z}\right) + \hat{\mathbf{y}}\left(\frac{\partial A_x}{\partial z} - \frac{\partial A_z}{\partial x}\right) + \hat{\mathbf{z}}\left(\frac{\partial A_y}{\partial x} - \frac{\partial A_x}{\partial y}\right)$$

$$\nabla^2 V = \frac{\partial^2 V}{\partial x^2} + \frac{\partial^2 V}{\partial y^2} + \frac{\partial^2 V}{\partial z^2}$$

CYLINDRICAL COORDINATES (r, ϕ, z)

$$\nabla V = \hat{\mathbf{r}}\frac{\partial V}{\partial r} + \hat{\boldsymbol{\phi}}\frac{1}{r}\frac{\partial V}{\partial \phi} + \hat{\mathbf{z}}\frac{\partial V}{\partial z}$$

$$\nabla \cdot \mathbf{A} = \frac{1}{r}\frac{\partial}{\partial r}(rA_r) + \frac{1}{r}\frac{\partial A_\phi}{\partial \phi} + \frac{\partial A_z}{\partial z}$$

$$\nabla \times \mathbf{A} = \frac{1}{r}\begin{vmatrix} \hat{\mathbf{r}} & \hat{\boldsymbol{\phi}}r & \hat{\mathbf{z}} \\ \frac{\partial}{\partial r} & \frac{\partial}{\partial \phi} & \frac{\partial}{\partial z} \\ A_r & rA_\phi & A_z \end{vmatrix} = \hat{\mathbf{r}}\left(\frac{1}{r}\frac{\partial A_z}{\partial \phi} - \frac{\partial A_\phi}{\partial z}\right) + \hat{\boldsymbol{\phi}}\left(\frac{\partial A_r}{\partial z} - \frac{\partial A_z}{\partial r}\right) + \hat{\mathbf{z}}\frac{1}{r}\left[\frac{\partial}{\partial r}(rA_\phi) - \frac{\partial A_r}{\partial \phi}\right]$$

$$\nabla^2 V = \frac{1}{r}\frac{\partial}{\partial r}\left(r\frac{\partial V}{\partial r}\right) + \frac{1}{r^2}\frac{\partial^2 V}{\partial \phi^2} + \frac{\partial^2 V}{\partial z^2}$$

SPHERICAL COORDINATES (R, θ, ϕ)

$$\nabla V = \hat{\mathbf{R}}\frac{\partial V}{\partial R} + \hat{\boldsymbol{\theta}}\frac{1}{R}\frac{\partial V}{\partial \theta} + \hat{\boldsymbol{\phi}}\frac{1}{R\sin\theta}\frac{\partial V}{\partial \phi}$$

$$\nabla \cdot \mathbf{A} = \frac{1}{R^2}\frac{\partial}{\partial R}(R^2 A_R) + \frac{1}{R\sin\theta}\frac{\partial}{\partial \theta}(A_\theta \sin\theta) + \frac{1}{R\sin\theta}\frac{\partial A_\phi}{\partial \phi}$$

$$\nabla \times \mathbf{A} = \frac{1}{R^2\sin\theta}\begin{vmatrix} \hat{\mathbf{R}} & \hat{\boldsymbol{\theta}}R & \hat{\boldsymbol{\phi}}R\sin\theta \\ \frac{\partial}{\partial R} & \frac{\partial}{\partial \theta} & \frac{\partial}{\partial \phi} \\ A_R & RA_\theta & (R\sin\theta)A_\phi \end{vmatrix}$$

$$= \hat{\mathbf{R}}\frac{1}{R\sin\theta}\left[\frac{\partial}{\partial \theta}(A_\phi \sin\theta) - \frac{\partial A_\theta}{\partial \phi}\right] + \hat{\boldsymbol{\theta}}\frac{1}{R}\left[\frac{1}{\sin\theta}\frac{\partial A_R}{\partial \phi} - \frac{\partial}{\partial R}(RA_\phi)\right] + \hat{\boldsymbol{\phi}}\frac{1}{R}\left[\frac{\partial}{\partial R}(RA_\theta) - \frac{\partial A_R}{\partial \theta}\right]$$

$$\nabla^2 V = \frac{1}{R^2}\frac{\partial}{\partial R}\left(R^2\frac{\partial V}{\partial R}\right) + \frac{1}{R^2\sin\theta}\frac{\partial}{\partial \theta}\left(\sin\theta\frac{\partial V}{\partial \theta}\right) + \frac{1}{R^2\sin^2\theta}\frac{\partial^2 V}{\partial \phi^2}$$

INTEL-1014
U.S. Patent 7,151,430

SOME USEFUL VECTOR IDENTITIES

$\mathbf{A}\cdot\mathbf{B} = AB\cos\theta_{AB}$ Scalar (or dot) product

$\mathbf{A}\times\mathbf{B} = \hat{\mathbf{n}}AB\sin\theta_{AB}$ Vector (or cross) product, $\hat{\mathbf{n}}$ normal to plane containing $\mathbf{A}$ and $\mathbf{B}$

$\mathbf{A}\cdot(\mathbf{B}\times\mathbf{C}) = \mathbf{B}\cdot(\mathbf{C}\times\mathbf{A}) = \mathbf{C}\cdot(\mathbf{A}\times\mathbf{B})$

$\mathbf{A}\times(\mathbf{B}\times\mathbf{C}) = \mathbf{B}(\mathbf{A}\cdot\mathbf{C}) - \mathbf{C}(\mathbf{A}\times\mathbf{B})$

$\nabla(U+V) = \nabla U + \nabla V$

$\nabla(UV) = U\nabla V + V\nabla U$

$\nabla\cdot(\mathbf{A}+\mathbf{B}) = \nabla\cdot\mathbf{A} + \nabla\cdot\mathbf{B}$

$\nabla\cdot(U\mathbf{A}) = U\nabla\cdot\mathbf{A} + \mathbf{A}\cdot\nabla U$

$\nabla\times(U\mathbf{A}) = U\nabla\times\mathbf{A} + \nabla U\times\mathbf{A}$

$\nabla\times(\mathbf{A}+\mathbf{B}) = \nabla\times\mathbf{A} + \nabla\times\mathbf{B}$

$\nabla\cdot(\mathbf{A}\times\mathbf{B}) = \mathbf{B}\cdot(\nabla\times\mathbf{A}) - \mathbf{A}\cdot(\nabla\times\mathbf{B})$

$\nabla\cdot(\nabla\times\mathbf{A}) = 0$

$\nabla\times\nabla V = 0$

$\nabla\cdot\nabla V = \nabla^2 V$

$\nabla\times\nabla\times\mathbf{A} = \nabla(\nabla\cdot\mathbf{A}) - \nabla^2\mathbf{A}$

$\int_{\mathcal{V}}(\nabla\cdot\mathbf{A})\,d\mathcal{V} = \oint_S \mathbf{A}\cdot d\mathbf{s}$ Divergence theorem (S encloses $\mathcal{V}$)

$\int_S(\nabla\times\mathbf{A})\cdot d\mathbf{s} = \oint_C \mathbf{A}\cdot d\mathbf{l}$ Stokes's theorem (S bounded by C)

INTEL-1014
U.S. Patent 7,151,430

END USER LICENSE AGREEMENT

You should carefully read the following terms and conditions before breaking the seal on the CD-ROM envelope. Among other things, this Agreement licenses the enclosed software to you and contains warranty and liability disclaimers. By breaking the seal on the CD-ROM envelope, you are accepting and agreeing to the terms and conditions of this Agreement. If you do not agree to the terms of this Agreement, do not break the seal. You should promptly return the package unopened.

LICENSE

Prentice-Hall, Inc. (the "Company") provides this Software to you and licenses its use as follows:

a. use the Software on a single computer of the type identified on the package;

b. make one copy of the Software in machine-readable form solely for back-up purposes.

LIMITED WARRANTY

The Company warrants the physical CD-ROM(s) on which the Software is furnished to be free from defects in materials and workmanship under normal use for a period of sixty (60) days from the date of purchase as evidenced by a copy of your receipt.

DISCLAIMER

THE SOFTWARE IS PROVIDED "AS IS" AND COMPANY SPECIFICALLY DISCLAIMS ALL WARRANTIES OF ANY KIND, EITHER EXPRESS OR IMPLIED, INCLUDING, BUT NOT LIMITED TO, THE IMPLIED WARRANTIES OF MERCHANTABILITY AND FITNESS FOR A PARTICULAR PURPOSE. IN NO EVENT WILL COMPANY BE LIABLE TO YOU FOR ANY DAMAGES, INCLUDING ANY LOSS OF PROFIT OR OTHER INCIDENTAL, SPECIAL OR CONSEQUENTIAL DAMAGES EVEN IF COMPANY HAS BEEN ADVISED OF THE POSSIBILITY OF SUCH DAMAGES.

SOME STATE DO NOT ALLOW THE EXCLUSION OF IMPLIED WARRANTIES OR LIMITATION OR EXCLUSION OF LIABILITY FOR INCIDENTAL OR CONSEQUENTIAL DAMAGES, SO THE ABOVE EXCLUSIONS AND/OR LIMITATIONS MAY NOT APPLY TO YOU.

LIMITATIONS OF REMEDIES

The Company's entire liability and your exclusive remedy shall be:

1. the replacement of such CD-ROM if you return a defective CD-ROM during the limited warranty period, or

2. if the Company is unable to deliver a replacement CD-ROM that is free of defects in materials or workmanship, you may terminate this Agreement by returning the Software.

GENERAL

You may not sublicense, assign, or transfer the license of the Software or make or distribute copies of the Software. Any attempt otherwise to sublicense, assign, or transfer any of the rights, duties, or obligations hereunder is void.

Should you have any questions concerning this Agreement, you may contact Prentice-Hall, Inc. by writing to:

Prentice Hall
Engineering
One Lake Street
Upper Saddle River, NJ 07458
Attention: Mechanical Engineering Editor

YOU ACKNOWLEDGE THAT YOU HAVE READ THIS AGREEMENT, UNDERSTAND IT, AND AGREE TO BE BOUND BY ITS TERMS AND CONDITIONS. YOU FURTHER AGREE THAT IT IS THE COMPLETE AND EXCLUSIVE STATEMENT OF THE AGREEMENT BETWEEN US THAT SUPERSEDES ANY PROPOSAL OR PRIOR AGREEMENT, ORAL OR WRITTEN, AND ANY OTHER COMMUNICATIONS BETWEEN US RELATING TO THE SUBJECT MATTER OF THIS AGREEMENT.

INTEL-1014
U.S. Patent 7,151,430



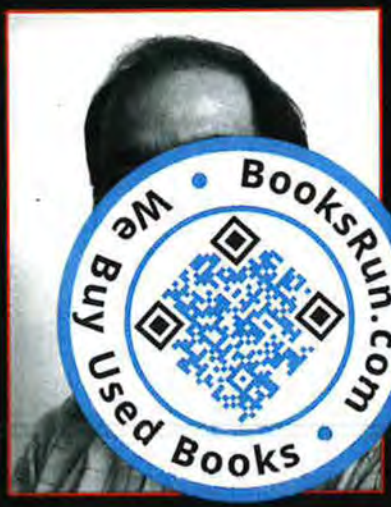
THIS CD-ROM CONTAINS:

(a) A generic copy of the Smith Chart used in Chapter 2
(b) Solutions of selected end-of-chapter problems
(c) Copies of all figures in the book

INTEL-1014
U.S. Patent 7,151,430

1999 Edition

CD-ROM Included



FUNDAMENTALS OF APPLIED ELECTROMAGNETICS

FAWWAZ T. ULABY

Fawwaz T. Ulaby was born in Damascus, Syria and grew up in Beirut, Lebanon. After receiving his B.S. degree in Physics from the American University of Beirut, he pursued graduate studies at the University of Texas at Austin from which he received his Ph.D. degree in electrical engineering in 1968. He then spent the next 16 years as a member of the Electrical Engineering faculty at the University of Kansas where he was involved in the development of radar sensor technology for environmental and industrial applications.

In 1984, Professor Ulaby moved to the University of Michigan in Ann Arbor where he is now the R. Jamison and Betty Williams Distinguished Professor of Electrical Engineering and Computer Science. His research experience includes the design of microwave systems for measuring the dielectric properties of materials; characterization of radar scattering and microwave emission from terrain; development of computer algorithms for identifying terrain features using Earth-observing satellite radar systems; and the development of millimeter-wave radar sensors for automotive applications. He has published several books on microwave sensor technology, imaging radar design, and the physics of radar scattering from terrain. He is Fellow of IEEE and a member of the National Academy of Engineering.

ISBN 0-13-011554-1
$86.25
9 780130 115546

PRENTICE HALL
Upper Saddle River, NJ 07458
http://www.prenhall.com

INTEL-1014
U.S. Patent 7,151,430